frontiers | Research Topics

Ferroptosis in cancer and beyond, volume II

Edited by
Yanqing Liu, Guo Chen, Chaoyun Pan and Xin Wang

Published in
Frontiers in Molecular Biosciences
Frontiers in Immunology
Frontiers in Oncology

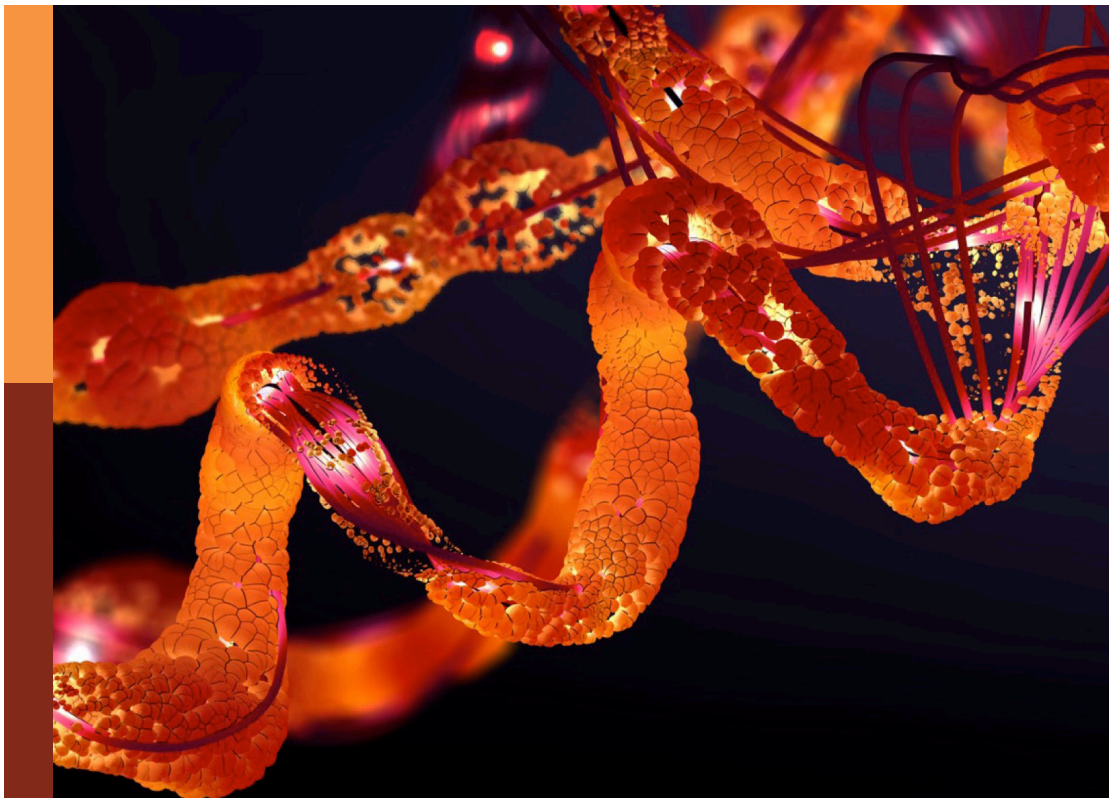

ISSN 1664-8714
ISBN 978-2-8325-3466-3
DOI 10.3389/978-2-8325-3466-3

About Frontiers

Frontiers is more than just an open access publisher of scholarly articles: it is a pioneering approach to the world of academia, radically improving the way scholarly research is managed. The grand vision of Frontiers is a world where all people have an equal opportunity to seek, share and generate knowledge. Frontiers provides immediate and permanent online open access to all its publications, but this alone is not enough to realize our grand goals.

Frontiers journal series

The Frontiers journal series is a multi-tier and interdisciplinary set of open-access, online journals, promising a paradigm shift from the current review, selection and dissemination processes in academic publishing. All Frontiers journals are driven by researchers for researchers; therefore, they constitute a service to the scholarly community. At the same time, the *Frontiers journal series* operates on a revolutionary invention, the tiered publishing system, initially addressing specific communities of scholars, and gradually climbing up to broader public understanding, thus serving the interests of the lay society, too.

Dedication to quality

Each Frontiers article is a landmark of the highest quality, thanks to genuinely collaborative interactions between authors and review editors, who include some of the world's best academicians. Research must be certified by peers before entering a stream of knowledge that may eventually reach the public - and shape society; therefore, Frontiers only applies the most rigorous and unbiased reviews. Frontiers revolutionizes research publishing by freely delivering the most outstanding research, evaluated with no bias from both the academic and social point of view. By applying the most advanced information technologies, Frontiers is catapulting scholarly publishing into a new generation.

What are Frontiers Research Topics?

Frontiers Research Topics are very popular trademarks of the *Frontiers journals series*: they are collections of at least ten articles, all centered on a particular subject. With their unique mix of varied contributions from Original Research to Review Articles, Frontiers Research Topics unify the most influential researchers, the latest key findings and historical advances in a hot research area.

Find out more on how to host your own Frontiers Research Topic or contribute to one as an author by contacting the Frontiers editorial office: frontiersin.org/about/contact

Ferroptosis in cancer and beyond, volume II

Topic editors

Yanqing Liu — Columbia University, United States
Guo Chen — China Pharmaceutical University, China
Chaoyun Pan — Sun Yat-sen University, China
Xin Wang — National Institutes of Health (NIH), United States

Citation

Liu, Y., Chen, G., Pan, C., Wang, X., eds. (2023). *Ferroptosis in cancer and beyond, volume II*. Lausanne: Frontiers Media SA. doi: 10.3389/978-2-8325-3466-3

Table of contents

frontiers | Frontiers in Molecular Biosciences

TYPE Editorial
PUBLISHED 29 August 2023
DOI 10.3389/fmolb.2023.1265127

OPEN ACCESS

EDITED AND REVIEWED BY
William C. Cho,
QEH, Hong Kong SAR, China

*CORRESPONDENCE
Guo Chen,
gchen84@cpu.edu.cn
Chaoyun Pan,
panchy27@mail.sysu.edu.cn
Yanqing Liu,
lyanqing321@163.com

†These authors have contributed equally to this work

RECEIVED 22 July 2023
ACCEPTED 25 July 2023
PUBLISHED 29 August 2023

CITATION
Wang X, Lu J, Chen G, Pan C and Liu Y (2023), Editorial: Ferroptosis in cancer and Beyond—volume II.
Front. Mol. Biosci. 10:1265127.
doi: 10.3389/fmolb.2023.1265127

Editorial: Ferroptosis in cancer and Beyond—volume II

Xin Wang[1†], Jordan Lu[2†], Guo Chen[3*], Chaoyun Pan[4*] and Yanqing Liu[2*]

[1]National Institute of Neurological Disorders and Stroke, Bethesda, MD, United States, [2]Herbert Irving Comprehensive Cancer Center, Columbia University, New York, NY, United States, [3]School of Biopharmacy, China Pharmaceutical University, Nanjing, China, [4]Department of Biochemistry and Molecular Biology, Zhongshan School of Medicine, Sun Yat-Sen University, Guangzhou, China

KEYWORDS

ferroptosis, oxidative stress, cancer, iron, disease treatment

Editorial on the Research Topic
Ferroptosis in cancer and Beyond—volume II

Introduction

It has been 11 years since Brent Stockwell identified and named ferroptosis (Dixon et al., 2012). Ferroptosis results from iron-dependent lipoxidation at various cellular membrane structures. Searching the PubMed database by using the keyword “ferroptosis” results in more than 8,000 papers. Why has ferroptosis received such intensive attention? There are at least three fundamental reasons. First, ferroptosis has a unique mechanism distinct from other known regulated cell death types. Ferroptosis is tightly associated with cell metabolism, such as amino acid, iron, and ROS metabolism. There are three key elements for ferroptosis: substrate of lipid peroxidation, executor of lipid peroxidation, and anti-ferroptosis system (Liu and Gu, 2022a). The balance between the three elements dictates the sensitivity of a cell to ferroptosis. Second, there are multiple ways to induce ferroptosis meaning it has a complex regulatory network. Many pathways are involved in ferroptosis mediation. Key factors regulating ferroptosis, including GPX4, p53, FSP1, and ALOXs have been identified (Dixon and Stockwell, 2019; Liu et al., 2019; Liu and Gu, 2022a; Liu and Gu, 2022b). However, new pathways and regulators are still emerging. Third, ferroptosis participates in the regulation of numerous physiological or pathological processes, such as normal development, degenerative diseases, ischemic injuries, immune system activities, and particularly cancer. This means that ferroptosis has amazing potential as a therapeutic target in many diseases (Stockwell et al., 2020).

To examine progress in the ferroptosis field and advances in basic research and clinical applications focusing on ferroptosis, we launched a Research Topic named Ferroptosis in Cancer and Beyond in early 2022, which was a great success. Given the rapid progression in this field, we opened a second call for this same Research Topic in late 2022, which has now been successfully closed. This second volume brings together 13 papers, including 6 research articles and 7 reviews. These articles outline recent information about ferroptosis from both basic research and clinical translation angles. The papers are briefly introduced below.

To comprehensively understand the contribution of iron regulatory proteins (IRPs) to ferroptosis, McKale Montgomery and Cameron Cardona reviewed the regulatory processes

regarding iron homeostasis, from absorption, metabolism to its participation in ferroptosis, and discussed the essential roles of various IRPs in ferroptosis and their potentials to be therapeutically maneuvered in cancer treatment. To explore how ferroptosis is regulated at the post-translational level, Zhang et al. introduce emerging evidence for the O-GlcNAc modification (O-GlcNAcylation) in ferroptosis in a review article and discuss the crosstalk between O-GlcNAcylation and ROS and related antioxidant defense systems. The authors elucidate the role of O-GlcNAcylation in proteins involved in iron metabolism and the regulation of lipid metabolism and peroxidation during ferroptosis. Furthermore, the underlying mechanisms including mitochondria dysfunction and endoplasmic reticulum alteration brought by O-GlcNAcylation are discussed. In their original research study, Nikulin et al. identified *ELOVL5* and *IGFBP6* may modulate the sensitivity of breast cancer cells to ferroptosis, possibly via enhancing the activity of GPX4, an antioxidant enzyme that plays a critical role in ferroptosis. Through analysis of the transcriptomic database and validation with HPLC-MS, the knockdown of either *ELOVL5* or *IGFBP6* was shown to cause remarkable changes in the production of long and very long fatty acids. In addition, the knockdown of *ELOVL5* or *IGFBP6* in MDA-MB-231 cells promotes cell death induced by PUFAs, and the potential benefit of PUFAs addition for improving chemotherapeutic effects was proposed in the condition of low *IGFBP6* (and maybe *ELOVL5*) gene expression.

Glutathione S-transferase P1 (GSTP1) was proposed to be a potential target to tackle radioresistance in cancer therapy by Tan et al. GSTP1 is fundamental to maintaining cellular oxidative homeostasis and is involved in ferroptosis. Based on increasing evidence showing that iron metabolism, lipid peroxidation, and GSH level are modulated by radiotherapy, the authors elaborated on the potential to control GSTP1 levels to enhance the efficacy of radiotherapy in cancer treatment. More pathways in ferroptosis induced by radiotherapy and their implications for radiotherapy were reviewed by Giovanni Luca Beretta and Nadia Zaffaroni, and other strategies were proposed to improve the efficacy of radiotherapy, including enhancing ionizing radiation by other reagents or selectively inducing ferroptosis with metal-based nanoparticles. Lu et al. introduced all kinds of therapies for glioblastoma, including immunotherapy, radiotherapy, and chemotherapy, and discussed how ferroptosis participates and affects the efficacy of different therapeutic treatments. In an original research article, Shi et al. found that dihydroartemisinin (DHA), an adjuvant drug-enhancing chemotherapy, induced cervical cancer death via initiating ferroptosis and explored the involvement of ferritinophagy induced by DHA. Furthermore, DHA was also shown to have a synergistic role with doxorubicin (DOX) in promoting cervical cancer cell death.

Growing evidence has revealed the impact of T cell infiltration in the development of various types of cancer. Jiang et al. analyzed the differential gene expression in $CD8^+$ T cells from $CD8^+$ highly or low infiltrated samples in acute myeloid leukemia (AML) and conducted extensive bioinformatics analysis, and six ferroptosis-related genes (FRGs) were identified to generate a prognostic prediction model, which was validated to be helpful to risk stratification and prognostic prediction of AML patients. Han et al. identified several ferroptosis-related genes (FRGs) which correlate well with the immune microenvironment and establish a model to predict the prognosis of cervical cancer patients. Further mechanisms underlying iron homeostasis, ROS and lipid peroxidation, GPX4-GSH, and other regulator systems in cervical cancer were discussed in a review by Xiangyu Chang and Jinwei Miao. In another review, Lai et al. specifically elaborated on the influence of steroid hormone signaling on ferroptosis and discuss the involvement of ferroptosis in gynecologic cancers and potential therapies targeting ferroptosis for the treatment of gynecologic cancers.

With data from FerrDb and TCGA database, Li et al. established a prognostic prediction model for colorectal cancer (CRC) patients with 8 FRGs among which NOS2 is one of the most significantly affected examples and was validated with the CRC mouse model and the involvement of NF-κB pathway was elucidated. To investigate whether ferroptosis is associated with colon adenocarcinoma (COAD), Baldi et al. identified a 4-gene signature that distinguishes high-risk and low-risk patients, and those FRGs were further shown to be implicated in many pathological related pathways and a variety of miRNAs and transcription factors were found to be involved. These researches consolidated the idea that disease-associated cell death has a specific gene expression profile relevant to the prognosis of the patient (Liu et al., 2022; Ye et al., 2022; Liu et al., 2023).

Taken together, this second volume of the Research Topic Ferroptosis in Cancer and Beyond adds new knowledge to this field, furthering research and the clinical translation of ferroptosis.

Author contributions

XW: Writing–original draft. JL: Writing–original draft. GC: Writing–review and editing. CP: Writing–review and editing. YL: Conceptualization, Writing–original draft.

Acknowledgments

We are grateful to all the authors and reviewers for their contributions to this Research Topic.

Conflict of interest

The authors declare that the research was conducted in the absence of any commercial or financial relationships that could be construed as a potential conflict of interest.

Publisher's note

References

Dixon, S. J., Lemberg, K. M., Lamprecht, M. R., Skouta, R., Zaitsev, E. M., Gleason, C. E., et al. (2012). Ferroptosis: an iron-dependent form of nonapoptotic cell death. *Cell* 149 (5), 1060–1072. doi:10.1016/j.cell.2012.03.042

Dixon, S. J., and Stockwell, B. R. (2019). The hallmarks of ferroptosis. *Annu. Rev. Canc Biol.* 3, 35–54. doi:10.1146/annurev-cancerbio-030518-055844

Liu, Y., and Gu, W. (2022a). p53 in ferroptosis regulation: the new weapon for the old guardian. *Cell death Differ.* 29 (5), 895–910. doi:10.1038/s41418-022-00943-y

Liu, Y., and Gu, W. (2022b). The complexity of p53-mediated metabolic regulation in tumor suppression. *Seminars cancer Biol.* 85, 4–32. doi:10.1016/j.semcancer.2021.03.010

Liu, Y. L. Y., Ye, S., Feng, H., and Ma, L. (2023). A new ferroptosis-related signature model including messenger RNAs and long non-coding RNAs predicts the prognosis of gastric cancer patients. *J. Transl. Intern Med.* 11 (2), 145–155. doi:10.2478/jtim-2023-0089

Liu, Y. Q., Liu, Y., Ye, S. J., Feng, H. J., and Ma, L. J. (2022). Development and validation of cuproptosis-related gene signature in the prognostic prediction of liver cancer. *Front. Oncol.* 12, 985484. doi:10.3389/fonc.2022.985484

Liu, Y. Q., Tavana, O., and Gu, W. (2019). p53 modifications: exquisite decorations of the powerful guardian. *J. Mol. Cell Biol.* 11 (7), 564–577. doi:10.1093/jmcb/mjz060

Stockwell, B. R., Jiang, X. J., and Gu, W. (2020). Emerging mechanisms and disease relevance of ferroptosis. *Trends Cell Biol.* 30 (6), 478–490. doi:10.1016/j.tcb.2020.02.009

Ye, S., Liu, Y., Zhang, T., Feng, H., Liu, Y., and Ma, L. (2022). Analysis of the correlation between non-alcoholic fatty liver disease and the risk of colorectal neoplasms. *Front. Pharmacol.* 13, 1068432. doi:10.3389/fphar.2022.1068432

frontiers | Frontiers in Molecular Biosciences

TYPE Original Research
PUBLISHED 13 December 2022
DOI 10.3389/fmolb.2022.1102735

OPEN ACCESS

EDITED BY
Yanqing Liu,
Columbia University, United States

REVIEWED BY
Jun Shang,
Cincom System, Inc., United States
Yufei Liu,
Huashan Hospital, Fudan University, China
Shiqiang Jin,
Bristol Myers Squibb, United States

*CORRESPONDENCE
Salem Baldi,
salimlaboratory@gmail.com
Yaping Gao,
gaoyp@tsinghua-sz.org
Hui Tian,
hui.tian@axbio.cn

SPECIALTY SECTION
This article was submitted to Molecular Diagnostics and Therapeutics, a section of the journal Frontiers in Molecular Biosciences

RECEIVED 19 November 2022
ACCEPTED 30 November 2022
PUBLISHED 13 December 2022

CITATION
Baldi S, He Y, Ivanov I, Sun Y, Feng W, Refat M, Mohammed SAD, Adlat S, Tian Z, Wang Y, Gao Y and Tian H (2022), Novel characterization discoveries of ferroptosis-associated molecules in COAD microenvironment based TCGA data.
Front. Mol. Biosci. 9:1102735.
doi: 10.3389/fmolb.2022.1102735

Novel characterization discoveries of ferroptosis-associated molecules in COAD microenvironment based TCGA data

Salem Baldi[1]*, Yun He[1], Igor Ivanov[1], Yaping Sun[2], Wei Feng[1], Moath Refat[3], Shadi A. D. Mohammed[4], Salah Adlat[5], Zixuan Tian[1], Yi Wang[1], Yaping Gao[2]* and Hui Tian[1]*

[1]Research Center of Molecular Diagnostics and Sequencing, Axbio Biotechnology (Shenzhen) Co., Ltd., Shenzhen, China, [2]Research Center of Molecular Diagnostics and Sequencing, Research Institute of Tsinghua University in Shenzhen, Shenzhen, China, [3]Department of Biochemistry and Molecular Biology, The Key Laboratory of Environment and Genes Related to Disease of Ministry of Education, Health Science Center, Xi'an Jiaotong University, Xi'an, China, [4]Graduate School of Heilongjiang University of Chinese Medicine, Harbin, China, [5]Department of Gastroenterology and Hepatology, Mayo Clinic, Rochester, MN, United States

Background and Objective: One of the most recent forms of programmed cell death, ferroptosis, is crucial in tumorigenesis. Ferroptosis is characterized by iron-dependent oxidative destruction of cellular membranes following the antioxidant system's failure. However, it is unknown whether ferroptosis-related genes (FRGs) are associated with colon adenocarcinoma (COAD) metastasis, immune cell infiltration, and oxidative stress in COAD. The current study concentrated on FRGs expression in colon cancer metastasis, their relationship to immune cell infiltration (ICI), and potential pathological pathways in COAD.

Methods and Results: Clinical information and mRNA expression patterns for patients with COAD metastasis were obtained from the public TCGA database. Patients with low mRNA levels showed good overall survival than patients with high mRNA levels. The genomic-clinicopathologic nomogram was subsequently created by combining risk score and clinicopathological features. Absolute Shrinkage and Selection Operator have shown a 4 gene signature that can stratify cancer patients into high-risk versus low-risk. These four FRGs were found to be significantly linked to the overall survival of COAD patients and predicted high risk score. Next, age, stage, and PTNM were combined in univariate and multivariate cox regression models to perform a filtering procedure. The receiver operating characteristic (ROC) and calibration curves indicated that constructed signature model exhibited high prediction accuracy and clinical relevance in COAD. ARID3A showed a strong negative correlation with a wide range of immune tumour-infiltrating cells in COAD microenvironment. According to the single sample gene set enrichment

analysis (ssGSEA) results, FRGs are involved in variety of pathological pathways including PI3K-AKT-mTOR pathway, reactive oxygen species (ROS) pathway, response to hypoxia pathway, and other inflammation related pathways. Moreover, dysregulation of FRGs in COAD patients showed a significance correlation with wide range of miRNAs and transcription factors (TFs).

Conclusion: We identified new diagnostic biomarkers and established prognostic models for ferroptosis related programmed cell death in COAD metastasis. FRGs may improve tumor cell survival by activating the TGFB pathway, which can stimulate ROS production, accelerates ECM breakdown, and promote tumor progression and invasion. Genes implicated in ferroptosis, as revealed by the Kaplan Meier and a genomic-clinicopathologic nomogram, are potential therapeutic targets and prognosis indications for metastasis COAD patients.

KEYWORDS

COAD microenvironment, metastasis, ferroptosis, immune cell infiltration, TCGA

1 Introduction

1.1 Colon cancer

Colon cancer is the third most frequently diagnosed cancer in males and females worldwide, with 80, 690 (8%), 70,340 (8%) new cases and 28,400 (9%), 24,180 (8%) deaths in male and female, respectively (Siegel et al., 2022). The high incidence rate or mortality is because of the lack of early detection and the fact that it is often diagnosed in its later stages (Zhou et al., 2019). The 5-year overall survival (OS) rate for COAD patients is still low, despite the availability of various targeted medicines and immunotherapies in recent years. Therefore, studying the molecular mechanism of the occurrence and development of colorectal cancer is an important subject of clinical research. Preventive measures, such as screening and finding new therapeutic targets, are also critical to improve patients' survival and prognosis of colon cancer.

1.2 Iron death

Various human diseases can be prevented by targeting regulated cell death, which includes necroptosis, pyroptosis, ferroptosis, entotic cell death, lysosome-dependent cell death, and autophagy-dependent cell death. Ferroptosis is iron-dependent programmed cell death, first postulated by Dixon in 2012; it differs from apoptosis, pyrolysis, and autophagy at levels of cell morphology, biochemical features, and regulation and occurs through Fe(II)-dependent lipid peroxidation to insufficient cellular reducing capacity (Dixon et al., 2012; Jiang et al., 2020). Several studies have connected ferroptosis to cancer development and progression (Xia et al., 2019; Jiang et al., 2020). Since tumor cells can maintain or acquire ferroptosis sensitivity while surviving cell death, ferroptosis therapy for cancer is gaining attention. Wei et al. found that small molecule drugs that activated p53 had potent inhibitory action against HCT116 cells by inducing ferroptosis (Wei et al., 2018). Combinatorial therapy with ferroptosis medicine and tumor necrosis factor-related apoptosis-inducing ligands led to synergistic apoptosis and growth regression of CRC (Lee et al., 2019). Thereby, ferroptosis-related genes (FRGs) are very significant in cancer patients (Jiang et al., 2015; Ou et al., 2016; Bersuker et al., 2019; Doll et al., 2019; Li et al., 2020) and could be promising therapeutic targets and prognostic indicators in colon adenocarcinoma (COAD).

1.3 Working hypothesis

Our working hypothesis was that FRGs promotes colon cancer metastasis and play a role in oxidative stress.

1.4 Study design

Based on above mentioned hypothesis we developed prognostic model, validated, and explored the mechanism by which FRGs promotes COAD progression and invasion. Our results showed that there are solid predictive genes and offered a novel, personalized approach to treating COAD.

2 Materials and methods

2.1 Data acquisition and identification of differentially expressed genes (DEGs)

Ferroptosis-related genes were derived from Ze-Xian Liu et al. RNA-sequencing expression (level 3) profiles and corresponding clinical information for COAD were downloaded from the TCGA

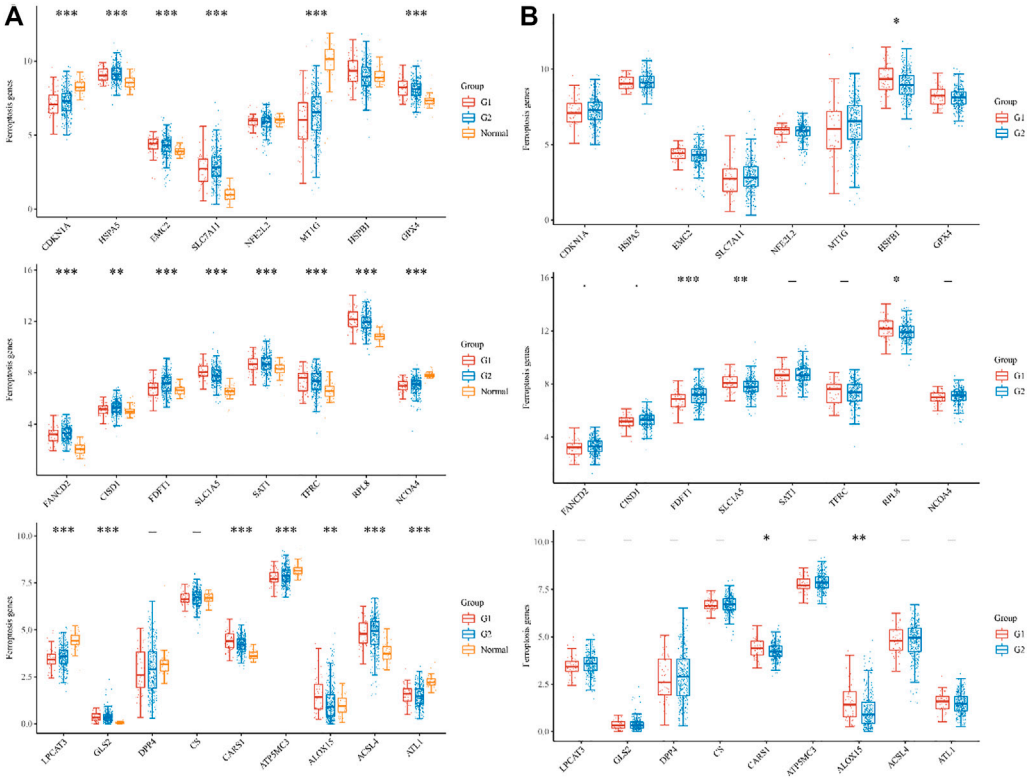

FIGURE 1
The expression distribution of ferroptosis-related mRNA in tumor tissues and normal tissues. **(A)** histogram shows the dysregulation of iron death in metastasis G1, non-metastases G2, and Normal samples, respectively. **(B)**histogram shows the number of significantly differentially expressed genes in metastasis G1, non-metastases G2, respectively. *$p < 0.05$, **$p < 0.01$, ***$p < 0.001$.

dataset (https://portal.gdc.com). R package, version 4.0.3 was used to implement the analysis. Genes with a *p*-value of less than 0.05 and log FC > 1 were chosen for further investigation. Only patients who had M1 metastases and higher were considered for participation in the trial according to the inclusion criteria for patient selection.

2.2 Nomogram construction

The Cox regression analysis was conducted to determine if risk scores and relevant clinical indicators could be identified as prospective predictors of OS for COAD patients. Based on the Cox regression analysis results, a prognostic nomogram was built using the stepwise Cox regression model to predict the 1, 3, and 5-year OS of COAD patients included in the TCGA dataset. This was done to determine the probability of survival. The area under the curve was used to evaluate the nomogram's ability to discriminate between categories (AUC). Using the calibration curve, a graph comparing the expected OS of the nomogram to the observed survival rates was constructed.

2.3 Correlation between genes and pathways in COAD

The genes found in the associated pathways were gathered and examined using the R software's GSVA package, with the parameter method set to the ssGSEA algorithm' as the final step. Finally, Spearman correlation was used to examine the correlation between the genes and the pathway score. The analysis methods and R packages were implemented by R version 4.0.3. *p*-value < 0.05 was considered statistically significant.

2.4 Regulatory network of FRGs

We predicted the potential ironoptosis-associated non-coding RNAs by performing co-expression analysis with identified iron-related genes in COAD. We predicted miRNAs that target FGRs using the GSCA-hosted TCGA database (GSCA - Gene Set Cancer Analysis (hust.edu.cn). We then utilized the knockTF database to identify FRGs-specific transcription factors (TFs) that significantly

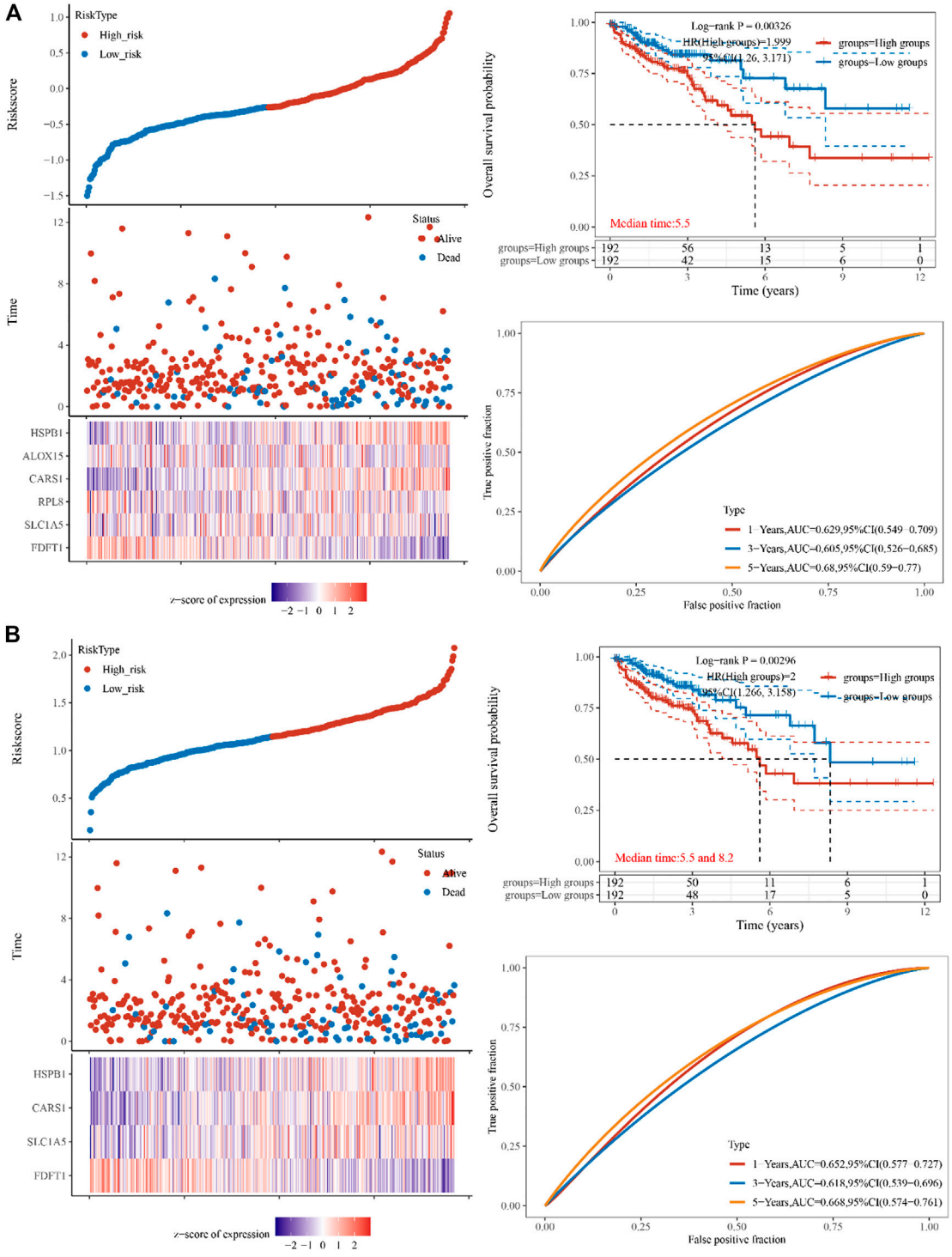

FIGURE 2
Constructing the TCGA cohort's genes. **(A)** The multi-factor cox regression analysis showed six prognosis related genes in colon cancer **(B)** The forest analysis showed four prognosis related genes in colon cancer using 10x cross-validation ($p < 0.05$) The top scatters represent TCGA cohort's risk score distribution from low to high. Kaplan-Meier survival analysis of the risk model from dataset, comparison among different groups was made by log-rank test. HR (High exp) represents the hazard ratio of the low-expression sample relatives to the high-expression sample. HR > 1 indicates the genes are a risk factor, and HR < 1 indicates the genes are a protective factor. HR (95%CI). Heatmap is the gene expression from the signature. Prognostic performance was evaluated using the AUC of the time-dependent ROC curve analysis for OS in the TCGA cohort.

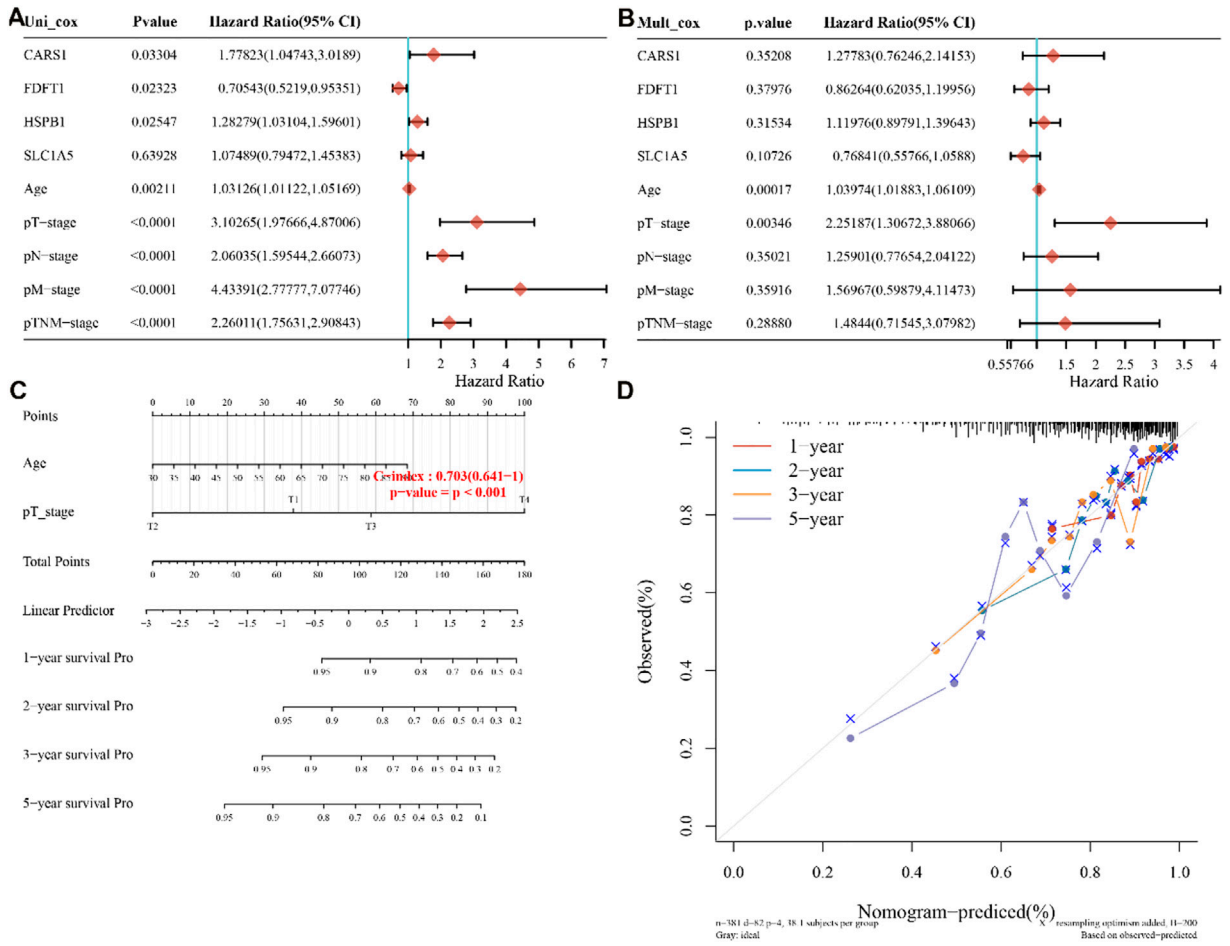

FIGURE 3
four-genes prognostic value and predictive nomogram. **(A,B)** Multivariate and univariate Cox regression analysis of the four genes is both available, **(C)** Nomogram development based on independent prognostic value for the 4-genes, **(D)** Predicting 1–5-year survival using a nomogram. pT,pN, pM are pathological stages where T is the stage (generally related to the size and depth of the tumor), N is lymph node metastasis, and M is distant metastasis. pTNM stands for Pathological tumor-node-metastasis (pTNM) staging.

influence FGRs based on expression and ChIP-seq/motif evidence (KnockTF-Search (licpathway.net)).

3 Results

3.1 Identification of DEGs related to ferroptosis in the TCGA cohort

In total, 426 sample, 52 metastases, 333 non-metastases COAD patients and 41 normal samples from TCGA cohorts were considered for inclusion in the study (Supplementary Table S1). We investigated RNA-seq data from the TCGA dataset to determine the expression differences of ferroptosis-related genes between tumor tissues and neighboring normal tissues. Among the 25 ferroptosis-related genes that were investigated, tumor tissues and adjacent normal tissues displayed significant differences in 21 genes. CDKN1A, HSPA5, EMC2, SLC7A11, MT1G, GPX4, FANCD2, CISD1, FDFT1, SLC1A5, SAT1, TFRC, RPL8, NCOA4, LPCAT3, GLS2, CARS1, ATP5MC3, ALOX15, ACSL4, and ATL1 (Figure 1A). To be more specific the differential expressed gene in metastases and non-metastases tissues were identified. Among the above-mentioned genes, the following genes were identified FDFT1, SLC1A5, RPL8, CARS1, and ALOX15 in addition to HSPB1.

3.2 Prognostic genes identified in the TCGA COAD cohort

To reduce dimensionality and construct prognostic models based on Cox and lasso regression methods, iron death-related

TABLE 1 Pathways correlated to FGRs genes in COAD.

Symbol	Pathway	Cor	*p*_value
FDFT1	Tumor_Inflammation_Signature	−0.05	0.321
FDFT1	Cellular_response_to_hypoxia	0.23	7.39e−07
FDFT1	Tumor_proliferation_signature	0.31	1.22e−11
FDFT1	EMT_markers	−0.06	0.177
FDFT1	ECM−relatted_genes	−0.08	0.091
FDFT1	Apoptosis	0.08	0.102
FDFT1	Angiogenesis	−0.04	0.376
FDFT1	DNA_repair	0.12	0.011
FDFT1	G2M_checkpoint	0.020275	8.36e−08
FDFT1	Inflammatory_response	0.06	0.174
FDFT1	PI3K_AKT_mTOR_pathway	0.05	0.283
FDFT1	P53_pathway	0.19	3.26e−05
FDFT1	MYC_targets	0.20	1.24e−05
FDFT1	TGFB	−0.08	0.106
FDFT1	IL−10_Anti−inflammatory_Signaling_Pathway	0.11	0.022
FDFT1	Genes_up−regulated_by_reactive_oxigen_species_(ROS)	0.09	0.063
FDFT1	DNA_replication	0.19	3.36e−05
FDFT1	Collagen_formation	−0.09	0.063
FDFT1	Degradation_of_ECM	−0.03	0.533
FDFT1	Ferroptosi	0.07	0.123
CARS1	Tumor_Inflammation_Signature	−0.05	0.321
CARS1	Cellular_response_to_hypoxia	0.18	1.48e−04
CARS1	Tumor_proliferation_signature	0.24	1.74e−07
CARS1	EMT_marker	0.09	0.066
CARS1	ECM−relatted_genes	0.05	0.254
CARS1	Angiogenesis	0.09	0.046
CARS1	Apoptosis	0.08	0.089
CARS1	DNA_repair	0.26	1.59e−08
CARS1	G2M_checkpoint	0.34	5.04e−14
CARS1	Inflammatory_response	0	0.958
CARS1	PI3K_AKT_mTOR_pathway	0.23	7.03e−07
CARS1	P53_pathway	0.03	0.57
CARS1	MYC_targets	0.33	2.85e−13
CARS1	TGFB	0.04	0.381
CARS1	IL−10_Anti−inflammatory_Signaling_Pathway	−0.01	0.896
CARS1	Genes_up−regulated_by_reactive_oxigen_species_(ROS)	−0.04	0.432

(Continued on following page)

TABLE 1 (*Continued*) Pathways correlated to FGRs genes in COAD.

Symbol	Pathway	Cor	*p*_value
CARS1	DNA_replication	0.3	3.21e−11
CARS1	Collagen_formation	0.09	0.06
CARS1	Degradation_of_ECM	0.08	0.082
CARS1	Ferroptosi	0.19	6.32e−05
HSPB1	Tumor_Inflammation_Signature	−0.06	0.237
HSPB1	Cellular_response_to_hypoxia	0.02	0.716
HSPB1	umor_proliferation_signature	−0.25	5.2e−08
HSPB1	EMT_markers	0.28	1.4e−09
HSPB1	ECM−relatted_genes	0.13	0.005
HSPB1	Angiogenesis	0.19	4.91e−05
HSPB1	Apoptosis	0.09	0.063
HSPB1	DNA_repair	−0.03	0.491
HSPB1	G2M_checkpoint	−0.26	1.87e−08
HSPB1	Inflammatory_response	0.03	0.526
HSPB1	PI3K_AKT_mTOR_pathway	0	0.991
HSPB1	P53_pathway	0.28	1.08e−09
HSPB1	MYC_targets	−0.24	2.89e−07
HSPB1	TGFB	0.14	0.003
HSPB1	L−10_Anti−inflammatory_Signaling_Pathway	0.05	0.327
HSPB1	Genes_up−regulated_by_reactive_oxigen_species_(ROS)	0.25	4.3e−08
HSPB1	DNA_replication	−0.16	0.001
HSPB1	Collagen_formation	0.24	3.05e−07
HSPB1	Degradation_of_ECM	0.21	4.03e−06
HSPB1	Ferroptosis	0.17	1.95e−04
SLC1A5	Tumor_Inflammation_Signature	−0.21	9.87e−06
SLC1A5	Cellular_response_to_hypoxia	−0.03	0.542
SLC1A5	Tumor_proliferation_signature	0.01	0.767
SLC1A5	EMT_markers	0.533	0.533
SLC1A5	ECM−relatted_genes	−0.08	0.11
SLC1A5	Angiogenesis	−0.03	0.542
SLC1A5	Apoptosis	−0.18	1.52e−04
SLC1A5	DNA_repair	0.18	1.39e−04
SLC1A5	G2M_checkpoint	0.1	0.043
SLC1A5	Inflammatory_response	−0.18	9.07e−05
SLC1A5	PI3K_AKT_mTOR_pathway	0.03	0.559
SLC1A5	P53_pathway	−0.01	0.906

(Continued on following page)

TABLE 1 (*Continued*) Pathways correlated to FGRs genes in COAD.

Symbol	Pathway	Cor	*p*_value
SLC1A5	MYC_targets	0.11	0.021
SLC1A5	TGFB	−0.04	0.372
SLC1A5	IL−10_Anti−inflammatory_Signaling_Pathway	−0.20	1.6e−05
SLC1A5	Genes_up−regulated_by_reactive_oxigen_species_(ROS)	0.05	0.259
SLC1A5	DNA_replication	0.2	1.57e−05
SLC1A5	Collagen_formation	0.04	0.427
SLC1A5	Degradation_of_ECM	−0.03, 0.16	0.163
SLC1A5	Ferroptosis	0.657	−0.02

Note: cor, correlation.

gene difference analysis results were utilized to evaluate the prognosis of these genes on CAOD tumor patients. Based on the median cut-off value, high- and low-risk patients were separated into two groups. The following formula was used to determine the risk score of the outcome = $\sum_{i=1}^{n}$ (coefi × Expri). The prognostic model constructed using multi-factor cox regression analysis is represented in Figure 2A. AIC = 793.6083 Riskscore= (-0.3887)*FDFT1+(-0.2156)*SLC1A5+(-0.0725)*RPL8+(0.6781)*CARS1+(-0.0524)*ALOX15+(0.253)*HSPB1. LASSO regression identified (FDFT1, HSPB1, SLC1A5, and CARS1 a signature model gene. lambda. min = 0.0151, (Riskscore= (-0.2482) *FDFT1+(-0.03) *SLC1A5+(0.4137) *CARS1+(0.1543) *HSPB1 (Figure 2B).

3.3 Independent prognostic value of the FRGs gene in COAD

The TCGA dataset was used to do univariate and multivariate Cox regression analysis on the identified 4 genes signature to determine whether the ability of the prognostic significant in predicting OS was independent. The effect of the 4 genes and clinical factors on prognosis was investigated with the help of the Cox regression analysis. These factors included age, pT, pM, pN, and Pathological tumor-node-metastasis (pTNM) staging. The variable was significant in the univariate Cox regression analysis and was thought to be related to prognosis (Figure 3A). Multivariate Cox regression analysis found these variables to be non-significant, except for age and pT stage and of the four discovered genes, CARS1 and HSPB1 had a hazard ratio greater than 1 (Figure 3B). Based on the independent prognostic factors for the OS of multi-factor Cox regression analysis, we developed a nomogram for predicting 1, 2, 3, and 5-year survival rates (Figures 3C, D). In the TCGA dataset, the calibration curve for the probability of 1, 2, 3, and 5-year OS exhibited the best agreement between observation and prediction. After bias adjustment, the C-index was found to be 0.703, $p < 0.001$ indicating a strong level of clinical diagnosis performance for the model signature genes. As a result, the identified ferroptosis-related gene impacts the prognosis of COAD and may serve as a possible diagnostic factor for COAD patients.

3.4 Characterization of ferroptosis-associated molecules in COAD microenvironment

The enrichment fraction of each sample on each pathway was calculated in turn using the ssGSEA algorithm to obtain the connection between the sample and the pathway, and we then obtained the relationship between the gene and the pathway by calculating the correlation between gene expression and pathway score using spearman analysis. The tumor cell proliferation signature score was found to be positively correlated with CARS1 and FDFT1, indicating that the signature model has a high proliferation rate. Furthermore, we found a statistically significant activation of the cellular response to hypoxia signature and the G2M checkpoint in SLC1A5, CARS1, and FDFT1 (Table1).

3.5 FRGs correlate with immune cell infiltration in COAD

An increasing number of studies have suggested an interaction between immune response and pathophysiological processes. GSCA was performed to evaluate the correlation between FRGs and the available immune cells in COAD. FRFs correlated negatively with the infiltration of immune cells, including B cells, CD4-T, CD8-T, central memory, NKT, Tfh, Th17, Th2, and other immune cells presented in Table 2. These results indicated that dysregulation of FRGs expression is associated with worse immune cell infiltration in the COAD microenvironment.

TABLE 2 FRGs and immune cell infiltration.

Cancer type	Gene symbol	Cell_type	Corrrelation	*p*_value	Fdr
COAD	CARS1	Bcell	−0.21337	0.000096037	0.000327
COAD	CARS1	CD4_T	−0.19581	0.000353103	0.000764
COAD	CARS1	CD4_naive	0.029763	0.59063182	0.904695
COAD	CARS1	CD8_T	−0.12105	0.028142976	0.06217
COAD	CARS1	CD8_naive	0.045845	0.407207002	0.511177
COAD	CARS1	Central_memory	−0.15803	0.004057678	0.019381
COAD	CARS1	Cytotoxic	0.002643	0.961910357	0.973297
COAD	CARS1	DC	0.117239	0.033522256	0.074959
COAD	CARS1	Effector_memory	0.028785	0.602898028	0.727797
COAD	CARS1	Exhausted	0.189201	0.000560693	0.00198
COAD	CARS1	Gamma_delta	0.17752	0.001223319	0.004746
COAD	CARS1	InfiltrationScore	−0.06767	0.22090454	0.287603
COAD	CARS1	MAIT	−0.20101	0.000242966	0.000602
COAD	CARS1	Macrophage	0.01099	0.842588283	0.891323
COAD	CARS1	Monocyte	0.209679	0.0001274	0.00041
COAD	CARS1	NK	−0.0985	0.074396025	0.105847
COAD	CARS1	NKT	−0.12172	0.027277463	0.05036
COAD	CARS1	Neutrophil	0.092057	0.09552524	0.154205
COAD	CARS1	Tfh	−0.19943	0.000272399	0.000714
COAD	CARS1	Th1	0.172121	0.001727179	0.007843
COAD	CARS1	Th17	−0.21842	0.000064685	0.000325
COAD	CARS1	Th2	−0.19984	0.000264373	0.000571
COAD	CARS1	Tr1	−0.12894	0.019301647	0.042031
COAD	CARS1	iTreg	0.019994	0.717866105	0.79491
COAD	CARS1	nTreg	0.195468	0.000361876	0.000824
COAD	FDFT1	Bcell	−0.11041	0.045370724	0.077487
COAD	FDFT1	CD4_T	−0.09759	0.07711229	0.110747
COAD	FDFT1	CD4_naive	0.005977	0.913988751	0.975471
COAD	FDFT1	CD8_T	0.067299	0.223438049	0.331996
COAD	FDFT1	CD8_naive	−0.11569	0.035950323	0.068571
COAD	FDFT1	Central_memory	0.122809	0.02591327	0.08246
COAD	FDFT1	Cytotoxic	0.031068	0.574448762	0.658329
COAD	FDFT1	DC	−0.03072	0.578734951	0.694377
COAD	FDFT1	Effector_memory	0.135348	0.014011419	0.040757
COAD	FDFT1	Exhausted	0.079108	0.15223709	0.238354
COAD	FDFT1	Gamma_delta	−0.09062	0.100848862	0.185006

(Continued on following page)

TABLE 2 (*Continued*) FRGs and immune cell infiltration.

Cancer type	Gene symbol	Cell_type	Corrrelation	*p*_value	Fdr
COAD	FDFT1	InfiltrationScore	−0.12446	0.02396175	0.039701
COAD	FDFT1	MAIT	0.065499	0.236098889	0.305429
COAD	FDFT1	Macrophage	−0.09246	0.094058982	0.163471
COAD	FDFT1	Monocyte	−0.1559	0.004590939	0.01021
COAD	FDFT1	NK	0.039389	0.476457385	0.547267
COAD	FDFT1	NKT	−0.04362	0.430394011	0.526828
COAD	FDFT1	Neutrophil	−0.08117	0.141813904	0.21543
COAD	FDFT1	Tfh	0.046057	0.405031918	0.489801
COAD	FDFT1	Th1	0.151289	0.005967945	0.021079
COAD	FDFT1	Th17	0.105758	0.055320302	0.106168
COAD	FDFT1	Th2	−0.03301	0.550702397	0.616684
COAD	FDFT1	Tr1	−0.10243	0.063502854	0.11671
COAD	FDFT1	iTreg	−0.0131	0.81287067	0.867349
COAD	FDFT1	nTreg	0.201106	0.000241193	0.000564
COAD	HSPB1	Bcell	0.016112	0.770935023	0.823707
COAD	HSPB1	CD4_T	0.11569	0.035950057	0.055578
COAD	HSPB1	CD4_naive	0.033855	0.540600482	0.887885
COAD	HSPB1	CD8_T	0.009588	0.862452846	0.90608
COAD	HSPB1	CD8_naive	0.089716	0.104293081	0.16892
COAD	HSPB1	Central_memory	−0.10655	0.053513211	0.142356
COAD	HSPB1	Cytotoxic	0.050055	0.365454017	0.457639
COAD	HSPB1	DC	0.038725	0.48393356	0.611192
COAD	HSPB1	Effector_memory	3.41E-05	0.99950775	0.999508
COAD	HSPB1	Exhausted	−0.09535	0.084202724	0.146841
COAD	HSPB1	Gamma_delta	−0.00273	0.960653853	0.975942
COAD	HSPB1	InfiltrationScore	0.107573	0.051244212	0.078929
COAD	HSPB1	MAIT	0.115156	0.036820715	0.059061
COAD	HSPB1	Macrophage	0.066933	0.225973178	0.330497
COAD	HSPB1	Monocyte	−0.05647	0.307179661	0.39625
COAD	HSPB1	NK	0.102513	0.063276701	0.091338
COAD	HSPB1	NKT	0.117307	0.033419966	0.060221
COAD	HSPB1	Neutrophil	−0.07423	0.179239336	0.26232
COAD	HSPB1	Tfh	−0.01071	0.846477576	0.88167
COAD	HSPB1	Th1	−0.19059	0.000509289	0.002927
COAD	HSPB1	Th17	0.036326	0.511433304	0.622967
COAD	HSPB1	Th2	0.167214	0.002343114	0.004378

(Continued on following page)

TABLE 2 (*Continued*) FRGs and immune cell infiltration.

Cancer type	Gene symbol	Cell_type	Corrrelation	*p*_value	Fdr
COAD	HSPB1	Tr1	−0.02527	0.647847324	0.737746
COAD	HSPB1	iTreg	−0.11985	0.02974044	0.062032
COAD	HSPB1	nTreg	−0.17044	0.001918694	0.003871
COAD	SLC1A5	Bcell	−0.24097	9.89224E-06	4.42E-05
COAD	SLC1A5	CD4_T	−0.31704	4.07515E-09	1.65E-08
COAD	SLC1A5	CD4_naive	0.055306	0.317257076	0.806027
COAD	SLC1A5	CD8_T	−0.20955	0.000128657	0.000662
COAD	SLC1A5	CD8_naive	0.13924	0.011461408	0.025583
COAD	SLC1A5	Central_memory	−0.11411	0.038573732	0.110974
COAD	SLC1A5	Cytotoxic	−0.15461	0.0049438	0.01088
COAD	SLC1A5	DC	0.022538	0.683790646	0.778397
COAD	SLC1A5	Effector_memory	−0.05282	0.339523746	0.48725
COAD	SLC1A5	Exhausted	0.160205	0.003572487	0.009971
COAD	SLC1A5	Gamma_delta	0.142781	0.009507343	0.026696
COAD	SLC1A5	InfiltrationScore	−0.25754	2.20581E-06	7.13E-06
COAD	SLC1A5	MAIT	−0.30951	9.81186E-09	5.85E-08
COAD	SLC1A5	Macrophage	−0.11209	0.04217849	0.083998
COAD	SLC1A5	Monocyte	0.267512	8.48819E-07	4.74E-06
COAD	SLC1A5	NK	−0.33351	5.47551E-10	2.67E-09
COAD	SLC1A5	NKT	−0.21394	0.000091869	0.000321
COAD	SLC1A5	Neutrophil	0.258419	2.03021E-06	9.46E-06
COAD	SLC1A5	Tfh	−0.33927	2.63682E-10	2.36E-09
COAD	SLC1A5	Th1	0.042495	0.442362903	0.583992
COAD	SLC1A5	Th17	−0.22282	0.000045489	0.00024
COAD	SLC1A5	Th2	−0.33281	5.97566E-10	2.8E-09
COAD	SLC1A5	Tr1	−0.15019	0.006347942	0.015927
COAD	SLC1A5	iTreg	0.094444	0.087197264	0.152343
COAD	SLC1A5	nTreg	0.326751	1.26625E-09	6.72E-09

Note: cor, correlation.

3.5 Prediction of FRGs' regulation network

MiRNAs have been linked to the regulation of tumor-associated genes in a variety of cancer types, although their role in the deregulation of FGRs remains uncertain. We initially identified the FGRs miRNAs network in COAD using the GSCALite tool. Figure 4 depicts evidence that miRNAs target FGRs identified by the GSCALite program. Using ChIP-seq datasets, we also discovered transcription factors that may posttranscriptionally modulate FGRs expression (Table 3). Hsa miR- 37–3p has experimentally verified to target ironoptosis-related SLC1A5 in melanoma (doi: 10.1038/s41418-017-0053-8). These consistent results suggest that anticipated miRNAs may have a role in COAD as well.

4 Discussion

Colon cancer is the most prevalent primary malignant tumor that is characterized by rapid growth and treatment resistance,

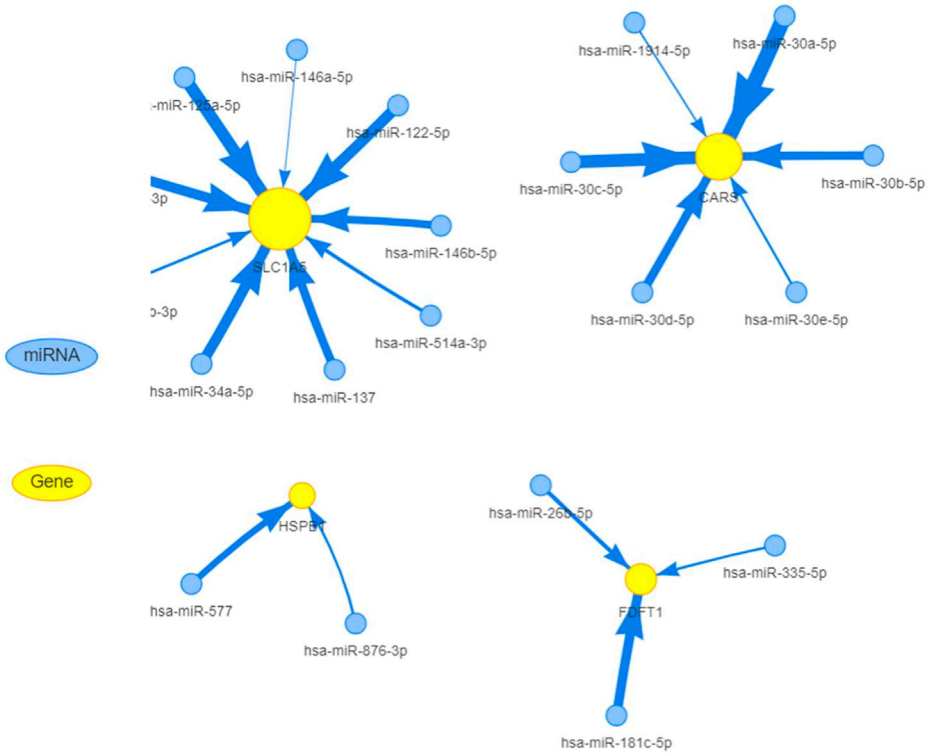

FIGURE 4
MiRNAs target FGRs in colon cancer. FGRs can be controlled by miRNAs in COAD.

resulting in significant mortality and morbidity. Iron death is a pattern of cell death caused by the accumulation of active oxygen species (ROS) of iron and lipids within cells and plays a vital role in tumorigenesis and development. (Dixon, 2017; Jiang et al., 2021). A number of studies have shown that ferroptosis can be used to treat cells that have developed resistance to drugs, which emphasized the importance of ferroptosis in the treatment of CRC patients (Friedmann Angeli et al., 2019; Wang et al., 2021). However, the underlying mechanisms and biomarkers of iron death in cancer remain to be studied. In the current study, we used bioinformatics and statistical methods to screen TCGA for information relevant to ferroptosis in COAD metastasis. We also created a risk for ferroptosis, which we believe could serve as a possible diagnostic biomarker. Using the TCGA data collection, we initially evaluated DEGs ferroptosis genes in primary and next in metastasis COAD patients. According to the findings of the Kaplan Meier survival analysis four genes having a significant correlation with OS. The prognostic accuracy of these ferroptosis-related genes in COAD patients was examined using univariate and multivariate Cox regression. Patients with COAD who were classified as high risk had a lower overall survival time than those who were classified as low risk. Studies have shown that fatal lipid peroxidation [20] is a cause of ferroptotic cell death (Gao et al., 2015). The accumulation of intracellular iron resulting from the depletion of ferritin or iron transporters and the subsequent peroxidation causes the formation of lipid peroxides and iron hypertrophy (Stockwell and Jiang, 2019). Four ferroptosis-related genes (FDFT1, HSPB1, SLC1A5, and CARS1 were identified in this investigation. Two genes involved in ferroptosis and lipid metabolism, FDFT1 and HSPB1, have been related to a poor prognosis in colorectal cancer, which is congruent with our own findings in COAD metastases (Liu et al., 2021; Yang et al., 2021). In addition to being increased in CRC, HSPB1 was also revealed to be related to worse survival in the present study (Wang et al., 2012; Konda et al., 2017). However, neither CARS1 nor SLC1A5 have previously been documented in CRC, therefore our results suggest that this area requires additional investigation. One of the most important regulators of cell survival is the PI3K/Akt/mTOR pathway. ROS can activate this pathway either by oxidizing kinases directly or by oxidizing the negative phosphatase regulators of this system, including phosphatase and tensin homolog (PTEN), protein-tyrosine phosphatase 1B (PTP1B), and protein phosphatase 2 (PP2) (PP2A). The effects of above mentioned FRGs on ROS can cause an increase in activity of the PI3K/Akt/mTOR signaling cascade. Furthermore,

TABLE 3 Regulation of FGRs expression by transcription factors identified using Chip-Seq data.

Promoter _Chr	Promoter _Start	Promoter _End	TF	Motif_ID	Motif _Start	Motif _End	Motif _Strand	Score	P.Value
chr11	3076681	3080681	TFAP4	Transfac.V$AP4_01	3077993	3078010	+	18.3577	5.74E-07
chr11	3076681	3080681	SP1	Transfac.V$SP1_Q6	3078348	3078360	–	16.4079	9.18E-07
chr11	3076681	3080681	SP1	Transfac.V$SP1_Q6_01	3078349	3078358	–	15.9857	6.78E-07
chr11	3076681	3080681	TFAP2C	Transfac.V$TFAP2C_01	3076752	3076763	+	15.7424	0.00000035
chr11	3076681	3080681	TFAP2C	Transfac.V$TFAP2C_01	3076752	3076763	–	16.7576	3.11E-08
chr11	3076681	3080681	TFAP2C	JASPAR2014.MA0524.1	3076752	3076766	–	17.5306	0.00000024
chr11	3076681	3080681	TFAP2C	Jolma2013.TFAP2C_DBD	3076752	3076763	+	16.6972	2.08E-07
chr11	3076681	3080681	TFAP2C	Jolma2013.TFAP2C_DBD	3076752	3076763	–	17.3853	3.11E-08
chr11	3076681	3080681	TFAP2C	Jolma2013.TFAP2C_full	3076752	3076763	+	15.6869	3.19E-07
chr11	3076681	3080681	TFAP2C	Jolma2013.TFAP2C_full	3076752	3076763	–	16.6869	3.11E-08
chr8	11658189	11662189	MYC	JASPAR2014.MA0147.2	11661289	11661298	+	15.5455	9.09E-07
chr19	47289842	47293842	NFYA	Transfac.V$NFYA_Q5	47291924	47291937	–	18.3026	6.79E-08
chr19	47289842	47293842	TFAP2C	Transfac.V$TFAP2C_03	47292525	47292535	+	15.1774	8.11E-07
chr19	47289842	47293842	TFAP2C	Jolma2013.TFAP2C_DBD_2	47292525	47292535	+	16.2755	6.13E-07
chr19	47289842	47293842	TFAP2C	Jolma2013.TFAP2C_full_3	47292525	47292535	+	15.1327	8.11E-07
chr7	75929874	75933874	TFAP4	Transfac.V$AP4_Q6_02	75932064	75932076	–	15.102	7.72E-07
chr7	75929874	75933874	TFAP4	Transfac.V$AP4_Q6_02	75932169	75932181	–	15.8265	2.75E-07
chr7	75929874	75933874	FOXP1	Transfac.V$FOXP1_01	75930287	75930306	+	17.5952	3.63E-08
chr7	75929874	75933874	FOXP1	Transfac.V$FOXP1_01	75931150	75931169	+	7.60714	0.00000053
chr7	75929874	75933874	HSF1	Transfac.V$HSF1_Q6	75932933	75932949	–	20.5688	7.59E-08
chr7	75929874	75933874	HSF1	Transfac.V$HSF1_Q6	75932940	75932956	+	17.9817	7.28E-07
chr7	75929874	75933874	SP1	Transfac.V$SP1_02	75932674	75932684	–	19	7.65E-08
chr7	75929874	75933874	SP1	Transfac.V$SP1_03	75933079	75933088	+	17.0674	7.52E-07
chr7	75929874	75933874	SP1	Transfac.V$SP1_05	75931838	75931848	+	16.5385	4.69E-07
chr7	75929874	75933874	SP1	Transfac.V$SP1_Q2_01	75932676	75932685	+	16.0921	6.78E-07
chr7	75929874	75933874	SP1	Transfac.V$SP1_Q4_01	75931837	75931849	–	16.9737	2.79E-07
chr7	75929874	75933874	SP1	Transfac.V$SP1_Q6	75931837	75931849	–	17.0132	0.0000005
chr7	75929874	75933874	SP1	Transfac.V$SP1_Q6_01	75932675	75932684	–	15.9857	6.78E-07
chr7	75929874	75933874	SP1	Transfac.V$SP1_Q6_02	75932195	75932211	+	15.2816	5.48E-07
chr7	75929874	75933874	SP1	Transfac.V$SP1_Q6_02	75932196	75932212	+	14.9029	8.55E-07
chr7	75929874	75933874	SP1	Transfac.V$SP1_Q6_02	75932198	75932214	+	16.3592	1.41E-07
chr7	75929874	75933874	SP1	Transfac.V$SP1_Q6_02	75932668	75932684	+	16.4806	0.00000012
chr7	75929874	75933874	SP1	Transfac.V$SP1_Q6_02	75932669	75932685	+	18.3883	7.35E-09
chr7	75929874	75933874	SP1	Transfac.V$SP1_Q6_02	75932671	75932687	+	14.9563	8.04E-07
chr7	75929874	75933874	SP1	Transfac.V$SP1_Q6_02	75932672	75932688	+	14.8786	0.00000088
chr7	75929874	75933874	SP1	Transfac.V$SP1_Q6_02	75932673	75932689	+	15.9466	2.41E-07
chr7	75929874	75933874	SP1	Transfac.V$SP1_Q6_02	75932674	75932690	+	17.8058	1.81E-08
chr7	75929874	75933874	HSF1	JASPAR2014.MA0486.1	75932935	75932949	–	18.9286	2.34E-07
chr7	75929874	75933874	HSF1	JASPAR2014.MA0486.1	75932940	75932954	+	18.7429	2.78E-07
chr7	75929874	75933874	TP63	JASPAR2014.MA0525.1	75931308	75931327	+	17.0577	0.00000077
chr7	75929874	75933874	SP1	Jolma2013.SP1_DBD	75931838	75931848	+	16.5	4.69E-07

Note: chr11 indicates CARS1 location, chr8 indicates FDFT1 location, chr19 represents SLC1A5 location, chr 7 represents HSPB1 location.

Curcumin's anti-cancer effects in colon cancer cells are modulated by HSPB1's ability to induce reactive oxygen species (ROS) generation and autophagy (Liang et al., 2018). The above results appeared to support the existing results that FRGs contributed to colon cancer progression and invasion *via* oxidative phosphorylation. FGRs may act as ROS-inducing agents and can activate TGFB, which is known to promote tumorigenesis, angiogenesis, and metastasis. Additionally, TGFB regulates the genes responsible for inflammation, cell proliferation, differentiation, and survival. Hypoxia is known to stimulate the production of mitochondrial reactive oxygen species (mROS), which in turn increases and stabilizes hypoxia-inducible factor-1 (HIF1a), which contributes to the survival and progression of tumors by upregulating the genes that regulate tumor angiogenesis and metastasis. On the other hand, several distinct DNA repair systems collaborate to decrease the risk that this damage may lead to dangerous mutations. There is a link between FRGs and genes involved in DNA repair pathways, allowing cells to be more resistant to DNA damage. FGRs showed positive correlation with a checkpoint control pathway and enhanced the activity of genes involved in DNA replication pathway that would normally prohibit cells from initiating DNA replication when breaks are present. Previous research reported that increasing SLC7A11 and GPX4 expression in HCT116 inhibited iron-induced lipid peroxidation and protected cells from ferroptosis (Yuan et al., 2021).

The infiltration of different types of immune cells is a principal determining factor for the immune response at primary and secondary tumor sites in the tumor microenvironment. We further analyzed the influence of CARS1 level on immune cell infiltration. The levels of FRGs significantly affects the infiltration level of B cells, CD4-T, CD8-T, central memory, NKT, Tfh, Th17, Th2, and Tr1cells. These results indicated that FRGs had a key regulatory effect on the immune cells in COAD patients. This is a preliminary exploration, but we intend to follow it up with experimental confirmation and biogenesis research.

Study limitation: All the findings in this manuscript were of speculation based on the transcriptional analyses using bioinformatics analysis. *In vitro* and *in vivo* investigations should be conducted to confirm the functional involvement in COAD. In conclusion, based on bioinformatics and statistical analysis, this study revealed associations between ferroptosis-related genes (FRGs) and colon adenocarcinoma (COAD). Prognostic models for ferroptosis-related programmed cell death in COAD metastasis were developed by identifying 4 signature genes, constructing a nomogram based on univariate and multivariate Cox regression model, and analyzing related pathways, immune cell infiltration, and regulatory networks.

Data availability statement

The original contributions presented in the study are included in the article/Supplementary Material, further inquiries can be directed to the corresponding authors.

Author contributions

SB conceived the idea, designed the study, and wrote the original draft. YH and II validated the results. YS, WF, YG, and HT reviewed and edited the paper. MR and SA performed statistical analysis. All authors discussed the results and contributed to the final manuscript.

Funding

The work is paid by 2021Szvup096, Shenzhen Science and Technology Innovation Strategic Research and Technology Transfer Promotion Center. This work is also supported by Grant no, LHTD20170002, Science and Technology Innovation Bureau of Nanshan district, Shenzhen.

Conflict of interest

Authors SB, YH, II, YS, WF, ZT, YW, and HT were employed by Research Center of Molecular Diagnostics and Sequencing, Axbio Biotechnology (Shenzhen) Co., Ltd.

The remaining authors declare that the research was conducted in the absence of any commercial or financial relationships that could be construed as a potential conflict of interest.

Publisher's note

Supplementary material

The Supplementary Material for this article can be found online at: https://www.frontiersin.org/articles/10.3389/fmolb.2022.1102735/full#supplementary-material

References

Bersuker, K., Hendricks, J. M., Li, Z., Magtanong, L., Ford, B., Tang, P. H., et al. (2019). The CoQ oxidoreductase FSP1 acts parallel to GPX4 to inhibit ferroptosis. *Nature* 575 (7784), 688–692. doi:10.1038/s41586-019-1705-2

Dixon, S. J. (2017). Ferroptosis: Bug or feature? *Immunol. Rev.* 277 (1), 150–157. doi:10.1111/imr.12533

Dixon, S. J., Lemberg, K. M., Lamprecht, M. R., Skouta, R., Zaitsev, E. M., Gleason, C. E., et al. (2012). Ferroptosis: An iron-dependent form of nonapoptotic cell death. *Cell* 149 (5), 1060–1072. doi:10.1016/j.cell.2012.03.042

Doll, S., Freitas, F. P., Shah, R., Aldrovandi, M., da Silva, M. C., Ingold, I., et al. (2019). FSP1 is a glutathione-independent ferroptosis suppressor. *Nature* 575 (7784), 693–698. doi:10.1038/s41586-019-1707-0

Friedmann Angeli, J. P., Krysko, D. V., and Conrad, M. (2019). Ferroptosis at the crossroads of cancer-acquired drug resistance and immune evasion. *Nat. Rev. Cancer* 19 (7), 405–414. doi:10.1038/s41568-019-0149-1

Gao, M., Monian, P., and Jiang, X. (2015). Metabolism and iron signaling in ferroptotic cell death. *Oncotarget* 6 (34), 35145–35146. doi:10.18632/oncotarget.5671

Jiang, L., Kon, N., Li, T., Wang, S. J., Su, T., Hibshoosh, H., et al. (2015). Ferroptosis as a p53-mediated activity during tumour suppression. *Nature* 520 (7545), 57–62. doi:10.1038/nature14344

Jiang, M., Qiao, M., Zhao, C., Deng, J., Li, X., and Zhou, C. (2020). Targeting ferroptosis for cancer therapy: Exploring novel strategies from its mechanisms and role in cancers. *Transl. Lung Cancer Res.* 9 (4), 1569–1584. doi:10.21037/tlcr-20-341

Jiang, X., Stockwell, B. R., and Conrad, M. (2021). Ferroptosis: Mechanisms, biology and role in disease. *Nat. Rev. Mol. Cell Biol.* 22 (4), 266–282. doi:10.1038/s41580-020-00324-8

Konda, J. D., Olivero, M., Musiani, D., Lamba, S., and Di Renzo, M. F. (2017). Heat-shock protein 27 (HSP27, HSPB1) is synthetic lethal to cells with oncogenic activation of MET, EGFR and BRAF. *Mol. Oncol.* 11 (6), 599–611. doi:10.1002/1878-0261.12042

Lee, Y. S., Lee, D. H., Jeong, S. Y., Park, S. H., Oh, S. C., Park, Y. S., et al. (2019). Ferroptosis-inducing agents enhance TRAIL-induced apoptosis through upregulation of death receptor 5. *J. Cell. Biochem.* 120 (1), 928–939. doi:10.1002/jcb.27456

Li, J., Cao, F., Yin, H. L., Huang, Z. J., Lin, Z. T., Mao, N., et al. (2020). Ferroptosis: Past, present and future. *Cell Death Dis.* 11 (2), 88. doi:10.1038/s41419-020-2298-2

Liang, H. H., Huang, C. Y., Chou, C. W., Makondi, P. T., Huang, M. T., Wei, P. L., et al. (2018). Heat shock protein 27 influences the anti-cancer effect of curcumin in colon cancer cells through ROS production and autophagy activation. *Life Sci.* 209, 43–51. doi:10.1016/j.lfs.2018.07.047

Liu, Y., Guo, F., Guo, W., Wang, Y., Song, W., and Fu, T. (2021). Ferroptosis-related genes are potential prognostic molecular markers for patients with colorectal cancer. *Clin. Exp. Med.* 21 (3), 467–477. doi:10.1007/s10238-021-00697-w

Ou, Y., Wang, S. J., Li, D., Chu, B., and Gu, W. (2016). Activation of SAT1 engages polyamine metabolism with p53-mediated ferroptotic responses. *Proc. Natl. Acad. Sci. U. S. A.* 113 (44), E6806–E6812. doi:10.1073/pnas.1607152113

Siegel, R. L., Miller, K. D., Fuchs, H. E., and Jemal, A. (2022). Cancer statistics, 2016. *Ca. Cancer J. Clin.* 72 (1), 7–30. doi:10.3322/caac.21332

Stockwell, B. R., and Jiang, X. (2019). A physiological function for ferroptosis in tumor suppression by the immune system. *Cell Metab.* 30 (1), 14–15. doi:10.1016/j.cmet.2019.06.012

Wang, J. J., Liu, Y., Zheng, Y., Lin, F., Cai, G. F., and Yao, X. Q. (2012). Comparative proteomics analysis of colorectal cancer. *Asian pac. J. Cancer Prev.* 13 (4), 1663–1666. doi:10.7314/apjcp.2012.13.4.1663

Wang, Y., Zhao, G., Condello, S., Huang, H., Cardenas, H., Tanner, E. J., et al. (2021). Frizzled-7 identifies platinum-tolerant ovarian cancer cells susceptible to ferroptosis. *Cancer Res.* 81 (2), 384–399. doi:10.1158/0008-5472.CAN-20-1488

Wei, G., Sun, J., Hou, Z., Luan, W., Wang, S., Cui, S., et al. (2018). Novel antitumor compound optimized from natural saponin Albiziabioside A induced caspase-dependent apoptosis and ferroptosis as a p53 activator through the mitochondrial pathway. *Eur. J. Med. Chem.* 157, 759–772. doi:10.1016/j.ejmech.2018.08.036

Xia, X., Fan, X., Zhao, M., and Zhu, P. (2019). The relationship between ferroptosis and tumors: A novel landscape for therapeutic approach. *Curr. Gene Ther.* 19 (2), 117–124. doi:10.2174/1566523219666190628152137

Yang, C., Huang, S., Cao, F., and Zheng, Y. (2021). A lipid metabolism-related genes prognosis biomarker associated with the tumor immune microenvironment in colorectal carcinoma. *BMC cancer* 21 (1), 1182. doi:10.1186/s12885-021-08902-5

Yuan, Y., Ni, S., Zhuge, A., Li, B., and Li, L. (2021). Iron regulates the warburg effect and ferroptosis in colorectal cancer. *Front. Oncol.* 11, 614778. doi:10.3389/fonc.2021.614778

Zhou, J. W., Wang, M., Sun, N. X., Qing, Y., Yin, T. F., Li, C., et al. (2019). Sulforaphane-induced epigenetic regulation of Nrf2 expression by DNA methyltransferase in human Caco-2 cells. *Oncol. Lett.* 18 (3), 2639–2647. doi:10.3892/ol.2019.10569

frontiers | Frontiers in Molecular Biosciences

TYPE Review
PUBLISHED 16 December 2022
DOI 10.3389/fmolb.2022.1102158

OPEN ACCESS

EDITED BY
Yanqing Liu,
Columbia University, United States

REVIEWED BY
Qian Wang,
College of Staten Island, United States
Bing Feng,
Pennington Biomedical Research Center, United States
Xiaoying Chen,
Washington University in St. Louis, United States

*CORRESPONDENCE
Xiao Lei,
18601758966@163.com
Baolin Qu,
baolinqu301@163.com

†These authors have contributed equally to this work

SPECIALTY SECTION
This article was submitted to Molecular Diagnostics and Therapeutics, a section of the journal Frontiers in Molecular Biosciences

RECEIVED 18 November 2022
ACCEPTED 06 December 2022
PUBLISHED 16 December 2022

CITATION
Tan X, Huang X, Niu B, Guo X, Lei X and Qu B (2022), Targeting GSTP1-dependent ferroptosis in lung cancer radiotherapy: Existing evidence and future directions.
Front. Mol. Biosci. 9:1102158.
doi: 10.3389/fmolb.2022.1102158

Targeting GSTP1-dependent ferroptosis in lung cancer radiotherapy: Existing evidence and future directions

Xin Tan[1,2†], Xiang Huang[1†], Baolong Niu[1†], Xingdong Guo[1,2], Xiao Lei[1*] and Baolin Qu[1*]

[1]Department of Radiation Oncology, The First Medical Center of Chinese PLA General Hospital, Beijing, China, [2]Medical School of Chinese PLA, Beijing, China

Radiotherapy is applied in about 70% patients with tumors, yet radioresistance of tumor cells remains a challenge that limits the efficacy of radiotherapy. Ferroptosis, an iron-dependent lipid peroxidation regulated cell death, is involved in the development of a variety of tumors. Interestingly, there is evidence that ferroptosis inducers in tumor treatment can significantly improve radiotherapy sensitivity. In addition, related studies show that Glutathione S-transferase P1 (GSTP1) is closely related to the development of ferroptosis. The potential mechanism of targeting GSTP1 to inhibit tumor cells from evading ferroptosis leading to radioresistance has been proposed in this review, which implies that GSTP1 may play a key role in radiosensitization of lung cancer *via* ferroptosis pathway.

KEYWORDS

ferroptosis, radiotherapy, lung cancer, GSTP1, mechanism

1 Background

Lung cancer is a malignancy with the highest mortality rate, with no treatment method that could effectively prolong the long-term survival rate of lung cancer patients (Sung et al., 2021). Therefore, finding ways to improve the survival rate of lung cancer patients has become the current focus in clinical research. Radiotherapy is a common treatment method for lung cancer and plays an increasingly important role. With the development of precision radiotherapy technology, the efficacy of radiotherapy and its status in tumor treatment have significantly increased (Santivasi and Xia, 2014). Although radiotherapy is the main method of tumor treatment, it produces unsatisfactory therapeutic results. These poor outcomes are diverse in pattern and associated with DNA repair, cell energetics, gene mutations, complex tumor microenvironment and immune response meditated by radiotherapy. All of the above factors ultimately contribute to tumor resistance to radiotherapy (Raghav et al., 2012; Buckley et al., 2020; Chandra et al., 2021; Busato et al., 2022). Currently, radioresistance has become one of the leading causes of treatment failure in lung cancer patients. Ferroptosis is an iron-dependent form of cell death marked by excessive accumulation of lipid peroxides, which

is significantly different from apoptosis, necroptosis and autophagy in morphology, genetic and biochemical characteristics fields (Dixon et al., 2012). The discovery of ferroptosis has led to new insights into tumor therapy, in which it has been found that ferroptosis might be involved in radiotherapy-induced cell death (Lang et al., 2019; Lei et al., 2020a; Ye et al., 2020). Glutathione S-transferase P1 (GSTP1) is a member of the glutathione-S-transferase (GST) family, which is capable of detoxifying cells from endogenous and exogenous toxic compounds by using glutathione (GSH) or by acting as a ligand (Mian et al., 2016). Studies have shown that GSTP1 plays a crucial role in maintaining cellular oxidative homeostasis and regulating cell proliferation and apoptosis (Holley et al., 2007). In addition, it has been surprisingly found that GSTP1 is involved in tumor development through ferroptosis pathway (Tew et al., 2011). Therefore, exploring the interaction of GSTP1 and ferroptosis in tumor radioresistance may provide us with a new approach to tumor radiosensitization. In this review, we discuss recent research advances on the role of ferroptosis and GSTP1 in lung cancer radiotherapy.

2 The potential role and its mechanisms of ferroptosis in radiotherapy

The mechanism of ferroptosis involves a confrontation between the intracellular ferroptosis execution system and the ferroptosis defense system. When the cellular activity promoting ferroptosis significantly exceeds the antioxidant buffering capacity provided by the ferroptosis defense system, there is an excessive accumulation of lipid peroxides on the cell membrane and subsequent membrane rupture, leading to cellular ferroptosis (Stockwell et al., 2020; Zheng and Conrad, 2020). The damage to the cellular structure by radiotherapy is mainly divided into two ways: direct way and indirect way. The direct way is mainly the direct action of high energy X-rays on the DNA double strand of the cell, causing it to break and inducing cell cycle arrest, senescence and cell death (Baskar et al., 2012). In addition to direct damage to DNA, ionizing radiation can also act on organisms through indirect effects. For example, after absorption of ionizing radiation by living cells, ionizing radiation can cause cellular damage by generating chemicals such as reactive oxygen species (ROS) (Azzam et al., 2012; Santivasi and Xia, 2014; Pouget et al., 2018). However, multiple tumors have evolved strategies to avoid cell death, such as loss of TP53 tumor suppressor function, increased expression of antiapoptotic regulators (Bcl-2, Bcl-xL) or survival signals (Igf1/2), thus exhibiting radioresistance to radiotherapy, which undoubtedly one of the main factors affecting patient outcome as well as prognosis (Hanahan and Weinberg, 2011). The concept of ferroptosis, first proposed by Prof. Stockwell's team in 2012, is a regulated cell death process caused by excessive accumulation of iron ions and reactive oxygen species-induced dysregulated accumulation of cellular lipid peroxidation metabolism (Dixon et al., 2012; Stockwell et al., 2017). It is morphologically characterized by mitochondrial wrinkling and a decrease in the number of mitochondrial cristae, an increase in membrane density and thickness, insignificant morphological changes in the nucleus (Stockwell et al., 2017). It is characterized by excessive accumulation of lipid peroxides and is closely associated with intracellular iron overload, free radical production, fatty acid supply and lipid peroxidation (Li et al., 2020; Stockwell, 2022). Radiotherapy can induce ferroptosis in the specified cancers through several pathways as following.

2.1 Radiotherapy might affect ferroptosis through iron metabolism

Iron overload is associated with the development of lung cancer, and there is a significant positive correlation between high iron intake and lung cancer risk. Datas from a clinical trial show that serum iron, ferritin and total iron binding are significantly higher in lung cancer patients than in healthy controls (Sukiennicki et al., 2019). The higher the serum iron concentration, the greater the risk of developing lung cancer (Sukiennicki et al., 2019; Ward et al., 2019). Under normal conditions, extracellular iron bounding to transferrin to form a complex is mediated by transferrin receptor 1 (TfR1) on the cell membrane into the intracellular compartment, where it is converted to ferrous ions by ferric reductase and subsequently stored in the intracellular unstable iron pool *via* the divalent metal transporter protein divalent metal transporter 1 (DMT1), and the excess iron ions are stored as inert iron in ferritin in the cell, maintaining intracellular iron homeostasis (Masaldan et al., 2018; Lei et al., 2020a). When iron ions are overloaded, the iron ions entering the cell react with reactive oxygen species in the Fenton reaction, peroxidizing polyunsaturated fatty acids on the cell membrane and generating lipid peroxides, leading to damage of the cell membrane structure and eventually triggering cell death (Conrad and Proneth, 2019). Under ionizing radiation and oxidative stress or certain other pathological conditions, iron homeostasis can be severely altered. This alteration can manifest itself in several ways, one of which is an increase in intracellular levels of potentially harmful unstable iron pools leading to oxidative membrane damage and cell death of cells (Aroun et al., 2012). Therefore, radiotherapy may also affect the occurrence of ferroptosis by modulating iron metabolism. Ivanov et al. significantly improved the efficiency of radiotherapy in glioma-bearing mice by adding mineralized iron water to the tumor-bearing animals, which reduced monocytes and tumor volume in glioma-bearing mice under radiotherapy. Further addition of iron chelators weakened the tumor suppressive effect of radiotherapy because of blocking

radiation-induced ferroptosis (Ivanov et al., 2013; Ivanov et al., 2015). Qin et al. found all-lactoferrin Holo-Lf was able to increase the expression of transferrin receptor, ferritin and ferroregulin, indicating increased iron uptake, storage and output, combined with radiotherapy could promote ROS production and increase lipid peroxidation end product malondialdehyde (MDA), thereby enhancing ferroptosis in MDA-MB-231 cells (Zhang et al., 2021a). Sato et al. shown that mitochondrial dysfunction increased intracellular H_2O_2, Fe^{2+} levels and might lead to increased production of -OH, resulting in lipid peroxidation and ferroptosis (Takashi et al., 2020). Zheng et al. found that the deubiquitinating enzyme USP35 regulated ferroptosis in lung cancer by targeting FPN (Tang et al., 2021a). Jun et al. disclosured that in ischemia-reperfusion-treated rat hearts, ubiquitin-specific protease seven could increase iron uptake and thus promoted ferroptosis by activating p53 leading to upregulation of TfR1 (Tang et al., 2021b). Tomita K et al. unfolded that miR-7-5p could impede Fe^{2+} transport into mitochondria by inhibiting mitoglobin under radiation, leading to the onset of intracellular hydroxyl radical levels and Fenton reaction-induced cytoplasmic membrane oxidation, ultimately causing radiation-induced ferroptosis (Tomita et al., 2019). In addition, Jaewang Lee et al. found that PCBP1, as a ferric ion chaperone protein, could inhibit iron-mediated ferritin phagocytosis and lipid peroxidation and was an important regulator of ferroptosis. Further experiments demonstrated that downregulation of PCBP1 increased the sensitivity of head and neck cancer to ferroptosis (Lee et al., 2022). In addition, many other researchers found that radiotherapy might affect ferroptosis by mediating the expression of iron metabolism-related proteins such as iron ion-related carriers like ferritin, FPN, regulatory iron regulators, membrane iron transport auxiliary protein (Hephaestin) and copper cyanobacteria by mediating hypoxia-inducible factor 1α (HIF-1α) or HIF-2α (Shah et al., 2009; Singhal et al., 2021; Yang et al., 2022). Therefore, we consider that the regulation of intracellular iron ion content by radiation to cause iron overload to enhance ferroptosis sensitivity in tumor cells is expected to be an effective way to enhance radiosensitivity.

2.2 Radiotherapy induces ferroptosis by promoting lipid peroxidation

Hyperoxidation of phospholipids containing polyunsaturated fatty acids (PUFA-PL) catalyzed by iron is the core feature of ferroptosis. Lipid peroxidation of PUFA generates a variety of oxidation products. Among them, lipid hydroperoxides (LOOHs) are the initial products of peroxidation. The secondary products are aldehydes, of which MDA and 4-hydroxynonenal (4-HNE) are the most abundant (Feng and Stockwell, 2018). Yang et al. finds that ferroptosis can be driven by peroxidation of polyunsaturated fatty acids (PUFA) at the diallyl site, which is pretreated with PUFA containing the heavy hydrogen isotope deuterium (D-) at the peroxidation site. Pretreatment of cells with PUFA containing the heavy hydrogen isotope deuterium (D-PUFA) at the peroxidation site prevents PUFA peroxidation and ferroptosis (Yang et al., 2016). Therefore, the content of intracellular PUFAs determines the degree of lipid peroxidation and the susceptibility of cells to ferroptosis (Lei et al., 2021a). Driven by the highly reactive OH • radicals generated by the Fenton reaction and the presence of a large amount of the bis-allylic, PUFA are the most susceptible to damage by exposure to high doses of radiation. In contrast, monounsaturated fatty acids (MUFA) are less susceptible to peroxidation due to the absence of the bis-allylic, which could inhibit lipid peroxidation and ferroptosis by replacing polyunsaturated fatty acids in the cell membrane (Feng and Stockwell, 2018). Therefore, cancer cells can be sensitized to ferroptosis by modulating the activities of enzymes involved in MUFA-PL synthesis, such as SCD1 and ACSL3. Polyunsaturated fatty acids containing diallyl provide substrates that are peroxidized to drive ferroptosis (Tesfay et al., 2019; Zou et al., 2020). Acyl coenzyme A synthase long chain family member 4 (ACSL4) esterifies CoA to free fatty acids, especially polyunsaturated fatty acids, and radiotherapy can collectively promote lipid peroxidation and ultimately ferroptosis by generating large amounts of ROS and upregulating the expression of the key enzyme ACSL4. In addition, knockdown of the ACSL4 gene in tumor cells leads to significant radioresistance (Doll et al., 2017; Lei et al., 2020a). Meanwhile, radiation is able to significantly increase the staining of C11-BODIPY, lipid peroxidation markers MDA and 4-HNE in cancer cells and tumor samples, indicating that radiation induces lipid peroxidation (Lei et al., 2020a; Zhang et al., 2021a; Zhou et al., 2022). Similarly, irradiated cells exhibit increased expression of the ferroptosis marker gene prostaglandin endoperoxide synthase 2 (PTGS2) (Busato et al., 2022; Yang et al., 2022). Furthermore, Seiji Torii et al. shows that knockdown of Arachidonate 15-Lipoxygenase (ALOX15) decreases erastin-induced and RSL3-induced cellular ferroptosis, on the contrary exogenous overexpression of ALOX15 enhances the effects of these compounds. This suggests that LOX-catalyzed lipid hydroperoxide production in the cell membrane promotes tumor ferroptosis (Shintoku et al., 2017). In contrast, treatment with baicalin (ALOX15 inhibitor) after irradiation restores normal levels of systemic irradiation-induced inflammatory cytokines and improves survival in mice (Thermozier et al., 2020). Dixon and Angeli et al. finds that the free radical scavenger statin Ferrostatin and the lipid peroxidase inhibitor/fat-soluble antioxidant vitamin E, among other lipophilic antioxidants and iron chelator drugs can modulate the occurrence of cellular ferroptosis by inhibiting the process of lipid peroxidation (Dixon et al., 2012; Angeli et al., 2017). Therefore, it is reasonable to assume that radiotherapy can

influence the onset of ferroptosis by mediating the biosynthesis of polyunsaturated fatty acids in cell membranes to promote the accumulation of lipid peroxides.

2.3 Radiotherapy induces ferroptosis by depleting GSH and inhibiting the synthesis of GPX4

Glutathione which is synthesized from glycine, glutamate and cysteine is an important non-enzymatic antioxidant for intracellular scavenging of ROS, and its metabolic balance is closely related to the regulation of ferroptosis. Glutathione peroxidase 4 (GPX4) as a selenoperoxidase is a key upstream regulator of ferroptosis which plays two simultaneous roles, one in converting reduced GSH to glutathione disulfide (GSSG) and the other is to inhibit ferroptosis by reducing phospholipid hydroperoxides (PLOOHs) to the corresponding alcohols (PLOHs), thereby preventing the accumulation of lipid peroxides (Jiang et al., 2021). The cysteine-glutamate reverse transporter (System-Xc) is a dimer composed of the transporter-active transmembrane protein solute carrier family seven member 11(SLC7A11) and the transmembrane regulatory protein solute carrier family three member 2 (SLC3A2), in which cysteine is the rate-limiting precursor for GSH synthesis. Inhibition of SystemXc-function can lead to GSH depletion and indirectly affect the ability of GPX4 to catalyze lipid peroxide reduction reactions, resulting in ROS accumulation and triggering ferroptosis (Yang et al., 2016). Zou et al. finds that Interferon (IFNγ) secreted by $CD8^+$ T cells and ATM activated by radiotherapy can synergistically inhibit SLC7A11 expression to limit cystine uptake by tumor cells, leading to reduced GSH synthesis and thus promoting lipid peroxidation and ferroptosis (Lang et al., 2019). Wang et al. finds that RBMS1 inhibits SLC7A11 translation, reduces SLC7A11-mediated cystine uptake and promotes ferroptosis in lung cancer cells (Zhang et al., 2021b). Cobler et al. finds that inhibition of SLC7A11 after Erastin treatment increases radiosensitivity in $SLC7A11^+$ breast cancer cells *in vitro* and *in vivo*, while it has no effect on $SLC7A11^-$ cancer cells, this process accompanied by a decrease in intracellular GSH synthesis that promotes cell death (Cobler et al., 2018). Li finds that nuclear factor erythroid 2-related factor 2 (NRF2) can inhibit radiation-induced ferroptosis by regulating SLC7A11 in esophageal squamous cell carcinoma (ESCC), promoting radioresistance in ESCC (Feng et al., 2021). Ye LF finds that ferroptosis is a mechanism of radiation-induced cancer cell death. When tumors have evolved specific resistance mechanisms such as a resistant state susceptible to GPX4 inhibition and ferroptotic cell death, the combination of ferroptosis inducers and radiotherapy has potential applications in cancers, especially those who have undergone EMT (Ye et al., 2020). In addition, Yu et al. finds that knockdown of GPX4 can reduce radiotherapy resistance in NSCLC cells by inducing ferroptosis (Pan et al., 2019). Gao et al. confirms that knockdown Ribonucleotide reductase subunit M1 (RRM1) promotes the occurrence of radiation-induced lipid peroxidation, decreases GSH levels, increases GSSH levels and elevates MDA levels. It is believed that targeting RRM1 can disrupt the antioxidant resistance system of tumor cells to mediate the onset of ferroptosis and thus radiosensitize tumor cells (Gao et al., 2022). Thus we have the same expectations for GSTP1. Shibata et al. also demonstrates the radiosensitizing effect of erastin on lung adenocarcinoma cells NCI-H1975 and tumor xenograft models accompanied by lower levels of glutathione (Shibata et al., 2019). Therefore, inhibition of the GSH/GPX4 pathway by SLC7A11 in combination with radiotherapy induces ferroptosis in tumor cells has strong application. When such ferroptosis inducers act as a radiosensitizer, in addition to the DNA double-strand damage effect, more ROS can be generated in tumor cells through other additional pathways, thus aggravating lipid peroxidation and cell death. In addition, there may be other regulatory mechanisms for the maintenance of intracellular GSH/GPX4 homeostasis, further studies targeting other influences on this pathway to induce ferroptosis and enhance radiosensitivity provide a broad scope for exploration.

3 GSTP1 as a potential regulator in radiotherapy of cancer

Radiotherapy exerts its anti-tumor effects mainly by generating oxidative stress (Mukha et al., 2021), thus oxidative stress-related enzymes may affect the effect of radiotherapy in cancer patients. Enzymes involved in the ROS neutralization pathway include glutathione-S-transferase (GST), manganese superoxide dismutase (MnSOD) and catalase (CAT) (Hayes and Pulford, 1995). Enzymes such as MPO and endothelial nitric oxide synthase (eNOS) are involved in the generation pathway of ROS (Rehman et al., 2020). MPO catalyzes a reaction between H_2O_2 and chloride to generate hypochlorous acid, a potent oxidizing agent (Peng et al., 2022). A Re et al. shows that a combinatorial complex between estrogen receptor (ER)-β and endothelial nitric oxide synthase (eNOS) could repress transcription of prognostic genes that are down-regulated in prostate tumors, such as the glutathione transferase gene GSTP1 (Re et al., 2011). Kecheng Lei et al. shows that inactivation of both NQO1 and GSTP1 result in imbalanced redox homeostasis, leading to apoptosis and mitigate cancer proliferation in glioblastoma (Lei et al., 2020b). Claudia Bănescu et al. illuminats that CAT, GPX, MnSOD, and glutathione S-transferase M1 (GSTM1) and glutathione S-transferase T1 (GSTT1) gene polymorphisms are not associated with the risk of chronic myeloid leukemia (CML) except GSTP1 depending on its strong restoring ability (Bănescu et al., 2014). Therefore, in this review we focus on GSTP1, which could be a potential

effective regulator in radiotherapy of cancer in GST family. Glutathione S-transferases (GST), a group of isoenzymes, were discovered in rat liver in 1960 and have gained attention for their detoxification function in catalyzing the reaction of GSH with electrophile substances (Booth et al., 1961). GSTs are found in cells mainly in the cytoplasm, mitochondria and microsomes, mainly divide into α (GSTA), π (GSTP), μ (GSTM), σ (GSTS), θ (GSTT), ζ (GSTZ), and ω (GSTO) seven isoforms. Among them, GSTP1 is the most widely studied member of the GST family (Chatterjee and Gupta, 2018; Kogawa et al., 2021). The gene encoding GSTP1 is localized on chromosome 11q13 and is approximately 3.2 kb long, which contains 9 exons and 6 introns. It has high G + C and CpG content near its 5′ end, typical of HTF (HpaII microfragment islands) (Cowell et al., 1988). GSTP1 is a phase II metabolizing enzyme that is widely found in mammalian liver, lung, kidney and other tissues. Its main function is to catalyze the binding of glutathione to various electrophilic hydrophobic substances to form water-soluble compounds for excretion from the body (Awasthi et al., 2017). Structurally, it is a dimeric protein containing 210 amino acids per subunit and two binding sites. G site specifically binds GSH and H site catalyzes the reaction of GSH with electrophile substances (FeiFei et al., 2019). GSTP1 is involved in the metabolism of various chemotherapeutic drugs and protects normal cells from carcinogens and electrophile compounds. With the continuous research on GSTP1, it has been found that besides its catalytic detoxification function, it also has various functions such as anti-apoptosis, regulation of inflammatory response, regulation of cell signaling pathways, and it is closely related to the development of tumors (van de Wetering et al., 2021). GSTP1 exists widely in the body, and its catalytic detoxification activity is believed to protect the body from carcinogenic factors. Many studies have confirmed that the expression level of GSTP1 is associated with an increased risk of various cancers. Ritchie et al. treated GSTP1 knockout mice and wild-type mice with benzopyrene, 3-methylcholanthrene, and urethane, respectively, and found that GSTP1 gene deletion increased the incidence of lung adenocarcinoma in mice exposed to these three compounds, respectively 8.3 times, 4.3 times and 8.7 times (Ritchie et al., 2007). GSTP1 may exert its protective effect on the organism by protecting normal organ tissues from carcinogenic factors due to its functions such as detoxification and regulation of inflammation. However, a large number of studies have found that the expression level of GSTP1 in most tumor cells is significantly higher than that in normal tissues, and high expression of GSTP1 is associated with poorer prognosis of tumors. Ali-Osman et al. analyzed the expression level and subcellular localization of GSTP1 in 61 primary gliomas, and analyzed the correlation between the results and tumor stage, patient age and patient survival rate. The relative risk of death in tumor patients was 3.2 times that of patients with low GSTP1 expression, and the relative risk of death in patients with GSTP1 expression in glioma nuclei was 3.9 times that in patients without GSTP1 expression in the nucleus (Ali-Osman et al., 1997). This shows that overexpression of GSTP1 protein in tumor cells and its nuclear localization are closely associated with more advanced tumor staging and worse prognosis. Pljesa-Ercegovac, M. et al. collected tumor and adjacent tissues from 84 patients with bladder transitional cell carcinoma. Through immunohistochemical analysis, they found that the apoptosis inhibitory protein Bcl-2 was highly expressed in most tumors with high GSTP1 expression, while the expression of GSTP1 was high. The level was significantly negatively correlated with the activator of apoptosis-enforcing protein caspase-3, indicating that the high expression of GSTP1 inhibited the apoptosis signaling pathway, thereby inhibiting tumor apoptosis (Pljesa-Ercegovac et al., 2011). The role of GSTP1 was explained by Savic et al.'s study on the antioxidant capacity of bladder transitional cell carcinoma. The researchers detected the activity of antioxidant enzymes in tumors and adjacent tissues of 30 patients with bladder transitional cell carcinoma, and found that γ-glutamyl cysteine synthase (γ-GCS) and glutathione in tumor tissue. The activity of peptide reductase (GR) was 4-fold and 2-fold higher than that of the paracancerous tissue, respectively, and the expression level of GSTP1 was significantly positively correlated with the activity of γ-GCS and GR. GSTP1 may participate in the regulation of cellular redox state by catalyzing the reaction of glutathione with intracellular reactive oxygen species and other electrophiles, thereby improving the antioxidant capacity of tumor cells and helping tumor cells to resist external killing factors (Savic-Radojevic et al., 2007). Our lab colleagues previously did a study on the response of GSTP1 to radiation. We found that both GSTP1 expression and its glutathione catalase activity were decreased after radiation (Lei et al., 2021b). Previous scholars have found that GSTP1 could be directly activated by NRF2 (Ikeda et al., 2002; Fang et al., 2020). At the same time, under some stress conditions (such as ionizing radiation and oxidative stress), the stress-responsive transcription factor NRF2 can induce the regulation of the SLC7A11 subunit with transport activity on System-Xc, increasing the uptake of cystine to promote further Synthesis and utilization of prototypical GSH to protect cells from ferroptosis under stressful conditions, the specific underlying mechanisms will be further explained in the outlook (Dong et al., 2021; Feng et al., 2021; Liu et al., 2022).

Till now, a specific radiosensitizer that sensitizes tumors without affecting normal tissues has not been found all over the world. Ferroptosis is a recently discovered form of cell death driven by iron-dependent lipid peroxidation which is mechanistically different from other forms of cell death. Previous studies have found that the expression of GSTP1 in tumor tissues is higher than that in normal tissues, which provides a good research entry point for us to study the potential role of GSTP1 in tumor radiotherapy through ferroptosis.

TABLE 1 The potential role of GSTP1 in ferroptosis pathway for tumor treatment.

Study	Year	Sample	Summary	Potential target	Possibly associated with radiotherapy
Biomimetic photosensitizer nanocrystals trigger enhanced ferroptosis for improving cancer treatment (Wu et al., 2022)	2022	Mice and HSC-3 cells	AE could induce ferroptosis by inhibiting the activity of GSTP1	LPO/GSTP1	Possible
Glutathione peroxidase 4-dependent glutathione high-consumption drives acquired platinum chemoresistance in lung cancer-derived brain (Liu et al., 2021)	2021	Immunodeficient mice and PC9-BrM3 cells	GPX4 regulated the level of GSTM1 by protein stabilization, which is an isoenzyme with GSTP1	GSTM1	Mostly possible
Activation of mouse Pi-class glutathione S-transferase gene by Nrf2(NF-E2-related factor 2) and androgen (Ikeda et al., 2002)	2002	Mice bearing HSC-3 tumors and HepG2 cells	Nrf2 and the androgen receptor directly bind to and activate the mouse GSTP1 gene	Nrf2	Mostly possible
A targetable CoQ-FSP1 axis drives ferroptosis- and radiation-resistance in KEAP1 inactive lung cancers (Koppula et al., 2022)	2022	H1299, H23, H460, H2126 and A549	The CoQ-FSP1 axis as a key downstream effector of the KEAP1-NRF2 pathway to mediate ferroptosis -and radiation-resistance in KEAP1 deficient lung cancers	Keap1-Nrf2/FSP1-CoQ/GSTP1	Mostly possible
Activation of anti-oxidant Keap1/Nrf2 pathway modulates efficacy of dihydroartemisinin-based monotherapy and combinatory therapy with ionizing radiation (Bader et al., 2021)	2021	HCT116 cells l and NCI–H460 cells	In Keap1-wildtype cells, radiotherapy and DHA more efficiently eradicated clonogenic cells than either therapy alone	Keap1-Nrf2/GSTP1	Mostly possible
Enhanced GSTP1 expression in transitional cell carcinoma of urinary bladder is associated with altered apoptotic pathways (Pljesa-Ercegovac et al., 2011)	2011	Patients with transitional cell carcinoma	The GSTP1 expression in transitional cell carcinoma of urinary bladder is associated with altered apoptotic pathways	GSTP1	Slightly possible
Role of KEAP1/NRF2 and TP53 Mutations in Lung Squamous Cell Carcinoma Development and Radiation Resistance (Jeong et al., 2017)	2017	mice	KEAP1/NRF2 mutation status predicted risk of local recurrence after RT in non-small lung cancer patients	KEAP1/NRF2/GSTP1	Mostly possible
STK11/LKB1 Mutations in NSCLC Are Associated with KEAP1/NRF2-Dependent Radiotherapy Resistance Targetable by Glutaminase Inhibition (Sitthideatphaiboon et al., 2021)	2021	Stage III patients with NSCLC	Targeting the KEAP1/NRF2 pathway or GLS inhibition are potential approaches to radiosensitize LKB1-deficient tumors	KEAP1/NRF2/GSTP1	Mostly possible
Glutathione S-transferase-P1 expression correlates with increased antioxidant capacity in transitional cell carcinoma of the urinary bladder (Savic-Radojevic et al., 2007)	2007	Patients with transitional cell carcinoma	GSTP1 expression in tumor tissues correlated positively not only with GSH levels γ-GCS and GR activity, but also with GPX and SOD activity in TCC.	GPX/GSTP1	Mostly possible
Expression of glutathione S-transferase P1-1 in leukemic cells is regulated by inducible AP-1 binding (Duvoix et al., 2004)	2004	K562 cells	High GSTP1 gene expression could be exploited to leukaemia through binding activity to AP-1 in leukemia cells	GSTP1/AP-1	Possible
Glutathione transferases P1/P2 regulate the timing of signaling pathway activations and cell cycle progression during mouse liver regeneration (Pajaud et al., 2015)	2015	Gstp1/2 knockout mice in C57BL6/J	The invalidation of Gstp1/p2 affects multiple key events of the hepatocyte cell cycle	GSTP1	Slightly possible

(Continued on following page)

TABLE 1 (*Continued*) The potential role of GSTP1 in ferroptosis pathway for tumor treatment.

Study	Year	Sample	Summary	Potential target	Possibly associated with radiotherapy
Regulation of glutathione S-transferase P1-1 gene expression by NF-kappaB in tumor necrosis factor alpha-treated K562 leukemia cells (Morceau et al., 2004)	2004	K562 cell	The regulation of the GSTP1-1 gene expression in the K562 cell line by NF-kappaB and TNFα	GSTP1	Slightly possible
GSTP1 Loss results in accumulation of oxidative DNA base damage and promotes prostate cancer cell survival following exposure to protracted oxidative stress (Mian et al., 2016)	2016	LNCaP cells	Silencing of GSTP1 in prostate cancer results in enhanced survival and accumulation of potentially promutagenic DNA adducts following exposure of cells to protracted oxidative injury	GSTP1	Mostly possible

AE, aloe-emodin; LPO, lipid peroxidation; FSP1, ferroptosis suppressor protein 1; CoQ, coenzyme Q(10); GSTM1, Glutathione S-transferase M1; Keap1, kelch-like ECH associated protein 1; Nrf2, nuclear factor erythroid 2-related factor 2; RT, radiation therapy; GSTP1, Glutathione S-transferase P1; GSH, glutathione; GPX4, glutathione peroxidase 4; LKB1, live kinase B1; γ-GCS, γ-glutamyl cysteine synthase; SOD, superoxide dismutase; TCC, transitional cell carcinoma; TNFα, tumor necrosis factor alpha.

4 Perspective

Cells exposed to ionizing radiation may generate a large amount of reactive oxygen species and free radicals, which can lead to protein, lipid membrane and DNA damage, resulting in apoptosis, necrosis, teratogenicity or carcinogenesis (Smith et al., 2017). As a protein isoform in the glutathione S-transferase family, GSTP1 plays an important role in maintaining cellular oxidative balance, regulating cell proliferation and apoptosis. In tumor-related studies, it has been found that the high expression of GSTP1 promotes the chemoresistance of various tumors. In addition, the expression level of GSTP1 in most tumor cells is significantly higher than that in normal tissues, and high expression of GSTP1 is associated with poor prognosis of tumors (Simic et al., 2009; Fujikawa et al., 2018). Glutathione peroxidase 4 (GPX4), a potent antioxidant, utilizes glutathione as a cofactor to scavenge ROS and reduce oxidized lipid species to inhibit ferroptosis. It has been reported that glutathione metabolism in brain metastases from NSCLC is regulated by glutathione peroxidase and glutathione S-transferase; among them, GPX4 and GSTM1 are overexpressed in BM subsets, and cause massive consumption of GSH in brain metastases of lung cancer (Liu et al., 2021). Further studies find that GPX4 regulates the expression level of GSTM1 by enhancing protein stability, and the overexpression of GPX4 and its regulatory target protein GSTM1 acquires chemoresistance by inhibiting ferroptosis (Liu et al., 2021). Inhibition of GPX4 expression and its activity *in vitro* and *in vivo* enhances the anticancer effect of platinum drugs in brain metastatic cells (Liu et al., 2021). In human lung tissue, GSTP1 is the most abundant protein isoform in the GST protein family. Therefore, we speculate that GSTP1, which is a GSTM1 isoenzyme, may also be closely associated with the regulation of ferroptosis. Related studies have been listed in Table 1.

Ferroptosis is an iron-dependent lipid peroxidation-mediated cell death. Researchers find that autophagy inhibitors can protect HepG2 cells from alcohol-induced ferroptosis by activating the p62-Keap1-Nrf2 pathway (Zhao et al., 2021). It has also been found that Keap1/Nrf2 mutation status predicts the risk of local recurrence after radiotherapy in NSCLC patients, and Keap1/Nrf2 mutant lung cancers may be radiotherapy resistant to radaition due to enhanced expression of ROS clearance and detoxification pathways (Jeong et al., 2017). Keap1 is a negative regulator of Nrf2, and Nrf2 is a major effector of the ARE system. Activation of the ARE system through negative regulation of Keap1 protein induces the expression of a range of antioxidant genes, including Nrf2 and GSTP 1 (Fang et al., 2020; Umamaheswari et al., 2021). The function of GSTP1 is to catalyze the binding of GSH to various electrophilic hydrophobic substances to form water-soluble compounds for excretion from the body (Ikeda et al., 2002; Cui et al., 2020). Lei et al. further demonstrats that Keap1 deficiency in lung cancer cells promotes radioresistance in lung squamous cell carcinoma in part through SLC7A11 inhibition of ferroptosis (Lei et al., 2020a). Interestingly, it is found that GSTP1 expression is regulated by the Keap1-Nrf2-ARE pathway and GSTP1 catalyzes the S-glutathionylation of cysteine residues of Keap1 protein, while S-glutathionylation of Keap1 leads to Nrf2 activation and increases the expression of GSTP1 (Carvalho et al., 2016). It has also been found that the promoter of the mouse GSTP1 gene contains at least three Nrf2 binding sites, demonstrating that Nrf2 directly activates the gene and that GSTP1 gene expression directly affects the Nrf2-dependent response to the hormone diselenide (Ikeda et al., 2002; Bartolini et al., 2015).

Therefore, we speculate that lung cancer cells might form a GSTP1-Keap1-Nrf2 positive feedback loop under ionizing radiation or oxidative stress, and play an anti-oxidative damage effect. At the same time, SLC7A11 is up-regulated by the transcription of Nrf2, thereby increasing the resistance to ionizing radiation. GSTP1 catalyzes the reaction of glutathione with electrophiles, including intracellular reactive oxygen species, hydroxyl radicals, and inhibits its oxidation of polyunsaturated

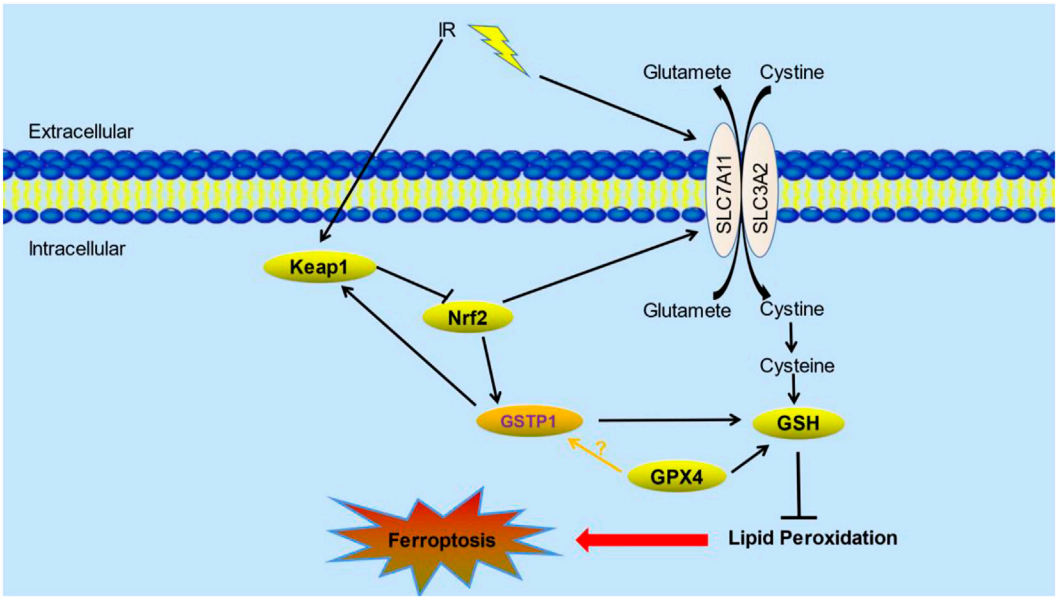

FIGURE 1
The potential role of GSTP1 and its mechanisms of ferroptosis in radiotherapy. Keap1-Nrf2-GSTP1 positive feedback loop interacts with GPX4 and SLC7A11 which are the core proteins in ferroptosis pathway under radiation. Their interactions affect lipid peroxidation, thus inhibiting the occurrence of ferroptosis (Liu et al., 2021; Wu et al., 2022). (IR: ionizing radiation; Keap1: kelch-like ECH associated protein 1; Nrf2: nuclear factor erythroid 2-related factor 2; GSTP1: Glutathione S-transferase P1; GSH: glutathione; GPX4: glutathione peroxidase 4).

fatty acids on the cell membrane to fight ferroptosis. In addition, GSTP1 may also interact with GPX4 to play a synergistic role in inhibiting the occurrence of ferroptosis, thereby enhancing the radioresistance of tumors. The potential mechanism is shown as following (Figure 1). Moreover, GSTP1 is involved in ferroptosis regulatory mechanisms possibly similar to GPX4 as part of the ferroptosis pathway. Targeting downregulation of GSTP1 expression under tumor radiotherapy would increase radiosensitivity of lung tumors and thus promoting radiation-induced ferroptosis. On the one hand, it may act from promoting lipid metabolism through the ferroptosis execution system, on the other hand, it may weaken the ferroptosis defense system by reduce the ability of cells to use GSH to counteract ROS. In addition, radiation may make the interaction between GSTP1 and GPX4 decreased, which further promotes the occurrence of ferroptosis. However, the exact mechanism still need to be confirmed by further experiments.

Although no experimental studies have shown that GSTP1 plays a key role in the radiosensitization of ferroptosis in lung cancer, previous studies by our group showed that the levels of MDA, the lipid peroxide breakdown product, were significantly increased in cells with knockdown of GSTP1 after radiation treatment. In addition, multiple studies have shown that higher serum iron concentrations and ferritin levels are positively associated with lung cancer morbidity and mortality. It also laid a theoretical foundation for our subsequent exploration of the mechanism by which GSTP1 may protect lung cancer cells and inhibit ferroptosis after tumor radiation therapy.

5 Conclusion

In conclusion, GSTP1 may be a novel negative regulator of ferroptosis other than GPX4, may play an important role in lung cancer radiotherapy by inhibiting ferroptosis. The reasons are as follows. Firstly, as a potent antioxidant, GPX4 utilizes glutathione as a cofactor to scavenge ROS and reduces oxidized lipid species to inhibit ferroptosis (Friedmann Angeli et al., 2014; Stockwell et al., 2020). It has been reported that glutathione metabolism in brain metastases from NSCLC is regulated by glutathione peroxidase and glutathione S-transferase; among them, GPX4 and GSTM1 are overexpressed in BM subsets, and cause massive consumption of GSH in brain metastases of lung cancer (Liu et al., 2021). Further studies find that GPX4 regulates the expression level of GSTM1 by enhancing protein stability, and the overexpression of GPX4 and its regulatory target protein GSTM1 acquires chemoresistance by inhibiting ferroptosis. Inhibition of GPX4 expression and its activity *in vitro* and *in vivo* enhances the anticancer effect of

platinum drugs in brain metastatic cells (Liu et al., 2021). Secondly, as a member of GSTs, GSTP1 could participate in the metabolism of lipids and DNA products derived from oxidative stress. The core of ferroptosis is the excessive accumulation of intracellular lipid peroxides, which is caused by the imbalance of lipid metabolism from various causes (Luo et al., 2022). Besides, Zhao et al. find that GSTP1 is a key protein for ferroptosis. And the photosensitizer aloe-emodin (AE) could induce cellular ferroptosis based on its specific inhibiting activity to GSTP1 (Wu et al., 2022). The underlying mechanism of GSTP1 in the induction of ferroptosis in lung cancer radiotherapy has been proposed in a hypothetical pathway map (Figure 1). In addition, although relevant studies have shown that GSTP1 is closely related to the occurrence and development of tumors, there is no specific experimental study to prove the role and mechanism of GSTP1 in ferroptosis radiotherapy. This provides us with a research entry point to develop better personalized treatment strategies for the clinic. So far, there are multiple evidences that targeting GSTP1 can have a synergistic effect with chemotherapeutic drugs, but there is no correlation between GSTP1 and radiation-induced ferroptosis. If the changes of GSTP1 protein expression or activity can be controlled, thereby increasing the ferroptosis effect of radiotherapy on lung tissue tumors, while reducing radiation damage to normal lung tissue, it has extremely important medical significance for the treatment and prognosis of thoracic tumor patients. This is the core purpose of this review.

Author contributions

XT and XH made the manuscript. BN and XG did the perspective and conclusion parts. XL and BQ participated in the writing of paper and revision of manuscript. All authors read and approved the final manuscript.

Funding

This study was supported in part by the grants from National Natural Science Foundation of China (No. 82003387) and Military Research Plan (No. 20BJZ40).

Conflict of interest

The authors declare that the research was conducted in the absence of any commercial or financial relationships that could be construed as a potential conflict of interest.

Publisher's note

All claims expressed in this article are solely those of the authors and do not necessarily represent those of their affiliated organizations, or those of the publisher, the editors and the reviewers. Any product that may be evaluated in this article, or claim that may be made by its manufacturer, is not guaranteed or endorsed by the publisher.

References

Ali-Osman, F., Brunner, J. M., Kutluk, T. M., and Hess, K. (1997). Prognostic significance of glutathione S-transferase pi expression and subcellular localization in human gliomas. *Clin. Cancer Res.* 3 (12), 2253–2261.

Angeli, J. P. F., Shah, R., Pratt, D. A., and Conrad, M. (2017). Ferroptosis inhibition: Mechanisms and opportunities. *Trends Pharmacol. Sci.* 38 (5), 489–498. doi:10.1016/j.tips.2017.02.005

Aroun, A., Zhong, J. L., Tyrrell, R. M., and Pourzand, C. (2012). Iron, oxidative stress and the example of solar ultraviolet A radiation. *Photochem. Photobiol. Sci.* 11 (1), 118–134. doi:10.1039/c1pp05204g

Awasthi, Y. C., Ramana, K. V., Chaudhary, P., Srivastava, S. K., and Awasthi, S. (2017). Regulatory roles of glutathione-S-transferases and 4-hydroxynonenal in stress-mediated signaling and toxicity. *Free Radic. Biol. Med.* 111, 235–243. doi:10.1016/j.freeradbiomed.2016.10.493

Azzam, E. I., Jay-Gerin, J. P., and Pain, D. (2012). Ionizing radiation-induced metabolic oxidative stress and prolonged cell injury. *Cancer Lett.* 327 (1-2), 48–60. doi:10.1016/j.canlet.2011.12.012

Bader, S., Wilmers, J., Pelzer, M., Jendrossek, V., and Rudner, J. (2021). Activation of anti-oxidant Keap1/Nrf2 pathway modulates efficacy of dihydroartemisinin-based monotherapy and combinatory therapy with ionizing radiation. *Free Radic. Biol. Med.* 168, 44–54. doi:10.1016/j.freeradbiomed.2021.03.024

Bănescu, C., Trifa, A. P., Voidazan, S., Moldovan, V. G., Macarie, I., Benedek Lazar, E., et al. (2014). CAT, GPX1, MnSOD, GSTM1, GSTT1, and GSTP1 genetic polymorphisms in chronic myeloid leukemia: A case-control study. *Oxid. Med. Cell. Longev.* 2014, 875861. doi:10.1155/2014/875861

Bartolini, D., Commodi, J., PiroddiM.Incipini, L., Sancineto, L., Santi, C., et al. (2015). Glutathione S-transferase pi expression regulates the Nrf2-dependent response to hormetic diselenides. *Free Radic. Biol. Med.* 88, 466–480. doi:10.1016/j.freeradbiomed.2015.06.039

Baskar, R., Lee, K. A., Yeo, R., and Yeoh, K. W. (2012). Cancer and radiation therapy: Current advances and future directions. *Int. J. Med. Sci.* 9 (3), 193–199. doi:10.7150/ijms.3635

Booth, J., Boyland, E., and Sims, P. (1961). An enzyme from rat liver catalysing conjugations with glutathione. *Biochem. J.* 79 (3), 516–524. doi:10.1042/bj0790516

Buckley, A. M., Lynam-Lennon, N., O'Neill, H., and O'Sullivan, J. (2020). Targeting hallmarks of cancer to enhance radiosensitivity in gastrointestinal cancers. *Nat. Rev. Gastroenterol. Hepatol.* 17 (5), 298–313. doi:10.1038/s41575-019-0247-2

Busato, F., Khouzai, B. E., and Mognato, M. (2022). Biological mechanisms to reduce radioresistance and increase the efficacy of radiotherapy: State of the art. *Int. J. Mol. Sci.* 23 (18), 10211. doi:10.3390/ijms231810211

Carvalho, A. N., S-Glutathionylation of Keap1Guedes, R. C., Castro-Caldas, M., Rodrigues, E., van Horssen, J., et al. (2016). S-glutathionylation of Keap1: A new role for glutathione S-transferase pi in neuronal protection. *FEBS Lett.* 590 (10), 1455–1466. doi:10.1002/1873-3468.12177

Chandra, R. A., Keane, F. K., Voncken, F. E. M., and Thomas, C. R., Jr (2021). Contemporary radiotherapy: Present and future. *Lancet* 398 (10295), 171–184. doi:10.1016/S0140-6736(21)00233-6

Chatterjee, A., and Gupta, S. (2018). The multifaceted role of glutathione S-transferases in cancer. *Cancer Lett.* 433, 33–42. doi:10.1016/j.canlet.2018.06.028

Cobler, L., Zhang, H., Suri, P., Park, C., and Timmerman, L. A. (2018). xCT inhibition sensitizes tumors to γ-radiation via glutathione reduction. *Oncotarget* 9 (64), 32280–32297. doi:10.18632/oncotarget.25794

Conrad, M., and Proneth, B. (2019). Broken hearts: Iron overload, ferroptosis and cardiomyopathy. *Cell Res.* 29 (4), 263–264. doi:10.1038/s41422-019-0150-y

Cowell, I. G., Dixon, K. H., Pemble, S. E., Ketterer, B., and Taylor, J. B. (1988). The structure of the human glutathione S-transferase pi gene. *Biochem. J.* 255 (1), 79–83. doi:10.1042/bj2550079

Cui, J., Li, G., Yin, J., Li, L., Tan, Y., Wei, H., et al. (2020). GSTP1 and cancer: Expression, methylation, polymorphisms and signaling (Review). *Int. J. Oncol.* 56 (4), 867–878. doi:10.3892/ijo.2020.4979

Dixon, S. J., Lemberg, K. M., Lamprecht, M. R., Skouta, R., Zaitsev, E. M., Gleason, C. E., et al. (2012). Ferroptosis: An iron-dependent form of nonapoptotic cell death. *Cell* 149 (5), 1060–1072. doi:10.1016/j.cell.2012.03.042

Doll, S., Proneth, B., Tyurina, Y. Y., Panzilius, E., Kobayashi, S., Ingold, I., et al. (2017). ACSL4 dictates ferroptosis sensitivity by shaping cellular lipid composition. *Nat. Chem. Biol.* 13 (1), 91–98. doi:10.1038/nchembio.2239

Dong, H., Xia, Y., Jin, S., Xue, C., Wang, Y., Hu, R., et al. (2021). Nrf2 attenuates ferroptosis-mediated IIR-ALI by modulating TERT and SLC7A11. *Cell Death Dis.* 12 (11), 1027. doi:10.1038/s41419-021-04307-1

Duvoix, A., Schnekenburger, M., Delhalle, S., Blasius, R., Borde-Chiche, P., Morceau, F., et al. (2004). Expression of glutathione S-transferase P1-1 in leukemic cells is regulated by inducible AP-1 binding. *Cancer Lett.* 216 (2), 207–219. doi:10.1016/j.canlet.2004.05.004

Fang, Y., Ye, J., Zhao, B., Sun, J., Gu, N., Chen, X., et al. (2020). Formononetin ameliorates oxaliplatin-induced peripheral neuropathy via the KEAP1-NRF2-GSTP1 axis. *Redox Biol.* 36, 101677. doi:10.1016/j.redox.2020.101677

FeiFei, W., HongHai, X., YongRong, Y., PingXiang, W., JianHua, W., XiaoHui, Z., et al. (2019). FBX8 degrades GSTP1 through ubiquitination to suppress colorectal cancer progression. *Cell Death Dis.* 10 (5), 351. doi:10.1038/s41419-019-1588-z

Feng, H., and Stockwell, B. R. (2018). Unsolved mysteries: How does lipid peroxidation cause ferroptosis? *PLoS Biol.* 16 (5), e2006203. doi:10.1371/journal.pbio.2006203

Feng, L., Zhao, K., Sun, L., Yin, X., Zhang, J., Liu, C., et al. (2021). SLC7A11 regulated by NRF2 modulates esophageal squamous cell carcinoma radiosensitivity by inhibiting ferroptosis. *J. Transl. Med.* 19 (1), 367. doi:10.1186/s12967-021-03042-7

Friedmann Angeli, J. P., Schneider, M., Proneth, B., Tyurina, Y. Y., Tyurin, V. A., Hammond, V. J., et al. (2014). Inactivation of the ferroptosis regulator Gpx4 triggers acute renal failure in mice. *Nat. Cell Biol.* 16 (12), 1180–1191. doi:10.1038/ncb3064

Fujikawa, Y., Nampo, T., Mori, M., Kikkawa, M., and Inoue, H. (2018). Fluorescein diacetate (FDA) and its analogue as substrates for Pi-class glutathione S-transferase (GSTP1) and their biological application. *Talanta* 179, 845–852. doi:10.1016/j.talanta.2017.12.010

Gao, Y., Chen, B., Wang, R., Xu, A., Wu, L., Lu, H., et al. (2022). Knockdown of RRM1 in tumor cells promotes radio-/chemotherapy induced ferroptosis by regulating p53 ubiquitination and p21-GPX4 signaling axis. *Cell Death Discov.* 8 (1), 343. doi:10.1038/s41420-022-01140-z

Hanahan, D., and Weinberg, R. A. (2011). Hallmarks of cancer: The next generation. *Cell* 144 (5), 646–674. doi:10.1016/j.cell.2011.02.013

Hayes, J. D., and Pulford, D. J. (1995). The glutathione S-transferase supergene family: Regulation of GST and the contribution of the isoenzymes to cancer chemoprotection and drug resistance. *Crit. Rev. Biochem. Mol. Biol.* 30 (6), 445–600. doi:10.3109/10409239509083491

Holley, S. L., Fryer, A. A., Haycock, J. W., Grubb, S. E. W., Strange, R. C., and Hoban, P. R. (2007). Differential effects of glutathione S-transferase pi (GSTP1) haplotypes on cell proliferation and apoptosis. *Carcinogenesis* 28 (11), 2268–2273. doi:10.1093/carcin/bgm135

Ikeda, H., Serria, M. S., Kakizaki, I., Hatayama, I., Satoh, K., Tsuchida, S., et al. (2002). Activation of mouse Pi-class glutathione S-transferase gene by Nrf2(NF-E2-related factor 2) and androgen. *Biochem. J.* 364 (2), 563–570. doi:10.1042/BJ20011756

Ivanov, S. D., Semenov, A. L., Kovan'ko, E. G., and Yamshanov, V. A. (2015). Effects of iron ions and iron chelation on the efficiency of experimental radiotherapy of animals with gliomas. *Bull. Exp. Biol. Med.* 158 (6), 800–803. doi:10.1007/s10517-015-2865-1

Ivanov, S. D., Semenov, A. L., Mikhelson, V. M., Kovan'ko, E. G., and Iamshanov, V. A. (2013). Effects of iron ion additional introduction in radiation therapy of tumor-bearing animals. *Radiats. Biol. Radioecol.* 53 (3), 296–303. doi:10.7868/s0869803113030065

Jeong, Y., Hoang, N. T., Lovejoy, A., Stehr, H., Newman, A. M., Gentles, A. J., et al. (2017). Role of KEAP1/NRF2 and TP53 mutations in lung squamous cell carcinoma development and radiation resistance. *Cancer Discov.* 7 (1), 86–101. doi:10.1158/2159-8290.CD-16-0127

Jiang, X., Stockwell, B. R., and Conrad, M. (2021). Ferroptosis: Mechanisms, biology and role in disease. *Nat. Rev. Mol. Cell Biol.* 22 (4), 266–282. doi:10.1038/s41580-020-00324-8

Kogawa, T., Sato, Y., Shimoyama, R., Kurata, W., Tashiro, Y., and Niitsu, Y. (2021). Chemoprevention of pancreatic cancer by inhibition of glutathione-S transferase P1. *Invest. New Drugs* 39 (6), 1484–1492. doi:10.1007/s10637-021-01129-y

Koppula, P., Lei, G., Zhang, Y., Yan, Y., Mao, C., Kondiparthi, L., et al. (2022). A targetable CoQ-FSP1 axis drives ferroptosis- and radiation-resistance in KEAP1 inactive lung cancers. *Nat. Commun.* 13 (1), 2206. doi:10.1038/s41467-022-29905-1

Lang, X., Green, M. D., Wang, W., Yu, J., Choi, J. E., Jiang, L., et al. (2019). Radiotherapy and immunotherapy promote tumoral lipid oxidation and ferroptosis via synergistic repression of SLC7A11. *Cancer Discov.* 9 (12), 1673–1685. doi:10.1158/2159-8290.CD-19-0338

Lee, J., You, J. H., and Roh, J. L. (2022). Poly(rC)-binding protein 1 represses ferritinophagy-mediated ferroptosis in head and neck cancer. *Redox Biol.* 51, 102276. doi:10.1016/j.redox.2022.102276

Lei, G., Mao, C., Yan, Y., Zhuang, L., and Gan, B. (2021). Ferroptosis, radiotherapy, and combination therapeutic strategies. *Protein Cell* 12 (11), 836–857. doi:10.1007/s13238-021-00841-y

Lei, G., Zhang, Y., Koppula, P., Liu, X., Zhang, J., Lin, S. H., et al. (2020). The role of ferroptosis in ionizing radiation-induced cell death and tumor suppression. *Cell Res.* 30 (2), 146–162. doi:10.1038/s41422-019-0263-3

Lei, K., Gu, X., Alvarado, A. G., Du, Y., Luo, S., Ahn, E. H., et al. (2020). Discovery of a dual inhibitor of NQO1 and GSTP1 for treating glioblastoma. *J. Hematol. Oncol.* 13 (1), 141. doi:10.1186/s13045-020-00979-y

Lei, X., Du, L., Yu, W., Wang, Y., Ma, N., and Qu, B. (2021). GSTP1 as a novel target in radiation induced lung injury. *J. Transl. Med.* 19 (1), 297. doi:10.1186/s12967-021-02978-0

Li, J., Cao, F., Yin, H. L., Huang, Z. J., Lin, Z. T., Mao, N., et al. (2020). Ferroptosis: Past, present and future. *Cell Death Dis.* 11 (2), 88. doi:10.1038/s41419-020-2298-2

Liu, J., Huang, C., Liu, J., Meng, C., Gu, Q., Du, X., et al. (2022). Nrf2 and its dependent autophagy activation cooperatively counteract ferroptosis to alleviate acute liver injury. *Pharmacol. Res.* 187, 106563. doi:10.1016/j.phrs.2022.106563

Liu, W., Zhou, Y., Duan, W., Song, J., Wei, S., Xia, S., et al. (2021). Glutathione peroxidase 4-dependent glutathione high-consumption drives acquired platinum chemoresistance in lung cancer-derived brain metastasis. *Clin. Transl. Med.* 11 (9), e517. doi:10.1002/ctm2.517

Luo, M., Yan, J., Hu, X., Li, H., Li, H., Liu, Q., et al. (2022). Targeting lipid metabolism for ferroptotic cancer therapy. *Apoptosis.* doi:10.1007/s10495-022-01795-0

Masaldan, S., Clatworthy, S. A. S., Gamell, C., Meggyesy, P. M., Rigopoulos, A. T., Haupt, S., et al. (2018). Iron accumulation in senescent cells is coupled with impaired ferritinophagy and inhibition of ferroptosis. *Redox Biol.* 14, 100–115. doi:10.1016/j.redox.2017.08.015

Mian, O. Y., Khattab, M. H., Hedayati, M., Coulter, J., Abubaker-Sharif, B., Schwaninger, J. M., et al. (2016). GSTP1 Loss results in accumulation of oxidative DNA base damage and promotes prostate cancer cell survival following exposure to protracted oxidative stress. *Prostate* 76 (2), 199–206. doi:10.1002/pros.23111

Morceau, F., Duvoix, A., Delhalle, S., Schnekenburger, M., Dicato, M., and Diederich, M. (2004). Regulation of glutathione S-transferase P1-1 gene expression by NF-kappaB in tumor necrosis factor alpha-treated K562 leukemia cells. *Biochem. Pharmacol.* 67 (7), 1227–1238. doi:10.1016/j.bcp.2003.10.036

Mukha, A., Kahya, U., Linge, A., Chen, O., Lock, S., Lukiyanchuk, V., et al. (2021). GLS-driven glutamine catabolism contributes to prostate cancer radiosensitivity by regulating the redox state, stemness and ATG5-mediated autophagy. *Theranostics* 11 (16), 7844–7868. doi:10.7150/thno.58655

Pajaud, J., Ribault, C., Ben Mosbah, I., RauCh, C., Henderson, C., Bellaud, P., et al. (2015). Glutathione transferases P1/P2 regulate the timing of signaling pathway activations and cell cycle progression during mouse liver regeneration. *Cell Death Dis.* 6 (1), e1598. doi:10.1038/cddis.2014.562

Pan, X., Lin, Z., Jiang, D., Yu, Y., Yang, D., Zhou, H., et al. (2019). Erastin decreases radioresistance of NSCLC cells partially by inducing GPX4-mediated ferroptosis. *Oncol. Lett.* 17 (3), 3001–3008. doi:10.3892/ol.2019.9888

Peng, J., Pan, J., Mo, J., and Peng, Y. (2022). MPO/HOCl facilitates apoptosis and ferroptosis in the SOD1(g93a) motor neuron of amyotrophic lateral sclerosis. *Oxid. Med. Cell. Longev.* 2022, 8217663. doi:10.1155/2022/8217663

Pljesa-Ercegovac, M., Savic-Radojevic, A., Dragicevic, D., Mimic-Oka, J., Matic, M., Sasic, T., et al. (2011). Enhanced GSTP1 expression in transitional cell carcinoma of urinary bladder is associated with altered apoptotic pathways. *Urol. Oncol.* 29 (1), 70–77. doi:10.1016/j.urolonc.2008.10.019

Pouget, J. P., Georgakilas, A. G., and Ravanat, J. L. (2018). Targeted and off-target (bystander and abscopal) effects of radiation therapy: Redox mechanisms and risk/benefit analysis. *Antioxid. Redox Signal.* 29 (15), 1447–1487. doi:10.1089/ars.2017.7267

Raghav, K. P., Gonzalez-Angulo, A. M., and Blumenschein, G. R., Jr. (2012). Role of HGF/MET axis in resistance of lung cancer to contemporary management. *Transl. Lung Cancer Res.* 1 (3), 179–193. doi:10.3978/j.issn.2218-6751.2012.09.04

Re, A., Aiello, A., Nanni, S., Grasselli, A., BenVenuti, V., Pantisano, V., et al. (2011). Silencing of GSTP1, a prostate cancer prognostic gene, by the estrogen receptor-β and endothelial nitric oxide synthase complex. *Mol. Endocrinol.* 25 (12), 2003–2016. doi:10.1210/me.2011-1024

Rehman, M. U., Rashid, S., Arafah, A., Qamar, W., Alsaffar, R. M., Ahmad, A., et al. (2020). Piperine regulates nrf-2/keap-1 signalling and exhibits anticancer effect in experimental colon carcinogenesis in wistar rats. *Biol. (Basel)* 9 (9), 302. doi:10.3390/biology9090302

Ritchie, K. J., Henderson, C. J., Wang, X. J., Vassieva, O., Carrie, D., Farmer, P. B., et al. (2007). Glutathione transferase pi plays a critical role in the development of lung carcinogenesis following exposure to tobacco-related carcinogens and urethane. *Cancer Res.* 67 (19), 9248–9257. doi:10.1158/0008-5472.CAN-07-1764

Santivasi, W. L., and Xia, F. (2014). Ionizing radiation-induced DNA damage, response, and repair. *Antioxid. Redox Signal.* 21 (2), 251–259. doi:10.1089/ars.2013.5668

Savic-Radojevic, A., Mimic-Oka, J., Pljesa-Ercegovac, M., Opacic, M., Dragicevic, D., Kravic, T., et al. (2007). Glutathione S-transferase-P1 expression correlates with increased antioxidant capacity in transitional cell carcinoma of the urinary bladder. *Eur. Urol.* 52 (2), 470–477. doi:10.1016/j.eururo.2007.01.046

Shah, Y. M., Matsubara, T., Ito, S., Yim, S. H., and Gonzalez, F. J. (2009). Intestinal hypoxia-inducible transcription factors are essential for iron absorption following iron deficiency. *Cell Metab.* 9 (2), 152–164. doi:10.1016/j.cmet.2008.12.012

Shibata, Y., Yasui, H., Higashikawa, K., Miyamoto, N., and Kuge, Y. (2019). Erastin, a ferroptosis-inducing agent, sensitized cancer cells to X-ray irradiation via glutathione starvation *in vitro* and *in vivo*. *PLoS One* 14 (12), e0225931. doi:10.1371/journal.pone.0225931

Shintoku, R., Takigawa, Y., Yamada, K., Kubota, C., Yoshimoto, Y., Takeuchi, T., et al. (2017). Lipoxygenase-mediated generation of lipid peroxides enhances ferroptosis induced by erastin and RSL3. *Cancer Sci.* 108 (11), 2187–2194. doi:10.1111/cas.13380

Simic, T., Savic-Radojevic, A., Pljesa-Ercegovac, M., Matic, M., and Mimic-Oka, J. (2009). Glutathione S-transferases in kidney and urinary bladder tumors. *Nat. Rev. Urol.* 6 (5), 281–289. doi:10.1038/nrurol.2009.49

Singhal, R., Mitta, S. R., Das, N. K., Kerk, S. A., Sajjakulnukit, P., Solanki, S., et al. (2021). HIF-2α activation potentiates oxidative cell death in colorectal cancers by increasing cellular iron. *J. Clin. Invest.* 131 (12), e143691. doi:10.1172/JCI143691

Sitthideatphaiboon, P., Galan-Cobo, A., Negrao, M. V., Qu, X., Poteete, A., Zhang, F., et al. (2021). STK11/LKB1 mutations in NSCLC are associated with KEAP1/NRF2-dependent radiotherapy resistance targetable by glutaminase inhibition. *Clin. Cancer Res.* 27 (6), 1720–1733. doi:10.1158/1078-0432.CCR-20-2859

Smith, T. A., Kirkpatrick, D. R., Smith, S., Smith, T. K., Pearson, T., Kailasam, A., et al. (2017). Radioprotective agents to prevent cellular damage due to ionizing radiation. *J. Transl. Med.* 15 (1), 232. doi:10.1186/s12967-017-1338-x

Stockwell, B. R. (2022). Ferroptosis turns 10: Emerging mechanisms, physiological functions, and therapeutic applications. *Cell* 185 (14), 2401–2421. doi:10.1016/j.cell.2022.06.003

Stockwell, B. R., Friedmann Angeli, J. P., Bayir, H., Bush, A. I., Conrad, M., Dixon, S. J., et al. (2017). Ferroptosis: A regulated cell death nexus linking metabolism, redox biology, and disease. *Cell* 171 (2), 273–285. doi:10.1016/j.cell.2017.09.021

Stockwell, B. R., Jiang, X., and Gu, W. (2020). Emerging mechanisms and disease relevance of ferroptosis. *Trends Cell Biol.* 30 (6), 478–490. doi:10.1016/j.tcb.2020.02.009

Sukiennicki, G. M., Marciniak, W., Muszynska, M., Baszuk, P., Gupta, S., Bialkowska, K., et al. (2019). Iron levels, genes involved in iron metabolism and antioxidative processes and lung cancer incidence. *PLoS One* 14 (1), e0208610. doi:10.1371/journal.pone.0208610

Sung, H., Ferlay, J., Siegel, R. L., Laversanne, M., Soerjomataram, I., Jemal, A., et al. (2021). Global cancer statistics 2020: GLOBOCAN estimates of incidence and mortality worldwide for 36 cancers in 185 countries. *CA. Cancer J. Clin.* 71 (3), 209–249. doi:10.3322/caac.21660

Takashi, Y., Tomita, K., Kuwahara, Y., Roudkenar, M. H., Roushandeh, A. M., Igarashi, K., et al. (2020). Mitochondrial dysfunction promotes aquaporin expression that controls hydrogen peroxide permeability and ferroptosis. *Free Radic. Biol. Med.* 161, 60–70. doi:10.1016/j.freeradbiomed.2020.09.027

Tang, L. J., Zhou, Y. J., Xiong, X. M., Li, N. S., Zhang, J. J., Luo, X. J., et al. (2021). Ubiquitin-specific protease 7 promotes ferroptosis via activation of the p53/TfR1 pathway in the rat hearts after ischemia/reperfusion. *Free Radic. Biol. Med.* 162, 339–352. doi:10.1016/j.freeradbiomed.2020.10.307

Tang, Z., Jiang, W., Mao, M., Zhao, J., Chen, J., and Cheng, N. (2021). Deubiquitinase USP35 modulates ferroptosis in lung cancer via targeting ferroportin. *Clin. Transl. Med.* 11 (4), e390. doi:10.1002/ctm2.390

Tesfay, L., Paul, B. T., Konstorum, A., Deng, Z., Cox, A. O., Lee, J., et al. (2019). Stearoyl-CoA desaturase 1 protects ovarian cancer cells from ferroptotic cell death. *Cancer Res.* 79 (20), 5355–5366. doi:10.1158/0008-5472.CAN-19-0369

Tew, K. D., Manevich, Y., Grek, C., Xiong, Y., Uys, J., and Townsend, D. M. (2011). The role of glutathione S-transferase P in signaling pathways and S-glutathionylation in cancer. *Free Radic. Biol. Med.* 51 (2), 299–313. doi:10.1016/j.freeradbiomed.2011.04.013

Thermozier, S., Hou, W., Zhang, X., Shields, D., Fisher, R., Bayir, H., et al. (2020). Anti-ferroptosis drug enhances total-body irradiation mitigation by drugs that block apoptosis and necroptosis. *Radiat. Res.* 193 (5), 435–450. doi:10.1667/RR15486.1

Tomita, K., Fukumoto, M., Itoh, K., Kuwahara, Y., Igarashi, K., Nagasawa, T., et al. (2019). MiR-7-5p is a key factor that controls radioresistance via intracellular Fe(2+) content in clinically relevant radioresistant cells. *Biochem. Biophys. Res. Commun.* 518 (4), 712–718. doi:10.1016/j.bbrc.2019.08.117

Umamaheswari, S., Priyadarshinee, S., Kadirvelu, K., and Ramesh, M. (2021). Polystyrene microplastics induce apoptosis via ROS-mediated p53 signaling pathway in zebrafish. *Chem. Biol. Interact.* 345, 109550. doi:10.1016/j.cbi.2021.109550

van de Wetering, C., Elko, E., Berg, M., Schiffers, C. H. J., Stylianidis, V., van den Berge, M., et al. (2021). Glutathione S-transferases and their implications in the lung diseases asthma and chronic obstructive pulmonary disease: Early life susceptibility? *Redox Biol.* 43, 101995. doi:10.1016/j.redox.2021.101995

Ward, H. A., Whitman, J., Muller, D. C., Johansson, M., Jakszyn, P., Weiderpass, E., et al. (2019). Haem iron intake and risk of lung cancer in the European Prospective Investigation into Cancer and Nutrition (EPIC) cohort. *Eur. J. Clin. Nutr.* 73 (8), 1122–1132. doi:10.1038/s41430-018-0271-2

Wu, M., Ling, W., Wei, J., Liao, R., Sun, H., Li, D., et al. (2022). Biomimetic photosensitizer nanocrystals trigger enhanced ferroptosis for improving cancer treatment. *J. Control. Release* 352, 1116–1133. doi:10.1016/j.jconrel.2022.11.026

Yang, M., Wu, D., Sun, H., Wang, L. K., and Chen, X. F. (2022). A metabolic plasticity-based signature for molecular classification and prognosis of lower-grade glioma. *Brain Sci.* 76 (5), 1138–1150. doi:10.3390/brainsci12091138

Yang, W. S., Kim, K. J., Gaschler, M. M., Patel, M., Shchepinov, M. S., and Stockwell, B. R. (2016). Peroxidation of polyunsaturated fatty acids by lipoxygenases drives ferroptosis. *Proc. Natl. Acad. Sci. U. S. A.* 113 (34), E4966–E4975. doi:10.1073/pnas.1603244113

Ye, L. F., Chaudhary, K. R., Zandkarimi, F., Harken, A. D., Kinslow, C. J., Upadhyayula, P. S., et al. (2020). Radiation-induced lipid peroxidation triggers ferroptosis and synergizes with ferroptosis inducers. *ACS Chem. Biol.* 15 (2), 469–484. doi:10.1021/acschembio.9b00939

Zhang, W., Sun, Y., Bai, L., Zhi, L., Yang, Y., Zhao, Q., et al. (2021). RBMS1 regulates lung cancer ferroptosis through translational control of SLC7A11. *J. Clin. Invest.* 131 (22), e152067. doi:10.1172/JCI152067

Zhang, Z., Lu, M., Chen, C., Tong, X., Li, Y., Yang, K., et al. (2021). Holo-lactoferrin: The link between ferroptosis and radiotherapy in triple-negative breast cancer. *Theranostics* 11 (7), 3167–3182. doi:10.7150/thno.52028

Zhao, Y., Lu, J., Mao, A., Zhang, R., and Guan, S. (2021). Autophagy inhibition plays a protective role in ferroptosis induced by alcohol via the p62-keap1-nrf2 pathway. *J. Agric. Food Chem.* 69 (33), 9671–9683. doi:10.1021/acs.jafc.1c03751

Zheng, J., and Conrad, M. (2020). The metabolic underpinnings of ferroptosis. *Cell Metab.* 32 (6), 920–937. doi:10.1016/j.cmet.2020.10.011

Zhou, H., Zhou, Y. L., Mao, J. A., Tang, L. F., Xu, J., Wang, Z. X., et al. (2022). NCOA4-mediated ferritinophagy is involved in ionizing radiation-induced ferroptosis of intestinal epithelial cells. *Redox Biol.* 55, 102413. doi:10.1016/j.redox.2022.102413

Zou, Y., Henry, W. S., Ricq, E. L., Graham, E. T., Phadnis, V. V., Maretich, P., et al. (2020). Plasticity of ether lipids promotes ferroptosis susceptibility and evasion. *Nature* 585 (7826), 603–608. doi:10.1038/s41586-020-2732-8

frontiers | Frontiers in Molecular Biosciences

TYPE Original Research
PUBLISHED 13 January 2023
DOI 10.3389/fmolb.2023.1075704

OPEN ACCESS

EDITED BY
Yanqing Liu,
Columbia University, United States

REVIEWED BY
Anna Lewinska,
University of Rzeszow, Poland
Yanan Ma,
Memorial Sloan Kettering Cancer Center, United States
Yunting Wang,
University of Houston, United States

*CORRESPONDENCE
Sergey Nikulin,
snikulin@hse.ru

SPECIALTY SECTION
This article was submitted to Molecular Diagnostics and Therapeutics, a section of the journal Frontiers in Molecular Biosciences

RECEIVED 20 October 2022
ACCEPTED 03 January 2023
PUBLISHED 13 January 2023

CITATION
Nikulin S, Razumovskaya A, Poloznikov A, Zakharova G, Alekseev B and Tonevitsky A (2023), *ELOVL5* and *IGFBP6* genes modulate sensitivity of breast cancer cells to ferroptosis.
Front. Mol. Biosci. 10:1075704.
doi: 10.3389/fmolb.2023.1075704

ELOVL5 and *IGFBP6* genes modulate sensitivity of breast cancer cells to ferroptosis

Sergey Nikulin[1]*, Alexandra Razumovskaya[1], Andrey Poloznikov[2], Galina Zakharova[3], Boris Alekseev[2] and Alexander Tonevitsky[1,4]

[1]Faculty of Biology and Biotechnologies, Higher School of Economics, Moscow, Russia, [2]P. A. Hertsen Moscow Oncology Research Center, Branch of the National Medical Research Radiological Center, Ministry of Health of the Russian Federation, Moscow, Russia, [3]World-Class Research Center "Digital Biodesign and Personalized Healthcare", Sechenov First Moscow State Medical University, Moscow, Russia, [4]Shemyakin-Ovchinnikov Institute of Bioorganic Chemistry, Russian Academy of Sciences, Moscow, Russia

Introduction: Relapse of breast cancer is one of the key obstacles to successful treatment. Previously we have shown that low expression of *ELOVL5* and *IGFBP6* genes in breast cancer tissue corresponded to poor prognosis. *ELOVL5* participates directly in the elongation of polyunsaturated fatty acids (PUFAs) that are considered to play an important role in cancer cell metabolism. Thus, in this work we studied the changes in lipid metabolism in breast cancer cells with reduced expression of either *ELOVL5* or *IGFBP6* gene.

Methods: MDA-MB-231 cells with a stable knockdown of either *ELOVL5* or *IGFBP6* gene were used in this study. Transcriptomic and proteomic analysis as well as RT-PCR were utilized to assess gene expression. Content of individual fatty acids in the cells was measured with HPLC-MS. HPLC was used for analysis of the kinetics of PUFAs uptake. Cell viability was measured with MTS assay. Flow cytometry was used to measure activation of apoptosis. Fluorescent microscopy was utilized to assess accumulation of ROS and formation of lipid droplets. Glutathione peroxidase activity was measured with a colorimetric assay.

Results: We found that the knockdown of *IGFBP6* gene led to significant changes in the profile of fatty acids in the cells and in the expression of many genes associated with lipid metabolism. As some PUFAs are known to inhibit proliferation and cause death of cancer cells, we also tested the response of the cells to single PUFAs and to combinations of docosahexaenoic acid (DHA, a n-3 PUFA) with standard chemotherapeutic drugs. Our data suggest that external PUFAs cause cell death by activation of ferroptosis, an iron-dependent mechanism of cell death with excessive lipid peroxidation. Moreover, both knockdowns increased cells' sensitivity to ferroptosis, probably due to a significant decrease in the activity of the antioxidant enzyme GPX4. Addition of DHA to commonly used chemotherapeutic drugs enhanced their effect significantly, especially for the cells with low expression of *IGFBP6* gene.

Discussion: The results of this study suggest that addition of PUFAs to the treatment regimen for the patients with low expression of *IGFBP6* and *ELOVL5* genes can be potentially beneficial and is worth testing in a clinically relevant setting.

KEYWORDS

breast cancer, *ELOVL5*, *IGFBP6*, PUFA, ferroptosis

1 Introduction

Breast cancer (BC) continues to remain the leading cause of morbidity and mortality of women from malignant neoplasms in the world (Sung et al., 2021). Recurrence of BC happens in around 40% of the patients (Gerber et al., 2010; Lafourcade et al., 2018). One of the promising treatment strategies relies on identifying patients with high risk of recurrence with the help of gene-expression signatures in the early stages of the disease and intensifying treatment regimen for them (Kwa et al., 2017). Previously, our group reported a new method for predicting outcomes based on prognostic markers, in which the expression levels of two genes: Insulin Like Growth Factor Binding Protein 6 (*IGFBP6*) and Elongation Of Very Long chain fatty acids protein 5 (*ELOVL5*) made it possible to predict breast cancer recurrence in the first 5 years of follow-up with high sensitivity (81.8%) and specificity (62.5%), while high expression of *ELOVL5* and *IGFBP6* corresponded to a favorable prognosis (Galatenko et al., 2015).

ELOVL5 is a human elongase of long-chain polyunsaturated fatty acids (LC-PUFAs) located in the endoplasmic reticulum membrane (Leonard et al., 2000; Wang et al., 2008; Moon et al., 2009). It is known that n-3 and n-6 polyunsaturated fatty acids can affect the development of breast cancer, and in some cases they can cause death of breast cancer cells (Liput et al., 2021). Moreover, polyunsaturated fatty acids alter breast cancer cell adhesion and metastasis in n-6 and n-3 PUFA-treated nude mice and affect mRNA expression in breast cancer cells that encode metastasis-associated metalloproteinases (Johanning and Lin, 1995).

On the other hand, *IGFBP6* is a secreted protein that binds to insulin-like growth factors (*IGFs*), preventing their action on cells (Bach et al., 2013). Particular attention was paid to the study of the role of IGFBP6 in tumor metastasis. For example, it was shown that the expression level of IGFBP6 in colon cancer cells with a high metastatic potential is lower than in the cells with a low metastatic potential, and the expression of IGFBP6 in secondary squamous cell carcinomas of the head and neck is lower than in primary ones, which indirectly indicates that that IGFBP6 reduces the metastatic potential of tumor cells (Bach, 2015). Acting as a transcription factor, IGFBP6 is able to enter the nucleus through the NLS sequence and importin-α (Bach, 2016). In the nucleus, IGFBP6 binds to the EGR-1 gene promoter and stimulates its expression. Expression of EGR1 leads to inhibition of migration and invasion, as well as inhibition of proliferation and triggering of apoptosis.

IGFBP6 can also reduce cell viability through other IGF-independent mechanisms. In particular, it is known that IGFBP6 locks the Ku80 protein in the cytosol, preventing it from entering the nucleus, where it is involved in the repair of DNA double-strand breaks (Bach, 2016). In turn, the accumulation of DNA defects promotes apoptosis. Finally, a recent study identified a relationship between the GPR81 lactate receptor and the IGFBP6 protein, which is able to modulate lactate metabolism and oxidative stress in human MDA-MB-231 cells, thus influencing breast cancer growth (Longhitano et al., 2022).

Recently we have found that knockdown of either *ELOVL5* or *IGFBP6* in breast cancer cell line MDA-MB-231 led to a strong increase in the expression of the matrix metalloproteinase (MMP) *MMP1*, as well as to a change in the expression of a group of genes involved in the formation of intercellular contacts (Nikulin et al., 2021). Analysis of spheroid formation confirmed that intercellular adhesion decreased as a result of both *ELOVL5* and *IGFBP6* knockdowns, thus suggesting that malignant breast tumors with reduced expression of *ELOVL5* or *IGFBP6* gene may metastasize more actively due to more efficient tumor cell invasion (Nikulin et al., 2021).

In addition to the changes in cell adhesion, we also noted changes in the fatty acid metabolism pathway for both knockdown lines (Nikulin et al., 2021). *ELOVL5* is directly involved in LC-PUFAs' metabolism and changes in fatty acids composition were expected for cells with *ELOVL5* knockdown. However, to our surprise, the decrease in *IGFBP6* expression also altered PUFAs' profile (Nikulin et al., 2021).

It is well known that PUFAs can affect the behavior of cancer cells. In particular, n-3 and n-6 LC-PUFAs change gene expression profile in tumor cells in different ways (Hammamieh et al., 2007). A number of studies have also shown that introduction of n-3 LC-PUFAs into the culture medium inhibits proliferation, migration, and invasion of tumor cells (Chamras et al., 2002; Ding et al., 2013; Huang et al., 2017). Data on the effects of n-6 LC-PUFAs on cancer cells are contradictory. Different studies reported that inhibitory effects of n-6 LC-PUFAs on tumor cells are less pronounced than those of n-3 LC-PUFAs, absent altogether, and even found stimulating effects of n-6 LC-PUFAs on tumor cells (Connolly and Rose, 1993; Schley et al., 2005; Gonzalez-Reyes et al., 2017).

One of the effects of LC-PUFAs on cancer cells that can potentially be utilized for therapy is induction of ferroptotic cell death (Chen et al., 2021a; Dierge et al., 2021). Ferroptosis is an iron-dependent, non-apoptotic mode of cell death characterized by the accumulation of lipid-reactive oxygen species (ROS). Ferroptosis does not have the morphological features of typical necrosis, such as swelling of the cytoplasm and organelles, and rupture of the cell membrane, nor does it have the characteristics of traditional cellular apoptosis, such as cell shrinkage, chromatin condensation, formation of apoptotic bodies, and disintegration of the cytoskeleton. And unlike in autophagy, the formation of classical closed bilayer membrane structures (autophagic vacuoles) does not occur during ferroptosis (Li et al., 2020). Morphologically, ferroptosis is mainly manifested in the apparent contraction of mitochondria with increased membrane density and reduction or disappearance of mitochondrial cristae, which differs from other modes of cell death (Dixon et al., 2012).

PUFAs peroxidation in cell membrane leads to disruption of cell integrity. Long-term excessive accumulation of fatty acids from the environment medium triggers ferroptosis (Chen et al., 2021a; Dierge et al., 2021). Ferroptosis can also be induced by inhibition of antioxidants (GPx4) that normally prevent lipid peroxidation (Seibt et al., 2019). During lipid peroxidation free radicals predominantly attack PUFAs. This fact is explained by the greatest susceptibility of multiple double bonds to peroxidation. (Dierge et al., 2021).

In this study, we focused on the role of *ELOVL5* and *IGFBP6* genes in the metabolism of LC-PUFAs in breast cancer cells. We also assessed the influence of *ELOVL5* and *IGFBP6* gene knockdowns on ferroptosis induction and on cell response to excess of various LC-PUFAs. For this study we chose 2 shorter PUFAs (n-6 linoleic acid and n-3 α-linolenic acid) and 2 longer ones (n-6 arachidonic acid and n-3 docosahexaenoic acid) as their impact on breast cancer has been extensively studied previously in different setups (Banni, 1999; Bocca et al., 2008; Yee et al., 2010; Zhou et al., 2016; Geng et al., 2017; Huang et al., 2022). And finally, we tested how the knockdowns of *ELOVL5* and *IGFBP6* affect the cell response to standard of care (SOC) chemotherapeutics when they are combined with ferroptosis inducers.

2 Materials and methods

2.1 Cell culture

Stable knockdowns of *ELOVL5* and *IGFBP6* genes were performed using RNA interference (Schwankhaus et al., 2014; Nikulin et al., 2018; 2021; Maltseva et al., 2020). DNA oligonucleotides selected for the target sequences in the *ELOVL5* and *IGFBP6* genes were ligated into the pLVX shRNA1 lentiviral vector (Clontech Laboratories) according to the manufacturer's protocol. To obtain the control MDA-MB-231 cells, we used the same lentiviral vector pLVX shRNA1 containing shRNA to the *Photinus pyralis* firefly luciferase gene. Viral particles were obtained in the form of cell-free supernatants using transient transfection of HEK-293T cell line according to the previously described method (Weber et al., 2010; 2012). Supernatants were collected 24 h after transfection, filtered using .45 μm syringe filters and stored at −80°C. Then, $5{\cdot}10^4$ MDA-MB-231 cells were cultured in the wells of a 24-well culture plate in 0.5 mL of cell culture medium. After 24 h, 10 μL of the supernatant containing viral particles was added to the wells, and the plate was placed in a cell culture incubator for 24 h. Then the cell culture medium was changed and the cells were incubated for another 24 h. After that, the selection with 1 μg/mL puromycin (Gibco) was carried out for 2 weeks.

Cells were cultured in a complete culture medium consisting of DMEM 4.5 g/L glucose (Gibco) supplemented with 10% vol. fetal bovine serum (Gibco) and 1% vol. antibiotic-antimycotic solution (Gibco). The cells were incubated in a cell culture incubator at 37°C, 5% CO_2 (Sanyo). Subcultivation was performed every 2–3 days using trypsin-EDTA solution (PanEco). Cells were counted after trypan blue (Gibco) staining using Countess automated cell counter (Invitrogen) according to the manufacturer's protocol.

2.2 Analysis of transcriptomic and proteomic data

We analyzed further the transcriptomic data that we have previously published (Nikulin et al., 2021) and deposited it as GSE165854 dataset. GSE165854 contains Human Transcriptome Array 2.0 microarray (Affymetrix) data for MDA-MB-231 cells with shRNA mediated knockdown of either *ELOVL5* or *IGFBP6* genes and for control MDA-MB-231(LUC) cells. ANOVA with Benjamin-Hochberg correction for multiple comparisons were used to access statistical significance of the differences observed between these cell lines.

The following datasets (Supplementary Table S1) from GEO (Gene Expression Omnibus) were used for correlation analysis: GSE102484 (Cheng et al., 2017), GSE22220 (Camps et al., 2008), GSE3494 (Miller et al., 2005), GSE58644 (Miller et al., 2005), GSE6532 (Loi et al., 2008). We also used data obtained by the METABRIC consortium (Cerami et al., 2012; Curtis et al., 2012) and The Cancer Genome Atlas (TCGA) program (Weinstein et al., 2013).

TAC 4.0 software (Thermo Fisher Scientific) was applied to preprocess raw data from Affymetrix microarrays. To carry out correlation analysis and statistical data processing, we employed the R 4.1 programming language with the RStudio 1.4 integrated development environment. The values of the Pearson correlation coefficient R and the p-values (the significance of the difference of R from zero) were calculated using the "cor.test" function. Correction for multiple comparisons was performed with the Benjamini-Hochberg method. The correlation coefficients with p-values less than .05 were considered significant.

Proteomic data from PXD023892 dataset was analyzed as well. NanoHPLC-MS/MS system coupled with a Q Exactive Orbitrap mass spectrometer (Thermo Fisher Scientific) was utilized to measure expression of proteins in the cells. Student's t-test with Benjamin-Hochberg correction for multiple comparisons were used to access statistical significance of the observed changes. Detailed procedure was described earlier (Nikulin et al., 2021).

2.3 RT-PCR

Real-time PCR was used to confirm the changes in the expression of individual genes. RNA isolation was performed using miRNeasy Micro Kit (Qiagen) according to the manufacturer's protocol. RNA concentration was measured with NanoDrop ND-1000 spectrophotometer (Thermo Fisher Scientific). Reverse transcription of RNA was performed using the MMLV RT kit (Evrogen) according to the manufacturer's protocol. The obtained cDNA samples were stored at −20°C. qPCRmix-HS SYBR (Evrogen) was used for RT-PCR performed with DTprime detecting amplifier (DNA Technology).

The oligonucleotide primers used for RT-PCR were designed based on the mRNA sequences of the studied genes from the UCSC Genome Browser database (Kent et al., 2002). Primer selection was performed using Primer-BLAST software (Ye et al., 2012). The possibility of the formation of secondary structures (hairpins), homo- and heterodimers by the primers was assessed using OligoAnalyzer 3.1 software (Owczarzy et al., 2008). *EEF1A1* and *ACTB* were selected as reference genes (Maltseva et al., 2013). The sequences of the primers are presented in Supplementary Table S2. The evaluation of the differences in the expression of the selected genes was carried out using the software REST 2009 v.2.0.13 (Pfaffl et al., 2002; Vandesompele et al., 2002). For each group 3 independently obtained samples of RNA were used to assess expression levels of the selected genes.

2.4 Gene Ontology enrichment analysis

Analysis of the enriched biological processes among the genes with increased and decreased expression was carried out using Gene Ontology (GO) database (Ashburner et al., 2000; Gene and Consortium, 2019) and "topGO" package for R programming language. The results were obtained using "weight01″ algorithm, p-values were calculated using Fisher's exact test.

2.5 Analysis of cellular fatty acids composition

To analyze the composition of intracellular fatty acids, the cells were cultured in culture flasks with surface area of 25 cm^2 in 5 mL of complete nutrient medium for 48 h. Samples containing pellets of 1.5×10^6 million cells were prepared for HPLC-MS analysis following a protocol based on a previously published method (Valianpour et al., 2003). The experiment was carried out in two biological replicates.

2.6 Analysis of the kinetics of PUFAs uptake

To study the kinetics of absorption of LC-PUFAs by the cells from the nutrient medium, 2×10^5 cells were seeded into the wells of 24-well

culture plates in 500 µL of complete cell culture medium. The plates were then incubated in a cell culture incubator at 37°C, 5% CO_2 (Sanyo) for 24 h. After that, the nutrient medium was replaced with a medium containing 50 µM of one of the studied LC-PUFAs (linoleic acid: LA, α-linolenic acid: ALA, arachidonic acid: AA, and docosahexaenoic acid: DHA) and the plates were incubated in the cell culture incubator until the end of the experiment. Sampling of the nutrient medium for analysis of the concentration of LC-PUFAs was carried out after 2, 4, 9, 22 and 27 h The experiment was carried out in two biological replicates.

To analyze the content of free fatty acids in the selected samples, each of them was combined 1:1 with methanol, thoroughly mixed by vortexing, and incubated at room temperature for 5 min. Next, the samples were centrifuged at 13,000 g for 5 min and the supernatant was transferred into chromatographic vials for analysis.

The composition of fatty acids in the samples was analyzed by HPLC using an Infinity 1200 chromatograph (Agilent Technologies) with a UV detector. Separation of fatty acids was carried out on a ZORBAX Eclipse XDB-C18 reverse-phase chromatographic column (length 150 mm, inner diameter 4.6 mm, sorbent particle diameter 5 µm) (Agilent Technologies), in the gradient elution mode (Supplementary Table S3). Phase A was deionized water with 0.1% vol. formic acid and phase B was acetonitrile with 0.1% vol. formic acid. The flow rate of the mobile phase was constant and equal to 1.5 mL/min. Fatty acid chromatograms were recorded with the UV detector at 194 nm. Concentrations of the analyzed PUFAs in the samples were determined based on the external calibration curves (Supplememtary Figure S1).

2.7 GPx4 activity assay

GPx4 activity analysis was performed with the Colorimetric Glutathione Peroxidase Assay Kit (Abcam) according to the standard protocol. Cell suspensions of 2×10^6 were used for each test. GPx4 activity was assessed by measurement of the decrease in NADPH absorbance at 340 nm with X-mark plate reader (BioRad). One unit is defined as the amount of enzyme that will cause the oxidation of 1.0 µmol of NADPH to NADP+ under the assay kit condition per minute at 25°C.

2.8 ROS accumulation assay

The cells were seeded into 96-well plates (20,000 cells/well) and incubated overnight. After 24 h, PUFAs in different concentrations were added into the wells and the plates were incubated for 4 h. Next, the culture medium was removed from the wells, the cells were washed with DPBS, and solution of the dye-indicator of reactive oxygen species H2DCFDA (cell-permeant 2′,7′-dichlorodihydrofluorescein diacetate, final concentration 10 µM) was added, and the plates were incubated for 30 min. After 30 min, the dye was removed, the wells were washed with DPBS and fresh DPBS was added into each well. Then integral fluorescence signal (excitation at 485 nm, emission at 535 nm) was measured on the SpectraMax i3 Plate Reader (Molecular Devices). Photomicrographs of cells were obtained using an inverted fluorescent microscope Axio Observer Z1 (Carl Zeiss).

2.9 Lipid droplets formation assay

MDA-MB-231 cells were seeded in a 96-well plate ($15{\cdot}10^3$ cells per well), grown overnight and then cultured with 50 µM of various LC-PUFAs for 24 h.

For lipid droplets staining by Oil Red O, cells were washed twice with PBS, fixed with 10% formalin for 45 min, and then rinsed twice in water for 1 min, followed by 5 min in 60% isopropanol. The cells were stained with Oil Red O (1.8 mg/mL in 60% isopropanol) for 15 min and rinsed 5 times with ddH_2O to remove excess stain. Oil Red O stained cells were directly visualized and imaged using an inverted fluorescent microscope Axio Observer Z1 (Carl Zeiss). Quantification of lipid accumulation was achieved by Oil Red O extraction with 100% isopropanol and gentle agitation for 5 min at room temperature. Then the extracts were transferred to a new 96-well plate and absorbance was measured at 492 nm using X-mark plate reader (BioRad).

For lipid droplet staining with BODIPY, cells were washed twice with DPBS, fixed with 10% formalin for 45 min and then washed twice with DPBS for 1 min. Cells were incubated with 2 µM BOBIPY (Lumiprobe) in the dark at 37°C for 60 min and then washed 3 times with DPBS to remove excess dye. Cells stained with BOBIPY were visualized directly with an inverted fluorescent microscope Axio Observer Z1 (Carl Zeiss).

2.10 Cell viability assay

The viability of tumor cells in all cases was determined using the CellTiter 96® AQueous One Solution (Promega) according to the manufacturer's recommendations. Optical density was measured at 490 nm with X-mark plate reader (BioRad). All analyzed LC-PUFAs were dissolved in ethanol and all other small molecules were dissolved in DMSO.

For the experiments with 2D cultures, 1×10^4 MDA-MB-231 cells per well were seeded into 96-well plates and incubated (37°C, 5% CO2) for 24 h with a tested compound or a combination of compounds. Then the viability was measured. Working concentrations of Erastin and Ferrostatin-1 were choosen based on previously published data (2–80 µM for Erastin and 0.1–2 µM for Ferrostatin-1) (Dixon et al., 2014; Yu et al., 2019; Anthonymuthu et al., 2021; Li et al., 2021; Chen et al., 2022; Wang et al., 2022).

To generate spheroids, MDA-MB-231 cells were cultured in Matrigel Growth Factor Reduced (GFR) Basement Membrane Matrix (Corning) in 24-well plates for 48 h. Then the spheroids were diluted in Matrigel Growth Factor Reduced (GFR) Basement Membrane Matrix (Corning) and seeded into 96-well plate. After solidification of the gel, complete cell culture medium was added into each well.

After 24 h, the cell culture medium was replaced with the control medium or the medium containing single standard of care (SOC) drugs. Clinically relevant concentrations were used in the assay: 371.7 µM for 5-FU, 5.47 µM for Docetaxel, 6.73 µM for Doxorubicin, 89.3 µM for Gemcitabine, 1.75 µM for Methotrexate, and 811 nM for Vinorelbine (Liston and Davis, 2017). Then the cells were incubated for 3 h in cell culture incubator (37°C, 5% CO2), and the medium was replaced with fresh complete cell culture medium or the medium containing Erastin (1 µM) or DHA (100 µM). Then plates were incubated in cell culture incubator (37°C, 5% CO2) for 72 h, and

TABLE 1 Significantly changed ($p < 0.05$) Gene Ontology biological processes after knockdown of *IGFBP6* gene according to the transcriptomic analysis.

Up-regulated genes		Down-regulated genes	
GO ID	Description	GO ID	Description
GO:0046949	fatty-acyl-CoA biosynthetic process	GO:0046320	regulation of fatty acid oxidation
GO:0008654	phospholipid biosynthetic process	GO:0019216	regulation of lipid metabolic process
GO:0046479	glycosphingolipid catabolic process	GO:0046474	glycerophospholipid biosynthetic process
		GO:0010888	negative regulation of lipid storage
		GO:0045332	phospholipid translocation
		GO:0046839	phospholipid dephosphorylation

TABLE 2 Significantly changed ($p < 0.05$) Gene Ontology biological processes after knockdown of *IGFBP6* gene according to the proteomic analysis.

Up-regulated genes		Down-regulated genes	
GO ID	Description	GO ID	Description
GO:0008654	phospholipid biosynthetic process	GO:0006633	fatty acid biosynthetic process
		GO:0019217	regulation of fatty acid metabolic process
		GO:0071398	cellular response to fatty acid
		GO:0032365	intracellular lipid transport
		GO:0045017	glycerolipid biosynthetic process
		GO:0046890	regulation of lipid biosynthetic process
		GO:0019915	lipid storage

relative number of viable cells was measured. Growth rate of cancer cells was calculated as described previously (Hafner et al., 2016).

ANOVA with Tukey *post hoc* test has been used to assess statistical significance of the changes in viability or growth rate. The differences were considered statistically significant if *p*-values were less than 0.05.

2.11 Apoptosis assay

To study the activation of apoptosis Dead Cell Apoptosis Kit with Annexin V Alexa Fluor ™ 488 & Propidium Iodide (PI) (Thermo Fisher Scientific) was used according to the manufacturer's instructions. Cells were treated with different PUFAs then detached and analyzed as described earlier (Nikulin et al., 2021). Analysis of raw data was carried out using FlowJo 10.6.1 software. Chi-squared test with Bonferroni correction for multiple comparisons were used to access statistical significance of the changes in different populations.

3 Results

3.1 Knockdown of *IGFBP6* gene leads to multiple changes in lipid metabolism

As one gene from our prognostic pair, *ELOVL5*, is directly involved in the elongation of fatty acids, we reanalyzed our previously published transcriptomic (GSE165854) and proteomic (PXD023892) data for a more detailed view of the changes in the molecular pathways related to lipid metabolism Surprisingly, we found a number of biological processes associated with lipid metabolism that were significantly changed not only after knockdown of *ELOVL5*, but of *IGFBP6* as well (Table 1; Table 2). In addition, a lot of the genes involved in these processes changed their expression by at least 1.5 times (FDR $p < 0.05$) after the knockdown of *IGFBP6* gene (Supplementary Figures S2–S16).

Fatty acid biosynthesis was one of the altered biological processes. Elongation is the key step of this pathway (Figure 1A). In the first stage, the condensation reaction of acyl-CoA with malonyl-CoA catalyzed by ELOVL1-7 enzymes occurs, followed by three consecutive reactions catalyzed by enzymes 3-ketoacyl-CoA reductase (*HSD17B12* gene), 3-hydroxyacyl-CoA dehydratase (*HACD1-4* genes), and trans-2,3-enoyl-CoA reductase (*TECR* gene) (Moon and Horton, 2003; Leonard et al., 2004; Ikeda et al., 2008). Malonyl-CoA, necessary for the elongation of long fatty acids, is synthesized by enzyme acetyl-CoA carboxylase (*ACACA* and *ACACB* genes).

According to the transcriptomic analysis (Figure 1B), expression of several genes from the fatty acids elongation pathway decreased as a result of the knockdown of *IGFBP6* gene in MDA-MB-231 cells; namely: *ACACB* (2.1 times, FDR $p = 6.3{\cdot}10^{-9}$), *HACD2* (2.1 times, FDR $p = 1.6{\cdot}10^{-8}$), and *TECR* (2.0 times, FDR $p = 5.8{\cdot}10^{-6}$). At the same time, the expression of

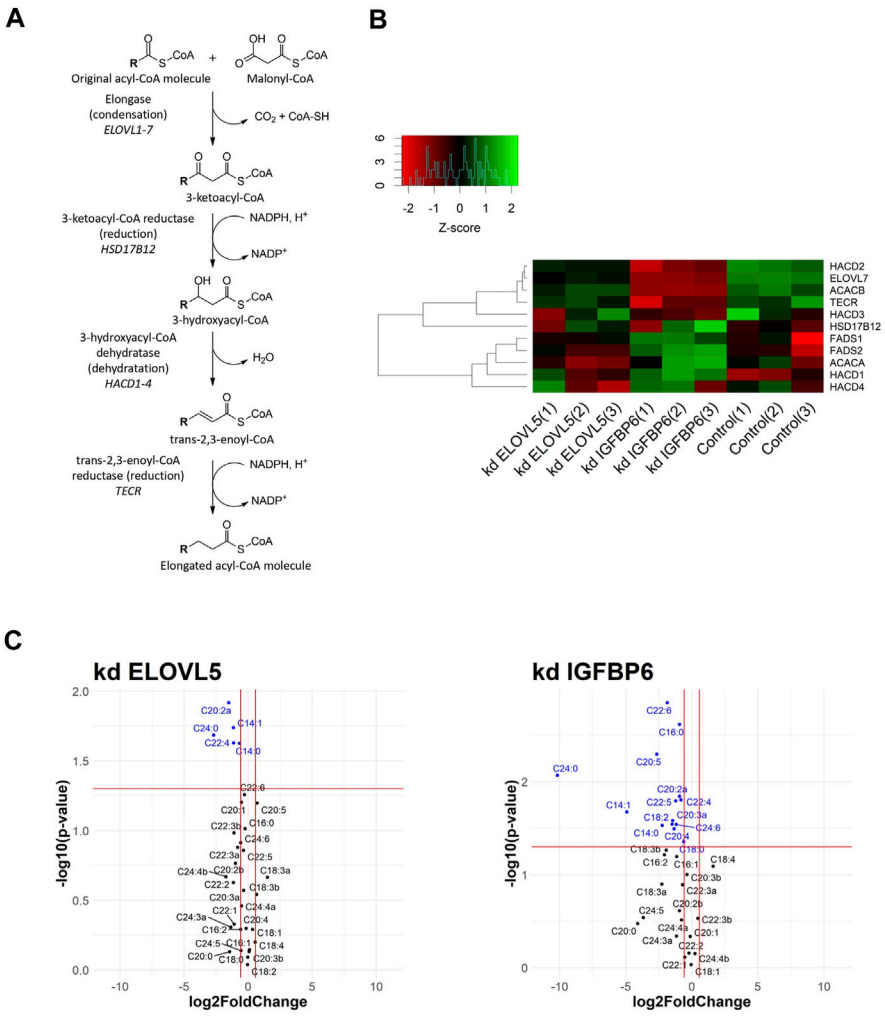

FIGURE 1
(A) Schematic drawing of fatty acid elongation. R represents a fatty acid with a varying length. **(B)** Heatmap of gene expression for selected genes from fatty acids elongation pathway. **(C)** Volcano plots showing fold changes and *p*-values of fatty acids content (kd *ELOVL5* vs. Control and kd *IGFBP6* vs. Control).

the *HACD1* gene slightly increased (1.6 times, FDR $p = 2.8{\cdot}10^{-3}$). A decrease in the content of the TECR protein in MDA-MB-231 cells with the knockdown of *IGFBP6* gene was also confirmed by proteomic analysis (1.9 times, FDR $p = 2.0{\cdot}10^{-2}$).

Interestingly, according to the transcriptomic analysis the expression of one of the fatty acids elongases, *ELOVL7*, substantially dropped as a result of the knockdown of *IGFBP6* gene (4.2 times, FDR $p = 2{,}4{\cdot}10^{-10}$), and it was confirmed by RT-PCR (10.4 times, $p = 2{,}6{\cdot}10^{-2}$). Moreover, similar but less prominent effect was observed after knockdown of *ELOVL5* gene. In this case expression of *ELOVL7* decreased 1.8 times (FDR $p = 6{,}0{\cdot}10^{-4}$). *ELOVL7* catalyzes elongation of very long chain saturated as well as unsaturated fatty acids, including n-3 and n-6 PUFAs (Naganuma et al., 2011).

Expression of several enzymes from the pathway of elongation of n-3 and n-6 polyunsaturated fatty acids, which include *ELOVL5*, changed after the knockdown of *IGFBP6* gene (Leonard et al., 2000; Wang et al., 2008; Moon et al., 2009). A slight but statistically significant increase in the expression of *ELOVL5*, *FADS1*, and *FADS2* genes after the knockdown of *IGFBP6* has been noted (*ELOVL5* 1.4 times, FDR $p = 2.0{\cdot}10^{-2}$; *FADS1* 1.3 times, FDR $p = 2.0{\cdot}10^{-2}$ and *FADS2* 1.5 times, FDR $p = 3.0{\cdot}10^{-4}$). The increase in *FADS1* and *FADS2* mRNAs was confirmed by RT-PCR (*FADS1* 2.7 times, $p = 3.5{\cdot}10^{-2}$ and *FADS2* 2.0 times, $p = 3.3{\cdot}10^{-2}$), and the increase in FADS2 protein level in MDA-MB-231 with knockdown of *IGFBP6* gene was also confirmed by proteomic analysis (3.4 times, FDR $p = 4.2{\cdot}10^{-3}$).

All described changes suggest that *IGFBP6* can be involved in the regulation of lipid metabolism in breast cancer cells. To our knowledge, there are no previously published data on the role of *IGFBP6* in the lipid metabolism; therefore, we performed additional experiments to test this relation.

We found that knockdowns of both *ELOVL5* and *IGFBP6* genes led to a significant change in the content of individual long and very long fatty acids in MDA-MB-231 cells (Figure 1C; Supplementary Table S4). In particular, when the *ELOVL5* gene is knocked down, the content of fatty acids C22:4n-6, C20:2 (peak "a", n-6 or n-9) decreased. Also, when either of the genes was knocked down, there was a significant decrease in the content of very long saturated fatty acid C24:0 in the cells. This result is in good agreement with the results of

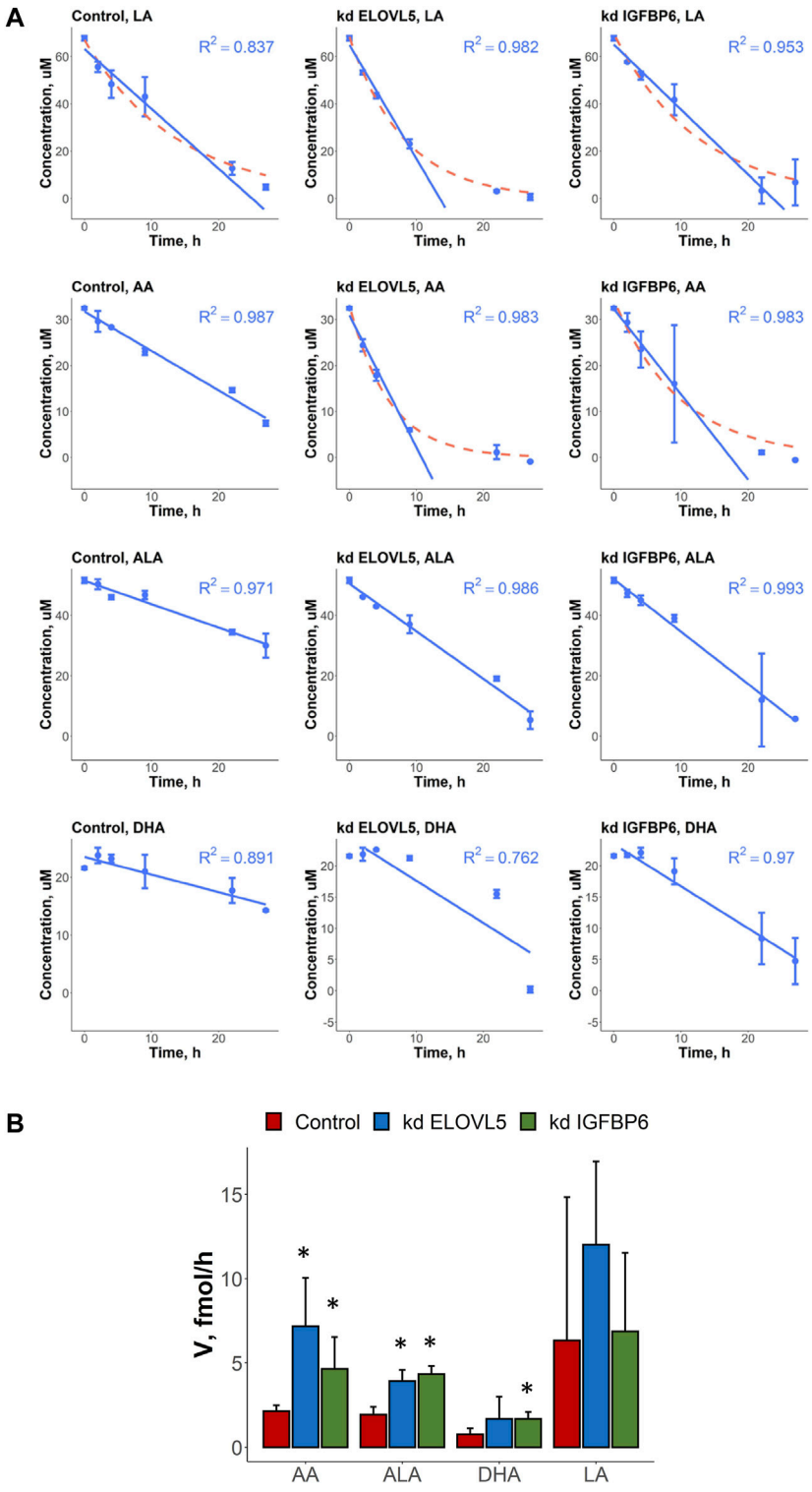

FIGURE 2
(A) Kinetics of changes in the concentration of various PUFAs (LA, AA, ALA and DHA) in cell culture medium in the presence of control MDA-MB-231 cells and the cells with knockdown of *ELOVL5* and *IGPBP6* genes. Error bars represent standard deviation (SD, $n = 2$). **(B)** Calculated uptake rates (per one cell) of various PUFAs (LA, AA, ALA and DHA) for control MDA-MB-231 cells and for the cells with knockdown of *ELOVL5* and *IGPBP6* genes. Error bars represent 95% confidence intervals. *—statistically significant difference versus control cells.

transcriptomic analysis, which demonstrated a decrease in the expression of the *ELOVL7* gene in both stable cell lines. Interestingly, after the knockdown of the *IGFBP6* gene, a significant decrease in the content of n-3 eicosapentaenoic (EPA, C20:5n-3) and docosahexaenoic (DHA, C22:6n-3) acids in cells was also noted.

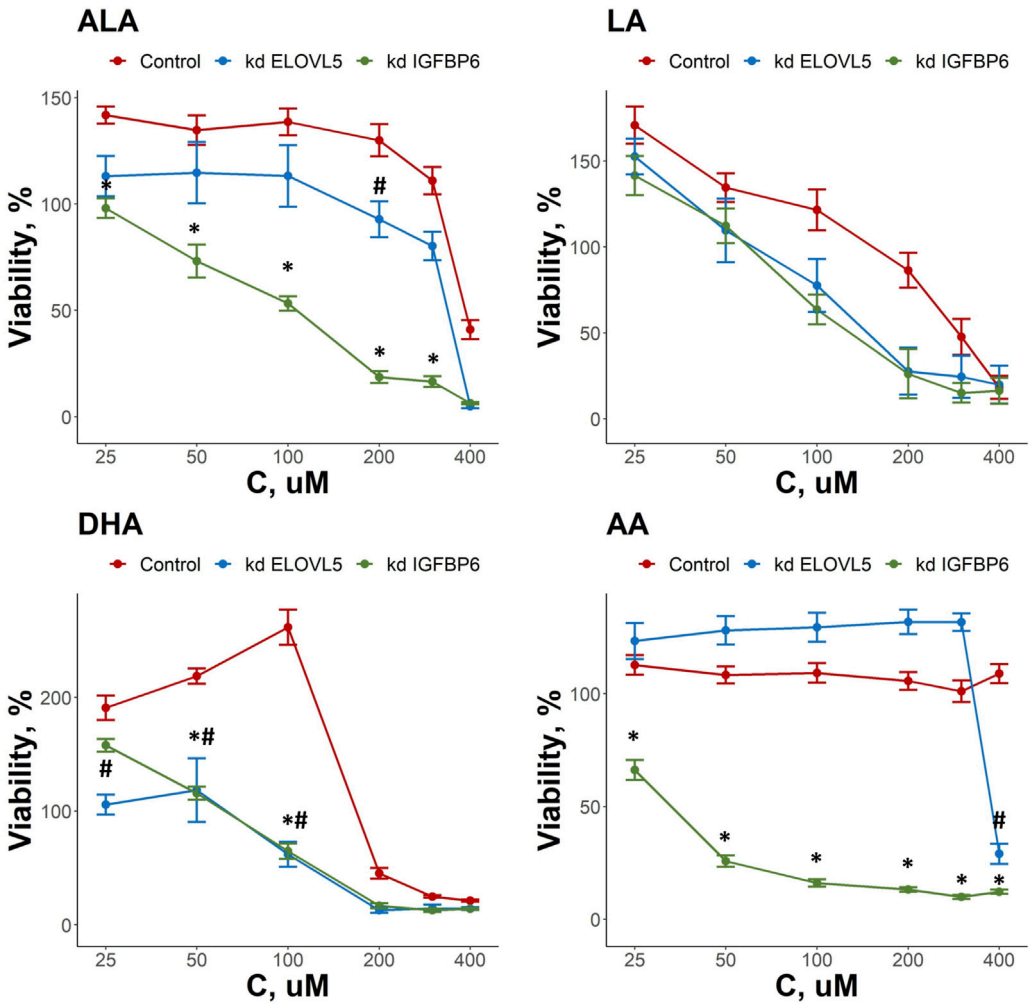

FIGURE 3
Effect of various LC-PUFA on the viability of control MDA-MB-231 cells and the cells with knockdown of *ELOVL5* and *IGFBP6* genes. Error bars represent standard error of mean (SEM, $n = 3$). *—$p < 0.05$ kd *IGPBP6* versus control cells. #—$p < 0.05$ kd *ELOVL5* versus control cells.

In this work we also measured uptake rates of four different PUFAs (LA, AA, ALA and DHA) by the control MDA-MB-231 cells and by the cells with knockdowns of *ELOVL5* and *IGFBP6* genes. In most cases, the kinetics of changes of PUFAs' concentrations in cell culture medium could be accurately approximated by the linear model with constant uptake rate over the whole time range (Figure 2A; Supplementary Table S5). At the same time, an exponential model was a better alternative in several cases. Indicating a more efficient uptake, the cases following exponential kinetics evidently benefit from transport molecules and/or specific enzymes utilizing the fatty acid not becoming rate-limiting as the fatty acid concentration decreases. In particular, the kinetics of AA's uptake quantitatively and qualitatively changed as a result of the knockdown of *ELOVL5* and *IGFBP6* genes. In both cases the cells with knockdowns demonstrated more efficient consumption.

To compare uptake rates of different PUFAs by different cells in cases of both linear and exponential kinetics, we approximated the initial parts of the exponential curves by straight lines and so obtained maximum initial uptake rates for those cases. We detected significant differences in the PUFAs' uptake rates after the knockdowns of *ELOVL5* and *IGFBP6* genes (Figure 2B). For example, we found that uptake rate of AA increased 3.3 times as a result of the decrease in expression of *ELOVL5* gene. Similar, but less prominent change (2.2 times) was observed for *IGFBP6* gene. In addition, the consumption of ALA was 1.8 and 2.2 times faster after the knockdown of *ELOVL5* and *IGFBP6* genes respectively. And finally, uptake rate of DHA was significantly higher (2.2 times) for the cells with the knockdown of *IGFBP6* gene in comparison to the control cells. All other changes were statistically insignificant.

Interestingly, the expression of genes involved in the transport of fatty acids into the cell (Liu et al., 2015; Zhang et al., 2018) did not change significantly (FDR $p > .05$) after the knockdown of *ELOVL5* or *IGFBP6* gene (CD36, SLC27A1-6, FABP1-9 and FABP12 genes were analyzed). The observed changes in uptake rates are thus probably due to the changes in metabolism of LC-PUFAs.

3.2 Knockdowns of both *ELOVL5* and *IGFBP6* genes change the response of breast cancer cells to external fatty acids

As both *ELOVL5* and *IGFBP6* genes affect lipid metabolism, we examined the changes in the response of MDA-MB-231 cells to

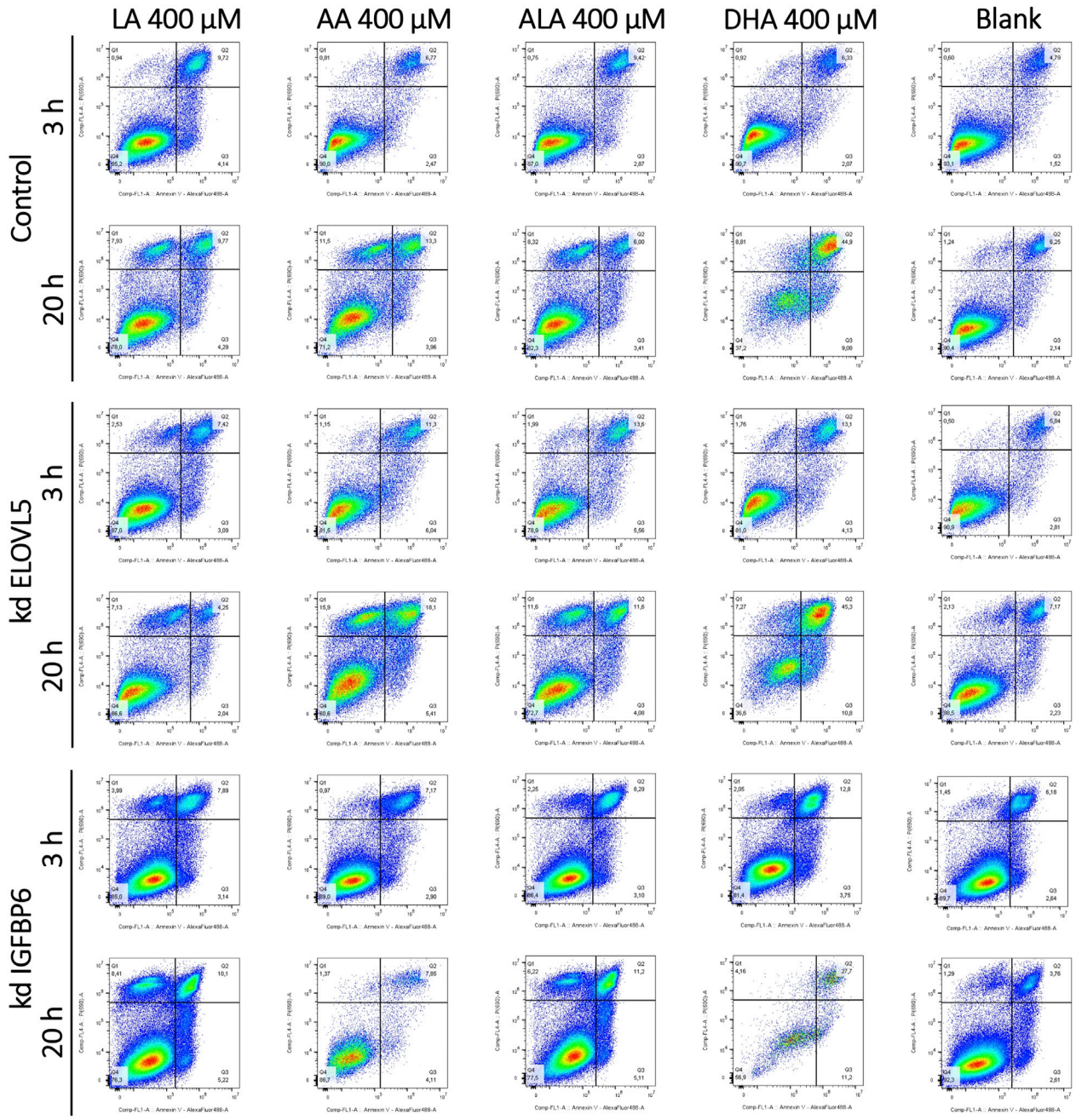

FIGURE 4
Effect of various LC-PUFAs on the activation of apoptosis in MDA-MB-231 cells. Two-dimensional plots of the integral fluorescence intensity of the annexin V conjugate with Alexa Fluor 488 dye (horizontal axis), and the integral fluorescence intensity of propidium iodide (vertical axis) in the cells with the knockdown of *ELOVL5* or *IGFBP6* genes, as well as in controls cells.

external LC-PUFAs in the culture medium. Overall, we observed that all LC-PUFAs studied can decrease viability of breast cancer cells *in vitro* (Figure 3). The viability of the cells with the knockdown of *IGFBP6* gene was significantly lower in comparison to the control cells for ALA in the range of 25–300 μM ($p < 0.05$), for DHA in the range of 50–100 μM ($p < .05$), and for AA in the range of 25–400 μM ($p < .05$). For the cells with reduced expression of *ELOVL5* gene, similar but less prominent effects were seen. The viability of these cells was lower than that of the control cells only at 200 μM for ALA ($p < .05$), at 400 μM for AA ($p < 0.05$), and in the range of 25–100 μM ($p < .05$) for DHA. The effect of LA was not significantly changed by either knockdown ($p > .05$). While n-3 ALA and n-6 AA turned out to be the least cytotoxic towards both control and knockdown *ELOVL5* cells, n-6 AA and n-3 DHA were highly cytotoxic to the knockdown *IGFBP6* cells, in line with the significantly greater sensitivity of the latter to all LC-PUFAs, and in good agreement with previous research (Schley et al., 2005). In all, our data demonstrate that reduction in the expression of *ELOVL5* or *IGFBP6* genes can lead to an increase in the sensitivity of breast cancer cells to various PUFAs.

Interestingly, we also found that some LC-PUFAs have a stimulating effect on the growth of MDA-MB-231 cells. For example, an increase in the viability of the control cells was observed in the range 25–200 μM for ALA, 25–100 μM for DHA and at 25 μM for LA. At the same time, the stimulating effect of these fatty acids on MDA-MB-231 cells with either *ELOVL5* or *IGFBP6* knockdown was less pronounced or completely absent.

3.3 Cytotoxic effect of PUFAs cannot be explained by apoptosis

As all tested LC-PUFAs could decrease viability of the MDA-MB-231 breast cancer cells, we studied the effect of these LC-PUFAs on the activation of apoptosis in the cells. The analysis was carried out at 3 and 20 h after the addition of one of the LC-PUFAs (Figure 4; Supplementary Table S6). For the control MDA-MB-231 cells, 3 h after the addition of LA and ALA, a significant increase in the proportion of dead (AV + PI+) cells (from about 5% to 10%) was observed, accompanied by a decrease in the proportion of viable cells. When these fatty acids were added, the proportion of cells at the early stage of apoptosis also slightly increased from about 1.5% to 2.9%–4.1%. At 20 h after the addition of any LC-PUFA, there was a significant increase in the proportion of the control cells in the AV-PI+ region. Moreover, a pronounced peak with increased cell density was visualized in the two-dimensional density maps.

Objects in this area correspond to nuclear fragments without a cell membrane, which can result from necrosis (Sawai and Domae, 2011). Interestingly, during necrosis, cells can also first move into the AV + PI- region, mimicking the behavior of cells at an early stage of apoptosis, and only then move into the area of dead cells (AV + PI-) and into the area of nuclear fragments without a cell membrane. (AV-PI+) (Sawai and Domae, 2011). However, a significant increase in the proportion of cells in the AV-PI+ region is not characteristic of apoptosis, which makes it possible to distinguish between these two mechanisms of cell death (Wlodkowic et al., 2009; Sawai and Domae, 2011; Brauchle et al., 2015). An increase in the proportion of cells in the AV-PI+ is also characteristic of ferroptosis (Chen et al., 2017; Sun et al., 2018). At the same time the proportions of cells in the regions AV + PI+ and AV + PI- can also rise during ferroptosis (Chen et al., 2017; Sun et al., 2018).

The proportion of the control cells in the region corresponding to early apoptosis (AV + PI-) slightly increased 20 h after the addition of LA, ALA, and AA (from about 2% to 4%). The increase was more significant for the DHA (from about 2% to 9%). The proportion of dead cells also increased from 6% to 10%–13% for LA and AA, while the proportion of dead cells did not change for ALA. In case of DHA, most of the cells were in the AV + PI+ area of dead cells (about 45%), and not in the area corresponding to viable cells, as it was observed for other fatty acids.

For the knockdown *ELOVL5* cells, a significant increase in the proportion of dead cells and a decrease in the proportion of viable cells was observed 3 h after the addition of ALA, AA, and DHA. This effect was less pronounced for LA. After 20 h, the pattern for the knockdown *ELOVL5* cells was largely similar to the results observed in the control cells. One can notice a slightly increased sensitivity of the cells with the knockdown of *ELOVL5* gene to ALA and AA, which is in good agreement with the data of the MTS test.

Three hours after the addition of LA, the knockdown *IGFBP6* cells started to concentrate in the AV-PI+ region. Also, the number of dead knockdown *IGFBP6* cells became more pronounced when DHA was added, compared to the control cells. Other changes after 3 h were similar to the control cells. After 20 h, for shorter LA and ALA, clusters of the knockdown *IGFBP6* cells were observed in the AV-PI+ area. The proportions were similar to the control cells. For longer AA and DHA, much fewer events were observed and a significant increase of the proportion of the cells in the region of dead cells (AV + PI+) was also noticed. On the other hand, the increase of cell counts in the AV-PI+ area was less prominent.

Overall, the patterns of death observed here for all tested LC-PUFAs and the cell lines correspond more closely to necrosis or ferroptosis rather than apoptosis.

3.4 Knockdown of either *ELOVL5* or *IGFBP6* gene increases sensitivity to ferroptosis

To assess how the sensitivity of MDA-MB-231 cells to ferroptosis changes upon the knockdown of *ELOVL5* or *IGFBP6* genes, we treated the cells with ferroptosis inducer Erastin. A ferroptosis inhibitor Ferrostatin-1 was used to prevent the action of Erastin. Our data showed (Figure 5A) that the knockdown of both genes leads to a significant increase in sensitivity to ferroptosis of MDA-MB-231 cells ($p < 0.05$). Moreover, the effect of Erastin was significantly reduced when Ferrostatin-1 was added to both knockdown cells ($p < 0.05$), while the increase of viability was insignificant for the control cells ($p > 0.05$). Thus, the reduction in the expression of *ELOVL5* or *IGFBP6* genes leads to increased sensitivity to the induction of ferroptosis in breast cancer cells and at the same time makes them more responsive to its inhibition.

Next, we treated MDA-MB-231 cells with combinations of various LC-PUFAs and Ferrostatin-1. Ferrostatin concentrations were the same as in the previous experiment. The choice of working concentrations of fatty acids (300 μM for LA, AA, and ALA, and 200 μM for DHA) was made on the basis of the data obtained on the cellular response to external LC-PUFAs to ensure the cells showed a measurable decrease in viability.

We confirmed that increasing the content of LC-PUFAs in the nutrient medium decreases the viability of MDA-MB-231 cells (Figure 5B). This effect was significantly reduced by Ferrostatin-1 in the knockdown *IGFBP6* cells for all LC-PUFAs ($p < 0.05$) and in the knockdown *ELOVL5* for DHA ($p < 0.05$). Again, the action of Ferrostatin-1 was insignificant for the control cells ($p > 0.05$). Overall, these data suggest that the mechanisms of cell death induced by Erastin and LC-PUFAs are similar.

GPx4 peroxidase is one of the key enzymes involved in the glutathione pathway of ferroptosis inhibition. It oxidizes glutathione to form glutathione disulfide (GSSG) and reduces the cytotoxic lipid peroxides L-OOH to alcohols simultaneously. Disruption of GPx4 activity leads to a decrease in antioxidant capacity and, consequently, to ferroptosis. Our transcriptomic analysis revealed a significantly reduced level of GPx4 expression in knockdown *IGFBP6* cells compared to the control cells.

Therefore, the next important task was to check the activity of this enzyme in all three cell lines. In this assay, GSSG formed by GPx4 is reduced back to 2GSH by glutathione disulfide reductase (GR) using NADPH as a source of electrons and cumene hydroperoxide as a

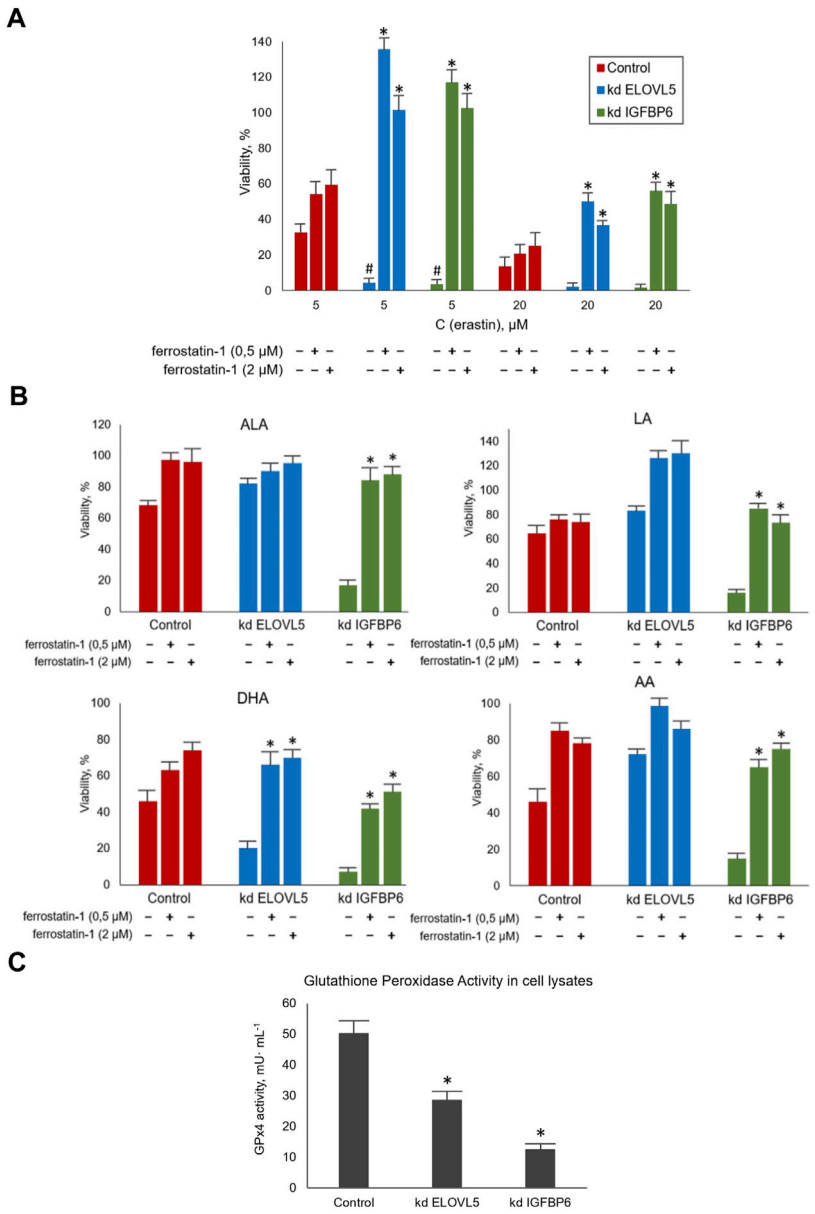

FIGURE 5
(A) Evaluation of the sensitivity of MDA-MB-231 cells to ferroptosis during their treatment with standard agents Erastin and Ferrostatin-1 in various combinations for 24 h. Error bars represent standard error of mean (SEM, $n = 3$). *—$p < 0.05$ versus pure Erastin. #—$p < 0.05$ versus control cells. **(B)** Evaluation of the sensitivity of MDA-MB-231 cells to ferroptosis during their treatment with LC-PUFA and Ferrostatin-1 for 24 h. The concentration for LA, AA, and ALA was 300 μM and for DHA 200 μM. Error bars represent standard error of mean (SEM, $n = 3$). *—$p < 0.05$ versus pure PUFA. **(C)** Glutathione Peroxidase Activity measured in cell lysates per one million cells after 10 min of incubation. Error bars represent standard error of mean (SEM, $n = 3$). *—$p < 0.05$ versus control cells.

substrate. The rate of oxidation of NADPH is directly reflects the activity of GPx4. This rate was determined by following the change in absorbance of NADPH at 340 nm with a spectrophotometer in kinetic mode and all reactants kept in excess so as to make the action of GPx4 rate limiting in the oxidation of NADPH.

The results obtained (Figure 5C) demonstrated a significant decrease in GPx4 activity in knockdown *IGFBP6* cells compared to the control ($p < 0.05$). These data are in good agreement with the transcriptomic analysis. It should also be noted that the activity of this enzyme also slightly changed after the knockdown of *ELOVL5* gene ($p < 0.05$). Thus, the decrease in GPx4 activity is likely to be the key to lowering antioxidant capacity and increasing cells' sensitivity to ferroptosis with the knockdowns.

Next, we tested whether the expression of *GPX4* gene can also decrease simultaneously with the expression of *IGFBP6* gene in breast cancer tissue. The analysis of the publicly available databases of transcriptomes of breast cancer samples showed that *GPX4* gene expression positively correlates with *IGFBP6* gene expression (i.e. decreases with a decrease in *IGFBP6* gene expression) in tumor samples from patients with ER+ breast cancer in 4 analyzed data sets (in total 10 datasets of ER+ breast cancer were analyzed) and in 5 datasets of ER-breast cancer patients (in total 7 datasets of ER-breast

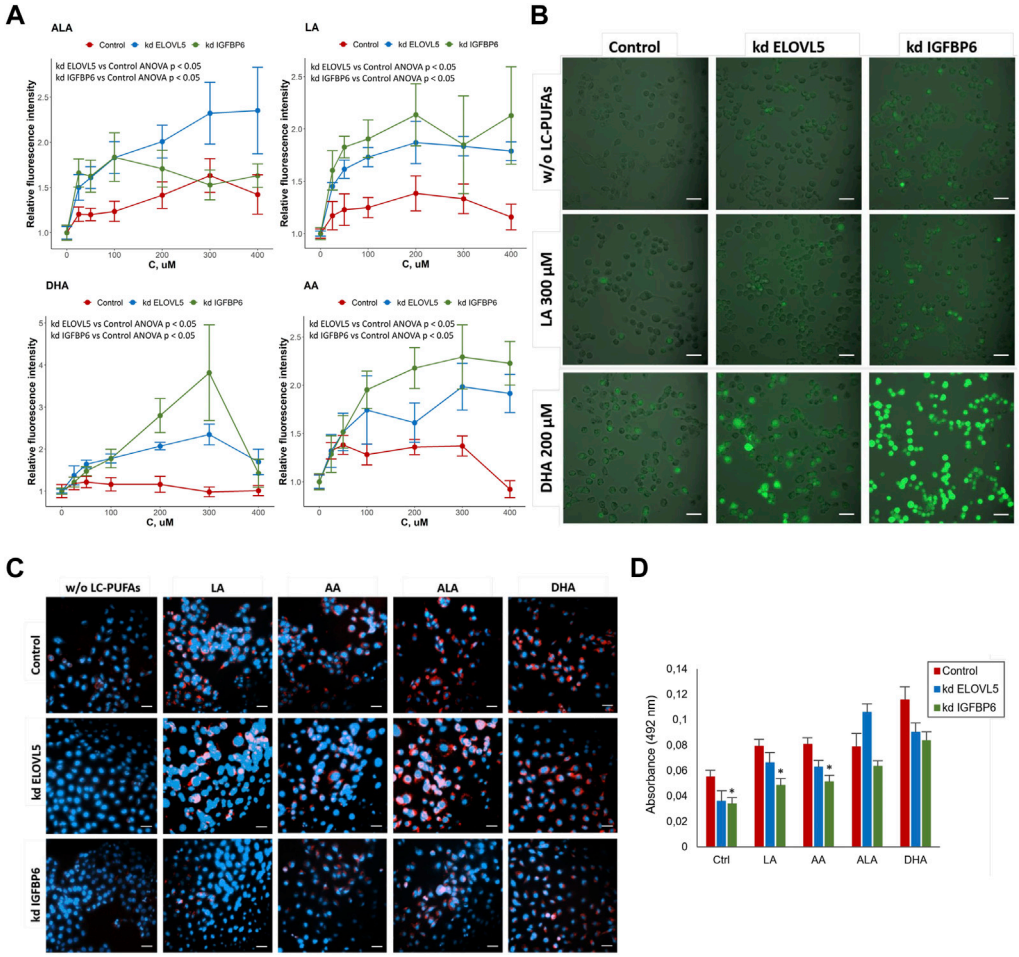

FIGURE 6
(A) Assessment of oxidative stress in MDA-MB-231 cells under the influence of various LC-PUFA by detection of reactive oxygen species (ROS) with H2DCFDA. Error bars represent standard error of mean (SEM, $n = 3$). **(B)** Photo of MDA-MB -231 cells in the cell culture medium without external LC-PUFAs and with addition of 300 μM LA or 200 μM DHA (staining with H2DCFDA). Scale bars indicate 50 μm. **(C)** Lipid droplets staining in MDA-MB-231 cells in control medium and in the medium containing 50 μM of LA, AA, ALA and DHA. Scale bars indicate 50 μm. Nuclei (blue) were stained with 4′,6-diamidino-2-phenylindole (DAPI), lipid droplets (red) were stained with Oil Red O. **(D)** Quantification of lipid droplets in MDA-MB-231 cells after treatment with various LC-PUFAs. The diagram represents absorbance of extracted Oil Red O. Error bars represent standard error of mean (SEM, $n = 3$).

cancer were analyzed). Negative correlations have not been observed in this study.

To check whether the knockdown of either *ELOVL5* or *IGFBP6* gene leads greater accumulation of reactive oxygen species (ROS) in the cells upon addition of external PUFAs, we used ROS indicator 2′,7′-dichlorodihydrofluorescein diacetate (DCFDA, also known as H2DCFDA, DCFH-DA, and DCFH). DCFDA is a cell-permeable chemically reduced form of fluorescein. After cleavage of the acetate groups by intracellular esterases and oxidation, the non-fluorescent form of DCFDA is converted to highly fluorescent DCF.

The results showed (Figure 6A) that for all tested PUFAs fluorescence intensity of DCF normalized to the control culture medium without external PUFAs was higher for the cells with reduced expression of *ELOVL5* (ANOVA $p < 0.05$) and *IGFBP6* gene (ANOVA $p < 0.05$), indicating greater accumulation of ROS in the knockdowns. In addition, knockdown *IGFBP6* cells with almost all fatty acids, and especially DHA, demonstrated the highest increase in fluorescence intensity. These data have been confirmed by microscopic observations (Figure 6B). Overall, the greater accumulation of ROS in the knockdowns is in good agreement with lower activity of GPx4 and higher sensitivity of these cells to PUFAs.

One possible way to prevent oxidation of PUFAs is to store them in lipid droplets (Wang et al., 2017; Dierge et al., 2021). We compared the accumulation of lipid droplets in the cells with knockdowns to the control cells with the help of lipid dye Oil Red O. The results (Figure 6C) showed an increase in the accumulation of lipids in MDA-MB-231 cells after addition of external PUFAs to the nutrient medium. Oil Red O extraction was carried out for quantification of lipid accumulation (Figure 6D). We found that knockdown of *IGFBP6* gene significantly reduces the formation of lipid droplets under the control conditions (p <0.05) and after treatment with LA ($p < 0.05$) and AA ($p < 0.05$). These data were confirmed by staining the cells with another lipid dye BODIPY (Figure S17).

These results are in good agreement with the transcriptomic analysis, which demonstrated significantly reduced expression levels

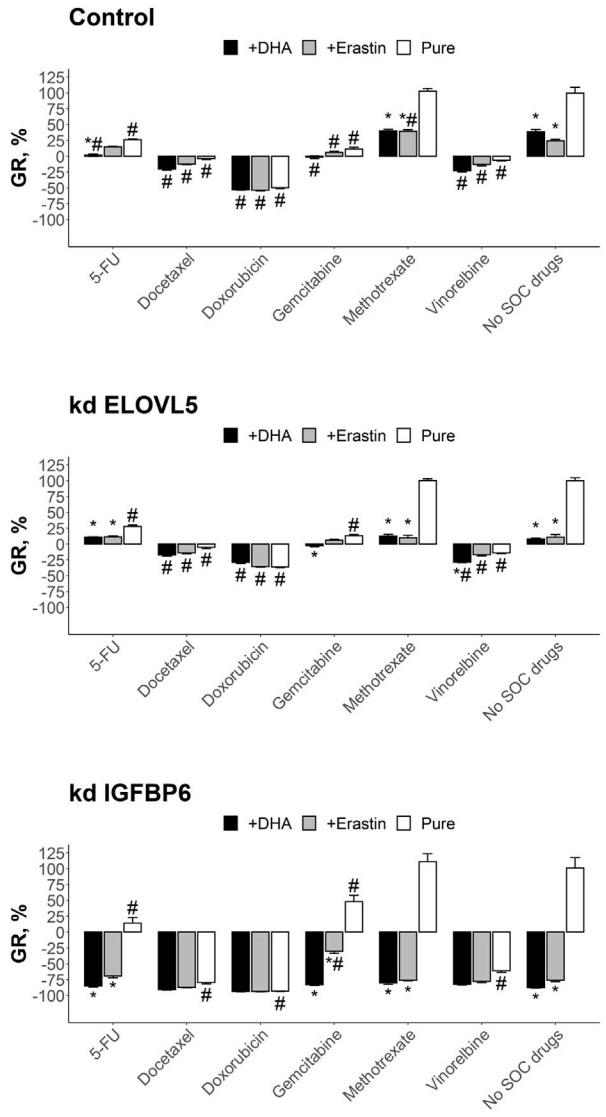

FIGURE 7
Results of the drug test for the tested SOC drugs and their combination with DHA and Erastin on the spheroids in Matrigel from MDA-MB-231 cells. Error bars represent standard error of mean (SEM, $n = 3$). *—$p < 0.05$ versus corresponding pure SOC treatment (without DHA or Erastin). #—$p < 0.05$ versus corresponding condition without SOC drugs (no SOC drugs).

of the *AGPAT3*, *GPAT2*, *GPAT3*, and *DGAT1* enzyme genes in the knockdown *IGFBP6* cells compared to the control cells (Supplementary Table S7). These enzymes play important roles in the regulation of triacylglycerol (TAG) biosynthesis: *AGPAT3* and *GPAT2* translocate TAG molecules from the endoplasmic reticulum (ER) into lipid droplets (LD) during membrane fusion; *GPAT3* catalyzes the conversion of glycerol-3-phosphate to lysophosphatidic acid during the synthesis of triacylglycerol; and *DGAT1* catalyzes the conversion of diacylglycerol and fatty acid esters of coenzyme A to triacylglycerols (Wilfling et al., 2014; Wang et al., 2017; Quiroga et al., 2021). Thus, disruption of TAG biosynthesis and lipid droplet formation in the knockdown *IGFBP6* cells appear to be one of the reasons for their increased sensitivity to external LC-PUFAs.

3.5 Combination of SOC drugs with inducers of ferroptosis

To find out whether induction of ferroptosis by a PUFA or Erastin can significantly improve cytotoxic effects of standard of care (SOC) chemotherapeutic drugs, we tested different combinations on 3D cell models from control MDA-MB-231 cells, as well as from the cells with the knockdowns. The cells were grown in Matrigel and formed spheroids. This method allows one to create more physiologically relevant environment and provides a more gradual access for the drugs to the cells, reflecting better the conditions *in vivo*.

Overall, almost all tested drugs at clinically relevant concentrations were able to significantly reduce growth rate or even cause cell death (Figure 7). The only exception was methotrexate which was inactive on all the three cell types ($p > 0.05$). As expected, breast cancer cells after the knockdown of either *ELOVL5* or *IGFBP6* gene were more sensitive to DHA ($p < 0.05$). Interestingly, after the knockdown of *IGFBP6* gene cells also became more sensitive to docetaxel, doxorubicin, vinorelbine and pure erastin ($p < 0.05$). On the other hand, decrease in the expression of *IGFBP6* gene led to higher resistance to gemcitabine ($p < 0.05$).

Analysis of the results of the combined treatment showed that combination of 5-FU with DHA resulted in better growth inhibition than pure 5-FU ($p < 0.05$) and pure DHA ($p < 0.05$) for control cells. The effect of this combination was still better than pure 5-FU for the cells with knockdown of *ELOVL5* ($p < 0.05$) or *IGFBP6* ($p < 0.05$) gene, however it was indistinguishable from pure DHA ($p > 0.05$), as DHA itself was much more potent for these cells. The effect of the combination of 5-FU with erastin on the control cells was almost the same as the effects of pure 5-FU ($p > 0.05$) and pure erastin ($p > 0.05$). However, erastin significantly improved the effect of 5-FU after the knockdown of *ELOVL5* ($p < 0.05$) or *IGFBP6* ($p < 0.05$) gene. But again, the result of the combination was indistinguishable from pure erastin ($p > 0.05$).

The inhibitory effect on growth of docetaxel in combination with either DHA or erasin was the same as the effect of pure docetaxel for all three cell types ($p > .05$). The same results were obtained for doxorubicin ($p > 0.05$). Very similar to these two drugs was vinorelbine with the exception for the cells with reduced expression of *ELOVL5* gene where the combination of vinorelbine with DHA resulted in slightly better growth inhibition than pure vinorelbine ($p < .05$) and pure DHA ($p < 0.05$). The effect of methotrexate in combination with DHA or erastin was in all cases better ($p < .05$) than the effect of pure methotrexate as it was not active as single drug. However, almost in all cases (with one exception for combination with erastin on the control cells) the effect did not differ from pure DHA ($p > 0.05$) or pure erastin ($p > 0.05$).

The results of the test for gemcitabine in combination with either DHA or erasin did not differ from pure gemcitabine on the control cells ($p > 0.05$). On the other hand, the combined treatment of gemcitabine with DHA outperformed pure gemcitabine after the knockdown of either *ELOVL5* ($p < 0.05$) or *IGFBP6* ($p < 0.05$) gene. However, as DHA was much more effective on these cells, the growth inhibitory effect of the combination was indistinguishable from pure DHA ($p > .05$). Addition of erastin to gemcitabine increased the effect of the later only on the cells with reduced expression of *IGFBP6* gene ($p < 0.05$).

Overall, these results clearly show that both DHA and erastin have the potential to inhibit growth of breast cancer cells. Moreover, in

some cases they can enhance the effect of the SOC drugs, especially if the cells have a decreased expression of *IGFBP6* gene.

4 Discussion

In our previous work, we identified new transcriptomic prognostic markers of breast cancer relapse (Galatenko et al., 2015). According to those results, low expression of *ELOVL5* and *IGFBP6* genes corresponded to poor prognosis, however, their role in metastasis was unknown. Next, we examined properties of breast cancer cells related to metastatic propensity after the knockdown of either *ELOVL5* or *IGFBP6* gene (Nikulin et al., 2021). We found sharp increase in the expression of metalloproteinases and a decrease in cell adhesion, both of which are likely to promote invasion of cancer cells. We also carried out a pathway analysis and found that the knockdown of *IGFBP6* gene led to downregulation of biosynthesis of some fatty acids in which *ELOVL5* participates directly.

ELOVL5 elongates n-3 and n-6 polyunsaturated fatty acids. It is known that its expression in breast cancer cells is elevated and that it directly affects the lipid composition in serum (Tomida et al., 2021). Moreover, the complete knockout of *ELOVL5* in the mouse breast carcinoma model led to a delay in tumor development and a decrease in tumor growth (Kieu et al., 2021). At the same time, the data on the impact of the *IGFBP6* gene on the lipid metabolism are limited. In this work we focused on the changes in lipid metabolism in breast cancer cells after both knockdowns, paying special attention to *IGFBP6*. Reanalysis of transcriptomic and proteomic data showed that the knockdown of *IGFBP6* gene significantly disrupted lipid metabolism at the mRNA and protein levels. Moreover, we detected significant changes in the composition of fatty acids in the cells after the knockdown of *IGFBP6* gene. Thus, our results suggest that *IGFBP6* can play an important role in the regulation of lipid metabolism in breast cancer cells.

Since blood plasma normally contains significant amount of fatty acids (Abdelmagid et al., 2015) and tumor cells often increase their consumption of fatty acids from the external environment as a result of metabolic reprogramming (Munir et al., 2019), we examined the rates of consumption of external LC-PUFAs and viability of MDA-MB-231 breast cancer cells in the presence of LC-PUFAs. We found significant increase in the uptake rates of several LC-PUFAs after the knockdown of either *ELOVL5* or *IGFBP6* gene. We also found that the effect of the LC-PUFAs is concentration dependent. At low concentration both n-3 and n-6 LC-PUFAs can stimulate growth of MDA-MB-231 breast cancer cells, but as the concentration rises, they become toxic for them. Interestingly, the toxicity was higher for the knockdown cells.

Overall, our results are in good agreement with previous data. n-3 LC-PUFAs have been previously shown to inhibit the proliferation, migration, and invasion of tumor cells *in vitro* (Chamras et al., 2002; Huang et al., 2017; Davison et al., 2018). On the other hand, n-6 LC-PUFAs can also induce cell death by increasing the content of reactive oxygen species (Zhang et al., 2015), but their inhibitory effects on tumor cells are either less pronounced compared to n-3 LC-PUFAs, or absent, or, on the contrary, stimulating effects are observed (Connolly and Rose, 1993; Gonzalez-Reyes et al., 2017). To date, there are also studies in the literature showing that subjects with a higher dietary n-3/n-6 ratio of LC-PUFAs have a significantly lower risk of breast cancer among the study populations (Zheng et al., 2013; Yang et al., 2014). However a recent meta-analysis found no effect of elevated n-3 LC-PUFAs levels on the risk of being diagnosed with any cancer (high-quality evidence) and likely on the risk of dying from cancer (Hanson et al., 2020). The key to this discrepancy can be the fact that the effect of LC-PUFAs is concentration dependent and the sensitivity of cancer cells to the action of LC-PUFAs depends on the transcriptional programs, in particular on the expression of the gene pair studied in this work.

To identify the cause of cell death caused by LC-PUFAs, we studied activation of apoptosis in the cells by flow cytometry. Overall, we observed very limited transition through the region of early apoptosis and a lot of cells in the region characteristic for other types of cell death. These results were notable as they indicated a non-apoptotic mode of cell death after exposure to external LC-PUFAs. Based on the previously published data, we considered that LC-PUFAs cause ferroptosis in breast cancer cells (Chen et al., 2021a; Dierge et al., 2021).

Ferroptosis is one of the mechanisms of programmed cell death, which is based on disturbance of the redox balance (Stockwell et al., 2017). Ferroptosis is fundamentally different from other programmed cell death mechanisms such as apoptosis, pyroptosis, and necroptosis. The term “ferroptosis” was introduced in 2012 to identify an iron-dependent mechanism of cell death with excessive lipid peroxidation followed by destruction of cell membrane. Since ferroptosis was discovered relatively recently, a number of aspects of its mechanism remain unknown to date. In particular, the effectors of this process have not yet been identified, although many of the signaling and metabolic cascades associated with ferroptosis are already known.

The molecular mechanism of ferroptosis is based on the regulation of the balance between oxidative damage and antioxidant protection (Chen et al., 2021b). The key stage in ferroptosis is elevated peroxidation of polyunsaturated fatty acids in phospholipids. There are several ways by which this process can be activated. Firstly, increased activity of the enzymes involved in the synthesis of polyunsaturated fatty acid esters, in particular ACSL4 and LPCAT3, can lead to an increase in peroxidation, since this increases the amount of available substrate for the reaction. Secondly, the activation of the enzymes that directly catalyze the oxidation reaction, for example, various lipoxygenases, can lead to the induction of ferroptosis. And finally, an increase in the concentration of reactive oxygen species due to the activation of proteins involved in their production, or by increasing the concentration of iron, also enhances peroxidation of polyunsaturated fatty acids. In addition, various antioxidant systems are involved in cell defense, in particular, the cascade of synthesis and utilization of glutathione (one of the key enzymes is glutathione peroxidase GPX4), as well as coenzyme Q. A decrease in the activity of these systems can also trigger ferroptosis.

Our data suggest that LC-PUFAs can trigger ferroptosis in breast cancer cells. Firstly, the results of the flow cytometry experiments were similar to the data published previously in the study of ferroptosis by this method (Chen et al., 2017; Sun et al., 2018). Secondly, our hypothesis was also supported by the experiments on the inhibition of the cell death caused by LC-PUFAs with canonical inhibitor of ferroptosis Ferrostatin-1, which can significantly increase cell viability in some cases. Moreover, we have found that the knockdown of either *ELOVL5* or *IGFBP6* gene significantly increases sensitivity of MDA-MB-231 cells to canonical inducer of ferroptosis Erastin, and again the cells can be rescued by Ferrostatin-1. Interestingly, previously it has been demonstrated that expression of *ELOVL5* gene can affect sensitivity to ferroptosis in gastric cancer (Lee et al., 2020).

The reason why the breast cancer cells with reduced expression of either *ELOVL5* or *IGFBP6* gene are more sensitive to ferroptosis is

complex. First of all, we found that the cells with the knockdowns accumulate more reactive oxygen species in response to external LC-PUFAs. Partly this can be explained by higher uptake of these LC-PUFAs from external medium. However, we also found that a significant decrease in the activity of one of the main antioxidant enzymes, GPX4, resulted from the knockdowns. Moreover, our data suggest that the cells with knockdown of *IGFBP6* gene are less efficient in storage of fatty acids in lipid droplets, and thus more substrate for peroxidation can be available in these cells. In addition, there is evidence in the literature that an increase in *IGFBP6* may improve mitochondrial fitness and redox status based on a decrease in mitochondrial ROS production (Longhitano et al., 2022).

At present, it is known that tumor cells are often resistant to classical mechanisms of programmed cell death, such as apoptosis. At the same time, ferroptosis is considered as a promising alternative means to destroy the tumor (Wu et al., 2020; Chen et al., 2021b). The accumulated information indicates that therapy-resistant tumor cells (in particular, the cells that have undergone epithelial to mesenchymal transformation or tumor stem cells) are sensitive to the induction of ferroptosis (Viswanathan et al., 2017; Cosialls et al., 2021). The influence of the expression of the genes associated with ferroptosis on the prognosis of some tumors (in particular, prostate cancer and colorectal cancer) has also been established (Wang Y. et al., 2021; Lv et al., 2021). Based on these data, ferroptosis inducers are considered to be a promising new class of anticancer drugs (Wang H. et al., 2021). Moreover, it has been proven that some of the approved drugs also trigger ferroptosis in tumor cells (Su et al., 2020).

Despite the fact that the effect of n-3 LC-PUFAs on non-tumorogenic cells is not fully understood, some studies showed that at concentrations which inhibit the growth of tumor cells, n-3 LC-PUFAs have little or no cytotoxic effect on normal breast cells (Grammatikos et al., 1994; Bernard-Gallon et al., 2002). Thus, as induction of ferroptosis is considered to be a promising means to kill cancer cells and potential harm of LC-PUFAs to normal cells is low, we studied combinations of the standard of care (SOC) chemotherapeutic drugs with DHA (an n-3 LC-PUFA). Our results showed that in some cases induction of ferroptosis can enhance the effect of the SOC drugs, especially if the cells have decreased expression of *IGFBP6* gene. Thus, it would be worthwhile to test LC-PUFAs in combination with anti-cancer drugs in more clinically relevant settings.

5 Conclusion

In this work we showed that, to our surprise, the knockdown of *IGFBP6* gene, a member of the IGF-binding protein family, led to significant changes in lipid metabolism in MDA-MB-231 cells. It was also found that a decrease in the expression of either *IGFBP6* or *ELOVL5* gene increases sensitivity of MDA-MB-231 breast cancer cells to LC-PUFAs and our data suggest that they cause cell death by activation of ferroptosis. We suspect a significant drop in the activity of the main antioxidant enzyme GPX4 in the cells after the knockdowns is the key reason for this phenomenon. Moreover, observed changes in the lipid metabolism after the knockdown of *IGFBP6* gene and increased uptake of some PUFAs can also contribute to it. Use of standard chemotherapeutics in combination with ferroptosis inducers showed that in some cases the latter can significantly enhance the effect of the drugs, especially for the cells with low expression of *IGFBP6* gene. Thus, for the breast cancer patients with low expression of *IGFBP6* and *ELOVL5* genes in cancer tissue the addition of PUFAs to the chemotherapy regimen can be potentially beneficial and should be tested in more clinically relevant settings.

Data availability statement

Publicly available datasets were analyzed in this study. This data can be found here: https://www.ncbi.nlm.nih.gov/geo/query/acc.cgi?acc=GSE165854 https://www.ebi.ac.uk/pride/archive/projects/PXD023892.

Author contributions

The study was supervised by AT and BA. SN, GZ, and AP designed the study. SN, AR, and GZ performed the experiments and analyzed the data. SN and AR wrote the manuscript. AT, AP, and BA revised the manuscript. All authors contributed to the article and approved the submitted version.

Funding

This work was financially supported by HSE University Basic Research Program and in part (experiments on the combinational treatment) by the Russian Science Foundation (Project No. 19-15-00397).

Acknowledgments

The authors thank Dr. Maxim Shkurnikov for the discussion of the obtained results and Dr. Vladimir Bezuglov for the help with BODIPY staining.

Conflict of interest

The authors declare that the research was conducted in the absence of any commercial or financial relationships that could be construed as a potential conflict of interest.

Publisher's note

Supplementary material

The Supplementary Material for this article can be found online at: https://www.frontiersin.org/articles/10.3389/fmolb.2023.1075704/full#supplementary-material

References

Abdelmagid, S. A., Clarke, S. E., Nielsen, D. E., Badawi, A., El-Sohemy, A., Mutch, D. M., et al. (2015). Comprehensive profiling of plasma fatty acid concentrations in young healthy Canadian adults. *PLoS One* 10, e0116195. doi:10.1371/journal.pone.0116195

Anthonymuthu, T. S., Tyurina, Y. Y., Sun, W.-Y., Mikulska-Ruminska, K., Shrivastava, I. H., Tyurin, V. A., et al. (2021). Resolving the paradox of ferroptotic cell death: Ferrostatin-1 binds to 15LOX/PEBP1 complex, suppresses generation of peroxidized ETE-PE, and protects against ferroptosis. *Redox Biol.* 38, 101744. doi:10.1016/j.redox.2020.101744

Ashburner, M., Ball, C. A., Blake, J. A., Botstein, D., Butler, H., Cherry, J. M., et al. (2000). Gene ontology: Tool for the unification of biology. The gene ontology consortium. *Nat. Genet.* 25, 25–29. doi:10.1038/75556

Bach, L. A. (2016). Current ideas on the biology of IGFBP-6: More than an IGF-II inhibitor? *Growth Horm. IGF Res.* 30–31, 81–86. doi:10.1016/j.ghir.2016.09.004

Bach, L. A., Fu, P., and Yang, Z. (2013). Insulin-like growth factor-binding protein-6 and cancer. *Clin. Sci.* 124, 215–229. doi:10.1042/CS20120343

Bach, L. A. (2015). Recent insights into the actions of IGFBP-6. *J. Cell Commun. Signal.* 9, 189–200. doi:10.1007/s12079-015-0288-4

Banni, S., Angioni, E., Casu, V., Melis, M. P., Carta, G., Corongiu, F. P., et al. (1999). Decrease in linoleic acid metabolites as a potential mechanism in cancer risk reduction by conjugated linoleic acid. *Carcinogenesis* 20, 1019–1024. doi:10.1093/carcin/20.6.1019

Bernard-Gallon, D. J., Vissac-Sabatier, C., Antoine-Vincent, D., Rio, P. G., Maurizis, J.-C., Fustier, P., et al. (2002). Differential effects of n-3 and n-6 polyunsaturated fatty acids on BRCA1 and BRCA2 gene expression in breast cell lines. *Br. J. Nutr.* 87, 281–289. doi:10.1079/BJNBJN2002522

Bocca, C., Bozzo, F., Martinasso, G., Canuto, R. A., and Miglietta, A. (2008). Involvement of PPARalpha in the growth inhibitory effect of arachidonic acid on breast cancer cells. *Br. J. Nutr.* 100, 739–750. doi:10.1017/S0007114508942161

Brauchle, E., Thude, S., Brucker, S. Y., and Schenke-Layland, K. (2015). Cell death stages in single apoptotic and necrotic cells monitored by Raman microspectroscopy. *Sci. Rep.* 4, 4698. doi:10.1038/srep04698

Camps, C., Buffa, F. M., Colella, S., Moore, J., Sotiriou, C., Sheldon, H., et al. (2008). Hsa-miR-210 is induced by hypoxia and is an independent prognostic factor in breast cancer. *Clin. Cancer Res.* 14, 1340–1348. doi:10.1158/1078-0432.CCR-07-1755

Cerami, E., Gao, J., Dogrusoz, U., Gross, B. E., Sumer, S. O., Aksoy, B. A., et al. (2012). The cBio cancer genomics portal: An open platform for exploring multidimensional cancer genomics data. *Cancer Discov.* 2, 401–404. doi:10.1158/2159-8290.CD-12-0095

Chamras, H., Ardashian, A., Heber, D., and Glaspy, J. a ((2002). Fatty acid modulation of MCF-7 human breast cancer cell proliferation, apoptosis and differentiation. *J. Nutr. Biochem.* 13, 711–716. doi:10.1016/S0955-2863(02)00230-9

Chen, C., Xie, B., Li, Z., Chen, L., Chen, Y., Zhou, J., et al. (2022). Fascin enhances the vulnerability of breast cancer to erastin-induced ferroptosis. *Cell Death Dis.* 13, 150. doi:10.1038/s41419-022-04579-1

Chen, D., Eyupoglu, I. Y., and Savaskan, N. (2017). *Ferroptosis and cell death analysis by flow cytometry*, 71–77. doi:10.1007/978-1-4939-6960-9_6

Chen, X., Comish, P. B., Tang, D., and Kang, R. (2021a). Characteristics and biomarkers of ferroptosis. *Front. Cell Dev. Biol.* 9, 637162. doi:10.3389/fcell.2021.637162

Chen, X., Kang, R., Kroemer, G., and Tang, D. (2021b). Broadening horizons: The role of ferroptosis in cancer. *Nat. Rev. Clin. Oncol.* 18, 280–296. doi:10.1038/s41571-020-00462-0

Cheng, S. H.-C., Huang, T.-T., Cheng, Y.-H., Tan, T. B. K., Horng, C.-F., Wang, Y. A., et al. (2017). Validation of the 18-gene classifier as a prognostic biomarker of distant metastasis in breast cancer. *PLoS One* 12, e0184372. doi:10.1371/journal.pone.0184372

Connolly, J. M., and Rose, D. P. (1993). Effects of fatty acids on invasion through reconstituted basement membrane ('Matrigel') by a human breast cancer cell line. *Cancer Lett.* 75, 137–142. doi:10.1016/0304-3835(93)90198-I

Cosialls, E., El Hage, R., Dos Santos, L., Gong, C., Mehrpour, M., and Hamaï, A. (2021). Ferroptosis: Cancer stem cells rely on iron until "to die for" it. *Cells* 10, 2981. doi:10.3390/cells10112981

Curtis, C., Shah, S. P., Chin, S.-F., Turashvili, G., Rueda, O. M., Dunning, M. J., et al. (2012). The genomic and transcriptomic architecture of 2, 000 breast tumours reveals novel subgroups. *Nature* 486, 346–352. doi:10.1038/nature10983

Davison, Z., Nicholson, R. I., Hiscox, S., and Heard, C. M. (2018). Co-administration of fish Oil with signal transduction inhibitors has anti-migration effects in breast cancer cell lines, *in vitro*. *Open biochem. J.* 12, 130–148. doi:10.2174/1874091X01812010130

Dierge, E., Debock, E., Guilbaud, C., Corbet, C., Mignolet, E., Mignard, L., et al. (2021). Peroxidation of n-3 and n-6 polyunsaturated fatty acids in the acidic tumor environment leads to ferroptosis-mediated anticancer effects. *Cell Metab.* 33, 1701–1715.e5. e5. doi:10.1016/j.cmet.2021.05.016

Ding, C., Chan, D. W., Liu, W., Liu, M., Li, D., Song, L., et al. (2013). Proteome-wide profiling of activated transcription factors with a concatenated tandem array of transcription factor response elements. *Proc. Natl. Acad. Sci. U. S. A.* 110, 6771–6776. doi:10.1073/pnas.1217657110

Dixon, S. J., Lemberg, K. M., Lamprecht, M. R., Skouta, R., Zaitsev, E. M., Gleason, C. E., et al. (2012). Ferroptosis: An iron-dependent form of nonapoptotic cell death. *Cell* 149, 1060–1072. doi:10.1016/j.cell.2012.03.042

Dixon, S. J., Patel, D. N., Welsch, M., Skouta, R., Lee, E. D., Hayano, M., et al. (2014). Pharmacological inhibition of cystine–glutamate exchange induces endoplasmic reticulum stress and ferroptosis. *Elife* 3, e02523. doi:10.7554/eLife.02523

Galatenko, V. V., Shkurnikov, M. Y., Samatov, T. R., Galatenko, A. V., Mityakina, I. A., Kaprin, A. D., et al. (2015). Highly informative marker sets consisting of genes with low individual degree of differential expression. *Sci. Rep.* 5, 14967. doi:10.1038/srep14967

Gene, T., and Consortium, O. (2019). The gene ontology resource: 20 years and still GOing strong. *Nucleic Acids Res.* 47, D330–D338. doi:10.1093/nar/gky1055

Geng, L., Zhou, W., Liu, B., Wang, X., and Chen, B. (2017). DHA induces apoptosis of human malignant breast cancer tissues by the TLR-4/PPAR-α pathways. *Oncol. Lett.* 15, 2967–2977. doi:10.3892/ol.2017.7702

Gerber, B., Freund, M., and Reimer, T. (2010). Recurrent breast cancer: Treatment strategies for maintaining and prolonging good quality of life. *Dtsch. Aerzteblatt Online* 107, 85–91. doi:10.3238/arztebl.2010.0085

Gonzalez-Reyes, C., Marcial-Medina, C., Cervantes-Anaya, N., Cortes-Reynosa, P., and Salazar, E. P. (2017). Migration and invasion induced by linoleic acid are mediated through fascin in MDA-MB-231 breast cancer cells. *Mol. Cell. Biochem.* 1, 1–10. doi:10.1007/s11010-017-3205-8

Grammatikos, S., Subbaiah, P., Victor, T., and Miller, W. (1994). n-3 and n-6 fatty acid processing and growth effects in neoplastic and non-cancerous human mammary epithelial cell lines. *Br. J. Cancer* 70, 219–227. doi:10.1038/bjc.1994.283

Hafner, M., Niepel, M., Chung, M., and Sorger, P. K. (2016). Growth rate inhibition metrics correct for confounders in measuring sensitivity to cancer drugs. *Nat. Methods* 13, 521–527. doi:10.1038/nmeth.3853

Hammamieh, R., Chakraborty, N., Miller, S.-A., Waddy, E., Barmada, M., Das, R., et al. (2007). Differential effects of omega-3 and omega-6 fatty acids on gene expression in breast cancer cells. *Breast Cancer Res. Treat.* 101, 7–16. doi:10.1007/s10549-006-9269-x

Hanson, S., Thorpe, G., Winstanley, L., Abdelhamid, A. S., and Hooper, L. (2020). Omega-3, omega-6 and total dietary polyunsaturated fat on cancer incidence: Systematic review and meta-analysis of randomised trials. *Br. J. Cancer* 122, 1260–1270. doi:10.1038/s41416-020-0761-6

Huang, L.-H., Chung, H.-Y., and Su, H.-M. (2017). Docosahexaenoic acid reduces sterol regulatory element binding protein-1 and fatty acid synthase expression and inhibits cell proliferation by inhibiting pAkt signaling in a human breast cancer MCF-7 cell line. *BMC Cancer* 17, 890. doi:10.1186/s12885-017-3936-7

Huang, W., Guo, X., Wang, C., Alzhan, A., Liu, Z., Ma, X., et al. (2022). α-Linolenic acid induces apoptosis, inhibits the invasion and metastasis, and arrests cell cycle in human breast cancer cells by inhibiting fatty acid synthase. *J. Funct. Foods* 92, 105041. doi:10.1016/j.jff.2022.105041

Ikeda, M., Kanao, Y., Yamanaka, M., Sakuraba, H., Mizutani, Y., Igarashi, Y., et al. (2008). Characterization of four mammalian 3-hydroxyacyl-CoA dehydratases involved in very long-chain fatty acid synthesis. *FEBS Lett.* 582, 2435–2440. doi:10.1016/j.febslet.2008.06.007

Johanning, G. L., and Lin, T. (1995). Unsaturated fatty acid effects on human breast cancer cell adhesion. *Nutr. Cancer* 24, 57–66. doi:10.1080/01635589509514393

Kent, W. J., Sugnet, C. W., Furey, T. S., Roskin, K. M., Pringle, T. H., Zahler, A. M., et al. (2002). The human Genome browser at UCSC. *Genome Res.* 12, 996–1006. doi:10.1101/gr.229102

Kieu, T. L. V., Pierre, L., Perrey, S., Derangere, V., Truntzer, C., Jalil, A., et al. (2021). 164P Effect of ELOVL5 expression on breast cancer development. *Ann. Oncol.* 32, S432. doi:10.1016/j.annonc.2021.08.445

Kwa, M., Makris, A., and Esteva, F. J. (2017). Clinical utility of gene-expression signatures in early stage breast cancer. *Nat. Rev. Clin. Oncol.* 14, 595–610. doi:10.1038/nrclinonc.2017.74

Lafourcade, A., His, M., Baglietto, L., Boutron-Ruault, M.-C., Dossus, L., and Rondeau, V. (2018). Factors associated with breast cancer recurrences or mortality and dynamic prediction of death using history of cancer recurrences: The French E3N cohort. *BMC Cancer* 18, 171. doi:10.1186/s12885-018-4076-4

Lee, J.-Y., Nam, M., Son, H. Y., Hyun, K., Jang, S. Y., Kim, J. W., et al. (2020). Polyunsaturated fatty acid biosynthesis pathway determines ferroptosis sensitivity in gastric cancer. *Proc. Natl. Acad. Sci.* 117, 32433–32442. doi:10.1073/pnas.2006828117

Leonard, A. E., Bobik, E. G., Dorado, J., Kroeger, P. E., Chuang, L. T., Thurmond, J. M., et al. (2000). Cloning of a human cDNA encoding a novel enzyme involved in the elongation of long-chain polyunsaturated fatty acids. *Biochem. J.* 350 (3), 765–770. doi:10.1042/bj3500765

Leonard, A. E., Pereira, S. L., Sprecher, H., and Huang, Y.-S. (2004). Elongation of long-chain fatty acids. *Prog. Lipid Res.* 43, 36–54. doi:10.1016/S0163-7827(03)00040-7

Li, J., Cao, F., Yin, H., Huang, Z., Lin, Z., Mao, N., et al. (2020). Ferroptosis: Past, present and future. *Cell Death Dis.* 11, 88. doi:10.1038/s41419-020-2298-2

Li, S., Zhou, C., Zhu, Y., Chao, Z., Sheng, Z., Zhang, Y., et al. (2021). Ferrostatin-1 alleviates angiotensin II (Ang II)- induced inflammation and ferroptosis in astrocytes. *Int. Immunopharmacol.* 90, 107179. doi:10.1016/j.intimp.2020.107179

Liput, K. P., Lepczyński, A., Ogłuszka, M., Nawrocka, A., Poławska, E., Grzesiak, A., et al. (2021). Effects of dietary n–3 and n–6 polyunsaturated fatty acids in inflammation and cancerogenesis. *Int. J. Mol. Sci.* 22, 6965. doi:10.3390/ijms22136965

Liston, D. R., and Davis, M. (2017). Clinically relevant concentrations of anticancer drugs: A guide for nonclinical studies. *Clin. Cancer Res.* 23, 3489–3498. doi:10.1158/1078-0432.CCR-16-3083

Liu, J. J., Green, P., John Mann, J., Rapoport, S. I., and Sublette, M. E. (2015). Pathways of polyunsaturated fatty acid utilization: Implications for brain function in neuropsychiatric health and disease. *Brain Res.* 1597, 220–246. doi:10.1016/j.brainres.2014.11.059

Loi, S., Haibe-Kains, B., Desmedt, C., Wirapati, P., Lallemand, F., Tutt, A. M., et al. (2008). Predicting prognosis using molecular profiling in estrogen receptor-positive breast cancer treated with tamoxifen. *BMC Genomics* 9, 239. doi:10.1186/1471-2164-9-239

Longhitano, L., Forte, S., Orlando, L., Grasso, S., Barbato, A., Vicario, N., et al. (2022). The crosstalk between GPR81/IGFBP6 promotes breast cancer progression by modulating lactate metabolism and oxidative stress. *Antioxidants* 11, 275. doi:10.3390/antiox11020275

Lv, Z., Wang, J., Wang, X., Mo, M., Tang, G., Xu, H., et al. (2021). Identifying a ferroptosis-related gene signature for predicting biochemical recurrence of prostate cancer. *Front. Cell Dev. Biol.* 9, 1–19. doi:10.3389/fcell.2021.666025

Maltseva, D., Raygorodskaya, M., Knyazev, E., Zgoda, V., Tikhonova, O., Zaidi, S., et al. (2020). Knockdown of the α5 laminin chain affects differentiation of colorectal cancer cells and their sensitivity to chemotherapy. *Biochimie* 174, 107–116. doi:10.1016/j.biochi.2020.04.016

Maltseva, D. V., Khaustova, N. a., Fedotov, N. N., Matveeva, E. O., Lebedev, A. E., Shkurnikov, M. U., et al. (2013). High-throughput identification of reference genes for research and clinical RT-qPCR analysis of breast cancer samples. *J. Clin. Bioinforma.* 3, 13. doi:10.1186/2043-9113-3-13

Miller, L. D., Smeds, J., George, J., Vega, V. B., Vergara, L., Ploner, A., et al. (2005). An expression signature for p53 status in human breast cancer predicts mutation status, transcriptional effects, and patient survival. *Proc. Natl. Acad. Sci.* 102, 13550–13555. doi:10.1073/pnas.0506230102

Moon, Y.-A., and Horton, J. D. (2003). Identification of two mammalian reductases involved in the two-carbon fatty acyl elongation cascade. *J. Biol. Chem.* 278, 7335–7343. doi:10.1074/jbc.M211684200

Moon, Y., Hammer, R. E., and Horton, J. D. (2009). Deletion of ELOVL5 leads to fatty liver through activation of SREBP-1c in mice. *J. Lipid Res.* 50, 412–423. doi:10.1194/jlr.M800383-JLR200

Munir, R., Lisec, J., Swinnen, J. V., and Zaidi, N. (2019). Lipid metabolism in cancer cells under metabolic stress. *Br. J. Cancer* 120, 1090–1098. doi:10.1038/s41416-019-0451-4

Naganuma, T., Sato, Y., Sassa, T., Ohno, Y., and Kihara, A. (2011). Biochemical characterization of the very long-chain fatty acid elongase ELOVL7. *FEBS Lett.* 585, 3337–3341. doi:10.1016/j.febslet.2011.09.024

Nikulin, S. V., Raigorodskaya, M. P., Poloznikov, A. A., Zakharova, G. S., Schumacher, U., Wicklein, D., et al. (2018). *In vitro* model for studying of the role of IGFBP6 gene in breast cancer metastasizing. *Bull. Exp. Biol. Med.* 164, 688–692. doi:10.1007/s10517-018-4060-7

Nikulin, S., Zakharova, G., Poloznikov, A., Raigorodskaya, M., Wicklein, D., Schumacher, U., et al. (2021). Effect of the expression of ELOVL5 and IGFBP6 genes on the metastatic potential of breast cancer cells. *Front. Genet.* 12, 662843. doi:10.3389/fgene.2021.662843

Owczarzy, R., Tataurov, A. V., Wu, Y., Manthey, J. A., McQuisten, K. A., Almabrazi, H. G., et al. (2008). IDT SciTools: A suite for analysis and design of nucleic acid oligomers. *Nucleic Acids Res.* 36, W163–W169. doi:10.1093/nar/gkn198

Pfaffl, M. W., Horgan, G. W., and Dempfle, L. (2002). Relative expression software tool (REST) for group-wise comparison and statistical analysis of relative expression results in real-time PCR. *Nucleic Acids Res.* 30, e36. doi:10.1093/nar/30.9.e36

Sawai, H., and Domae, N. (2011). Discrimination between primary necrosis and apoptosis by necrostatin-1 in Annexin V-positive/propidium iodide-negative cells. *Biochem. Biophys. Res. Commun.* 411, 569–573. doi:10.1016/j.bbrc.2011.06.186

Schley, P. D., Jijon, H. B., Robinson, L. E., and Field, C. J. (2005). Mechanisms of omega-3 fatty acid-induced growth inhibition in MDA-MB-231 human breast cancer cells. *Breast Cancer Res. Treat.* 92, 187–195. doi:10.1007/s10549-005-2415-z

Schwankhaus, N., Gathmann, C., Wicklein, D., Riecken, K., Schumacher, U., and Valentiner, U. (2014). Cell adhesion molecules in metastatic neuroblastoma models. *Clin. Exp. Metastasis* 31, 483–496. doi:10.1007/s10585-014-9643-8

Seibt, T. M., Proneth, B., and Conrad, M. (2019). Role of GPX4 in ferroptosis and its pharmacological implication. *Free Radic. Biol. Med.* 133, 144–152. doi:10.1016/j.freeradbiomed.2018.09.014

Stockwell, B. R., Friedmann Angeli, J. P., Bayir, H., Bush, A. I., Conrad, M., Dixon, S. J., et al. (2017). Ferroptosis: A regulated cell death nexus linking metabolism, redox biology, and disease. *Cell* 171, 273–285. doi:10.1016/j.cell.2017.09.021

Su, Y., Zhao, B., Zhou, L., Zhang, Z., Shen, Y., Lv, H., et al. (2020). Ferroptosis, a novel pharmacological mechanism of anti-cancer drugs. *Cancer Lett.* 483, 127–136. doi:10.1016/j.canlet.2020.02.015

Sun, Y., Zheng, Y., Wang, C., and Liu, Y. (2018). Glutathione depletion induces ferroptosis, autophagy, and premature cell senescence in retinal pigment epithelial cells. *Cell Death Dis.* 9, 753. doi:10.1038/s41419-018-0794-4

Sung, H., Ferlay, J., Siegel, R. L., Laversanne, M., Soerjomataram, I., Jemal, A., et al. (2021). Global cancer statistics 2020: GLOBOCAN estimates of incidence and mortality worldwide for 36 cancers in 185 countries. *Ca. Cancer J. Clin.* 71, 209–249. doi:10.3322/caac.21660

Tomida, S., Goodenowe, D. B., Koyama, T., Ozaki, E., Kuriyama, N., Morita, M., et al. (2021). Plasmalogen deficiency and overactive fatty acid elongation biomarkers in serum of breast cancer patients pre- and post-surgery—new insights on diagnosis, risk assessment, and disease mechanisms. *Cancers (Basel).* 13, 4170. doi:10.3390/cancers13164170

Valianpour, F., Selhorst, J. J. M., van Lint, L. E. M., van Gennip, A. H., Wanders, R. J. A., and Kemp, S. (2003). Analysis of very long-chain fatty acids using electrospray ionization mass spectrometry. *Mol. Genet. Metab.* 79, 189–196. doi:10.1016/S1096-7192(03)00098-2

Vandesompele, J., De Preter, K., Pattyn, F., Poppe, B., Van Roy, N., De Paepe, A., et al. (2002). Accurate normalization of real-time quantitative RT-PCR data by geometric averaging of multiple internal control genes. *Genome Biol.* 3, RESEARCH0034. doi:10.1186/gb-2002-3-7-research0034

Viswanathan, V. S., Ryan, M. J., Dhruv, H. D., Gill, S., Eichhoff, O. M., Seashore-Ludlow, B., et al. (2017). Dependency of a therapy-resistant state of cancer cells on a lipid peroxidase pathway. *Nature* 547, 453–457. doi:10.1038/nature23007

Wang, H., Airola, M. V., and Reue, K. (2017). How lipid droplets "TAG" along: Glycerolipid synthetic enzymes and lipid storage. *Biochim. Biophys. Acta - Mol. Cell Biol. Lipids* 1862, 1131–1145. doi:10.1016/j.bbalip.2017.06.010

Wang, H., Lin, D., Yu, Q., Li, Z., Lenahan, C., Dong, Y., et al. (2021a). A promising future of ferroptosis in tumor therapy. *Front. Cell Dev. Biol.* 9, 1–13. doi:10.3389/fcell.2021.629150

Wang, H., Wang, P., and Zhu, B. T. (2022). Mechanism of erastin-induced ferroptosis in MDA-MB-231 human breast cancer cells: Evidence for a critical role of protein disulfide isomerase. *Mol. Cell. Biol.* 42, e0052221. doi:10.1128/mcb.00522-21

Wang, Y., Torres-Gonzalez, M., Tripathy, S., Botolin, D., Christian, B., and Jump, D. B. (2008). Elevated hepatic fatty acid elongase-5 activity affects multiple pathways controlling hepatic lipid and carbohydrate composition. *J. Lipid Res.* 49, 1538–1552. doi:10.1194/jlr.M800123-JLR200

Wang, Y., Xia, H., Chen, Z., Meng, L., and Xu, A. (2021b). Identification of a ferroptosis-related gene signature predictive model in colon cancer. *World J. Surg. Oncol.* 19, 135. doi:10.1186/s12957-021-02244-z

Weber, K., Mock, U., Petrowitz, B., Bartsch, U., Fehse, B., and Bartsch, U. (2010). Lentiviral gene ontology (LeGO) vectors equipped with novel drug-selectable fluorescent proteins: New building blocks for cell marking and multi-gene analysis. *Gene Ther.* 17, 511–520. doi:10.1038/gt.2009.149

Weber, K., Thomaschewski, M., Benten, D., and Fehse, B. (2012). RGB marking with lentiviral vectors for multicolor clonal cell tracking. *Nat. Protoc.* 7, 839–849. doi:10.1038/nprot.2012.026

Weinstein, J. N., Collisson, E. A., Mills, G. B., Shaw, K. R. M., Ozenberger, B. A., Ellrott, K., et al. (2013). The cancer Genome Atlas pan-cancer analysis project. *Nat. Genet.* 45, 1113–1120. doi:10.1038/ng.2764

Wlodkowic, D., Skommer, J., and Darzynkiewicz, Z. (2009). "Flow cytometry-based apoptosis detection," in Business *methods in molecular biology*. Editors P. Erhardt, and A. Toth (Totowa, NJ: Humana Press), 19–32. doi:10.1007/978-1-60327-017-5_2

Wu, Y., Yu, C., Luo, M., Cen, C., Qiu, J., Zhang, S., et al. (2020). Ferroptosis in cancer treatment: Another way to rome. *Front. Oncol.* 10, 571127. doi:10.3389/fonc.2020.571127

Yang, B., Ren, X.-L., Fu, Y.-Q., Gao, J.-L., and Li, D. (2014). Ratio of n-3/n-6 PUFAs and risk of breast cancer: A meta-analysis of 274135 adult females from 11 independent prospective studies. *BMC Cancer* 14, 105. doi:10.1186/1471-2407-14-105

Ye, J., Coulouris, G., Zaretskaya, I., Cutcutache, I., Rozen, S., and Madden, T. L. (2012). Primer-BLAST: A tool to design target-specific primers for polymerase chain reaction. *BMC Bioinforma.* 13, 134. doi:10.1186/1471-2105-13-134

Yee, L. D., Lester, J. L., Cole, R. M., Richardson, J. R., Hsu, J. C., Li, Y., et al. (2010). Omega-3 fatty acid supplements in women at high risk of breast cancer have dose-dependent effects on breast adipose tissue fatty acid composition. *Am. J. Clin. Nutr.* 91, 1185–1194. doi:10.3945/ajcn.2009.29036

Yu, M., Gai, C., Li, Z., Ding, D., Zheng, J., Zhang, W., et al. (2019). Targeted exosome-encapsulated erastin induced ferroptosis in triple negative breast cancer cells. *Cancer Sci.* 110, 3173–3182. doi:10.1111/cas.14181

Zhang, C., Yu, H., Shen, Y., Ni, X., Shen, S., and Das, U. N. (2015). Polyunsaturated fatty acids trigger apoptosis of colon cancer cells through a mitochondrial pathway. *Arch. Med. Sci.* 11, 1081–1094. doi:10.5114/aoms.2015.54865

Zhang, W., Chen, R., Yang, T., Xu, N., Chen, J., Gao, Y., et al. (2018). Fatty acid transporting proteins: Roles in brain development, aging, and stroke. *Prostagl. Leukot. Essent. Fat. Acids* 136, 35–45. doi:10.1016/j.plefa.2017.04.004

Zheng, J.-S., Hu, X.-J., Zhao, Y.-M., Yang, J., and Li, D. (2013). Intake of fish and marine n-3 polyunsaturated fatty acids and risk of breast cancer: meta-analysis of data from 21 independent prospective cohort studies. *BMJ* 346, f3706. doi:10.1136/bmj.f3706

Zhou, Y., Wang, T., Zhai, S., Li, W., and Meng, Q. (2016). Linoleic acid and breast cancer risk: A meta-analysis. *Public Health Nutr.* 19, 1457–1463. doi:10.1017/S136898001500289X

frontiers | Frontiers in Molecular Biosciences

TYPE Review
PUBLISHED 13 January 2023
DOI 10.3389/fmolb.2022.1068437

OPEN ACCESS

EDITED BY
Xin Wang,
National Institutes of Health (NIH), United States

REVIEWED BY
Wenqiang Li,
First Affiliated Hospital of Zhengzhou University, China
Jianhua Peng,
The Affiliated Hospital of Southwest Medical University, China

*CORRESPONDENCE
Hu Zhou,
602856636@qq.com
Tao Li,
taoli_kh@163.com

†These authors have contributed equally to this work

SPECIALTY SECTION
This article was submitted to Molecular Diagnostics and Therapeutics, a section of the journal Frontiers in Molecular Biosciences

RECEIVED 12 October 2022
ACCEPTED 02 December 2022
PUBLISHED 13 January 2023

CITATION
Lu Q, Lu X, Zhang Y, Huang W, Zhou H and Li T (2023), Recent advances in ferroptosis and therapeutic strategies for glioblastoma.
Front. Mol. Biosci. 9:1068437.
doi: 10.3389/fmolb.2022.1068437

Recent advances in ferroptosis and therapeutic strategies for glioblastoma

Qixiong Lu[1†], Xiaoyang Lu[2†], Yuansheng Zhang[1†], Wei Huang[2], Hu Zhou[2*] and Tao Li[2*]

[1]The Affiliated Hospital of Kunming University of Science and Technology, Department of Neurosurgery, The First People's Hospital of Yunnan Province, Kunming, Yunnan, China, [2]Department of Neurosurgery, The First People's Hospital of Yunnan Province, The Affiliated Hospital of Kunming University of Science and Technology, Kunming, Yunnan, China

Ferroptosis is an emerging form of cell death characterized by the over-accumulation of iron-dependent lipid peroxidation. Ferroptosis directly or indirectly disturbs glutathione peroxidases cycle through diverse pathways, impacting the cellular antioxidant capacities, aggravating accumulation of reactive oxygen species in lipid, and it finally causes oxidative overload and cell death. Ferroptosis plays a significant role in the pathophysiological processes of many diseases. Glioblastoma is one of the most common primary malignant brain tumors in the central nervous system in adults. Although there are many treatment plans for it, such as surgical resection, radiotherapy, and chemotherapy, they are currently ineffective and the recurrent rate is almost up to 100%. The therapies abovementioned have a strong relationship with ferroptosis at the cellular and molecular level according to the results reported by numerous researchers. The regulation of ferroptosis can significantly determine the outcome of the cells of glioblastoma. Thus ferroptosis, as a regulated form of programed cell death, has the possibility for treating glioblastoma.

KEYWORDS

ferroptosis, glioblastoma, iron metabolism, chemotherapy, radiotherapy, immunotherapy

Introduction

Ferroptosis is an emerging form of regulatable programed cell death compared with apoptosis, necroptosis, and pyroptosis [(Zhang et al., 2021a); (Shi et al., 2022a); (Zhou et al., 2019); (Bertheloot et al., 2021); (Li and Huang, 2022)]. In 2012, Dixon et al. named this regulatable cell death mode which could be inhibited by iron chelating agent as iron death on the basis of summarizing previous studies on cell deaths (Dixon et al., 2012). It is a metabolic process (Xu et al., 2021), not an active one that requires transcription induction or post-translational modification by specific death effectors in response to lethal stimuli. On the contrary, it is considered to be part of cell destruction or cell clearance.

Different from the previously described cell death modes, ferroptosis showed necrosis-like morphology: shrunk mitochondria, increased membrane density and narrowed crista, and ruptured cell membrane, whereas morphological changes were not evident in the nucleus; this kind of programmed cell death is initiated by abnormal metabolism of iron ions in cells, which causes the breakdown of the steady state of oxidoreduction reaction. The inhibition of the synthesis of reduced glutathione (GSH) and the intensification of oxidation reaction are the main causes of ferroptosis. A series of reactions that cause ferroptosis are iron dependent, triggered by intracellular changes in iron metabolism, leading to lipid peroxidation and finally cell death. (Lu et al., 2017; Mou et al., 2020; Aguilera et al., 2022). This mechanism is involved in pathophysiological conditions (Tang et al., 2018), including inflammation, tissue injuries, and cancerous transformation (Zhang et al., 2021a), among which glioblastoma (GBM) is one.

GBM, known for its devastating progression and dismal prognosis (Martínez-Garcia et al., 2018), is the most common primary malignant brain tumor in adults and accounts for over 50% of all high-grade gliomas (Martínez-Garcia et al., 2018). Its main characteristics are high malignancy, aggressive invasion, frequent brain or spinal cord metastasis and inevitable recurrence (Gu et al., 2016). According to the WHO grading system, GBM is classified as a Grade IV astrocytoma consisting of mostly low differentiated neoplastic astrocytes mixed with cells having different extent of differentiation (Ou-Yang et al., 2018) This is mainly due to the coexistence of multiple tumor cell populations with different degrees of differentiation, especially tumor cells that showing stem cell-like characteristics (Wang et al., 2019). Glioma stem cells have pretty strong renewal ability (Adamo et al., 2017), low differentiation, and high resistance to radiation and chemotherapy [(Broadley et al., 2011); (Sesé et al., 2022); (Liu et al., 2017)]. At present, there is no effective drug to treat it efficaciously, and surgery can only resect part of the tumor if it locates at functional or cranial base areas. Even if it can be removed completely with a negative intraoperative pathological edge, it virtually recurs through the mechanism we have not known yet. Therefore, the treatment scheme for recurrence can only remove the tumor to the maximum extent, and then carry out subsequent adjuvant chemotherapy and radiotherapy to destroy the tumor cells and inhibit the growth of tumor cells as much as possible (Berardinelli et al., 2019). However, the residual tumor cells are very easy to generate tolerance to radiotherapy and chemotherapy, and thus the recurrence rate of the tumor is as high as 100% [(Chanez et al., 2022); (Dissaux et al., 2021)]. After a series of changes in the internal structure of recurrent tumor cells, clonal evolution trees showed higher heterogeneity (Yang et al., 2020), and their malignancy is higher than the first time; that may be the reason why now no clinically available methods can effectively treat it. The average survival time of GBM patients after diagnosis is 12–15 months (Shi et al., 2015). It is urgent to develop molecular targeted drugs that are capable of effectively controlling the growth of GBM tumor cells based on their metabolic pathways.

Although few studies on the relationship between ferroptosis and GBM have been reported, especially using ferroptosis as a treatment or/and diagnostic method and the exploration of the relevant mechanism on cell death, recurrence and drug resistance between the two. We believe it is valuable to discuss this issue and it is what we attempted to deliver through this review.

Iron metabolism affects the ferroptosis

Iron is a vital element for the survival of organisms. It is indispensable for the metabolism of many substances in the body [(Dutt et al., 2022); (Stallhofer et al., 2022)]. Iron in the digestive tract is mainly absorbed in the duodenum and upper jejunum in the form of Fe^{2+} (Karaskova et al., 2021). Then, in the epithelial cells of small intestinal mucosa, Fe^{2+} is oxidized to Fe^{3+}, and part of Fe^{3+} in the blood is further bound to the transported by transferrin (TF) and receptor (TFR) on the cell membrane and transported into the cell [(Piskin et al., 2022); (Zhao et al., 2022)], which reacts with the metal reductase Six-transmembrane epithelial antigen of prostate 3 (STEAP3) in the endoplasmic reticulum to form Fe^{2+}; Fe^{2+} is transported to cells through transferrin receptor protein 1 (TFR1). The body regulates the storage of iron ions through the expression of ferritin and its related genes according to its own needs, such as ferritin heavy chain 1 (FTH1), ferritin light chain (FTL) and heat shock protein B1 (HSPB1) (Yang et al., 2022a); HSPB1 inhibits the expression of TFR1, thereby reducing the intracellular iron concentration. Therefore, overexpression of HSPB1 will inhibit ferroptosis [(Yuan et al., 2022); (Liu et al., 2021)]. In addition, the expression of FTL and FTH1 is regulated by iron responsive element binding protein 2 (IREBP2), and the overexpression of IREBP2 will inhibit iron death induced by erastin as well. The biological toxicity of iron ions is mediated by Fenton reaction, which transforms Fe^{2+} into Fe^{3+} and generates hydroxyl radicals, oxidative proteins et cetera (Zhang et al., 2022a; Gong et al., 2022). Knockout of *Tf* gene or down-regulation of TF can inhibit iron overload and cell apoptosis. Autophagy can regulate the amount of transferrin and lipid in cells to regulate iron metabolism, and ultimately affect iron death sensitivity, while ferritin selective autophagy can also regulate fine ferroptosis sensitivity. Other proteins may as well affect iron sensitivity in iron metabolism (Zhu and Fan, 2021) (Figure 1).

Lipid metabolism and reactive oxygen species accumulation regulate ferroptosis

Under normal circumstances, the substance in the organism is in a dynamic change process. When the body is disturbed by

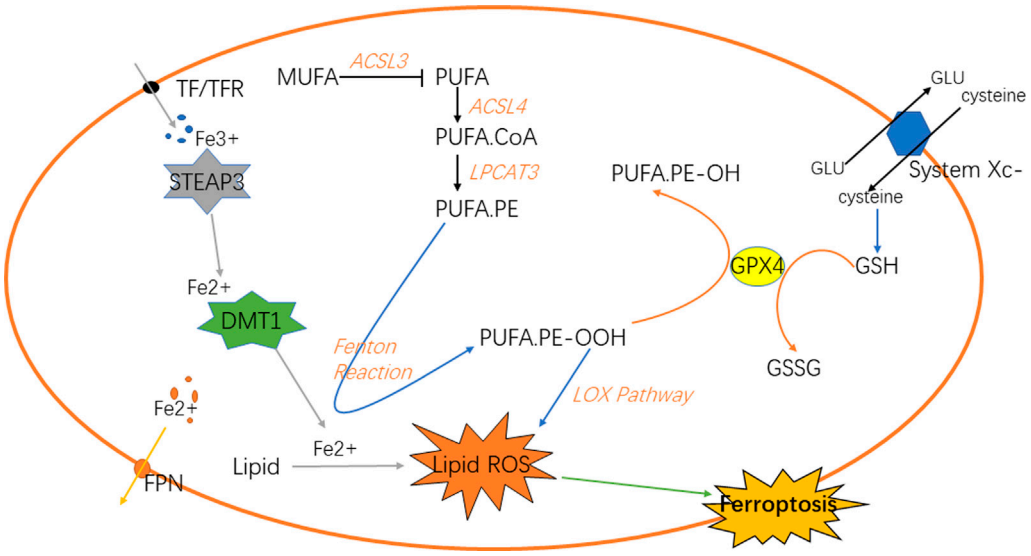

FIGURE 1
Classic signaling pathways of ferroptosis in cells.

external or internal irresistible stimulus, the balance of homeostasis will be impaired (Badr et al., 2020). For example, oxidoreduction reaction disbalance and production of reactive oxygen species (ROS) in GBM (Reichert et al., 2020), the normal physiological conditions are disturbed, and the antioxidant capacity of cells will be relatively reduced (Burić et al., 2019; McNamee et al., 2021). A series of chain reactions of peroxidation will lead to the accumulation of lipid peroxidation in cells. Lipid peroxidation is a key step in ferroptosis (Lee and Roh, 2022), which can be divided into the synthesis of phospholipids with polyunsaturated fatty acids (PUFAs) as the substrate and the two peroxidation reactions. PUFAs are the key substances in lipid peroxidation (Yang et al., 2016). Firstly, PUFA.coenzyme A (PUFA.CoA) was synthesized with PUFAs under the action of acetyl CoA synthetase long-chain family member 4 (ACSL4) and then PUFA-phospholipids (PUFA-PL) was generated under the action of lysophospholipidacyltransferase 3 (LPCAT3) and incorporated into the cell components. PUFA-PL will participate in the next series of chain reactions as the substrate of peroxidation. Next, it can be divided into two ways to generate free radicals with strong oxidation capacity. Fenton reaction and lipoxygenase pathway will generate a large number of hydroxyl radicals and oxygen radicals (Xing et al., 2021). These free radicals will attack PUFA-PL, forming a cycle of peroxidation. Because cells are in a state of imbalance, this reaction will be terminated only when the substrate is exhausted. As one of the components of cells, its large consumption will inevitably lead to the damage of cell structure. In the lipoxygenase pathway (Tomita et al., 2019), 15-lipoxygenase (15-LOX) first combines with phosphatidylethanolamine binding protein 1 (PEBP1), and then oxidizes PUFA on the cell membrane to PUFA.phosphatidylethanolamines-OOH (PUFA.PE-OOH), thus causing ferroptosis (Kagan et al., 2020; Anthonymuthu et al., 2021; Mikulska-Ruminska et al., 2021). In addition to the end-products that will destroy the normal structure of cells and generate lipid peroxidation (Chng et al., 2021), the above peroxidation reactions will also produce some cytotoxic active aldehydes, which will attack phospholipids, proteins and even nucleic acids in cells (Gao et al., 2018; Liu et al., 2020; Zhao et al., 2020). NF-E2-relatedfactor2 (NRF2) plays an important role in regulating the homeostasis of cells and a key factor in oxidoreduction reaction (Zhang et al., 2016; Fan et al., 2017). Relevant studies have shown that when NRF2 is up-regulated in tumors, it is closely related to the poor prognosis of primary malignant brain tumors (Chew et al., 2021); the NRF2-Keap1 system regulates the expression of human antioxidant proteins, which is a typical antioxidant reaction pathway. Fe^{2+} is regulated by NRF2. Normally, it is inactive. When the intracellular peroxide increases, it will stimulate NRF2 to activate the downstream antioxidant enzymes to inhibit the oxidation reaction. Glutathione peroxidase 4 (GPX4) is also a key factor in the antioxidant system, which converts the lipid peroxide into non-toxic aliphatic alcohol and reduces H_2O_2 (Shin et al., 2018; Wu et al., 2022).

Lipid peroxidation in ferroptosis is regulated by several regulatory axes. Among them, GPX4 is recognized as the key

regulatory target (Hayashima and Katoh, 2022). GSH and GPX4 in the signal axis of cystine/glutathione/glutathione peroxidase 4 can associate with each other to reduce PUFA-PL-OOH to PUFA-PL-OH, resultantly preventing the continuation of ferroptosis (Li et al., 2022a). Cystine is one of the components of glutathione, which requires the reverse transporter system Xc- to transport from outside the cell. Therefore, this transporter is also an important site for regulating ferroptosis. The signal axis of ferroptosis suppressor protein 1 (FSP1) and coenzyme Q10 (CoQ10) is also one of the regulatory sites of ferroptosis. When the GPX4 system is lacking (Doll et al., 2019), the increased expression of FSP1 can up-regulate the NADH dependent CoQ10 reduction reaction, so that the oxygen free radicals in the peroxidation cycle reaction caused by it are reduced to prevent ferroptosis (Santoro, 2020; Yang et al., 2022b). GTP cyclohydrolase 1 (GCH1)/tetrahydrobiopterin (BH4)/dihydrofolate reductase (DHFR) signal axis, in which the overexpression of GCH1 can selectively protect membrane phospholipids with two PUFA tails from peroxidation, preventing ferroptosis from occurring as well (Hu et al., 2022; Jiang et al., 2022) (Figure 1).

Immunotherapy for glioblastoma

Iron is pivotal for cell survival. Cancer cells are more prone to undergo ferroptosis than normal cells, and oxidized membrane lipids on ferroptotic cells can mediate the phagocytosis of macrophages to keep immune response. In addition, immune detection point inhibitor treatment may make cancer cells sensitive to ferroptosis (Shi et al., 2022b), it is expected to overcome chemical resistance and strengthen the death of immunogenicity cells. Enhanced ferroptosis was shown to induce activation and infiltration of immune cells, but to weaken the cytotoxicity of anti-tumor cells. It was found that tumor-associated macrophages were involved in ferroptosis-mediated immunosuppression (Liu et al., 2022a), which provides a new vision for immunotherapy for GBM (Yu et al., 2022).

Inhibition of asparagine-linked glycosylation 3 (ALG3) stimulates cancer cell immunogenic ferroptosis to potentiate immunotherapy. ALG3 is an a-1, 3-mannosyltransferase involved in protein glycosylation in the endoplasmic reticulum. Liu et al. reported that inhibition of ALG3 would induce defects in post-translational N-linked glycosylation modification and lead to excessive lipid accumulation through sterol regulatory element binding proteins (SREBPs)-dependent adipogenesis in cancer cells. Lipid peroxidation mediated by N-linked glycosylation deficiency induces the immunogenic ferroptosis of cancer cells and promotes the pro-inflammatory microenvironment, thus enhancing the anti-tumor immune response (Liu et al., 2022b).

Ir(III) complex containing a ferrocene-modified diphosphine ligand that localizes in lysosomes. Under the acidic environments of lysosomes, Ir(III) can effectively catalyze a Fenton-like reaction, produce hydroxyl radicals, induce lipid peroxidation, down-regulate GPX4, resulting in ferroptosis, and thus inhibit tumor cell growth (Wang et al., 2022).

In recent years, immunotherapy has raised fervent attention. One strategy is to activate lymphocytes that can recognize the tumor cells specifically and induce the cancer cells' death by releasing perforin and granzyme. Accordingly, relevant studies pointed out that active $CD8^+$ T cells release IFNγ that down-regulate the expression of Solute carrier (SLC) family 7 member 11 (SLC7A11) and SLC family 3 member 2 (SLC3A2), thereby inhibiting the absorption of cystine and enhancing lipid peroxidation and ferroptosis of tumor cells (Figure 2).

Radiotherapy for glioblastoma

Ionizing radiation can produce a lot of free radicals in irradiated cells. These free radicals are the factors that cause side effects when ionizing radiation is used to treat diseases. Among them, lipid peroxidation is an important influence of ionizing radiation on cell membranes, which is one of the key targets of radiation. On the other hand, lipid peroxidation is an important metabolic pathway for ferroptosis. Therefore, the effect of ionizing radiation on tumor cells should be related to the ferroptotic process to a large extent (Agrawal and Kale, 2001). It was found that after radiotherapy, the tumor cells showed typical morphological changes of ferroptosis such as changed density of mitochondria, shrunk cell membranes, and decreased mitochondrial cristae. It indicates that radiotherapy can increase the expression of key enzymes by generating a large number of ROS, thus promoting lipid peroxidation, and ultimately leading to ferroptosis (Zhang et al., 2022b). CuS@mSiO_2@MnO_2 nanocomposite, as a radiosensitizer that can effectively exhaust GSH was used *in vitro*; it uses up GSH and induces ferroptosis and apoptosis. The experiment performed *in vivo* also showed that tumor cells were damaged. Therefore, it is speculated that radiotherapy may induce ferroptosis after the depletion of GSH to play its role in the treatment of tumors (Li et al., 2021) (Figure 2).

Chemotherapy for glioblastoma

Temozolomide (TMZ) is the first-line drug for clinical chemotherapy for GBM in recent decades. Although it is the most effective drug for GBM for now, resistance to it especially in recurrent GBM can be noted very common. Drug resistance is one of the most significant factors which bring about a poor prognosis. NRF2 is an important transcription factor involved in chemotherapy resistance, and it can play a key role in inducing ferroptosis through GSH regulation. According to the

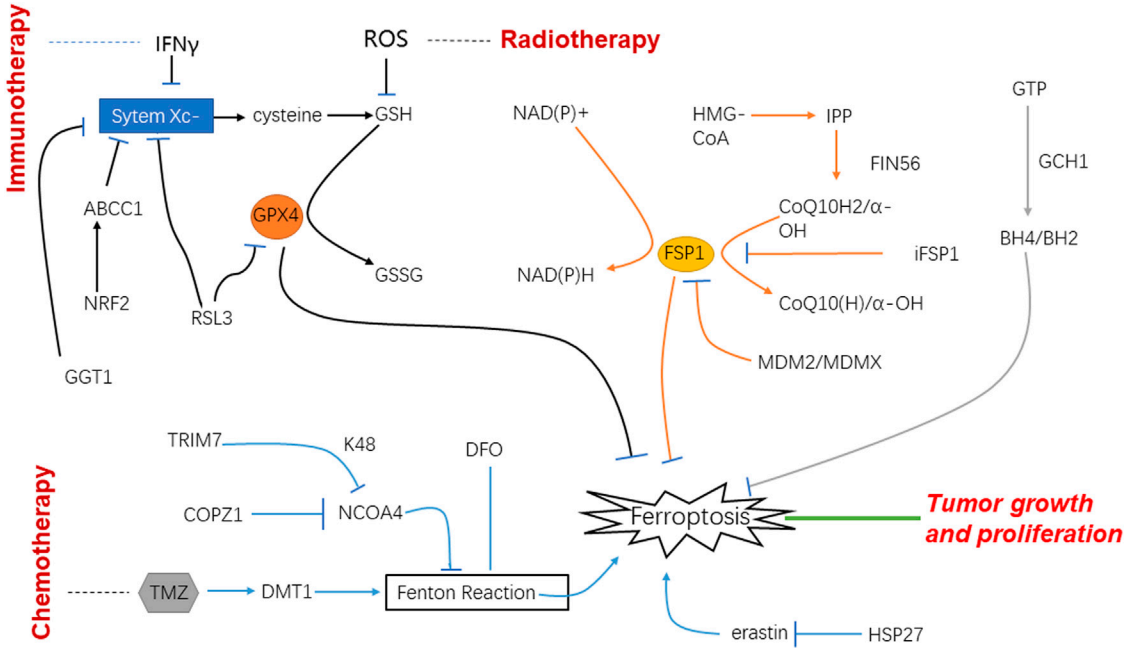

FIGURE 2
Schematic of mechanisms of ferroptosis and glioblastoma under the treatment of immunotherapy, radiotherapy and chemotherapy.

experimental data, high-level of NRF2 leads to the resistance to TMZ therapy for GBM through the up-regulation of ATP-binding cassette subfamily C member 1 (ABCC1) which is the target of NRF2 and able to antagonize ferroptosis. For this rationale, ferroptosis induction may be an important treatment strategy to reverse the drug resistance of GBM with high NRF2 and ABCC1 expression (de Souza et al., 2022). Most chemotherapy medicines exert efficacy on tumor cells through signaling transduction which are bound up with oxygen-free radicals and ROS; under the circumstance, ferroptosis will play important role in the therapy of malignant tumors. Nowadays, TMZ is a new medicine for GBM and considered the most effective one, and thus widely used for patients in clinical practice (Zhou and Ma, 2022). There have been *in vitro* studies using TG905 cells showing that the divalent metal transporter 1 (DMT1) and ROS in GBM increases when treated with TMZ, whereas GPX4 is decreased (Su et al., 2022), in the meantime it observes an iron-independent cells death. Thus, we have good reason to believe that TMZ can induce the ferroptosis by targeting the expression of DMT1 in GBM cells and inhibiting tumor cells growth (Song et al., 2021).

It is reported that heat shock protein 27 (HSP27) is the new regulator of ferroptosis in tumor cells (Liu et al., 2021); GBM cells are protected by overexpression of HSP27 to escape from ferroptosis that is induced by erastin (Yuan et al., 2022). Therefore, HSP27 can be a regulatory spot of ferroptosis and used as a potential therapy target for GBM.

Clinical studies have shown that programmed cell death one (PD-1)/programmed cell death ligand one (PD-L1) have low efficacy on GBM due to low immunogenicity. In the experiment, Fe_3O_4-siPD-L1@M-BV2 increases the siPD-L1 and Fe^{2+} of the drug-resistant GBM in mice tissue. Fe_3O_4-siPD-L1@M-BV2 is associated with ferroptosis and immune activation, inhibiting the growth of drug-resistant GBM (Liu et al., 2022c).

Chen et al. reported that IONP@PTX can inhibit cell migration and invasion after incubating with cells. They made the conclusion that the level of iron ions, ROS and lipid peroxidation in cells is increased, suggesting that IONP@PTX might affect GBM through ferroptosis. More importantly, the influence of IONP@PTX on GBM can be regulated by other external factors such as 3-methyladenine (3-MA) and rapamycin. Another advantage is that IONP@PTX has no obvious toxic effect on GBM xenotransplantation mice, which may make IONP@PTX a potential treatment for GBM with high safety based on ferroptosis (Chen and Wen, 2022).

Some scholars reported that NF-κB activation protein (NKAP) knockout will increase the level of lipid peroxidation in naive T cells and induce cell death in colon cancer cells. Another experiment showed the consistent results that knockout of NKAP induces the death of GBM; silencing NKAP increases the sensitivity of cells to iron death inducers, and exogenous overexpression of NAKP can positively regulate an iron death defense protein, SLC7A11 to reduce the sensitivity of cells to iron death inducers. RNA and protein immunoprecipitation can

prove that NKAP and N6-methyladenosine (m6A) interact on SLC7A11 transcription. Thus, inhibiting NKAP expression or knocking out its gene will increase the level of ferroptosis in cells, and may become a potential therapeutic direction to the treatment of GBM (Sun et al., 2022).

Ferroptosis is mainly caused by an imbalance of ROS and lipid peroxidation. One of the processes of lipid peroxidation can be inhibited by GPX4. In consequence, blocking the expression of GPX4 or reducing its production will greatly increase the degree of ferroptosis. γ-glutamine transferase 1 (GGT1) can inhibit the formation of the substrate in the process of synthesizing GPX4. Given this, GGT inhibitor is a potential treatment scheme for GBM, and it will be more effective if it is supplemented with iron death inducers (Hayashima and Katoh, 2022).

Based on the analysis of existing data, the overexpression of coatomer protein complex subunit zeta 1 (COPZ1) is related to the increase in tumor grade and poor prognosis of GBM patients. Via immunohistochemistry and western blot analysis, it is noted that the expression of COPZ1 protein in GBM was significantly higher than that in normal tissues. Knockout of *Copz1* gene using iRNA could inhibit the growth of GBM *in vitro*, but also lead to a series of intracellular metabolic disorders, including the imbalance of iron metabolism. Therefore, COPZ1 can be a key regulatory point of ferroptosis, and become a potential therapeutic target for GBM (Zhang et al., 2021b).

Dihydroartemisinin (DHA) has the advantages of selective cytotoxicity and low drug resistance. These characteristics make DHA one of the new research directions of anti-tumor therapy. Through the effect of DHA on normal cells and GBM, it is found that GPX4 in tumor cells is significantly reduced, ROS and peroxidative lipids are increased, and these effects can be reversed by using ferroptosis inhibitors, which demonstrates DHA can inhibit tumor growth by changing the intracellular GPX4 to cause ferroptosis. DHA is one of the potential drugs for GBM (Yi et al., 2020) (Figure 2).

Ferroptosis in glioblastoma

The main component of brain tissue is lipid. At present, there is no effective treatment for GBM, and the recurrence rate and mortality rate are nearly 100% (Mitre et al., 2022). Currently, ferroptosis as the research field remains many unrevealed areas, which may become a potentially effective treatment scheme. The brain is more vulnerable to oxidative stress than other tissues, because the activity of antioxidant enzymes is low and the content of PUFAs is high, which makes it prone to lipid peroxidation (Rao et al., 2000). The disorder of lipid metabolism is the key link of ferroptosis. It was found that expression of tripartite motif protein 7 (TRIM7) is more in GBM cells than in normal cells. When the TRIM7 is silent, the growth and development of the body is inhibited, but the level of ferroptosis is increased; while the TRIM7 is overexpressed, it can promote the growth and development of the body and inhibit the death of GBM cells. It can be concluded that when the ferroptosis level is inhibited, the death of GBM cells is also reduced, and there is a positive correlation between them. This experiment also indicates that when TRIM7 is missing, GBM is sensitive to the treatment of TMZ. As a potential treatment scheme for GBM, it is uncertain whether the sensitivity of TRIM7 to ferroptosis will make the treatment of TMZ more effective (Li et al., 2022b). Some experiments also found that the use of iron inducers can increase the sensitivity of TMZ. TMZ is a first-line drug for GBM (Song et al., 2021), and it is clear that its mechanism is to cause base pair mismatch, leading to cell apoptosis. However, several reports suggest that, it can activate nuclear factor NRF2 and transcription factor 4 (ATF4) at the same time to inhibit iron death. To sum up, ferroptosis participated not only in the sensitivity of TMZ in the treatment of GBM, but also in the formation of drug resistance (Chen et al., 2017; Hu et al., 2020; Li et al., 2022b; de Souza et al., 2022). Iron overload is another key link of ferroptosis. The high degree of malignancy of tumors is characterized by rapid growth and proliferation and strong invasiveness. Genes and proteins related to growth and development are overexpressed, such as poly(C)-binding protein 2 (PCBP2), DMT1, STEAP3, FTH and FTL, which can change iron storage capacity (Cheng et al., 2018); the expression of TF and TFR also increased significantly. A large amount of free iron would be transported and absorbed into the cells through selective endocytosis, and excessive iron would increase lipid peroxidation accordingly. In GBM cells with overloaded iron and rich PUFAs, plenty of peroxides can rapidly accumulate and lead to ferroptosis (Park et al., 2019). STEAP3 can promote TFR1 expression and increase cell iron content by activating STAT3-forkhead box protein M1 (FOXM1) axis (Sendamarai et al., 2008; Isobe et al., 2011), thus inducing epithelial mesenchymal transformation (EMT) in GBM, which is a route for GBM invasion and metastasis (Chang et al., 2017; Terry et al., 2017).

Expectation

Ferroptosis is a newly discovered iron dependent programmed cell death in recent years, which is different from apoptosis, necrosis and necroptosis. It has a unique mechanism of occurrence and effectiveness. It will be a potential therapeutic scheme in tumor treatment, and more and more targeted ferroptosis therapies are under study. Relevant pharmaceutical industries are also actively exploring the specific mechanism of iron death, trying to link it with cancer treatment to find a breakthrough. So far, although ferroptosis has made some theoretical achievements and curative effect in animal experiments, it has not made virtual progress. As aforementioned, some scholars proposed even contradictory conclusions. Some pointed out that TMZ

treatment could strengthen ferroptosis and might be one of the mechanisms of tumor cell killing, whereas other researchers opposed this kind of conclusion and observed the opposite that TMZ might inhibit ferroptosis to result in drug resistance. This is an interesting phenomenon, and we speculate that TMZ treatment indeed up-regulates ferroptosis and causes the death of tumor cells. However, at the late stage of the course, the GBM cells may induce numerous ferroptotic inhibitors and the ferroptosis is significantly suppressed. This is worthy of being studied in the future. GBM, as one of the most common primary malignant tumors in adults, has not only a high recurrence rate but also an approximately mortality rate of 100%. Increasing evidence indicates that ferroptosis plays a certain role in immunotherapy, radiotherapy and chemotherapy for GBM. However, the research on its regulation and the mechanism of ferroptosis treatment has not made significant progress. It is still necessary to take persistent efforts to clarify the mechanism of the relationship between ferroptosis and GBM, to provide new ideas for the treatment, and in the meantime to bring up prevention or early diagnosis methods.

Author contributions

QL, XL, and YZ initiated the idea and wrote the manuscript; WH made valuable suggestions; HZ and TL revised the paper and coordinated the study and are shared correspondence.

Funding

This work was funded by the National Natural Science Foundation of China (Grant No. 82001278), The Fund for Young Doctors with the First People's Hospital of Yunnan Province (Grant No. KHBS-2020-014), Yunnan Fundamental Research Projects (Grant No. 202101AU070106), and Joint Projects of Yunnan Provincial Science and Technology Department and Kunming Medical University for Applied Basic Research (Grant No. 202101AY070001-252), The Fund for Young Doctors with the First People's Hospital of Yunnan Province (Grant No. KHBS-2022-018).

Conflict of interest

The authors declare that the research was conducted in the absence of any commercial or financial relationships that could be construed as a potential conflict of interest.

Publisher's note

All claims expressed in this article are solely those of the authors and do not necessarily represent those of their affiliated organizations, or those of the publisher, the editors and the reviewers. Any product that may be evaluated in this article, or claim that may be made by its manufacturer, is not guaranteed or endorsed by the publisher.

References

Adamo, A., Fiore, D., De Martino, F., Roscigno, G., Affinito, A., Donnarumma, E., et al. (2017). RYK promotes the stemness of glioblastoma cells via the WNT/β-catenin pathway. *Oncotarget* 8, 13476–13487. doi:10.18632/oncotarget.14564

Agrawal, A., and Kale, R. K. (2001). Radiation induced peroxidative damage: Mechanism and significance. *Indian J. Exp. Biol.* 39, 291–309.

Aguilera, A., Berdun, F., Bartoli, C., Steelheart, C., Alegre, M., Bayir, H., et al. (2022). C-ferroptosis is an iron-dependent form of regulated cell death in cyanobacteria. *J. Cell Biol.* 221, e201911005. null. doi:10.1083/jcb.201911005

Anthonymuthu, T. S., Tyurina, Y. Y., Sun, W. Y., Mikulska-Ruminska, K., Shrivastava, I. H., Tyurin, V. A., et al. (2021). Resolving the paradox of ferroptotic cell death: Ferrostatin-1 binds to 15LOX/PEBP1 complex, suppresses generation of peroxidized ETE-PE, and protects against ferroptosis. *Redox Biol.* 38, 101744. doi:10.1016/j.redox.2020.101744

Badr, C. E., Silver, D. J., Siebzehnrubl, F. A., and Deleyrolle, L. P. (2020). Metabolic heterogeneity and adaptability in brain tumors. *Cell. Mol. Life Sci.* 77, 5101–5119. doi:10.1007/s00018-020-03569-w

Berardinelli, F., Tanori, M., Muoio, D., Buccarelli, M., di Masi, A., Leone, S., et al. (2019). G-quadruplex ligand RHPS4 radiosensitizes glioblastoma xenograft *in vivo* through a differential targeting of bulky differentiated- and stem-cancer cells. *J. Exp. Clin. Cancer Res.* 38, 311. doi:10.1186/s13046-019-1293-x

Bertheloot, D., Latz, E., and Franklin, B. S. (2021). Necroptosis, pyroptosis and apoptosis: An intricate game of cell death. *Cell. Mol. Immunol.* 18, 1106–1121. doi:10.1038/s41423-020-00630-3

Broadley, K. W., Hunn, M. K., Farrand, K. J., Price, K. M., Grasso, C., Miller, R. J., et al. (2011). Side population is not necessary or sufficient for a cancer stem cell phenotype in glioblastoma multiforme. *Stem cells* 29, 452–461. doi:10.1002/stem.582

Burić, S. S., Podolski-Renić, A., Dinić, J., Stanković, T., Jovanović, M., Hadžić, S., et al. (2019). Modulation of antioxidant potential with coenzyme Q10 suppressed invasion of temozolomide-resistant rat glioma *in vitro* and *in vivo*. *Oxid. Med. Cell. Longev.* 2019, 3061607. doi:10.1155/2019/3061607

Chanez, B., Appay, R., Guille, A., Lagarde, A., Colin, C., Adelaide, J., et al. (2022). Genomic analysis of paired IDHwt glioblastomas reveals recurrent alterations of MPDZ at relapse after radiotherapy and chemotherapy. *J. Neurol. Sci.* 436, 120207. doi:10.1016/j.jns.2022.120207

Chang, L., Li, K., and Guo, T. (2017). miR-26a-5p suppresses tumor metastasis by regulating EMT and is associated with prognosis in HCC. *Clin. Transl. Oncol.* 19, 695–703. doi:10.1007/s12094-016-1582-1

Chen, D., Rauh, M., Buchfelder, M., Eyupoglu, I. Y., and Savaskan, N. (2017). The oxido-metabolic driver ATF4 enhances temozolamide chemo-resistance in human gliomas. *Oncotarget* 8, 51164–51176. doi:10.18632/oncotarget.17737

Chen, H., and Wen, J. (2022). Iron oxide nanoparticles loaded with paclitaxel inhibits glioblastoma by enhancing autophagy-dependent ferroptosis pathway. *Eur. J. Pharmacol.* 921, 174860. doi:10.1016/j.ejphar.2022.174860

Cheng, C., Geng, F., Cheng, X., and Guo, D. (2018). Lipid metabolism reprogramming and its potential targets in cancer. *Cancer Commun.* 38, 27. doi:10.1186/s40880-018-0301-4

Chew, L. Y., Zhang, H., He, J., and Yu, F. (2021). The Nrf2-Keap1 pathway is activated by steroid hormone signaling to govern neuronal remodeling. *Cell Rep.* 36, 109466. doi:10.1016/j.celrep.2021.109466

Chng, C. P., Sadovsky, Y., Hsia, K. J., and Huang, C. (2021). Site-specific peroxidation modulates lipid bilayer mechanics. *Extreme Mech. Lett.* 42, 101148. null. doi:10.1016/j.eml.2020.101148

de Souza, I., Monteiro, L. K. S., Guedes, C. B., Silva, M. M., Andrade-Tomaz, M., Contieri, B., et al. (2022). High levels of NRF2 sensitize temozolomide-resistant glioblastoma cells to ferroptosis via ABCC1/MRP1 upregulation. *Cell Death Dis.* 13, 591. doi:10.1038/s41419-022-05044-9

Dissaux, G., Dissaux, B., Bourhis, D., Schick, U., and Querellou, S. (2021). 18F-FET PET/CT in early subventricular zone recurrence of adult glioblastoma. *Clin. Nucl. Med.* 46, 499–500. doi:10.1097/RLU.0000000000003639

Dixon, S. J., Lemberg, K. M., Lamprecht, M. R., Skouta, R., Zaitsev, E. M., Gleason, C. E., et al. (2012). Ferroptosis: An iron-dependent form of nonapoptotic cell death. *Cell* 149, 1060–1072. doi:10.1016/j.cell.2012.03.042

Doll, S., Freitas, F. P., Shah, R., Aldrovandi, M., da Silva, M. C., Ingold, I., et al. (2019). FSP1 is a glutathione-independent ferroptosis suppressor. *Nature* 575, 693–698. doi:10.1038/s41586-019-1707-0

Dutt, S., Hamza, I., and Bartnikas, T. B. (2022). Molecular mechanisms of iron and heme metabolism. *Annu. Rev. Nutr.* 42, 311–335. doi:10.1146/annurev-nutr-062320-112625

Fan, Z., Wirth, A. K., Chen, D., Wruck, C. J., Rauh, M., Buchfelder, M., et al. (2017). Nrf2-Keap1 pathway promotes cell proliferation and diminishes ferroptosis. *Oncogenesis* 6, e371. doi:10.1038/oncsis.2017.65

Gao, M., Meng, X., Guo, X., Zhu, J., Fan, A., Wang, Z., et al. (2018). All-active antitumor micelles via triggered lipid peroxidation. *J. Control. Release* 286, 381–393. doi:10.1016/j.jconrel.2018.08.003

Gong, C., Zhai, J., Wang, X., Zhu, W., Yang, D., Luo, Y., et al. (2022). Synergistic improving photo-Fenton and photo-catalytic degradation of carbamazepine over FeS2/Fe2O3/organic acid with H2O2*in-situ* generation. *Chemosphere* 307, 136199. doi:10.1016/j.chemosphere.2022.136199

Gu, H., Feng, J., Wang, H., Qian, Y., Yang, L., Chen, J., et al. (2016). Celastrus orbiculatus extract inhibits the migration and invasion of human glioblastoma cells *in vitro*. *BMC Complement. Altern. Med.* 16, 387. doi:10.1186/s12906-016-1232-8

Hayashima, K., and Katoh, H. (2022). Expression of gamma-glutamyltransferase 1 in glioblastoma cells confers resistance to cystine deprivation-induced ferroptosis. *J. Biol. Chem.* 298, 101703. doi:10.1016/j.jbc.2022.101703

Hu, Q., Wei, W., Wu, D., Huang, F., Li, M., Li, W., et al. (2022). Blockade of GCH1/BH4 Axis activates ferritinophagy to mitigate the resistance of colorectal cancer to erastin-induced ferroptosis. *Front. Cell Dev. Biol.* 10, 810327. doi:10.3389/fcell.2022.810327

Hu, Z., Mi, Y., Qian, H., Guo, N., Yan, A., Zhang, Y., et al. (2020). A potential mechanism of temozolomide resistance in glioma-ferroptosis. *Front. Oncol.* 10, 897. doi:10.3389/fonc.2020.00897

Isobe, T., Baba, E., Arita, S., Komoda, M., Tamura, S., Shirakawa, T., et al. (2011). Human STEAP3 maintains tumor growth under hypoferric condition. *Exp. Cell Res.* 317, 2582–2591. doi:10.1016/j.yexcr.2011.07.022

Jiang, Y., Zhao, J., Li, R., Liu, Y., Zhou, L., Wang, C., et al. (2022). CircLRFN5 inhibits the progression of glioblastoma via PRRX2/GCH1 mediated ferroptosis. *J. Exp. Clin. Cancer Res.* 41, 307. doi:10.1186/s13046-022-02518-8

Kagan, V. E., Tyurina, Y. Y., Vlasova, II, Kapralov, A. A., Amoscato, A. A., Anthonymuthu, T. S., et al. (2020). Redox epiphospholipidome in programmed cell death signaling: Catalytic mechanisms and regulation. *Front. Endocrinol.* 11, 628079. doi:10.3389/fendo.2020.628079

Karaskova, E., Pospisilova, D., Velganova-Veghova, M., Geryk, M., Volejnikova, J., Holub, D., et al. (2021). Importance of hepcidin in the etiopathogenesis of anemia in inflammatory bowel disease. *Dig. Dis. Sci.* 66, 3263–3269. doi:10.1007/s10620-020-06652-1

Lee, J., and Roh, J. L. (2022). Induction of ferroptosis in head and neck cancer: A novel bridgehead for fighting cancer resilience. *Cancer Lett.* 546, 215854. doi:10.1016/j.canlet.2022.215854

Li, F. J., Long, H. Z., Zhou, Z. W., Luo, H. Y., Xu, S. G., and Gao, L. C. (2022). System Xc -/GSH/GPX4 axis: An important antioxidant system for the ferroptosis in drug-resistant solid tumor therapy. *Front. Pharmacol.* 13, 910292. doi:10.3389/fphar.2022.910292

Li, K., Chen, B., Xu, A., Shen, J., Li, K., Hao, K., et al. (2022). TRIM7 modulates NCOA4-mediated ferritinophagy and ferroptosis in glioblastoma cells. *Redox Biol.* 56, 102451. doi:10.1016/j.redox.2022.102451

Li, S., and Huang, Y. (2022). Ferroptosis: An iron-dependent cell death form linking metabolism, diseases, immune cell and targeted therapy. *Clin. Transl. Oncol.* 24, 1–12. doi:10.1007/s12094-021-02669-8

Li, X., Wang, Q., Yu, S., Zhang, M., Liu, X., Deng, G., et al. (2021). Multifunctional MnO2-based nanoplatform-induced ferroptosis and apoptosis for synergetic chemoradiotherapy. *Nanomedicine* 16, 2343–2361. doi:10.2217/nnm-2021-0286

Liu, B., Ji, Q., Cheng, Y., Liu, M., Zhang, B., Mei, Q., et al. (2022). Biomimetic GBM-targeted drug delivery system boosting ferroptosis for immunotherapy of orthotopic drug-resistant GBM. *J. Nanobiotechnology* 20, 161. doi:10.1186/s12951-022-01360-6

Liu, C. C., Li, H. H., Lin, J. H., Chiang, M. C., Hsu, T. W., Li, A. F., et al. (2021). Esophageal cancer stem-like cells resist ferroptosis-induced cell death by active hsp27-GPX4 pathway. *Biomolecules* 12, 48. null. doi:10.3390/biom12010048

Liu, P., Feng, Y., Li, H., Chen, X., Wang, G., Xu, S., et al. (2020). Ferrostatin-1 alleviates lipopolysaccharide-induced acute lung injury via inhibiting ferroptosis. *Cell. Mol. Biol. Lett.* 25, 10. doi:10.1186/s11658-020-00205-0

Liu, P., Lin, C., Liu, Z., Zhu, C., Lin, Z., Xu, D., et al. (2022). Inhibition of ALG3 stimulates cancer cell immunogenic ferroptosis to potentiate immunotherapy. *Cell. Mol. Life Sci.* 79, 352. doi:10.1007/s00018-022-04365-4

Liu, T., Zhu, C., Chen, X., Guan, G., Zou, C., Shen, S., et al. (2022). Ferroptosis, as the most enriched programmed cell death process in glioma, induces immunosuppression and immunotherapy resistance. *Neuro. Oncol.* 24, 1113–1125. doi:10.1093/neuonc/noac033

Liu, Y., Shen, Y., Sun, T., and Yang, W. (2017). Mechanisms regulating radiosensitivity of glioma stem cells. *Neoplasma* 64, 655–665. doi:10.4149/neo_2017_502

Lu, B., Chen, X. B., Ying, M. D., He, Q. J., Cao, J., and Yang, B. (2017). The role of ferroptosis in cancer development and treatment response. *Front. Pharmacol.* 8, 992. doi:10.3389/fphar.2017.00992

Martínez-Garcia, M., Álvarez-Linera, J., Carrato, C., Ley, L., Luque, R., Maldonado, X., et al. (2018). SEOM clinical guidelines for diagnosis and treatment of glioblastoma (2017). *Clin. Transl. Oncol.* 20, 22–28. doi:10.1007/s12094-017-1763-6

McNamee, J. P., Grybas, V. S., Qutob, S. S., and Bellier, P. V. (2021). Effects of 1800 MHz radiofrequency fields on signal transduction and antioxidant proteins in human A172 glioblastoma cells. *Int. J. Radiat. Biol.* 97, 1316–1323. doi:10.1080/09553002.2021.1934751

Mikulska-Ruminska, K., Anthonymuthu, T. S., Levkina, A., Shrivastava, I. H., Kapralov, A. A., Bayır, H., et al. (2021). NO● represses the oxygenation of arachidonoyl PE by 15lox/PEBP1: Mechanism and role in ferroptosis. *Int. J. Mol. Sci.* 22, 5253. null. doi:10.3390/ijms22105253

Mitre, A. O., Florian, A. I., Buruiana, A., Boer, A., Moldovan, I., Soritau, O., et al. (2022). Ferroptosis involvement in glioblastoma treatment. *Medicina* 58, 319. null. doi:10.3390/medicina58020319

Mou, Y. W., Li, Z. Y., Yang, X., Chen, S. Y., Hou, S. S., Zhang, E. G., et al. (2020). Research progress of ferroptosis-related mechanism and diseases. *Zhonghua Lao Dong Wei Sheng Zhi Ye Bing Za Zhi* 38, 797–800. doi:10.3760/cma.j.cn121094-20190925-00392

Ou-Yang, Q., He, X., Yang, A., Li, B., and Xu, M. (2018). Interference with NTSR1 expression exerts an anti-invasion effect via the jun/miR-494/SOCS6 Axis of glioblastoma cells. *Cell. Physiol. biochem.* 49, 2382–2395. doi:10.1159/000493838

Park, K. J., Kim, J., Testoff, T., Adams, J., Poklar, M., Zborowski, M., et al. (2019). Quantitative characterization of the regulation of iron metabolism in glioblastoma stem-like cells using magnetophoresis. *Biotechnol. Bioeng.* 116, 1644–1655. doi:10.1002/bit.26973

Piskin, E., Cianciosi, D., Gulec, S., Tomas, M., and Capanoglu, E. (2022). Iron absorption: Factors, limitations, and improvement methods. *ACS omega* 7, 20441–20456. doi:10.1021/acsomega.2c01833

Rao, G. M., Rao, A. V., Raja, A., Rao, S., and Rao, A. (2000). Role of antioxidant enzymes in brain tumours. *Clin. Chim. Acta.* 296, 203–212. doi:10.1016/s0009-8981(00)00219-9

Reichert, C. O., de Freitas, F. A., Sampaio-Silva, J., Rokita-Rosa, L., Barros, P. L., Levy, D., et al. (2020). Ferroptosis mechanisms involved in neurodegenerative diseases. *Int. J. Mol. Sci.* 21, 8765. null. doi:10.3390/ijms21228765

Santoro, M. M. (2020). The antioxidant role of non-mitochondrial CoQ10: Mystery solved. *Cell Metab.* 31, 13–15. doi:10.1016/j.cmet.2019.12.007

Sendamarai, A. K., Ohgami, R. S., Fleming, M. D., and Lawrence, C. M. (2008). Structure of the membrane proximal oxidoreductase domain of human Steap3, the dominant ferrireductase of the erythroid transferrin cycle. *Proc. Natl. Acad. Sci. U. S. A.* 105, 7410–7415. doi:10.1073/pnas.0801318105

Sesé, B., Íñiguez-Muñoz, S., Ensenyat-Mendez, M., Llinàs-Arias, P., Ramis, G., Orozco, J. I. J., et al. (2022). Glioblastoma embryonic-like stem cells exhibit immune-evasive phenotype. *Cancers* 14, 2070. null. doi:10.3390/cancers14092070

Shi, J., Yang, N., Han, M., and Qiu, C. (2022). Emerging roles of ferroptosis in glioma. *Front. Oncol.* 12, 993316. doi:10.3389/fonc.2022.993316

Shi, L., Liu, Y., Li, M., and Luo, Z. (2022). Emerging roles of ferroptosis in the tumor immune landscape: From danger signals to anti-tumor immunity. *FEBS J.* 289 (2022), 3655–3665. doi:10.1111/febs.16034

Shi, Z. X., Rao, W., Wang, H., Wang, N. D., Si, J. W., Zhao, J., et al. (2015). Modeled microgravity suppressed invasion and migration of human glioblastoma U87 cells through downregulating store-operated calcium entry. *Biochem. Biophys. Res. Commun.* 457, 378–384. doi:10.1016/j.bbrc.2014.12.120

Shin, D., Kim, E. H., Lee, J., and Roh, J. L. (2018). Nrf2 inhibition reverses resistance to GPX4 inhibitor-induced ferroptosis in head and neck cancer. *Free Radic. Biol. Med.* 129, 454–462. doi:10.1016/j.freeradbiomed.2018.10.426

Song, Q., Peng, S., Sun, Z., Heng, X., and Zhu, X. (2021). Temozolomide drives ferroptosis via a DMT1-dependent pathway in glioblastoma cells. *Yonsei Med. J.* 62, 843–849. doi:10.3349/ymj.2021.62.9.843

Stallhofer, J., Veith, L., Diegelmann, J., Probst, P., Brand, S., Schnitzler, F., et al. (2022). Iron deficiency in inflammatory bowel disease is associated with low levels of vitamin D modulating serum hepcidin and intestinal ceruloplasmin expression. *Clin. Transl. Gastroenterol.* 13, e00450. doi:10.14309/ctg.0000000000000450

Su, J., Li, Y., Liu, Q., Peng, G., Qin, C., and Li, Y. (2022). Identification of SSBP1 as a ferroptosis-related biomarker of glioblastoma based on a novel mitochondria-related gene risk model and *in vitro* experiments. *J. Transl. Med.* 20, 440. doi:10.1186/s12967-022-03657-4

Sun, S., Gao, T., Pang, B., Su, X., Guo, C., Zhang, R., et al. (2022). RNA binding protein NKAP protects glioblastoma cells from ferroptosis by promoting SLC7A11 mRNA splicing in an m6A-dependent manner. *Cell Death Dis.* 13, 73. doi:10.1038/s41419-022-04524-2

Tang, Q., Bai, L., Zou, Z., Meng, P., Xia, Y., Cheng, S., et al. (2018). Ferroptosis is newly characterized form of neuronal cell death in response to arsenite exposure. *Neurotoxicology* 67, 27–36. doi:10.1016/j.neuro.2018.04.012

Terry, S., Savagner, P., Ortiz-Cuaran, S., Mahjoubi, L., Saintigny, P., Thiery, J. P., et al. (2017). New insights into the role of EMT in tumor immune escape. *Mol. Oncol.* 11, 824–846. doi:10.1002/1878-0261.12093

Tomita, K., Takashi, Y., Ouchi, Y., Kuwahara, Y., Igarashi, K., Nagasawa, T., et al. (2019). Lipid peroxidation increases hydrogen peroxide permeability leading to cell death in cancer cell lines that lack mtDNA. *Cancer Sci.* 110, 2856–2866. doi:10.1111/cas.14132

Wang, K. Y., Huang, R. Y., Tong, X. Z., Zhang, K. N., Liu, Y. W., Zeng, F., et al. (2019). Molecular and clinical characterization of TMEM71 expression at the transcriptional level in glioma. *CNS Neurosci. Ther.* 25, 965–975. doi:10.1111/cns.13137

Wang, W. J., Ling, Y. Y., Zhong, Y. M., Li, Z. Y., Tan, C. P., and Mao, Z. W. (2022). Ferroptosis-enhanced cancer immunity by a ferrocene-appended iridium(III) diphosphine complex. *Angew. Chem. Int. Ed. Engl.* 61, e202115247. doi:10.1002/anie.202115247

Wu, H., Luan, Y., Wang, H., Zhang, P., Liu, S., Wang, P., et al. (2022). Selenium inhibits ferroptosis and ameliorates autistic-like behaviors of BTBR mice by regulating the Nrf2/GPx4 pathway. *Brain Res. Bull.* 183, 38–48. doi:10.1016/j.brainresbull.2022.02.018

Xing, L., Liu, X. Y., Zhou, T. J., Wan, X., Wang, Y., and Jiang, H. L. (2021). Photothermal nanozyme-ignited Fenton reaction-independent ferroptosis for breast cancer therapy. *J. Control. Release* 339, 14–26. doi:10.1016/j.jconrel.2021.09.019

Xu, H., Ye, D., Ren, M., Zhang, H., and Bi, F. (2021). Ferroptosis in the tumor microenvironment: Perspectives for immunotherapy. *Trends Mol. Med.* 27, 856–867. doi:10.1016/j.molmed.2021.06.014

Yang, F. C., Wang, C., Zhu, J., Gai, Q. J., Mao, M., He, J., et al. (2022). Inhibitory effects of temozolomide on glioma cells is sensitized by RSL3-induced ferroptosis but negatively correlated with expression of ferritin heavy chain 1 and ferritin light chain. *Lab. Invest.* 102, 741–752. doi:10.1038/s41374-022-00779-7

Yang, F., Zou, Y., Gong, Q., Chen, J., Li, W. D., and Huang, Q. (2020). From astrocytoma to glioblastoma: A clonal evolution study. *FEBS open bio* 10, 744–751. doi:10.1002/2211-5463.12815

Yang, M., Tsui, M. G., Tsang, J. K. W., Goit, R. K., Yao, K. M., So, K. F., et al. (2022). Involvement of FSP1-CoQ10-NADH and GSH-GPx-4 pathways in retinal pigment epithelium ferroptosis. *Cell Death Dis.* 13, 468. doi:10.1038/s41419-022-04924-4

Yang, W. S., Kim, K. J., Gaschler, M. M., Patel, M., Shchepinov, M. S., and Stockwell, B. R. (2016). Peroxidation of polyunsaturated fatty acids by lipoxygenases drives ferroptosis. *Proc. Natl. Acad. Sci. U. S. A.* 113, E4966–E4975. doi:10.1073/pnas.1603244113

Yi, R., Wang, H., Deng, C., Wang, X., Yao, L., Niu, W., et al. (2020). Dihydroartemisinin initiates ferroptosis in glioblastoma through GPX4 inhibition. *Biosci. Rep.* 40, BSR20193314. null. doi:10.1042/BSR20193314

Yu, Y., Huang, Z., Chen, Q., Zhang, Z., Jiang, H., Gu, R., et al. (2022). Iron-based nanoscale coordination polymers synergistically induce immunogenic ferroptosis by blocking dihydrofolate reductase for cancer immunotherapy. *Biomaterials* 288, 121724. doi:10.1016/j.biomaterials.2022.121724

Yuan, F., Sun, Q., Zhang, S., Ye, L., Xu, Y., Xu, Z., et al. (2022). HSP27 protects against ferroptosis of glioblastoma cells. *Hum. Cell* 35, 238–249. doi:10.1007/s13577-021-00645-6

Zhang, J. J., Du, J., Kong, N., Zhang, G. Y., Liu, M. Z., and Liu, C. (2021). Mechanisms and pharmacological applications of ferroptosis: A narrative review. *Ann. Transl. Med.* 9, 1503. doi:10.21037/atm-21-1595

Zhang, X., Li, X., Zheng, C., Yang, C., Zhang, R., Wang, A., et al. (2022). Ferroptosis, a new form of cell death defined after radiation exposure. *Int. J. Radiat. Biol.* 98, 1201–1209. doi:10.1080/09553002.2022.2020358

Zhang, Y., Hou, Y., Liu, C., Li, Y., Guo, W., Wu, J. L., et al. (2016). Identification of an adaptor protein that facilitates Nrf2-Keap1 complex formation and modulates antioxidant response. *Free Radic. Biol. Med.* 97, 38–49. doi:10.1016/j.freeradbiomed.2016.05.017

Zhang, Y., Kong, Y., Ma, Y., Ni, S., Wikerholmen, T., Xi, K., et al. (2021). Loss of COPZ1 induces NCOA4 mediated autophagy and ferroptosis in glioblastoma cell lines. *Oncogene* 40, 1425–1439. doi:10.1038/s41388-020-01622-3

Zhang, Z., Pan, Y., Cun, J. E., Li, J., Guo, Z., Pan, Q., et al. (2022). A reactive oxygen species-replenishing coordination polymer nanomedicine disrupts redox homeostasis and induces concurrent apoptosis-ferroptosis for combinational cancer therapy. *Acta Biomater.* 151, 480–490. doi:10.1016/j.actbio.2022.07.055

Zhao, J., Wang, Y., Tao, L., and Chen, L. (2022). Iron transporters and ferroptosis in malignant brain tumors. *Front. Oncol.* 12, 861834. doi:10.3389/fonc.2022.861834

Zhao, X., Liu, Z., Gao, J., Li, H., Wang, X., Li, Y., et al. (2020). Inhibition of ferroptosis attenuates busulfan-induced oligospermia in mice. *Toxicology* 440, 152489. doi:10.1016/j.tox.2020.152489

Zhou, L., and Ma, J. (2022). MIR99AHG/miR-204-5p/TXNIP/Nrf2/ARE signaling pathway decreases glioblastoma temozolomide sensitivity. *Neurotox. Res.* 40, 1152–1162. doi:10.1007/s12640-022-00536-0

Zhou, Y., Shen, Y., Chen, C., Sui, X., Yang, J., Wang, L., et al. (2019). The crosstalk between autophagy and ferroptosis: What can we learn to target drug resistance in cancer? *Cancer Biol. Med.* 16, 630–646. doi:10.20892/j.issn.2095-3941.2019.0158

Zhu, T., and Fan, Y. (2021). Autophagy regulates the sensitivity of acute lymphoblastic leukemia cells to ferroptosis activator by influencing iron homeostasis. *Zhongguo shi yan xue ye xue za zhi* 29, 1380–1386. doi:10.19746/j.cnki.issn.1009-2137.2021.05.003

frontiers | Frontiers in Molecular Biosciences

TYPE Mini Review
PUBLISHED 21 March 2023
DOI 10.3389/fmolb.2023.1164398

OPEN ACCESS

EDITED BY
Yanqing Liu,
Columbia University, United States

REVIEWED BY
Yutong Liu,
Harvard University, United States
Chenchen Li,
University of Pennsylvania, United States

*CORRESPONDENCE
Jinwei Miao,
jinweimiao@ccmu.edu.cn

SPECIALTY SECTION
This article was submitted to Molecular Diagnostics and Therapeutics, a section of the journal Frontiers in Molecular Biosciences

RECEIVED 12 February 2023
ACCEPTED 10 March 2023
PUBLISHED 21 March 2023

CITATION
Chang X and Miao J (2023), Ferroptosis: Mechanism and potential applications in cervical cancer.
Front. Mol. Biosci. 10:1164398.
doi: 10.3389/fmolb.2023.1164398

Ferroptosis: Mechanism and potential applications in cervical cancer

Xiangyu Chang and Jinwei Miao*

Department of Gynecologic Oncology, Beijing Obstetrics and Gynecology Hospital, Capital Medical University, Beijing, China

Ferroptosis is a distinct form of cell death mechanism different from the traditional ones. Ferroptosis is characterized biochemically by lipid peroxidation, iron accumulation, and glutathione deficiency. It has already demonstrated significant promise in antitumor therapy. Cervical cancer (CC) progression is closely linked to iron regulation and oxidative stress. Existing research has investigated the role of ferroptosis in CC. Ferroptosis could open up a new avenue of research for treating CC. This review will describe the factors and pathways and the research basis of ferroptosis, which is closely related to CC. Furthermore, the review may provide potential future directions for CC research, and we believe that more studies concerning the therapeutic implications of ferroptosis in CC will come to notice.

KEYWORDS

cervical cancer, ferroptosis, lipid peroxidation, iron accumulation, treatment

Introduction

Cervical cancer (CC) is one of the most common gynecological tumors worldwide, and 311,000 women died of cervical cancer in 2018 (Bray et al., 2018). Based on the clinical stage and pathological risk factors, surgery or a combination of chemotherapy and radiation therapy is commonly used to treat CC (Koh et al., 2019). Patients with advanced-stage CC have a poor prognosis with a low 5-year mortality rate of only 17% (Pfaendler and Tewari, 2016). However, cisplatin-based first-line chemotherapy has shown little or no response (Monk et al., 2009). Significant adverse effects and narrow therapeutic windows limit the use of systemic chemotherapy. The FDA has approved atezolizumab, pembrolizumab, bleomycin sulfate, and topotecan hydrochloric acid for patients with metastatic or recurrent CC. The standard first-line therapy for CC is platinum-based chemotherapy with bevacizumab (Rallis et al., 2021); non-etheless, the failure of this treatment indicates a high likelihood of subsequent treatment failure. Therefore, it is necessary to develop novel therapeutics for the treatment of CC.

High-risk human papillomavirus (hrHPV) infection, age, smoking, and childbirth are important risk factors for CC (Gaffney et al., 2018). Among all these risk factors, persistent hrHPV infection appears to be the main risk factor responsible for the carcinogenesis and progression of CC (Crosbie et al., 2013). HPV16 is the most common HPV subtype found in CC, causing more than 50% of all cervical cancer cases (Jiang et al., 2018). hrHPV can cause cancer by expressing multiple oncoproteins, including E6 and E7 proteins, which induce carcinogenesis and malignant transformation of cervical epithelial cells (Taghizadeh et al., 2019). HrHPV infiltrates the cervical epithelium and integrates into the host genome, inactivating tumor suppressor genes and activating oncogenes. HPV oncoproteins E6 and E7 regulate the function of several tumor-related proteins, including EGFR family members,

p53, and retinoblastoma protein (pRb). HPV oncoproteins also affect the function of various cellular organelles, including mitochondria (Cruz-Gregorio et al., 2019; Cruz-Gregorio et al., 2020). A study has found that HPV infection can induce chronic oxidative stress by promoting the production of reactive oxygen species (ROS) in the tissue microenvironment in patients with CC (Banerjee et al., 2019), which regulates different cellular signaling pathways (Yeo-Teh et al., 2018; Cruz-Gregorio and Aranda-Rivera, 2021) and cellular processes, such as autophagy (Aranda-Rivera et al., 2021) and apoptosis (Jiang and Yue, 2014). The concept of ferroptosis has been recently introduced as an iron-dependent form of oxidative cell death, and ferroptosis is distinct from other known forms of cell death modalities. Ferroptosis primarily occurs in cancer cells and neurons and contributes to the progression of many diseases (Dixon et al., 2012). Ferroptosis was observed in hrHPV-infected squamous intraepithelial lesions, indicating that it is likely to be associated with the development of CC. Cancer cells are more iron-dependent for growth and more sensitive to the iron deficiency than non-cancer cells. Ferroptosis is first reported in ovarian cancer (Wang et al., 2021a), which is another well-known gynecologic malignancy. Ferroptosis has also been reported in liver cancer (Yang et al., 2020), glioma (Zhuo et al., 2020), osteosarcoma (Liu and Wang, 2019), and renal cell carcinoma (Markowitsch et al., 2020); however, the pathogenic mechanism of ferroptosis in the progression of CC is poorly understood and needs further exploration.

Potential mechanism of iron death and iron homeostasis in cervical cancer

Iron metabolism plays a vital role in the development of CC. A meta-analysis showed that Chinese patients with CC exhibited lower serum iron levels suggesting that higher serum iron levels may play a protective role in CC (Chen et al., 2020). The study by Braun et al., on the other hand, demonstrated that iron deficiency has profound antiviral and antiproliferative effects on HPV-positive cancer cells. The internal reason may be that tumor cells typically reprogram various cellular processes that ultimately lead to enhanced iron influx and reduced iron efflux, and iron ions enter the cells and the serum concentration of iron ions in the extracellular fluid decreases. They proposed that iron chelators, such as CPX, function as HPV inhibitors, pro-senescence agents, and pro-apoptotic agents in both normoxia and hypoxia environments. The study also demonstrated the therapeutic potential of iron chelators in cancer therapy (Braun et al., 2020). Iron is essential in many physiological processes and an essential component of hemoglobin; therefore, iron is required for oxygen transport in the body (Paul et al., 2017). Transferrin receptor 1 (TfR1) and transferrin (TF) are well-known cellular regulators of iron transport, and they control intracellular iron levels by transporting Fe^{3+} into the cell (Qian et al., 2002). Nan et al. first reported that TfR1 regulates the expression of many genes at the transcriptional and post-transcriptional levels. The results suggest that TfR1 is involved in the progression of CC by affecting the expression and alternative splicing (AS) of several genes involved in cancer-related pathways (Huang et al., 2022), but whether these pathways are related to ferroptosis has not been elucidated so far.

Although most of the intracellular iron is stored in ferritin, there is still a small cytosolic pool of weakly bound iron available for a variety of interactions with other molecules in the cell; the catalytic activity of weakly bound iron (Fe^{2+}) is almost unlimited since Fe^{2+} can capture electrons to form peroxides (Dev and Babitt, 2017). These ferrous ions (Fe^{2+}) are called labile iron pool (LIP) (Espósito et al., 2002; Petrat et al., 2002). Fe^{2+} is a metal ion with a high redox potential. It is the most important catalyst in the lipid peroxidation chain reaction, but it can also generate free radicals from hydrogen peroxide *via* the Fenton reaction in cells that produce a lot of ROS (Kajarabille and Latunde-Dada, 2019). Reactive oxygen species (ROS) are a group of molecules that contain partially reduced oxygen, including peroxide, superoxide, singlet oxygen, hydroxyl radicals, and free radicals. The dramatic increase of ROS in cells renders cells more prone to ferroptosis (Lin et al., 2018; Liang et al., 2019). High iron level in the cytoplasm significantly promotes ferroptosis susceptibility (Hassannia et al., 2019). Moreover, ferroptosis also participates in the regulation of iron homeostasis in the cell.

Genes involved in iron homeostasis (input, output, and storage of iron ions) have also been shown to modulate the sensitivity to ferroptosis. Preliminary research has been conducted on the ferroptosis regulatory factors that are involved in the release of ferric ions. The overexpression of TF and TfR1 increases iron uptake, making cells susceptible to ferroptosis; conversely, silencing TfR1 inhibited erastin-induced ferroptosis. A recent study found that heat shock protein beta-1 (HSPB1) significantly inhibits ferroptosis by inhibiting TfR1 expression and thus lowering intracellular iron levels (Li et al., 2020). Additionally, nitrogen fixation inhibitor 1 (NFS1), a cysteine desulfurase that mobilizes sulfur from cysteine to synthesize iron-sulfur clusters, is activated by simultaneously increasing TfR1 levels and decreasing ferritin levels, causing the iron starvation response, thereby sensitizing cells to ferroptosis (Alvarez et al., 2017). In addition, iron is mainly exported through ferroportin 1 (FPN1); accordingly, inhibition of FPN1 resulted in enhanced ferroptosis (Geng et al., 2018). Furthermore, the major route of iron release from ferritin is mediated by the incorporation of ferritin into the lysosomes through nuclear receptor coactivator 4 (NCOA4), and knockdown of NCOA4 decreases the ferritinophagy leading to the restricted use of free intracellular iron. NCOA4-mediated ferritin deposition is linked to neurodegeneration, as shown by Quiles et al. (Brown et al., 2019; Quiles Del Rey and Mancias, 2019). Ferritin degradation occurs through NCOA4-mediated ferritinophagy, which induces ferroptosis by releasing free iron from ferritin (Hou et al., 2016). Hemin was used as an intracellular iron source to promote ferroptosis in platelets *via* ROS-regulated proteasome activity (Naveen Kumar et al., 2019). According to one study on lung cancer, hemin causes ferroptosis in lung cancer cells while protecting normal lung cells after exposure to fractionated doses of ionizing radiation (Chen et al., 2020). Nrf2 is a transcription factor, and the activation of Nrf2 regulates iron metabolism; it reduces cellular iron uptake and limits the production of reactive oxygen species. Thus, Nrf2 inhibits ferroptosis and promotes the progression of cancer. In liver cancer cell lines, p62 can bind to Keap1 and disrupts the interaction of Keap1 with Nrf2 when exposed to compounds inducing iron toxicity. The disruption of Keap1-Nrf2 interaction by ferroptosis-inducing compounds leads to the accumulation of Nrf2, ultimately reducing cancer cell susceptibility to ferroptosis (Sun et al., 2016). In a study by Xiong et al., hypoxia upregulated KDM4A *via*

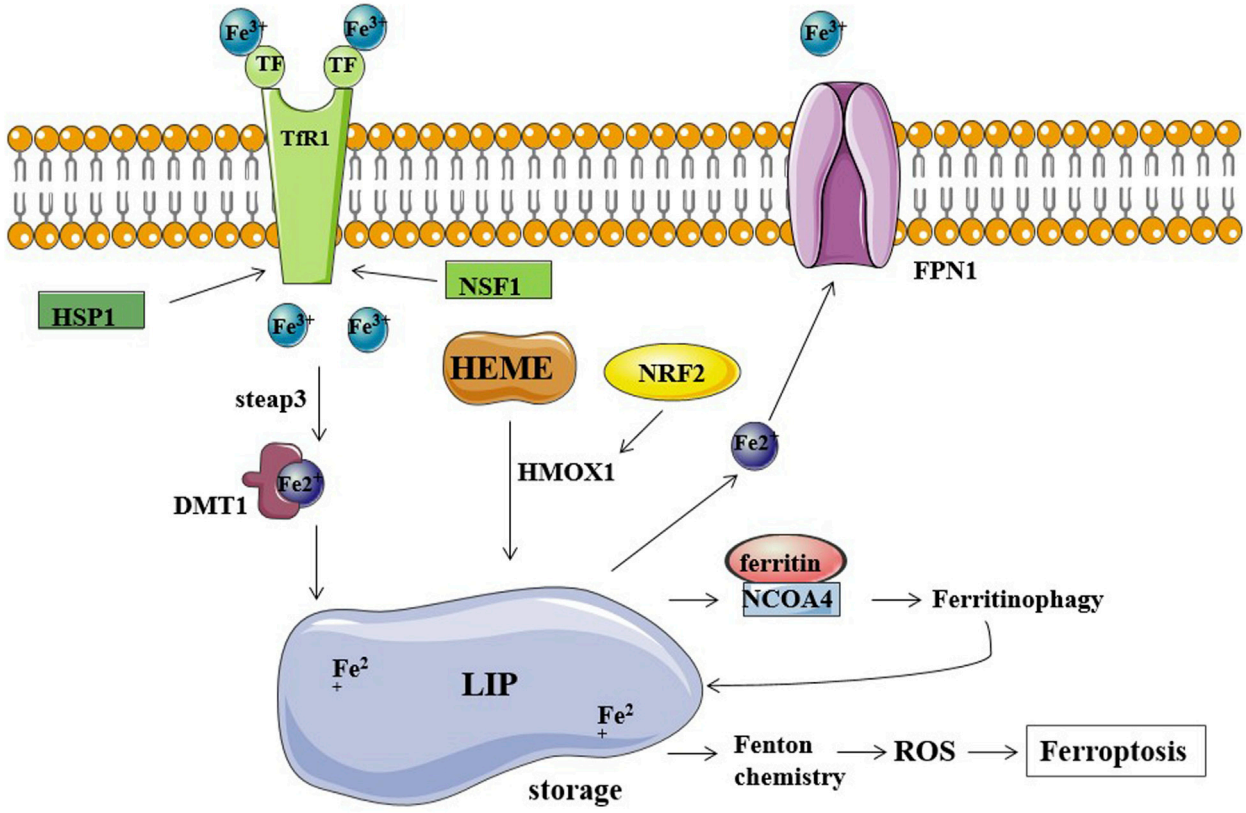

FIGURE 1
Iron metabolism and ferroptosis. Fe^{2+} storage in LIP (labile iron pool) participates in the Fenton reaction producing ROS and causing ferroptosis. TfR1, TF, and FPN1 are the major regulators of cellular iron balance on the cell membrane. TF transports Fe^{3+} into cells by TfR1-mediated endocytosis. HSP1 inhibits this process by inhibiting TfR1, while NSF1 can increase TfR1 levels. Fe^{3+} is converted to Fe^{2+} by STEAP3 and released into the cytoplasm *via* DMT1. FPN1 exports and decreases intracellular iron levels. Ferritin stores iron and limits the iron-catalyzed Fenton reaction. NCOA4 binds ferritin mediating its autophagic degradation in a process called ferritinophagy.

H3K9me3t, which enhanced HIF1 transcription, activated HRE sequences (5′-ACGTG-3′) in TfR1, activated DMT1 promoter, and induced ferroptosis resistance in CC cells (Xiong et al., 2022) (Figure 1).

ROS and lipid peroxidation in cervical cancer

The activation of protooncogenes in tumor cells results in the production of ROS. Furthermore, tumor cells require a large amount of nutrients and energy to maintain rapid proliferation, and tumor cells undergo metabolic reprogramming and abnormal mitochondrial function, all of which contribute to the production of more ROS. ROS have been shown to transmit proliferative signals and promote tumor development (Wang et al., 2019). Non-etheless, high levels of ROS can cause cell death, and tumor cells must increase their antioxidant activity to maintain cellular redox balance. One of the most noticeable features of ferroptosis is lipid peroxidation. Ferroptosis is a regulated cell death mechanism that results in glutathione (GSH) depletion. Ferroptosis reduces glutathione peroxidase (GPX4) activity and cellular antioxidant capacity, resulting in increased lipid peroxidation (Dixon et al., 2012; Yang et al., 2014). Sanguinarine treatment increased the generation of reactive oxygen species (ROS), and blocking ROS production inhibited the induction of both apoptosis and ferroptosis. PUFA (polyunsaturated fatty acid)-containing membrane phospholipids are vulnerable to peroxidation under intracellular environment rich in iron and reactive oxygen species. This accumulation of lipid peroxides in the cell membranes eventually destroys membrane integrity leading to ferroptosis (Stockwell et al., 2017). Ferroptosis induces specific morphological changes in mitochondria, including mitochondrial shrinkage, increased membrane density, outer membrane rupture, cristae shrinkage or disappearance, membrane potential drop, etc. Erastin-mediated inhibition of intracellular cystine causes the depletion of intracellular glutathione (GSH), eventually leading to the inactivation of GPX4 and accumulation of lipid peroxidation, inducing cell death. RSL3, a well-known inhibitor of GPX4, can also directly promote these effects, and the regulatory mechanisms of RSL3 include GSH/GPX4 axis, system Xc-, ACSL4, FSP1, etc. (Bridges et al., 2012; Yuan et al., 2016; Doll et al., 2019).

Glutathione reductase (GR), also known as Glutathione-disulfide reductase (GSR), is a key enzyme that catalyzes the reduction of GSH by glutathione disulfide (GSSG), and the inhibition of GSR results in increased ROS activity. In a previous

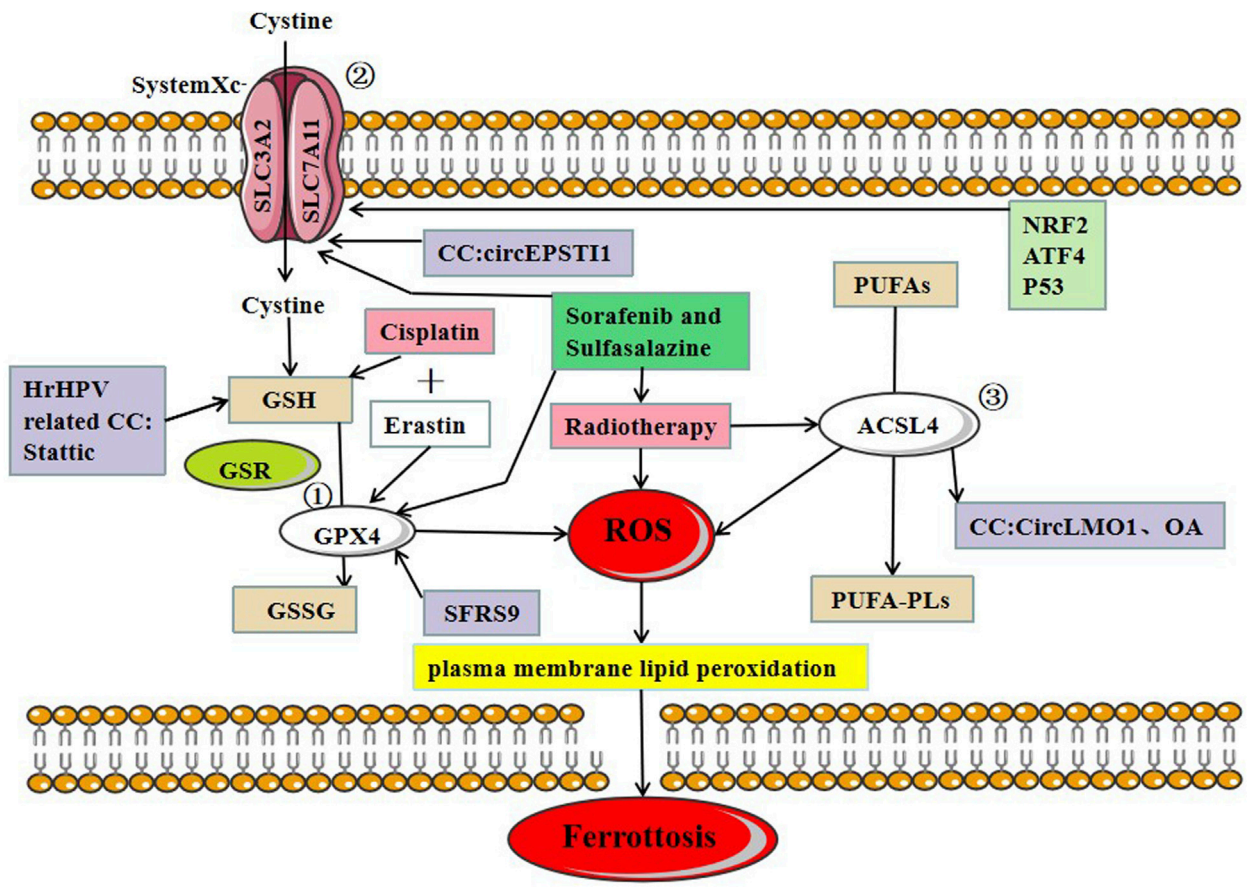

FIGURE 2
Three major regulatory mechanisms of ferroptosis in cervical cancer. ①GPX4 pathway: the SLC7A11-GSH-GPX4 (solute carrier family 7 members 11-glutathione-GPX4) signaling axis accounts for the predominant ferroptosis defense system. Cysteine serves as the rate-limiting precursor for the biosynthesis of GSH, a critical cofactor for GPX4 to detoxify lipid peroxides, ② SystemXc-: SLC7A11 is a core component of the cystine-glutamate antiporter system (system Xc-) and mediates the antiport activity of system xc– by importing extracellular cystine and exporting out intracellular glutamate, ③ ACSL4: PUFAs derived from lipid bilayers are metabolized by ACSL4 leading to the production of ROS. Recent research on ferroptosis in CC has primarily focused on these three protein complexes. The main treatments for ferroptosis-related CC are cisplatin and radiotherapy.

study of ROS in the development of CC, Xia Y et al. demonstrated that the expression of GSR level was increased in human CC tissues, inhibiting the enzymatic activity of GSR and inducing cell death in CC through a ROS-dependent mechanism. Furthermore, this study demonstrates the potential of ROS as an effective antitumor modality for the treatment of CC (Fan et al., 2020). HPV oncoproteins induce oxidative stress (OS), which in turn promotes lipid peroxidation and cellular damage resulting in various types of cell death, including ferroptosis (Di Domenico et al., 2018). It has been demonstrated that the pathogenesis of HPV-mediated CC progression is linked to ferroptosis. Ferroptosis was found in low-grade cervical squamous intraepithelial lesions (SIL) with hrHPV infection in a study on the relationship between ferroptosis and HPV-induced cervical disease. Persistent ferroptosis aided in developing squamous intraepithelial lesions (SIL), which resulted in anti-ferroptotic effects. Many other studies have identified the critical role of lipid peroxidation in the progression of CC, providing us with new ideas for treating CC by targeting ferroptosis (Wang et al., 2022).

Role of GPX4-GSH pathway in ferroptosis of cervical cancer

GPX4 plays a critical role in regulating ferroptosis, and the inhibition of GPX4 induces ferroptosis. GSH is a substrate of GPX4, and the deletion of GPX4 induces ferroptosis. Erastin inhibits ferroptosis by reducing intracellular GSH levels. RSL3 can also directly bind to GPX4 and inhibits its activity, leading to the accumulation of intracellular reactive oxygen species and ferroptosis induction (Yang and Stockwell, 2008). P53, a well-known tumor suppressor gene, can inhibit the induction of system Xc-through the classical pathway and enhances ferroptosis by inhibiting dipeptidyl-peptidase 4 through the non-canonical pathway (Jiang et al., 2015a). hrHPV protein E6 induces p53 degradation by activating hTERT (human telomerase reverse transcriptase), avoiding apoptosis and cell immortalization (Vande Pol and Klingelhutz, 2013). However, the involvement of ferroptosis in this process needs to be further verified. In cervical and bladder cancers, SFRS9 (Serine and arginine-rich splicing factor 9) has been identified as a protooncogene. SFRC9 can inhibit ferroptosis in

TABLE 1 Overview of ferroptosis-associated chemotherapeutic agents in CC.

Chemotherapeutic agents	*In vitro*	*In vivo*	Inhibitors and inducers of ferroptosis	Effect
Oxaliplatin Chen et al. (2016)	Oxaliplatin-resistant human cervical cancer cell line, S3	SiHa and S3 tumor xenograft mouse models Chen et al. (2016)	Deferoxamine/DFO	The synergistic killing effect
Cisplatin Roh et al. (2016); Guo et al. (2018)	Human ovarian cancer cell line (A2780 and its CDDP-resistant variant A2780DDP), HNC cell lines (AMC-HN3R, -HN4R, and -HN9R), A549, HCT116 cells	HN9-cisR mouse models Roh et al. (2016)	Erastin	The synergistic killing effect, enhancing the anticancer activity
Paclitaxel/PTX Ye et al. (2019)	mtp53 HPSCC	None	RSL3	Enhance the anticancer activity
Gemcitabine Zhu et al. (2017)	PANC1, CFPAC1, MiaPaCa2, Panc2.03, and Panc02 cells	PANC1 nude mouse model	Erastin	Enhance sensitivity
Cytarabine, Doxorubicin Zhu et al. (2017)	HL-60 cells	None	Erastin	Enhance the anticancer activity

colorectal cancer (CRC) by binding to GPX4 mRNA, and another study suggests that inhibiting SFRC9 in CRC may have therapeutic implications (Wang et al., 2021b). MiR-193a-5p targets GPX4 mRNA and reduces GPX4 expression in cervical cancer cells. Circular RNA circACAP2 increases GPX4 expression by targeting miR-193a-5p, thereby repressing ferroptosis in cervical cancer during malignant progression by miR-193a-5p/GPX4. Indeed, limited studies have been conducted to identify the role of GPX4 in inducing ferroptosis in cervical cancer cells. Further studies are required to understand the precise role of GPX4 in CC progression (Figure 2).

Role of system Xc- in ferroptosis of cervical cancer

System Xc- is an amino acid transporter widely distributed on the cell membrane and mainly consists of SLC7A11 and SLC3A2. System Xc- transports cystine into the cytosol in exchange for the same amount of glutamate being transported out of the cell. Inhibiting the activity of system Xc- can reduce cystine absorption and decrease glutathione synthesis, eventually leading to oxidative damage and ferroptosis (Bridges et al., 2012). ATF4 (activating transcription factor 4) and NRF2 (nuclear factor erythroid 2-related factor 2) represent two major transcription factors mediating stress-induced transcription of SLC7A11, and it has been shown that SLC7A11 drives ferroptosis resistance (Ye et al., 2014). Erastin and sorafenib induce ferroptosis by inhibiting System Xc-. Multiple studies suggest that p53 downregulates the expression of SLC7A11 as demonstrated in polymorphic mutants of p53, and the mechanism of p53-mediated tumor suppression is governed by the inhibition of SLC7A11 function, conferring resistance to ferroptosis (Jiang et al., 2015b; Jennis et al., 2016; Wang et al., 2016).

A recent study of CC found that the circEPSTI1-miR-375/409–3P/515–5p/SLC7A11 axis influenced CC proliferation *via* the competing endogenous RNAs (ceRNA) mechanism and was involved in ferroptosis. Wu et al. provided experimental evidence, which revealed that circEPSTI1 might act as a new and useful prognostic and predictive biomarker for CC (Wu et al., 2021) (Figure 2).

Role of ACSL4 in ferroptosis of cervical cancer

ACSL4 (Long-chain acyl-CoA synthetase 4) belongs to the acyl-CoA synthetase protein family, which catalyzes the covalent addition of a CoA moiety to fatty acid groups in an ATP-dependent manner. Mouse embryonic fibroblasts from ACSL4 knock-out mice undergo ferroptosis in response to RSL3 (RAS-selective lethal 3). Thus, ACSL4 plays a crucial role in iron-dependent oxidative stress (Yuan et al., 2016). Cortical neurons (Seiler et al., 2008), fibroblasts (Wortmann et al., 2013), vascular cells (Wortmann et al., 2013), T cells, and erythroid cells (Canli et al., 2016) did not survive in the absence of GPX4. ACSL4 and GPX4 double KO cells, on the other hand, survived and proliferated normally in cell culture for an extended period of time, highlighting the critical functional interaction between GPX4 and ACSL4.

In CC, CircLMO1, a newly identified circRNA, induced ferroptosis in CC cells by upregulating ACSL4 expression. Overexpression of miR-4291 or knockdown of ACSL4 reversed the effect of circLMO1 in facilitating ferroptosis, repressing proliferation, and decreasing tumor invasion of CC cells (Wu et al., 2021). Oleanolic acid (OA) promotes ACSL4-dependent ferroptosis in HeLa cells (Xiaofei et al., 2021) (Figure 2).

Potential applications of ferroptosis in cervical cancer

Besides surgery, the first-line chemotherapy drugs for CC currently include cisplatin, paclitaxel, carboplatin, etc. The second-line chemotherapy drugs include gemcitabine, epirubicin, etc. Among various anticancer drugs, cisplatin is one of the most widely used and effective anticancer agent in the treatment of

different types of solid tumors, but unfortunately, repeated platinum therapy after tumor recurrence is often ineffective. Cisplatin resistance may develop through the following molecular mechanisms: increased DNA repair capacity, altered cellular aggregation of the drug, and cytoplasmic inactivation of the drugs (Richon et al., 1987; Ferry et al., 2000; Amable, 2016). These cell death mechanisms are involved in apoptosis, but whether ferroptosis occurs through similar mechanisms is unclear. Ferroptosis is a novel cell death mechanism that differs greatly from traditional apoptosis; thus, targeting ferroptosis may be an effective therapeutic strategy for overcoming tumor resistance to cisplatin. Given that elastin induces ferroptosis, combining elastin (GSH inhibitor) with cisplatin (genotoxic agent) may have a synergistic effect on cancer therapy (Figure 2). Cisplatin combined with elastin showed a significant additive effect on antitumor activity in human ovarian cancer, head, and neck cancer (HNC), lung carcinoma (A549), and colon carcinoma (HCT116) cell lines, according to Guo et al. and Roh et al. (Roh et al., 2016; Guo et al., 2018). In oxaliplatin-resistant human cervical cancer cell lines, a combination treatment of iron chelator desferal (DFO) and oxaliplatin can overcome oxaliplatin resistance (Chen et al., 2016); a combination of low-concentration of PTX and RSL3 synergistically inhibits tumor cell growth by inducing ferroptosis (Ye et al., 2019); both *in vivo* and *in vitro* experiments confirmed that a combination of gemcitabine and erastin can inhibit the HSPA5-GPX4 signaling pathway and displays a synergistic antitumor effect on pancreatic cancer cells. A low concentration of elastin enhances the sensitivity of HL-60 cells to cytarabine and doxorubicin (Zhu et al., 2017) (Table 1).

Radiation therapy is another effective modality for the treatment of CC, but some patients develop resistance to radiation therapy. Various ferroptosis inducers, such as sorafenib and sulfasalazine, can act as radiosensitizers by inhibiting SLC7A11 and GPX4 activity. Lei et al. (Lei et al., 2020) found that radiotherapy can induce tumor cells to produce a large amount of lipid ROS and ACSL4 leading to the increased accumulation of lipid peroxides and increased occurrence of ferroptosis (Figure 2). The study further reported the activity of SLC7A11 and GPX4 in combination with ferroptosis inducers to cervical cancer *in vitro* and *in vivo* experiments, and found that tumor cells were considerably more sensitive to radiotherapy. The study also suggested that suitable ferroptosis inducers can serve as effective radiosensitizers to improve the efficacy of radiotherapy on tumor cells.

Conclusion

In other studies investigating the role of ferroptosis in cervical cancer, Wang et al. show that Cdc25A (cell division cycle 25) upregulates ErbB2 (epidermal growth factor receptor) level through dephosphorylation of PKM2, thereby inhibiting autophagy-dependent ferroptosis in CC cells (Wang et al., 2021c). Zhao et al. demonstrate that propofol and paclitaxel exert synergistic anticancer effects on cervical cancer cells (Zhao et al., 2022). Qi et al. established a four-gene (TFRC. ACACA, SQLE, and PHKG2) prognostic signature based on ferroptosis related genes (FRGs), providing new targets for CC involving ferroptosis (Qi et al., 2021). Xing et al. discovered eight ferroptosis- and immune-related differentially expressed genes (FI-DEGs) and developed a risk assessment model to predict outcomes in CESC patients (Cervical squamous cell carcinoma). Therefore, these eight genes have the potential to be prognostic and predictive biomarkers for cancer. Indeed, more research is needed to confirm the findings in the field of CC (Xing et al., 2021). Jiang et al. established a new predictive model that integrated 7 lncRNAs related to ferroptosis through analysis, which improve the predictive value and guided personalized treatment in patients with CC (Jiang et al., 2022). In the study by Zou et al., the ferroptosis-related gene PTGS2 turned out to be a key prognostic gene for an early-stage CC model associated with the immune microenvironment (Zou et al., 2022). Li et al. established a ferroptosis score (FerroScore) that was used to predict the sensitivity to chemotherapy and responses to immunotherapy in patients with CC. All these methods have a potential application for ferroptosis in CC.

Cancer incidence has been rising in recent years. According to current research, the ability of cells to avoid apoptosis is the primary cause of tumor resistance to treatment. Because ferroptosis differs from apoptosis, it provides a novel therapeutic option for cancer treatment. Due to the important roles of iron in cellular metabolism and increased oxidative stress in cervical cancer, it is worth exploring whether ferroptosis plays an important role in the pathogenesis of cervical cancer. In addition to the above-mentioned proteins and non-coding RNAs, several other compounds and proteins also play important roles in the occurrence of ferroptosis, regulating the biological characteristics of CC cells. HPV infection is closely related to the early diagnosis of CC, and HPV infection is also associated with oxidative stress, which is a key process promoting cell death by ferroptosis. Therefore, understanding the underlying mechanism of ferroptosis in the progression of CC may have implications for early diagnosis of CC.

In addition, the present study demonstrates that ferroptosis significantly affects the sensitization of tumor cells to chemoradiotherapy. Depending on the clinical status of CC, many patients with CC are resistant to traditional treatments. Therefore, as a newly discovered cell death mechanism, ferroptosis has excellent research value in antitumor therapy. However, antitumor therapy for ferroptosis faces numerous challenges. Several studies on the mechanism of ferroptosis in CC are currently being conducted, but the clinical application of the ferroptotic pathway in cancer therapy is very limited. Ferroptosis research in CC is currently ongoing, and the future application prospects of ferroptosis are limitless.

Author contributions

All authors listed have made a substantial, direct, and intellectual contribution to the work and approved it for publication.

Funding

National Natural Science Foundation of China, No. 82271677 Beijing Hospitals Authority's Ascent Plan, Code: DFL20221201; Beijing Municipal Health Commission, demonstration construction project of Clinical Research ward (NO: BCRW202109); Gynecological Tumor Precise Diagnosis and Treatment Innovaticn Studio; Funds received for open access publication fees from Beijing Obstetrics and Gynecology Hospital,

Capital Medical University, Beijing Maternal and Child Health Care Hospital.

Conflict of interest

The authors declare that the research was conducted in the absence of any commercial or financial relationships that could be construed as a potential conflict of interest.

Publisher's note

References

Alvarez, S. W., Sviderskiy, V. O., Terzi, E. M., Papagiannakopoulos, T., Moreira, A. L., Adams, S., et al. (2017). NFS1 undergoes positive selection in lung tumours and protects cells from ferroptosis. *Nature* 551 (7682), 639–643. doi:10.1038/nature24637

Amable, L. (2016). Cisplatin resistance and opportunities for precision medicine. *Pharmacol. Res.* 106, 27–36. doi:10.1016/j.phrs.2016.01.001

Aranda-Rivera, A. K., Cruz-Gregorio, A., Briones-Herrera, A., and Pedraza-Chaverri, J. (2021). Regulation of autophagy by high- and low-risk human papillomaviruses. *Rev. Med. virology* 31 (2), e2169. doi:10.1002/rmv.2169

Banerjee, N. S., Moore, D., Parker, C. J., Broker, T. R., and Chow, L. T. (2019). Targeting DNA damage response as a strategy to treat HPV infections. *Int. J. Mol. Sci.* 20 (21), 5455. doi:10.3390/ijms20215455

Braun, J. A., Herrmann, A. L., Blase, J. I., Frensemeier, K., Bulkescher, J., Scheffner, M., et al. (2020). Effects of the antifungal agent ciclopirox in HPV-positive cancer cells: Repression of viral E6/E7 oncogene expression and induction of senescence and apoptosis. *Int. J. cancer* 146 (2), 461–474. doi:10.1002/ijc.32709

Bray, F., Ferlay, J., Soerjomataram, I., Siegel, R. L., Torre, L. A., and Jemal, A. (2018). Global cancer statistics 2018: GLOBOCAN estimates of incidence and mortality worldwide for 36 cancers in 185 countries. *CA a cancer J. Clin.* 68 (6), 394–424. doi:10.3322/caac.21492

Bridges, R. J., Natale, N. R., and Patel, S. A. (2012). System xc^- cystine/glutamate antiporter: An update on molecular pharmacology and roles within the CNS. *Br. J. Pharmacol.* 165 (1), 20–34. doi:10.1111/j.1476-5381.2011.01480.x

Brown, C. W., Amante, J. J., Chhoy, P., Elaimy, A. L., Liu, H., Zhu, L. J., et al. (2019). Prominin2 drives ferroptosis resistance by stimulating iron export. *Dev. Cell* 51 (5), 575–586. doi:10.1016/j.devcel.2019.10.007

Canli, Ö., Alankuş, Y. B., Grootjans, S., Vegi, N., Hültner, L., Hoppe, P. S., et al. (2016). Glutathione peroxidase 4 prevents necroptosis in mouse erythroid precursors. *Blood* 127 (1), 139–148. doi:10.1182/blood-2015-06-654194

Chen, S. J., Kuo, C. C., Pan, H. Y., Tsou, T. C., Yeh, S. C., and Chang, J. Y. (2016). Desferal regulates hCtr1 and transferrin receptor expression through Sp1 and exhibits synergistic cytotoxicity with platinum drugs in oxaliplatin-resistant human cervical cancer cells *in vitro* and *in vivo*. *Oncotarget* 7 (31), 49310–49321. doi:10.18632/oncotarget.10336

Chen, S., Shen, L., Luo, S., Lan, X., and Wang, L. (2020). Association between serum iron levels and the risk of cervical cancer in Chinese: A meta-analysis. *J. Int. Med. Res.* 48 (3), 300060519882804. doi:10.1177/0300060519882804

Crosbie, E. J., Einstein, M. H., Franceschi, S., and Kitchener, H. C. (2013). Human papillomavirus and cervical cancer. *Lancet (London, Engl.* 382 (9895), 889–899. doi:10.1016/S0140-6736(13)60022-7

Cruz-Gregorio, A., and Aranda-Rivera, A. K. (2021). Redox-sensitive signalling pathways regulated by human papillomavirus in HPV-related cancers. *Rev. Med. virology* 31 (6), e2230. doi:10.1002/rmv.2230

Cruz-Gregorio, A., Aranda-Rivera, A. K., Aparicio-Trejo, O. E., Coronado-Martínez, I., Pedraza-Chaverri, J., and Lizano, M. (2019). E6 oncoproteins from high-risk human papillomavirus induce mitochondrial metabolism in a head and neck squamous cell carcinoma model. *Biomolecules* 9 (8), 351. doi:10.3390/biom9080351

Cruz-Gregorio, A., Aranda-Rivera, A. K., and Pedraza-Chaverri, J. (2020). Human papillomavirus-related cancers and mitochondria. *Virus Res.* 286, 198016. doi:10.1016/j.virusres.2020.198016

Dev, S., and Babitt, J. L. (2017). Overview of iron metabolism in health and disease. *Hemodial. Int. Int. Symposium Home Hemodial.* 21 (1), S6–S20. doi:10.1111/hdi.12542

Di Domenico, M., Giovane, G., Kouidhi, S., Iorio, R., Romano, M., De Francesco, F., et al. (2018). HPV epigenetic mechanisms related to Oropharyngeal and Cervix cancers. *Cancer Biol. Ther.* 19 (10), 850–857. doi:10.1080/15384047.2017.1310349

Dixon, S. J., Lemberg, K. M., Lamprecht, M. R., Skouta, R., Zaitsev, E. M., Gleason, C. E., et al. (2012). Ferroptosis: An iron-dependent form of nonapoptotic cell death. *Cell* 149 (5), 1060–1072. doi:10.1016/j.cell.2012.03.042

Doll, S., Freitas, F. P., Shah, R., Aldrovandi, M., da Silva, M. C., Ingold, I., et al. (2019). FSP1 is a glutathione-independent ferroptosis suppressor. *Nature* 575 (7784), 693–698. doi:10.1038/s41586-019-1707-0

Espósito, B. P., Epsztejn, S., Breuer, W., and Cabantchik, Z. I. (2002). A review of fluorescence methods for assessing labile iron in cells and biological fluids. *Anal. Biochem.* 304 (1), 1–18. doi:10.1006/abio.2002.5611

Fan, H. J., Tan, Z. B., Wu, Y. T., Feng, X. R., Bi, Y. M., Xie, L. P., et al. (2020). The role of ginsenoside Rb1, a potential natural glutathione reductase agonist, in preventing oxidative stress-induced apoptosis of H9C2 cells. *J. ginseng Res.* 44 (2), 258–266. doi:10.1016/j.jgr.2018.12.004

Ferry, K. V., Hamilton, T. C., and Johnson, S. W. (2000). Increased nucleotide excision repair in cisplatin-resistant ovarian cancer cells: Role of ERCC1-XPF. *Biochem. Pharmacol.* 60 (9), 1305–1313. doi:10.1016/s0006-2952(00)00441-x

Gaffney, D. K., Hashibe, M., Kepka, D., Maurer, K. A., and Werner, T. L. (2018). Too many women are dying from cervix cancer: Problems and solutions. *Gynecol. Oncol.* 151 (3), 547–554. doi:10.1016/j.ygyno.2018.10.004

Geng, N., Shi, B. J., Li, S. L., Zhong, Z. Y., Li, Y. C., Xua, W. L., et al. (2018). Knockdown of ferroportin accelerates erastin-induced ferroptosis in neuroblastoma cells. *Eur. Rev. Med. Pharmacol. Sci.* 22 (12), 3826–3836. doi:10.26355/eurrev_201806_15267

Guo, J., Xu, B., Han, Q., Zhou, H., Xia, Y., Gong, C., et al. (2018). Ferroptosis: A novel antitumor action for cisplatin. *Cancer Res. Treat.* 50 (2), 445–460. doi:10.4143/crt.2016.572

Hassannia, B., Vandenabeele, P., and Vanden Berghe, T. (2019). Targeting ferroptosis to iron out cancer. *Cancer Cell* 35 (6), 830–849. doi:10.1016/j.ccell.2019.04.002

Hou, W., Xie, Y., Song, X., Sun, X., Lotze, M. T., Zeh, H. J., 3rd, et al. (2016). Autophagy promotes ferroptosis by degradation of ferritin. *Autophagy* 12 (8), 1425–1428. doi:10.1080/15548627.2016.1187366

Huang, N., Wei, Y., Cheng, Y., Wang, X., Wang, Q., Chen, D., et al. (2022). Iron metabolism protein transferrin receptor 1 involves in cervical cancer progression by affecting gene expression and alternative splicing in HeLa cells. *Genes and genomics* 44 (6), 637–650. doi:10.1007/s13258-021-01205-w

Jennis, M., Kung, C. P., Basu, S., Budina-Kolomets, A., Leu, J. I., Khaku, S., et al. (2016). An African-specific polymorphism in the TP53 gene impairs p53 tumor suppressor function in a mouse model. *Genes and Dev.* 30 (8), 918–930. doi:10.1101/gad.275891.115

Jiang, P., and Yue, Y. (2014). Human papillomavirus oncoproteins and apoptosis (Review). *Exp. Ther. Med.* 7 (1), 3–7. doi:10.3892/etm.2013.1374

Jiang, L., Hickman, J. H., Wang, S. J., and Gu, W. (2015). Dynamic roles of p53-mediated metabolic activities in ROS-induced stress responses. *Cell cycleGeorget. Tex)* 14 (18), 2881–2885. doi:10.1080/15384101.2015.1068479

Jiang, L., Kon, N., Li, T., Wang, S. J., Su, T., Hibshoosh, H., et al. (2015). Ferroptosis as a p53-mediated activity during tumour suppression. *Nature* 520 (7545), 57–62. doi:10.1038/nature14344

Jiang, P., Wang, L., Hou, B., Zhu, J., Zhou, M., Jiang, J., et al. (2018). A novel HPV16 E7-affitoxin for targeted therapy of HPV16-induced human cervical cancer. *Theranostics* 8 (13), 3544–3558. doi:10.7150/thno.24607

Jiang, Z., Li, J., Feng, W., Sun, Y., and Bu, J. (2022). A ferroptosis-related lncRNA model to enhance the predicted value of cervical cancer. *J. Oncol.* 2022, 6080049. doi:10.1155/2022/6080049

Kajarabille, N., and Latunde-Dada, G. O. (2019). Programmed cell-death by ferroptosis: Antioxidants as mitigators. *Int. J. Mol. Sci.* 20 (19), 4968. doi:10.3390/ijms20194968

Koh, W. J., Abu-Rustum, N. R., Bean, S., Bradley, K., Campos, S. M., Cho, K. R., et al. (2019). Cervical cancer, version 3.2019, NCCN clinical practice guidelines in oncology. *J. Natl. Compr. Cancer Netw. JNCCN* 17 (1), 64–84. doi:10.6004/jnccn.2019.0001

Lei, G., Zhang, Y., Koppula, P., Liu, X., Zhang, J., Lin, S. H., et al. (2020). The role of ferroptosis in ionizing radiation-induced cell death and tumor suppression. *Cell Res.* 30 (2), 146–162. doi:10.1038/s41422-019-0263-3

Li, J., Cao, F., Yin, H. L., Huang, Z. J., Lin, Z. T., Mao, N., et al. (2020). Ferroptosis: Past, present and future. *Cell death Dis.* 11 (2), 88. doi:10.1038/s41419-020-2298-2

Liang, C., Zhang, X., Yang, M., and Dong, X. (2019). Recent progress in ferroptosis inducers for cancer therapy. *Adv. Mater. Deerf. Beach, Fla)* 31 (51), e1904197. doi:10.1002/adma.201904197

Lin, L. S., Song, J., Song, L., Ke, K., Liu, Y., Zhou, Z., et al. (2018). Simultaneous fenton-like ion delivery and glutathione depletion by MnO(2) -based nanoagent to enhance chemodynamic therapy. *Angewandte Chemie Int. ed Engl.* 57 (18), 4902–4906. doi:10.1002/anie.201712027

Liu, Q., and Wang, K. (2019). The induction of ferroptosis by impairing STAT3/Nrf2/GPx4 signaling enhances the sensitivity of osteosarcoma cells to cisplatin. *Cell Biol. Int.* 43 (11), 1245–1256. doi:10.1002/cbin.11121

Markowitsch, S. D., Schupp, P., Lauckner, J., Vakhrusheva, O., Slade, K. S., Mager, R., et al. (2020). Artesunate inhibits growth of sunitinib-resistant renal cell carcinoma cells through cell cycle arrest and induction of ferroptosis. *Cancers* 12 (11), 3150. doi:10.3390/cancers12113150

Monk, B. J., Sill, M. W., McMeekin, D. S., Cohn, D. E., Ramondetta, L. M., Boardman, C. H., et al. (2009). Phase III trial of four cisplatin-containing doublet combinations in stage IVB, recurrent, or persistent cervical carcinoma: A gynecologic oncology group study. *J. Clin. Onco. J. Am. Soci. Clin. Onco.* 27 (28), 4649–4655. doi:10.1200/JCO.2009.21.8909

Naveen Kumar, S. K., Hemshekhar, M., Kemparaju, K., and Girish, K. S. (2019). Hemin-induced platelet activation and ferroptosis is mediated through ROS-driven proteasomal activity and inflammasome activation: Protection by Melatonin. *Biochimica biophysica acta Mol. basis Dis.* 1865 (9), 2303–2316. doi:10.1016/j.bbadis.2019.05.009

Paul, B. T., Manz, D. H., Torti, F. M., and Torti, S. V. (2017). Mitochondria and iron: Current questions. *Expert Rev. Hematol.* 10 (1), 65–79. doi:10.1080/17474086.2016.1268047

Petrat, F., de Groot, H., Sustmann, R., and Rauen, U. (2002). The chelatable iron pool in living cells: A methodically defined quantity. *Biol. Chem.* 383 (3–4), 489–502. doi:10.1515/BC.2002.051

Pfaendler, K. S., and Tewari, K. S. (2016). Changing paradigms in the systemic treatment of advanced cervical cancer. *Am. J. obstetrics Gynecol.* 214 (1), 22–30. doi:10.1016/j.ajog.2015.07.022

Qi, X., Fu, Y., Sheng, J., Zhang, M., Zhang, M., Wang, Y., et al. (2021). A novel ferroptosis-related gene signature for predicting outcomes in cervical cancer. *Bioengineered* 12 (1), 1813–1825. doi:10.1080/21655979.2021.1925003

Qian, Z. M., Li, H., Sun, H., and Ho, K. (2002). Targeted drug delivery via the transferrin receptor-mediated endocytosis pathway. *Pharmacol. Rev.* 54 (4), 561–587. doi:10.1124/pr.54.4.561

Quiles Del Rey, M., and Mancias, J. D. (2019). NCOA4-Mediated ferritinophagy: A potential link to neurodegeneration. *Front. Neurosci.* 13, 238. doi:10.3389/fnins.2019.00238

Rallis, K. S., Lai Yau, T. H., and Sideris, M. (2021). Chemoradiotherapy in cancer treatment: Rationale and clinical applications. *Anticancer Res.* 41 (1), 1–7. doi:10.21873/anticanres.14746

Richon, V. M., Schulte, N., and Eastman, A. (1987). Multiple mechanisms of resistance to cis-diamminedichloroplatinum(II) in murine leukemia L1210 cells. *Cancer Res.* 47 (8), 2056–2061.

Roh, J. L., Kim, E. H., Jang, H. J., Park, J. Y., and Shin, D. (2016). Induction of ferroptotic cell death for overcoming cisplatin resistance of head and neck cancer. *Cancer Lett.* 381 (1), 96–103. doi:10.1016/j.canlet.2016.07.035

Seiler, A., Schneider, M., Förster, H., Roth, S., Wirth, E. K., Culmsee, C., et al. (2008). Glutathione peroxidase 4 senses and translates oxidative stress into 12/15-lipoxygenase dependent- and AIF-mediated cell death. *Cell metab.* 8 (3), 237–248. doi:10.1016/j.cmet.2008.07.005

Stockwell, B. R., Friedmann Angeli, J. P., Bayir, H., Bush, A. I., Conrad, M., Dixon, S. J., et al. (2017). Ferroptosis: A regulated cell death nexus linking metabolism, redox biology, and disease. *Cell* 171 (2), 273–285. doi:10.1016/j.cell.2017.09.021

Sun, X., Ou, Z., Chen, R., Niu, X., Chen, D., Kang, R., et al. (2016). Activation of the p62-Keap1-NRF2 pathway protects against ferroptosis in hepatocellular carcinoma cells. *Hepatol. Baltim. Md)* 63 (1), 173–184. doi:10.1002/hep.28251

Taghizadeh, E., Jahangiri, S., Rostami, D., Taheri, F., Renani, P. G., Taghizadeh, H., et al. (2019). Roles of E6 and E7 human papillomavirus proteins in molecular pathogenesis of cervical cancer. *Curr. protein and peptide Sci.* 20 (9), 926–934. doi:10.2174/1389203720666190618101441

Vande Pol, S. B., and Klingelhutz, A. J. (2013). Papillomavirus E6 oncoproteins. *Virology* 445 (1–2), 115–137. doi:10.1016/j.virol.2013.04.026

Wang, S. J., Li, D., Ou, Y., Jiang, L., Chen, Y., Zhao, Y., et al. (2016). Acetylation is crucial for p53-mediated ferroptosis and tumor suppression. *Cell Rep.* 17 (2), 366–373. doi:10.1016/j.celrep.2016.09.022

Wang, K., Jiang, J., Lei, Y., Zhou, S., Wei, Y., and Huang, C. (2019). Targeting metabolic-redox circuits for cancer therapy. *Trends Biochem. Sci.* 44 (5), 401–414. doi:10.1016/j.tibs.2019.01.001

Wang, Y., Zhao, G., Condello, S., Huang, H., Cardenas, H., Tanner, E. J., et al. (2021). Frizzled-7 identifies platinum-tolerant ovarian cancer cells susceptible to ferroptosis. *Cancer Res.* 81 (2), 384–399. doi:10.1158/0008-5472.CAN-20-1488

Wang, R., Xing, R., Su, Q., Yin, H., Wu, D., Lv, C., et al. (2021). Knockdown of SFRS9 inhibits progression of colorectal cancer through triggering ferroptosis mediated by GPX4 reduction. *Front. Oncol.* 11, 683589. doi:10.3389/fonc.2021.683589

Wang, C., Zeng, J., Li, L. J., Xue, M., and He, S. L. (2021). Cdc25A inhibits autophagy-mediated ferroptosis by upregulating ErbB2 through PKM2 dephosphorylation in cervical cancer cells. *Cell death Dis.* 12 (11), 1055. doi:10.1038/s41419-021-04342-y

Wang, T., Gong, M., Cao, Y., Zhao, C., Lu, Y., Zhou, Y., et al. (2022). Persistent ferroptosis promotes cervical squamous intraepithelial lesion development and oncogenesis by regulating KRAS expression in patients with high risk-HPV infection. *Cell death Discov.* 8 (1), 201. doi:10.1038/s41420-022-01013-5

Wortmann, M., Schneider, M., Pircher, J., Hellfritsch, J., Aichler, M., Vegi, N., et al. (2013). Combined deficiency in glutathione peroxidase 4 and vitamin E causes multiorgan thrombus formation and early death in mice. *Circulation Res.* 113 (4), 408–417. doi:10.1161/CIRCRESAHA.113.279984

Wu, P., Li, C., Ye, D. M., Yu, K., Li, Y., Tang, H., et al. (2021). Circular RNA circEPSTI1 accelerates cervical cancer progression via miR-375/409–3P/515–5p-SLC7A11 axis. *Aging* 13 (3), 4663–4673. doi:10.18632/aging.202518

Xiaofei, J., Mingqing, S., Miao, S., Yizhen, Y., Shuang, Z., Qinhua, X., et al. (2021). Oleanolic acid inhibits cervical cancer Hela cell proliferation through modulation of the ACSL4 ferroptosis signaling pathway. *Biochem. biophysical Res. Commun.* 545, 81–88. doi:10.1016/j.bbrc.2021.01.028

Xing, C., Yin, H., Yao, Z. Y., and Xing, X. L. (2021). Prognostic signatures based on ferroptosis- and immune-related genes for cervical squamous cell carcinoma and endocervical adenocarcinoma. *Front. Oncol.* 11, 774558. doi:10.3389/fonc.2021.774558

Xiong, J., Nie, M., Fu, C., Chai, X., Zhang, Y., He, L., et al. (2022). Hypoxia enhances HIF1α transcription activity by upregulating KDM4A and mediating H3K9 me3; thus, inducing ferroptosis resistance in cervical cancer cells. *Stem cells Int.* 2022, 1608806. doi:10.1155/2022/1608806

Yang, W. S., and Stockwell, B. R. (2008). Synthetic lethal screening identifies compounds activating iron-dependent, nonapoptotic cell death in oncogenic-RAS-harboring cancer cells. *Chem. Biol.* 15 (3), 234–245. doi:10.1016/j.chembiol.2008.02.010

Yang, W. S., SriRamaratnam, R., Welsch, M. E., Shimada, K., Skouta, R., Viswanathan, V. S., et al. (2014). Regulation of ferroptotic cancer cell death by GPX4. *Cell* 156 (1–2), 317–331. doi:10.1016/j.cell.2013.12.010

Yang, Y., Lin, J., Guo, S., Xue, X., Wang, Y., Qiu, S., et al. (2020). RRM2 protects against ferroptosis and is a tumor biomarker for liver cancer. *Cancer Cell Int.* 20 (1), 587. doi:10.1186/s12935-020-01689-8

Ye, P., Mimura, J., Okada, T., Sato, H., Liu, T., Maruyama, A., et al. (2014). Nrf2-and ATF4-dependent upregulation of xCT modulates the sensitivity of T24 bladder carcinoma cells to proteasome inhibition. *Mol. Cell. Biol.* 34 (18), 3421–3434. doi:10.1128/MCB.00221-14

Ye, J., Jiang, X., Dong, Z., Hu, S., and Xiao, M. (2019). Low-concentration PTX and RSL3 inhibits tumor cell growth synergistically by inducing ferroptosis in mutant p53 hypopharyngeal squamous carcinoma. *Cancer Manag. Res.* 11, 9783–9792. doi:10.2147/CMAR.S217944

Yeo-Teh, N. S. L., Ito, Y., and Jha, S. (2018). High-risk human papillomaviral oncogenes E6 and E7 target key cellular pathways to achieve oncogenesis. *Int. J. Mol. Sci.* 19 (6), 1706. doi:10.3390/ijms19061706

Yuan, H., Li, X., Zhang, X., Kang, R., and Tang, D. (2016). Identification of ACSL4 as a biomarker and contributor of ferroptosis. *Biochem. biophysical Res. Commun.* 478 (3), 1338–1343. doi:10.1016/j.bbrc.2016.08.124

Zhao, M. Y., Liu, P., Sun, C., Pei, L. J., and Huang, Y. G. (2022). Propofol augments paclitaxel-induced cervical cancer cell ferroptosis *in vitro*. *Front. Pharmacol.* 13, 816432. doi:10.3389/fphar.2022.816432

Zhu, S., Zhang, Q., Sun, X., Zeh, H. J., 3rd, Lotze, M. T., Kang, R., et al. (2017). HSPA5 regulates ferroptotic cell death in cancer cells. *Cancer Res.* 77 (8), 2064–2077. doi:10.1158/0008-5472.CAN-16-1979

Zhuo, S., Chen, Z., Yang, Y., Zhang, J., Tang, J., and Yang, K. (2020). Clinical and biological significances of a ferroptosis-related gene signature in glioma. *Front. Oncol.* 10, 590861. doi:10.3389/fonc.2020.590861

Zou, C., Xu, F., Shen, J., and Xu, S. (2022). Identification of a ferroptosis-related prognostic gene PTGS2 based on risk modeling and immune microenvironment of early-stage cervical cancer. *J. Oncol.* 2022, 3997562. doi:10.1155/2022/3997562

frontiers | Frontiers in Molecular Biosciences

TYPE Original Research
PUBLISHED 31 March 2023
DOI 10.3389/fmolb.2023.1156062

OPEN ACCESS

EDITED BY
Yanqing Liu,
Columbia University, United States

REVIEWED BY
Valentina Bosello Travain,
University of Padua, Italy
Li-Xing Yang,
National Cheng Kung University, Taiwan

*CORRESPONDENCE
Yanbo Shi,
shiyanbocas@163.com

SPECIALTY SECTION
This article was submitted to Molecular Diagnostics and Therapeutics, a section of the journal Frontiers in Molecular Biosciences

RECEIVED 01 February 2023
ACCEPTED 22 March 2023
PUBLISHED 31 March 2023

CITATION
Shi H, Xiong L, Yan G, Du S, Liu J and Shi Y (2023), Susceptibility of cervical cancer to dihydroartemisinin-induced ferritinophagy-dependent ferroptosis. *Front. Mol. Biosci.* 10:1156062. doi: 10.3389/fmolb.2023.1156062

Susceptibility of cervical cancer to dihydroartemisinin-induced ferritinophagy-dependent ferroptosis

Hanqiang Shi[1,2], Lie Xiong[1,2], Guang Yan[3], Shuqin Du[1,4], Jie Liu[5] and Yanbo Shi[1,2]*

[1]Central Laboratory of Molecular Medicine Research Center, Jiaxing Traditional Chinese Medicine Hospital Affiliated to Zhejiang Chinese Medical University, Jiaxing, China, [2]Jiaxing Key Laboratory of Diabetic Angiopathy Research, Jiaxing, China, [3]Department of Urology, Nanfang Hospital, Southern Medical University, Guangzhou, China, [4]School of Pharmacy, Zhejiang University of Technology, Hangzhou, China, [5]Oncology Department, Jiaxing Traditional Chinese Medicine Hospital Affiliated to Zhejiang Chinese Medical University, Jiaxing, China

The clinical therapeutics of cervical cancer is limited due to the drug resistance and metastasis of tumor. As a novel target for antitumor therapy, ferroptosis is deemed to be more susceptible for those cancer cells with resistance to apoptosis and chemotherapy. Dihydroartemisinin (DHA), the primary active metabolites of artemisinin and its derivatives, has exhibited a variety of anticancer properties with low toxicity. However, the role of DHA and ferroptosis in cervical cancer remained unclear. Here, we showed that DHA could time-dependently and dose-dependently inhibit the proliferation of cervical cancer cells, which could be alleviated by the inhibitors of ferroptosis rather than apoptosis. Further investigation confirmed that DHA treatment initiated ferroptosis, as evidenced by the accumulation of reactive oxygen species (ROS), malondialdehyde (MDA) and liquid peroxidation (LPO) levels and simultaneously depletion of glutathione peroxidase 4 (GPX4) and glutathione (GSH). Moreover, nuclear receptor coactivator 4 (NCOA4)-mediated ferritinophagy was also induced by DHA leading to subsequent increases of intracellular labile iron pool (LIP), exacerbated the Fenton reaction resulting in excessive ROS production, and enhanced cervical cancer ferroptosis. Among them, we unexpectedly found that heme oxygenase-1 (HO-1) played an antioxidant role in DHA-induced cell death. In addition, the results of synergy analysis showed that the combination of DHA and doxorubicin (DOX) emerged a highly synergistic lethal effect for cervical cancer cells, which was related also to ferroptosis. Overall, our data revealed the molecular mechanisms that DHA triggered ferritinophagy-dependent ferroptosis and sensitized to DOX in cervical cancer, which may provide novel avenues for future therapy development.

KEYWORDS

cervical cancer, dihydroartemisinin, ferroptosis, ferritinophagy, heme oxygenase-1, doxorubicin

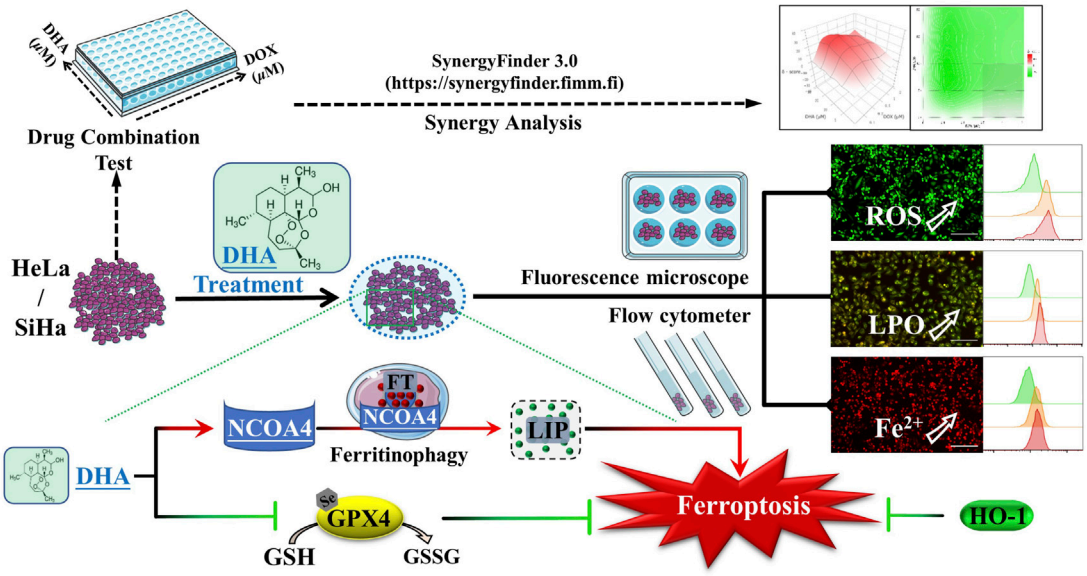

GRAPHICAL ABSTRACT

1 Introduction

Cervical cancer is one of the most common and lethal gynecological malignancy, affecting millions of women worldwide (Arbyn et al., 2020). Despite the vigorous promotion of HPV vaccine and the continuous improvement of screening technology, it is still the leading cause of death in women in underdeveloped countries or areas (Sung et al., 2021). And because of China's large population, women's death from cervical cancer accounts for 12% of women's death worldwide. Even more alarming, its incidence rate is rising, and the incidence age is getting younger (Zhou et al., 2016; Xia et al., 2018). At present, the combined chemotherapy with targeted therapy is a standard treatment for cervical cancer, which significantly improves the survival of patients compared with chemotherapy alone (Hill, 2020). So far, the clinical outcomes of cervical cancer patients in early stages have significantly improved by standard treatments. However, due to the drug resistance and metastasis of tumor, those patients at an advanced stage or recurrent cervical cancer have a poor prognosis with limited treatment options and the therapy remains far from satisfactory (Abu-Rustum et al., 2020; Zhang et al., 2021). As a result, nowadays, the demand for new therapies with more secure, effective and feasible is becoming more and more urgent.

Ferroptosis is a new form of programmed cell death that characterized by an iron-dependent accumulation of lethal lipid peroxidation (LPO) (Dixon et al., 2012; Stockwell, 2022). And it is different from apoptosis, necrosis, and autophagy at morphological, biochemical, and genetical levels. From the perspective of antioxidant, ferroptosis is caused by a redox imbalance between the production of oxidants and antioxidants, which is driven by the abnormal expression and activity of multiple redox-active enzymes that produce or detoxify free radicals and lipid oxidation products (Tang et al., 2021a; Liu and Gu, 2022). Emerging evidences have shown that cancer cells are sensitive to ferroptosis and targeting ferroptosis has great potential to be an effective strategy and approach for cancer therapy (Hassannia et al., 2019; Chen et al., 2022). It has been reported that ferroptosis inducer RAS-selective lethal small molecule 3 (RSL3) could enhance the antitumor effect of cisplatin *via* the inhibition of glutathione peroxidase 4 (GPX4) (Zhang et al., 2020a). Noteworthy, activation of certain autophagy pathways can promote ferroptosis, which is called autophagy-dependent ferroptotic cell death, such as nuclear receptor coactivator 4 (NCOA4)-facilitated ferritinophagy, beclin 1 (BECN1)-mediated glutamate antiporter (system Xc^-) inhibition (Zhou et al., 2020). In cervical cancer cells, the anti-cancer drug sorafenib has been shown to induce autophagy-dependent ferroptosis through the Cdc25A/PKM2/ErbB2 axis (Wang et al., 2021a). It has also been found that non-coding RNAs can affect the occurrence of ferroptosis in cervical cancer cells (Wu et al., 2021; Liu et al., 2022). And the bioinformatics analysis about ferroptosis-related genes suggests that targeting ferroptosis may represent a promising approach for the treatment in cervical cancer (Qi et al., 2021). Although the roles of ferroptosis in cervical cancer are remain rarely explored and unclear, it may be a potential therapeutic direction.

Dihydroartemisinin (DHA), first-generation derivative of artemisinin and also the primary active metabolites of artemisinin and its derivatives, is an effective antimalarial drug with low toxicity (Yu et al., 2021). Beyond the widely acknowledged anti-malarial effect, DHA has shown a variety of anticancer properties including apoptosis, autophagy and ferroptosis in different cancers, as well as enhances the efficacy of chemotherapy and targeted therapy (Dai et al., 2021; Li et al., 2021). Previous studies have confirmed that DHA has a potent lethal effect in cervical cancer cells (Lu et al., 2020), and can sensitize HeLa cells to doxorubicin (DOX) -induced apoptosis (Tai et al., 2016). Meanwhile, a clinical study also found that Artenimol-R (the succinate ester of DHA) treatment in patients with advanced cervical cancer showed an improvement of the clinical symptoms

and a good tolerability (Jansen et al., 2011). Nevertheless, there is little literature to confirm the existence and importance of ferroptosis in the DHA-induced cervical cancer cell death. Thus, in the present study, we investigated the effect and mechanism of DHA on the proliferation and ferroptosis of cervical cancer cells, as well as the sensitization effect on DOX.

2 Materials and methods

2.1 Reagent and antibodies

Dihydroartemisinin (DHA, D140839, purity: ≥98%), hemin (H140872) and chloroquine (CQ, C193834) were purchased from Aladdin (China). Dimethyl sulfoxide (DMSO, A503039) and ferric ammonium citrate (FAC, A500061) were got from Sangon Biotech (China). Deferoxamine (DFO, D9533) and protoporphyrin IX zinc(II) (ZnPPIX, 282820) were purchased from Sigma-Aldrich (United States). Z-VAD-FMK (HY-16658B), ferrostatin-1 (Fer-1, HY-100579) and doxorubicin hydrochloride (DOX, HY-15142) were purchased from MedChemExpress (United States). And the antibody to ACSL4 (ab155282), GPX4 (ab125066), xCT (ab175186), HO-1 (ab82585), TfR1 (ab84036), FTH1 (ab65080) and NCOA4 (ab86707) were all purchased from Abcam (United Kingdom). Anti-β-actin and goat anti-rabbit IgG H&L were purchased from Bioker (China).

2.2 Cell culture and drug configuration

Human cervical cancer cells HeLa (adenocarcinoma) and SiHa (squamous cell carcinoma) were purchased from National Infrastructure of Cell Line Resource (NICR, China) and then were maintained in RPMI-1640 and MEM medium (Gibco, United States), respectively, supplemented with 10% FBS (Gibco, United States) and 100 IU/mL penicillin and 100 mug/mL streptomycin (Sangon, China) at a 37°C incubator with 5% CO_2. DHA was prepared as a DMSO stocking solution with a concentration of 200 mM. After sub packaging, it was frozen at −20°C.

2.3 Cell viability assay

DHA cytotoxicity was detected by the Cell Counting Kit-8 (CCK-8; BBI, China). 5×10^3 cells were seeded into each well of the 96-well plate. Then various concentrations of DHA (0, 5, 10, 20, 40 and 80 μM) were added to the plates and followed by another 24, or 48-h incubation in a 37°C, 5% CO_2 incubator. Then 10 μL CCK-8 solution was added to each well and further 1 h's incubation was carried out. The optical density (OD) was measured at 450 nm, and then the cell viability was calculated.

2.4 Determination of intracellular reactive oxygen species (ROS)

The fluorescent probe DCFH-DA (Sigma-Aldrich, United States) was used to evaluate the intracellular ROS levels. The methods used are according to the manufacturer's instructions. Cells were inoculated into 6-well plates at 2×10^5 cells/well and grown overnight, then incubated with different concentration of DHA for 24 h. Thereafter, the cells were stained with DCFH-DA probe at 37°C for 30 min in the dark. After washing with serum-free medium for three times, the fluorescence of cells was photographed under fluorescence inverted microscope Axio Observer D1 (ZEISS, Germany) and detected by the flow cytometer BD FACS Canto II (BD Biosciences, United States).

2.5 Detection of intracellular malondialdehyde (MDA)

Intracellular MDA levels in the cells were measured using micro MDA assay kit (Solarbio, China) following the instruction by the manufacturer. Briefly, the cells of each group were collected and disrupted by an ultrasonic cell pulverize. The cell suspension was centrifuged and then 100 μL sample was added for the measurement, followed by the addition of 400 μL of the MDA test solution. After mixing and reacting in a 100°C-water bath for 30 min, the mixture was cooled to room temperature and centrifuged. Next the supernatant was taken out and measured absorbance at 450, 532, and 600 nm wavelength with a full-wavelength microplate reader (Thermo, United States).

2.6 Redox status determination

2×10^5 cells were seeded into each well of the 6-well plate and intervened with 0, 40 and 80 μM DHA for 24 h. To assess the status of antioxidant, the collected cells were measured using the commercial assay kits of superoxide dismutase (SOD; Sangon Biotech, China), catalase (CAT; Sangon Biotech, China), reduced glutathione (GSH; Jiancheng, China) and glutathione peroxidase (GPx; Beyotime, China) strictly following the manufacturer's instructions.

2.7 Lipid peroxidation (LPO) assay

LPO was investigated by BODIPY™ 581/591 C11 dye (Thermo, United States), which shifts fluorescence properties from red signals to green signals upon oxidation (Yi et al., 2022). Briefly, cells were seeded in 6-well plates at 2×10^5 cells/well and grown overnight. After treatments, cells were loaded with 2.5 μM BODIPY™ 581/591 C11 at 37°C for 30 min in the dark. After washing with serum-free medium for three times, the fluorescence of cells was photographed under fluorescence inverted microscope Axio Observer D1 (ZEISS, Germany) and detected by the flow cytometer BD FACS Canto II (BD Biosciences, United States).

2.8 RNA extraction and quantitative PCR (qPCR)

RNA was extracted and quantified according to the previous operation methods of our research group (Du et al., 2022). Total

TABLE 1 The primer sequences.

Target gene		Primer sequence (5′to 3′)		Size (bp)
Name	Id	Forward	Reverse	
ACSL4	2,182	ATACCTGGACTGGGACCGAA	TGCTGGACTGGTCAGAGAGT	145
TfR1	7,037	TGGAGACTTTGGATCGGTTGGTG	CAGTGGCTGGCAGAAACCTTG	138
NCOA4	8031	GGGCAACCTCAGCCAGTTAT	CAAACTGCAGGGAGGCCATA	139
FTH1	2,495	CCAGAACTACCACCAGGACTC	CAAAGCCACATCATCGCGG	118
GPX4	2,879	CAGTGAGGCAAGACCGAAGT	CCGAACTGGTTACACGGGAA	104
xCT	23657	CATCTCTCCTAAGGGCGTGC	TAGTGACAGGACCCCACACA	85
H O -1	3162	CCGCATGAACTCCCTGGAGATG	CTGGATGTTGAGCAGGAACGCAG	85
β-*actin*	60	CCTGGCACCCAGCACAAT	GGGCCGGACTCGTCATAC	114

ACSL4: acyl-CoA, synthetase long-chain family member 4; *NCOA4*: nuclear receptor coactivator 4; *FTH1*: ferritin heavy chain 1; *GPX4*: glutathione peroxidase 4; *H O -1*: heme oxygenase 1; *xCT*: cystine-glutamate antiporter; *TfR1*: transferrin receptor 1.

RNA was extracted from cells using TRIzol reagent (Takara, Japan) according to the manufacturer's introduction and then converted to cDNA using a PrimeScript™ RT reagent kit (Takara, Japan; 37°C for 15 min, 85°C for 5 s). The qPCR assay was performed with TB Green® Premix Ex Taq™ II (Takara, Japan; 95°C for 30 s, 1 cycle; 95°C for 5 s, 60°C for 34 s, 40 cycles) on the 7,500 Real-Time PCR system (Applied Biosystems, United States), and *β-actin* was used as an internal control. The primer sequences were listed in Table 1 and the relative expression levels were determined using the $2^{-\Delta\Delta Ct}$ method.

2.9 Western blotting analysis

The cells were harvested and whole cell lysates were extracted with RIPA buffer (Solarbio, China) supplemented with protease inhibitor. Protein concentrations were determined using the BCA protein assay (Sangon, China). After quantification, equal amounts of proteins were subjected to SDS-polyacrylamide gel electrophoresis and transferred to the nitrocellulose membrane. Blocking with 5% non-fat dry milk at room temperature for 1 h, then the membrane was incubated with primary (4°C overnight) and secondary antibodies (37°C for 1 h). Then protein blots were incubated with ECL luminescence reagent (Sangon, China) and visualized using Tanon 5,200 multi System (Tannon, China).

2.10 Measurement of intracellular labile iron pool (LIP)

Intracellular LIP was measured by BioTracker 575 Red Fe^{2+} Dye (Sigma-Aldrich, United States; also named FeRhoNox™-1), an activatable fluorescent probe that specifically detects labile ferrous ion in living cells (Niwa et al., 2014). In brief, firstly, the cells were exposed to 5 μM FeRhoNox™-1 for 37°C, 5% CO_2 for 30 min after twice PBS washing. Then rinsed the cells with PBS three times and observed cells by fluorescence inverted microscope Axio Observer D1 (ZEISS, Germany). The stained cells were quantified by the flow cytometer BD FACSCanto II (BD Biosciences, United States).

2.11 Drug combination test and synergy analysis

HeLa and SiHa cells were treated with different concentrations of DOX (0, 0.1, 0.2, 0.5, 1 and 2 μM) with or without DHA (0, 5, 10, 20 and 40 μM). After 48 h of treatment, the cell viability of HeLa and SiHa cells was measured. The online SynergyFinder software (https://synergyfinder.fimm.fi) was used to calculate drug synergy scoring by four separate reference models (Zero Interaction Potency (ZIP) model, Bliss Independence model, Loewe Additivity model, and Highest Single Agent (HSA) model) (Ianevski et al., 2022). Based on these reference models, if 3 or more models agreed, the combination was synergistic. And the synergy score value > 10 is considered synergistic, between −10 and +10 is considered additive, and a synergy score <−10 is considered antagonistic (Neal et al., 2021).

2.12 Statistical analysis

Data analysis was performed using SPSS 24.0. All experimental data were represented as mean ± standard deviation, and the differences between which were analyzed for significance using independent sample *t*-test or one-way analysis of variance (ANOVA) for multivariate analysis. Differences with $p < 0.05$ were deemed statistically significant.

3 Results

3.1 DHA inhibits the proliferation of cervical cancer cells by inducing ROS

DHA is an endoperoxide sesquiterpene lactone and can generate cytotoxic radical species *via* cleavage of the endoperoxide bond (Figure 1A). To investigate the effect of DHA on the proliferation of cervical cancer cells and to select the appropriate intervening time and concentration, cytotoxicity assays were performed with CCK-8 kit. As shown in Figure 1B, the

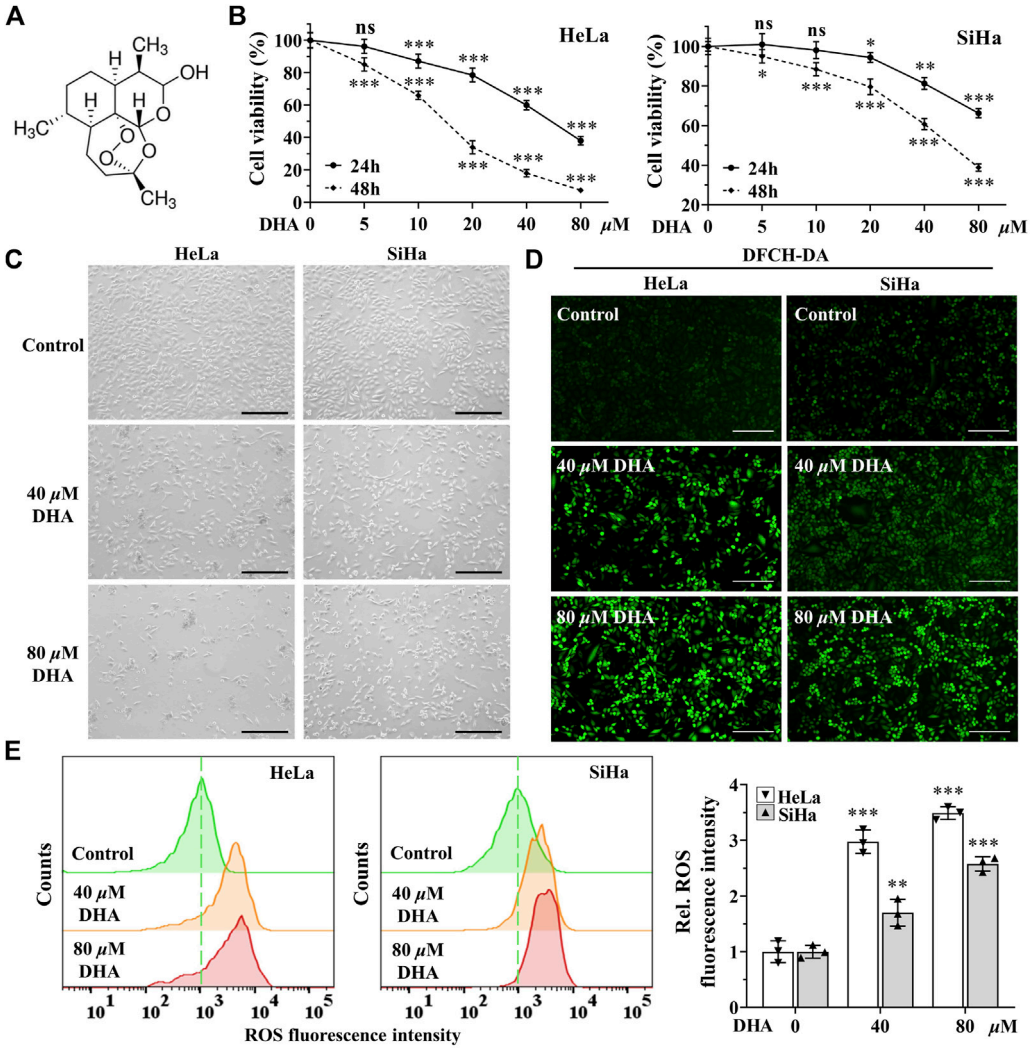

FIGURE 1
DHA inhibits the proliferation of cervical cancer cells by inducing ROS. **(A)** DHA structure. **(B)** Effects of various concentrations of DHA for 24 or 48 h on the cell viability of HeLa and SiHa cells. **(C)** Morphological changes of HeLa and SiHa cells after 24 h DHA treatment (100×; Scale bar: 200 μm). **(D)** The images and **(E)** fluorescence intensity of intracellular ROS stained by DCFH-DA (100×; Scale bar: 200 μm). DHA: dihydroartemisinin; Rel. relative; ROS: reactive oxygen species. (*, $p < 0.05$; **, $p < 0.01$; ***, $p < 0.001$ compared with control group; ns: no significance.).

cell viability of HeLa and SiHa cells were significantly inhibited by DHA treatment, which showed a concentration-dependent and time-dependent manner. At concentration of 80 μM DHA, HeLa cells were almost completely killed (inhibition reached 95.36%), while SiHa cells survived less than 40% after 48 h of DHA intervention. To further evaluate the effect of DHA on cell death, cell morphology was observed. The results suggested DHA greatly increased the number of dead cells, and its inhibitory effect on HeLa cells was much greater than that of SiHa cells (Figure 1C). Based on these data, we carried out the subsequent experiments with the concentration of 40 and 80 μM to further elaborate the detailed mechanism of DHA. Besides, DCHF-DA staining showed dramatical increase in fluorescence intensity along with the concentration of DHA (Figures 1D,E) in both cervical cancer cells, reflecting intracellular ROS excessive accumulation. These results indicated that the inhibitory effect of DHA on cervical cancer cell proliferation was related to the induction and accumulation of ROS.

3.2 DHA enhances oxidative stress in cervical cancer cells

Higher levels of ROS have been found to promote anticancer signaling by initiating oxidative stress-induced cancer cell death (Arfin et al., 2021). To determine the effect of DHA on oxidative stress in cervical cancer cells, the indexes of oxidative stress including MDA, SOD, CAT and LPO were examined. First, after 24 h of DHA intervention, MDA, one of the most important products of membrane lipid peroxidation, was also prominently increased in both cervical cancer cells (Figure 2A). On the contrary, SOD and CAT activities, two kinds of most important antioxidants,

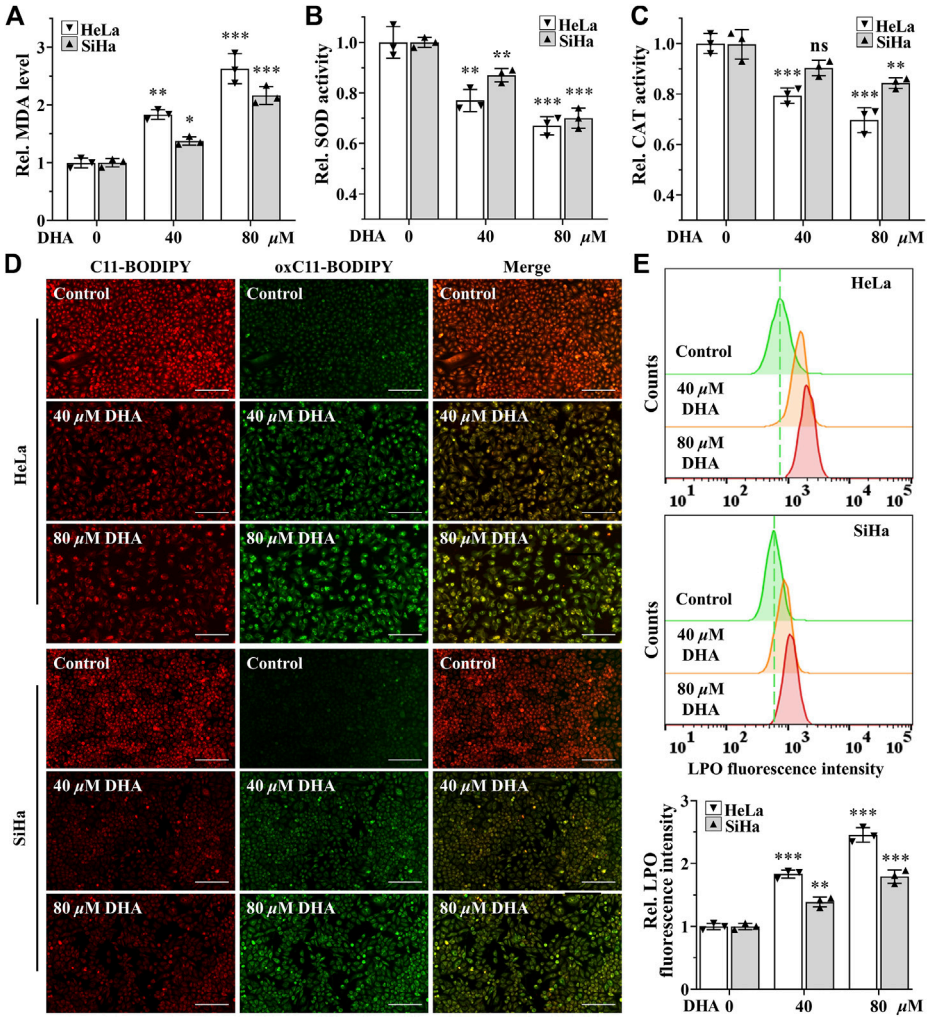

FIGURE 2
DHA enhances oxidative stress in cervical cancer cells. Levels of **(A)** MDA, **(B)** SOD and **(C)** CAT in HeLa and SiHa cells treated with 0, 40 and 80 μM DHA for 24 h. **(D)** The images and **(E)** fluorescence intensity of intracellular LPO stained by BODIPY™ 581/591 C11 (100×; Scale bar: 200 μm). C11-BODIPY represents the level of staining with the probe (unoxidized), while oxC11-BODIPY (oxidized) represents the level of LPO. DHA: dihydroartemisinin; Rel. relative; MDA: malondialdehyde; SOD: superoxide dismutase; CAT: catalase; LPO: liquid peroxidation. (*, $p < 0.05$; **, $p < 0.01$; ***, $p < 0.001$ compared with control group; ns: no significance.).

were significantly decreased in DHA groups of HeLa and SiHa cells and the ratios of decrease were positively proportional to the concentration (Figures 2B,C). Next, the changes of LPO after DHA intervention were detected with the specific fluorescent probe BODIPY™ 581/591 C11. C11-BODIPY staining showed that the levels of oxC11-BODIPY (oxidized) rose significantly in DHA groups compared with control group in HeLa and SiHa cells (Figures 2D,E), representing DHA exacerbated LPO levels. These assays suggested that DHA enhanced oxidative stress in cervical cancer cells.

3.3 DHA triggers cervical cancer cells ferroptosis

Excessive accumulation of LPO is one of the characteristic features of ferroptosis (Dixon et al., 2012). To further determine whether ferroptosis contributed to the cell death induced by DHA, apoptosis inhibitor Z-VAD-FMK (50 μM), ferroptosis inhibitors Fer-1 (5 μM) or iron chelator DFO (50 μM) was co-treated with 80 μM DHA for 24 h. From Figure 3A, it was obvious that the inhibition effect induced by DHA was alleviated by the addition of Fer-1, and even completely reversed in adding DFO group, while Z-VAD-FMK could not reverse DHA-induced cell death in HeLa and SiHa cells. Correspondingly, ferroptosis inhibitors also significantly reduced the high level of MDA induced by DHA, but apoptosis inhibitor had no effect (Figure 3B). These results indicated that ferroptosis may as the central method that contributed to DHA-caused cell death.

To further verify the occurrence of ferroptosis, next we detected the expression of ferroptosis related genes. The detection revealed that, compared with control group, the mRNA and protein expression of gene *GPX4* were both downregulated in a concentration-dependent manner after 24 h of DHA treatment in

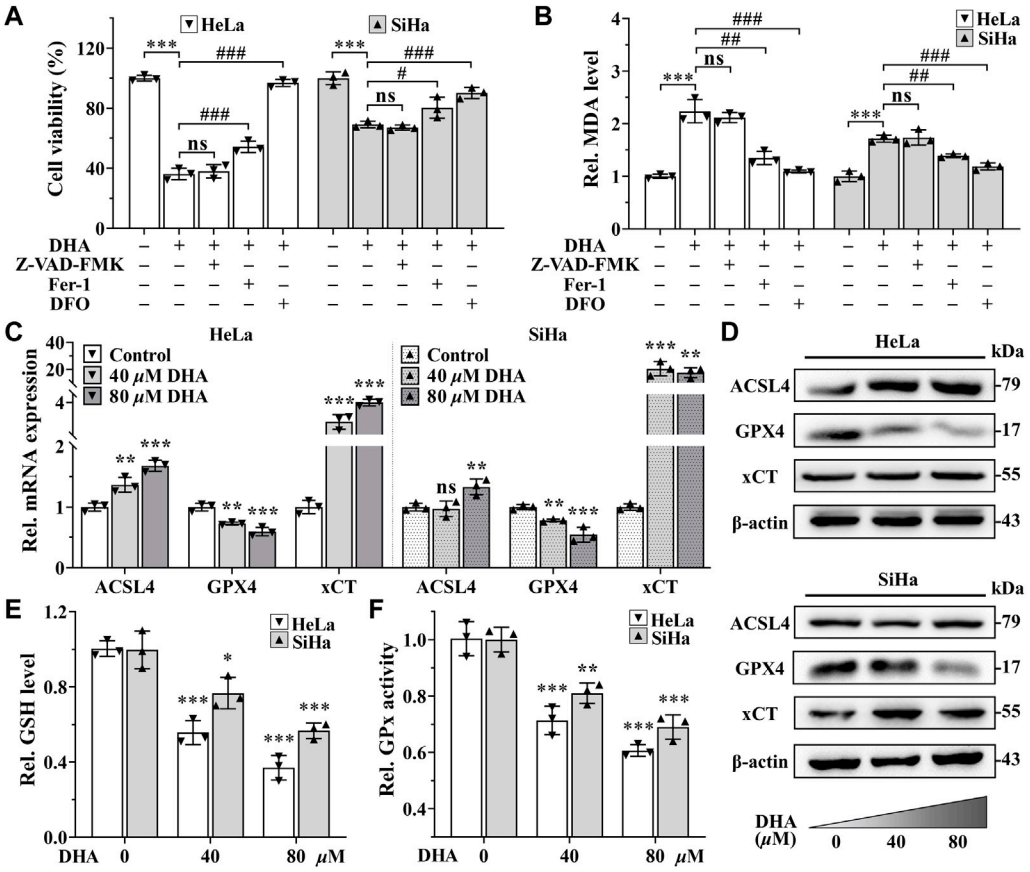

FIGURE 3
DHA triggers cervical cancer cells ferroptosis. Effects on **(A)** cell viability and **(B)** MDA level of HeLa and SiHa cells after 24 h of DHA treatment with or without Z-VAD-FMK, Fer-1 or DFO. **(C)** The transcriptional levels of *ACSL4*, *GPX4* and *xCT* after DHA treatment. **(D)** The protein expressions of ACSL4, GPX4 and xCT after DHA treatment, compared with β-actin. Levels of **(E)** GSH and **(F)** GPx in HeLa and SiHa cells treated with 0, 40 and 80 μM DHA for 24 h. Rel. relative; DHA: dihydroartemisinin; MDA: malondialdehyde; Fer-1: ferrostatin-1; DFO: deferoxamine; ACSL4: acyl-CoA synthetase long-chain family member 4; GPX4: glutathione peroxidase 4; xCT: cystine-glutamate antiporter; GSH: glutathione; GPx: glutathione peroxidase. (*, $p < 0.05$; **, $p < 0.01$; ***, $p < 0.001$ compared with control group; #, $p < 0.05$; ##, $p < 0.01$; ###, $p < 0.001$ compared with DHA group; ns: no significance.).

both cell lines (Figures 3C,D), while the expression of gene *Acyl-CoA synthetase long-chain family member 4 (ACSL4)* were opposite (Figures 3C,D). In SiHa cells, the transcriptional and protein levels of cystine-glutamate antiporter (xCT) gene were both significantly elevated after DHA intervention, even the highest upregulated in mRNA level more than 20 times (Figures 3C,D). Although *xCT* was also highly expressed at mRNA level in HeLa cells (Figure 3C), the protein change was inconspicuous (Figure 3D). In the meantime, GSH and GPx, which exert anti-ferroptosis effects, also decreased after DHA treatment in a concentration-dependent manner in both cell lines (Figures 3E,F). Altogether, these results confirmed that DHA triggered cervical cancer cells ferroptosis, which was related to GPX4 depletion.

3.4 DHA induces ferritinophagy-dependent ferroptosis in cervical cancer cells

Since iron is an important part of ferroptosis (Stockwell, 2022), and combined with previous results that the iron chelator DFO was more efficient than Fer-1 in inhibiting DHA-induced cell death, we speculated that iron may play a momentous role in DHA-induced ferroptosis. So, the impact of DHA treatment on intracellular LIP was evaluated. As shown in Figures 4A,B, the fluorescence intensities of DHA groups reinforced remarkably compared with control group in cervical cancer cells, suggesting that DHA significantly increased the levels of LIP, which could promote cell ferroptosis (Lu et al., 2021).

Then, we further examined the effect of DHA on iron metabolism. The data from qPCR showed that DHA intervention elevated the mRNA expression of *transferrin receptor 1* (*TFR1*), *NCOA4* and *ferritin heavy chain 1* (*FTH1*) in both cell lines (Figure 4C). And at the protein level, the trend of TfR1 was consistent with mRNA (Figure 4D). However, the protein expression of FTH1 and NCOA4 displayed the opposite trend with mRNA (Figure 4D). It is noteworthy that FTH1 degradation exhibited a synergistic effect with NCOA4 depletion according to Western blotting results (Figure 4D), which may be caused by the delivery of ferritin by NCOA4 to lysosomes and subsequent the ferritinophagy occurred.

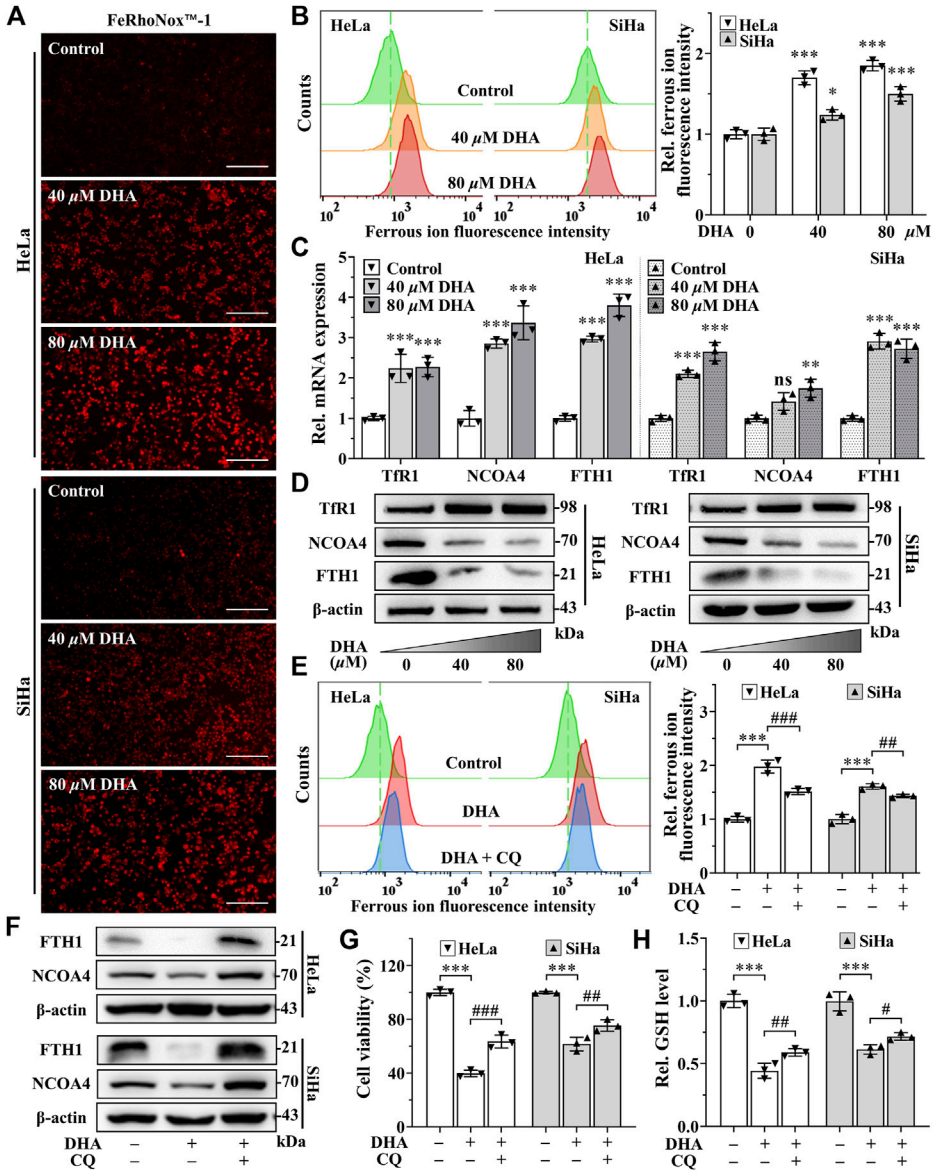

FIGURE 4
DHA induces ferritinophagy-dependent ferroptosis in cervical cancer cells. **(A)** The images and **(B)** fluorescence intensity of intracellular ferrous ion stained by FeRhoNox™-1 (100×; Scale bar: 200 μm). **(C)** The transcriptional levels of *TfR1*, *NCOA4* and *FTH1* after DHA treatment. **(D)** The protein expressions of TfR1, NCOA4 and FTH1 after DHA treatment, compared with β-actin. Effects on **(E)** intracellular ferrous ion level, **(F)** FTH1 and NCOA4 protein expressions, **(G)** cell viability and **(H)** GSH level of HeLa and SiHa cells after 24 h of DHA treatment with or without CQ. DHA: dihydroartemisinin; Rel. relative; TfR1: transferrin receptor 1; NCOA4: nuclear receptor coactivator 4; FTH1: ferritin heavy chain 1; CQ: chloroquine; GSH: glutathione. (*, $p < 0.05$; **, $p < 0.01$; ***, $p < 0.001$ compared with control group; #, $p < 0.05$; ##, $p < 0.01$; ###, $p < 0.001$ compared with DHA group; ns: no significance.).

Since the ferritin degradation was *via* autophagy, autophagy inhibitor CQ (25 μM) was co-cultured with 80 μM DHA for 24 h to verify whether autophagy contributes to DHA-induced FTH1 degradation and ferroptosis. As expected, CQ addition could significantly inhibit the degradation of FTH1 and the depletion of NCOA4 (Figure 4F), and reduce LIP levels (Figure 4E). At the same time, the inhibitory effect of DHA on HeLa and SiHa cells also alleviated by CQ (Figure 4G), accompanied by a decrease in GSH consumption (Figure 4H). All these data indicated that ferritinophagy-dependent ferroptosis contribute to DHA-induced cell death.

3.5 HO-1 against DHA-induced ferroptosis in cervical cancer cells

In addition, the extremely high expression of heme oxygenase-1 (HO-1) after DHA treatment, especially in

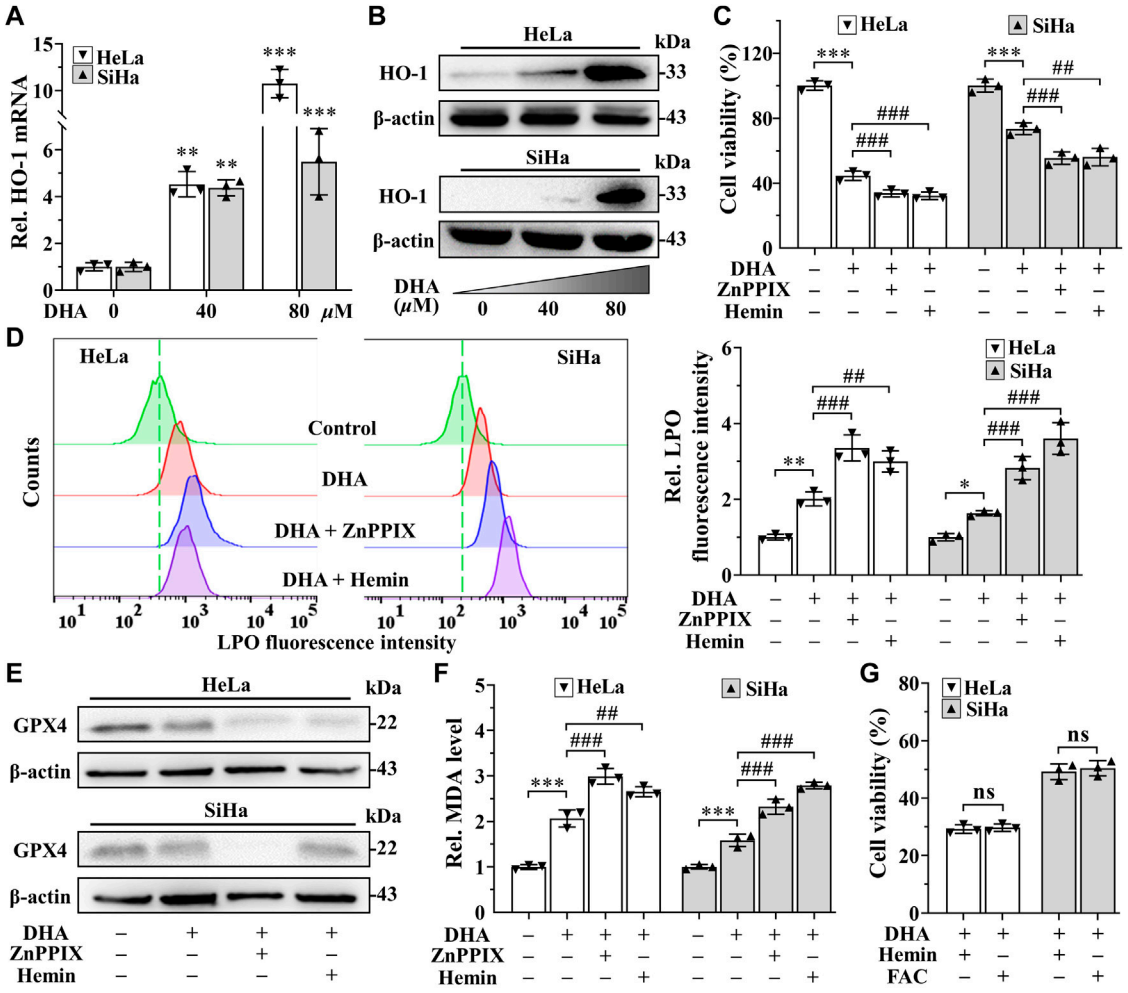

FIGURE 5
HO-1 against DHA-induced ferroptosis in cervical cancer cells. **(A)** The transcriptional level and **(B)** protein expression of HO-1 of HeLa and SiHa cells after 24 h of treatment with DHA. Effects on **(C)** cell viability, **(D)** LPO level, **(E)** GPX4 protein expression and **(F)** MDA level of HeLa and SiHa cells after 24 h of DHA treatment with or without ZnPPIX or hemin. **(G)** The cell viability of HeLa and SiHa cells treated with DHA supplemented Hemin or FAC. Rel. relative; DHA: dihydroartemisinin; HO-1: heme oxygenase-1; ZnPPIX: protoporphyrin IX zinc(II); LPO: liquid peroxidation; GPX4: glutathione peroxidase 4; MDA: malondialdehyde. (*, $p < 0.05$; **, $p < 0.01$; ***, $p < 0.001$ compared with control group; #, $p < 0.05$; ##, $p < 0.01$; ###, $p < 0.001$ compared with DHA group; ns: no significance.).

80 μM DHA group (Figures 5A,B), attracted our attention. Considering the dual function of HO-1 (Ryter, 2021), its inhibitor ZnPPIX and agonists hemin were used to investigate its role in DHA-induced ferroptosis. Confusingly, incubation of DHA with either ZnPPIX (10 μM) or hemin (25 μM) both significantly increased the cell growth inhibition rates in cervical cancer cells (Figure 5C), along with higher levels of LPO and MDA (Figures 5D,F). And the protein level of GPX4 were further suppressed in both combination groups (Figure 5E). Given the critical role of iron in ferroptosis, we surmised that the boosting anticancer action of ZnPPIX with DHA should be through inhibition of HO-1, while the unexpected performance of hemin may not be related to HO-1 but mediated by iron. To address this question, FAC, a commonly used mono-iron compound, was chosen as a control to explore the effect of iron on DHA. At the same concentrations, we compared the consequences of incubating DHA with hemin or FAC. As Figure 5G shown, the cell viability showed no significant difference between DHA + hemin group and DHA + FAC group in both cell lines, hinting that iron rather than HO-1 was the dominant factor for hemin to increase DHA inhibitory effect on cervical cancer cells. Thus, these results suggested that HO-1 may play a role in resisting ferroptosis in DHA-induced cervical cancer cell death.

3.6 DHA sensitizes cervical cancer to DOX-induced cell death

SynergyFinder is a web-application for interactive analysis and visualization of multi-drug combination response data (Ianevski et al., 2022). In HeLa cells, synergy scoring of treatment with DHA

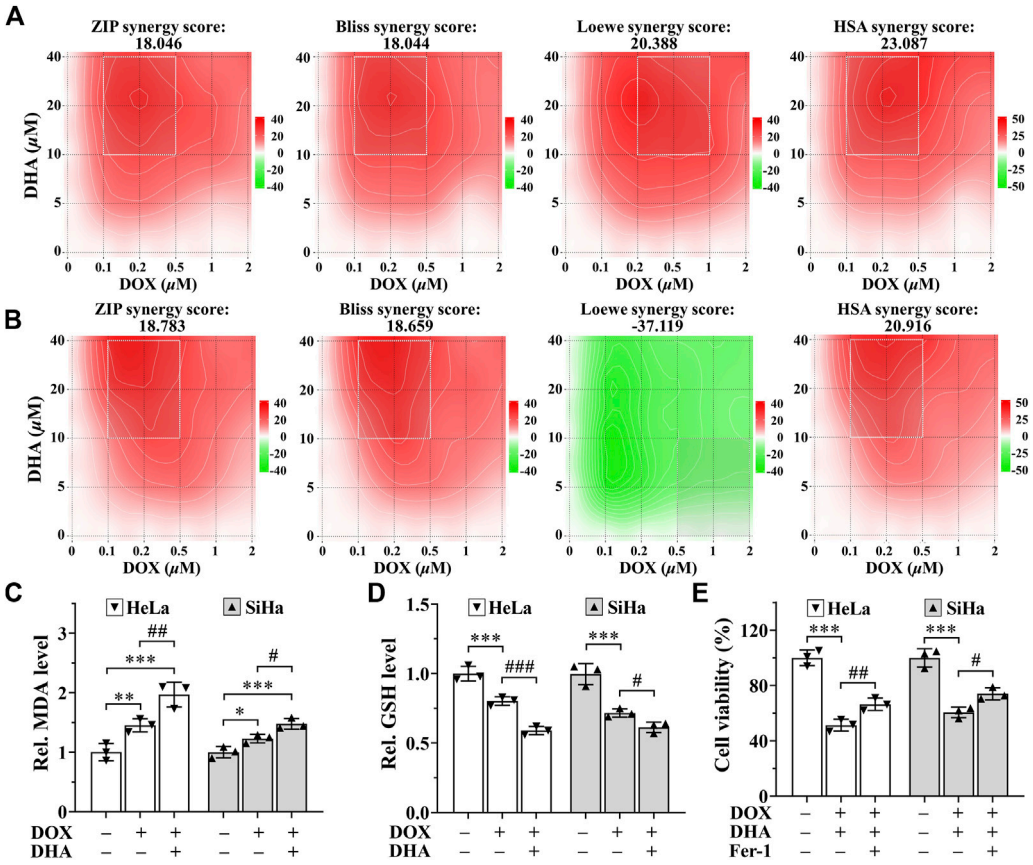

FIGURE 6
DHA sensitizes cervical cancer to DOX-induced cell death. **(A, B)** Heatmaps of drug combination responses. Synergy score >10 is considered synergistic, between −10 and +10 is considered additive, <−10 is considered antagonistic. The gradation of the red regions indicates the intensity of synergism. The white rectangle indicates the concentrations encompassing the region of highest synergy. Effects on the levels of **(C)** MDA and **(D)** GSH in HeLa and SiHa cells after 24 h of treatment with DOX with or without DHA. **(E)** Effects of Fer-1 on cell viability of HeLa and SiHa cells treated with DOX and DHA. Rel. relative; DHA: dihydroartemisinin; DOX: doxorubicin; MDA: malondialdehyde; GSH: glutathione; Fer-1: ferrostatin-1. (*, $p < 0.05$; **, $p < 0.01$; ***, $p < 0.001$ compared with control group; #, $p < 0.05$; ##, $p < 0.01$; ###, $p < 0.001$ compared with DOX group).

and DOX calculated by four separate reference models were all >10, which was considered strongly synergistic between DHA and DOX. And except Loewe Additivity model, the other three reference models all revealed highly synergistic effect between DHA and DOX in inhibiting SiHa cell proliferation (synergy scores >10). Under the previous rule, we also expected this to be synergistic. As shown in Figures 6A,B, the white rectangle indicates the concentrations encompassing the region of the maximum synergistic area. The data indicated that 10 μM for DHA and 0.2 μM for DOX were the lowest concentrations encompassing the region of highest synergy, which were selected as the best-combined concentration for DHA and DOX. Therefore, this synergistic combination of DHA and DOX was used in our following experiments. After 24 h of treatment, it could be seen that, compared with DOX group, the level of MDA in DHA + DOX group of HeLa and SiHa cells were increased obviously, while the level of GSH were significantly lower (Figures 6C,D). In addition, the inhibition effect induced by DHA + DOX could also be alleviated by Fer-1 (Figure 6E). The results indicated that the synergistic lethal effect of DHA with DOX in cervical cancer was also related to ferroptosis.

4 Discussion

Cervical cancer is still one of the most common and lethal gynecological malignancy and the clinical therapeutics is limited due to the drug resistance and metastasis of tumor, seriously threating women health (Arbyn et al., 2020; Sung et al., 2021). Therefore, it is imperative and prevalent to explore more efficient and safer therapeutic targets and therapies. As mentioned previously, cancer cells are more susceptible to ferroptosis (Chen et al., 2022). The most likely reason to explain this phenomenon is that the rapid growth and metabolism lead to the intense iron demand (Torti and Torti, 2013) and high levels of intracellular ROS (Dixon and Stockwell, 2014) in cancer cells. Furthermore, encouragingly, researchers have found that the cancer cells with resistance to apoptosis and chemotherapy are also exquisitely susceptible to ferroptosis (Hangauer et al., 2017; Tsoi et al., 2018), which further emphasize the prospect of ferroptosis as a novel target for antitumor therapy. In addition, NCOA4-mediated ferritinophagy can enhance ferroptosis by inducing the degradation of ferritin and increasing LIP (Zhou et al., 2020; Yu et al., 2022). In recent years, the role of ferroptosis in cervical carcinogenesis, progression and immunity has been gradually concerned (Qi et al., 2021; Yang et al.,

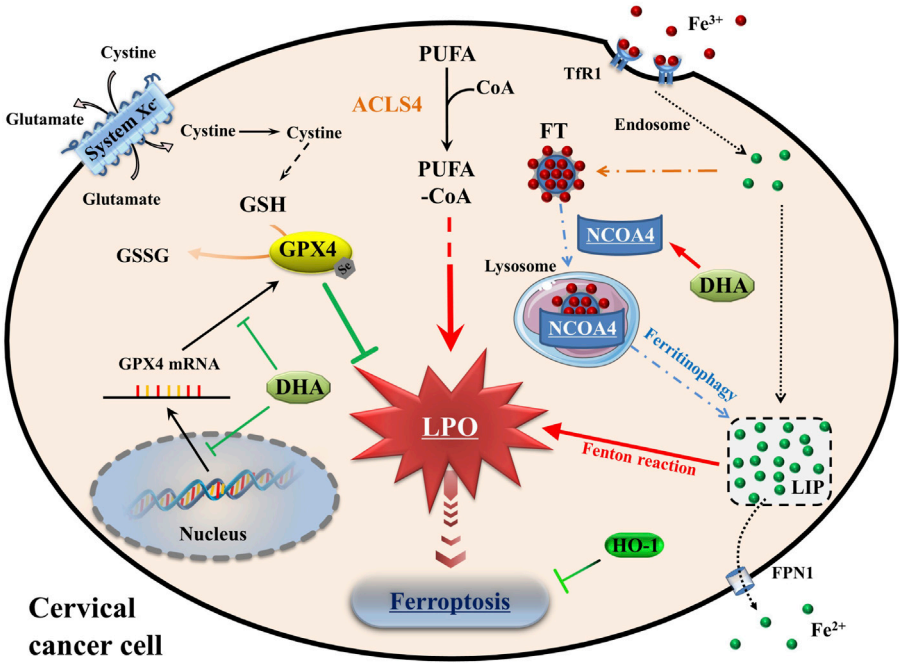

FIGURE 7
Schematic depicting DHA-induced ferroptosis in cervical cancer cells. DHA: dihydroartemisinin; GPX4: glutathione peroxidase 4; GSH: glutathione; GSSG: oxidized glutathione; CoA: coenzyme A; PUFA: polyunsaturated fatty acids; ACSL4: acyl-CoA synthetase long-chain family member 4; PLO: liquid peroxidation; Fe^{3+}, ferric iron; Fe^{2+}, ferrous iron; TfR1: transferrin receptor 1; Steap3: six transmembrane epithelial antigen of the prostate 3; FT: ferritin; NCOA4: nuclear receptor coactivator 4; LIP: labile iron pool; FPN1: Ferroportin1; HO-1: heme oxygenase-1.

2022). Except sorafenib, natural product oleanolic acid inhibited cervical cancer Hela cell proliferation through modulation of the ACSL4 ferroptosis signaling pathway (Xiaofei et al., 2021). As a natural ferroptosis inducer, DHA could react with ferrous ions to produce cytotoxic ROS and played an important role in inducing ferroptosis (Lin et al., 2016; Shen et al., 2020). And in the present study, we reveal the molecular mechanisms that DHA triggered ferritinophagy-dependent ferroptosis in cervical cancer and sensitized to DOX, which may provide novel avenues for future therapy development.

Since structural diversity and biological prevalidation, natural products are indispensable sources of clinical drug research and development (Hong et al., 2020; Kim et al., 2021). In the field of cancer therapy, natural products also show potential anticancer effects, and its use has facilitated the development of effective and safer anti-cancer drugs. Currently, a large number of studies have been reported on natural products to treat cancer and overcome tumor drug resistance (Zhang et al., 2020b; Dahmardeh Ghalehno et al., 2022). DHA, a natural anticancer drug, has exhibited a variety of anticancer properties such as inducing apoptosis or autophagy and even can reverse drug resistance of certain cancer cell lines and greatly enhance the anticancer effect in combination with a variety of chemotherapeutic drugs (Dai et al., 2021). Moreover, no obvious toxicity in normal cells has been found after DHA treatment, indicating that DHA is a potential ideal anti-cancer drug (Li et al., 2021). With the deepening of research, its role in inducing ferroptosis was gradually discovered (Hong et al., 2020; Kim et al., 2021). For cervical cancer cells, it is confirmed that DHA has a potent lethal effect and synergistic effect with chemotherapeutic drugs (Tai et al., 2016; Tang et al., 2021b), while the self-assembled DHA nanoparticles are a highly promising delivery system for targeted cancer treatment (Lu et al., 2020). However, it remains rarely explored and unclear in cervical cancer about the roles of DHA for ferroptosis.

At the cellular level, the pathways of iron, amino acids and lipid metabolism are involved in the initiation and execution of ferroptosis (Du et al., 2022). As Figure 7 shown, iron, transported into cells by TfR1, is either stored in ferritin or exported by FPN1. The excess cellular iron, particularly ferrous iron, can react directly with cellular oxidants to produce cytotoxic hydroxyl radicals *via* the Fenton reaction, which in turn promotes ferroptosis (Dixon and Stockwell, 2014). And the key enzyme of lipid peroxidation ACSL4 plays a role in responsible for the esterification of coenzyme A to polyunsaturated fatty acids (Killion et al., 2018). It is considered to be an essential component for ferroptosis execution, as its renders the cell more susceptible to ferroptosis (Doll et al., 2017). GPX4 is the only known GPX that can catalyze toxic lipid hydroperoxides into non-toxic lipid alcohols under normal physiological conditions, with its substrate GSH (Ingold et al., 2018). With the System Xc^-, GPX4 constitutes the main cellular pathway to protect cells from undergoing ferroptosis.

Oxidative stress is caused by an imbalance between cellular oxidants and antioxidants (Arfin et al., 2021). When ferroptosis occurs, cellular oxidative stress is intensified. So, the oxidative stress levels were assessed firstly to understand the cellular state. In cervical cancer cells, DHA treatment aggravated the levels of oxidative stress, which was manifested by the accumulation of ROS, LPO and MDA, and the upregulation of ACSL4. And the cell death of cervical cancer cells caused by DHA, accompanied with depletion of GPX4 and GSH,

could be attenuated by ferroptosis inhibitors. In accordance with these data, we concluded that DHA triggered ferroptosis, which was related to GPX4 depletion. Likewise, in glioblastoma and lung cancer cells, DHA induced ferroptosis by inhibiting xCT/GPX4 axis in different ways (Yi et al., 2020; Yuan et al., 2020), indicating that the mechanisms of DHA-induced ferroptosis in various cells were different. Simultaneously, in HeLa and SiHa cells, the synergistic lethal effect between DHA and DOX, used as a first-line drug to treat cervical cancer (Wang et al., 2022), was related to ferroptosis. This suggested that DHA may have potential as an adjunct to chemotherapy.

Besides, Fenton reaction, caused by the interaction between excessive ferrous iron and peroxide leading to the production of highly active hydroxyl radicals (Dixon and Stockwell, 2014), was also a predisposing factor of ferroptosis. Notably, many cellular processes change the sensitivity of cells to ferroptosis by altering cellular LIP levels (Xiao et al., 2020; Lu et al., 2021). Among them, ferritinophagy mediated by selective cargo receptor NCOA4 is a major pathway to regulate intracellular LIP levels, which delivers ferritin to lysosomes *via* macroautophagy to release stored iron for cellular utilization (Mancias et al., 2014). On one hand, due to the siderophilic properties of cancer, NCOA4-mediated ferritinophagy may promote the progression of some tumors (Santana-Codina et al., 2022). On the other hand, excessive LIP accumulation by ferritinophagy could initiate ferritinophagy-dependent ferroptosis and played an anticancer role (Wang et al., 2021b; Li et al., 2022b; Stockwell, 2022). As mentioned previously, the degradation of ferritin induced by DHA was an important consideration leading to ferroptosis (Du et al., 2019; Chen et al., 2020). Indeed, the significant degradation of FTH1 and subsequent increases of intracellular ferrous iron were observed in our study, which may be due to the increased efficiency of NCOA4-mediated ferritinophagy caused by DHA. Thus, DHA-induced ferritinophagy may be one of the causes of initiating and enhancing ferroptosis in cervical cancer cells. However, the specific mechanism remains to be further studied.

As we known, HO-1 is an oxidative stress inducing enzyme that catalyzes the degradation of heme into biliverdin, carbon monoxide and ferrous iron. Given the dual role of HO-1 in regulating iron and ROS homeostasis, its contradictory role in ferroptosis may depend on the degree of ROS production and the following oxidative damage (Ryter, 2021). Gloria et al. found that Siramesine and Lapatinib induced a synergistic ferroptosis through reduced HO-1 Levels (Villalpando-Rodriguez et al., 2019). However, luteolin, a natural compound monomer, triggered ferroptosis in clear cell renal cell carcinoma by excessively up-regulating HO-1 expression and activating LIP (Han et al., 2022). Currently, pharmacological and genetic tools have proposed cancer therapy strategies of targeting HO-1 (Chiang et al., 2018). The extremely high expression of HO-1 induced by DHA was seen in HeLa and SiHa cells, which was similar to the result in glioblastoma and was worthy of further research (Yi et al., 2020). After using specific HO-1 inhibitor ZnPPIX, the degree of DHA-induced ferroptosis was aggravated. So, another important conclusion of our work is the fact that HO-1 exerted antioxidant effects against DHA-induced ferroptosis. On the other hand, it had been reported that DOX could downregulate Nrf2 to inhibit HO-1 and GPX4 levels (Li et al., 2022a), which may be one of the important reasons for its synergism with DHA to induce ferroptosis. The combination of DHA and HO-1 inhibitors may have a potential application in cancer therapy by mediating the induction of ferroptosis.

However, there are several limitations to our work. Due to limited resources, our research was conducted only in cell lines without animal experiments. The mechanisms of ferroptosis are delicate and complicated. In addition to the metabolism of iron, amino acids and lipid, mitochondria also act a critical role in regulating ferroptosis (Takashi et al., 2020), which are not included in this study. Hence, further evaluations of the specific molecular mechanism underlying DHA-mediated regulation of ferroptosis and its effect on upstream pathway-related proteins is needed. In the next step, future studies will focus on these deficiencies and carry out more in-depth research.

5 Conclusion

Taken together, our study demonstrated evidence that the inhibitory effect of DHA on the proliferation of cervical cancer is related to ferroptosis, mediated by the GPX4 inhibition and ferritinophagy, whereas HO-1 expression is anti-ferroptosis. Furthermore, the synergistic lethal effect of DHA with chemotherapeutic agents makes it possible to be a potential adjuvant drug for chemotherapy. All these findings paved the way for further research and provided the theoretical basis for its clinical application.

Data availability statement

The original contributions presented in the study are included in the article/supplementary material, further inquiries can be directed to the corresponding author.

Author contributions

YS and HS contributed to conception and design of the study. HS conducted most of the experiments and data analysis, and wrote the manuscript. LX and SD participated in collecting data and helped to draft the manuscript. YS, GY and JL edited and revised the manuscript. All authors contributed to the article and approved the submitted version.

Funding

This research was funded by grants from Basic Public Welfare Research Program of Zhejiang Province (LGF18H200004), Science and Technology Bureau of Jiaxing City (2020AY10002 and 2020AY30003), Scientific Research Project of Affiliated Hospital of Zhejiang University of Traditional Chinese Medicine (2022FSYYZY18) and Jiaxing Key Laboratory of Diabetic Angiopathy (2019ZDSYS).

Conflict of interest

The authors declare that the research was conducted in the absence of any commercial or financial relationships that could be construed as a potential conflict of interest.

Publisher's note

References

Abu-Rustum, N. R., Yashar, C. M., Bean, S., Bradley, K., Campos, S. M., Chon, H. S., et al. (2020). NCCN guidelines insights: Cervical cancer, version 1.2020. *J. Natl. Compr. Canc Netw.* 18 (6), 660–666. doi:10.6004/jnccn.2020.0027

Arbyn, M., Weiderpass, E., Bruni, L., de Sanjosé, S., Saraiya, M., Ferlay, J., et al. (2020). Estimates of incidence and mortality of cervical cancer in 2018: A worldwide analysis. *Lancet Glob. Health* 8 (2), e191–e203. doi:10.1016/S2214-109X(19)30482-6

Arfin, S., Jha, N. K., Jha, S. K., Kesari, K. K., Ruokolainen, J., Roychoudhury, S., et al. (2021). Oxidative stress in cancer cell metabolism. *Antioxidants (Basel)* 10 (5), 642. doi:10.3390/antiox10050642

Chen, G. Q., Benthani, F. A., Wu, J., Liang, D., Bian, Z. X., and Jiang, X. (2020). Artemisinin compounds sensitize cancer cells to ferroptosis by regulating iron homeostasis. *Cell Death Differ.* 27 (1), 242–254. doi:10.1038/s41418-019-0352-3

Chen, H., Wang, C., Liu, Z., He, X., Tang, W., He, L., et al. (2022). Ferroptosis and its multifaceted role in cancer: Mechanisms and therapeutic approach. *Antioxidants (Basel)* 11 (8), 1504. doi:10.3390/antiox11081504

Chiang, S. K., Chen, S. E., and Chang, L. C. (2018). A dual role of heme oxygenase-1 in cancer cells. *Int. J. Mol. Sci.* 20 (1), 39. doi:10.3390/ijms20010039

Dahmardeh Ghalehno, A., Boustan, A., Abdi, H., Aganj, Z., Mosaffa, F., and Jamialahmadi, K. (2022). The potential for natural products to overcome cancer drug resistance by modulation of epithelial-mesenchymal transition. *Nutr. Cancer* 74 (8), 2686–2712. doi:10.1080/01635581.2021.2022169

Dai, X., Zhang, X., Chen, W., Chen, Y., Zhang, Q., Mo, S., et al. (2021). Dihydroartemisinin: A potential natural anticancer drug. *Int. J. Biol. Sci.* 17 (2), 603–622. doi:10.7150/ijbs.50364

Dixon, S. J., Lemberg, K. M., Lamprecht, M. R., Skouta, R., Zaitsev, E. M., Gleason, C. E., et al. (2012). Ferroptosis: An iron-dependent form of nonapoptotic cell death. *Cell* 149 (5), 1060–1072. doi:10.1016/j.cell.2012.03.042

Dixon, S. J., and Stockwell, B. R. (2014). The role of iron and reactive oxygen species in cell death. *Nat. Chem. Biol.* 10 (1), 9–17. doi:10.1038/nchembio.1416

Doll, S., Proneth, B., Tyurina, Y. Y., Panzilius, E., Kobayashi, S., Ingold, I., et al. (2017). ACSL4 dictates ferroptosis sensitivity by shaping cellular lipid composition. *Nat. Chem. Biol.* 13 (1), 91–98. doi:10.1038/nchembio.2239

Du, J., Wang, T., Li, Y., Zhou, Y., Wang, X., Yu, X., et al. (2019). DHA inhibits proliferation and induces ferroptosis of leukemia cells through autophagy dependent degradation of ferritin. *Free Radic. Biol. Med.* 131, 356–369. doi:10.1016/j.freeradbiomed.2018.12.011

Du, S., Shi, H., Xiong, L., Wang, P., and Shi, Y. (2022). Canagliflozin mitigates ferroptosis and improves myocardial oxidative stress in mice with diabetic cardiomyopathy. *Front. Endocrinol.* 13, 1011669. doi:10.3389/fendo.2022.1011669

Han, S., Lin, F., Qi, Y., Liu, C., Zhou, L., Xia, Y., et al. (2022). HO-1 contributes to luteolin-triggered ferroptosis in clear cell renal cell carcinoma via increasing the labile iron pool and promoting lipid peroxidation. *Oxid. Med. Cell Longev.* 2022, 3846217. doi:10.1155/2022/3846217

Hangauer, M. J., Viswanathan, V. S., Ryan, M. J., Bole, D., Eaton, J. K., Matov, A., et al. (2017). Drug-tolerant persister cancer cells are vulnerable to GPX4 inhibition. *Nature* 551 (7679), 247–250. doi:10.1038/nature24297

Hassannia, B., Vandenabeele, P., and Vanden Berghe, T. (2019). Targeting ferroptosis to iron out cancer. *Cancer Cell* 35 (6), 830–849. doi:10.1016/j.ccell.2019.04.002

Hill, E. K. (2020). Updates in cervical cancer treatment. *Clin. Obstet. Gynecol.* 63 (1), 3–11. doi:10.1097/GRF.0000000000000507

Hong, B., Luo, T., and Lei, X. (2020). Late-stage diversification of natural products. *ACS Cent. Sci.* 6 (5), 622–635. doi:10.1021/acscentsci.9b00916

Ianevski, A., Giri, A. K., and Aittokallio, T. (2022). SynergyFinder 3.0: An interactive analysis and consensus interpretation of multi-drug synergies across multiple samples. *Nucleic Acids Res.* 50 (1), W739–W743. doi:10.1093/nar/gkac382

Ingold, I., Berndt, C., Schmitt, S., Doll, S., Poschmann, G., Buday, K., et al. (2018). Selenium utilization by GPX4 is required to prevent hydroperoxide-induced ferroptosis. *Cell* 172 (3), 409–422.e21. doi:10.1016/j.cell.2017.11.048

Jansen, F. H., Adoubi, I., De Cnodder, T., Jansen, N., Tschulakow, A., et al. (2011). First study of oral Artenimol-R in advanced cervical cancer, clinical benefit., tolerability and tumor markers. *Anticancer Res.* 31 (12), 4417–4422.

Killion, E. A., Reeves, A. R., El Azzouny, M. A., Yan, Q. W., Surujon, D., Griffin, J. D., et al. (2018). A role for long-chain acyl-CoA synthetase-4 (ACSL4) in diet-induced phospholipid remodeling and obesity-associated adipocyte dysfunction. *Mol. Metab.* 9, 43–56. doi:10.1016/j.molmet.2018.01.012

Kim, A., Ha, J., Kim, J., Cho, Y., Ahn, J., Cheon, C., et al. (2021). Natural products for pancreatic cancer treatment, from traditional medicine to modern drug discovery. *Nutrients* 13 (11), 3801. doi:10.3390/nu13113801

Li, K., Chen, B., Xu, A., Shen, J., Li, K., Hao, K., et al. (2022a). TRIM7 modulates NCOA4-mediated ferritinophagy and ferroptosis in glioblastoma cells. *Redox Biol.* 56, 102451. doi:10.1016/j.redox.2022.102451

Li, Q., Ma, Q., Cheng, J., Zhou, X., Pu, W., Zhong, X., et al. (2021). Dihydroartemisinin as a sensitizing agent in cancer therapies. *Onco Targets Ther.* 14, 2563–2573. doi:10.2147/OTT.S297785

Li, X., Liang, J., Qu, L., Liu, S., Qin, A., Liu, H., et al. (2022b). Exploring the role of ferroptosis in the doxorubicin-induced chronic cardiotoxicity using a murine model. *Chem. Biol. Interact.* 363, 110008. doi:10.1016/j.cbi.2022.110008

Lin, R., Zhang, Z., Chen, L., Zhou, Y., Zou, P., Feng, C., et al. (2016). Dihydroartemisinin (DHA) induces ferroptosis and causes cell cycle arrest in head and neck carcinoma cells. *Cancer Lett.* 381 (1), 165–175. doi:10.1016/j.canlet.2016.07.033

Liu, Y., and Gu, W. (2022). p53 in ferroptosis regulation: the new weapon for the old guardian. *Cell Death Differ.* 29 (5), 895–910. doi:10.1038/s41418-022-00943-y

Liu, Y., Li, L., Yang, Z., Wen, D., and Hu, Z. (2022). Circular RNA circACAP2 suppresses ferroptosis of cervical cancer during malignant progression by miR-193a-5p/GPX4. *J. Oncol.* 2022, 5228874. doi:10.1155/2022/5228874

Lu, S., Song, Y., Luo, R., Li, S., Li, G., Wang, K., et al. (2021). Ferroportin-dependent iron homeostasis protects against oxidative stress-induced nucleus pulposus cell ferroptosis and ameliorates intervertebral disc degeneration *in vivo*. *Oxid. Med. Cell Longev.* 2021, 6670497. doi:10.1155/2021/6670497

Lu, Y., Wen, Q., Luo, J., Xiong, K., Wu, Z., Wang, B., et al. (2020). Self-assembled dihydroartemisinin nanoparticles as a platform for cervical cancer chemotherapy. *Drug Deliv.* 27 (1), 876–887. doi:10.1080/10717544.2020.1775725

Mancias, J. D., Wang, X., Gygi, S. P., Harper, J. W., and Kimmelman, A. C. (2014). Quantitative proteomics identifies NCOA4 as the cargo receptor mediating ferritinophagy. *Nature* 509 (7498), 105–109. doi:10.1038/nature13148

Neal, A., Lai, T., Singh, T., Rahseparian, N., Grogan, T., Elashoff, D., et al. (2021). Combining ReACp53 with carboplatin to target high-grade serous ovarian cancers. *Cancers (Basel).* 13 (23), 5908. doi:10.3390/cancers13235908

Niwa, M., Hirayama, T., Okuda, K., and Nagasawa, H. (2014). A new class of high-contrast Fe(II) selective fluorescent probes based on spirocyclized scaffolds for visualization of intracellular labile iron delivered by transferrin. *Org. Biomol. Chem.* 12 (34), 6590–6597. doi:10.1039/c4ob00935e

Qi, X., Fu, Y., Sheng, J., Zhang, M., Zhang, M., Wang, Y., et al. (2021). A novel ferroptosis-related gene signature for predicting outcomes in cervical cancer. *Bioengineered* 12 (1), 1813–1825. doi:10.1080/21655979.2021.1925003

Ryter, S. W. (2021). Heme oxgenase-1: A cardinal modulator of regulated cell death and inflammation. *Cells* 10 (3), 515. doi:10.3390/cells10030515

Santana-Codina, N., Del Rey, M. Q., Kapner, K. S., Zhang, H., Gikandi, A., Malcolm, C., et al. (2022). NCOA4-Mediated ferritinophagy is a pancreatic cancer dependency via maintenance of iron bioavailability for iron-sulfur cluster proteins. *Cancer Discov.* 12 (9), 2180–2197. doi:10.1158/2159-8290.CD-22-0043

Shen, Y., Zhang, B., Su, Y., Badshah, S. A., Wang, X., Li, X., et al. (2020). Iron promotes dihydroartemisinin cytotoxicity via ROS production and blockade of autophagic flux via lysosomal damage in osteosarcoma. *Front. Pharmacol.* 11, 444. doi:10.3389/fphar.2020.00444

Stockwell, B. R. (2022). Ferroptosis turns 10: Emerging mechanisms, physiological functions, and therapeutic applications. *Cell* 185 (14), 2401–2421. doi:10.1016/j.cell.2022.06.003

Sung, H., Ferlay, J., Siegel, R. L., Laversanne, M., Soerjomataram, I., Jemal, A., et al. (2021). Global cancer statistics 2020: GLOBOCAN estimates of incidence and mortality worldwide for 36 cancers in 185 countries. *CA Cancer J. Clin.* 71 (3), 209–249. doi:10.3322/caac.21660

Tai, X., Cai, X. B., Zhang, Z., and Wei, R. (2016). *In vitro* and *in vivo* inhibition of tumor cell viability by combined dihydroartemisinin and doxorubicin treatment., and the underlying mechanism. *Oncol. Lett.* 12 (5), 3701–3706. doi:10.3892/ol.2016.5187

Takashi, Y., Tomita, K., Kuwahara, Y., Roudkenar, M. H., Roushandeh, A. M., Igarashi, K., et al. (2020). Mitochondrial dysfunction promotes aquaporin expression that controls hydrogen peroxide permeability and ferroptosis. *Free Radic. Biol. Med.* 161, 60–70. doi:10.1016/j.freeradbiomed.2020.09.027

Tang, D., Chen, X., Kang, R., and Kroemer, G. (2021a). Ferroptosis: Molecular mechanisms and health implications. *Cell Res.* 31 (2), 107–125. doi:10.1038/s41422-020-00441-1

Tang, T., Xia, Q., and Xi, M. (2021b). Dihydroartemisinin and its anticancer activity against endometrial carcinoma and cervical cancer, involvement of apoptosis., autophagy and transferrin receptor. *Singap. Med. J.* 62 (2), 96–103. doi:10.11622/smedj.2019138

Torti, S. V., and Torti, F. M. (2013). Iron and cancer: More ore to be mined. *Nat. Rev. Cancer* 13 (5), 342–355. doi:10.1038/nrc3495

Tsoi, J., Robert, L., Paraiso, K., Galvan, C., Sheu, K. M., Lay, J., et al. (2018). Multi-stage differentiation defines melanoma subtypes with differential vulnerability to drug-induced iron-dependent oxidative stress. *Cancer Cell* 33 (5), 890–904.e5. doi:10.1016/j.ccell.2018.03.017

Villalpando-Rodriguez, G. E., Blankstein, A. R., Konzelman, C., and Gibson, S. B. (2019). Lysosomal destabilizing drug siramesine and the dual tyrosine kinase inhibitor Lapatinib induce a synergistic ferroptosis through reduced heme oxygenase-1 (HO-1) levels. *Oxid. Med. Cell Longev.* 2019, 9561281. doi:10.1155/2019/9561281

Wang, C., Zeng, J., Li, L. J., Xue, M., and He, S. L. (2021a). Cdc25A inhibits autophagy-mediated ferroptosis by upregulating ErbB2 through PKM2 dephosphorylation in cervical cancer cells. *Cell Death Dis.* 12 (11), 1055. doi:10.1038/s41419-021-04342-y

Wang, X., Wang, H., Mou, X., Xu, Y., Han, W., Huang, A., et al. (2022). Lysophosphatidic acid protects cervical cancer HeLa cells from apoptosis induced by doxorubicin hydrochloride. *Oncol. Lett.* 24 (2), 267. doi:10.3892/ol.2022.13387

Wang, X., Xu, S., Zhang, L., Cheng, X., Yu, H., Bao, J., et al. (2021b). Vitamin C induces ferroptosis in anaplastic thyroid cancer cells by ferritinophagy activation. *Biochem. Biophys. Res. Commun.* 551, 46–53. doi:10.1016/j.bbrc.2021.02.126

Wu, P., Li, C., Ye, D. M., Yu, K., Li, Y., Tang, H., et al. (2021). Circular RNA circEPSTI1 accelerates cervical cancer progression via miR-375/409-3P/515-5p-SLC7A11 axis. *Aging (Albany NY)* 13 (3), 4663–4673. doi:10.18632/aging.202518

Xia, L., Su, X., Shen, J., Meng, Q., Yan, J., Zhang, C., et al. (2018). ANLN functions as a key candidate gene in cervical cancer as determined by integrated bioinformatic analysis. *Cancer Manag. Res.* 10, 663–670. doi:10.2147/CMAR.S162813

Xiao, C., Fu, X., Wang, Y., Liu, H., Jiang, Y., Zhao, Z., et al. (2020). Transferrin receptor regulates malignancies and the stemness of hepatocellular carcinoma-derived cancer stem-like cells by affecting iron accumulation. *PLoS One* 15 (12), e0243812. doi:10.1371/journal.pone.0243812

Xiaofei, J., Mingqing, S., Miao, S., Yizhen, Y., Shuang, Z., Qinhua, X., et al. (2021). Oleanolic acid inhibits cervical cancer Hela cell proliferation through modulation of the ACSL4 ferroptosis signaling pathway. *Biochem. Biophys. Res. Commun.* 545, 81–88. doi:10.1016/j.bbrc.2021.01.028

Yang, X., Yin, F., Liu, Q., Ma, Y., Zhang, H., Guo, P., et al. (2022). Ferroptosis-related genes identify tumor immune microenvironment characterization for the prediction of prognosis in cervical cancer. *Ann. Transl. Med.* 10 (2), 123. doi:10.21037/atm-21-6265

Yi, L., Hu, Y., Wu, Z., Li, Y., Kong, M., Kang, Z., et al. (2022). TFRC upregulation promotes ferroptosis in CVB3 infection via nucleus recruitment of Sp1. *Cell Death Dis.* 13 (7), 592. doi:10.1038/s41419-022-05027-w

Yi, R., Wang, H., Deng, C., Wang, X., Yao, L., Niu, W., et al. (2020). Dihydroartemisinin initiates ferroptosis in glioblastoma through GPX4 inhibition. *Biosci. Rep.* 40 (6), BSR20193314. doi:10.1042/BSR20193314

Yu, F., Zhang, Q., Liu, H., Liu, J., Yang, S., Luo, X., et al. (2022). Dynamic O-GlcNAcylation coordinates ferritinophagy and mitophagy to activate ferroptosis. *Cell Discov.* 8 (1), 40. doi:10.1038/s41421-022-00390-6

Yu, R., Jin, G., and Fujimoto, M. (2021). Dihydroartemisinin: A potential drug for the treatment of malignancies and inflammatory diseases. *Front. Oncol.* 11, 722331. doi:10.3389/fonc.2021.722331

Yuan, B., Liao, F., Shi, Z. Z., Ren, Y., Deng, X. L., Yang, T. T., et al. (2020). Dihydroartemisinin inhibits the proliferation., colony formation and induces ferroptosis of lung cancer cells by inhibiting PRIM2/slc7a11 Axis. *Onco Targets Ther.* 13, 10829–10840. doi:10.2147/OTT.S248492

Zhang, B., Tian, L., Xie, J., Chen, G., and Wang, F. (2020b). Targeting miRNAs by natural products: A new way for cancer therapy. *Biomed. Pharmacother.* 130, 110546. doi:10.1016/j.biopha.2020.110546

Zhang, C., Liu, P., Huang, J., Liao, Y., Pan, C., Liu, J., et al. (2021). Circular RNA hsa_circ_0043280 inhibits cervical cancer tumor growth and metastasis via miR-203a-3p/PAQR3 axis. *Cell Death Dis.* 12 (10), 888. doi:10.1038/s41419-021-04193-7

Zhang, X., Sui, S., Wang, L., Li, H., Zhang, L., Xu, S., et al. (2020a). Inhibition of tumor propellant glutathione peroxidase 4 induces ferroptosis in cancer cells and enhances anticancer effect of cisplatin. *J. Cell Physiol.* 235 (4), 3425–3437. doi:10.1002/jcp.29232

Zhou, B., Liu, J., Kang, R., Klionsky, D. J., Kroemer, G., and Tang, D. (2020). Ferroptosis is a type of autophagy-dependent cell death. *Semin. Cancer Biol.* 66, 89–100. doi:10.1016/j.semcancer.2019.03.002

Zhou, M., Wang, H., Zhu, J., Chen, W., Wang, L., Liu, S., et al. (2016). Cause-specific mortality for 240 causes in China during 1990-2013: A systematic subnational analysis for the global burden of disease study 2013. *Lancet* 387 (10015), 251–272. doi:10.1016/S0140-6736(15)00551-6

frontiers | Frontiers in Immunology

TYPE Original Research
PUBLISHED 17 April 2023
DOI 10.3389/fimmu.2023.1149513

OPEN ACCESS

EDITED BY
Yanqing Liu,
Columbia University, United States

REVIEWED BY
Mingrong Zuo,
Sichuan University, China
Di He,
Memorial Sloan Kettering Cancer Center, United States
Yichao Shen,
Baylor College of Medicine, United States

*CORRESPONDENCE
Kai Xue
xuekaishanghai@126.com
Xiaoyang Li
lxy11811@rjh.com.cn
Junmin Li
drlijunmin@126.com

SPECIALTY SECTION
This article was submitted to Cancer Immunity and Immunotherapy, a section of the journal Frontiers in Immunology

RECEIVED 22 January 2023
ACCEPTED 28 March 2023
PUBLISHED 17 April 2023

CITATION
Jiang G, Jin P, Xiao X, Shen J, Li R, Zhang Y, Li X, Xue K and Li J (2023) Identification and validation of a novel CD8+ T cell-associated prognostic model based on ferroptosis in acute myeloid leukemia.
Front. Immunol. 14:1149513.
doi: 10.3389/fimmu.2023.1149513

Identification and validation of a novel CD8+ T cell-associated prognostic model based on ferroptosis in acute myeloid leukemia

Ge Jiang[1], Peng Jin[1], Xiao Xiao[2], Jie Shen[1], Ran Li[1], Yunxiang Zhang[1], Xiaoyang Li[1]*, Kai Xue[1]* and Junmin Li[1]*

[1]State Key Laboratory of Medical Genomics, Shanghai Institute of Hematology, National Research Center for Translational Medicine at Shanghai, Ruijin Hospital Affiliated to Shanghai Jiao Tong University School of Medicine, Shanghai, China, [2]Department of Orthopedic, Shanghai Tenth People's Hospital, Tongji University School of Medicine, Shanghai, China

Acute myeloid leukemia (AML) is a highly aggressive cancer with great heterogeneity and variability in prognosis. Though European Leukemia Net (ELN) 2017 risk classification has been widely used, nearly half of patients were stratified to "intermediate" risk and requires more accurate classification *via* excavating biological features. As new evidence showed that CD8+ T cell can kill cancer cells through ferroptosis pathway. We firstly use CIBERSORT algorithm to divide AMLs into CD8+ ^{high} and CD8+ ^{low} T cell groups, then 2789 differentially expressed genes (DEGs) between groups were identified, of which 46 ferroptosis-related genes associated with CD8+ T cell were sorted out. GO, KEGG analysis and PPI network were conducted based on these 46 DEGs. By jointly using LASSO algorithm and Cox univariate regression, we generated a 6-gene prognostic signature comprising *VEGFA*, *KLHL24*, *ATG3*, *EIF2AK4*, *IDH1* and *HSPB1*. Low-risk group shows a longer overall survival. We then validated the prognostic value of this 6-gene signature using two independent external datasets and patient sample collection dataset. We also proved that incorporation of the 6-gene signature obviously enhanced the accuracy of ELN risk classification. Finally, gene mutation analysis, drug sensitive prediction, GSEA and GSVA analysis were conducted between high-risk and low-risk AML patients. Collectively, our findings suggested that the prognostic signature based on CD8+ T cell-related ferroptosis genes can optimize the risk stratification and prognostic prediction of AML patients.

KEYWORDS

CD8+ T cell, acute myeloid leukemia (AML), prognosis, ferroptosis, European Leukemia Net (ELN) 2017

Introduction

Acute myeloid leukemia (AML), which is highly heterogeneous in adults, represents the most common hematologic malignancy worldwide (1–3). The American Cancer Society has reported a diagnoses rate of more than 20000 new cases of AML in 2021 in the United States alone, while the 5-year overall survival rate is lower than 30% (4). A recent, advanced risk stratification model for AML based on risk classification by the European Leukemia Net (ELN) 2017 categorizes AML patients into three groups for prediction of treatment responses and prognosis (5, 6). Despite its extensive use, the increasing availability of multi-omics data presents an opportunity for improvements to the ELN2017 model through the incorporation of molecular expression data (7–9), which could facilitate higher accuracy patient stratification and therapeutic decision-making. In particular, the use of transcriptomic data that contain the underlying molecular basis responsible for AML pathophysiology could further improve prognosis and enable the identification of novel therapeutic targets.

The strategies for treating AML have remained relatively unchanged over the past three decades. While the "7+3" combined chemotherapy regimen reportedly leads to complete remission in 60-80% in patients younger than 60-years-old and 40%-60% in patients older than 60 years of age (10), in addition to the durable complete remission in the limited group of patients eligible for allogeneic hematopoietic stem cell transplantation (HSCT), both HSCT and chemotherapy treatments have long been associated with high relapse rates (11). Emerging tumor immunotherapy approaches that rely on T cell activation (including CAR-T, TCR-T, or cancer vaccines, etc.) have also shown promise for improved treatment response and clinical outcomes in AML patients (12). These immunotherapeutic approaches rely on the potent effects of CD8+ T cell activation to combat hematopoietic malignancies, since these cells perform essential functions in mediating tumor adaptive immunity (13, 14). Generally, CD8+ T cells exert their killing effects through two main pathways for inducing apoptosis in tumor cells: granzyme-perforin and Fas-FasL (15).

In addition to the canonical apoptotic routes, ferroptosis is an iron-dependent program for regulated cell death (RCD) induced by oxidative disruption of the intracellular microenvironment, which has been implicated as a determining factor in pathogenic progression and treatment response in AML (16, 17). Ferroptosis-related genes can therefore enhance predictive accuracy in AML prognosis over that of apoptosis-related genes since cancer cells exhibit marked sensitivity to ferroptosis due to the necessity of related factors such as iron accumulation and fatty acid synthesis, among others, for tumor growth (16, 18, 19).

Interestingly, correlation between CD8+ T cell and ferroptosis has been unveiled recently. For example, Wang et al. provided direct evidence that CD8+ T cells can mediate resistance to cancer cells *via* the ferroptosis pathway (20). Another research conducted by Liao et al. further proved that polyunsaturated fatty acids (PUFAs) and CD8+ T cell-derived interferon (IFN) γ work together as a natural ferroptosis inducer (FIN) to cause tumor ferroptosis and boost anti-tumor immunity (21).

Inspired by the correlation, our work innovatively investigated CD8+ T cell-related ferroptosis prognostic model in AML, which has a potential to optimize ELN 2017 classification and enable the identification of new and effective therapeutic strategies.

Materials and methods

Patient sample collection and RNA-sequencing

A total of 157 bone marrow (BM) aspirates were collected from 157 *de novo* AML patients diagnosed between June 2019 and September 2020 at Ruijin Hospital affiliated to Shanghai Jiao Tong University School of Medicine. Following the Declaration of Helsinki, the Institutional Review Board of Ruijin Hospital approved the collection of the specimens, and all patients provided written informed consent for specimen collection and research. Total RNA was extracted and RNA-seq libraries were constructed using the TruSeq RNA Sample Preparation Kit v2 (Illumina, San Diego, CA, USA). Paired-end sequencing (150-bp) was performed on the NovaSeq 6000 platform (Illumina). Adapter sequences were trimmed from raw sequencing reads using Trim-galore and then aligned with STAR aligner. Cleaned reads were quantified with HT-Seq count through mapping to the GRCh38 human reference genome assembly. Gene expression estimates were normalized to Transcripts Per Kilobase of exon model per Million mapped reads (TPM) using a customed script. The cohort was named 'RJAML' below.

Data collection

Gene expression and mutation data from the TCGA-LAML cohort (N=151) were obtained from the GDC data portal. Similarly, the gene expression profiles of the GSE12417 (GPL570, N=78) and GSE71014 (N=104) datasets were downloaded from the GEO database. Subsequently, we obtained 259 ferroptosis-related genes from FerrDb DATABASE (http://www.zhounan.org/ferrdb/index.html).

Estimation of immune cell infiltration

CIBERSORT algorithm (22) was used to examine the relative proportions of the 22 immune infiltrating cell types including CD8+ T cell. Correlation between gene expression and immune cell population data were analyzed using the Spearman correlation method, with $p < 0.05$ regarded statistically significant.

Pathway enrichment analysis of CD8+ T cell-related ferroptosis genes

To explore the potential biological functions and pathways related to CD8+ T cell-related ferroptosis genes, DEG analysis

was performed using the edgeRR package between CD8+ ^{high} and CD8+ ^{low} T cell groups. A cutoff of |logFC| > 1, and $p< 0.05$ was used to define DEGs, of which 46 DEGs were related to ferroptosis. Gene Ontology (GO) and Kyoto Encyclopedia of Genes and Genomes (KEGG) were used to make a comprehensive investigation for the CD8+ T cell-related ferroptosis genes based on "Cluster Profiler" (R3.6). GO and KEGG enrichment pathways with both *p*- and *q*-value< 0.05 were considered as significant.

Construction and validation of a prognostic ferroptosis-related gene signature

Univariate cox analysis of overall survival (OS) was performed to screen for ferroptosis-related genes with potential prognostic value. To construct a prognostic model that minimized the risk of overfitting, we used LASSO-penalized Cox regression analysis based on partial likelihood deviance and lambda values, with the value of lambda corresponding to the lowest partial likelihood deviance. After normalizing the expression values of each specific gene, a risk score formula was generated for each patient as follows,

$$\begin{aligned} Risk\ Score\ =\ & VEGFA*(-0.136)\ +KLHL24*(-0.034) \\ & +ATG3*0.031\ +EIF2AK4*\ \ 0.146\ +IDH1*0.186 \\ & +HSPB1*0.297 \end{aligned}$$

and scores were weighted with the regression coefficient estimated by the lasso regression analysis. Based on the above risk score formula, patients were assigned to high-risk or low-risk groups, and the median risk score was used as the cut-off value. The difference in overall survival (OS) between the two groups was assessed by Kaplan-Meier and compared using log-rank statistics. The role of risk scores in predicting patient prognosis was examined using lasso regression analysis and stratified analysis. The accuracy of model predictions was examined using ROC curves.

Improving the European Leukemia Net 2017 risk stratification system

According to the ELN2017 classification system and the 6-gene signature, we refined ELN2017 risk classification by reclassifying patients with favorable ELN and low 6-gene scores as a favorable group; those with favorable ELN and high 6-gene scores or intermediate ELN and low 6-gene scores were included in the intermediate group, while the other three subgroups were included in the adverse group.

Drug sensitivity analysis

We used the R package 'pRRophetic' to predict the chemosensitivity of each tumor sample *via* the largest pharmacogenomic database (Genomics Database for Cancer Drug Sensitivity, GDSC). The IC50 estimations for each individual chemotherapeutic drug treatment were calculated using the regression method, and ten cross-validations with the GDSC training set were carried out to test the accuracy of the regression and prediction. All parameters, including a 'combat' to eliminate batch effects and an average of duplicate gene expression, were set to their default values.

Gene set enrichment analysis

Gene sets were filtered using a minimum and maximum gene set size of 20 and 500 genes, respectively. After performing 1,000 alignments, enriched gene sets were obtained based on a $p< 0.05$ and a false discovery rate (FDR) value of 0.25. At last, significantly enriched GO terms and KEGG pathways were demonstrated.

Statistical analysis

Survival curves were generated by the Kaplan-Meier method and significance was determined by log-rank tests. Multivariate analysis was carried out using the Cox proportional-hazards model. All statistical analyses were performed using the R software package (version 3.6). All statistical tests were two-sided with $p< 0.05$ considered statistically significant.

Results

Identification of CD8+ T cell-related ferroptosis genes in AML

The flowchart of the entire study is shown in Figure 1. Firstly, we quantified the proportion of immune infiltrating cells for each patient using the CIBERSORT algorithm and divided the samples (TCGA-LAML cohort, N=151) into CD8+ ^{high} and CD8+ ^{low} T cell groups based on the median percentage of infiltrating CD8+ T cells. Patients with high infiltration of CD8+ T cells had significantly higher cytolytic scores, which reflected cytolytic cell abundance, as previous reported (Figure 2A) (23). Figure 1S demonstrates the accordance of flow cytometry enumeration with CIBERSORT deconvolution for 6 AML samples (The experimental method is described in the Supplementary Data Sheet 1). We then performed differential expression analysis between high and low CD8+ T cell infiltration groups, which revealed a total of 2,798 differentially expressed genes (DEGs, |logFC| > 1, and $p<$ 0.05), including 1,415 up-regulated and 1,383 down-regulated genes (Figure 2B). Notably, 46 of the DEGs were associated with ferroptosis (Figure 2C). Supplementally, the expression of these 46 CD8+ T cell-related ferroptosis genes in the CD8+ ^{high} and CD8+ ^{low} T cell groups is presented in the Supplementary Data Sheet 2.

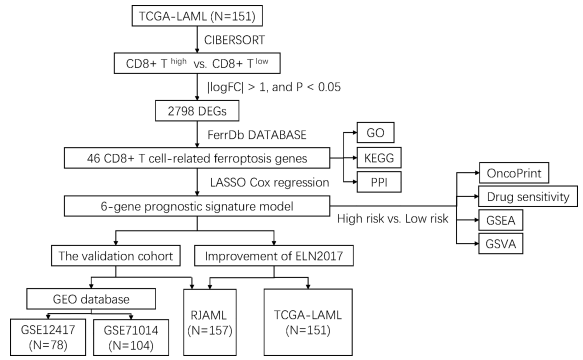

FIGURE 1
Flowchart of study design.

Pathways related to 'response to oxidative stress', 'cellular response to oxidative stress', 'protein kinase complex', and 'secondary lysosome' etc. were enriched by GO analysis. In the process of KEGG analysis, pathways related to 'acute myeloid leukemia', 'PD-L1 expression' and 'PD-1 checkpoint pathway in cancer' etc. were enriched (Figure 3B). As shown in Figure 3C, we constructed a protein-protein interaction (PPI) network using Cytoscape based on the 46 CD8+ T cell-related ferroptosis genes.

Defining a prognostic ferroptosis-related gene signature for CD8+ T cells in AML

To establish a ferroptosis-related gene expression signature, we integrated clinical information from TCGA-LAML cohort and randomly divided these patients into training and validation sets

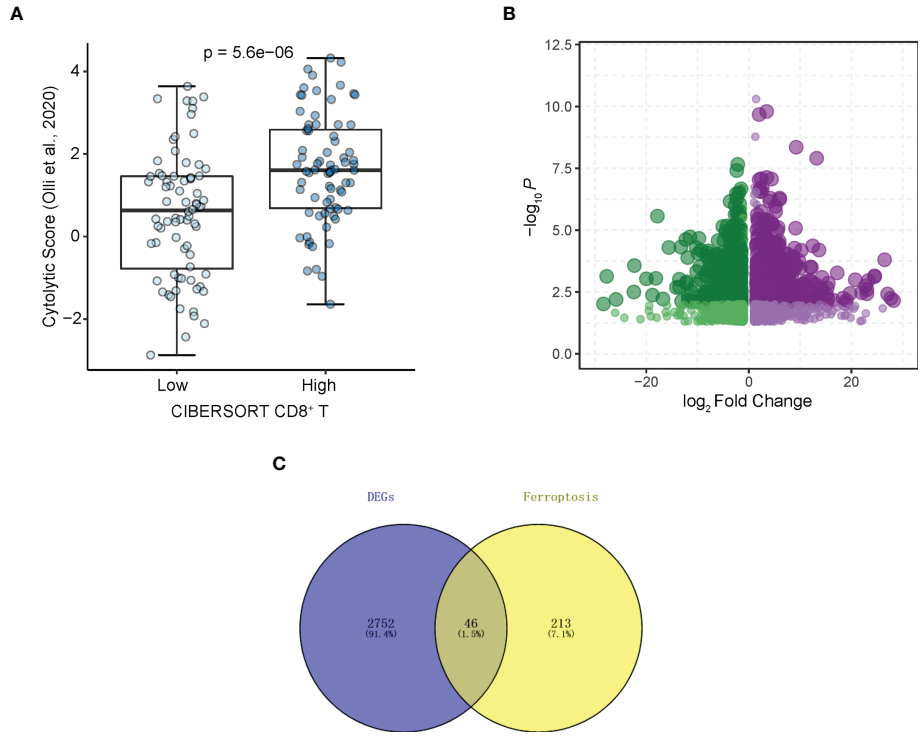

FIGURE 2
Identifying CD8+ T cell-related ferroptosis genes in AML. **(A)** Cytolytic scores (Olli et al., 2020) of patients from CD8+ T cell high and low groups divided by CIBERSORT. **(B)** Volcano plot of DEGs. Plots represents differentially expressed genes between CD8+ T cell high and low groups. **(C)** DEGs associated with ferroptosis.

Molecular functions and pathways enriched by CD8+ T cell-related ferroptosis genes *via* GO and KEGG Analysis; construction of protein-protein interaction (PPI) network analysis based on CD8+ T cell-related ferroptosis genes

We further investigated the differences in biological processes and pathways in 46 ferroptosis-related differentially expressed genes (DEGs) between CD8+ ^{high} and CD8+ ^{low} T cell groups (Figure 3A).

using a 4:1 ratio. By jointly using univariate Cox regression and LASSO regression analysis (Figures 4A, B), we generated an optimal six-gene prognostic signature (Gene6): Risk Score = VEGFA x (-0.136195304538939) + KLHL24 x (-0.0344312172907215) + ATG3 x 0.0306216446230082 + EIF2AK4 x 0.146417351223169 + IDH1 x 0.186205021011148 + HSPB1 x 0.296526705974414 (Figure 4C). The distribution of risk score was then analyzed (Figures 4D, E), which demonstrates that prognostic model has the ability to distinguish high- and low-risk groups of AML patients. Based on the median risk score, patients were classified

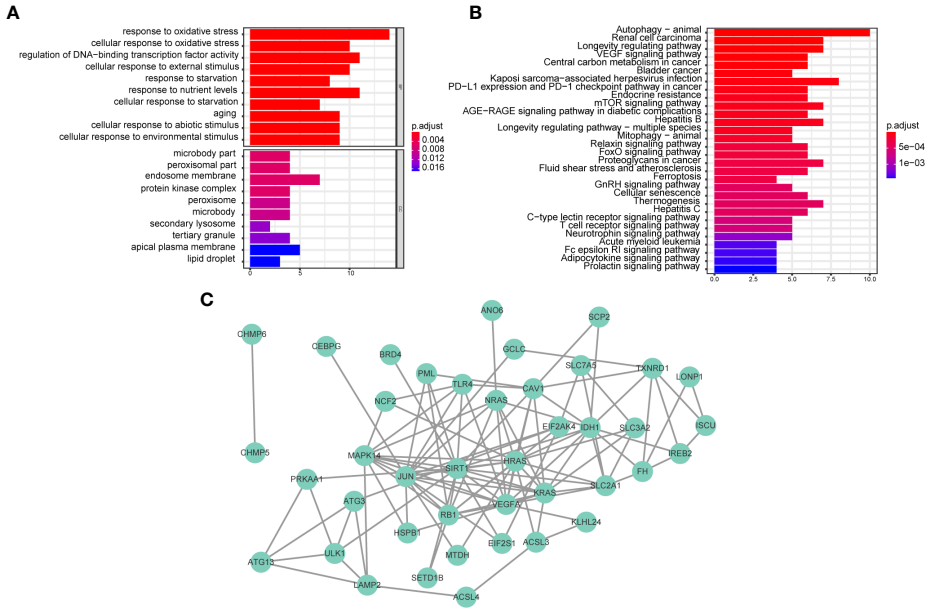

FIGURE 3
Biological functional and pathway enrichment analysis of CD8+ T cell-related ferroptosis genes. **(A, B)** GO and KEGG analysis on CD8+ T cell-related ferroptosis genes. **(C)** Network of co-expressed CD8+ T cell-related ferroptosis genes visualized by Cytoscape.

into high-risk and low-risk groups, and Kaplan-Meier curves were utilized to analyze the data. In both the validation and training sets, OS was considerably lower in the high-risk group (Figures 4F, G). Additionally, the AUC values at 1, 2, and 3 years were greater than 0.7 in both the testing and training datasets, as shown by the ROC curves, suggesting that the model had robust predictive power (Figures 4H, I).

Independent validation of the prognostic six-gene signature

To further evaluate the association of the six-gene signature with patient survival, we obtained the gene expression and clinical data from the GSE12417 (GPL570) (24) and GSE71014 (25) independent patient cohorts. Compared with low-risk scores, patients with high-risk scores had significantly poorer OS than those, according to Kaplan-Meier analysis (Figures 5A, B). ROC analysis also showed that the six-gene model had high accuracy in predicting patient prognoses (AUC values > 0.6 at 1, 2, and 3 years in the GSE12417 dataset; AUC values > 0.7 at 1, 2, and 3 years in the GSE71014 dataset) (Figures 5C, D). Similarly, differences in survival between the high- and low-risk groups remained significant in RJAML cohort, indicated by shorter OS and event-free survival (EFS), in high-risk patients (Figures 5E, F). Collectively, these results demonstrated the prognostic power of the six-gene signature. Incorporation of the six-gene signature into the ELN2017 scheme resulted in generating three new risk groups, as follows: patients with Gene6$^{low\text{-}risk}$/ELN-favorable were re-classified into the favorable-risk group, whereas Gene6$^{high\text{-}risk}$/ELN-favorable, Gene6$^{low\text{-}risk}$/ELN-intermediate and Gene6$^{low\text{-}risk}$/ELN-adverse patients were re-classified as the intermediate-risk group, and Gene6$^{high\text{-}risk}$/ELN-intermediate patients were re-assigned to the adverse-risk group (Figure 5G). Based on the median OS value, these resulting ELN2017 plus Gene6 scores contributed to improved risk segregation and substantially refined ELN2017 classification in TCGA-LAML cohort, evidenced by the more significant *p*-value (Figure 5H). Similar results were obtained when these analyses were performed independently in the RJAML cohort, regardless of OS or EFS (Figures 5I, J). Taken together, these results demonstrated that the Gene6 signature could improve the prognostic efficacy of ELN2017 classification. In addition, we analyzed the association of 6 signature genes expression with the infiltration of 22 major immune cell types and the response to immunotherapy in AML (Figures 2S, 3S).

Gene mutation, drug sensitivity, GSEA, and GSVA analysis between high-risk group and low-risk group classified by CD8+ T cell-related ferroptosis prognostic signature in AML

General information on AML-related gene mutations in high- versus low-risk groups is shown in Figure 6A. DNMT3A (14%), NPM1 (14%), TP53 (11%), RUNX1 (8%) and PTPN11 (8%) rank top five on gene mutation frequencies in high-risk group. The top five genes in the low-risk group with the highest mutation frequencies were IDH2 (11%), TET2 (8%), NPM1 (8%), DNMT3A (8%) and FLT3 (5%). We contrasted the estimated IC50 levels of drugs in AMLs from two groups. Figure 6B shows four representative drugs. Epothilone.B and Cytarabine were

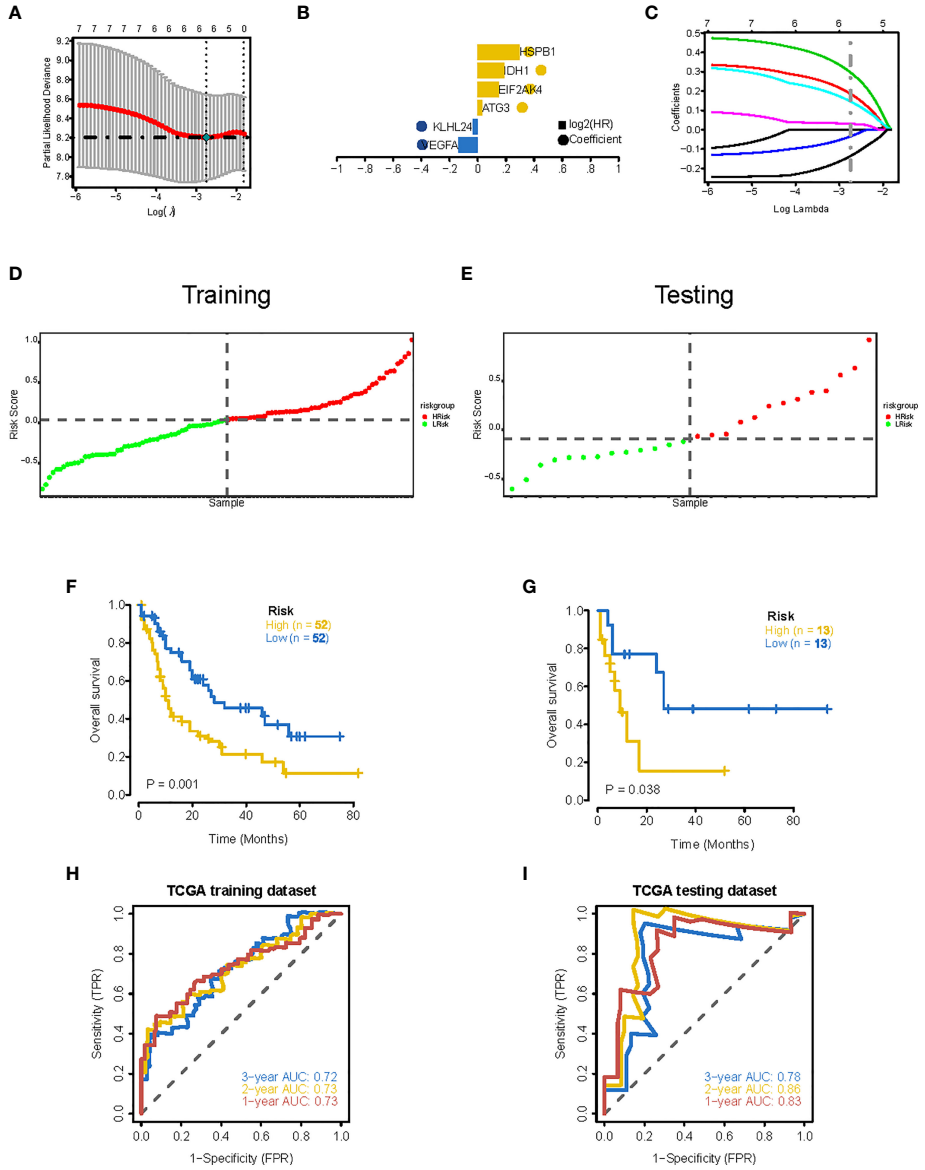

FIGURE 4
Construction of 6-gene prognostic signature. **(A)** Determination of the minimum lambda value with ten-fold cross validation of tuning parameter selection in the LASSO model. **(B)** Distribution of LASSO coefficients for prognosis-related genes and the gene combinations at the minimum lambda value. **(C)** Coefficients of Lasso genes. **(D, E)** The distribution of the risk scores in the training and testing datasets. **(F, G)** Survival curves of TCGA training dataset and testing dataset. **(H, I)** ROC curves of TCGA training dataset and testing dataset (AUC values at 1, 2 and 3 years in both the training and testing datasets were greater than 0.7).

identified to be potential treatment options for patients in high-risk group. Conversely, OSI.906, CCT007093 turn out not ideal drugs for AMLs stratified to high-risk group by Gene6. We then characterized the biological phenotypes associated with each Gene6 risk score through gene set enrichment analysis (GSEA). Indicated by GSEA, upregulated genes were enriched in pathways related to 'cellular response to exogenous dsRNA' and 'valine, leucine, and isoleucine degradation', while down-regulated genes were involved in pathways related to 'intermediate filament organization', 'glycosaminoglycan biosynthesis - heparan sulfate' in the high-risk patient group (Figures 7A, B). Further gene set variation analysis (GSVA) showed that altered pathways in the high-risk patient group were mainly involved in 'adipogenesis', 'PI3K/AKT/MTOR signaling', 'IL2/STAT5 signaling', 'mTORC1 signaling' and others (Figure 7C).

Discussion

In the current work, we first quantified the fraction of various immune infiltrating cells in each patient sample with CIBERSORT (22) to divide the samples into CD8+ ^{high} and CD8+ ^{low} T cell groups by the median percentage of infiltrating CD8+ T cells. We then identified ferroptosis-related genes that were differentially

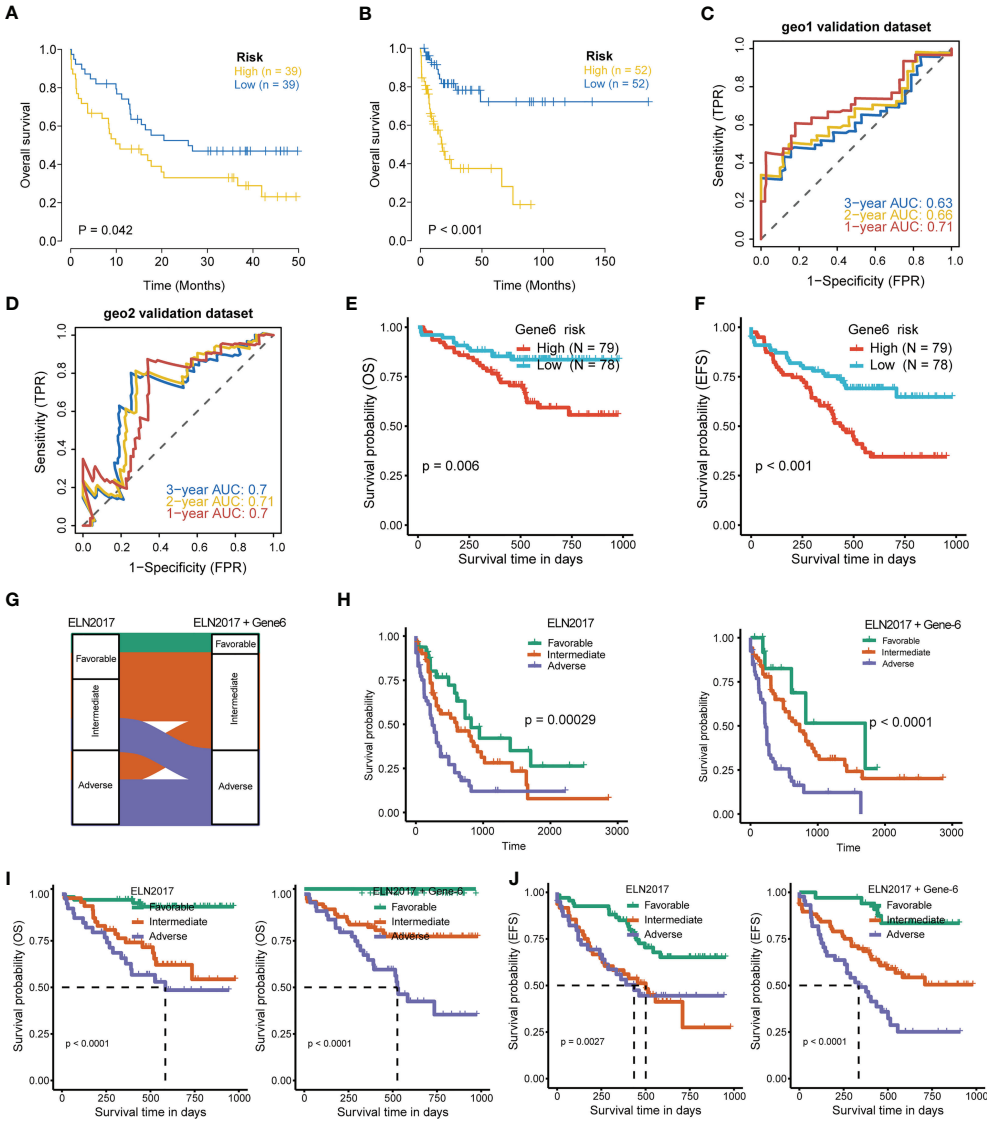

FIGURE 5
Validation of 6-gene prognostic signature. **(A, B)** Kaplan-Meier curves for OS of high- and low-risk groups in validation datasets (GSE12417 dataset, geo1; GSE71014 dataset, geo2). **(C, D)** ROC curves of the risk score in geo1 and geo2 validation gene set (AUC values > 0.6 at 1, 2, and 3 years in the geo1 validation dataset; AUC values > 0.7 at 1, 2, and 3 years in the geo2 validation dataset). **(E, F)** OS and EFS of high- and low-risk groups in RJAML cohort. **(G)** Improvement of the ELN2017 classification incorporating with Gene6 signature. **(H)** Comparison of OS segregation between different risk classifications in ELN2017 vs ELN2017 plus Gene6 at TCGA-LAML cohort. **(I, J)** Comparison of OS and EFS segregation between different risk classifications in ELN2017 vs ELN2017 plus Gene6 at RJAML cohort.

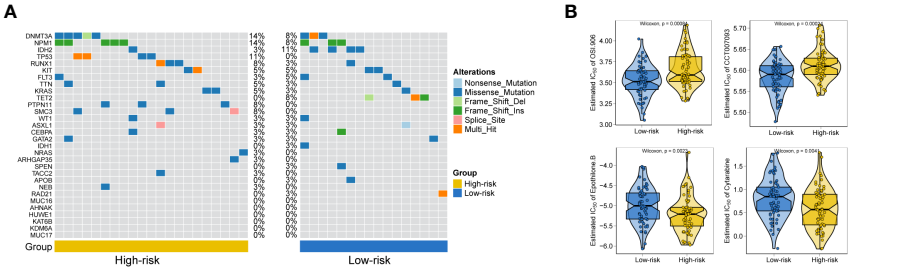

FIGURE 6
Gene mutation analysis and drug sensitive prediction in AML patients. **(A)** Oncoplots showing AML-related gene mutation frequencies among high-risk group and low-risk group in AML patients. **(B)** Violinplots showing the mean differences in estimated IC50 values of 4 representative drugs (OSI.906, CCT007093, Epothilone.B, Cytarabine) between the two risk groups.

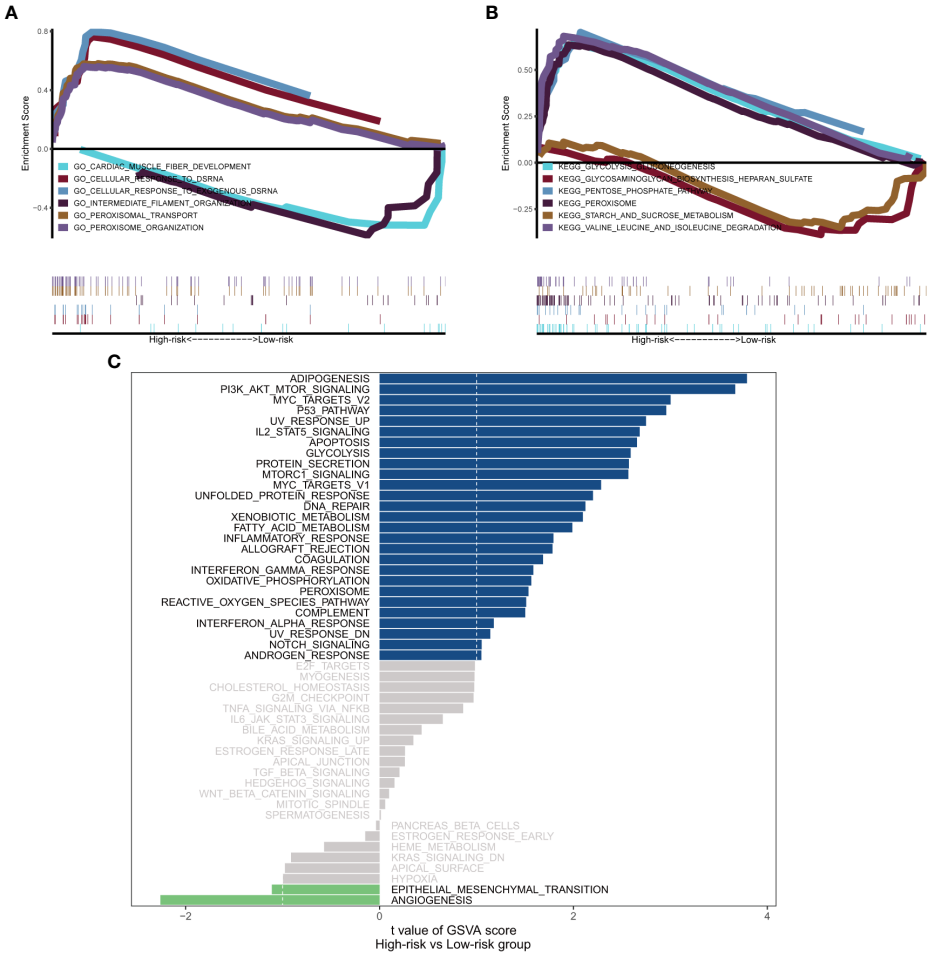

FIGURE 7
Biological phenotypes associated with Gene6 risk score. **(A, B)** GSEA results of Gene6 risk score in GO and KEGG. **(C)** GSVA result of Gene6 risk score.

expressed in CD8+ ^{high} and CD8+ ^{low} T cell groups. We then collected clinical information from each AML patient, identified AML-related signature genes, and used LASSO regression to obtain a panel of genes that provided optimal risk scores for subsequent analysis. To validate the accuracy of the model, we conducted ROC analysis using two external datasets downloaded from GEO database and RNA-seq data from 157 bone marrow (BM) samples aspirated from 157 *de novo* AML patients diagnosed at Ruijin Hospital. It is noteworthy that combining our Gene6 model can improve the accuracy of ELN2017 in classifying the prognosis of AML patients (26).

The prognostic model proposed in this study consists of 6 CD8+ T cell infiltration-related ferroptosis genes (*HSPB1*, *IDH1*, *EIF2AK4*, *ATG3*, *KLHL24*, *VEGFA*). Consistent with the strong connection between this prognostic model and CD8+ T cell immunity, several previous reports revealed that HSPB1 plays a part in the control of CD8+ T cell (27–29). On the other hand, HSPB1 phosphorylation protects tumor cells from ferroptosis by reducing lipid ROS production mediated by iron (30). Glutathione oxidase 4 (GPX4) is a key enzyme in the removing lipid reactive oxygen species (ROS) and ferroptosis. In fact, prior to the recent publication of direct evidence that CD8 can function in cancer *via* ferroptosis (20), numerous previous works unveiled that ferroptosis enhances anti-cancer immunity by boosting cancer immunosurveillance and deciding the fate of CD8+ T cells *via* glutathione oxidase 4 (GPX4), which is a key enzyme in the removing lipid reactive oxygen species (ROS) and ferroptosis (31, 32). IDH1 mutation affects the prognosis of AMLs (33) through regulating the protein level of GPX4 and so has a connection with CD8+ T cell either (34). EIF2AK4 (or GCN2) has been found to affect the survival of tumor patients by suppressing cancer immunology (35, 36). In addition, EIF2AK4 mediates anergy induction and proliferative arrest in T cell through detecting and responding to the immunoregulatory signal generated by Indoleamine 2,3 dioxygenase (IDO) (37). This may support the finding that GCN2 is positively associated with risk of AMLs in our prognostic model based on CD8+ T cell-associated ferroptosis gene. Besides, demonstrated by PPI network of CD8+ T cell-associated ferroptosis genes in Figure 3C, both IDH1 and EIF2AK4 are co-expressed with *Solute Carrier Family 7 Member 5* (SLC7A5), a type of system L transporter. Previous research revealed that T cells require SLC7A5 for methionine uptake even though methionine

can also be produced *de novo* in mammalian cells as well (38, 39). Hence in combination with the previous research, the co-expression result not only reflects the fact that the two genes in Gene6 (IDH1 and EIF2AK4) are associated with CD8+ T cell but also indicates that this association may be mediated by SLC7A5. Jia et al. demonstrated that survival of naïve CD8+ T cell is defective in ATG3-deficient T lymphocytes, which indicated ATG3 is associated with CD8+ T cell (40). Meanwhile, ferroptosis also has been known as a type of cell death depending on autophagy in which ATG3 is a key player (41, 42). In a study conducted by Altman et al, ATG3 deficiency prevented BCR-abl-dependent leukemia by blocking the autophagic pathway (43). KLHL24 found in acute myeloid leukemia as an autophagy-related gene to inform prognostic assessment (38, 44). Despite the lack of previous evidence showed that KLHL24 directly correlated with CD8+ T cell, we speculate KLHL24 indirectly associated with CD8+ T cell *via* autophagy, as autophagy act a pivotal part in the cellular and metabolic reprogramming progresses of CD8+ T cell (45). VEGFA, has been widely recognized as a pro-angiogenic factor in vertebrates and a promoter of tumor progression for decades (46). However, in a research of Palazon et al., they found deletion of VEGFA in CD8+ T cell enhanced tumor growth, which was explained by the VEGF-deficient CTLs' intrinsic defect in acquisition of effector phenotypes (47). Furthermore, in one of the latest studies, researchers found that the absence of CDS2 enhanced the level of VEGFA secreted by the tumor, thereby trapping the tumor in a condition of VEGFA-induced vascular regression, leading to inhibition of tumor growth, which may result in activation of ferroptosis-related pathways (48). Consistent with above mentioned reports, these 6 genes in our model are all directly or indirectly associated with both CD8+ T cell and ferroptosis in cancer and jointly affect the prognosis of AMLs.

As shown by the analysis of AML-related gene mutation between high and low-risk groups (Figure 6A), the adverse-risk gene mutations such as TP53, SMC3 and PTPN11 mutations (26, 49, 50) have obviously higher frequency in high-risk group. This study also excavated altered biological phenotypes including 'cellular response to exogenous dsRNA', 'PI3K/AKT/MTOR signaling' and so on in high- versus low-risk patient group by GSEA and GSVA. Consistently, exogenous dsRNA participates in driving Type I IFN induction *via* targeting RNA-sensing PRR pathways, including RIG-I/MDA5-IPS-1, TLR7-MyD88 and TLR3-TICAM-1 in dendritic cell subset, so as to evoke and amplify CD8+ T cell anti-tumor immunity (51). In contrast to subcutaneously grown leukemic tumors, diffused leukemia is known for its failure to produce type I IFN, which prevents it from generating cellular antitumor immunity (52, 53). FLT3-ITD was previously reported to synergistically activate the mTORC1/S6K/4EBP1 pathway through the PI3K/AKT and STAT5/PIM pathways to enhance eIF4F complex formation and promote the proliferation and survival of tumor cells, while FLT3-ITD is the most common tyrosine kinase mutation associated with poor prognosis in AML (54). The association of other pathways with prognosis was also illustrated in previous reports (55–57). These findings suggested that perturbation of these signaling pathways may underpin the survival differences between the high-risk and low-risk patient groups.

In general, this study was the first to establish a prognostic model of AML based on $CD8^+$ T cell-associated ferroptosis genes that exhibited certain guiding effects in predicting OS and EFS in patients with AML and further optimize the classification of ELN2017 scheme, which is proved by multiple data sets, especially our patient sample data. In order to reduce the limitations of the study, we hope that the utility of the model constructed will also be validated in the future with larger scale of clinical samples and studies. Additionally, the complex mechanisms underlying the prognostic function of 6 CD8+ T cell-related ferroptosis genes in AML need being further investigated in the following work.

Data availability statement

The datasets presented in this study can be found in online repositories. The names of the repository/repositories and accession number(s) can be found below: Gene Expression Omnibus (GEO) *via* GSE201492.

Ethics statement

The study was approved by the Ethics Review Committee of Ruijin Hospital affiliated to Shanghai Jiao Tong University School of Medicine. The patients/participants provided their written informed consent to participate in this study.

Author contributions

JL, GJ, XL and KX designed the study. GJ, PJ, JS and XX drafted the paper. YZ, GJ, RL collected the samples. GJ, XX and PJ integrated and analyzed the data. GJ, PJ, XX and KX edited and revised the paper. All authors contributed to the article and approved the submitted version.

Funding

National Natural Science Foundation of China (81870110, 82200158), National Key R&D Program of China (2019YFA0905900), Shanghai Science Technology and Innovation Action Plan-Key Program on Medical Innovation Research (21Y31920400), Medical-Engineering Cross Foundation of Shanghai Jiao Tong University (ZH2018ZDA02).

Conflict of interest

The authors declare that the research was conducted in the absence of any commercial or financial

relationships that could be construed as a potential conflict of interest.

Publisher's note

Supplementary material

The Supplementary Material for this article can be found online at: https://www.frontiersin.org/articles/10.3389/fimmu.2023.1149513/full#supplementary-material

References

1. Newell LF, Cook RJ. Advances in acute myeloid leukemia. *BMJ* (2021) 375:n2026. doi: 10.1136/bmj.n2026

2. De Kouchkovsky I, Abdul-Hay M. 'Acute myeloid leukemia: A comprehensive review and 2016 update'. *Blood Cancer J* (2016) 6(7):e441. doi: 10.1038/bcj.2016.50

3. Lowenberg B, Downing JR, Burnett A. Acute myeloid leukemia. *N Engl J Med* (1999) 341(14):1051–62. doi: 10.1056/NEJM199909303411407

4. Siegel RL, Miller KD, Fuchs HE, Jemal A. Cancer statistics, 2021. *CA Cancer J Clin* (2021) 71(1):7–33. doi: 10.3322/caac.21654

5. Döhner H, Estey E, Grimwade D, Amadori S, Appelbaum FR, Büchner T, et al. Diagnosis and management of aml in adults: 2017 eln recommendations from an international expert panel. *Blood* (2017) 129(4):424–47. doi: 10.1182/blood-2016-08-733196

6. Horibata S, Gui G, Lack J, DeStefano CB, Gottesman MM, Hourigan CS. Heterogeneity in refractory acute myeloid leukemia. *Proc Natl Acad Sci USA* (2019) 116(21):10494–503. doi: 10.1073/pnas.1902375116

7. Ng SW, Mitchell A, Kennedy JA, Chen WC, McLeod J, Ibrahimova N, et al. A 17-gene stemness score for rapid determination of risk in acute leukaemia. *Nature* (2016) 540(7633):433–7. doi: 10.1038/nature20598

8. Jin P, Tan Y, Zhang W, Li J, Wang K. Prognostic alternative mrna splicing signatures and associated splicing factors in acute myeloid leukemia. *Neoplasia* (2020) 22(9):447–57. doi: 10.1016/j.neo.2020.06.004

9. Ijurko C, González-García N, Galindo-Villardón P, Hernández-Hernández Á. A 29-gene signature associated with Nox2 discriminates acute myeloid leukemia prognosis and survival *Am J Hematol* (2022) 97(4):448–57 doi: 10.1002/ajh.26477

10. Dohner H, Estey EH, Amadori S, Appelbaum FR, Buchner T, Burnett AK, et al. Diagnosis and management of acute myeloid leukemia in adults: Recommendations from an international expert panel, on behalf of the European leukemianet. *Blood* (2010) 115(3):453–74. doi: 10.1182/blood-2009-07-235358

11. Koenig K, Mims A. Relapsed or primary refractory aml: Moving past mec and flag-Ida. *Curr Opin Hematol* (2020) 27(2):108–14. doi: 10.1097/moh.0000000000000561

12. Tawara I, Kageyama S, Miyahara Y, Fujiwara H, Nishida T, Akatsuka Y, et al. Safety and persistence of Wt1-specific T-cell receptor gene-transduced lymphocytes in patients with aml and mds. *Blood* (2017) 130(18):1985–94. doi: 10.1182/blood-2017-06-791202

13. Zou W, Wolchok JD, Chen L. Pd-L1 (B7-H1) and pd-1 pathway blockade for cancer therapy: Mechanisms, response biomarkers, and combinations. *Sci Trans Med* (2016) 8(328):328rv4. doi: 10.1126/scitranslmed.aad7118

14. Chen DS, Mellman I. Oncology meets immunology: The cancer-immunity cycle. *Immunity* (2013) 39(1):1–10. doi: 10.1016/j.immuni.2013.07.012

15. Golstein P, Griffiths GM. An early history of T cell-mediated cytotoxicity. *Nat Rev Immunol* (2018) 18(8):527–35. doi: 10.1038/s41577-018-0009-3

16. Yu Y, Xie Y, Cao L, Yang L, Yang M, Lotze MT, et al. The ferroptosis inducer erastin enhances sensitivity of acute myeloid leukemia cells to chemotherapeutic agents. *Mol Cell Oncol* (2015) 2(4):e1054549. doi: 10.1080/23723556.2015.1054549

17. Dixon SJ, Lemberg KM, Lamprecht MR, Skouta R, Zaitsev EM, Gleason CE, et al. Ferroptosis: An iron-dependent form of nonapoptotic cell death. *Cell* (2012) 149(5):1060–72. doi: 10.1016/j.cell.2012.03.042

18. Chen X, Kang R, Kroemer G, Tang D. Broadening horizons: The role of ferroptosis in cancer. *Nat Rev Clin Oncol* (2021) 18(5):280–96. doi: 10.1038/s41571-020-00462-0

19. Zhu S, Zhang Q, Sun X, Zeh HJ3rd, Lotze MT, Kang R, et al. Hspa5 regulates ferroptotic cell death in cancer cells. *Cancer Res* (2017) 77(8):2064–77. doi: 10.1158/0008-5472.Can-16-1979

20. Wang W, Green M, Choi JE, Gijon M, Kennedy PD, Johnson JK, et al. Cd8(+) T cells regulate tumour ferroptosis during cancer immunotherapy. *Nature* (2019) 569(7755):270–4. doi: 10.1038/s41586-019-1170-y

21. Liao P, Wang W, Wang W, Kryczek I, Li X, Bian Y, et al. Cd8(+) T cells and fatty acids orchestrate tumor ferroptosis and immunity *via* Acsl4. *Cancer Cell* (2022) 40(4):365–78.e6. doi: 10.1016/j.ccell.2022.02.003

22. Newman AM, Liu CL, Green MR, Gentles AJ, Feng W, Xu Y, et al. Robust enumeration of cell subsets from tissue expression profiles. *Nat Methods* (2015) 12(5):453–7. doi: 10.1038/nmeth.3337

23. Dufva O, Pölönen P, Brück O, Keränen MAI, Klievink J, Mehtonen J, et al. Immunogenomic landscape of hematological malignancies. *Cancer Cell* (2020) 38(3):424–8. doi: 10.1016/j.ccell.2020.08.019

24. Metzeler KH, Hummel M, Bloomfield CD, Spiekermann K, Braess J, Sauerland MC, et al. An 86-Probe-Set gene-expression signature predicts survival in cytogenetically normal acute myeloid leukemia. *Blood* (2008) 112(10):4193–201. doi: 10.1182/blood-2008-02-134411

25. Chuang MK, Chiu YC, Chou WC, Hou HA, Tseng MH, Kuo YY, et al. An mrna expression signature for prognostication in *De novo* acute myeloid leukemia patients with normal karyotype. *Oncotarget* (2015) 6(36):39098–110. doi: 10.18632/oncotarget.5390

26. Cancer Genome Atlas Research N, Ley TJ, Miller C, Ding L, Raphael BJ, Mungall AJ, et al. Genomic and epigenomic landscapes of adult *De novo* acute myeloid leukemia. *N Engl J Med* (2013) 368(22):2059–74. doi: 10.1056/NEJMoa1301689

27. Breed ER, Hilliard CA, Yoseph B, Mittal R, Liang Z, Chen CW, et al. The small heat shock protein Hspb1 protects mice from sepsis. *Sci Rep* (2018) 8(1):12493. doi: 10.1038/s41598-018-30752-8

28. Marotta D, Karar J, Jenkins WT, Kumanova M, Jenkins KW, Tobias JW, et al. *In vivo* profiling of hypoxic gene expression in gliomas using the hypoxia marker Ef5 and laser-capture microdissection. *Cancer Res* (2011) 71(3):779–89. doi: 10.1158/0008-5472.Can-10-3061

29. Wood KL, Voss OH, Huang Q, Parihar A, Mehta N, Batra S, et al. The small heat shock protein 27 is a key regulator of Cd8+ Cd57+ lymphocyte survival. *J Immunol* (2010) 184(10):5582–8. doi: 10.4049/jimmunol.0902953

30. Sun X, Ou Z, Xie M, Kang R, Fan Y, Niu X, et al. Hspb1 as a novel regulator of ferroptotic cancer cell death. *Oncogene* (2015) 34(45):5617–25. doi: 10.1038/onc.2015.32

31. Jiang X, Stockwell BR, Conrad M. Ferroptosis: Mechanisms, biology and role in disease. *Nat Rev Mol Cell Biol* (2021) 22(4):266–82. doi: 10.1038/s41580-020-00324-8

32. Matsushita M, Freigang S, Schneider C, Conrad M, Bornkamm GW, Kopf M. T Cell lipid peroxidation induces ferroptosis and prevents immunity to infection. *J Exp Med* (2015) 212(4):555–68. doi: 10.1084/jem.20140857

33. Patel JP, Gönen M, Figueroa ME, Fernandez H, Sun Z, Racevskis J, et al. Prognostic relevance of integrated genetic profiling in acute myeloid leukemia. *New Engl J Med* (2012) 366(12):1079–89. doi: 10.1056/NEJMoa1112304

34. Wang TX, Liang JY, Zhang C, Xiong Y, Guan KL, Yuan HX. The oncometabolite 2-hydroxyglutarate produced by mutant Idh1 sensitizes cells to ferroptosis. *Cell Death Dis* (2019) 10(10):755. doi: 10.1038/s41419-019-1984-4

35. Donnelly N, Gorman AM, Gupta S, Samali A. The Eif2α kinases: Their structures and functions. *Cell Mol Life Sci* (2013) 70(19):3493–511. doi: 10.1007/s00018-012-1252-6

36. Halaby MJ, Hezaveh K, Lamorte S, Ciudad MT, Kloetgen A, MacLeod BL, et al. Gcn2 drives macrophage and mdsc function and immunosuppression in the tumor microenvironment. *Sci Immunol* (2019) 4(42). doi: 10.1126/sciimmunol.aax8189

37. Munn DH, Sharma MD, Baban B, Harding HP, Zhang Y, Ron D, et al. Gcn2 kinase in T cells mediates proliferative arrest and anergy induction in response to indoleamine 2,3-dioxygenase. *Immunity* (2005) 22(5):633–42. doi: 10.1016/j.immuni.2005.03.013

38. Roy DG, Chen J, Mamane V, Ma EH, Muhire BM, Sheldon RD, et al. Methionine metabolism shapes T helper cell responses through regulation of epigenetic reprogramming. *Cell Metab* (2020) 31(2):250–66.e9. doi: 10.1016/j.cmet.2020.01.006

39. Sinclair LV, Howden AJM, Brenes A, Spinelli L, Hukelmann JL, Macintyre AN, et al. Antigen receptor control of methionine metabolism in T cells. *eLife* (2019) 8: e44210. doi: 10.7554/eLife.44210

40. Jia W, He YW. Temporal regulation of intracellular organelle homeostasis in T lymphocytes by autophagy. *J Immunol* (2011) 186(9):5313–22. doi: 10.4049/jimmunol.1002404

41. Zhou B, Liu J, Kang R, Klionsky DJ, Kroemer G, Tang D. Ferroptosis is a type of autophagy-dependent cell death. *Semin Cancer Biol* (2020) 66:89–100. doi: 10.1016/j.semcancer.2019.03.002

42. Qiu Y, Zheng Y, Grace CRR, Liu X, Klionsky DJ, Schulman BA. Allosteric regulation through a switch element in the autophagy E2, Atg3. *Autophagy* (2020) 16 (1):183–4. doi: 10.1080/15548627.2019.1688550

43. Altman BJ, Jacobs SR, Mason EF, Michalek RD, MacIntyre AN, Coloff JL, et al. Autophagy is essential to suppress cell stress and to allow bcr-Abl-Mediated leukemogenesis. *Oncogene* (2011) 30(16):1855–67. doi: 10.1038/onc.2010.561

44. Auberger P, Puissant A. Autophagy, a key mechanism of oncogenesis and resistance in leukemia. *Blood* (2017) 129(5):547–52. doi: 10.1182/blood-2016-07-692707

45. Xu X, Araki K, Li S, Han J-H, Ye L, Tan WG, et al. Autophagy is essential for effector Cd8+ T cell survival and memory formation. *Nat Immunol* (2014) 15 (12):1152–61. doi: 10.1038/ni.3025

46. Claesson-Welsh L, Welsh M. Vegfa and tumour angiogenesis. *J Internal Med* (2013) 273(2):114–27. doi: 10.1111/joim.12019

47. Palazon A, Tyrakis PA, Macias D, Veliça P, Rundqvist H, Fitzpatrick S, et al. An hif-1α/Vegf-a axis in cytotoxic T cells regulates tumor progression. *Cancer Cell* (2017) 32(5):669–83.e5. doi: 10.1016/j.ccell.2017.10.003

48. Zhao W, Cao L, Ying H, Zhang W, Li D, Zhu X, et al. Endothelial Cds2 deficiency causes vegfa-mediated vascular regression and tumor inhibition. *Cell Res* (2019) 29(11):895–910. doi: 10.1038/s41422-019-0229-5

49. Katti A, Diaz BJ, Caragine CM, Sanjana NE, Dow LE. Crispr in cancer biology and therapy. *Nat Rev Cancer* (2022) 22(5):259–79. doi: 10.1038/s41568-022-00441-w

50. Alfayez M, Issa GC, Patel KP, Wang F, Wang X, Short NJ, et al. The clinical impact of Ptpn11 mutations in adults with acute myeloid leukemia. *Leukemia* (2021) 35 (3):691–700. doi: 10.1038/s41375-020-0920-z

51. Iwasaki A, Medzhitov R. Regulation of adaptive immunity by the innate immune system. *Science* (2010) 327(5963):291–5. doi: 10.1126/science.1183021

52. Curran E, Chen X, Corrales L, Kline DE, Dubensky TWJr., Duttagupta P, et al. Sting pathway activation stimulates potent immunity against acute myeloid leukemia. *Cell Rep* (2016) 15(11):2357–66. doi: 10.1016/j.celrep.2016.05.023

53. Ruzicka M, Koenig LM, Formisano S, Boehmer DFR, Vick B, Heuer EM, et al. Rig-I-Based immunotherapy enhances survival in preclinical aml models and sensitizes aml cells to checkpoint blockade. *Leukemia* (2020) 34(4):1017–26. doi: 10.1038/s41375-019-0639-x

54. Watanabe D, Nogami A, Okada K, Akiyama H, Umezawa Y, Miura O. Flt3-itd activates Rsk1 to enhance proliferation and survival of aml cells by activating Mtorc1 and Eif4b cooperatively with pim or Pi3k and by inhibiting bad and bim. *Cancers* (2019) 11(12). doi: 10.3390/cancers11121827

55. Liu H, Zhai Y, Zhao W, Wan Y, Lu W, Yang S, et al. Consolidation chemotherapy prevents relapse by indirectly regulating bone marrow adipogenesis in patients with acute myeloid leukemia. *Cell Physiol Biochem Int J Exp Cell physiology biochemistry Pharmacol* (2018) 45(6):2389–400. doi: 10.1159/000488225

56. Akhter A, Farooq F, Elyamany G, Mughal MK, Rashid-Kolvear F, Shabani-Rad MT, et al. Acute myeloid leukemia (Aml): Upregulation of Baalc/Mn1/Mllt11/Evi1 gene cluster relate with poor overall survival and a possible linkage with coexpression of Myc/Bcl2 proteins. *Appl immunohistochemistry Mol Morphol AIMM* (2018) 26(7):483–8. doi: 10.1097/pai.0000000000000452

57. Nematollahi P, Baradaran A, Kasaei Koopaei Z, Sajjadieh H. Angiogenesis and minimal residual disease in patients with acute myeloid leukemia. *Int J Hematol-Oncol Stem Cell Res* (2020) 14(2):93–8.

frontiers | Frontiers in Molecular Biosciences

TYPE Original Research
PUBLISHED 28 April 2023
DOI 10.3389/fmolb.2023.1188027

OPEN ACCESS

EDITED BY
Yanqing Liu,
Columbia University, United States

REVIEWED BY
Jianmin Ding,
University of Texas Health Science Center at Houston, United States
Rongkang Yin,
Rice University, United States
Dan Yuan,
University of Washington, United States
Yichao Shen,
Baylor College of Medicine, United States
Senmiao Sun,
Harvard University, United States

*CORRESPONDENCE
Yangchun Feng,
fengyangchun@xjmu.edu.cn

†These authors have contributed equally to this work

RECEIVED 16 March 2023
ACCEPTED 17 April 2023
PUBLISHED 28 April 2023

CITATION
Han S, Wang S, Lv X, Li D and Feng Y (2023), Ferroptosis-related genes in cervical cancer as biomarkers for predicting the prognosis of gynecological tumors.
Front. Mol. Biosci. 10:1188027.
doi: 10.3389/fmolb.2023.1188027

Ferroptosis-related genes in cervical cancer as biomarkers for predicting the prognosis of gynecological tumors

Songtao Han[1,2†], Senyu Wang[1,3,4†], Xiang Lv[5†], Dan Li[6†] and Yangchun Feng[1,3*]

[1]Xinjiang Key Laboratory of Oncology, Tumor Hospital Affiliated to Xinjiang Medical University, Ürümqi, China, [2]Clinical Laboratory Center, Hospital of Traditional Chinese Medicine Affiliated to Xinjiang Medical University, Ürümqi, China, [3]Department of Laboratory Medicine, Tumor Hospital Affiliated to Xinjiang Medical University, Ürümqi, China, [4]Department of Laboratory Medicine, Second Hospital Affiliated to Xinjiang Medical University, Ürümqi, China, [5]Department of Laboratory Medicine, Jianyang People's Hospital, Chengdu, China, [6]Department of Encephalopathy, Hospital of Traditional Chinese Medicine Affiliated to Xinjiang Medical University, Ürümqi, China

Background: Ferroptosis has been identified as a potent predictor of cancer prognosis. Currently, cervical cancer ranks among the most prevalent malignant tumors in women. Enhancing the prognosis for patients experiencing metastasis or recurrence is of critical importance. Consequently, investigating the potential of ferroptosis-related genes (FRGs) as prognostic biomarkers for cervical cancer patients is essential.

Methods: In this study, 52 FRGs were obtained from the GSE9750, GSE7410, GSE63514, and FerrDb databases. Six genes possessing prognostic characteristics were identified: JUN, TSC22D3, SLC11A2, DDIT4, DUOX1, and HELLS. The multivariate Cox regression analysis was employed to establish and validate the prognostic model, while simultaneously performing a correlation analysis of the immune microenvironment.

Results: The prediction model was validated using TCGA-CESC and GSE44001 datasets. Furthermore, the prognostic model was validated in endometrial cancer and ovarian serous cystadenocarcinoma cases. KM curves revealed significant differences in OS between high-risk and low-risk groups. ROC curves demonstrated the stability and accuracy of the prognostic model established in this study. Concurrently, the research identified a higher proportion of immune cells in patients within the low-risk group. Additionally, the expression of immune checkpoints (TIGIT, CTLA4, BTLA, CD27, and CD28) was elevated in the low-risk group. Ultimately, 4 FRGs in cervical cancer were corroborated through qRT-PCR.

Conclusion: The FRGs prognostic model for cervical cancer not only exhibits robust stability and accuracy in predicting the prognosis of cervical cancer patients but also demonstrates considerable prognostic value in other gynecological tumors.

KEYWORDS

cervical cancer, ferroptosis, prognosis model, immune checkpoint, gynecological tumors

Introduction

Cervical cancer (CC) ranks as the fourth most common cancer among women worldwide (Sung et al., 2021). In 2020, approximately 600,000 new cases of this disease were reported, with around 340,000 deaths occurring globally (Sung et al., 2021). Persistent infection with human papillomavirus (HPV) can lead to precancerous cervical lesions, which may eventually progress to cancer (CrosbieEinsteinFranceschi and Kitchener, 2013). While the availability of HPV vaccines and cervical cancer screening has dramatically altered mortality and morbidity rates in high-income countries, coverage rates for these policies remain low in many low- and middle-income regions (only 10%) (Brüggmann et al., 2022; Bruni et al., 2022). The primary treatment for cervical cancer involves surgery or postoperative concurrent chemoradiotherapy. Metastasis or recurrence of the cancer substantially decreases the overall survival (OS) rate, which plummets to 5% at 4 years (Small et al., 2017). CC is considered one of the most lethal and threatening types of cancer among women globally, necessitating the development of novel tumor markers for accurate prognosis assessment.

Ferroptosis is an iron-dependent programmed cell death triggered by the accumulation of lipid-based reactive oxygen species (Dixon, 2017). Research has shown that the induction of ferroptosis can play various roles in signal transduction and bioregulation pathways, leading to tumor growth (Stockwell et al., 2017; Shen et al., 2018). Jiang et al. Xiaofei et al. (2021) discovered that the reduction in tumor size and decreased activity of Hela cells could be attributed to ACSL4-induced ferroptosis. Furthermore, FBXW7 (Zhang et al., 2020), G6PD (Dixon et al., 2012), and TP53 (Jiang et al., 2015a) promote ferroptosis in tumor cells, while CSD2 (Kim et al., 2018), GPX4 (Friedmann Angeli et al., 2014), and SLC7A11 (Jiang et al., 2015b) function as inhibitory factors to prevent ferroptosis. Wang et al. (2019) demonstrated that $CD8^+$ T cells' ability to enhance lipid peroxidation specific to ferroptosis could be harnessed for effective immunotherapies. The relationship between ferroptosis and immune cell infiltration holds potential for providing new insights into immunotherapeutic effectiveness.

Most current studies focus on bioinformatically analyzing the expression of ferroptosis-related genes or associated long non-coding RNAs (lncRNAs) in different cancer types to predict prognosis. Although ferroptosis-related genes (FRGs) have been identified as potential prognostic biomarkers for various cancer types, their evaluation in cervical cancer has not been conducted. The clinical information and expression data of patients were analyzed using the TCGA and GEO databases, with data from the FerrDb database also employed in the study. The aim of this study was to develop a prognostic model capable of evaluating the prognosis of women with cervical cancer and to test the model's applicability to other gynecological tumors. Furthermore, the correlation between the prognostic model of FRGs and the immune microenvironment was analyzed, with FRGs validated by quantitative real-time PCR (qRT-PCR). This study's objective was to establish a new strategy that could assist clinicians in predicting the prognosis of patients with cervical cancer.

Materials and methods

Sample and data collection

The research plan is illustrated in Figure 1A. RNA transcriptome data and clinical information were acquired from the GEO and TCGA databases (http://www.ncbi.nlm.nih.gov/projects/geo/, https://portal.gdc.cancer.gov/). All data were transformed using log2 to ensure normalization. Four databases, FerrDb (http://www.zhounan.org/ferrdb/), NCBI-gene (https://www.ncbi.nlm.nih.gov/gene), MSigDB (http://www.gsea-msigdb.org/gsea/msigdb/), and Genecard (https://www.genecards.org/), provided a total of 416 ferroptosis genes (Supplementary Tables S1, S2).

Differential expression and functional enrichment analysis

For the TCGA-CESC and GEO data, the R package edgeR conducted differential analysis on normal and cancer samples. The threshold was set at |Log (FC)|>1, p adj<0.05, and the intersection of differentially expressed genes and ferroptosis genes was determined (The criteria for selecting overlapping genes required their presence in at least two datasets, with one dataset being a ferroptosis gene set). The R package clusterProfiler (version 3.14.3) performed GO/KEGG enrichment analysis of differentially expressed FRGs.

Prognostic model Establishment and prognostic analysis

The R package (glmnet version 4.1.1) executed LASSO regression on the differentially expressed FRGs to filter out redundant factors. Subsequently, univariate/multivariate Cox regression analysis determined the prognostic genes and constructed a Risk score prognostic model (The majority of literature calculates Risk score based on the weighting of the product of gene expression and its coefficients. This study employed multivariate Cox regression to develop a model in which Risk score was determined as the weighting of the product of gene expression and its coefficients.). High-risk groups (n = 153) and low-risk groups (n = 153) were categorized according to the median of the Risk score. The R packages survival ROC (version 1.0.3) and rms (version 6.2.0) analyzed 1-year, 3-year, 5-year survival prognoses and prognostic risk performance.

$$riskscore = \sum_{i=1}^{n} \beta i \times \mathrm{Exp}(i)$$

Clinicopathological features and immune infiltration analysis

The correlation between the Risk score, constructed by FRGs, and clinicopathological characteristics was assessed. Immune

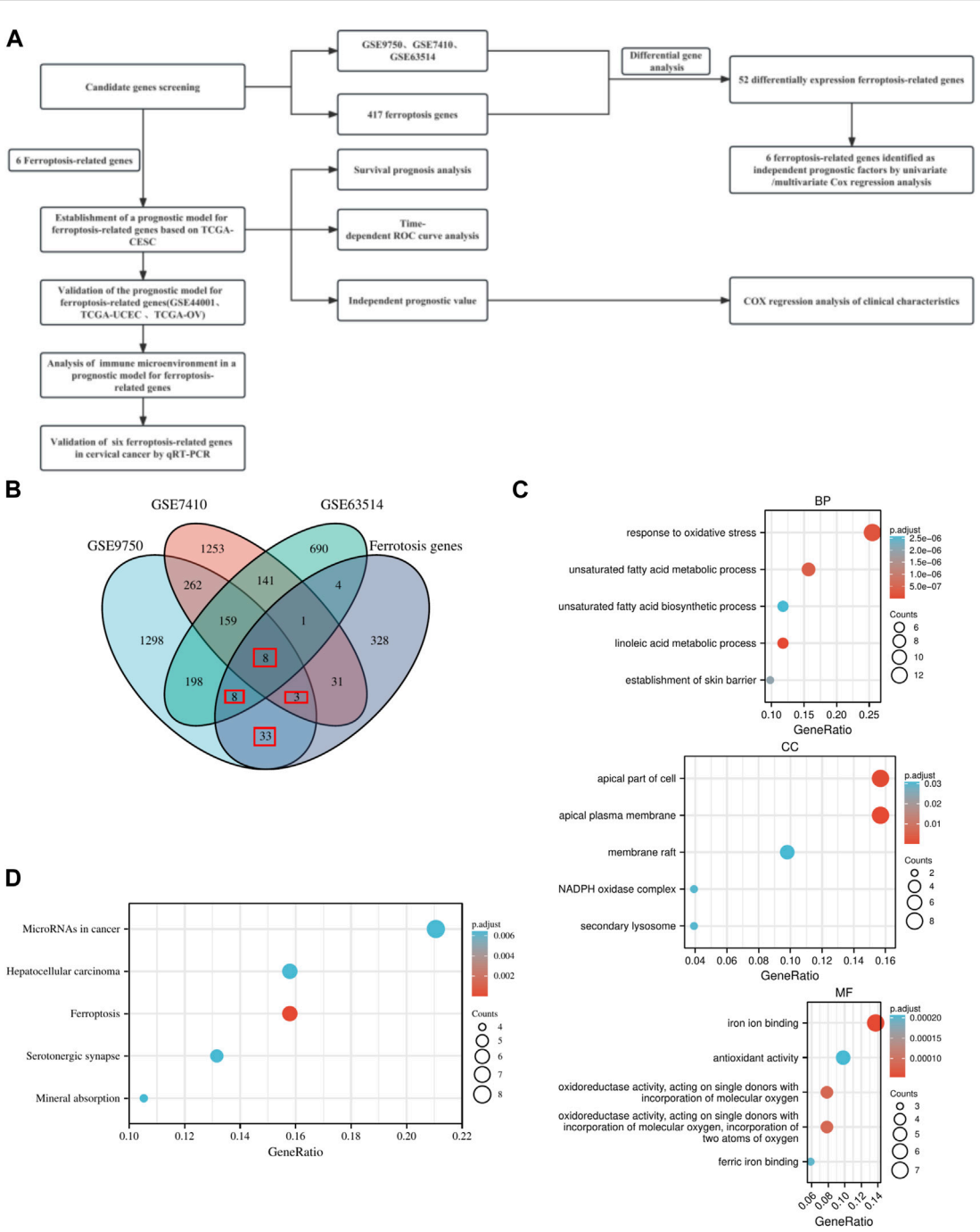

FIGURE 1
Research plan and Overview of FRGs signatures. **(A)** Research plan. **(B)** Venn diagram of differential genes and ferroptosis genes. **(C)** GO enrichment analysis of ferroptosis-related genes in BP, CC, and MF. **(D)** KEGG pathway enrichment analysis of ferroptosis-related genes.

infiltration analysis was performed by ssGSEA algorithm to obtain enrichment scores for each class of immune cells in each sample of TCGA-CESC and GSE44001. The Risk score was then divided into high and low risk groups based on the median of the Risk score among all samples. Differences in the enrichment scores of 24 immune cells (Gabriela et al., 2013) in high and low risk groups were assessed to infer the composition of immune cells in patients with cervical cancer under Risk score.

qRT-PCR detection

A total of 25 cervical cancer tissue samples were collected from surgical patients at the Tumor hospital affiliated with Xinjiang Medical University between 2015 and 2020, with signed informed consent forms. The study was approved by the Ethics Committee of the Tumor hospital affiliated with Xinjiang Medical University and conformed to the Helsinki Declaration and Clinical Practice Guidelines. Total RNA extraction from tissues was performed

TABLE 1 Univariate/multivariate Cox regression analysis of FRGs.

Characteristics	Total(N)	Univariate analysis		Multivariate analysis	
		Hazard ratio (95% CI)	*p*-value	Hazard ratio (95% CI)	*p*-value
JUN	306	1.873 (1.167–3.005)	**0.009**	1.879 (1.154–3.059)	**0.011**
DNAJB6	306	1.710 (1.070–2.735)	**0.025**	1.581 (0.973–2.569)	0.064
TSC22D3	306	0.605 (0.380–0.965)	**0.035**	0.457 (0.277–0.754)	**0.002**
SLC11A2	306	1.611 (1.004–2.585)	**0.048**	1.855 (1.129–3.048)	**0.015**
DDIT4	306	2.097 (1.294–3.398)	**0.003**	2.416 (1.413–4.130)	**0.001**
DUOX1	306	0.439 (0.270–0.712)	**<0.001**	0.454 (0.274–0.754)	**0.002**
CA9	306	1.644 (1.029–2.628)	**0.038**	1.128 (0.685–1.856)	0.635
HELLS	306	0.529 (0.329–0.851)	**0.009**	0.488 (0.288–0.828)	**0.008**

using TRIzol reagent (Invitrogen, United States), and cDNA synthesis occurred by reverse transcription using the PrimeScript real-time kit (Takara, Japan). qRT-PCRs were conducted using an ABI 7500 PRISM 7500 Platform (Applied Biosystems, United States). GAPDH served as a reference, and relative expression levels of target genes were calculated employing the $2^{-\Delta\Delta Ct}$ method. Primers for correlation analysis can be found in Supplementary Tables S3.

Statistical analysis

Differential analysis of normal and cancer samples was conducted using the R package edgeR, with a threshold of |Log (FC)|>1 and p adj<0.05. The R package implemented LASSO regression and univariate/multivariate Cox regression analysis on differentially expressed FRGs. The R packages survminer (version 0.4.9) and survival ROC (version 1.0.3) performed KM(Cox regression was used for analysis) and ROC curve analysis to predict the survival prognosis of patients with cervical cancer. Correlation analysis of survival Risk scores constructed from FRGs and clinicopathological characteristics utilized univariate and multivariate Cox regression analysis. Differences in genes were analyzed by independent samples t-test and visualized using GraphPad Prism 8. The test level was $\alpha = 0.05$, and a difference was considered statistically significant with $p < 0.05$.

Results

Screening and functional analysis of FRGs

Differential gene analysis yielded 1,969, 2,142, and 1,209 differential genes for GSE9750, GSE7410, and GSE63514, respectively (Supplementary Figure S1; Supplementary Table S2). In three distinct datasets, the DEGs were combined with ferroptosis genes to generate differentially expressed FRGs. A total of 52 FRGs were obtained (Figure 1B; Supplementary Tables S4). Ultimately, 52 FRGs underwent GO/KEGG enrichment analysis (Supplementary Tables S5). Enrichment analysis in biological process (BP), cellular component (CC), and molecular function (MF) domains indicated that the gene set was involved in various activities, including the apical part of the cell, iron ion binding, and response to oxidative stress (Figure 1C). KEGG pathway enrichment analysis revealed significant enrichment of the gene set in both ferroptosis and cancer-related pathways (Figure 1D).

Establishment and prognostic analysis of FRGs prognostic model in cervical cancer

TCGA-CESC data served as the training set. Initially, 15 FRGs were derived from LASSO analysis of the 52 FRGs (Supplementary Figure S2). Subsequently, Cox regression analysis results demonstrated that among eight FRGs, six exhibited independent effects on predicted outcomes, including JUN, TSC22D3, SLC11A2, DDIT4, DUOX1, and HELLS (Table 1). A prognostic model was developed based on these six genes and classified into two groups according to Risk score. Scatter plots of survival outcomes and survival time indicated that the high-risk group had more fatalities than the low-risk group (Figure 2A). The training set's KM curve showed that the OS of the low-risk group was longer than that of the high-risk group ($p < 0.001$, Figure 2B). ROC curves were employed to analyze the OS at 1, 3, and 5 years, with AUC values of 0.763, 0.782, and 0.827, respectively (Figure 2C). In conclusion, the model provided a stable and accurate prediction of patients' prognosis.

Prognostic analysis of clinicopathological features by FRGs prognostic model in cervical cancer

Clinicopathological features of the study were examined using univariate/multivariate Cox regression analyses. According to univariate analysis, clinical stage, TNM stage, and Risk score were significant factors predicting patient prognosis. In contrast, multivariate analysis revealed that Risk score was the sole independent factor predicting patient prognosis (Table 2). To ensure accurate patient prognosis, a nomogram incorporating various clinicopathologic parameters was generated (Figure 2D).

10.3389/fmolb.2023.1188027

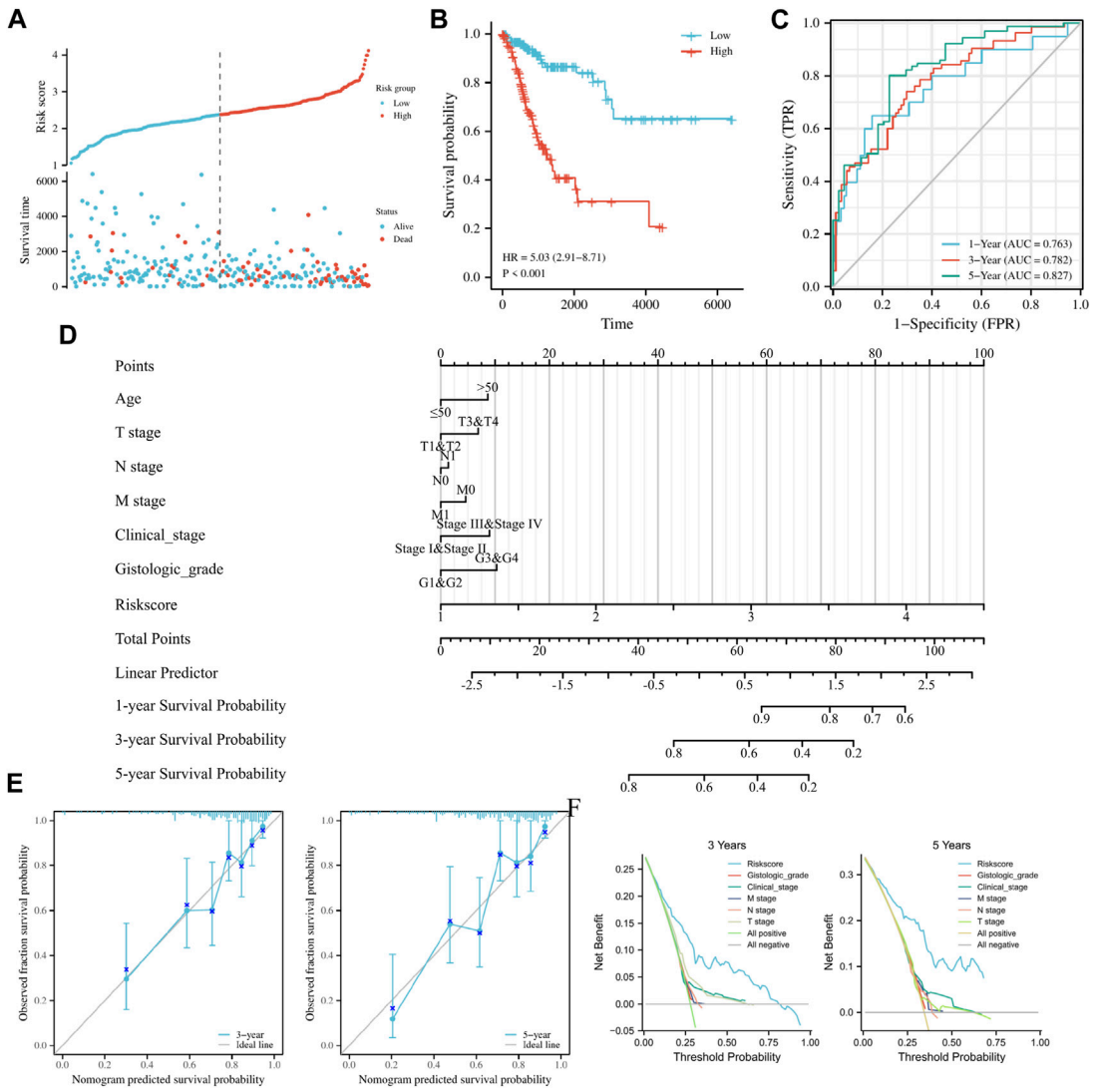

FIGURE 2
Establishment and prognostic analysis of FRGs prognostic model in cervical cancer. **(A)** Curve scatter plot of training set survival model efficacy assessment and cumulative scatter plot of survival mortality event risk. **(B)** KM curves show a significant difference in OS between high-risk and low-risk groups in the training set. **(C)** Time-dependent ROC curves were used to predict 1, 3 and 5 years survival. **(D)** 1, 3, and 5 years nomograms for predicting OS in cervical cancer. **(E)** Calibration curves showing the agreement between predicted and observed 3 and 5 years OS. **(F)** Decision curve analysis of the prognostic model in the training set at 3 and 5 years.

Additionally, DCA and calibration curves (Figures 2E, F) demonstrated the model's role in assessing patient outcomes. In summary, the model could be employed as a novel and powerful tool for predicting patient prognosis.

Validation and prognostic efficacy analysis of prognostic model of FRGs in cervical cancer

To validate the model's applicability, the GSE44001 dataset was used as the validation set. A prognostic model was developed based on the six aforementioned genes, which were divided into high and low groups according to median Risk score. Scatter plots of survival outcomes and survival time indicated that the high-risk group had more fatalities than the low-risk group (Figure 3A). The validation set's KM curve showed that the OS of the low-risk group was longer than that of the high-risk group ($p < 0.001$, Figure 3B). ROC curves were employed to analyze the OS at 1, 3, and 5 years, with AUC values of 0.667, 0.713, and 0.741, respectively (Figure 3C). The study results also indicated that the model was stable and accurate in the validation set. Univariate/multivariate Cox regression analyses were then employed with the dataset to further validate the model's clinicopathologic characteristics. According to univariate analysis results, Risk score and IB2 were the primary prognostic factors. In multivariate regression analysis, Risk score was considered an independent predictor of the study's outcome (Table 3). A nomogram was also used to evaluate the model's value in

TABLE 2 Univariate/multivariate Cox regression analysis of clinicopathological characteristics of TCGA-CESC.

Characteristics	Total (N)	Univariate analysis		Multivariate analysis	
		Hazard ratio (95% CI)	*p*-value	Hazard ratio (95% CI)	*p*-value
Age(>50 *vs.* ≤ 50)	306	1.289 (0.810–2.050)	0.284	0.577 (0.157–2.122)	0.408
T stage (T3&T4 *vs.* T1&T2)	243	3.863 (2.072–7.201)	**<0.001**	2.148 (0.325–14.219)	0.428
N stage(N1 *vs.* N0)	195	2.844 (1.446–5.593)	**0.002**	1.223 (0.352–4.248)	0.751
M stage(M1 *vs.* M0)	127	3.555 (1.187–10.641)	**0.023**	0.000 (0.000-Inf)	0.998
Clinical stage (Stage III&Stage IV *vs.* Stage I&Stage II)	299	2.369 (1.457–3.854)	**<0.001**	1.282 (0.133–12.361)	0.830
Histologic grade (G3&G4 *vs.* G1&G2)	274	0.866 (0.514–1.459)	0.589	2.396 (0.663–8.654)	0.182
RiskScore (High *vs.* Low)	294	8.191 (1.081–62.076)	**0.042**	14.075 (1.147–172.783)	**0.039**

assessing patient prognosis in the GSE44001 dataset (Figure 3D). DCA and calibration curves (Figures 3E, F) also demonstrated that the model had a consistent effect on patient prognosis assessment. In conclusion, the model's practicality and suitability for various datasets render it an ideal choice for determining cervical cancer patients' prognosis.

Validation and prognostic efficacy analysis of FRGs prognostic model for cervical cancer in other gynecological tumors

To confirm the model's universal applicability across different gynecological tumors, TCGA-UCEC and TCGA-OV datasets were employed as validation sets. Scatter plots of survival outcomes and survival time indicated that the high-risk group had more fatalities than the low-risk group (Figure 4A). The validation set's KM curve revealed that the OS of the low-risk group was longer than that of the high-risk group in TCGA-UCEC ($p < 0.001$, Figure 4B). ROC curves were utilized to analyze the OS at 1, 3, and 5 years, with AUC values of 0.758, 0.776, and 0.788, respectively (Figure 4C). The results demonstrated that the model exhibited excellent stability and accuracy in TCGA-UCEC. Clinicopathological features of the model were further verified using univariate/multivariate Cox regression analysis on the TCGA-UCEC dataset. Univariate/multivariate regression analysis revealed that Age, Clinical stage, Histologic grade, and risk score were prognostic factors for TCGA-UCEC (Table 4). Ultimately, a nomogram was established to predict the OS of cervical cancer patients in the TCGA-UCEC dataset at 1, 3, and 5 years (Figure 4D). The DCA diagram and calibration curve (Figures 4E, F) also confirmed that the nomogram combined with clinical features held significant clinical application value. Additionally, the same analysis was performed on the TCGA-OV dataset, which indicated that the cervical cancer prognostic model of iron death-related genes also possessed robust prognostic value in ovarian serous cystadenocarcinoma (Supplementary Figure S2; Supplementary Table S6). In conclusion, the cervical cancer prognostic model of iron death-related genes exhibits strong applicability and can serve as biomarkers to predict patient prognosis across different gynecological tumor datasets.

Correlation analysis between prognostic model of FRGs and immune microenvironment

We found that the low-risk group had significantly higher enrichment scores for B cells, DC, iDC, pDC, T cells, and TReg than the high-risk group ($p < 0.001$, Figure 5A). The enrichment scores in Cytotoxic cells, Mast cells, and T helper cells were slightly higher than the high-risk group ($p < 0.01$, Figure 5A). The enrichment scores for aDC, CD8+T cells, Neutrophils, and TFH were not significantly higher than the high-risk group ($p < 0.05$, Figure 5A). It can be seen that the immune microenvironment of cervical cancer patients under Risk score consists of immune cells such as B cells, T cells, DC and mast cells. Lastly, the correlations between 24 immune cells were assessed, and the correlations between different tumor-infiltrating immune cell subsets ranged from weak to moderate correlations (Figure 5B). The same analysis was conducted for GSE44001, with statistically significant enrichment scores for Macrophages, Mast cells, and Neutrophils, which also resembled the TCGA cohort (Supplementary Figure S4). The expression of various immune checkpoint inhibitors, such as CTLA4, BTLA, CD27, CD28, and CD40, in high and low-risk groups was also analyzed. The results demonstrated that the expression of TIGIT, CTLA4, BTLA, CD27, and CD28 were higher in the low-risk group than in the high-risk group, indicating improved immune efficacy for patients in the low-risk group. The level of expression of other checkpoint inhibitors was not significantly different between the two groups (Figure 5C). In conclusion, the model correlates with the prognosis of patients with cervical cancer from an immune infiltration perspective. Simultaneously, the high expression of immune checkpoint inhibitors in the low-risk group enhances the effectiveness of immunotherapy in patients.

Validation of FRGs expression levels

The expression levels of the model's six genes were validated using the TCGA database. The expression levels of DDIT4 and SLC11A2 were not significantly different when comparing noncancerous and cancerous tissues (Supplementary Figure S5).

10.3389/fmolb.2023.1188027

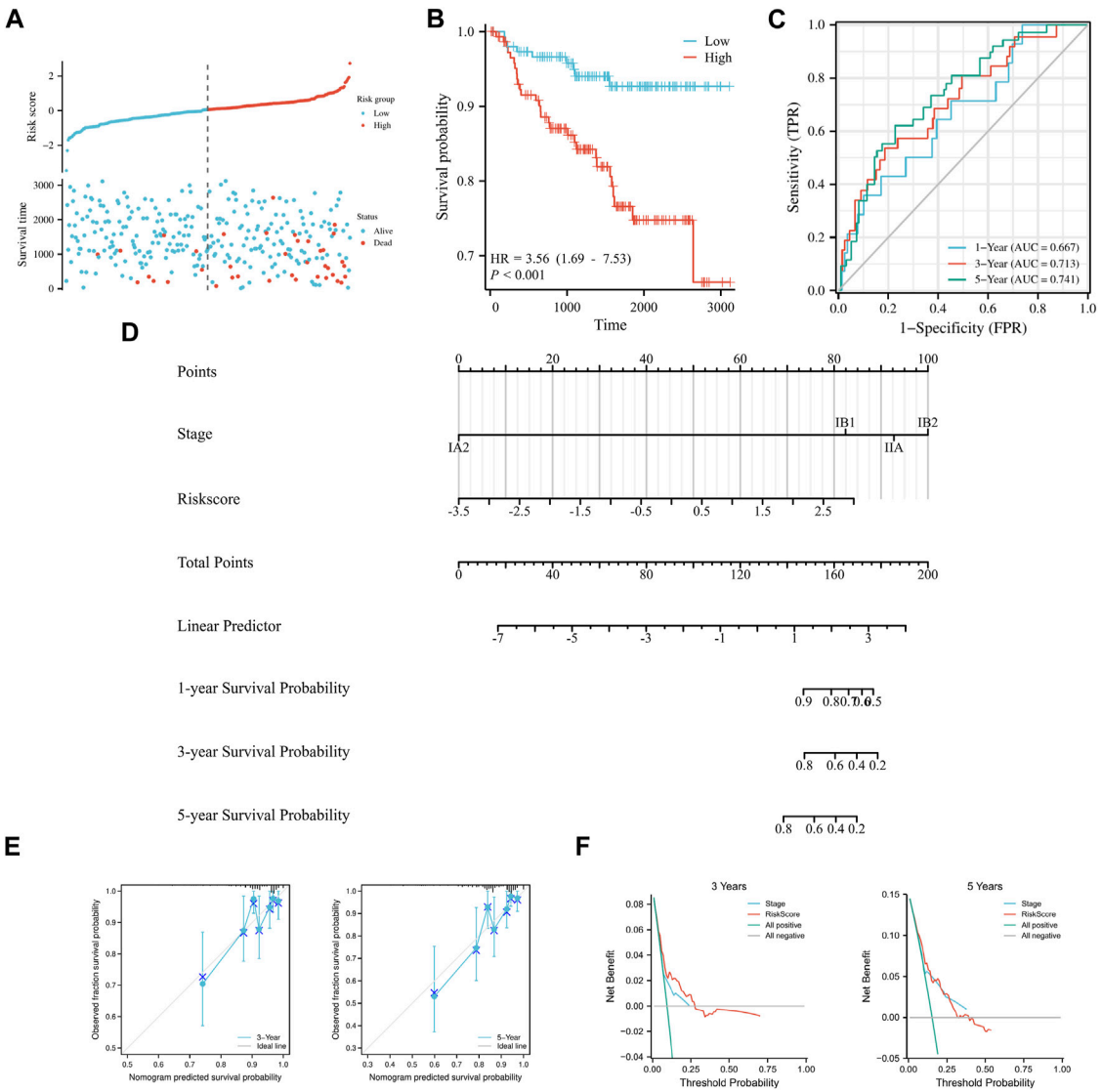

FIGURE 3
Validation of a prognostic model of FRGs in cervical cancer. **(A)** Curve scatter plot of validation set survival model efficacy assessment and cumulative scatter plot of survival mortality event risk. **(B)** KM curve shows that there is a significant difference in OS between high-risk and low-risk groups in GSE44001. **(C)** Time-dependent ROC curves were used to predict 1, 3, and 5 years survival. **(D)** 1, 3, and 5 years nomograms for predicting OS in cervical cancer. **(E)** Calibration curves showing the agreement between predicted and observed 3 and 5 years OS. **(F)** Decision curve analysis of the prognostic model in the validation set at 3 and 5 years.

TABLE 3 Univariate/multivariate Cox regression analysis of clinicopathological characteristics of GSE44001.

Characteristics	Total(N)	Univariate analysis		Multivariate analysis	
		Hazard ratio (95% CI)	*p*-value	Hazard ratio (95% CI)	*p*-value
Stage	300				
IB1	217	Reference			
IA2	13	0.000 (0.000-Inf)	0.996	0.000 (0.000-Inf)	0.996
IB2	28	3.953 (1.807–8.651)	**<0.001**	3.038 (1.334–6.920)	**0.008**
IIA	42	2.106 (0.932–4.758)	0.073	1.920 (0.844–4.369)	0.120
RiskScore (High *vs.* Low)	300	2.718 (1.810–4.081)	**<0.001**	2.270 (1.539–3.349)	**<0.001**

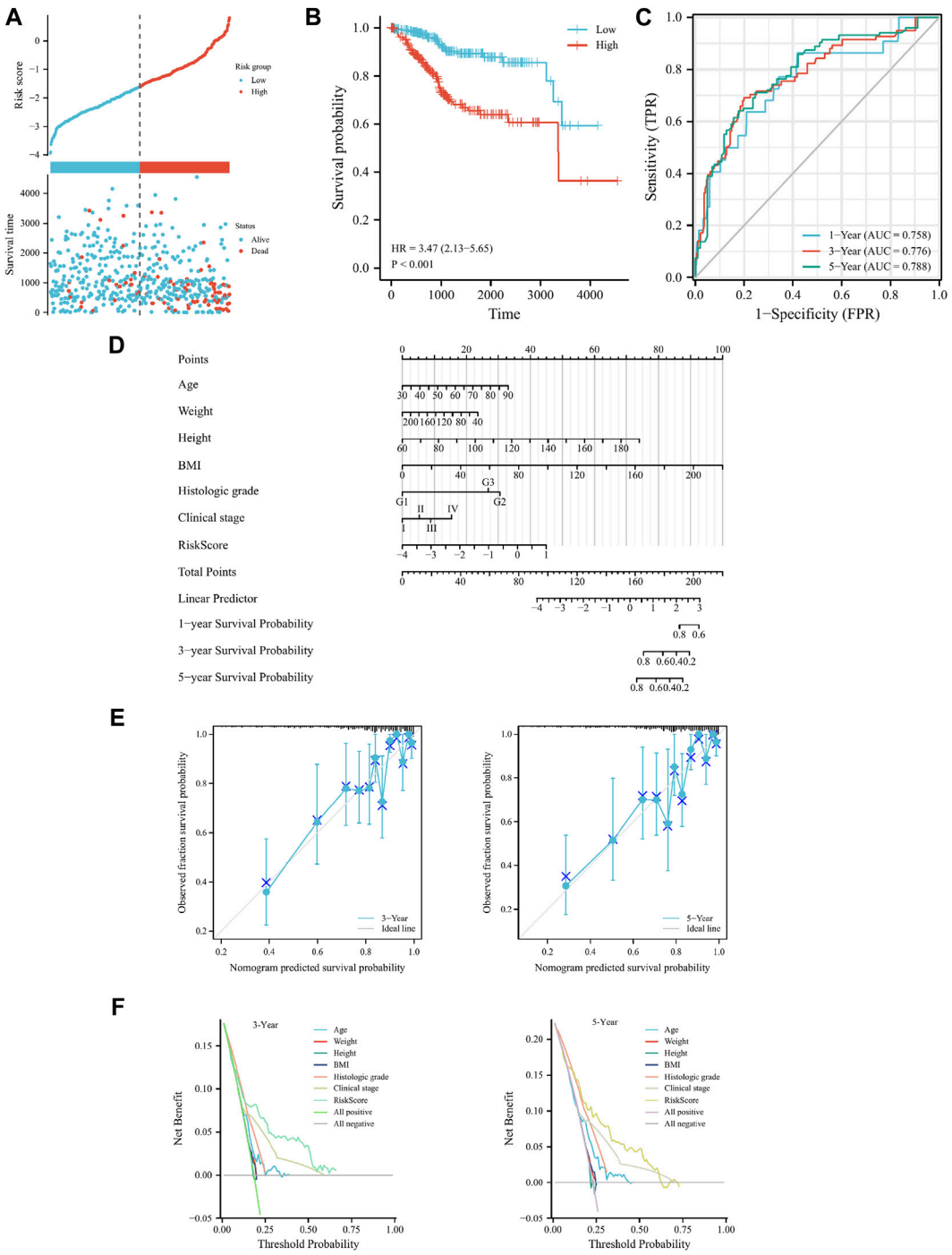

FIGURE 4
Cervical cancer FRGs prognosis model validation in the TCGA-UCEC. **(A)** Curve scatter plot of validation set survival model efficacy assessment and cumulative scatter plot of survival mortality event risk. **(B)** KM curve shows that there is a significant difference in OS between high-risk and low-risk groups in TCGA-UCEC. **(C)** Time-dependent ROC curves were used to predict 1, 3, and 5 years survival. **(D)** 1, 3 and 5 years nomograms for predicting OS in TCGA-UCEC. **(E)** Calibration curves showing the agreement between predicted and observed 3 and 5 years OS. **(F)** Decision curve analysis of the prognostic model in the validation set at 3 and 5 years.

qRT-PCR analysis was performed to assess the levels of the remaining genes in both cervical and non-cancerous tissues. Consequently, the expression levels of JUN and TSC22D3 in cervical cancer tissues displayed an overall downward trend compared with non-tumor tissues (Figures 6A, B). DUOX1 and HELLS exhibited an overall upward trend (Figures 6C, D). Furthermore, the relationship between four genes and B cells, CD8 T cells, DC, NK cells, and T cells was examined, revealing that TSC22D3 was positively correlated with the aforementioned cells; aside from NK cells, HELLS was negatively correlated with the

TABLE 4 Univariate and multivariate Cox regression analysis of clinicopathological characteristics of TCGA-UCEC.

Characteristics	Total (N)	Univariate analysis		Multivariate analysis	
		Hazard ratio (95% CI)	*p*-value	Hazard ratio (95% CI)	*p*-value
Age(>60 *vs.* <=60)	549	0.541 (0.340–0.862)	**0.010**	0.484 (0.293–0.799)	**0.005**
Weight(>80 *vs.* <=80)	527	0.944 (0.622–1.431)	0.784	0.519 (0.228–1.185)	0.119
Height(>160 *vs.* <=160)	522	0.868 (0.571–1.319)	0.507	0.907 (0.567–1.450)	0.682
BMI(>30 *vs.* <=30)	518	1.034 (0.680–1.572)	0.876	1.479 (0.674–3.243)	0.329
Clinical stage (Stage III&Stage IV *vs.* Stage I&Stage II)	551	0.282 (0.188–0.425)	**<0.001**	0.269 (0.171–0.424)	**<0.001**
Histologic grade (G3 *vs.* G1&G2)	540	0.305 (0.177–0.524)	**<0.001**	0.409 (0.232–0.719)	**0.002**
RiskScore (High *vs.* Low)	506	2.718 (2.124–3.479)	**<0.001**	2.060 (1.196–3.548)	**0.009**

other 4 cells; DUOX1 was negatively correlated with CD8+T cells and NK cells but positively correlated with DC; JUN was negatively correlated with B cells and showed no correlation with other cells (Supplementary Figure S6). In summary, the four genes exhibit specific expression in cervical cancer tissue, and there is a discernible correlation with immune infiltration.

Discussion

Despite the progress made in the prevention, screening, and treatment of cervical cancer, the outcomes of the disease have not significantly improved (Zeng et al., 2018). For cervical cancer patients with metastasis or recurrence, the 5-year OS is only 17% (Ouyang et al., 2020). Currently, the main research focus in ferroptosis is on the occurrence, development, and treatment of tumors. Several studies have demonstrated that ferroptosis-related biomarkers are strong predictors of cancer prognosis and treatment efficacy (Shi et al., 2019; Liang et al., 2020; Tang et al., 2020). Based on these findings, it is essential to systematically and comprehensively evaluate the prognostic role of FRGs in cervical cancer.

In this study, the impact of FRGs prognostic models on prognosis was investigated, while also examining the relationship between FRGs prognostic models and the immune microenvironment to determine if this model could be a potential biomarker for prognosis. Initially, the DEGs of the GSE9750, GSE7410, and GSE63514 datasets were analyzed. The intersection of the ferroptosis gene sets was obtained from the FerrDb, NCBI-gene, MSigDB, and Genecard databases. Notably, as the intersection of the four datasets yielded fewer genes, the intersection of each dataset was analyzed, resulting in a total of 52 FRGs. Then, functional analysis of these 52 FRGs showed that they were related to ferroptosis and oxidative stress processes. Univariate/multivariate Cox regression analysis was employed to identify FRGs with prognostic features and to establish a prognostic model for FRGs. Subsequently, the ssGSEA was used to study the differences between various immune cells. Statistically significant differences were found for B cells, DC, iDC, pDC, T cells, and TReg.

Ferroptosis is currently recognized as an immunogenic cell death characterized by the release of damage-associated molecular patterns (DAMPs) from deceased tumor cells (Tang et al., 2019; Wen et al., 2019; Wan et al., 2020). The analysis discovered that B cells, DC, T cells, and TReg exhibited higher abundances in the low-risk group compared to the high-risk group, which displayed a higher immune score. These correlation results demonstrate, to some extent, the relevance of FRGs prognostic models to the immune infiltration of cervical cancer. This can be combined with the finding by Wang et al. (2019) that the antitumor efficacy of immunotherapy can be achieved through enhanced ferroptosis-specific lipid peroxidation by $CD8^+$ T cells. Additionally, the analysis of immune checkpoint inhibitors revealed higher expression of TIGIT, CTLA4, BTLA, CD27, and CD28 in the low-risk group, suggesting that the efficacy of immunotherapy is better in the low-risk group than in the high-risk group. TIGIT, an emerging immune checkpoint, is widely expressed on lymphocytes (Harjunpää and Guillerey, 2020). It is capable of inhibiting every step of the cancer immune cycle (Manieri et al., 2017). TIGIT may prevent NK cells from releasing tumor antigens, impair DC-primed T cell priming, or inhibit CD8+T cell-mediated cancer cell killing (Harjunpää and Guillerey, 2020). Combined with the results of this study, it is plausible that TIGIT kills cancer cells in the low-risk group by reducing DC-triggered T-cell initiation, leading to immunotherapeutic benefits for patients in the low-risk group. However, further research is needed to elucidate the specific mechanism.

In this study, four FRGs, including JUN, TSC22D3, DUOX1, and HELLS, were experimentally validated and analyzed for correlation with immune cells. TSC22D3 is a transcriptional regulator that mediates immunosuppressive effects through NF-κB, RAS, and other pathway proteins, as well as heterodimerization ability (Ronchetti et al., 2015). It has been shown that elevated glucocorticoids due to stress induce the expression of TSC22D3, which blocks type I interferon (IFN) responses and IFN-γ+ T cell activation in dendritic cells (DCs), thereby disrupting immune surveillance (Yang et al., 2019a). Based on previous findings, and considering the positive correlation of TSC22D3 with immune cells in this study, it is reasonable to suspect that in cervical cancer, TSC22D3 expression may enhance the immunity of patients by stimulating the activation of immune cells, thereby prolonging their prognosis. DUOX1 is expressed at low levels in HCC and can be used as an important indicator for evaluating the therapeutic effect

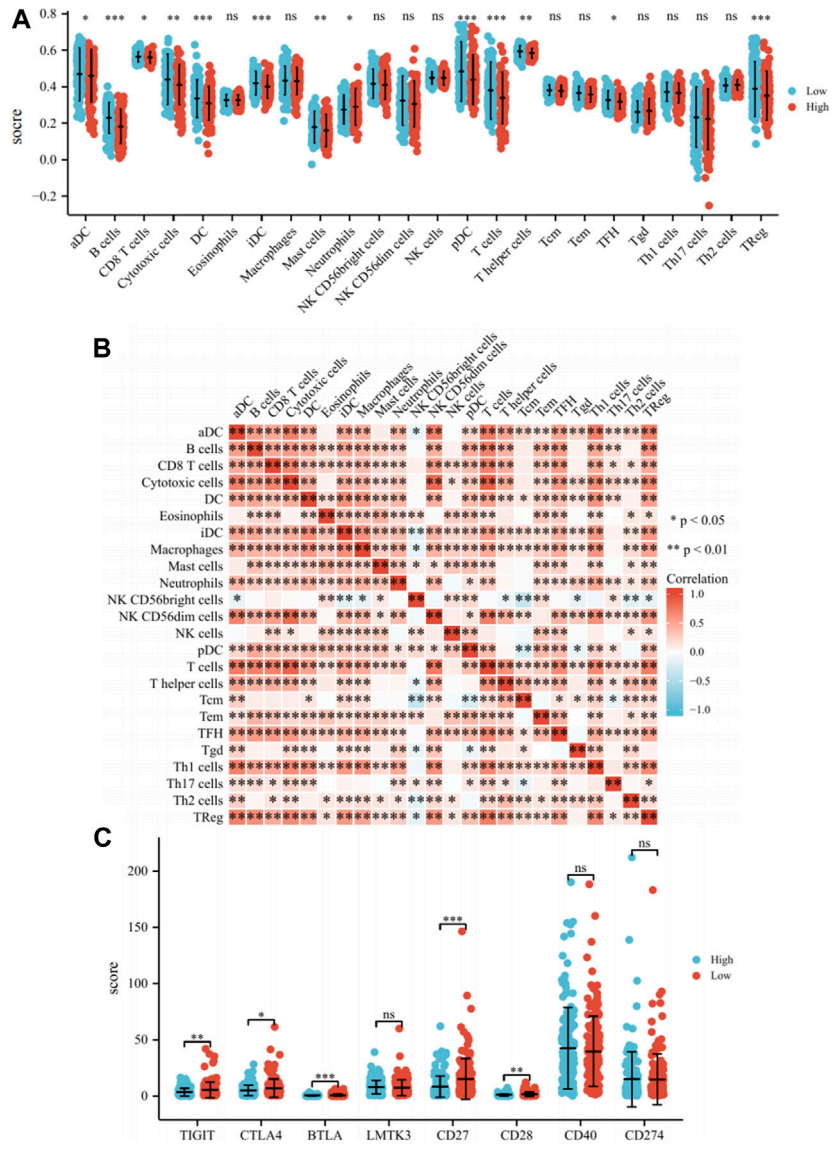

FIGURE 5
Analysis of the immune microenvironment. **(A)** Differences of 24 immune cells in different expression levels of Risk score. **(B)** Correlation between 24 immune cells. **(C)** Differences of immune checkpoint inhibitors in different expression levels of Risk score. Note: ns: no significant difference, *: $p < 0.05$, **: $p < 0.01$, ***: $p < 0.001$.

of HCC after surgery (Lu et al., 2011). However, DUOX1 is overexpressed in patients with cervical cancers (Cho et al., 2019). DUOX1 was strongly correlated with the ratios of $CD8^+$ T cells, DCs, and NK cells, indicating that its expression was highly associated with the innate immune cell response in cervical cancer. Furthermore, DUOX1 expression in innate lymphocytes suggests that DUOX1 has a broad host defense function (Habibovic et al., 2016; Cho et al., 2019), resulting in prolonged survival prognosis for patients with cervical cancer. HELLS is overexpressed in colorectal, HCC, nasopharyngeal, and lung cancers, leading to poorer prognosis, and therefore, HELLS can be useful as a prognostic marker in various cancers (He et al., 2016; Yang et al., 2019b; Law et al., 2019; Liu et al., 2019; Zhu et al., 2020; Xing et al., 2021). Zocchi et al. (2020) found that low expression of HELLS in retinoblastoma inhibited ectopic division of differentiated cells in the retina, leading to tumor development inhibition and, consequently, prolonging OS in patients (Zocchi et al., 2020; Xing et al., 2021). In conjunction with previous studies, HELLS displayed a negative correlation with B cells, CD8 T cells, DC, and T cells in this investigation, with high HELLS expression signifying reduced expression of immune cells and promotion of tumor progression. As a critical prognostic gene in this study, it is valuable to delve deeper into how patients' prognosis can be enhanced through the mechanism of HELLS.

In addition to this study, it is noteworthy that Du et al. (2022), Qin et al. (2022), Qi et al. (2021), and Xing et al. (2021) all investigated FRGs in cervical cancer. Du et al. (2022) constructed a prognostic model with excellent predictive performance based on

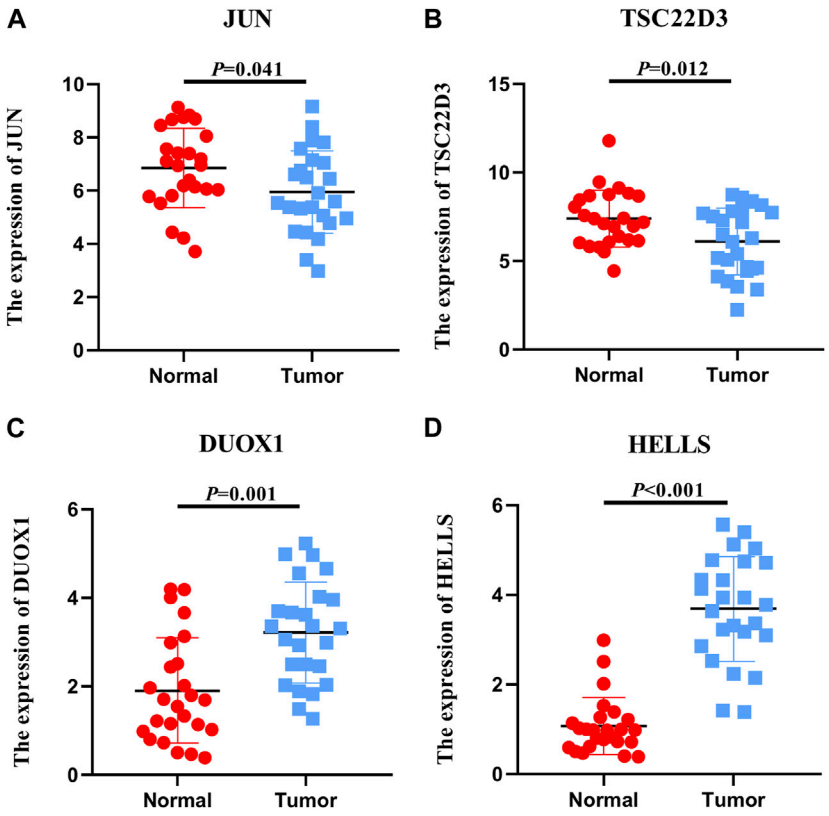

FIGURE 6
Expression levels of FRGs. Expression levels of 4 ferroptosis-related genes in 25 non-tumor tissues and 25 cervical cancer tissues.

FRGs. CA9/ULBP2 was also identified as a potential regulator of cervical carcinogenesis and progression. Qin et al. (2022) constructed a prognostic model with four iron death-associated genes and examined the immune microenvironment. Qi et al. (2021) developed a novel prognostic model with FRGs and validated the genes within the model. Xing et al. (2021) constructed a model with immune-associated genes and iron death genes related to OS in CESC patients, effectively predicting the outcome.

It is worth mentioning that most of the above studies selected 1-2 datasets for analysis and model construction. In this study, FRGs were obtained from multiple datasets, and a model was built. The model demonstrates good stability and accuracy in TCGA-CESC and GSE44001 datasets. Furthermore, it has significant predictive value and general applicability in other gynecological tumors. In addition, the expression of four genes, including JUN, TSC22D3, DUOX1, and HELLS, in cervical cancer tissues was verified by qRT-PCR. However, considering the limitations of previous related research, further study is necessary to explore the immune molecular mechanism between ferroptosis and cervical cancer and how this mechanism affects the prognosis of patients with cervical cancer.

Of course, this study had two limitations. First, one of the cohorts included relatively few indicators in clinical information, leading to insufficient validation of some results. Second, the study used retrospective data from public databases to construct and validate a prognostic model for FRGs. It would be more convincing to use prospective data to assess its clinical utility. Based on these two points, combined with the current lack of understanding of the mechanism of genes in cervical cancer, it is essential to further explore and study the biological functions of genes in cervical cancer in future research.

In conclusion, this study fills the gap in the FRGs prognostic model for cervical cancer prognosis. The constructed prognostic model possesses a strong ability to predict the survival outcome of patients with cervical cancer and has certain applicability to other gynecological tumors. Ultimately, the model demonstrates a correlation with the prognosis of cervical cancer patients in terms of immune infiltration, and the high expression of immune checkpoint inhibitors in the low-risk group is more conducive to immunotherapy efficacy. It is hoped that these findings will provide new insights for future research and clinical practice.

Conclusion

In this research, FRGs were derived from multiple datasets, and a cervical cancer prognostic model was developed. This model was validated not only in external cervical cancer datasets but also in datasets of other gynecological tumors. Simultaneously, 4 FRGs were confirmed using qRT-PCR. The association between immune

infiltration and patient prognosis, as well as the differences in the expression of immune checkpoint inhibitors under varying risk scores, were also determined in this study.

Data availability statement

The original contributions presented in the study are included in the article/Supplementary Material, further inquiries can be directed to the corresponding author.

Ethics statement

The studies involving human participants were reviewed and approved by the Ethics Committee of the Tumor hospital affiliated to Xinjiang Medical University. The patients/participants provided their written informed consent to participate in this study.

Author contributions

SH made substantial contributions to the study design, collection, and analysis of data and the writing of the article. SW and XL participated in drafting and revising the article critically for important intellectual content. SH and DL refined the data analysis. SH, SW, XL, DL, and YF were involved in revising the article. SH, SW, XL, and DL contributed to the study design and the final approval of the version to be published. All authors have read and approved the final manuscript.

Funding

This work was funded by Xinjiang Uygur Autonomous Region Science and Technology Support Project (2020E0280), State Key Laboratory of Pathogenesis, Prevention and Treatment of Central Asian High Incidence Diseases Fund (SKL-HIDCA-2021-15), The Postdoctoral Fund of Affilated Tumor hospital of Xinjiang Medical University (2021), Talent support project of Affilated Tumor hospital of Xinjiang Medical University (2021).

Acknowledgments

Thanks for all the help provided by each author in this research.

Conflict of interest

The authors declare that the research was conducted in the absence of any commercial or financial relationships that could be construed as a potential conflict of interest.

Publisher's note

Supplementary material

The Supplementary Material for this article can be found online at: https://www.frontiersin.org/articles/10.+3389/fmolb.2023.1188027/full#supplementary-material

SUPPLEMENTARY FIGURE S1
Volcano plot display for GSE9750, GSE7410, GSE63514 datasets.

SUPPLEMENTARY FIGURE S2
Lasso Cox analysis (A: Lasso coefficient B: Lasso variable track).

SUPPLEMENTARY FIGURE S3
Validation of FRGs in cervical cancer in TCGA-OV (A: Curve scatter plot of training set survival model efficacy assessment and cumulative scatter plot of survival mortality event risk. B: KM curves show a significant difference in OS between high-risk and low-risk groups in TCGA-OV. C: Time-dependent ROC curves were used to predict 1, 3, and 5 years survival. D: 1, 3, and 5 years nomograms for predicting OS in cervical cancer. E: Calibration curves showing the agreement between predicted and observed 3 and 5 years OS. F: Decision curve analysis of the prognostic model in the training set at 3 and 5 years.).

SUPPLEMENTARY FIGURE S4
GSE44001 immune infiltration analysis (A: Differences of 24 immune cells in different expression levels of Risk score. B: Correlation between 24 immune cells.).

SUPPLEMENTARY FIGURE S5
Six genes were analyzed in TCGA database (A: the expression of JUN B:the expression of TSC22D3 C: the expression of SLC11A2 D: the expression of DDIT4 E: the expression of DUOX1 F: the expression of HELLS).

SUPPLEMENTARY FIGURE S6
Analysis of immune infiltration of 4 genes (A: Correlation between JUN and immune cells B: Correlation between TSC22D3 and immune cells C: Correlation between DUOX1 and immune cells D: Correlation between HELLS and immune cells).

SUPPLEMENTARY TABLE S1
The information of datasets from the GEO database.

SUPPLEMENTARY TABLE S2
GSE9750, GSE7410, GSE63514 and Ferroptosis genes dataset differential genes display.

SUPPLEMENTARY TABLE S3
qRT-PCR primers for mRNA or miRNA expression analysis.

SUPPLEMENTARY TABLE S4
Wayne chart genetics showcase.

SUPPLEMENTARY TABLE S5
GO/KEGG enrichment analysis demonstration.

SUPPLEMENTARY TABLE S6
Univariate and multivariate Cox regression analysis of clinicopathological characteristics of TCGA-OV.

References

Brüggmann, D., Quinkert-Schmolke, K., Jaque, J. M., Quarcoo, D., Bohlmann, M. K., Klingelhöfer, D., et al. (2022). Global cervical cancer research: A scientometric density equalizing mapping and socioeconomic analysis. *Plos one* 17 (1), e0261503. doi:10.1371/journal.pone.0261503

Bruni, L., Serrano, B., Roura, E., Alemany, L., Cowan, M., Herrero, R., et al. (2022). Cervical cancer screening programmes and age-specific coverage estimates for 202 countries and territories worldwide: A review and synthetic analysis. *Lancet Glob. Health* 10 (8), e1115–e1127. doi:10.1016/S2214-109X(22)00241-8

Cho, S. Y., Kim, S., Son, M. J., Kim, G., Singh, P., Kim, H. N., et al. (2019). Dual oxidase 1 and NADPH oxidase 2 exert favorable effects in cervical cancer patients by activating immune response. *BMC cancer* 19 (1), 1078–1112. doi:10.1186/s12885-019-6202-3

Crosbie, E. J., Einstein, M. H., Franceschi, S., and Kitchener, H. C. (2013). Human papillomavirus and cervical cancer. *Gan Kagaku Ryoho Cancer & Chemother.* 382 (772), 889–899. doi:10.1016/S0140-6736(13)60022-7

Dixon, S. J. (2017). Ferroptosis: Bug or feature? *Immunol. Rev.* 277 (1), 150–157. doi:10.1111/imr.12533

Dixon, S. J., Lemberg, K. M., Lamprecht, M. R., Skouta, R., Zaitsev, E. M., Gleason, C. E., et al. (2012). Ferroptosis: An iron-dependent form of nonapoptotic cell death. *Cell* 149 (5), 1060–1072. doi:10.1016/j.cell.2012.03.042

Du, H., Tang, Y., Ren, X., Zhang, F., Yang, W., Cheng, L., et al. (2022). A prognostic model for cervical cancer based on ferroptosis-related genes. *Front. Endocrinol.* 13, 991178. doi:10.3389/fendo.2022.991178

Friedmann Angeli, J. P., Schneider, M., Proneth, B., Tyurina, Y. Y., Tyurin, V. A., Hammond, V. J., et al. (2014). Inactivation of the ferroptosis regulator Gpx4 triggers acute renal failure in mice. *Nat. Cell Biol.* 16 (12), 1180–1191. doi:10.1038/ncb3064

Gabriela, B., Mlecnik, B., Tosolini, M., Kirilovsky, A., Waldner, M., Obenauf, A. C., et al. (2013). Spatiotemporal dynamics of intratumoral immune cells reveal the immune landscape in human cancer. *Immunity* 39, 782–795. doi:10.1016/j.immuni.2013.10.003

Habibovic, A., Hristova, M., Heppner, D. E., Danyal, K., Ather, J. L., Janssen-Heininger, Y. M., et al. (2016). DUOX1 mediates persistent epithelial EGFR activation, mucous cell metaplasia, and airway remodeling during allergic asthma. *JCI Insight* 1 (18), e88811. doi:10.1172/jci.insight.88811

Harjunpää, H., and Guillerey, C. (2020). TIGIT as an emerging immune checkpoint. *Clin. Exp. Immunol.* 200 (2), 108–119. doi:10.1111/cei.13407

He, X., Yan, B., Liu, S., Jia, J., Lai, W., Xin, X., et al. (2016). Chromatin remodeling factor LSH drives cancer progression by suppressing the activity of fumarate hydratase. *Cancer Res.* 76 (19), 5743–5755. doi:10.1158/0008-5472.CAN-16-0268

Jiang, L., Hickman, J. H., Wang, S. J., and Gu, W. (2015). Dynamic roles of p53-mediated metabolic activities in ROS-induced stress responses. *Cell cycle* 14 (18), 2881–2885. doi:10.1080/15384101.2015.1068479

Jiang, L., Kon, N., Li, T., Wang, S. J., Su, T., Hibshoosh, H., et al. (2015). Ferroptosis as a p53-mediated activity during tumour suppression. *Nature* 520 (7545), 57–62. doi:10.1038/nature14344

Kim, E. H., Shin, D., Lee, J., Jung, A. R., and Roh, J. L. (2018). CISD2 inhibition overcomes resistance to sulfasalazine-induced ferroptotic cell death in head and neck cancer. *Cancer Lett.* 432, 180–190. doi:10.1016/j.canlet.2018.06.018

Law, C. T., Wei, L., Tsang, F. H. C., Chan, C. Y. K., Xu, I. M. J., Lai, R. K. H., et al. (2019). HELLS regulates chromatin remodeling and epigenetic silencing of multiple tumor suppressor genes in human hepatocellular carcinoma. *Hepatology* 69 (5), 2013–2030. doi:10.1002/hep.30414

Liang, J., Wang, D., Lin, H., Chen, X. X., Yang, H., Zheng, Y., et al. (2020). A novel ferroptosis-related gene signature for overall survival prediction in patients with hepatocellular carcinoma. *Int. J. Biol. Sci.* 16 (13), 2430–2441. doi:10.7150/ijbs.45050

Liu, X., Hou, X., Zhou, Y., Li, Q., Kong, F., Yan, S., et al. (2019). Downregulation of the helicase lymphoid-specific (HELLS) gene impairs cell proliferation and induces cell cycle arrest in colorectal cancer cells. *OncoTargets Ther.* 12, 10153–10163. doi:10.2147/OTT.S223668

Lu, C. L., Qiu, J. L., Huang, P. Z., Zou, R. H., Hong, J., Li, B. K., et al. (2011). NADPH oxidase DUOX1 and DUOX2 but not NOX4 are independent predictors in hepatocellular carcinoma after hepatectomy. *Tumor Biol.* 32 (6), 1173–1182. doi:10.1007/s13277-011-0220-3

Manieri, N. A., Chiang, E. Y., and Grogan, J. L. (2017). TIGIT: A key inhibitor of the cancer immunity cycle. *Trends Immunol.* 38 (1), 20–28. doi:10.1016/j.it.2016.10.002

Ouyang, D., Yang, P., Cai, J., Sun, S., and Wang, Z. (2020). Comprehensive analysis of prognostic alternative splicing signature in cervical cancer. *Cancer Cell Int.* 20 (1), 221–315. doi:10.1186/s12935-020-01299-4

Qi, X., Fu, Y., Sheng, J., Zhang, M., Zhang, M., Wang, Y., et al. (2021). A novel ferroptosis-related gene signature for predicting outcomes in cervical cancer. *Bioengineered* 12 (1), 1813–1825. doi:10.1080/21655979.2021.1925003

Qin, W., He, C., Jiang, D., Gao, Y., Chen, Y., Su, M., et al. (2022). Systematic construction and validation of a novel ferroptosis-related gene model for predicting prognosis in cervical cancer. *J. Immunol. Res.* 2022, 2148215. doi:10.1155/2022/2148215

Ronchetti, S., Migliorati, G., and Riccardi, C. (2015). GILZ as a mediator of the anti-inflammatory effects of glucocorticoids. *Front. Endocrinol.* 6, 170. doi:10.3389/fendo.2015.00170

Shen, Z., Song, J., Yung, B. C., Zhou, Z., Wu, A., and Chen, X. (2018). Emerging strategies of cancer therapy based on ferroptosis. *Adv. Mater.* 30 (12), 1704007. doi:10.1002/adma.201704007

Shi, Z. Z., Fan, Z. W., Chen, Y. X., Xie, X. F., Jiang, W., Wang, W. J., et al. (2019). Ferroptosis in carcinoma: Regulatory mechanisms and new method for cancer therapy. *OncoTargets Ther.* 12, 11291–11304. doi:10.2147/OTT.S232852

Small, W., Jr, Bacon, M. A., Bajaj, A., Chuang, L. T., Fisher, B. J., Harkenrider, M. M., et al. (2017). Cervical cancer: A global health crisis. *Cancer* 123 (13), 2404–2412. doi:10.1002/cncr.30667

Stockwell, B. R., Angeli, J. P. F., Bayir, H., Bush, A. I., Conrad, M., Dixon, S. J., et al. (2017). Ferroptosis: A regulated cell death nexus linking metabolism, redox biology, and disease. *Cell* 171 (2), 273–285. doi:10.1016/j.cell.2017.09.021

Sung, H., Ferlay, J., Siegel, R. L., Laversanne, M., Soerjomataram, I., Jemal, A., et al. (2021). Global cancer statistics 2020: GLOBOCAN estimates of incidence and mortality worldwide for 36 cancers in 185 countries. *CA a cancer J. Clin.* 71 (3), 209–249. doi:10.3322/caac.21660

Tang, B., Zhu, J., Li, J., Fan, K., Gao, Y., Cheng, S., et al. (2020). The ferroptosis and iron-metabolism signature robustly predicts clinical diagnosis, prognosis and immune microenvironment for hepatocellular carcinoma. *Cell Commun. Signal.* 18 (1), 174–218. doi:10.1186/s12964-020-00663-1

Tang, D., Kang, R., Berghe, T. V., Vandenabeele, P., and Kroemer, G. (2019). The molecular machinery of regulated cell death. *Cell Res.* 29 (5), 347–364. doi:10.1038/s41422-019-0164-5

Wan, C., Sun, Y., Tian, Y., Lu, L., Dai, X., Meng, J., et al. (2020). Irradiated tumor cell–derived microparticles mediate tumor eradication via cell killing and immune reprogramming. *Sci. Adv.* 6 (13), eaay9789. doi:10.1126/sciadv.aay9789

Wang, W., Green, M., Choi, J. E., Gijón, M., Kennedy, P. D., Johnson, J. K., et al. (2019). CD8+ T cells regulate tumour ferroptosis during cancer immunotherapy. *Nature* 569 (7755), 270–274. doi:10.1038/s41586-019-1170-y

Wen, Q., Liu, J., Kang, R., Zhou, B., and Tang, D. (2019). The release and activity of HMGB1 in ferroptosis. *Biochem. biophysical Res. Commun.* 510 (2), 278–283. doi:10.1016/j.bbrc.2019.01.090

Xiaofei, J., Mingqing, S., Miao, S., Yizhen, Y., Shuang, Z., Qinhua, X., et al. (2021). Oleanolic acid inhibits cervical cancer Hela cell proliferation through modulation of the ACSL4 ferroptosis signaling pathway. *Biochem. Biophysical Res. Commun.* 545, 81–88. doi:10.1016/j.bbrc.2021.01.028

Xing, C., Yin, H., Yao, Z. Y., and Xing, X. L. (2021). Prognostic signatures based on ferroptosis-and immune-related genes for cervical squamous cell carcinoma and endocervical adenocarcinoma. *Front. Oncol.* 11, 774558. doi:10.3389/fonc.2021.774558

Yang, H., Xia, L., Chen, J., Zhang, S., Martin, V., Li, Q., et al. (2019). Stress-glucocorticoid-TSC22D3 axis compromises therapy-induced antitumor immunity. *Nat. Med.* 25 (9), 1428–1441. doi:10.1038/s41591-019-0566-4

Yang, R., Liu, N., Chen, L., Jiang, Y., Shi, Y., Mao, C., et al. (2019). LSH interacts with and stabilizes GINS4 transcript that promotes tumourigenesis in non-small cell lung cancer. *J. Exp. Clin. Cancer Res.* 38 (1), 280–312. doi:10.1186/s13046-019-1276-y

Zeng, H., Chen, W., Zheng, R., Zhang, S., Ji, J. S., Zou, X., et al. (2018). Changing cancer survival in China during 2003-15:a pooled analysis of 17 population-based cancer registries. *Lancet Glob. Health* 6 (5), e555–e567. doi:10.1016/S2214-109X(18)30127-X

Zhang, Z., Guo, M., Li, Y., Shen, M., Kong, D., Shao, J., et al. (2020). RNA-binding protein ZFP36/TTP protects against ferroptosis by regulating autophagy signaling pathway in hepatic stellate cells. *Autophagy* 16 (8), 1482–1505. doi:10.1080/15548627.2019.1687985

Zhu, W., Li, L. L., Songyang, Y., and Shi, Z. (2020). Identification and validation of HELLS (Helicase, Lymphoid-Specific) and ICAM1 (Intercellular adhesion molecule 1) as potential diagnostic biomarkers of lung cancer. *PeerJ* 8, e8731. doi:10.7717/peerj.8731

Zocchi, L., Mehta, A., Wu, S. C., Wu, J., Gu, Y., Wang, J., et al. (2020). Chromatin remodeling protein HELLS is critical for retinoblastoma tumor initiation and progression. *Oncogenesis* 9 (2), 25–15. doi:10.1038/s41389-020-0210-7

frontiers | Frontiers in Molecular Biosciences

TYPE Review
PUBLISHED 11 May 2023
DOI 10.3389/fmolb.2023.1203269

OPEN ACCESS

EDITED BY
Yanqing Liu,
Columbia University, United States

REVIEWED BY
Yutong Liu,
Harvard University, United States
Jinghua Han,
Georgia State University, United States

*CORRESPONDENCE
Ying Kong,
yingkong@dmu.edu.cn
Youfei Guan,
guanyf@dmu.edu.cn

RECEIVED 10 April 2023
ACCEPTED 02 May 2023
PUBLISHED 11 May 2023

CITATION
Zhang H, Zhang J, Dong H, Kong Y and Guan Y (2023), Emerging field: *O*-GlcNAcylation in ferroptosis.
Front. Mol. Biosci. 10:1203269.
doi: 10.3389/fmolb.2023.1203269

Emerging field: *O*-GlcNAcylation in ferroptosis

Hongshuo Zhang[1], Juan Zhang[2], Haojie Dong[2], Ying Kong[2]* and Youfei Guan[1]*

[1]Advanced Institute for Medical Sciences, Dalian Medical University, Dalian, China, [2]Department of Biochemistry and Molecular Biology, College of Basic Medical Sciences, Dalian Medical University, Dalian, China

In 2012, researchers proposed a non-apoptotic, iron-dependent form of cell death caused by lipid peroxidation called ferroptosis. During the past decade, a comprehensive understanding of ferroptosis has emerged. Ferroptosis is closely associated with the tumor microenvironment, cancer, immunity, aging, and tissue damage. Its mechanism is precisely regulated at the epigenetic, transcriptional, and post-translational levels. *O*-GlcNAc modification (*O*-GlcNAcylation) is one of the post-translational modifications of proteins. Cells can modulate cell survival in response to stress stimuli, including apoptosis, necrosis, and autophagy, through adaptive regulation by *O*-GlcNAcylation. However, the function and mechanism of these modifications in regulating ferroptosis are only beginning to be understood. Here, we review the relevant literature within the last 5 years and present the current understanding of the regulatory function of *O*-GlcNAcylation in ferroptosis and the potential mechanisms that may be involved, including antioxidant defense system-controlled reactive oxygen species biology, iron metabolism, and membrane lipid peroxidation metabolism. In addition to these three areas of ferroptosis research, we examine how changes in the morphology and function of subcellular organelles (e.g., mitochondria and endoplasmic reticulum) involved in *O*-GlcNAcylation may trigger and amplify ferroptosis. We have dissected the role of *O*-GlcNAcylation in regulating ferroptosis and hope that our introduction will provide a general framework for those interested in this field.

KEYWORDS

ferroptosis, *O*-GlcNAcylation, ROS biology, iron metabolism, lipid peroxidation, subcellular organelle

1 Introduction

Cell death is an inevitable and important part of life, involving a series of biological processes. Historically, cell death has been divided into three types based on morphological changes: 1) type I cell death (apoptosis) is characterized by cytoplasmic shrinkage, plasma membrane blebbing, chromatin condensation; formation of apoptotic bodies; phagocytosis of apoptotic bodies by neighboring cells or macrophages (Galluzzi et al., 2018; Santagostino et al., 2021); 2) type II cell death (autophagy) exhibits extensive cytoplasmic vacuolization and accumulation of autophagic vacuoles (autophagosomes); no chromatin condensation; the fusion of autophagosomes with lysosomes (Lin et al., 2021); 3) type III cell death (necrosis), characterized by cell swelling, loss of membrane integrity, and "spillage" of intracellular contents (Moujalled et al., 2021). In a departure from traditional thinking, the Stockwell laboratory proposed the concept of a unique form of regulated cell death driven by iron-dependent lipid peroxidation, named ferroptosis (Dixon et al., 2012). As a new cell death modality, ferroptosis studies have increased in recent years; however, our

understanding of the regulatory mechanisms for ferroptosis is still incomplete. Recently, there has been increasing evidence that pathways closely related to epigenetic regulation and post-translational modification mechanisms influence the propensity of cells to undergo ferroptosis (Wei et al., 2020; Chen D. et al., 2021; Tang et al., 2021).

As one of the prevalent post-translational modifications, the O-linked β-N-acetylglucosamine (*O*-GlcNAc) modification consists of the addition of a single N-acetylglucosamine (GlcNAc) to serine or threonine residues of a protein. Unlike conventional *N*-/*O*-glycosylation, *O*-GlcNAcylation is not restricted to the extracellular structural domains of the endoplasmic reticulum (ER), Golgi apparatus, or secretory proteins (Hart, 2019). It also occurs in the cytoplasm, nuclear proteins, and mitochondria. Unlike kinases and phosphatases involved in phosphorylation, the regulation of *O*-GlcNAcylation has so far been the responsibility of only two enzymes, *O*-GlcNAc transferase (OGT) and *O*-GlcNAcase (OGA). OGT catalyzes the addition of the precursor uridine diphosphate-GlcNAc (UDP-GlcNAc) to proteins, and OGA removes GlcNAc by hydrolysis (Vocadlo, 2012). As a branch of glucose metabolism, UDP-GlcNAc is the end product of the hexosamine biosynthetic pathway (HBP), which links glucose, fatty acid, nucleic acid, and amino acid metabolic pathways. Therefore, *O*-GlcNAcylation is involved in various life processes as a nutrient sensor and signaling integrator. Our previous work showed that *O*-GlcNAcylation could redirect glucose metabolism and provide compensation for glycolysis via glycerol (Zhang H. et al., 2022). Our previous review also detailed the important role of *O*-GlcNAc modification on physiological and pathological processes such as glucose metabolism, lipid metabolism, and homeostasis maintenance (Zhang H. et al., 2021). In addition, *O*-GlcNAc modifications are highly sensitive to various stimuli, including physiological, chemical, and oxidative stress, heat shock, hypoxia, and ischemia (Zachara and Hart, 2004). Protein molecules respond to stress stimuli by transient and reversible regulation of *O*-GlcNAcylation, thereby improving the survival adaptability of cells and preventing cell death (Xue et al., 2022).

Although ferroptosis has been detected in various biological systems since 2012, understanding the role and mechanism of *O*-GlcNAcylation in regulating ferroptosis is just beginning; the first regulation study was reported in 2019 (Chen et al., 2019). We reviewed the relevant literature within the last 5 years. Here, we present the role of *O*-GlcNAcylation in regulating ferroptosis from the perspectives of antioxidant defense system-controlled ROS biology, iron metabolism, lipid metabolism and peroxidation, and the morphology and function of subcellular organelles (mitochondria, ER). We also describe the potential mechanisms that may be involved. We hope our review provides a general framework for those interested in this field.

2 Overview of ferroptosis

Ferroptosis is morphologically, functionally, and biochemically distinct from other forms of cell death, such as apoptosis, necrosis, and autophagy (Dixon et al., 2012; Xie et al., 2016). Morphologically, ferroptosis is mainly characterized by abnormalities in mitochondria, including a marked shrinkage of mitochondrial volume, increased bilayer density, reduction or disappearance of mitochondrial cristae, and rupture of the outer membrane (Li et al., 2020). In some cases, ferroptosis is accompanied by an increase in intracellular autophagosomes and cell detachment and aggregation (Yagoda et al., 2007; Friedmann Angeli et al., 2014). Moreover, ferroptosis occurring in one cell can rapidly spread to neighboring cells (Katikaneni et al., 2020; Riegman et al., 2020). Genetically, mutations or polymorphisms in some genes (e.g., P53 and RAS) are involved in the biological regulation of ferroptosis (Jiang et al., 2015). Biochemically, there are three main areas of research regarding the regulation of ferroptosis, including antioxidant defense system-controlled ROS biology (Figure 1), iron metabolism (Figure 2), and membrane lipid peroxidation metabolism (Figures 3, 4). The accumulation of reactive oxygen species (ROS) due to the inactivation of the antioxidant defense system seems to play a key role in ferroptosis; however, not all sources of ROS contribute equally to ferroptosis. Iron-dependent ROS production appears to be the main driver of ferroptosis induced by lipid peroxidation. The antioxidant defense system of ferroptosis consists of the classical System Xc/GSH/GPX4 pathway. Cystine (Cys2) and glutamate (Glu) enter and exit cells via System Xc in a 1:1 reverse transport, and the absorbed Cys2 can be oxidized to cysteine (Cys) for the synthesis of glutathione (GSH). Glutathione peroxidase 4 (GPX4) uses glutathione as a cofactor to reduce lipid peroxides to lipid alcohols. Inhibition of System Xc or reduced GPX4 activity leads to lipid ROS accumulation, promoting ferroptosis (Friedmann Angeli et al., 2014; Chen et al., 2021b). Several other GPX4-independent ferroptosis suppressor systems have been identified in recent years [e.g., the ferroptosis suppressor protein 1 (FSP1)/$CoQ_{10}H_2$ system, GTP cyclohydrolase 1 (GCH1)/tetrahydrobiopterin (BH4) system, and dihydroorotate dehydrogenase (DHODH) system] (Figure 1). The FSP1 (also known as apoptosis-inducing factor mitochondria-associated 2, AIFM2) oxidoreductase of the FSP1/$CoQ_{10}H_2$ system reduces ubiquinone (CoQ, common CoQ_{10}) to ubiquinol ($CoQ_{10}H_2$) using NADPH (Bersuker et al., 2019; Doll et al., 2019). $CoQ_{10}H_2$ can capture peroxyl radicals to scavenge lipid peroxidation intermediates (Bersuker et al., 2019). Furthermore, FSP1 participates in the repair of plasma membrane damage by activating the endosomal sorting complex required for transport III(ESCRT III) (Dai et al., 2020). In the GCH1/BH4 system, GCH1 produces the lipophilic antioxidant BH4, which functions similarly to $CoQ_{10}H_2$ to prevent lipid peroxidation and inhibit ferroptosis. GCH1 also causes remodeling of the lipid membrane environment to increase $CoQ_{10}H_2$ levels and deplete polyunsaturated fatty acid-phospholipids (PUFA-PLs), reducing ferroptosis sensitivity (Kraft et al., 2020; Soula et al., 2020). DHODH was identified in 2021 as a local mitochondrial defense system. When GPX4 is acutely inhibited, DHODH increases the flux of CoQ_{10} reduction to $CoQ_{10}H_2$, acting as an iron death inhibitor (Mao et al., 2021). Recent studies suggest that there may be other defense systems. In 2021, Zeitler et al. found that the metabolite indole-3-pyruvate (In3Py) could inhibit iron death by scavenging free radicals and attenuating ferroptosis-related gene expression (Zeitler et al., 2021).

Some iron regulatory-related proteins, including transferrin (TF), transferrin receptor (TFRC), and ferritin components (FTH1 and FTL), affect intracellular Fe^{2+} levels by regulating iron

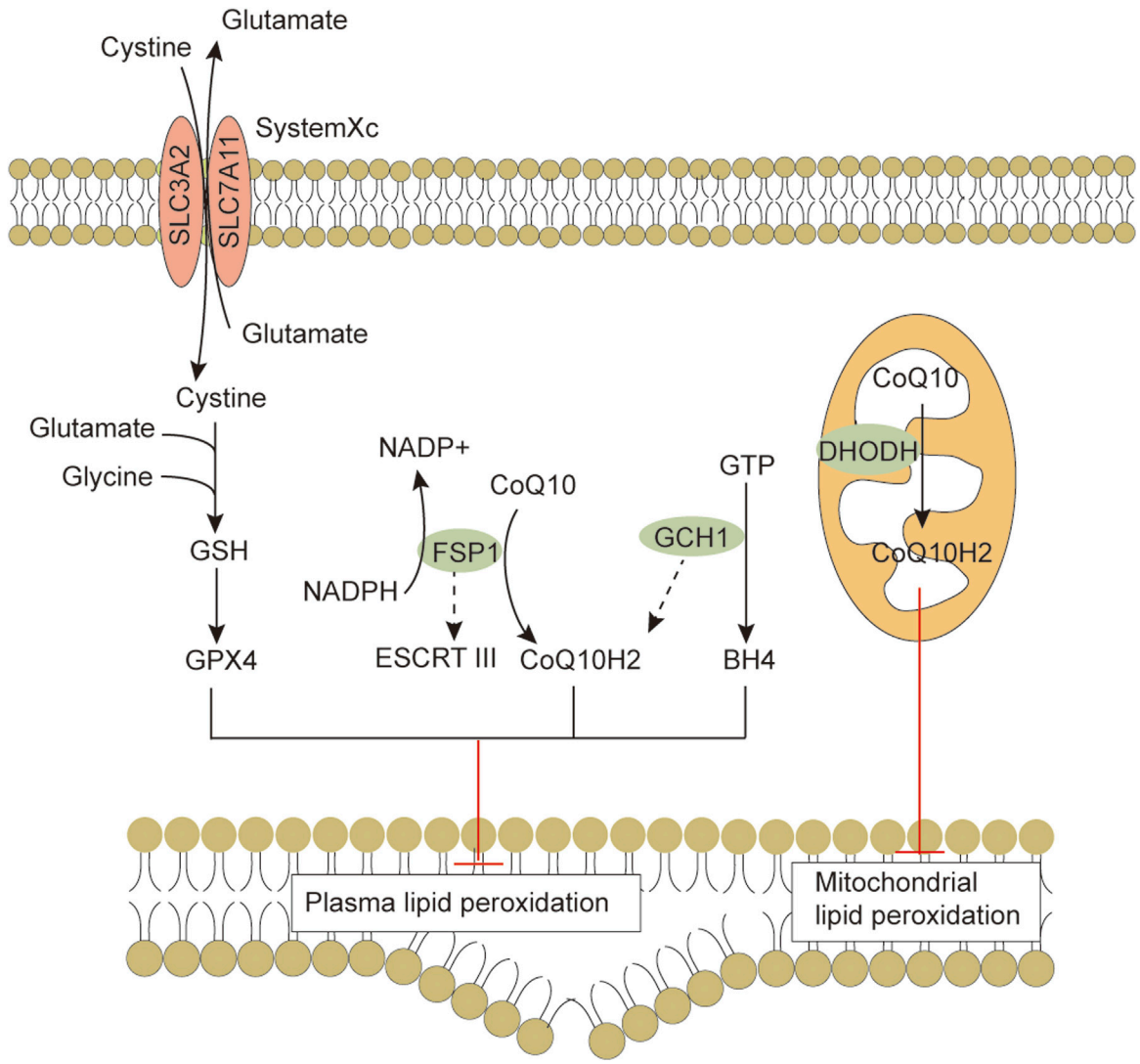

FIGURE 1
The antioxidant defense systems in ferroptosis. Cells have evolved at least four ferroptosis antioxidant defense systems mainly including the System Xc/GSH/GPX4 system, the FSP1/CoQ10H2 system, the GCH1/BH4 system and the DHODH/CoQH2 system. When the detoxification capacity provided by the cellular ROS defense system is insufficient, membrane lipid peroxidation leads to subsequent ferroptosis. Abbreviations: BH4, tetrahydrobiopterin; CoQ10, coenzyme Q10; CoQ10H2, ubiquinol; DHODH, dihydroorotate dehydrogenase; ESCRTIII, endosomal sorting complex required for transport III; FSP1, ferroptosis suppressor protein 1; GCH1, GTP cyclohydrolase 1; GPX4, Glutathione peroxidase 4; GSH, glutathione; SLC3A2, solute carrier family 3 member 2; SLC7A11, solute carrier family 7 member 11.

metabolism. Fe^{2+} oxidizes lipids in a Fenton-like manner, generating large amounts of ROS and promoting ferroptosis (Chen et al., 2021c). Free polyunsaturated fatty acids (PUFAs) generated by lipid anabolism and catabolism are sensitive to lipid peroxidation (Yang and Stockwell, 2016). Long-chain fatty acid-CoA synthetase 4 (ACSL4) promotes the activation of PUFAs (especially arachidonic acid and adrenergic acids) into PUFAs-CoA, lysophosphatidylcholine acyltransferase 3 (LPCAT3) promotes the binding of PUFAs-CoA to phospholipids to form membrane phospholipids and thus transmit ferroptosis signaling. Downregulation of ACSL4 and LPCAT3 reduces the accumulation of membrane phospholipid peroxide substrates, which inhibits ferroptosis (Kagan et al., 2017). These are the main biochemical features of ferroptosis.

3 *O*-GlcNAcylation regulates cell death

Numerous studies have demonstrated that *O*-GlcNAc modifications are involved in regulating cell death. For example, decreased *O*-GlcNAcylation caused by OGT inhibitor OSMI-1 enhances doxorubicin-induced apoptosis in hepatocellular carcinoma (HCC) cells (Lee and Kwon, 2020). Glucosamine enhances *O*-GlcNAc signaling and attenuates apoptosis in iohexanol-induced renal injury (Hu et al., 2017). Melatonin inhibits bladder cancer cell proliferation and promotes apoptosis by inhibiting *O*-GlcNAcylation (Wu et al., 2021). OGT deletion-mediated downregulation of *O*-GlcNAc modification levels causes excessive hepatocyte necrosis (Zhang et al., 2019). Sevoflurane postconditioning-induced enhancement of *O*-GlcNAcylation of

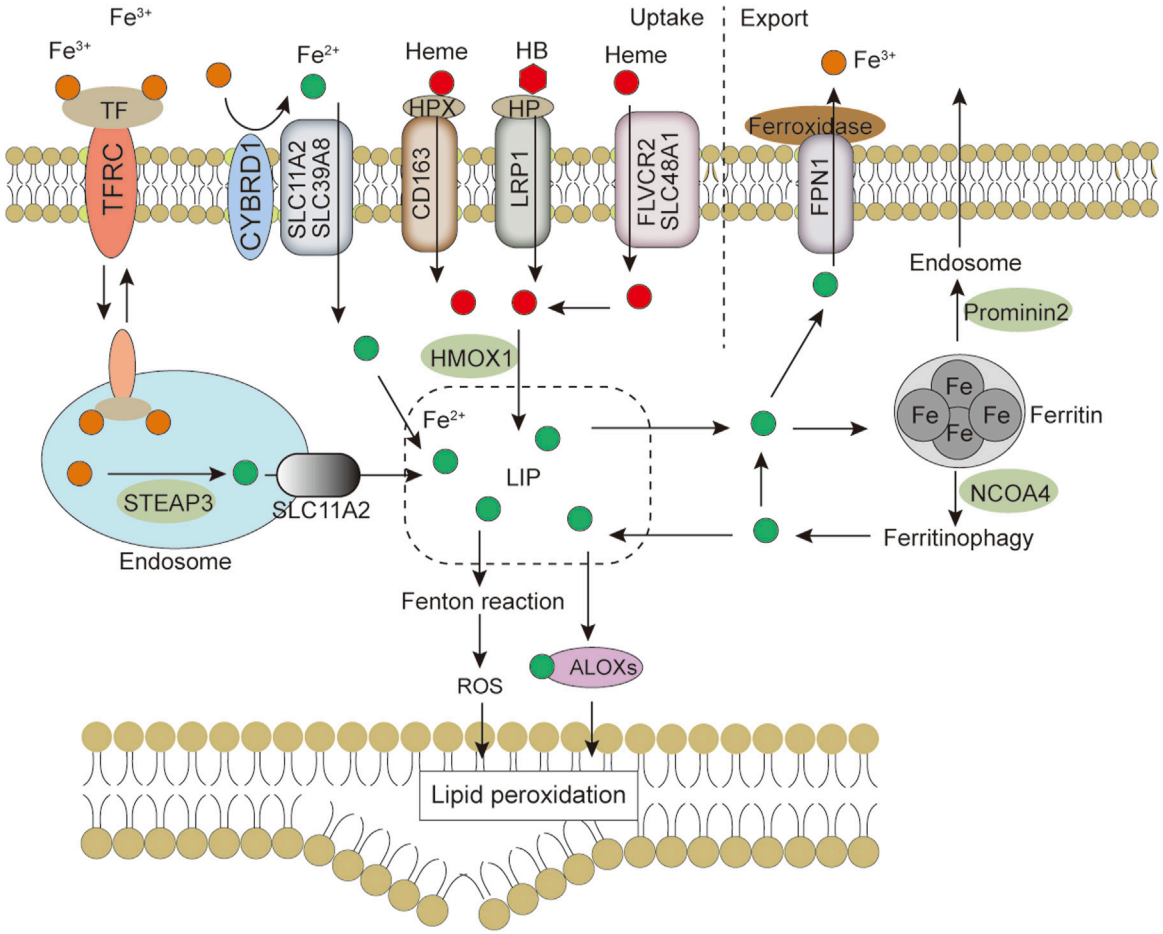

FIGURE 2
Iron metabolism and ferroptosis. Iron import is mainly mediated by the TF-TFRC, NTBI and heme pathways, intracellular iron is utilized from LIP, excess iron is stored back in ferritin, and iron is exported extracellularly via the FNP1 or exosome pathway. Changes in iron homeostasis regulate cell sensitivity to ferroptosis. Abbreviations: ALOXs, arachidonate lipoxygenase; CYBRD1, cytochrome B reductase 1; FLVCR2, feline leukemia virus subgroup C cellular receptor 2; FPN1, ferroportin 1; HB, hemoglobin; HMOX1, heme oxygenase 1; HP, haptoglobin; HPX, hemopexin; LIP, labile iron pool; LRP1, LDL receptor-related protein 1 receptor; NCOA4, nuclear receptor coactivator 4; ROS, reactive oxygen species; SLC11A2, solute carrier family 11 member 2; SLC39A8, solute carrier family 39 member 8; SLC48A1, solute carrier family 48 member 1; STEAP3, six-transmembrane epithelial antigen of the prostate 3; TF, transferrin; TFRC, transferrin receptor.

RIPK3 (necrosis regulatory protein) inhibits myocardial ischemia-reperfusion injury-mediated necrosis through inhibition of RIPK3/MLKL (a key mediator of necrosis) complex formation (Zhang et al., 2020). In addition, multiple mechanisms are likely involved in regulating cellular autophagy through *O*-GlcNAc signaling (Fahie and Zachara, 2016). For instance, *O*-GlcNAcylation can regulate autophagy by modifying CopII, a protein associated with autophagic vesicles (Dudognon et al., 2004). In HPV-infected head and neck squamous cell carcinomas, *O*-GlcNAc signaling elevates autophagy levels by regulating the autophagy-initiating enzyme ULK1 (Shi et al., 2022). Decreased *O*-GlcNAcylation levels in SNAP-29 induced by OGT downregulation promote the formation of autophagosomes and increase cisplatin resistance in ovarian cancer cells (Zhou et al., 2018). Although the mechanisms by which *O*-GlcNAcylation regulates cell death are slowly being revealed, the roles these modifications play under similar stimulation conditions may not be identical due to the effect of the spatiotemporal specificity of *O*-GlcNAc-modified proteins on the interactions between proteins and the regulatory complexity of site-specificity on altered protein function.

4 *O*-GlcNAcylation regulates antioxidant defense system-controlled ROS biology during ferroptosis

4.1 *O*-GlcNAcylation and ROS biology

Cells often encounter ROS-mediated stress. ROS act as signaling molecules and disrupt proteins, nucleic acids, and lipids, triggering cellular stress responses (Panieri and Santoro, 2016; Chen et al., 2018). Reports suggest a link between *O*-GlcNAcylation and ROS biology (Yang et al., 2010; Chen et al., 2018). For example, hydrogen peroxide enhances *O*-GlcNAcylation in mouse embryonic fibroblasts, which may be a strategy to promote cell survival in response to oxidative stress stimuli (Lee et al., 2016). Interestingly,

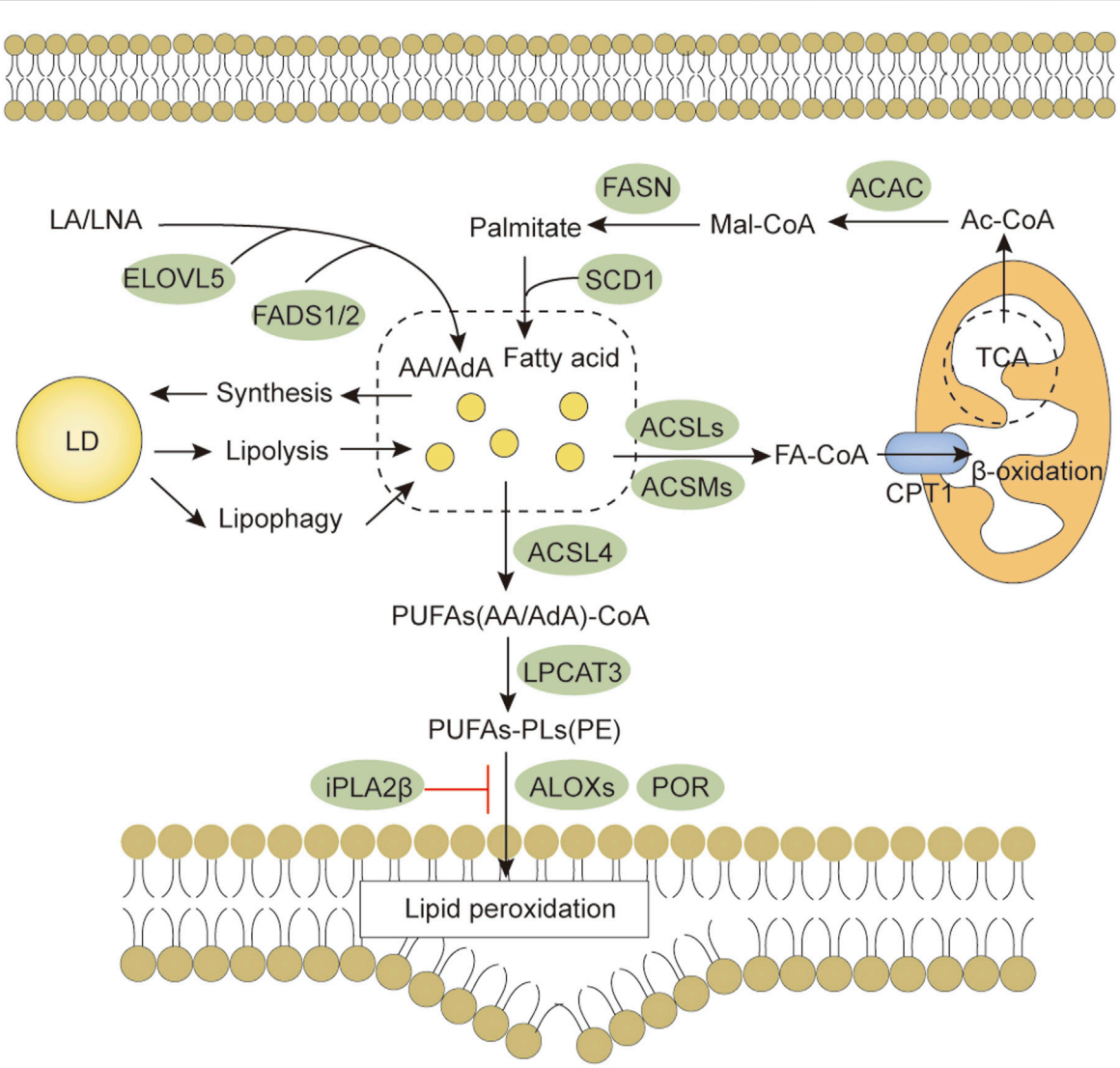

FIGURE 3
Lipid metabolism and ferroptosis. Both lipid anabolism and catabolism affect the content of lipid substrates for ferroptosis. PUFAs are activated by ACSL4, LPCAT3 promotes the synthesis of PUFAs-PL, and membrane PUFAs-PL are subsequently oxidized by oxygenases, such as ALOX and POR, to promote ferroptosis. Abbreviations: AA, arachidonic acid; ACAC, acetyl-CoA carboxylase; ACSLs, Long-chain fatty acid-CoA synthases; ACSMs, medium-chain acyl-CoA synthases; AdA, adrenic acid; ALOXs, arachidonate lipoxygenase; CPT1, carnitine palmitoyltransferase 1; LA, linoleic acid; LD, lipid droplet; LNA, α-linolenic acid; ELOVL5, elongation of very long-chain fatty acid protein 5; FADS1/2, fatty acid desaturases 1/2; FASN, fatty acid synthetase; LPCAT3, lysophosphatidylcholine acyltransferase 3; POR, Cytochrome P450 reductase.

modulation of *O*-GlcNAcylation can also affect the level of intracellular ROS. Decreased *O*-GlcNAc modifications inhibit high glucose-stimulated ROS production in rat mesangial cells (Goldberg et al., 2011). In addition, *O*-GlcNAcylation of phosphofructokinase 1 (PFK1, a key glycolytic enzyme) shifts glucose flux from glycolysis to the pentose phosphate pathway (PPP), leading to increased levels of NADPH and GSH and reduced accumulation of ROS in cancer cells (Yi et al., 2012). Similarly, glucose-6-phosphate dehydrogenase (G6PD, a rate-limiting enzyme of the PPP) activity and oligomerization are regulated by *O*-GlcNAcylation, and increased *O*-GlcNAcylation leads to dimeric G6PD accumulation, leading to increased PPP flux and NADPH and GSH levels and decreased ROS levels (Rao et al., 2015). This evidence demonstrates that the crosstalk between *O*-GlcNAcylation and ROS signaling is complex and reciprocal. Since ROS accumulation (especially inactivation of the System Xc/GSH/GPX4-dependent antioxidant defense system) is one of the essential conditions for ferroptosis, the crosstalk between abnormal ROS signaling and *O*-GlcNAc modifications may be related to ferroptosis.

4.2 *O*-GlcNAcylation and antioxidant defense systems

In 2019, Chen et al. (Chen et al., 2019) reported the first study on *O*-GlcNAcylation and the regulation of ferroptosis. They found that overall *O*-GlcNAc modification levels were

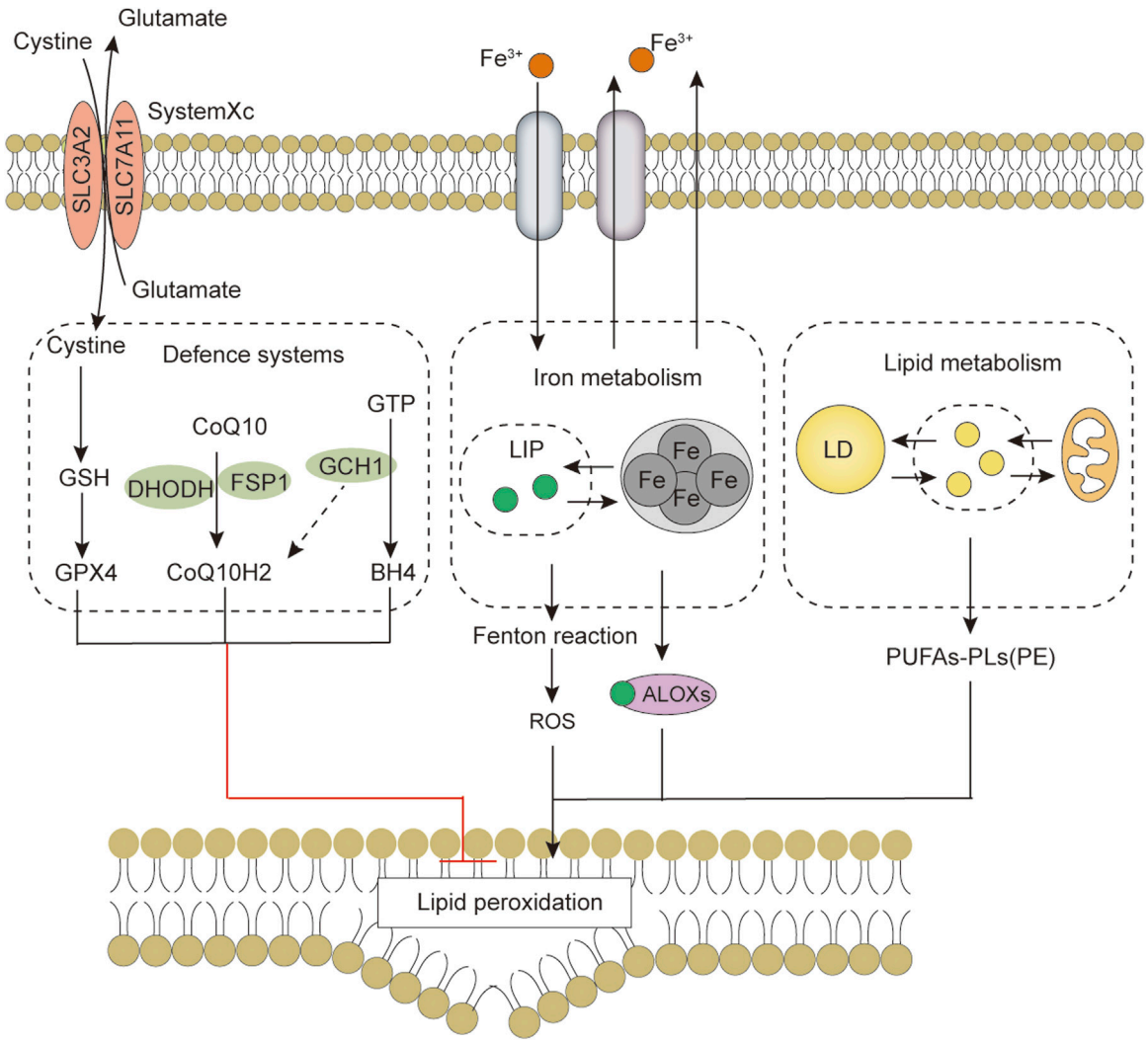

FIGURE 4
The core features of ferroptosis include the antioxidant defense system, iron metabolism, lipid metabolism and peroxidation. Abbreviations: ALOXs, arachidonate lipoxygenase; BH4, tetrahydrobiopterin; CoQ10, coenzyme Q10; CoQ10H2, ubiquinol; DHODH, dihydroorotate dehydrogenase; FSP1, ferroptosis suppressor protein 1; GCH1, GTP cyclohydrolase 1; GPX4, Glutathione peroxidase 4; GSH, glutathione; LD, lipid droplet; LIP, labile iron pool; PUFAs, Free polyunsaturated fatty acids; PUFAs-PL, PUFA-phospholipids; PUFAs-PE, PUFA-phosphatidylethanolamine; ROS, reactive oxygen species; SLC3A2, solute carrier family 3 member 2; SLC7A11, solute carrier family 7 member 11.

inhibited in hepatoma cells after erastin treatment. Erastin inhibited the binding of c-Jun to OGT. Moreover, *O*-GlcNAcylated c-Jun inhibited ferroptosis by directly binding to the promoters of key enzymes in the GSH synthesis pathway [i.e., phosphoserine aminotransferase 1 (PSAT1) and cystathionine β synthase (CBS)], activating their transcription, stimulating GSH synthesis, and decreasing ROS accumulation (Chen et al., 2019). This study opened the door to understanding the role of *O*-GlcNAc modifications in iron-dependent death (i.e., ferroptosis). However, for the classical ferroptosis antioxidant system (System Xc/GSH/GPX4 axis), System Xc and GPX4 may also be potential targets for regulation by *O*-GlcNAcylation. System Xc is an amino acid reverse transporter protein in the membrane phospholipid bilayer, consisting of two subunits, solute carrier family 7 member 11 (SLC7A11) and solute carrier family 3 member 2 (SLC3A2). The expression and activity of SLC7A11 affect cystine uptake by System Xc. They are positively regulated by the oxidative stress regulator nuclear factor erythroid 2-related factor 2 (NRF2) (Chen et al., 2017) and negatively regulated by tumor suppressor genes, such as P53 (Jiang et al., 2015), BAP1 (Zhang et al., 2018), and BECN1(Song et al., 2018). However, one study found that the OGA inhibitor Thiamet G (TMG) decreased NRF2 protein and transcript levels but increased the *O*-GlcNAcylation of NRF2(Tan et al., 2017). P53 activity is strictly regulated, and post-translational modifications are an important dimension of this regulation. P53 is modified by *O*-GlcNAc; *O*-GlcNAcylation of Ser149 stabilizes P53 by blocking ubiquitin-dependent protein degradation (Yang et al., 2006). Elevated *O*-GlcNAc modifications induced by TMG promote the activation and nuclear localization of P53 (de Queiroz et al., 2016). Furthermore, BAP1 and BECN1 can also

be modified by *O*-GlcNAc(Wang and Hanover, 2013; Moon et al., 2017). These examples suggest that *O*-GlcNAcylation indirectly regulate System Xc and may play a regulatory role in ferroptosis.

GPX4 directly reduces cytotoxic lipid peroxides (L-OOH) to non-toxic lipid alcohols (L-OH) in the membrane. Of the three GPX4 isoforms (mitochondrial, nuclear, and cytoplasmic isoforms), only the cytoplasmic isoform is required for ferroptosis, and its expression is regulated by transcription factors (i.e., stimulating protein 1, nuclear factor Y, and AP2) (Ursini and Maiorino, 2020; Zheng and Conrad, 2020), integrin α6β4 (Brown et al., 2017), and heat shock protein 90 (Wu et al., 2019). It is not clear whether these molecules undergo *O*-GlcNAcylation and regulate GPX4. *O*-GlcNAcylation is mainly in the cytoplasm and nucleus, while GPX4 is localized in the cytoplasm, mitochondria, and mitochondrial OGT has also been identified in recent years (Hanover et al., 2003). In addition, we used the *O*-GlcNAc modification site prediction website (https://services.healthtech.dtu.dk/service.php?YinOYang-1.2) for GPX4 and showed the highest potential at 67 threonine (NetPhos threshold>0.5), which implies that GPX4 may directly modified by *O*-GlcNAc. The above evidence implies that *O*-GlcNAc signaling homeostasis may affect ferroptosis sensitivity by regulating antioxidant defense system-controlled ROS biology through related molecules or direct modifications by transcription-dependent and -independent mechanisms.

When System Xc transfers Cys2 into cells, it also carries endogenous glutamate out of the cells. Therefore, inhibition of System Xc reduces Cys2 uptake while increasing endogenous glutamate accumulation, suggesting that intracellular glutamate metabolism may also be involved in regulating ferroptosis. In 2021, Zhang et al. investigated the mechanism that determines the sensitivity of lung adenocarcinoma cells to ferroptosis (Zhang X. et al., 2021) and found that the greater the inhibition of ferroptosis by erastin, the lower the Yes-associated protein (YAP) levels. Erastin induces polyubiquitination-mediated degradation of YAP by recruiting the ubiquitin E3 ligase βtrCP. However, RSL3, a ferroptosis stimulator targeting GPX4, failed to reduce YAP levels, suggesting that the reduction of YAP was caused by the inhibition of Systemic Xc. It was further found that cystine deficiency caused by System Xc inhibition is critical for triggering ferroptosis. Moreover, glutamate accumulation is required to determine ferroptosis sensitivity after System Xc inhibition, and the decrease in YAP is caused by endogenous glutamate accumulation. Phosphorylation of YAP S127 (the major phosphorylation site of the Hippo pathway) is increased by erastin in a glutamate-dependent manner, whereas the *O*-GlcNAcylation on T241 of YAP and total YAP are significantly decreased by this treatment (Zhang H. et al., 2021). In addition, there is evidence that the *O*-GlcNAcylation at T241 stabilizes YAP by antagonizing Hippo-dependent phosphorylation (Zhang et al., 2017). Decreased *O*-GlcNAcylation is a prerequisite for endogenous glutamate-induced reduction of YAP levels, and *O*-GlcNAcylation at T241 is critical for ferroptosis sensitivity (Zhang X. et al., 2021). However, there are no reports on *O*-GlcNAcylation and the three other antioxidant defense systems of ferroptosis independent of the System Xc/GSH/GPX4 axis. There may be synergistic or complementary effects among these antioxidant defense systems, and whether *O*-GlcNAcylation is involved in the direct or indirect regulation of these pathways or affect ferroptosis needs further investigation.

5 *O*-GlcNAcylation regulates iron metabolism during ferroptosis

5.1 *O*-GlcNAcylation and iron uptake

As an indispensable trace element in the human body, iron is essential in physiological concentrations for metabolic processes, such as oxygen transport and electron transfer. Iron promotes lipid peroxidation during ferroptosis by at least two mechanisms. Iron can produce ROS through the Fenton-like reaction and can also act as a cofactor to activate iron-containing enzymes [e.g., arachidonate lipoxygenase (ALOX) (Yang et al., 2016), Cytochrome P450 reductase (POR) (Koppula et al., 2021)] involved in lipid peroxidation. Thus, the regulation of iron metabolism (iron uptake, utilization, storage, efflux) (Figure 2) affects ferroptosis sensitivity (Chen P. H. et al., 2020).

Iron uptake into cells occurs by multiple mechanisms. The main mechanism of iron uptake is through the TF-bound iron uptake pathway (Ruff and Whittlesey, 1993; Wang J. et al., 2020; Chen D. et al., 2021). TF can bind two Fe^{3+} and subsequently bind to the TFRC, which causes membrane invagination to form specialized endosomes. The pH drop in the endosomes leads to the release of Fe^{3+} from TF. The metalloreductase six-transmembrane epithelial antigen of the prostate 3 (STEAP3) can reduce the released Fe^{3+} to Fe^{2+}, which then crosses the endosomal membrane via solute carrier family 11 member 2 (SLC11A2) into the cytoplasm. TF/TFRC then returns to the cell surface (Chen et al., 2021b). It is now generally accepted that TF has a limited transport capacity and that excess iron may enter the cytosol by other routes. One such route is the non-TF-bound iron (NTBI) uptake pathway. Iron reductase or the release of cellular reductants (e.g., cytochrome B reductase 1 [CYBRD1], ascorbate) (Lane et al., 2015) present on the cell surface can reduce iron to the ferrous form and translocate it into the cell via transmembrane transport proteins, such as SLC11A2, SLC39A8 or SLC39A14 (Knutson, 2019). The Heme and hemoglobin (HB) iron uptake pathway is another mechanism of iron transport into cells. Plasma-free heme and HB are captured by hemopexin (HPX) and haptoglobin (HP) and transferred into cells by binding to the LDL receptor-related protein 1 receptor (LRP1) and macrophage scavenger receptor CD163, respectively (Gozzelino and Soares, 2014). Finally, extracellular albumin-bound heme or non-protein-bound heme enters cells via multiple transporters [feline leukemia virus subgroup C cellular receptor 2 (FLVCR2), SLC48A1, and SLC46A1] and subsequently releases Fe^{2+} through the action of heme oxygenase 1 (HMOX1) (Knutson, 2019). Iron uptake-mediated iron metabolism is essential for ferroptosis, and there is evidence that TFRC knockdown prevents ferroptosis caused by erastin or Cys2 deprivation (Yang and Stockwell, 2008; Gao et al., 2015). Therefore, does *O*-GlcNAcylation regulate ferroptosis through iron uptake? Zhu et al. (2021) showed that *O*-GlcNAcylation increased RSL3-induced ferroptosis in HCC cells via YAP, and the OGA inhibitor PUGNAc-induced *O*-GlcNAcylation promoted YAP expression and nuclear

localization (Zhu et al., 2021). YAP can directly bind to the TFRC promoter region and increase TFRC expression, promoting cellular iron uptake (Torii et al., 2016). These findings suggest that *O*-GlcNAcylation can affect ferroptosis by modulating TFRC and enhancing cellular iron uptake.

5.2 *O*-GlcNAcylation and iron storage

Fe^{2+} released into the cytoplasm enters the metabolically active "labile iron pool" (LIP), which regulates the Fe^{2+} ion concentration in the cytoplasm and determines the exchange and utilization of Fe^{2+}. Excess iron is mainly stored in cytoplasmic ferritin, a complex composed of two isoforms, ferritin heavy chain (FTH1) and ferritin light chain (FTL). FTH1 is responsible for the oxidation of Fe^{2+} to Fe^{3+}, and FTL promotes iron nucleation and mineralization. Iron entering the inner cavity of ferritin is deposited as ferrihydrite (Chen et al., 2021c). Iron can be excreted through pores on the surface of ferritin; however, it is mainly bound to nuclear receptor coactivator 4 (NCOA4) and delivered to the lysosome for degradation (ferritinophagy), releasing stored iron (Mancias et al., 2014). Iron can also be released through ferritin degradation by the ubiquitin-proteasome system (De Domenico et al., 2006). Reduced FTH1 expression increases free Fe^{2+} in the LIP, promoting cellular ferroptosis (Chen X. et al., 2020). Increased iron storage by inhibiting NCOA4-mediated ferritinophagy limits ferroptosis in cancer cells (Hou et al., 2016). There is indirect evidence that *O*-GlcNAcylation regulates iron storage. First, reduced *O*-GlcNAcylation of YAP induced by endogenous glutamine accumulation in erastin-treated lung adenocarcinoma cells caused YAP degradation, and inhibition of YAP could not increase FTH1 expression via the transcription factor TFCP2, leading to elevated labile iron (Zhang H. et al., 2021). Second, Yu et al. (2022) showed that RSL3 caused biphasic changes in protein *O*-GlcNAcylation, which regulates ferroptosis by coordinating ferritinophagy and mitophagy (Yu et al., 2022). Specifically, *O*-GlcNAcylation increased sharply after RSL3 treatment and then gradually decreased during ferroptosis. Decreased *O*-GlcNAcylation strongly promoted RSL3-induced TFRC membrane transfer and increased ferroptosis sensitivity. Decreased *O*-GlcNAcylation also promoted FTH1 degradation and ferritinophagy, leading to increased labile iron levels. NCOA4 knockdown blocked ferritin co-localization with lysosomes. In contrast, de-*O*-GlcNAcylation of FTH1 at S179 increased its interaction with NCOA4 and promoted the transport of FTH1 to lysosomes, leading to ferritinophagy (Yu et al., 2022). This recent study demonstrated that *O*-GlcNAc modifications could affect ferroptosis by regulating iron storage.

5.3 *O*-GlcNAcylation and iron export

Iron export is mediated by the plasma membrane protein ferroportin 1 (FPN1, also known as solute carrier family 40 member 1, SLC40A1) and the ferro-oxidases (e.g., ceruloplasmin and hephaestin). FPN1 transports Fe^{2+} to the extracellular space, where it is oxidized by the ferro-oxidases to Fe^{3+} for export. In addition, ferritin and its stored iron can be released from the cell via the prominin-2-mediated exosome pathway (Brown et al., 2019), suggesting that intracellular iron export is also regulated by this secretory pathway. There is evidence that blocking the iron release pathway by inhibiting FPN1 on the cell membrane increases ferroptosis sensitivity (Brown et al., 2019; Shang et al., 2020). Moreover, NH_4Cl can increase *O*-GlcNAcylation and FPN1 expression (Görg et al., 2019), suggesting a potential link between *O*-GlcNAcylation and iron export. However, the specific mechanism is still unclear.

6 *O*-GlcNAcylation regulates lipid metabolism and peroxidation during ferroptosis

Ferroptosis is ultimately caused by the peroxidation of membrane lipids and involves complex lipid metabolic processes (Figure 3). Because the bis-allylic group (-CH = CH-CH2-CH = CH-) is more susceptible to oxidation, PUFAs are one of the main lipid targets for peroxidation. Fatty acids are important precursors of membrane lipids. For their *de novo* synthesis, acetyl-CoA carboxylase (ACAC) catalyzes the synthesis of malonyl-CoA from acetyl CoA, and then fatty acid synthetase (FASN) catalyzes the condensation of malonyl-CoA and acetyl CoA to form saturated fatty acids (e.g., palmitic acid). The saturated fatty acids are desaturated by desaturases (e.g., stearoyl-CoA desaturase-1, SCD1) to form monounsaturated fatty acids (e.g., palmitoleic acid). Essential PUFAs [α-linolenic acid (LNA) and linoleic acid (LA)] obtained from food are further processed by elongation reactions (e.g., elongation of very long-chain fatty acid protein 5, ELOVL5) and desaturation (e.g., fatty acid desaturases 1/2, FADS1/2) to other long-chain PUFAs (e.g., arachidonic acid). Inhibition of ACAC can inhibit ferroptosis caused by various stimuli (Lee H. et al., 2020). SCD1 knockdown sensitizes cells to ferroptosis (Tesfay et al., 2019). FADS1/2 and ELOVL5 can promote ferroptosis (Lee J. Y. et al., 2020), suggesting that PUFA synthesis also regulates ferroptosis. *O*-GlcNAc modifications have been associated with fatty acid synthesis. For example, Sodi et al. (2018) found that OGT downregulation inhibited fatty acid biosynthesis and led to cancer cell death by decreasing FASN expression (Sodi et al., 2018). However, there is still a lack of reports on whether *O*-GlcNAcylation affects ferroptosis by regulating fatty acid synthesis. Recently, Wang et al. (2022) found enhanced *O*-GlCNAcylation at Ser555 of transcription factor ZEB1 in mesenchymal pancreatic cancer cells, which promoted FASN and FADS2 transcriptional activity and lipid peroxidation-dependent ferroptosis in cancer cells (Wang et al., 2022). This study may be the only direct evidence so far that elevated *O*-GlcNAcylation regulates ferroptosis through lipid metabolism. Interestingly, FASN is modified by *O*-GlcNAc (Baldini et al., 2016). Whether elevated *O*-GlcNAcylation plays a role in regulating ferroptosis through FASN remains to be proven.

Excess lipids can be stored in lipid droplets composed of glycerol and cholesterol lipids. Lipid droplet formation increases fatty acid storage, and separating PUFA from membrane phospholipids limits ferroptosis precursor utilization (Bai et al., 2019). Enhanced selective autophagic degradation of lipid droplets increases the production of free fatty acids, promoting lipid peroxidation and increasing the ferroptosis sensitivity of HCC cells (Bai et al., 2019). Both anabolism and

TABLE 1 Effect of key *O*-GlcNAcylated proteins on ferroptosis.

Proteins	*O*-GlcNAcylation sites	Effect on its function	Mechanisms	Effect on ferroptosis	Sample types	Ref
c-Jun	Ser73	*O*-GlcNAcylation promotes protein expression, transcriptional activity and nuclear accumulation of c-Jun	*O*-GlcNAcylation of c-Jun stimulates GSH synthesis and reduces ROS accumulation	*O*-GlcNAcylation of c-Jun inhibits ferroptosis	Liver cancer	Chen et al. (2019)
YAP	Thr241	*O*-GlcNAcylation antagonizes Ser127 phosphorylation to inhibit the degradation of YAP	Reduced *O*-GlcNAcylation inhibit the transcription of FTH1 by YAP, resulting in elevated LIP	Decreased *O*-GlcNAcylation of YAP increased ferroptosis sensitivity	Lung adenocarcinoma	Zhang et al. (2021a)
YAP	Thr241	*O*-GlcNAcylation enhances and stabilizes the expression of YAP	*O*-GlcNAcylation of YAP increases TFRC transcription and leads to elevated Fe^{2+} concentration	Elevated YAP *O*-GlcNAcylation increases ferroptosis sensitivity	hepatocellular carcinoma	Zhu et al. (2021)
ZEB1	Ser555	*O*-GlcNAcylation enhances the stability and nuclear translocation of ZEB1	*O*-GlcNAcylation of ZEB1 promotes the transcriptional activity of adipogenesis-related genes FASN and FADS2, leading to increased synthesis of PUFAs	*O*-GlcNAcylation of ZEB1 promotes ferroptosis in mesenchymal pancreatic cancer cells	Mesenchymal pancreatic cancer cells	Wang et al. (2022)
FTH	Ser179	De-*O*-GlcNAcylation of FTH promoted the degradation of FTH	De-*O*-GlcNAcylation of FTH increases the interaction with NCOA4 and promotes ferritinophagy, leading to elevated LIP	Inhibition of *O*-GlcNAcylation of FTH activates ferroptosis	U2OS cells, HUVEC and HT1080 cells	Yu et al. (2022)

β-oxidative catabolism first require fatty acid activation. Fatty acids are converted to medium/long-chain acyl coenzyme A via medium/long-chain acyl-CoA synthetases (ACSMs, ACSLs) and subsequently enter the mitochondria for oxidative catabolism by carnitine palmitoyltransferase 1 (CPT1). Unsaturated fatty acids are saturated before being oxidatively catabolized, and 2,4-dienoyl-CoA reductase 1 (DECR1) catalyzes the reduction of PUFAs in mitochondria. Inhibition of CPT1 promotes ferroptosis induced by RLS3 (Kagan et al., 2017), and knockdown of DECR1 promotes ferroptosis in prostate cancer cells (Blomme et al., 2020). These examples suggest that PUFA depletion by β-oxidation may reduce ferroptosis oxidation precursors and inhibit ferroptosis. The importance of *O*-GlcNAcylation for lipid synthesis in cancer cells is self-evident. However, there is a lack of direct evidence on whether *O*-GlcNAcylation regulates lipolysis in relation to ferroptosis.

Initially, free PUFAs were thought to be ferroptosis drivers. However, further studies have revealed that PUFAs must undergo esterification and be incorporated into the membrane lipid environment and oxidized by oxygenases (e.g., lipoxygenases, ALOXs) to transmit ferroptosis signals. PUFAs (i.e., arachidonic acid or adrenergic acids) are catalyzed by ACSL4 into fatty acyl-CoA. LPCAT3 then promotes the esterification of fatty acyl-CoA bound to membrane phospholipids (e.g., phosphatidylethanolamine, phosphatidylcholine) into PUFA-phospholipids (e.g., PUFA-phosphatidylethanolamine, PUFA-PE; PUFA-phosphatidylcholine, PUFA-PC). The inactivation of ACSL4 and LPCAT3 renders cells resistant to ferroptosis (Dixon et al., 2015; Doll et al., 2017). Zhang H. et al. (2022) showed that phosphorylation of ACSL4 on Thr328 promotes its activation, drives PUFA incorporation into phospholipids, and promotes ferroptosis (Zhang H. L. et al., 2022). For other members of the ACSLs, ACSL1 generates conjugated linoleates (e.g., α-eleostearic acid) capable of triggering ferroptosis (Beatty et al., 2021). ACSL3-activated exogenous monounsaturated fatty acids promote cellular resistance to ferroptosis by reducing the sensitivity of membrane lipids to oxidation (Magtanong et al., 2019), suggesting that ACSLs may play different roles in ferroptosis regulation in a substrate-dependent manner. Furthermore, ACSL4 can be *O*-GlcNAcylated in HCC cells, and its silencing can eliminate the promoting effect of *O*-GlcNAcylation on apoptosis (Wang Y. et al., 2020). However, there is a competitive relationship between phosphorylation and *O*-GlcNAcylation. Therefore, researchers should explore whether *O*-GlcNAcylation and phosphorylation crosstalk affects the sensitivity of ACSL4 to ferroptosis.

Finally, oxygenases, such as the ALOXs, trigger ferroptosis by oxidizing membrane phospholipids (Kagan et al., 2017). In addition, cytochrome P450 oxidoreductase (POR) contributes to lipid peroxidation during ferroptosis (Zou et al., 2020). Recent studies have found that the calcium-independent phospholipase, iPLA2β, releases oxidized PUFAs from the membrane phospholipids to inhibit P53-driven ferroptosis under ROS-induced stress (Chen D. et al., 2021), indirectly showing that oxidized PUFA tails do not promote ferroptosis after separation from membrane phospholipids. The 2022 review by Stockwell concluded that ferroptosis should not be considered a general type of oxidative stress but rather a lethal accumulation of membrane-localized lipid

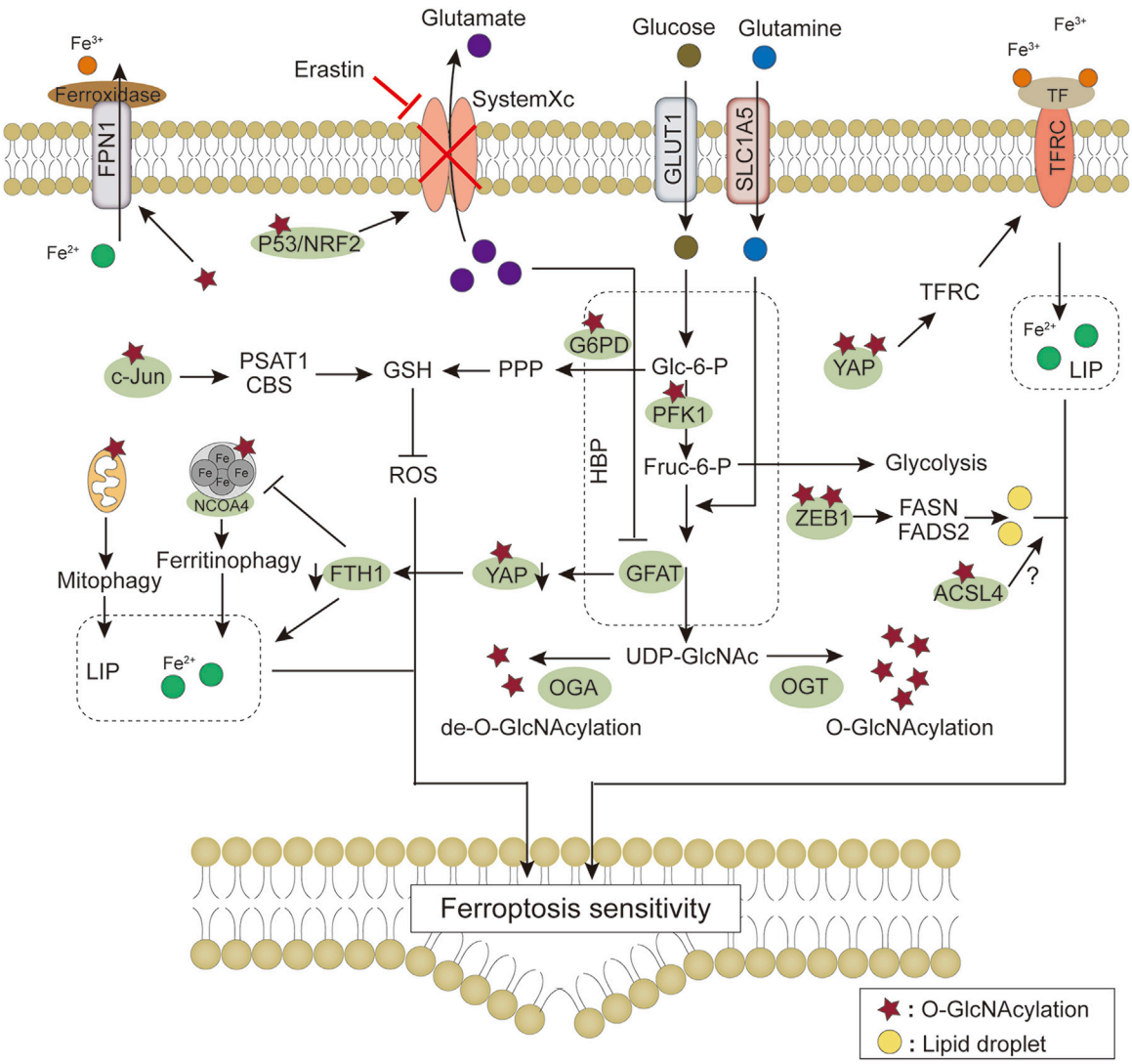

FIGURE 5
Modulation of ferroptosis signaling pathway by O-GlcNAc modification. HBP provides UDP-GlcNAc through glucose and glutamine, and regulation of O-GlcNAc modification homeostasis by OGT/OGA affects cellular sensitivity to ferroptosis through ROS production, iron metabolism, and fatty acid synthesis, respectively. Details of the molecular mechanism are provided in the main text. The star symbol represents O-GlcNAc modification, and the yellow orbs represent lipid droplets. Abbreviations: ACSL4, Long-chain fatty acid-CoA synthetase 4; CBS, cystathionine β synthase; FADS2, fatty acid desaturases 2; FASN, fatty acid synthetase; FPN1, ferroportin 1; Fruc-6-P, fructose-6-phosphate; FTH1, ferritin heavy chain 1; G6PD, glucose-6-phosphate dehydrogenase; GFAT, Glutamine-fructose-6-phosphate transaminase; Glc-6-P, Glucose-6-phosphate; GLUT1, Glucose transporter 1; GSH, glutathione; HBP, hexosamine biosynthetic pathway; LIP, labile iron pool; NRF2, Nuclear factor erythroid 2-related factor 2; OGA, *O*-GlcNAcase; OGT, *O*-GlcNAc transferase; PFK1, phosphofructokinase 1; PPP, pentose phosphate pathway; PSAT1, phosphoserine aminotransferase 1; SLC1A5, solute carrier family 1 member 5; TF, transferrin; TFRC, transferrin receptor; YAP, Yes-associated protein; ZEB1, zinc-finger E homeobox-binding 1.

peroxides (Stockwell, 2022). In lipid metabolism, the production of PUFAs increases ferroptosis sensitivity. Most fatty acids are consumed by β-oxidation, which reduces the rate of lipid peroxidation. Lipid droplet formation protects the PUFAs from lipid oxidation during ferroptosis (Chen et al., 2021b). These data suggest that PUFA-mediated lipid synthesis and catabolism play important roles in regulating ferroptosis. The regulation of lipid metabolism by *O*-GlcNAcylation has been widely studied; however, the role of *O*-GlcNAcylation in lipid metabolism-mediated ferroptosis is still unclear. Thus, a better understanding of the effect of *O*-GlcNAcylation on lipid peroxidation will help researchers clarify the complex regulatory processes for ferroptosis.

7 Effects of *O*-GlcNAcylation on the morphology and function of subcellular organelles during ferroptosis

7.1 *O*-GlcNAcylation and mitochondria

For subcellular organelles, changes in the morphology or function of subcellular organelles may either facilitate or accompany ferroptosis. In recent years, the roles of different subcellular organelles in ferroptosis have been identified. Morphologically, mitochondria shrink in size, cristae are reduced, and the outer membranes are ruptured during ferroptosis (Dixon

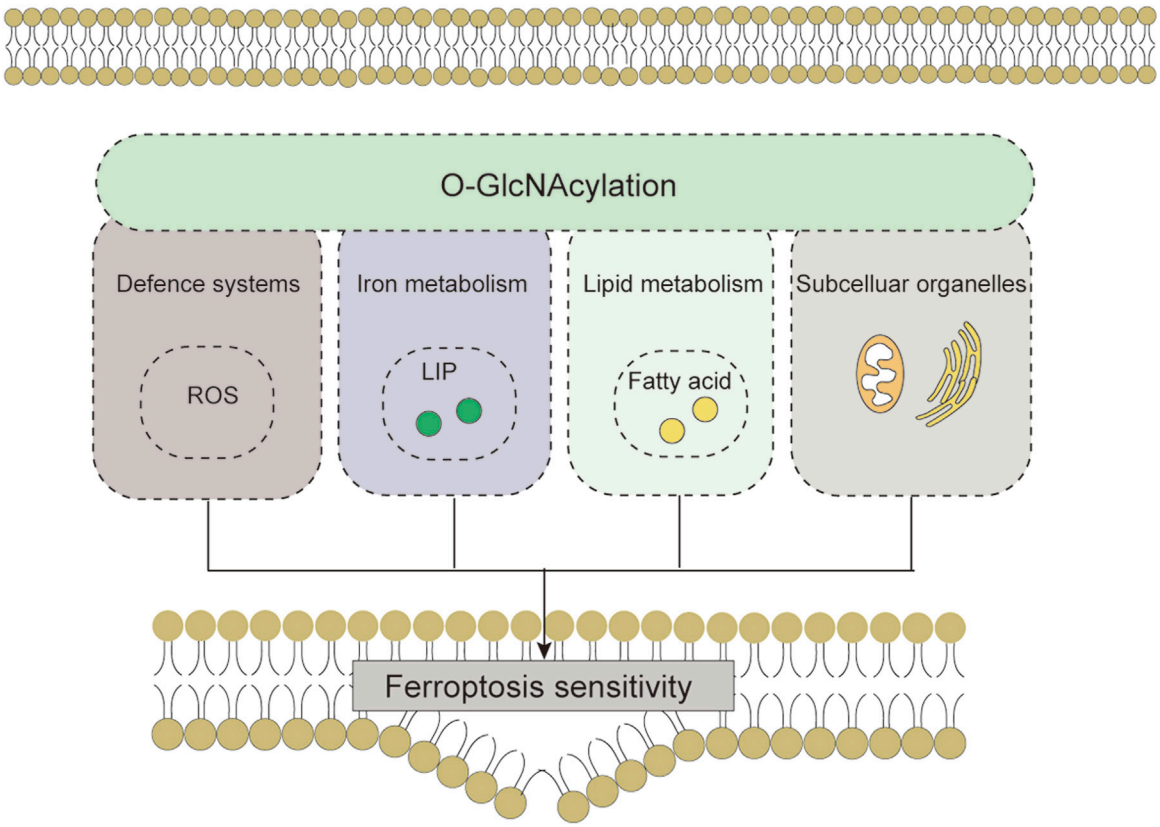

FIGURE 6
O-GlcNAcylation affects cellular sensitivity to ferroptosis through ROS biology, iron metabolism, lipid peroxidation and subcellular organelles. Abbreviations: ROS, reactive oxygen species; LIP, labile iron pool.

et al., 2012). Functionally, depletion of mitochondria or inhibition of the electron transport chain causes resistance to cystine starvation or erastin-induced ferroptosis (Gao et al., 2019). Voltage-dependent Anion channel 2 (VDAC2, responsible for the transport of ions and metabolites) of the outer mitochondrial membrane is a direct target of erastin, which causes mitochondrial dysfunction and massive oxide release via VDAC2 (Yagoda et al., 2007). In addition, mitochondria play an important role in iron metabolism. Iron in the LIP can be imported into mitochondria through channels in the outer mitochondrial membrane (e.g., SLC25A37 and SLC25A28) to synthesize heme and Fe-S clusters (Paradkar et al., 2009). Iron overload in the mitochondria can lead to mitochondrial autophagy (Li et al., 2018). Inhibition of the mitochondrial outer membrane protein CDGSH iron-containing domain-containing protein 1 (CISD1) increases mitochondrial iron accumulation and mitochondrial lipid peroxidation, promoting erastin-induced ferroptosis (Yuan et al., 2016). Ferroptosis may be initiated and amplified by damage to the mitochondrial morphology and function.

With the discovery of mitochondrial OGT (mOGT), the effect of *O*-GlcNAcylation on mitochondria has attracted widespread attention. Numerous publications have shown that *O*-GlcNAcylation is associated with mitochondrial dysfunction (Zhang X. et al., 2021; Xue et al., 2022). For example, Dontaine et al. (2022) found that acute elevation in mitochondrial *O*-GlcNAc modifications enhanced electron transport chain flux and complex I activity and decreased ROS release (Dontaine et al., 2022). Furthermore, many mitochondrial proteins involved in mitochondrial respiration, fatty acid metabolism, apoptosis, and other biological processes are substrates for mOGT (Jóźwiak et al., 2021). As mentioned above, Yu et al. found that inhibition of *O*-GlcNAcylation increased cellular ferritinophagy, and iron released from ferritinophagy was transported to the mitochondria. The investigators subsequently found that inhibition of *O*-GlcNAcylation increased mitochondrial fragmentation and autophagy, adding an additional source of iron for ferroptosis and making cells more sensitive to this mechanism of cell death (Yu et al., 2022). This study provides a different perspective on our understanding of ferroptosis in terms of the regulation of mitochondrial iron homeostasis by *O*-GlcNAcylation. It is unknown whether *O*-GlcNAcylation affects ferroptosis by regulating mitochondrial ROS.

7.2 *O*-GlcNAcylation and endoplasmic reticulum

Of the other subcellular organelles, the ER is worth mentioning. The efficacy of ferrostatin-1 (ferroptosis inhibitor) is derived from its ability to anchor to lipid

membranes, thereby capturing free radical intermediates during lipid peroxidation and reducing lipid hydroperoxides. Gaschler et al. (2018) observed Ferrostatin-1 aggregates in lysosomes, mitochondria, and the ER using stimulated Raman scattering microscopy. Ferrostatin-1 accumulation in the ER may be critical for inhibiting ferroptosis (Gaschler et al., 2018). Consistent with this hypothesis, the fluorescent lipid peroxidation probe LiperFluo was mainly localized in the ER (Kagan et al., 2017). Because the ER contains more than half of the lipid bilayers of a cell and is the source of most membrane lipids in other organelles, it is not surprising that the ER may be an important site of lipid peroxidation. Another study showed that erastin could induce ALOX5 translocation to the nuclear membrane, suggesting that lipid peroxidation also occurs in that membrane (Yang et al., 2016). Thus, membrane damage may involve multiple subcellular organelles, and cells exhibiting loss of plasma membrane integrity may be in a late stage of ferroptosis (Stockwell, 2022). The ESCRT III may repair the final stage of plasma membrane damage but may also simply slow the rate of iron death (Pedrera et al., 2021). The epidermal growth factor (EGF) domain-specific *O*-GlcNAc transferase (EOGT) in the ER catalyzes proteins in the lumen of the ER, implying the presence of extracellular *O*-GlcNAc modifications (Sakaidani et al., 2011; Ogawa et al., 2015). Abnormal *O*-GlcNAcylation in the ER tubular lumen is associated with the development of some diseases (e.g., Adams-Oliver syndrome and Walker-Warburg syndrome) (Manzini et al., 2012; Shaheen et al., 2013; Cohen et al., 2014). Recent studies have found that the OGT inhibitor OSMI-1 can activate apoptosis by inducing ER stress (Lee et al., 2021). *O*-GlcNAcylation promotes the formation of Coat Protein Complex II (COPII) vesicles and accelerates the cis-transport of vesicles in the ER-Golgi network (Cho and Mook-Jung, 2018). These reports suggest that *O*-GlcNAcylation is associated with stress response and vesicle transport in the ER. However, it is unclear what types of proteins are modified by *O*-GlcNAc in the ER lumen or what the effect of *O*-GlcNAcylation is on ER function, especially whether *O*-GlcNAcylation regulates ER lipid metabolism.

8 Prospects

The biological processes and sensitivity of ferroptosis are highly dependent on the ROS defense system, iron metabolism and membrane lipid peroxidation metabolism (Figure 4). Studies of these three processes have identified many direct and indirect regulatory factors regulated by transcription, translation, epigenetics, and post-translational modifications (e.g., phosphorylation, methylation, and acetylation) that also play an indispensable role in ferroptosis (Wei et al., 2020). *O*-GlcNAcylation also regulates ferroptosis, adding to our understanding of ferroptosis from another perspective. However, the role of *O*-GlcNAcylation in ferroptosis is only beginning to be elucidated, so there are still many unknowns and questions. For example, physiological and pathological states of *O*-GlcNAc modifications have different regulatory effects on ferroptosis, and *O*-GlcNAc modifications in different cell types under the same or similar conditions may play different roles, indicating the complexity and refinement of *O*-GlcNAcylation in regulating ferroptosis.

Although ferroptosis is not equivalent to general ROS accumulation, the accumulation of ROS is necessary for ferroptosis. There is a crosstalk between ROS and *O*-GlcNAcylation in the antioxidant defense system. It is unclear whether *O*-GlcNAcylation plays a role in regulating ferroptosis through other defense systems in addition to the System Xc/GSH/GPX4 axis. It is worth mentioning that $CoQ_{10}H_2$ functions in the plasma membrane. Does the ER, the main site of lipids, also have other defense systems? Whether *O*-GlcNAcylation in the ER is involved in the ROS defense system is a question well worth exploring.

The significance of iron uptake, utilization, storage, and efflux in ferroptosis is self-evident. Recent findings only suggest that *O*-GlcNAcylation regulates ferroptosis sensitivity through iron metabolism; however, whether *O*-GlcNAcylation is a direct driver of iron metabolism under physiological or pathological conditions is unclear.

Whether *O*-GlcNAcylation occurs in key enzymes in the membrane lipid peroxidative metabolism pathway during the synthesis of PUFAs needs to be further characterized. Lipid droplet synthesis and catabolism and fatty acid β-oxidation appear to regulate PUFA content; however, free PUFAs may not be inherently ferroptosis-toxic. Therefore, PUFA oxidation (especially membrane PUFAs) should be the focus of attention. In contrast, the regulation of lipid substrate production and oxidative processes by *O*-GlcNAcylation currently lacks relevant evidence. It is worth noting that not all unsaturated fatty acids induce ferroptosis, and it is also worth considering whether *O*-GlcNAcylation regulates the production of different fatty acids (e.g., monounsaturated fatty acids).

Finally, whether other subcellular organelles (e.g., the Golgi) regulate ferroptosis needs to be explored. *O*-GlcNAcylation has been observed in the Golgi (Ogawa et al., 2015). In addition, neighboring cells might transmit ferroptosis signals. Does this signaling involve exosomes even though OGT is present within the exosome (Yuan et al., 2021)?

9 Conclusion

In summary, adaptive regulation by *O*-GlcNAcylation in response to stress perturbations plays an important role in regulating ferroptosis sensitivity via the antioxidant defense system-controlled ROS biology, iron metabolism, and membrane lipid peroxidation metabolism (Table 1). These three processes synergistically interact with each other. In lipid metabolism, *O*-GlcNAcylation is involved in regulating the process of lipid substrate production; in iron metabolism, *O*-GlcNAcylation affects the efficiency of Fe^{2+} utilization; the crosstalk with ROS biology reflects the role of *O*-GlcNAcylation in the defense process of lipid peroxidation damage (Figure 5). In addition, changes in the morphology and function of subcellular organelles regulated by *O*-GlcNAc modification may trigger and amplify ferroptosis (Figure 6). These current studies on the roles of *O*-GlcNAcylation in ferroptosis are only the prologue, and since one key cannot open all locks, we are not limited to starting with the

above questions in the future. Exploring the environment-specific regulatory effects of *O*-GlcNAcylation is important for understanding the physiological and pathological mechanisms of ferroptosis.

Author contributions

HoZ: The conception and design of the study, drafting the article. JZ and HD: Review and edit the article. YK and YG: The conception and design of the study, revising the article critically for important intellectual content, and final approval of the version to be submitted. All authors contributed to the article and approved the submitted version.

Funding

This study was supported by the National Natural Science Foundation of China (grant no.31971209), and the Liaoning Provincial Program for Top Discipline of Basic Medical Sciences, and the Research Project of Education Department of Liaoning Province (LJKQZ20222417), and the Liaoning Revitalization Talents Program.

Conflict of interest

The authors declare that the research was conducted in the absence of any commercial or financial relationships that could be construed as a potential conflict of interest.

Publisher's note

All claims expressed in this article are solely those of the authors and do not necessarily represent those of their affiliated organizations, or those of the publisher, the editors and the reviewers. Any product that may be evaluated in this article, or claim that may be made by its manufacturer, is not guaranteed or endorsed by the publisher.

Supplementary material

The Supplementary Material for this article can be found online at: https://www.frontiersin.org/articles/10.3389/fmolb.2023.1203269/full#supplementary-material

References

Bai, Y., Meng, L., Han, L., Jia, Y., Zhao, Y., Gao, H., et al. (2019). Lipid storage and lipophagy regulates ferroptosis. *Biochem. Biophys. Res. Commun.* 508, 997–1003. doi:10.1016/j.bbrc.2018.12.039

Baldini, S. F., Wavelet, C., Hainault, I., Guinez, C., and Lefebvre, T. (2016). The nutrient-dependent O-GlcNAc modification controls the expression of liver fatty acid synthase. *J. Mol. Biol.* 428, 3295–3304. doi:10.1016/j.jmb.2016.04.035

Beatty, A., Singh, T., Tyurina, Y. Y., Tyurin, V. A., Samovich, S., Nicolas, E., et al. (2021). Ferroptotic cell death triggered by conjugated linolenic acids is mediated by ACSL1. *Nat. Commun.* 12, 2244. doi:10.1038/s41467-021-22471-y

Bersuker, K., Hendricks, J. M., Li, Z., Magtanong, L., Ford, B., Tang, P. H., et al. (2019). The CoQ oxidoreductase FSP1 acts parallel to GPX4 to inhibit ferroptosis. *Nature* 575, 688–692. doi:10.1038/s41586-019-1705-2

Blomme, A., Ford, C. A., Mui, E., Patel, R., Ntala, C., Jamieson, L. E., et al. (2020). 2,4-dienoyl-CoA reductase regulates lipid homeostasis in treatment-resistant prostate cancer. *Nat. Commun.* 11, 2508. doi:10.1038/s41467-020-16126-7

Brown, C. W., Amante, J. J., Chhoy, P., Elaimy, A. L., Liu, H., Zhu, L. J., et al. (2019). Prominin2 drives ferroptosis resistance by stimulating iron export. *Dev. Cell* 51, 575–586. doi:10.1016/j.devcel.2019.10.007

Brown, C. W., Amante, J. J., Goel, H. L., and Mercurio, A. M. (2017). The α6β4 integrin promotes resistance to ferroptosis. *J. Cell Biol.* 216, 4287–4297. doi:10.1083/jcb.201701136

Chen, D., Chu, B., Yang, X., Liu, Z., Jin, Y., Kon, N., et al. (2021a). iPLA2β-mediated lipid detoxification controls p53-driven ferroptosis independent of GPX4. *Nat. Commun.* 12, 3644. doi:10.1038/s41467-021-23902-6

Chen, D., Tavana, O., Chu, B., Erber, L., Chen, Y., Baer, R., et al. (2017). NRF2 is a major target of ARF in p53-independent tumor suppression. *Mol. Cell* 68, 224–232. doi:10.1016/j.molcel.2017.09.009

Chen, P. H., Chi, J. T., and Boyce, M. (2018). Functional crosstalk among oxidative stress and O-GlcNAc signaling pathways. *Glycobiology* 28, 556–564. doi:10.1093/glycob/cwy027

Chen, P. H., Wu, J., Ding, C. C., Lin, C. C., Pan, S., Bossa, N., et al. (2020a). Kinome screen of ferroptosis reveals a novel role of ATM in regulating iron metabolism. *Cell Death Differ.* 27, 1008–1022. doi:10.1038/s41418-019-0393-7

Chen, X., Kang, R., Kroemer, G., and Tang, D. (2021b). Broadening horizons: The role of ferroptosis in cancer. *Nat. Rev. Clin. Oncol.* 18, 280–296. doi:10.1038/s41571-020-00462-0

Chen, X., Li, J., Kang, R., Klionsky, D. J., and Tang, D. (2021c). Ferroptosis: Machinery and regulation. *Autophagy* 17, 2054–2081. doi:10.1080/15548627.2020.1810918

Chen, X., Yu, C., Kang, R., and Tang, D. (2020b). Iron metabolism in ferroptosis. *Front. Cell Dev. Biol.* 8, 590226. doi:10.3389/fcell.2020.590226

Chen, Y., Zhu, G., Liu, Y., Wu, Q., Zhang, X., Bian, Z., et al. (2019). O-GlcNAcylated c-Jun antagonizes ferroptosis via inhibiting GSH synthesis in liver cancer. *Cell. Signal.* 63, 109384. doi:10.1016/j.cellsig.2019.109384

Cho, H. J., and Mook-Jung, I. (2018). O-GlcNAcylation regulates endoplasmic reticulum exit sites through Sec31A modification in conventional secretory pathway. *FASEB J.* 32, 4641–4657. doi:10.1096/fj.201701523R

Cohen, I., Silberstein, E., Perez, Y., Landau, D., Elbedour, K., Langer, Y., et al. (2014). Autosomal recessive Adams-Oliver syndrome caused by homozygous mutation in EOGT, encoding an EGF domain-specific O-GlcNAc transferase. *Eur. J. Hum. Genet.* 22, 374–378. doi:10.1038/ejhg.2013.159

Dai, E., Zhang, W., Cong, D., Kang, R., Wang, J., and Tang, D. (2020). AIFM2 blocks ferroptosis independent of ubiquinol metabolism. *Biochem. Biophys. Res. Commun.* 523, 966–971. doi:10.1016/j.bbrc.2020.01.066

De Domenico, I., Vaughn, M. B., Li, L., Bagley, D., Musci, G., Ward, D. M., et al. (2006). Ferroportin-mediated mobilization of ferritin iron precedes ferritin degradation by the proteasome. *EMBO J.* 25, 5396–5404. doi:10.1038/sj.emboj.7601409

de Queiroz, R. M., Madan, R., Chien, J., Dias, W. B., and Slawson, C. (2016). Changes in O-linked N-acetylglucosamine (O-GlcNAc) homeostasis activate the p53 pathway in ovarian cancer cells. *J. Biol. Chem.* 291, 18897–18914. doi:10.1074/jbc.M116.734533

Dixon, S. J., Lemberg, K. M., Lamprecht, M. R., Skouta, R., Zaitsev, E. M., Gleason, C. E., et al. (2012). Ferroptosis: An iron-dependent form of nonapoptotic cell death. *Cell* 149, 1060–1072. doi:10.1016/j.cell.2012.03.042

Dixon, S. J., Winter, G. E., Musavi, L. S., Lee, E. D., Snijder, B., Rebsamen, M., et al. (2015). Human haploid cell genetics reveals roles for lipid metabolism genes in nonapoptotic cell death. *ACS Chem. Biol.* 10, 1604–1609. doi:10.1021/acschembio.5b00245

Doll, S., Freitas, F. P., Shah, R., Aldrovandi, M., da Silva, M. C., Ingold, I., et al. (2019). FSP1 is a glutathione-independent ferroptosis suppressor. *Nature* 575, 693–698. doi:10.1038/s41586-019-1707-0

Doll, S., Proneth, B., Tyurina, Y. Y., Panzilius, E., Kobayashi, S., Ingold, I., et al. (2017). ACSL4 dictates ferroptosis sensitivity by shaping cellular lipid composition. *Nat. Chem. Biol.* 13, 91–98. doi:10.1038/nchembio.2239

Dontaine, J., Bouali, A., Daussin, F., Bultot, L., Vertommen, D., Martin, M., et al. (2022). The intra-mitochondrial O-GlcNAcylation system rapidly modulates OXPHOS function and ROS release in the heart. *Commun. Biol.* 5, 349. doi:10.1038/s42003-022-03282-3

Dudognon, P., Maeder-Garavaglia, C., Carpentier, J. L., and Paccaud, J. P. (2004). Regulation of a COPII component by cytosolic O-glycosylation during mitosis. *FEBS Lett.* 561, 44–50. doi:10.1016/S0014-5793(04)00109-7

Fahie, K., and Zachara, N. E. (2016). Molecular functions of glycoconjugates in autophagy. *J. Mol. Biol.* 428, 3305–3324. doi:10.1016/j.jmb.2016.06.011

Friedmann Angeli, J. P., Schneider, M., Proneth, B., Tyurina, Y. Y., Tyurin, V. A., Hammond, V. J., et al. (2014). Inactivation of the ferroptosis regulator Gpx4 triggers acute renal failure in mice. *Nat. Cell Biol.* 16, 1180–1191. doi:10.1038/ncb3064

Galluzzi, L., Vitale, I., Aaronson, S. A., Abrams, J. M., Adam, D., Agostinis, P., et al. (2018). Molecular mechanisms of cell death: Recommendations of the nomenclature committee on cell death 2018. *Cell Death Differ.* 25, 486–541. doi:10.1038/s41418-017-0012-4

Gao, M., Monian, P., Quadri, N., Ramasamy, R., and Jiang, X. (2015). Glutaminolysis and transferrin regulate ferroptosis. *Mol. Cell* 59, 298–308. doi:10.1016/j.molcel.2015.06.011

Gao, M., Yi, J., Zhu, J., Minikes, A. M., Monian, P., Thompson, C. B., et al. (2019). Role of mitochondria in ferroptosis. *Mol. Cell* 73, 354–363. doi:10.1016/j.molcel.2018.10.042

Gaschler, M. M., Hu, F., Feng, H., Linkermann, A., Min, W., and Stockwell, B. R. (2018). Determination of the subcellular localization and mechanism of action of ferrostatins in suppressing ferroptosis. *ACS Chem. Biol.* 13, 1013–1020. doi:10.1021/acschembio.8b00199

Goldberg, H., Whiteside, C., and Fantus, I. G. (2011). O-linked β-N-acetylglucosamine supports p38 MAPK activation by high glucose in glomerular mesangial cells. *Am. J. Physiol. Endocrinol. Metab.* 301, E713–E726. doi:10.1152/ajpendo.00108.2011

Görg, B., Karababa, A., Schütz, E., Paluschinski, M., Schrimpf, A., Shafigullina, A., et al. (2019). O-GlcNAcylation-dependent upregulation of HO1 triggers ammonia-induced oxidative stress and senescence in hepatic encephalopathy. *J. Hepatol.* 71, 930–941. doi:10.1016/j.jhep.2019.06.020

Gozzelino, R., and Soares, M. P. (2014). Coupling heme and iron metabolism via ferritin H chain. *Antioxid. Redox Signal.* 20, 1754–1769. doi:10.1089/ars.2013.5666

Hanover, J. A., Yu, S., Lubas, W. B., Shin, S. H., Ragano-Caracciola, M., Kochran, J., et al. (2003). Mitochondrial and nucleocytoplasmic isoforms of O-linked GlcNAc transferase encoded by a single mammalian gene. *Arch. Biochem. Biophys.* 409, 287–297. doi:10.1016/s0003-9861(02)00578-7

Hart, G. W. (2019). Nutrient regulation of signaling and transcription. *J. Biol. Chem.* 294, 2211–2231. doi:10.1074/jbc.AW119.003226

Hou, W., Xie, Y., Song, X., Sun, X., Lotze, M. T., Zeh, H. J., 3rd, et al. (2016). Autophagy promotes ferroptosis by degradation of ferritin. *Autophagy* 12, 1425–1428. doi:10.1080/15548627.2016.1187366

Hu, J., Chen, R., Jia, P., Fang, Y., Liu, T., Song, N., et al. (2017). Augmented O-GlcNAc signaling via glucosamine attenuates oxidative stress and apoptosis following contrast-induced acute kidney injury in rats. *Free Radic. Biol. Med.* 103, 121–132. doi:10.1016/j.freeradbiomed.2016.12.032

Jiang, L., Kon, N., Li, T., Wang, S. J., Su, T., Hibshoosh, H., et al. (2015). Ferroptosis as a p53-mediated activity during tumour suppression. *Nature* 520, 57–62. doi:10.1038/nature14344

Jóźwiak, P., Ciesielski, P., Zakrzewski, P. K., Kozal, K., Oracz, J., Budryn, G., et al. (2021). Mitochondrial O-GlcNAc transferase interacts with and modifies many proteins and its up-regulation affects mitochondrial function and cellular energy homeostasis. *Cancers (Basel)* 13, 2956. doi:10.3390/cancers13122956

Kagan, V. E., Mao, G., Qu, F., Angeli, J. P., Doll, S., Croix, C. S., et al. (2017). Oxidized arachidonic and adrenic PEs navigate cells to ferroptosis. *Nat. Chem. Biol.* 13, 81–90. doi:10.1038/nchembio.2238

Katikaneni, A., Jelcic, M., Gerlach, G. F., Ma, Y., Overholtzer, M., and Niethammer, P. (2020). Lipid peroxidation regulates long-range wound detection through 5-lipoxygenase in zebrafish. *Nat. Cell Biol.* 22, 1049–1055. doi:10.1038/s41556-020-0564-2

Knutson, M. D. (2019). Non-transferrin-bound iron transporters. *Free Radic. Biol. Med.* 133, 101–111. doi:10.1016/j.freeradbiomed.2018.10.413

Koppula, P., Zhuang, L., and Gan, B. (2021). Cytochrome P450 reductase (POR) as a ferroptosis fuel. *Protein Cell* 12, 675–679. doi:10.1007/s13238-021-00823-0

Kraft, V., Bezjian, C. T., Pfeiffer, S., Ringelstetter, L., Müller, C., Zandkarimi, F., et al. (2020). GTP cyclohydrolase 1/tetrahydrobiopterin counteract ferroptosis through lipid remodeling. *ACS Cent. Sci.* 6, 41–53. doi:10.1021/acscentsci.9b01063

Lane, D. J., Merlot, A. M., Huang, M. L., Bae, D. H., Jansson, P. J., Sahni, S., et al. (2015). Cellular iron uptake, trafficking and metabolism: Key molecules and mechanisms and their roles in disease. *Biochim. Biophys. Acta* 1853, 1130–1144. doi:10.1016/j.bbamcr.2015.01.021

Lee, A., Miller, D., Henry, R., Paruchuri, V. D., O'Meally, R. N., Boronina, T., et al. (2016). Combined antibody/lectin enrichment identifies extensive changes in the O-GlcNAc sub-proteome upon oxidative stress. *J. Proteome Res.* 15, 4318–4336. doi:10.1021/acs.jproteome.6b00369

Lee, H., Zandkarimi, F., Zhang, Y., Meena, J. K., Kim, J., Zhuang, L., et al. (2020a). Energy-stress-mediated AMPK activation inhibits ferroptosis. *Nat. Cell Biol.* 22, 225–234. doi:10.1038/s41556-020-0461-8

Lee, J. Y., Nam, M., Son, H. Y., Hyun, K., Jang, S. Y., Kim, J. W., et al. (2020b). Polyunsaturated fatty acid biosynthesis pathway determines ferroptosis sensitivity in gastric cancer. *Proc. Natl. Acad. Sci. U.S.A.* 117, 32433–32442. doi:10.1073/pnas.2006828117

Lee, S. J., and Kwon, O. S. (2020). O-GlcNAc transferase inhibitor synergistically enhances doxorubicin-induced apoptosis in HepG2 cells. *Cancers (Basel)* 12, 3154. doi:10.3390/cancers12113154

Lee, S. J., Lee, D. E., Choi, S. Y., and Kwon, O. S. (2021). OSMI-1 enhances TRAIL-induced apoptosis through ER stress and NF-κB signaling in colon cancer cells. *Int. J. Mol. Sci.* 22, 11073. doi:10.3390/ijms222011073

Li, C., Zhang, Y., Cheng, X., Yuan, H., Zhu, S., Liu, J., et al. (2018). PINK1 and PARK2 suppress pancreatic tumorigenesis through control of mitochondrial iron-mediated immunometabolism. *Dev. Cell* 46, 441–455. doi:10.1016/j.devcel.2018.07.012

Li, J., Cao, F., Yin, H. L., Huang, Z. J., Lin, Z. T., Mao, N., et al. (2020). Ferroptosis: Past, present and future. *Cell Death Dis.* 11, 88. doi:10.1038/s41419-020-2298-2

Lin, L., Zhang, M. X., Zhang, L., Zhang, D., Li, C., and Li, Y. L. (2021). Autophagy, pyroptosis, and ferroptosis: New regulatory mechanisms for atherosclerosis. *Front. Cell Dev. Biol.* 9, 809955. doi:10.3389/fcell.2021.809955

Magtanong, L., Ko, P. J., To, M., Cao, J. Y., Forcina, G. C., Tarangelo, A., et al. (2019). Exogenous monounsaturated fatty acids promote a ferroptosis-resistant cell state. *Cell Chem. Biol.* 26, 420–432. doi:10.1016/j.chembiol.2018.11.016

Mancias, J. D., Wang, X., Gygi, S. P., Harper, J. W., and Kimmelman, A. C. (2014). Quantitative proteomics identifies NCOA4 as the cargo receptor mediating ferritinophagy. *Nature* 509, 105–109. doi:10.1038/nature13148

Manzini, M. C., Tambunan, D. E., Hill, R. S., Yu, T. W., Maynard, T. M., Heinzen, E. L., et al. (2012). Exome sequencing and functional validation in zebrafish identify GTDC2 mutations as a cause of Walker-Warburg syndrome. *Am. J. Hum. Genet.* 91, 541–547. doi:10.1016/j.ajhg.2012.07.009

Mao, C., Liu, X., Zhang, Y., Lei, G., Yan, Y., Lee, H., et al. (2021). DHODH-mediated ferroptosis defence is a targetable vulnerability in cancer. *Nature* 593, 586–590. doi:10.1038/s41586-021-03539-7

Moon, S., Lee, Y. K., Lee, S. W., and Um, S. J. (2017). Suppressive role of OGT-mediated O-GlcNAcylation of BAP1 in retinoic acid signaling. *Biochem. Biophys. Res. Commun.* 492, 89–95. doi:10.1016/j.bbrc.2017.08.029

Moujalled, D., Strasser, A., and Liddell, J. R. (2021). Molecular mechanisms of cell death in neurological diseases. *Cell Death Differ.* 28, 2029–2044. doi:10.1038/s41418-021-00814-y

Ogawa, M., Sawaguchi, S., Furukawa, K., and Okajima, T. (2015). N-acetylglucosamine modification in the lumen of the endoplasmic reticulum. *Biochim. Biophys. Acta* 1850, 1319–1324. doi:10.1016/j.bbagen.2015.03.003

Panieri, E., and Santoro, M. M. (2016). ROS homeostasis and metabolism: A dangerous liason in cancer cells. *Cell Death Dis.* 7, e2253. doi:10.1038/cddis.2016.105

Paradkar, P. N., Zumbrennen, K. B., Paw, B. H., Ward, D. M., and Kaplan, J. (2009). Regulation of mitochondrial iron import through differential turnover of mitoferrin 1 and mitoferrin 2. *Mol. Cell. Biol.* 29, 1007–1016. doi:10.1128/MCB.01685-08

Pedrera, L., Espiritu, R. A., Ros, U., Weber, J., Schmitt, A., Stroh, J., et al. (2021). Ferroptotic pores induce Ca2+ fluxes and ESCRT-III activation to modulate cell death kinetics. *Cell Death Differ.* 28, 1644–1657. doi:10.1038/s41418-020-00691-x

Rao, X., Duan, X., Mao, W., Li, X., Li, Z., Li, Q., et al. (2015). O-GlcNAcylation of G6PD promotes the pentose phosphate pathway and tumor growth. *Nat. Commun.* 6, 8468. doi:10.1038/ncomms9468

Riegman, M., Sagie, L., Galed, C., Levin, T., Steinberg, N., Dixon, S. J., et al. (2020). Ferroptosis occurs through an osmotic mechanism and propagates independently of cell rupture. *Nat. Cell Biol.* 22, 1042–1048. doi:10.1038/s41556-020-0565-1

Ruff, R. L., and Whittlesey, D. (1993). Na+ currents near and away from endplates on human fast and slow twitch muscle fibers. *Muscle Nerve* 16, 922–929. doi:10.1002/mus.880160906

Sakaidani, Y., Nomura, T., Matsuura, A., Ito, M., Suzuki, E., Murakami, K., et al. (2011). O-linked-N-acetylglucosamine on extracellular protein domains mediates epithelial cell-matrix interactions. *Nat. Commun.* 2, 583. doi:10.1038/ncomms1591

Santagostino, S. F., Assenmacher, C. A., Tarrant, J. C., Adedeji, A. O., and Radaelli, E. (2021). Mechanisms of regulated cell death: Current perspectives. *Vet. Pathol.* 58, 596–623. doi:10.1177/03009858211005537

Shaheen, R., Aglan, M., Keppler-Noreuil, K., Faqeih, E., Ansari, S., Horton, K., et al. (2013). Mutations in EOGT confirm the genetic heterogeneity of autosomal-recessive Adams-Oliver syndrome. *Am. J. Hum. Genet.* 92, 598–604. doi:10.1016/j.ajhg.2013.02.012

Shang, Y., Luo, M., Yao, F., Wang, S., Yuan, Z., and Yang, Y. (2020). Ceruloplasmin suppresses ferroptosis by regulating iron homeostasis in hepatocellular carcinoma cells. *Cell. Signal.* 72, 109633. doi:10.1016/j.cellsig.2020.109633

Shi, Y., Yan, S., Shao, G. C., Wang, J., Jian, Y. P., Liu, B., et al. (2022). O-GlcNAcylation stabilizes the autophagy-initiating kinase ULK1 by inhibiting chaperone-mediated autophagy upon HPV infection. *J. Biol. Chem.* 298, 102341. doi:10.1016/j.jbc.2022.102341

Sodi, V. L., Bacigalupa, Z. A., Ferrer, C. M., Lee, J. V., Gocal, W. A., Mukhopadhyay, D., et al. (2018). Nutrient sensor O-GlcNAc transferase controls cancer lipid metabolism via SREBP-1 regulation. *Oncogene* 37, 924–934. doi:10.1038/onc.2017.395

Song, X., Zhu, S., Chen, P., Hou, W., Wen, Q., Liu, J., et al. (2018). AMPK-mediated BECN1 phosphorylation promotes ferroptosis by directly blocking system Xc- activity. *Curr. Biol.* 28, 2388–2399. doi:10.1016/j.cub.2018.05.094

Soula, M., Weber, R. A., Zilka, O., Alwaseem, H., La, K., Yen, F., et al. (2020). Metabolic determinants of cancer cell sensitivity to canonical ferroptosis inducers. *Nat. Chem. Biol.* 16, 1351–1360. doi:10.1038/s41589-020-0613-y

Stockwell, B. R. (2022). Ferroptosis turns 10: Emerging mechanisms, physiological functions, and therapeutic applications. *Cell* 185, 2401–2421. doi:10.1016/j.cell.2022.06.003

Tan, E. P., McGreal, S. R., Graw, S., Tessman, R., Koppel, S. J., Dhakal, P., et al. (2017). Sustained O-GlcNAcylation reprograms mitochondrial function to regulate energy metabolism. *J. Biol. Chem.* 292, 14940–14962. doi:10.1074/jbc.M117.797944

Tang, D., Chen, X., Kang, R., and Kroemer, G. (2021). Ferroptosis: Molecular mechanisms and health implications. *Cell Res.* 31, 107–125. doi:10.1038/s41422-020-00441-1

Tesfay, L., Paul, B. T., Konstorum, A., Deng, Z., Cox, A. O., Lee, J., et al. (2019). Stearoyl-CoA desaturase 1 protects ovarian cancer cells from ferroptotic cell death. *Cancer Res.* 79, 5355–5366. doi:10.1158/0008-5472.CAN-19-0369

Torii, S., Shintoku, R., Kubota, C., Yaegashi, M., Torii, R., Sasaki, M., et al. (2016). An essential role for functional lysosomes in ferroptosis of cancer cells. *Biochem. J.* 473, 769–777. doi:10.1042/BJ20150658

Ursini, F., and Maiorino, M. (2020). Lipid peroxidation and ferroptosis: The role of GSH and GPx4. *Free Radic. Biol. Med.* 152, 175–185. doi:10.1016/j.freeradbiomed.2020.02.027

Vocadlo, D. J. (2012). O-GlcNAc processing enzymes: Catalytic mechanisms, substrate specificity, and enzyme regulation. *Curr. Opin. Chem. Biol.* 16, 488–497. doi:10.1016/j.cbpa.2012.10.021

Wang, J., Wang, Z., Yuan, J., Wang, J., and Shen, X. (2020a). The positive feedback between ACSL4 expression and O-GlcNAcylation contributes to the growth and survival of hepatocellular carcinoma. *Aging (Albany NY)* 12, 7786–7800. doi:10.18632/aging.103092

Wang, P., and Hanover, J. A. (2013). Nutrient-driven O-GlcNAc cycling influences autophagic flux and neurodegenerative proteotoxicity. *Autophagy* 9, 604–606. doi:10.4161/auto.23459

Wang, X., Liu, M., Chu, Y., Liu, Y., Cao, X., Zhang, H., et al. (2022). O-GlcNAcylation of ZEB1 facilitated mesenchymal pancreatic cancer cell ferroptosis. *Int. J. Biol. Sci.* 18, 4135–4150. doi:10.7150/ijbs.71520

Wang, Y., Liu, Y., Liu, J., Kang, R., and Tang, D. (2020b). NEDD4L-mediated LTF protein degradation limits ferroptosis. *Biochem. Biophys. Res. Commun.* 531, 581–587. doi:10.1016/j.bbrc.2020.07.032

Wei, X., Yi, X., Zhu, X. H., and Jiang, D. S. (2020). Posttranslational modifications in ferroptosis. *Oxid. Med. Cell Longev.* 2020, 8832043. doi:10.1155/2020/8832043

Wu, J., Tan, Z., Li, H., Lin, M., Jiang, Y., Liang, L., et al. (2021). Melatonin reduces proliferation and promotes apoptosis of bladder cancer cells by suppressing O-GlcNAcylation of cyclin-dependent-like kinase 5. *J. Pineal Res.* 71, e12765. doi:10.1111/jpi.12765

Wu, Z., Geng, Y., Lu, X., Shi, Y., Wu, G., Zhang, M., et al. (2019). Chaperone-mediated autophagy is involved in the execution of ferroptosis. *Proc. Natl. Acad. Sci. U.S.A.* 116, 2996–3005. doi:10.1073/pnas.1819728116

Xie, Y., Hou, W., Song, X., Yu, Y., Huang, J., Sun, X., et al. (2016). Ferroptosis: Process and function. *Cell Death Differ.* 23, 369–379. doi:10.1038/cdd.2015.158

Xue, Q., Yan, R., Ji, S., and Yu, S. (2022). Regulation of mitochondrial network homeostasis by O-GlcNAcylation. *Mitochondrion* 65, 45–55. doi:10.1016/j.mito.2022.04.007

Yagoda, N., von Rechenberg, M., Zaganjor, E., Bauer, A. J., Yang, W. S., Fridman, D. J., et al. (2007). RAS-RAF-MEK-dependent oxidative cell death involving voltage-dependent anion channels. *Nature* 447, 864–868. doi:10.1038/nature05859

Yang, W. H., Kim, J. E., Nam, H. W., Ju, J. W., Kim, H. S., Kim, Y. S., et al. (2006). Modification of p53 with O-linked N-acetylglucosamine regulates p53 activity and stability. *Nat. Cell Biol.* 8, 1074–1083. doi:10.1038/ncb1470

Yang, W. H., Park, S. Y., Ji, S., Kang, J. G., Kim, J. E., Song, H., et al. (2010). O-GlcNAcylation regulates hyperglycemia-induced GPX1 activation. *Biochem. Biophys. Res. Commun.* 391, 756–761. doi:10.1016/j.bbrc.2009.11.133

Yang, W. S., Kim, K. J., Gaschler, M. M., Patel, M., Shchepinov, M. S., and Stockwell, B. R. (2016). Peroxidation of polyunsaturated fatty acids by lipoxygenases drives ferroptosis. *Proc. Natl. Acad. Sci. U.S.A.* 113, E4966–E4975. doi:10.1073/pnas.1603244113

Yang, W. S., and Stockwell, B. R. (2016). Ferroptosis: Death by lipid peroxidation. *Trends Cell Biol.* 26, 165–176. doi:10.1016/j.tcb.2015.10.014

Yang, W. S., and Stockwell, B. R. (2008). Synthetic lethal screening identifies compounds activating iron-dependent, nonapoptotic cell death in oncogenic-RAS-harboring cancer cells. *Chem. Biol.* 15, 234–245. doi:10.1016/j.chembiol.2008.02.010

Yi, W., Clark, P. M., Mason, D. E., Keenan, M. C., Hill, C., Goddard, W. A., 3rd, et al. (2012). Phosphofructokinase 1 glycosylation regulates cell growth and metabolism. *Science* 337, 975–980. doi:10.1126/science.1222278

Yu, F., Zhang, Q., Liu, H., Liu, J., Yang, S., Luo, X., et al. (2022). Dynamic O-GlcNAcylation coordinates ferritinophagy and mitophagy to activate ferroptosis. *Cell Discov.* 8, 40. doi:10.1038/s41421-022-00390-6

Yuan, H., Li, X., Zhang, X., Kang, R., and Tang, D. (2016). CISD1 inhibits ferroptosis by protection against mitochondrial lipid peroxidation. *Biochem. Biophys. Res. Commun.* 478, 838–844. doi:10.1016/j.bbrc.2016.08.034

Yuan, Y., Wang, L., Ge, D., Tan, L., Cao, B., Fan, H., et al. (2021). Exosomal O-GlcNAc transferase from esophageal carcinoma stem cell promotes cancer immunosuppression through up-regulation of PD-1 in CD8+ T cells. *Cancer Lett.* 500, 98–106. doi:10.1016/j.canlet.2020.12.012

Zachara, N. E., and Hart, G. W. (2004). O-GlcNAc a sensor of cellular state: The role of nucleocytoplasmic glycosylation in modulating cellular function in response to nutrition and stress. *Biochim. Biophys. Acta* 1673, 13–28. doi:10.1016/j.bbagen.2004.03.016

Zeitler, L., Fiore, A., Meyer, C., Russier, M., Zanella, G., Suppmann, S., et al. (2021). Anti-ferroptotic mechanism of IL4i1-mediated amino acid metabolism. *Elife* 10, e64806. doi:10.7554/eLife.64806

Zhang, B., Li, M. D., Yin, R., Liu, Y., Yang, Y., Mitchell-Richards, K. A., et al. (2019). O-GlcNAc transferase suppresses necroptosis and liver fibrosis. *JCI Insight* 4, e127709. doi:10.1172/jci.insight.127709

Zhang, H. L., Hu, B. X., Li, Z. L., Du, T., Shan, J. L., Ye, Z. P., et al. (2022b). PKCβII phosphorylates ACSL4 to amplify lipid peroxidation to induce ferroptosis. *Nat. Cell Biol.* 24, 88–98. doi:10.1038/s41556-021-00818-3

Zhang, H., Li, Z., Wang, Y., and Kong, Y. (2021a). O-GlcNAcylation is a key regulator of multiple cellular metabolic pathways. *PeerJ* 9, e11443. doi:10.7717/peerj.11443

Zhang, H., Qi, J., Pei, J., Zhang, M., Shang, Y., Li, Z., et al. (2022a). O-GlcNAc modification mediates aquaporin 3 to coordinate endometrial cell glycolysis and affects embryo implantation. *J. Adv. Res.* 37, 119–131. doi:10.1016/j.jare.2021.06.022

Zhang, J., Yu, P., Hua, F., Hu, Y., Xiao, F., Liu, Q., et al. (2020). Sevoflurane postconditioning reduces myocardial ischemia reperfusion injury-induced necroptosis by up-regulation of OGT-mediated O-GlcNAcylated RIPK3. *Aging (Albany NY)* 12, 25452–25468. doi:10.18632/aging.104146

Zhang, X., Qiao, Y., Wu, Q., Chen, Y., Zou, S., Liu, X., et al. (2017). The essential role of YAP O-GlcNAcylation in high-glucose-stimulated liver tumorigenesis. *Nat. Commun.* 8, 15280. doi:10.1038/ncomms15280

Zhang, X., Yu, K., Ma, L., Qian, Z., Tian, X., Miao, Y., et al. (2021b). Endogenous glutamate determines ferroptosis sensitivity via ADCY10-dependent YAP suppression in lung adenocarcinoma. *Theranostics* 11, 5650–5674. doi:10.7150/thno.55482

Zhang, Y., Shi, J., Liu, X., Feng, L., Gong, Z., Koppula, P., et al. (2018). BAP1 links metabolic regulation of ferroptosis to tumour suppression. *Nat. Cell Biol.* 20, 1181–1192. doi:10.1038/s41556-018-0178-0

Zheng, J., and Conrad, M. (2020). The metabolic underpinnings of ferroptosis. *Cell Metab.* 32, 920–937. doi:10.1016/j.cmet.2020.10.011

Zhou, F., Yang, X., Zhao, H., Liu, Y., Feng, Y., An, R., et al. (2018). Down-regulation of OGT promotes cisplatin resistance by inducing autophagy in ovarian cancer. *Theranostics* 8, 5200–5212. doi:10.7150/thno.27806

Zhu, G., Murshed, A., Li, H., Ma, J., Zhen, N., Ding, M., et al. (2021). O-GlcNAcylation enhances sensitivity to RSL3-induced ferroptosis via the YAP/TFRC pathway in liver cancer. *Cell Death Discov.* 7, 83. doi:10.1038/s41420-021-00468-2

Zou, Y., Li, H., Graham, E. T., Deik, A. A., Eaton, J. K., Wang, W., et al. (2020). Cytochrome P450 oxidoreductase contributes to phospholipid peroxidation in ferroptosis. *Nat. Chem. Biol.* 16, 302–309. doi:10.1038/s41589-020-0472-6

frontiers | Frontiers in Oncology

TYPE Original Research
PUBLISHED 06 June 2023
DOI 10.3389/fonc.2023.1133946

OPEN ACCESS

EDITED BY
Xin Wang,
National Institutes of Health (NIH), United States

REVIEWED BY
Zhuoyu Wen,
University of Texas Southwestern Medical Center, United States
Shuiping Liu,
Hangzhou Normal University, China

*CORRESPONDENCE
Chengzhi Huang
huangchengzhi93@hotmail.com
Xueqing Yao
syyaoxueqing@scut.edu.cn

†These authors have contributed equally to this work

RECEIVED 08 February 2023
ACCEPTED 05 May 2023
PUBLISHED 06 June 2023

CITATION
Li H, Feng X, Hu Y, Wang J, Huang C and Yao X (2023) Development of a prognostic model based on ferroptosis-related genes for colorectal cancer patients and exploration of the biological functions of NOS2 *in vivo* and *in vitro*. *Front. Oncol.* 13:1133946. doi: 10.3389/fonc.2023.1133946

Development of a prognostic model based on ferroptosis-related genes for colorectal cancer patients and exploration of the biological functions of NOS2 *in vivo* and *in vitro*

Hongming Li[1,2,3†], Xiaochuang Feng[3†], Yong Hu[2†], Junjiang Wang[1,2†], Chengzhi Huang[4*] and Xueqing Yao[1,2*]

[1]The Second School of Clinical Medicine, Southern Medical University, Guangzhou, Guangdong, China, [2]Department of Gastrointestinal Surgery, Department of General Surgery, Guangdong Provincial People's Hospital (Guangdong Academy of Medical Sciences), Southern Medical University, Guangzhou, China, [3]Department of Colorectal Surgery, Guangdong Provincial Hospital of Chinese Medicine, Guangzhou, Guangdong, China, [4]School of Bioscience and Bioengineering, South China University of Technology, Guangzhou, Guangdong, China

Background: Ferroptosis is involved in many malignant tumors and has been implicated in important mechanisms of colorectal cancer (CRC) suppression. However, the prognostic and predictive values of the ferroptosis activation pattern in CRC patients have not been noted. Here, we aimed to construct and validate a prediction model based on ferroptosis-related genes (FRGs) for CRC patients and investigated the expression pattern and biological function of the most significantly altered gene.

Methods: A total of 112 FRGs were obtained from the FerrDb website, and the clinical characteristics of 545 CRC patients and their global gene expression profiles were downloaded from The Cancer Genome Atlas (TCGA) database. Survival-related FRGs were identified by Cox proportional hazards regression analysis. Finally, the expression pattern and biological function of NOS2, the most implicated gene was explored *in vitro* and *in vivo*.

Results: The prediction model was established based on 8 FRGs. Patients in the high- or low-risk group were stratified based on the median risk value calculated by our model, and patients in the high-risk group experienced poor overall survival ($p<0.01$). Further validation demonstrated that the FRG model acted as an independent prognostic indicator for CRC patients (HR=1.428, 95% CI, 1.341-1.627; $p<0.001$). The area under the receiver operating characteristic (ROC) curve (AUC) for 5-year survival was 0.741. NOS2 was one of the most significantly affected FRGs and was highly expressed in malignant tissue, but it inhibited tumor growth and induced tumor cell death *in vitro* and *in vivo*, possibly by repressing the NF-κB pathway.

Conclusion: Our study revealed that FRGs have potential prognostic value in CRC patients and that NOS2 suppresses tumor progression, providing a novel therapeutic target for CRC treatment based on ferroptosis.

KEYWORDS

colorectal cancer, ferroptosis, prognostic model, gene, NOS2

Introduction

CRC is the third most frequently diagnosed malignant tumor worldwide, accounting for approximately 10% of all cancers and leading to almost 9×10^5 deaths annually (1, 2). The incidence of CRC has been increasing over recent decades, and it is foreseeable that new cases will reach 2.5 million in 2035, and the treatment and management of CRC have become more difficult due to the increase in drug resistance (3–5). However, guiding prognostication and treatment decision-making with biomarkers would provide promising therapeutic targets for CRC (6).

Ferroptosis is an important and recently identified form of nonapoptotic cell death driven by iron-dependent lipid peroxidation that was first proposed in 2012 (7). Emerging evidence has gradually indicated the tumor-suppressive consequence of ferroptosis through cysteine deprivation and reactive oxygen species (ROS) production by p53 (8, 9). To date, ferroptosis has been shown to affect the immune microenvironment, metabolism, and cell proliferation in CRC and acts downstream of chemotherapy and targeted therapy in KRAS-mutated CRC cells (10–12). However, the diagnostic and prognostic values and underlying biological mechanisms involved in ferroptosis remain unclear in CRC.

As shown in previous studies, NOS2 (Enzyme Nitric Oxide Synthase 2) might act in the process of ferroptosis and have implications for patient stratification for prognosis (13, 14). NOS2 is a calcium-independent and inducible enzyme that contributes to the production of NO in cells; therefore, it is related to immune response facilitation, the vascular relaxation function, and inflammation (15, 16). In many types of cancer, the mechanisms by which NOS2 is involved are complex and poorly defined, with both promoting and inhibiting functions having been described (15, 17, 18). Several studies have addressed the mechanisms by which NOS2 promotes tumor progression by p53 and TNFα interactions within the tumor microenvironment (19, 20). However, NOS2 is essential for T cell immunotherapies to destroy tumors (21).

Our study analyzed the correlation between the expression pattern of FRGs and the survival of 545 CRC patients from the TCGA database, and a prognostic model based on the risk score of 8 FRGs identified by multivariate Cox regression analysis was established. Furthermore, we explored the expression pattern and the tumor suppressive role and mechanism of NOS2, which was one of the most significantly affected gene in our model.

Abbreviations: CRC, Colorectal cancer; FRGs, Ferroptosis-related genes; ROS, Reactive oxygen species; NOS2, Enzyme nitric oxide synthase 2; MTT, 3-(4, 5-dimethyl-thiahiazo-2-yl)-2, 5-di- phenytetrazoliumromide.

Materials and methods

Data sources

A total of 112 FRGs, including ferroptosis drivers, suppressors and markers, were obtained from the FerrDB website (http://www.zhounan.org/ferrdb/). We downloaded the mRNA expression data and clinical characteristics of 545 patients diagnosed with CRC from The Cancer Genome Atlas (TCGA) database (https://www.cancer.gov/).

Identification of differentially expressed FRGs and enrichment analysis

We ran the edgeR package to identify differentially expressed FRGs (fold change >2, adjusted p-value< 0.05) between CRC and normal tissues. Then, we used a parallel box diagram to visualize these eligible FRGs and conducted Gene Ontology (GO) and Kyoto Encyclopedia of Genes and Genomes (KEGG) analyses for gene functional enrichment analyses. “GO plot” and “KEGG plot” were used to visualize the results.

Establishment of the individualized prognostic model based on FRGs

We performed univariate Cox regression analysis to select the significant survival-related FRGs and avoid false positives and overfitting of the model by LASSO regression analysis. Next, we used multivariate Cox regression analysis to further identify FRGs that could independently predict survival. Finally, the prognostic model was established according to the relative expression levels of the screened FRGs and weighted according to regression coefficients (β) with a multivariate Cox regression model. The equation was as follows:

$$\text{Risk score} = \beta\text{gene}(1) \times \text{FRGexpression}(1) + \beta\text{gene}(2) \times \text{FRGexpression}(2) + \cdots + \beta\text{gene}(n) \times \text{FRGexpression}(n)$$

Calculating survival and the risk score

According to the median risk score, CRC patients were divided into the high- or low-risk group. Kaplan-Meier curves were generated to analyze the overall survival (OS) times between the two groups, and a time-dependent receiver operating characteristic (ROC) curve was used to evaluate the accuracy of the prediction model. Then, we drew a nomogram to demonstrate the predictive probability and observation rate of five-year OS in CRC patients.

Western blot analysis and quantitative real-time PCR

We used RIPA buffer (Amresco, America) to lyse cells and tissues, separated total proteins by 10% SDS-PAGE (Amresco, America) and transferred them to PVDF membranes. All membranes were incubated overnight with primary antibodies at 4°C and with the HRP-conjugated secondary antibody at room temperature for 1 h. All western blot results were quantified by software Image J (v1.8.0).

For qRT-PCR, total mRNA was extracted from tumor cells or tumor tissues using TRIzol reagent and reverse transcribed into cDNA with a PrimeScript RT-PCR Kit. cDNA was amplified using SYBR™ Premix Ex Taq™ (TaKaRa, Japan) on a LightCycler 96 Detection System (Roche). GAPDH CT values were used for normalization.

MTT proliferation and clonogenic assays

For the MTT (3-(4, 5-dimethyl-thiahiazo-2-yl)-2, 5-di-phenytetrazolium bromide) proliferation assay, transfected cells (1×10^3 cells per well) were seeded onto 96-well plates. After 24 h, we performed an MTT assay at fixed time points every day. For the clonogenic assay, 500 cells were cultivated per well into 6-well plates and maintained in RPMI 1640 medium with 10% fetal bovine serum at 37°C for 7 days.

In vivo subcutaneous xenograft models

All nude mice were purchased from Guangdong Medical Laboratory Animal Center. NOS2-overexpressing and control cell lines were transplanted subcutaneously into the bilateral flanks, and appropriate care was given to these animals. Tumor volume [(length × width^2)/2] was measured every 3 days, and all mice were sacrificed 21 days after injection.

Statistical analysis

All statistical analyses were performed using GraphPad Prism 8.0 and R 3.6.2. The R package edgeR was used for differential expression analysis, and then univariate LASSO and multivariate Cox regression analyses were performed to identify FRGs associated with prognosis and further introduced into the prognostic model. Differences in OS between CRC patients in the high-risk group and low-risk group were generated with the Kaplan-Meier method. The R package "survivalROC" was run to generate the ROC curve and the corresponding area under the ROC curve (AUC) for model evaluation. Relevant R packages used for statistical analysis referenced the method in (22).

Data are shown as the mean ± SD, and all tests were considered statistically significant only when $p< 0.05$ was achieved.

Results

Differentially expressed FRGs in CRC and functional enrichment

First, we downloaded RNA-seq and clinical data from 646 CRC tissue samples and 68 normal colorectal mucosa specimens (Paired colon samples were from partial colon resection for carcinoma) from the TCGA database. Altogether, 545 CRC patients with follow-up data were eligible (Table 1). A total of 112 FRGs were accessed from the FerrDB website (Figure 1), and 61 genes (40 upregulated and 21 downregulated) were obtained under the criteria FDR<0.05 and log2 (fold change) > 1 (Figures 2A, B). Box plot graph showing these differential genes expression between normal and tumor tissues (Figure 2C). These differentially expressed FRGs were then subjected to functional enrichment analysis, and the top 28 GO terms and 8 KEGG pathways are visualized in Figures 2D, E. The top ranked pathways according to enrichment score were "Ferroptosis" and "Response to toxic substance".

Identification of prognostic FRGs and construction of a predictive model

We selected the above 61 FRGs for further exploration and performed univariate Cox regression analysis. The results revealed that 14 differentially expressed FRGs were significantly correlated with OS (Table 2). Then, we conducted LASSO regression analysis to narrow the scope and avoid false positives and ultimately identified 8 FRGs independently associated with survival in CRC patients by multivariate Cox regression to construct a predictive model (Supplementary Table 1). A heatmap of the expression profiles of 8 FRGs is shown in Figure 3A.

According to the model, 545 patients were classified into the high- or low-risk group based on the median risk scores [Risk score = -0.144 ×NOS2 expression + 0.723 × DRD4 expression + (-0.561) × STAT3 expression + 1.208 × LINC0036 expression + 0.431 ×

TABLE 1 Specific baseline clinical characteristic of 545 colorectal cancer patients.

Characteristic	
Gender	
Male	291
Female	254
Age	
<60	153
≧60	392
Stage	
I/II	305
III/IV	225
unknow	15
Pathologic T stage	
T1-2	111
T3-4	433
Unknow	1
Pathologic N stage	
N0	322
N1-2	222
unknow	1
Pathologic M stage	
M0	406
M1	76
unknow	63
Survival time	
0-3 years	441
3-5 years	67
>5 years	37

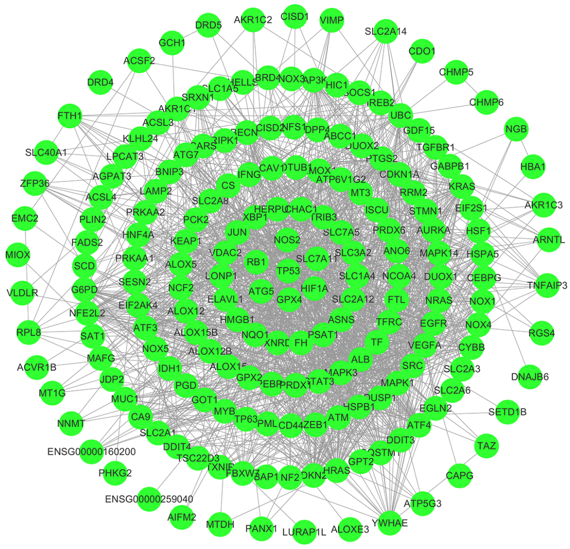

FIGURE 1
112 FRGs were obtained from the FerrDB website, and the interaction network was constructed by cyberscope software.

SLC2A3 expression + 0.707 × JDP2 expression + 0.770 × DUOX1 expression+ 0.996 × ISCU expression]. Subsequently, uni- and multivariate Cox regression analyses demonstrated that the risk score acted as an independent risk factor and an independent prognostic factor for the survival of CRC patients (Figures 3B, C). A K-M survival curve indicated that the survival rate of CRC patients in the high-risk group was significantly lower than that of CRC patients in the low-risk group (Figure 3D). The survival statuses of CRC patients in the two groups were presented in Figure 3E. The ROC curve for 5-year survival prediction and AUC for the risk score model showed good accuracy, and the area under the ROC curve was 0.741, which was higher than that of the ROC curve for age (0.637), sex (0.438), disease stage (0.709), T stage (0.676), N stage (0.654) and M stage (0.650) (Figure 3F).

Evaluation of the accuracy of the predictive model

To assess the prognostic efficacy of our model, we performed disease stage-based ROC curve analysis. The stage I/II and III/IV AUC values of the predictive model were 0.737 and 0.771, respectively, reflecting the superior performance of the FRG model for CRC prognostication (Figures 4A, B). Moreover, the K-M survival curve showed that the survival rates of CRC patients with stage I/II and III/IV disease in the high-risk group were distinctly lower than those in the low-risk group (Figures 4C, D). Finally, we constructed a nomogram to predict 1-year, 2-year and 3-year survival according to age, sex, clinical stage and our predictive model (Figure 4E).

NOS2 might act as a protective factor

Considering that NOS2 was one of the most significantly affected FRGs in our model (Supplementary Table 1) and the most obvious expression differences between patients in high risk and low risk groups (Figure 3A), we further investigated the role of NOS2 in ferroptosis-related tumor progression. The expression of NOS2 in 545 CRC patients with early or advanced TNM stages was detected. Overall, the expression of NOS2 gradually decreased as the TNM stage advanced (Figure 5A). Furthermore, the survival rates of CRC patients with high NOS2 expression were significantly higher than those of patients with low NOS2 expression (Figure 5B). Taken together, these data suggest that NOS2 might have a tumor suppressive function in CRC.

10.3389/fonc.2023.1133946

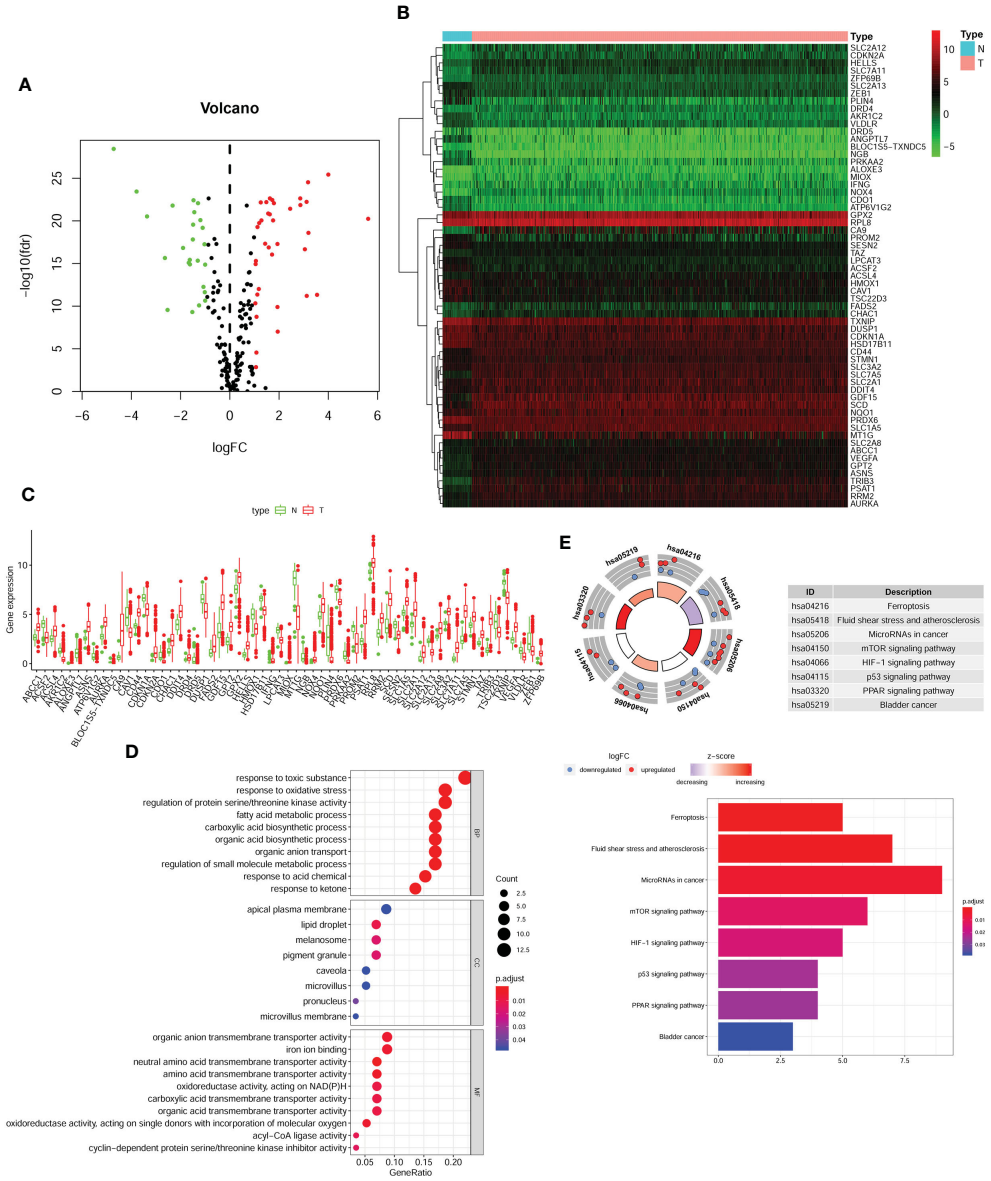

FIGURE 2
Differentially FRGs expressed in CRC and functional enrichment. Volcano plot **(A)**, heatmap **(B)** and expression bar chart **(C)** showing the 61 differentially expressed FRGs in CRC tissues compared with normal tissue. The red dots represented significantly up-regulated FRGs, green dots standed for FRGs with significantly downregulated and black dots standed for no significant differences FRGs. The GO analysis **(D)** and KGEE analysis **(E)** for molecular functions and potential pathways for differentially expressed FRGs involved in.

TABLE 2 Fourteen prognosis-related genes obtained based on univariate COX regression analysis.

Gene symbol	Hazard ratio	95%CI	*p*-Value
HSPB1	1.228	1.002–1.504	0.048
DDIT3	1.314	1.022–1.690	0.033
NOS2	0.852	v0.747–0.973	0.018
DRD4	1.719	1.162–2.542	0.007
STAT3	0.616	0.390–0.975	0.039
LINC00336	4.285	1.352–13.578	0.013

(Continued)

TABLE 2 Continued

Gene symbol	Hazard ratio	95%CI	*p*-Value
NOX4	1.612	1.015–2.561	0.043
ATP6V1G2	6.506	1.986–21.315	0.002
SLC2A3	1.348	1.102–1.649	0.004
JDP2	2.214	1.386–3.539	<0.001
DUOX1	1.800	1.177–2.752	0.007
SLC2A6	1.459	1.061–2.006	0.020
ISCU	1.865	1.043–3.334	0.036
ALOX12	2.561	1.196–5.482	0.015

NOS2 suppresses tumor proliferation *in vitro*

To further explore the biological functions of NOS2 in CRC, we first detected endogenous NOS2 expression in 11 CRC cell lines through qRT-PCR and western blot (Figures 6A, B). According to the results, NOS2 was relatively highly expressed in HCT116 and SW480 cells and weakly expressed in SW620 and CACO2 cells. Thus, we generated HCT116 and SW480 cell lines stably overexpressing NOS2 and SW620 and CACO2 cell lines with

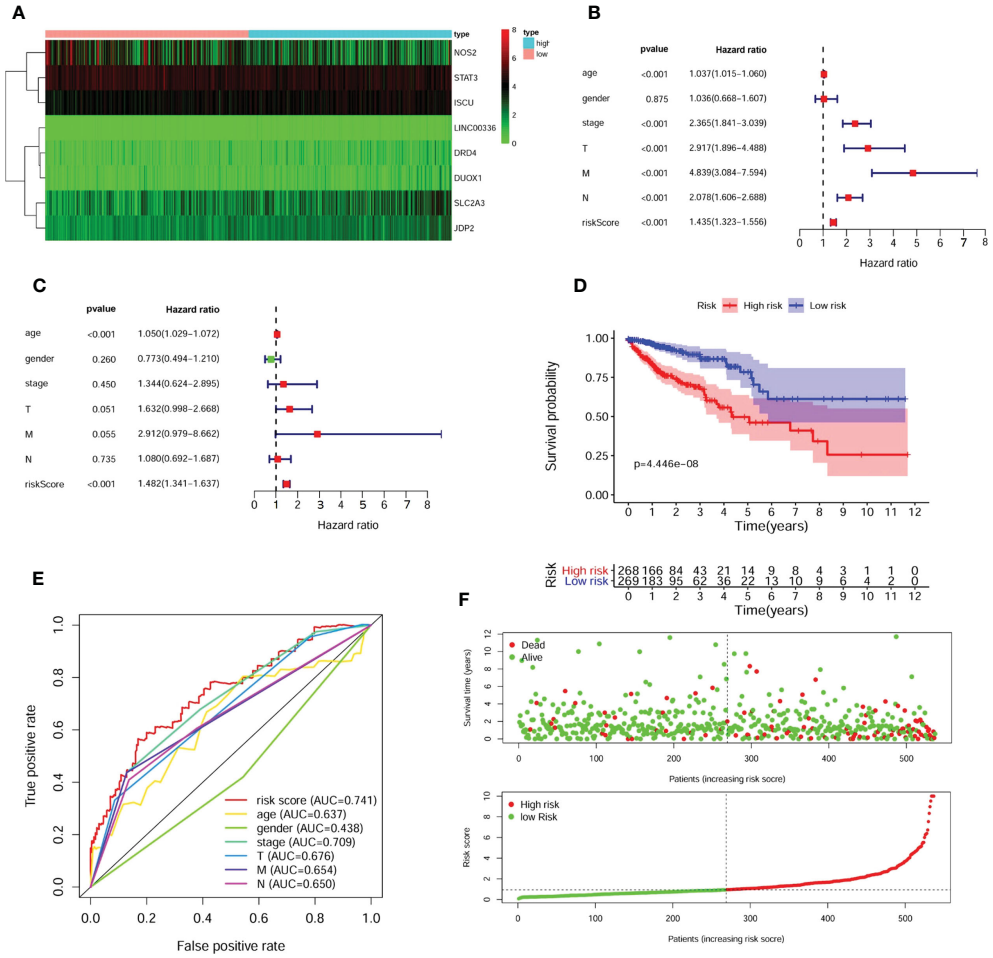

FIGURE 3
Identification of prognostic FRGs and construction of predictive model. **(A)** The heatmap of 8 included FGRs expression profile. A forest plot of univariate **(B)** and multivariate **(C)** Cox regression analysis for CRC patients. The K-M survival curve **(D)**, distribution of prognostic index and survival status **(E)** of 545 CRC patients in low- and high-risk groups. **(F)** The ROC curves validated the prognostic significance of risk score based on FRGs and other clinical indicators.

10.3389/fonc.2023.1133946

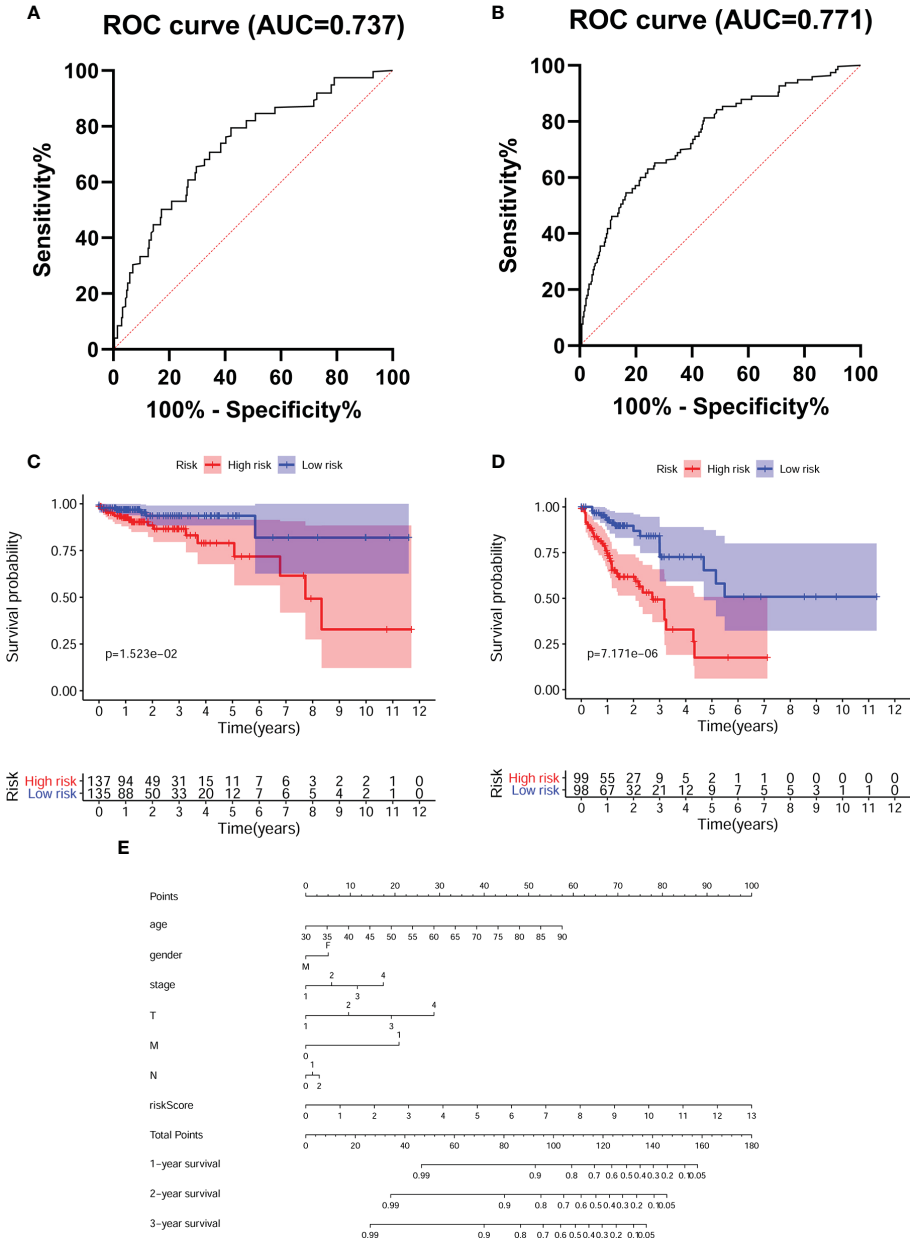

FIGURE 4
Evaluated the accuracy of the predictive model. Tumor stage-dependent ROC curve analysis **(A)**.I/II; **(B)** III/IV) for survival prediction based on the model. K-M survival curves for CRC patients with different tumor stage **(C)**.I/II; **(D)** III/IV) in low- and high- risk groups. **(E)** Nomogram predicts the probability of 3 years overall survival (OS) in CRC patients.

NOS2 knockdown. The lentiviral transfection efficiency of overexpression and knockdown was determined by qRT-PCR and western blot (Figure 6C).

Then, several experiments were performed to determine whether NOS2 affects the biological functions of CRC cells. The results of the MTT assay indicated that elevated NOS2 reduced cell proliferation, while the growth rate of cell lines increased when NOS2 was knocked down (Figure 6D).

To assess the function of NOS2 with respect to tumorigenic inhibition *in vivo*, SW620 NOS2 overexpression and control cell lines were used in subcutaneous tumorigenesis assays. The result demonstrated that elevated NOS2 expression decreased tumorigenicity in nude mice (Figure 6E). Together, these results suggest that NOS2 mainly functions as a tumor suppressor in CRC.

NOS2 inhibits the NF-κB signaling pathway

To further demonstrate the downstream molecular mechanism of NOS2, we used GSEA software to explore the related signaling pathways in microarray data from the TCGA, GSE17538 and GSE40967. The “NF-kappa B signaling pathway”, “IL6-STAT3 signaling pathway”, “c-MYC signaling pathway” and “oxidative

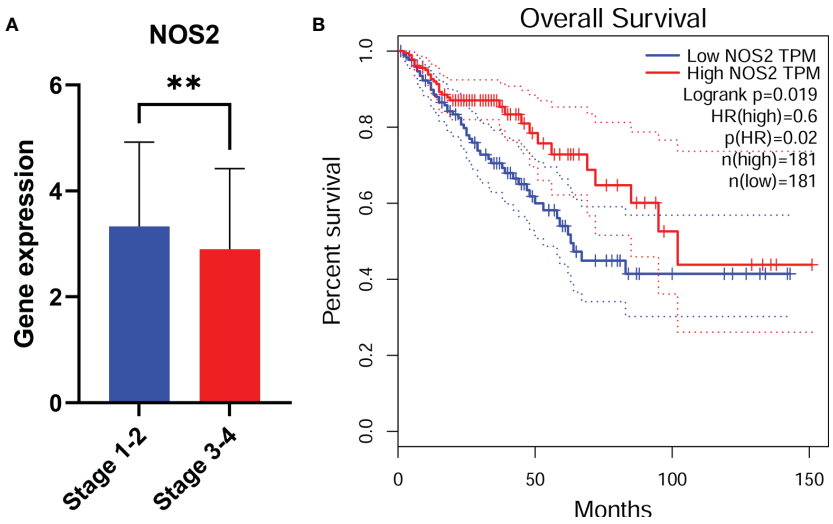

FIGURE 5
NOS2 might act as a protective factor. NOS2 expression among different tumor stage **(A)** in CRC. **(B)** CRC patients with low NOS2 expression had a shorter overall survival. **, p<0.01.

phosphorylation" were highly enriched and associated with NOS2 knockdown (Figure 7A).

We initially detected the relationship between NOS2 and STAT3, c-MYC pathways. Overall, NOS2 expression does not affect p-STAT3 and c-MYC changes (Supplementary Figure 1). Therefore we explored the association of NOS2 with NF-κB pathway.

Moreover, the western blot results suggested that NOS2 knockdown in SW480 and HCT116 cells increased the expression of p-P50 and p-P65, whereas NOS2 overexpression in SW620 and CACO2 cells reduced the expression of p-P50 and p-P65 (Figures 7B, C). Finally, to verify the regulatory relationship between NOS2 and ferroptosis, we conduct western blot and the outcome showed a higher level of GPX4 when NOS2 was knockdown, whereas NOS2 overexpression in CACO2 cells decreased the expression of GPX4 (Figures 7D, E).

In conclusion, NOS2 might inhibit CRC carcinogenicity *via* suppression of the NF-κB signaling pathway.

Discussion

Ferroptosis is a recently discovered type of nonapoptotic mechanism involved in excessive lipid peroxidation and iron-dependent damage to membrane lipids (23, 24). Numerous studies have shown that the peroxidation of phospholipids (PLs), especially arachidonic acid, is mainly responsible for ferroptosis induction, while cumulative GPX4 and the inactivation of ACSL4 can attenuate ferroptosis by reducing lipid alcohol conversion and PL biosynthesis, respectively (24–26). At the organoid level, significant changes in mitochondrial morphology usually lead to increased membrane density, condensation or swelling and rupture of the outer membrane (27, 28).

Accumulating studies have suggested that ferroptosis participates in human diseases through a variety of mechanisms, the most likely of which is tumor suppression (23). The underlying mechanism of tumor suppression through ferroptosis in CRC remains to be investigated. In KRAS-mutant CRC cells, combination treatment with β-elemene and cetuximab enhanced the cytotoxic effect against cancer cells by inducing ferroptosis and inhibiting EMT (29). Moreover, it has been reported that the compound IMCA can upregulate SLC7A11, resulting in ROS accumulation and promoting ferroptosis (30). GPX4 is the core marker of ferroptosis, which protects cells from oxidative stress, and degradation of GPX4 contributes to ferroptosis (31). In our research, GPX4 expression was negatively correlated with the survival of CRC patients, which demonstrated the tumor inhibition effect of ferroptosis in CRC (Supplementary Figure 2). Thus, ferroptosis-inducing agents might be a potential therapeutic option for CRC treatment (32).

The exploration of ferroptosis and FRGs aimed to develop effective biomarkers for CRC prognosis prediction and therapy monitoring. In this study, we identified 8 candidates FRGs from 214 FRGs according to the FerrDb website and TCGA database and constructed a CRC predictive model. Further calculations revealed a high correlation between the survival outcomes of CRC patients and the risk score, as confirmed by uni- and multivariate Cox regression analyses. The survival rate of CRC patients in the high-risk group was significantly lower than that of CRC patients in the low-risk group, and the ROC curve for 5-year survival prediction and AUC for the risk score model showed good accuracy. These results revealed that our prognostic model, which was retrospectively validated in CRC patients at risk for mortality, had a good fit and predictive ability.

According to previous studies, the 8 FRGs selected for model construction play an important role by functionally inhibiting or promoting tumor progression in different tumor types. According to

10.3389/fonc.2023.1133946

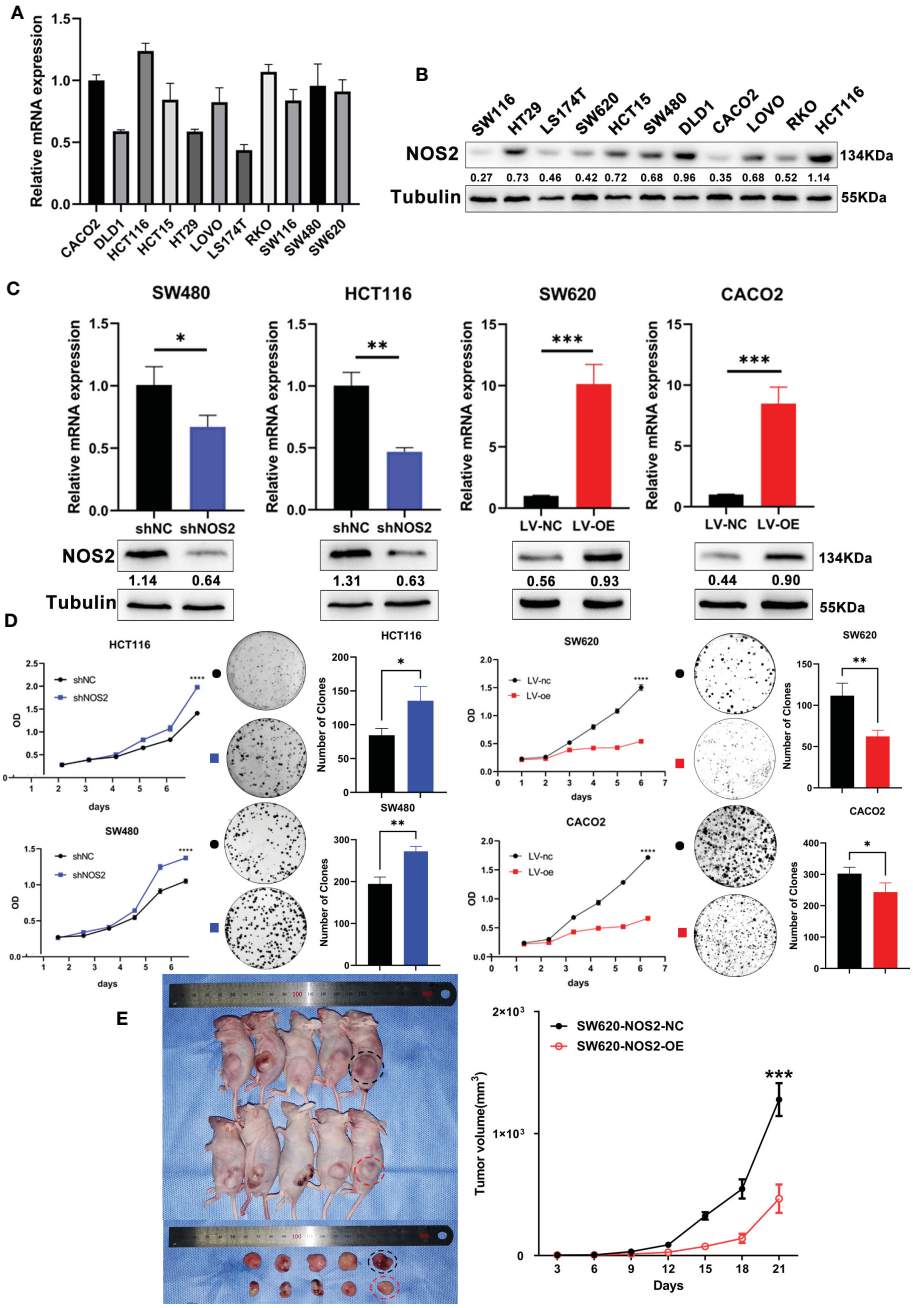

FIGURE 6
NOS2 suppresses tumor proliferation *in vitro* and vivo. **(A)** q-PCR and **(B)** western blot determined the endogenous expression of NOS2 in 11 CRC cell lines. **(C)** q-PCR and western blot results of NOS2 expression upon knockdown and overexpression of NOS2 in different cell lines. **(D)** MTT assay (Left) and clonogenic assay (Right) on cell proliferation ability. **(E)** Subcutaneous xenograft tumor model and growth rates of tumor xenografts inoculated subcutaneously. p>0.05; *, p<0.05; **, p<0.01; ***, p<0.001.

our data, NOS2 was one of the most significantly affected FRGs, and the most obvious expression differences between high risk and low risk groups patients, therefore we began to explore the biological functions and the molecular mechanism of NOS2 in CRC. NOS2 is an inducible isoform of NOS enzymes and functions as a key inflammatory enzyme responsible for nitric oxide biosynthesis (33). Recent studies connected NOS2 and ferroptosis were almost based on bioinformatic analysis, and NOS2 had been identified as the marker of ferroptosis functions in the process of HIF-1 signaling pathway, NOD-like receptor signaling pathway, central carbon metabolism and macrophage polarization (13, 34, 35). The dysregulation of NOS2 expression can be observed under pathological conditions, including cytokine exposure, inflammation and tumors (33, 36). A large number of studies have considered NOS2 to be a promoter and a prognostic indicator for malignancy progression. In hepatocellular carcinomas, NOS2 is a Wnt β-catenin/Tcf-4 target gene that promotes tumorigenesis (37).

10.3389/fonc.2023.1133946

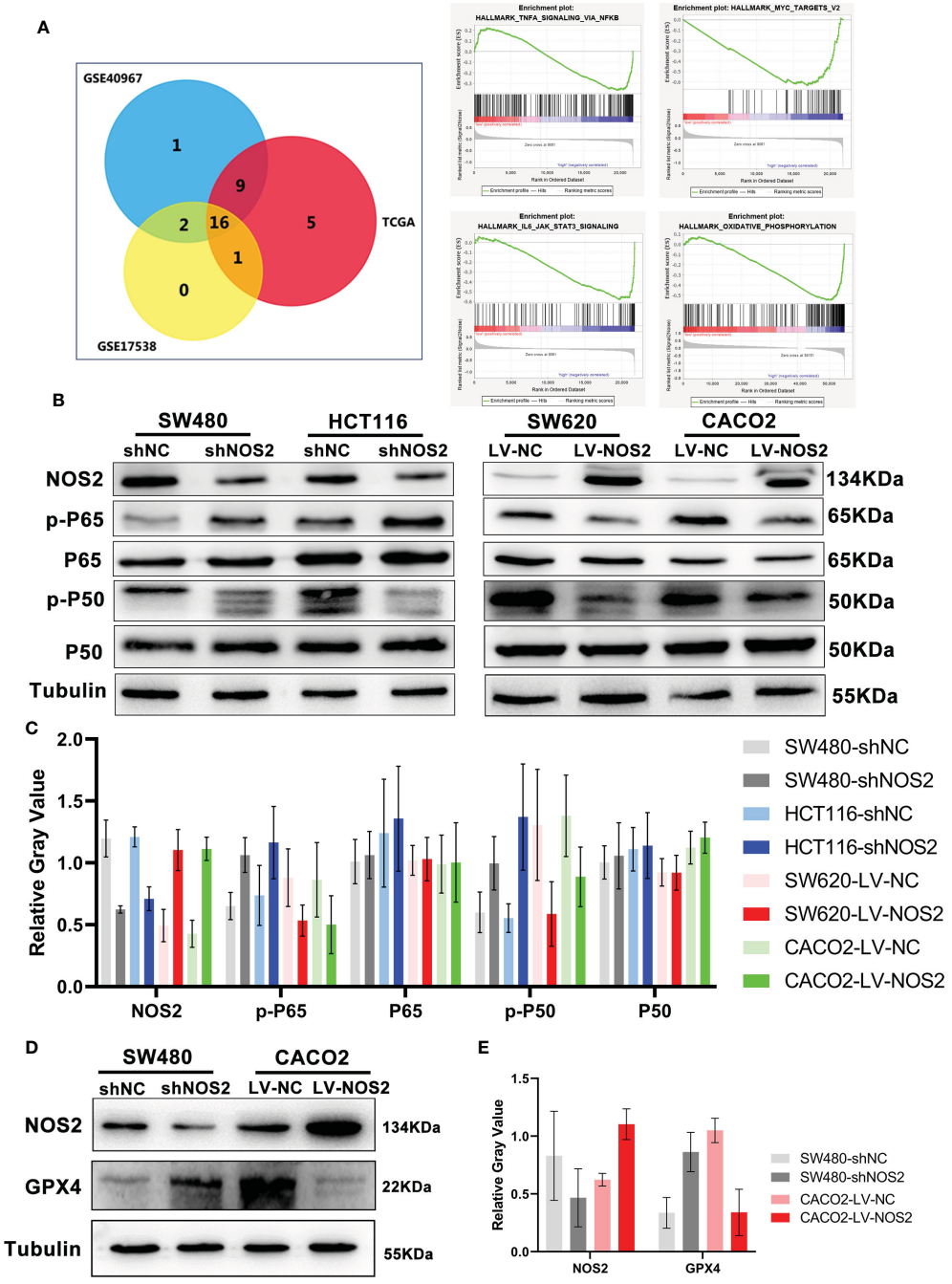

FIGURE 7
NOS2 inhibited NF-κB signaling pathway. **(A)** The wayne figures of overlapping and different enrichment pathways between different NOS2 expression samples in 3 databases. The NF-κB signaling pathway was the most significantly enriched pathway. **(B)** NF-κB activation in different cell lines with NOS2 knockdown and overexpression was monitored by western blot analysis. **(C)** Relative expression of NOS2 and NF-κB signaling proteins. The data were expressed as the ratio of specific protein level (gray value) to Tubulin protein level (gray value). **(D)** Western blot results of GPX4 expression upon knockdown and overexpression of NOS2 in CRC cells. **(E)** Relative expression of NOS2 and GPX4.

However, NOS2 has also been proven to have both antitumoricidal functions and tumor suppressive properties in various tumors.

It was shown that a high level of NO induced the phosphorylation and stabilization of p53 (38). In patients with ulcerative colitis or Crohn's disease, NOS2 and p-p53 are colocalized in tissues (36). Moreover, in several trials, selective or nonselective NOS2 inhibitors did not have a therapeutic benefit in some diseases (39–41). Thus, the underlying molecular mechanisms by which NOS2 promotes the progression of CRC have remained complex and need to be further explored. In our model, considering that NOS2 was the most prominent gene and that decreased NOS2 expression was clearly linked to a poor prognosis, we performed

biological function experiments *in vitro* and *in vivo*. The results suggested that elevated NOS2 significantly inhibited CRC cell proliferation and promoted apoptosis.

Though NOS2 had been reported involving in the development of tumors in our research, the underlying molecular mechanism is still unclearly elucidated. Our further exploration of the molecular mechanism preliminarily revealed that the inhibition of NF-κB signaling might be an important contributor to CRC when NOS2 is upregulated. In breast cancer, the co-expression of NOS2 and COX2 is involved in the regulation of oncogenic pathways such as ERK, PI3K and NF-κB results in a poor prognosis (42, 43). Among the inflammatory diseases, NOS2 might inhibit the phosphorylation of NF-κB (44). Our results showed that the expression level of NOS2 could induce the opposite expression of GPX4, which might demonstrate that NOS2 can participate in GPX4 synthesis or breakdown, repress NF-κB pathway by inhibiting the phosphorylation of the p50 and p65, and thus regulated the ferroptosis in CRC cells.

Nevertheless, this study was subject to several limitations. First, it was a retrospective study, and selection bias cannot be ruled out. Second, although effective external verification was performed, internal data validation is still lacking. In addition, the molecular mechanisms underlying the 8 identified FRGs need to be further explored.

In summary, our research demonstrated, for the first time to our knowledge, the potential prognostic value of FRGs in CRC patients. The construction of a predictive model based on FRGs may be helpful for decision-making in clinical practice. In addition, our results suggest that NOS2 might inhibit CRC cell growth and induce apoptosis by inhibiting NF-κB signaling pathways *in vitro* and *in vivo*.

Data availability statement

The original contributions presented in the study are included in the article/Supplementary Material, further inquiries can be directed to the corresponding authors.

Ethics statement

The animal study was reviewed and approved by Ethics Committee of Guangdong Provincial Hospital of Chinese Medicine.

Author contributions

XY and HL designed the study. XF, YH, and JW performed the molecular biology experiments and statistical analysis. XY, CH, and HL contributed to administrative, technical, or material support. HL and XF wrote the manuscript. All authors contributed to the article and approved the submitted version.

Funding

This study was supported by Leading Innovation Specialist Support Program of Guangdong Province, the Science and Technology Planning Project of Ganzhou (No. 202101074816), Scientific Research Project of Guangdong Provincial Traditional Chinese Medicine Bureau (No. 20211155), Medical Scientific Research Foundation of Guangdong Province (No. A2022305), National Key Clinical Specialty Construction Project (2021–2024, No. 2022YW030009), National Natural Science Foundation of China (No. 82260501), the Science and Technology Planning Project of Guangdong Provincial People's Hospital (Guangdong Academy of Medical Sciences, No. DFJH201913), CSCO-Roche Cancer Research Foundation (No. Y-2019Roche-190) and CSCO-Haosen Research Foundation (No.YHS2019/2–050).

Acknowledgments

Our authors deeply appreciate the editors and reviewers for their help with the manuscript.

Conflict of interest

The authors declare that the research was conducted in the absence of any commercial or financial relationships that could be construed as a potential conflict of interest.

Publisher's note

Supplementary material

The Supplementary Material for this article can be found online at: https://www.frontiersin.org/articles/10.3389/fonc.2023.1133946/full#supplementary-material

SUPPLEMENTARY FIGURE 1
Different NOS2 expression level hardly affected STAT3 and c-MYC signaling pathway.

SUPPLEMENTARY FIGURE 2
Kaplan-Meier survival curves of OS with GPX4 expression level.

References

1. Dekker E, Tanis PJ, Vleugels JLA, Kasi PM, Wallace MB. Colorectal cancer. *Lancet* (2019) 394(10207):1467–80. doi: 10.1016/S0140-6736(19)32319-0

2. Bray F, Ferlay J, Soerjomataram I, Siegel RL, Torre LA, Jemal A. Global cancer statistics 2018: GLOBOCAN estimates of incidence and mortality worldwide for 36 cancers in 185 countries. *CA Cancer J Clin* (2018) 68(6):394–424. doi: 10.3322/caac.21492

3. Arnold M, Sierra MS, Laversanne M, Soerjomataram I, Jemal A, Bray F. Global patterns and trends in colorectal cancer incidence and mortality. *Gut* (2017) 66(4):683–91. doi: 10.1136/gutjnl-2015-310912

4. Sharma R. An examination of colorectal cancer burden by socioeconomic status: evidence from GLOBOCAN 2018. *EPMA J* (2020) 11(1):95–117. doi: 10.1007/s13167-019-00185-y

5. Duffy MJ, Crown J. Drugging "undruggable" genes for cancer treatment: are we making progress? *Int J Cancer* (2020) 148(1):8–17. doi: 10.1002/ijc.33197

6. Sveen A, Kopetz S, Lothe RA. Biomarker-guided therapy for colorectal cancer: strength in complexity. *Nat Rev Clin Oncol* (2020) 17(1):11–32. doi: 10.1038/s41571-019-0241-1

7. Dixon SJ, Lemberg KM, Lamprecht MR, Skouta R, Zaitsev EM, Gleason CE, et al. Ferroptosis: an iron-dependent form of nonapoptotic cell death. *Cell* (2012) 149 (5):1060–72. doi: 10.1016/j.cell.2012.03.042

8. Liang C, Zhang X, Yang M, Dong X. Recent progress in ferroptosis inducers for cancer therapy. *Adv Mater* (2019) 31(51):e1904197. doi: 10.1002/adma.201904197

9. Xie Y, Zhu S, Song X, Sun X, Fan Y, Liu J, et al. The tumor suppressor p53 limits ferroptosis by blocking DPP4 activity. *Cell Rep* (2017) 20(7):1692–704. doi: 10.1016/j.celrep.2017.07.055

10. Chen P, Li X, Zhang R, Liu S, Xiang Y, Zhang M, et al. Combinative treatment of beta-elemene and cetuximab is sensitive to KRAS mutant colorectal cancer cells by inducing ferroptosis and inhibiting epithelial-mesenchymal transformation. *Theranostics* (2020) 10(11):5107–19. doi: 10.7150/thno.44705

11. Zhang Y, Song J, Zhao Z, Yang M, Chen M, Liu C, et al. Single-cell transcriptome analysis reveals tumor immune microenvironment heterogenicity and granulocytes enrichment in colorectal cancer liver metastases. *Cancer Lett* (2020) 470:84–94. doi: 10.1016/j.canlet.2019.10.016

12. Chapkin RS, Navarro SL, Hullar MAJ, Lampe JW. Diet and gut microbes act coordinately to enhance programmed cell death and reduce colorectal cancer risk. *Dig Dis Sci* (2020) 65(3):840–51. doi: 10.1007/s10620-020-06106-8

13. He J, Li X, Yu M. Bioinformatics analysis identifies potential ferroptosis key genes in the pathogenesis of pulmonary fibrosis. *Front Genet* (2021) 12:788417. doi: 10.3389/fgene.2021.788417

14. Chen Y, Li H. Prognostic and predictive models for left- and right- colorectal cancer patients: a bioinformatics analysis based on ferroptosis-related genes. *Front Oncol* (2022) 12:833834. doi: 10.3389/fonc.2022.833834

15. Vannini F, Kashfi K, Nath N. The dual role of iNOS in cancer. *Redox Biol* (2015) 6:334–43. doi: 10.1016/j.redox.2015.08.009

16. Somasundaram V, Gilmore AC, Basudhar D, Palmieri EM, Scheiblin DA, Heinz WF, et al. Inducible nitric oxide synthase-derived extracellular nitric oxide flux regulates proinflammatory responses at the single cell level. *Redox Biol* (2020) 28: 2213-17. doi: 10.1016/j.redox.2019.101354

17. Perwez Hussain S. Deciphering the complex biological interactions of nitric oxide in cancer. *Redox Biol* (2015) 5:413. doi: 10.1016/j.redox.2015.09.011

18. Thomas DD, Wink DA. NOS2 as an emergent player in progression of cancer. *Antioxid Redox Signal* (2017) 26(17):963–5. doi: 10.1089/ars.2016.6835

19. Fransen K, Elander N, Soderkvist P. Nitric oxide synthase 2 (NOS2) promoter polymorphisms in colorectal cancer. *Cancer Lett* (2005) 225(1):99–103. doi: 10.1016/j.canlet.2005.02.006

20. Speckmann B, Pinto A, Winter M, Förster I, Sies H, Steinbrenner H. Proinflammatory cytokines down-regulate intestinal selenoprotein P biosynthesis via NOS2 induction.. *Free Radic Biol Med.* (2010) 49(5):777–85. doi: 10.1016/j.freeradbiomed.2010.05.035

21. Marigo I, Zilio S, Desantis G, Mlecnik B, Agnellini AH, Ugel S, et al. T Cell cancer therapy requires CD40-CD40L activation of tumor necrosis factor and inducible nitric-Oxide-Synthase-Producing dendritic cells. *Cancer Cell* (2016) 30(4):651. doi: 10.1016/j.ccell.2016.09.009

22. Zhu Y, Wang R, Chen W, Chen Q, Zhou J. Construction of a prognosis-predicting model based on autophagy-related genes for hepatocellular carcinoma (HCC) patients. *Aging (Albany NY).* (2020) 12(14):14582–92. doi: 10.18632/aging.103507

23. Stockwell BR, Jiang X, Gu W. Emerging mechanisms and disease relevance of ferroptosis. *Trends Cell Biol* (2020) 30(6):478–90. doi: 10.1016/j.tcb.2020.02.009

24. Lei G, Zhang Y, Koppula P, Liu X, Zhang J, Lin SH, et al. The role of ferroptosis in ionizing radiation-induced cell death and tumor suppression. *Cell Res* (2020) 30 (2):146–62. doi: 10.1038/s41422-019-0263-3

25. Kagan VE, Mao G, Qu F, Angeli JP, Doll S, Croix CS, et al. Oxidized arachidonic and adrenic PEs navigate cells to ferroptosis. *Nat Chem Biol* (2017) 13(1):81–90. doi: 10.1038/nchembio.2238

26. Seibt TM, Proneth B, Conrad M. Role of GPX4 in ferroptosis and its pharmacological implication. *Free Radic Biol Med* (2019) 133:144–52. doi: 10.1016/j.freeradbiomed.2018.09.014

27. Tang D, Chen X, Kang R, Kroemer G. Ferroptosis: molecular mechanisms and health implications. *Cell Res* (2020). doi: 10.1038/s41422-020-00441-1

28. Gao M, Yi J, Zhu J, Minikes AM, Monian P, Thompson CB, et al. Role of mitochondria in ferroptosis. *Mol Cell* (2019) 73(2):354–363 e353. doi: 10.1016/j.molcel.2018.10.042

29. Chen P, Li X, Zhang R, Liu S, Xiang Y, Zhang M, et al. Combinative treatment of β-elemene and cetuximab is sensitive to KRAS mutant colorectal cancer cells by inducing ferroptosis and inhibiting epithelial-mesenchymal transformation. (2020) 10 (11):5107–19. doi: 10.7150/thno.44705

30. Zhang L, Liu W, Liu F, Wang Q, Song M, Yu Q, et al. Corrigendum to "IMCA induces ferroptosis mediated by SLC7A11 through the AMPK/mTOR pathway in colorectal cancer". (2020) 2020:6901472. doi: 10.1155/2020/6901472

31. Ursini F, Maiorino M. Lipid peroxidation and ferroptosis: the role of GSH and GPx4. *Free Radic Biol Med* (2020) 152:175–85. doi: 10.1016/j.freeradbiomed.2020.02.027

32. Weigand I, Schreiner J, Röhrig F, Sun N, Landwehr LS, Urlaub H, et al. Active steroid hormone synthesis renders adrenocortical cells highly susceptible to type II ferroptosis induction. *Cell Death Dis.* (2020) 11(3):192. doi: 10.1038/s41419-020-2385-4

33. Basudhar D, Bharadwaj G, Somasundaram V, Cheng RYS, Ridnour LA, Fujita M, et al. Understanding the tumour micro-environment communication network from an NOS2/COX2 perspective. *Br J Pharmacol* (2018) 176(2):155–76. doi: 10.1111/bph.14488

34. Fujii J, Osaki T. Involvement of nitric oxide in protecting against radical species and autoregulation of M1-polarized macrophages through metabolic remodeling. *Molecules* (2023) 28(2). doi: 10.3390/molecules28020814

35. Sun S, Wu Y, Maimaitijiang A, Huang Q, Chen Q. Ferroptotic cardiomyocyte-derived exosomes promote cardiac macrophage M1 polarization during myocardial infarction. *PeerJ* (2022) 10:e13717. doi: 10.7717/peerj.13717

36. Thomas DD, Heinecke JL, Ridnour LA, Cheng RY, Kesarwala AH, Switzer CH, et al. Signaling and stress: the redox landscape in NOS2 biology. *Free Radic Biol Med* (2015) 87:204–25. doi: 10.1016/j.freeradbiomed.2015.06.002

37. Wang R, Geller DA, Wink DA, Cheng B, Billiar TR. NO and hepatocellular cancer. *Br J Pharmacol.* (2020) 177(24):5459–66. doi: 10.1111/bph.14838

38. Hofseth LJ, Saito S, Hussain SP, Espey MG, Miranda KM, Araki Y, et al. Nitric oxide-induced cellular stress and p53 activation in chronic inflammation. *Proc Natl Acad Sci USA* (2003) 100(1):143–8. doi: 10.1073/pnas.0237083100

39. Dzavík V, Cotter G, Reynolds HR, Alexander JH, Ramanathan K, Stebbins AL, et al. Effect of nitric oxide synthase inhibition on haemodynamics and outcome of patients with persistent cardiogenic shock complicating acute myocardial infarction: a phase II dose-ranging study. *Eur Heart J.* (2007) 28(9):1109–16. doi: 10.1093/eurheartj/ehm075

40. Hansel TT, Kharitonov SA, Donnelly LE, Erin EM, Currie MG, Moore WM, et al. A selective inhibitor of inducible nitric oxide synthase inhibits exhaled breath nitric oxide in healthy volunteers and asthmatics.. *FASEB J.* (2003) 17(10):1298–300. doi: 10.1096/fj.02-0633fje

41. Hellio le Graverand MP, Clemmer RS, Redifer P, Brunell RM, Hayes CW, Brandt KD, et al. A 2-year randomised, double-blind, placebo-controlled, multicentre study of oral selective iNOS inhibitor, cindunistat (SD-6010), in patients with symptomatic osteoarthritis of the knee. *Ann Rheum Dis.* (2013) 72(2):187–95. doi: 10.1136/annrheumdis-2012-202239

42. Basudhar D, Glynn SA, Greer M, Somasundaram V, No JH, Scheiblin DA, et al. Coexpression of NOS2 and COX2 accelerates tumor growth and reduces survival in estrogen receptor-negative breast cancer. *Proc Natl Acad Sci USA* (2017) 114 (49):13030–5. doi: 10.1073/pnas.1709119114

43. Glynn SA, Boersma BJ, Dorsey TH, Yi M, Yfantis H, Ridnour L, et al. Increased NOS2 predicts poor survival in estrogen receptor-negative breast cancer patients. *J Clin Invest.* (2010) 120(11):3843–54. doi: 10.1172/JCI42059

44. Wei X, Zhang B, Liang X, Liu C, Xia T, Xie Y, et al. Higenamine alleviates allergic rhinitis by activating AKT1 and suppressing the EGFR/JAK2/c-JUN signaling. *Phytomedicine* (2021) 86:153565. doi: 10.1016/j.phymed.2021.153565

frontiers | Frontiers in Molecular Biosciences

TYPE Review
PUBLISHED 14 June 2023
DOI 10.3389/fmolb.2023.1216733

OPEN ACCESS

EDITED BY
Guo Chen,
China Pharmaceutical University, China

REVIEWED BY
Ana Cipak Gasparovic,
Rudjer Boskovic Institute, Croatia
Lixia Gao,
Chongqing University of Arts and Sciences, China

*CORRESPONDENCE
Nadia Zaffaroni,
nadia.zaffaroni@istitutotumori.mi.it

RECEIVED 04 May 2023
ACCEPTED 05 June 2023
PUBLISHED 14 June 2023

CITATION
Beretta GL and Zaffaroni N (2023), Radiotherapy-induced ferroptosis for cancer treatment.
Front. Mol. Biosci. 10:1216733.
doi: 10.3389/fmolb.2023.1216733

Radiotherapy-induced ferroptosis for cancer treatment

Giovanni L. Beretta and Nadia Zaffaroni*

Molecular Pharmacology Unit, Department of Experimental Oncology, Fondazione IRCCS Istituto Nazionale dei Tumori di Milano, Milan, Italy

Ferroptosis is a regulated cell death mechanism controlled by iron, amino acid and reactive oxygen species metabolisms, which is very relevant for cancer therapy. Radiotherapy-induced ferroptosis is critical for tumor suppression and several preclinical studies have demonstrated that the combination of ionizing radiation with small molecules or nano-systems is effective in combating cancer growth and overcoming drug or ionizing radiation resistance. Here, we briefly overview the mechanisms of ferroptosis and the cross-talk existing between the cellular pathways activated by ferroptosis and those induced by radiotherapy. Lastly, we discuss the recently reported combinational studies involving radiotherapy, small molecules as well as nano-systems and report the recent findings achieved in this field for the treatment of tumors.

KEYWORDS

ferroptosis, radiotherapy, reactive oxygen species, nanomedicine, drug combinations, gene signatures

1 Introduction

The accidental cell death (ACD) and the regulated cell death (RCD) govern the cell fate (Tang et al., 2019). Necrosis is the best representative of ACD, which is a passive mechanism allowing plasma membrane rupture, cytoplasm release and inducing inflammation reaction. Conversely, RCD is an active and regulated cell suicide, which can involve or not inflammation reaction, playing crucial functions in tissue homeostasis and in the pathogenesis of several diseases (Galluzzi et al., 2018; Tang et al., 2019). So far, two RCD categories are reported: apoptotic and non-apoptotic. Necroptosis, pyroptosis, autophagy and ferroptosis belong to the non-apoptotic RCD and are classified according to different molecular, morphological, biochemical and functional features (Galluzzi et al., 2018). RCD pathways are implicated in physiologic processes regulating the development of multicellular organisms and represent defense mechanisms against cancer transformation/development as well as against pathogen infections (Galluzzi et al., 2018; Tang et al., 2019). As suggested by its name, ferroptosis is stimulated by the lipid peroxidation provoked by the iron accumulated into the cells. Critical for ferroptosis is the content of polyunsaturated-fatty-acids (PUFA) composing the cellular membrane. PUFA represent a toxic reservoir that in iron- and reactive oxygen species (ROS)-rich conditions are susceptible to peroxidation, leading to membrane damage and cell death (Stockwell et al., 2017).

The induction of ferroptosis is a new interesting strategy for fighting cancer (Lei et al., 2022). This strategy is based on the condition known as iron addiction, which is typical of cancer cells that need higher levels of iron in comparison with healthy cells (Friedmann Angeli et al., 2019). Iron addiction renders cancer cells more sensitive to iron and to iron-induced ROS production (Fenton reaction) than normal cells (Torti and Torti, 2019). Though ferroptosis induction proved efficacy in overcoming resistance to apoptosis developed by tumors exposed to anticancer therapy, tumor cells challenged by

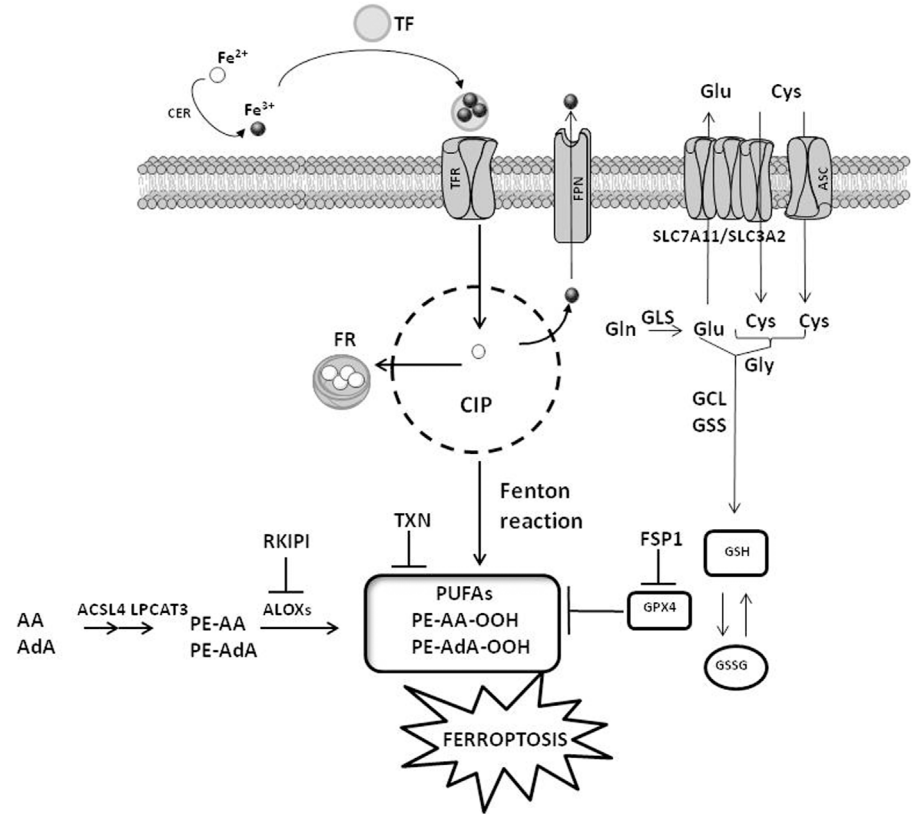

FIGURE 1
Cellular mechanisms of ferroptosis. The cellular pathways involving iron, amino acids and ROS metabolisms are reported. CIP, cellular iron pool; FR, ferritin; CER, ceruloplasmin; TF, transferrin; TFR, transferrin receptor; FPN, ferroportin; ACSL4, acyl-CoA synthetase long-chain family member 4; LPCAT3, lysophosphatidylcholine acyltransferase 3; ALOXs, arachidonate lipoxygenase; GPX4, glutathione peroxidase 4; ASC, alanine–serine–cysteine system; SLC7A11, solute carrier family 7 member 11; SLC3A2, solute carrier family 3 member 2; GLS, glutaminases; GSS, glutathione synthetase; GCL, glutamate-cysteine ligase; PUFAs, polyunsaturated fatty acids; FSP1, ferroptosis suppressor protein 1; TXN, thioredoxin. AA, arachidonoyl; AdA, adrenic acid; PE, phosphatidylethanolamines; RKIPI, Raf1 kinase inhibitory protein GSH, glutathione; GSSG, glutathione disulfide. The figure is prepared using tools from Servier Medical Art (http://www.servier.fr/servier-medical-art, accessed on March 2023).

ferroptosis inducers can evolve defense mechanisms that counteract ferroptosis and in turn preserving cell vitality (Stockwell et al., 2017; Hassannia et al., 2019; Zheng and Conrad, 2020). This implies that drugs hitting cellular pathways involved in resistance to ferroptosis potentiate pharmacological interventions (Liang et al., 2019).

Besides chemotherapy, tumors are treated by radiotherapy as well. The exposure to ionizing radiation (IR) induces DNA damage leading to cell death (Delaney et al., 2005; Jaffray, 2012). Besides direct DNA damage, IR hits water molecules contained into the cells favoring their radiolysis and, together with the activation of specific enzymes, stimulate ROS production. ROS, including peroxides (H_2O_2, ROOH), free radicals (HO•, HO_2•, R•, RO•, NO• and NO_2•), singlet oxygen ($^1O_2$) and superoxide (O_2–•), attack DNA, lipids, and proteins (Azzam et al., 2012; Reisz et al., 2014). DNA damages include nucleotide base damage, single strand breaks (SSBs), and double strand breaks (DSBs) (Baidoo et al., 2013). The cellular response to damaged DNA allows cell-cycle arrest, cellular senescence, and RCD. Although apoptosis is the most studied RCD induced by radiotherapy, other types of RCD are reported in radiotherapy-treated cells, including ferroptosis (Lang et al., 2019; Adjemian et al., 2020; Lei et al., 2020; Ye et al., 2020). Since for the treatment of tumors radiotherapy is administered in combination with chemotherapy, it is conceivable to study the radiotherapy and ferroptosis pathways as well as their cross-talk to set up combination strategies maximizing tumor response.

In this review we briefly overview the cellular pathways implicated in ferroptosis induced by radiotherapy and discuss the potential combination strategies with small molecules and nano-systems for enhancing radiotherapy antitumor activity.

2 General overview on ferroptosis

Compared to apoptosis, autophagy and necrosis, ferroptosis shows peculiar properties. Morphological alterations of mitochondria, including reduction in volume, increased density of the mitochondrial membranes as well as reduced mitochondrial cristae, characterize ferroptotic cells. Cells undergoing ferroptosis are rounded and floating with intact nuclei and uncondensed chromatin (Dixon et al., 2012; Stockwell et al., 2017). Conversely, the typical features of apoptosis (e.g., chromatin condensation and the production of apoptotic bodies)

as well as that of autophagy (e.g., the formation of autophagosomes) are not reported in ferroptotic cells. Agents that inhibit apoptosis, autophagy and necroptosis are ineffective on ferroptosis induction. Therefore, the sensitivity to drugs that induce ferroptosis is maintained by cells deficient in apoptotic-related factors (e.g., BAX, BAK, MLKL, and RIPK1/3). On the contrary, antioxidants and iron chelators inhibit ferroptosis (Vanden Berghe et al., 2010; Lei et al., 2019).

Ferroptosis is governed by three main cellular mechanisms, including i) iron metabolism, ii) amino acid metabolism and iii) ROS metabolism (Figure 1) (Liang et al., 2019).

2.1 Iron metabolism

Iron transport systems regulate iron accumulation and in turn ferroptosis induction. These transporters, including ceruloplasmin (CER), transferrin (TF), transferrin receptor (TFR), ferritin (FR) and ferroportin (FPN), impact on intracellular levels of iron. Adsorbed Fe^{2+} is oxidized to Fe^{3+} by CER and in this form is captured by TF. The interaction of TF with TFR favors the cellular uptake of iron. Upon reduction to Fe^{2+} by the sixtransmembrane epithelial antigen of the prostate 3 (STEAP3), iron is bound to FR or stored into the cellular iron pool (CIP). When cells are saturated by iron, exceeding amounts of Fe^{2+} are oxidized to Fe^{3+} and pumped out of the cells by FPN (Trujillo-Alonso et al., 2019). CIP is controlled by other two factors: the nuclear receptor coactivator 4 (NCOA4), which is a specific receptor favoring FR accumulation into the autophagosome, and the iron-responsive element binding protein 2 (IREB2), which is a transcription factor controlling the iron metabolism by regulating the level of FR (Dixon et al., 2012; Mancias et al., 2014; Tang et al., 2018). Interferences with the iron balance regulated by these mechanisms (e.g., increased uptake or reduced export) stimulate iron-mediated lipid peroxidation and ferroptosis (Yang and Stockwell, 2008; Stockwell et al., 2017).

2.2 Amino acid metabolism

The exchange of cystine/cystathionine across the plasma membranes depends on the red-ox state of the extracellular compartment. Under reducing conditions, the intracellular accumulation of cysteine is controlled by the alanine–serine–cysteine (ASC) system. Conversely, oxidative extracellular conditions stimulate the exchange of cystine/cystathionine with glutamate mediated by Xc–transporter system (Doll and Conrad, 2017). Two subunits linked via a disulfide bridge compose the Xc–, including the catalytic subunit solute carrier family 7 member 11 (SLC7A11) and the regulatory subunit solute carrier family 3 member 2 (SLC3A2). Intracellular glutamate levels, which are under the control of the enzymatic activity degrading glutamine (glutaminolysis) mediated by glutaminases (GLS) 1 and 2, impact on Xc–activity. Diminished cellular content of cysteine, which is stimulated by enhanced GLS activity or reduced SLC7A11 levels as well as reduced activation of spermidine/spermine N1 acetyltransferase 1 (SAT1), favors lipid peroxidation and ferroptosis induction (Jiang et al., 2015; Jennis et al., 2016; Ou et al., 2016; Zhang et al., 2018). Alterations in GLS, SLC7A11 or SAT1 activities, which result in reduced intracellular availability of cysteine, negatively impact on glutathione (GSH) levels triggering ferroptosis (Shah et al., 2017). The synthesis of GSH needs glutamate, cysteine, and glycine and is catalyzed by glutamate-cysteine ligase (GCL) and glutathione synthase (GSS). The erastin-mediated inhibition of Xc–, which reduces cystine uptake, or the inhibition of GSH biosynthesis via buthionine sulfoximine, deplete intracellular GSH levels leading to ferroptosis.

2.3 ROS metabolism

Besides DNA damage, ROS stimulate ferroptosis by provoking alterations in lipid metabolism (D'Herde and Krysko et al., 2017; Lin et al., 2018). The lipid peroxidation occurring in PUFA is among the most important type of cellular damage for ferroptosis induction, and cells with high levels of PUFA are very sensitive to ferroptosis (Yang et al., 2016; Yuan et al., 2016). The catalytic activity of two enzymes, acyl-CoA synthetase long-chain family member 4 (ACSL4) and lysophosphatidylcholine acyltransferase 3 (LPCAT3), which allows the esterification and incorporation of PUFA into membrane phospholipids, is crucial for sensitizing cells to ferroptosis. The accumulation of lipid peroxides enhances the formation of additional ROS that increases biomacromolecule damage leading to cell membrane destabilization and micelle formation, in turn enhancing ferroptosis induction (Gaschler and Stockwell, 2017; Feng and Stockwell, 2018). Two proteins are critical for ferroptosis induction as well, the small scaffolding protein Raf1 kinase inhibitory protein (RKIP1) and the seleno enzyme glutathione peroxidase 4 (GPX4) (Wenzel et al., 2017; Tang et al., 2018; Liang et al., 2019). By interacting with the iron-containing enzyme arachidonate lipoxygenase 15 (ALOX15), RKIP1interferes with the production of phospholipid alcohols regulating ferroptosis. Similarly, GPX4 is a detoxifying enzyme catalyzing the transformation of PUFA into non-toxic phospholipid alcohols. The red-ox reaction involving the oxidation of GSH into GSSG is required by GPX4 to accomplish its catalytic activity, and cells showing high levels of GPX4 are less susceptible to ferroptosis (Seibt et al., 2019). On the contrary, compounds impairing the activity of GPX4 by reducing its expression/activity are typical ferroptosis inducers (Tang et al., 2018; Liang et al., 2019). Since the activity of GPX4 needs selenocysteine tRNA, whose cellular amount is controlled by the mevalonate (MVA) pathway, the inhibition of MVA pathway favors ferroptosis by reducing the availability of selenocysteine tRNA (Kryukov et al., 2003). Another protein controlling GPX4 activity is the ferroptosis suppressor protein 1 (FSP1). FSP1 inhibits GPX4 and its expression is high in cells resistant to ferroptosis. Elevated levels of FSP1 protect cells against compounds that induce ferroptosis by targeting GPX4 (Bersuker et al., 2019; Doll et al., 2019). Upon myristoylation, the cytoplasmic FSP1 moves to the plasma membranes and in this peculiar cellular localization catalyzes the reduction of coenzyme Q10. This behavior, in presence of GSH as well as active GPX4, attenuates the

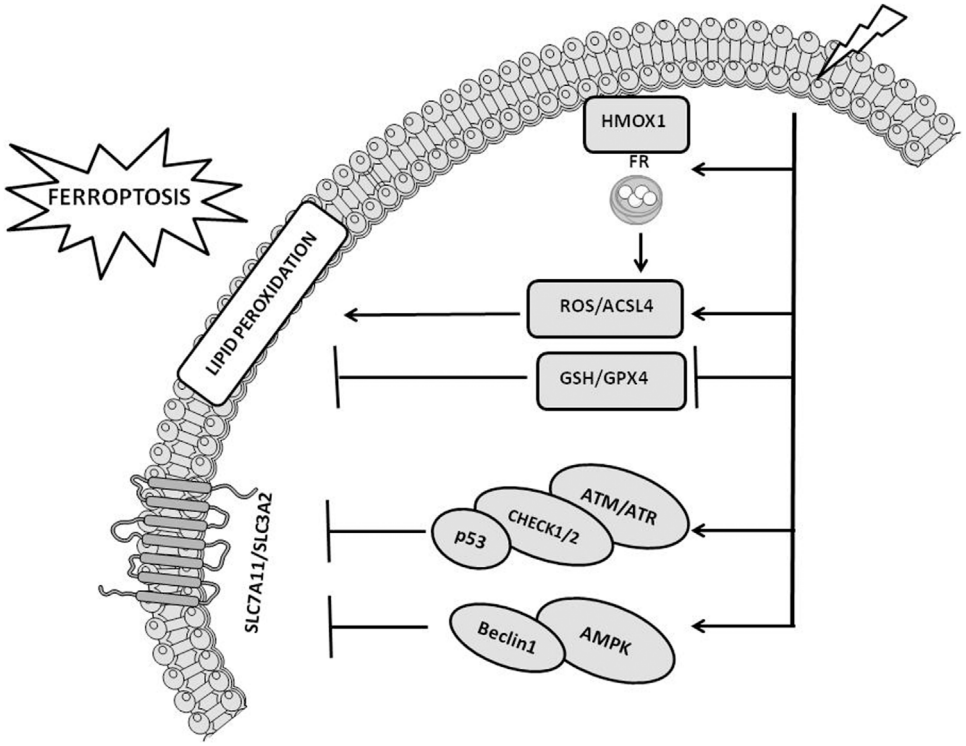

FIGURE 2
Cellular pathways implicated in radiotherapy-induced ferroptosis. The figure reports the cross-talk occurring between ionizing radiation and ferroptosis pathways, including ROS/ACSL4, GSH/GPX4, SLC7A11, ATM/ATR, and AMPK pathways. The figure is prepared using tools from Servier Medical Art (http://www.servier.fr/servier-medical-art, accessed on March 2023).

propagation of lipid peroxide production and reduces phospholipid peroxidation attenuating ferroptosis (Doll et al., 2019).

3 Cross-talk between radiotherapy and ferroptosis in cancer

Besides direct damage of biomacromolecules (e.g., DNA, proteins and lipids), radiotherapy generates ROS, which are the most important molecules responsible for lipid peroxide accumulation and ferroptosis. The relationship between radiotherapy and ferroptosis is corroborated by several evidence, including the specific staining (e.g., C11-BODIPY) as well as the increased expression of specific markers (e.g., MDA, 4-HNE and prostaglandin-endoperoxide synthase 2, PTGS2) reflecting lipid peroxidation observed in IR-exposed cancer cell lines and tumor samples. Moreover, irradiated cells show morphological alterations of mitochondria typical of ferroptosis (Lang et al., 2019). Of note, these features depend on IR doses administered. In support of the cross-talk between radiotherapy and ferroptosis is the observation that treatment of cells with iron chelators (e.g., deferoxamine) or with ferroptosis inhibitors (e.g., ferrostatin-1 and liproxstatin-1) before exposure to IR partially rescue their survival, and that this finding is more evident in comparison to what observed combining IR with compounds that inhibits other RCD (Lei et al., 2021).

Three major pathways regulate IR-mediated ferroptosis induction (Lang et al., 2019; Lei et al., 2020; Ye et al., 2020) (Figure 2), including 1) ROS and ACSL4. Increased ROS produced by IR are responsible for the formation of PUFA radicals that, following the interaction with oxygen (Fenton reaction), generate lipid hydroperoxides (PUFA-OOH) (Lei et al., 2020). This pathway is powered by the IR-induced ACSL4 expression (Figure 1) that, together with LPCAT3, favors the synthesis of phospholipid containing PUFA, which are also liable of peroxidation; 2) GSH and GPX4. IR exposure depletes GSH leading to reduced activity/expression of GPX4 and in such a way attenuating the GPX4-mediated detoxification functions leading to increased toxic effects of lipid peroxides (Ye et al., 2020) and 3) SLC7A11. Reduced levels of SLC7A11 favor ferroptosis by downregulating cystine uptake and in turn GSH synthesis and GPX4 functions (Figure 1). Through the activation of ataxia telangiectasia mutated serine/threonine kinase (ATM), IR represses SLC7A11 levels stimulating ferroptosis. Other studies have underlined that the expression of SLC7A11 is increased upon IR exposure leading to the interpretation that an adaptive cellular response to IR rescues the SLC7A11 expression or that the level of SLC7A11 upon IR exposure depends on a peculiar cellular context (Xie et al., 2011; Lei et al., 2020).

The activation of the cellular pathways induced by the DNA damage together with the stimulation of signaling pathways associated with alterations of lipids contained into the cellular membranes occurring upon radiotherapy exposure synergize each

other leading to enhanced tumor growth inhibition (Lei et al., 2020). IR-induced DNA damage increases the expression of sensor proteins, including ATM and ataxia telangiectasia and Rad3 related serine/threonine kinase (ATR) that recognize the altered DNA and stimulate DNA damage response signaling cascades (DDR). DDR activate checkpoint kinases 1/2 (chk1/2) and in turn stimulate the phosphorylation of p53 inducing cell-cycle arrest. The block of the cell-cycle is required by the cells to test the severity of the damage and "decide" their fate, 1) survive, upon the activation of the DNA repair machine in case the damage can be corrected, or 2) comit suicide, in case the damage is irreparable or not correctly repaired, triggering RCD, including ferroptosis (Maier et al., 2016; Huang and Zhou, 2020). Upon p53-mediated cell-cycle arrest, irradiated cells mostly activate senescence (Bieging et al., 2014; Maier et al., 2016). P53 mutation, which is a very common condition in tumors, engage an alternative senescence checkpoint protein, p16-retinoblastoma (RB) (Sabin and Anderson, 2011). Senescence can coexists with apoptosis and in case of prolonged p53 activation, IR preferentially stimulates both intrinsic (e.g., PUMA, BAX, NOXA, cytochrome C and caspase-9/3/7) and extrinsic apoptosis (e.g., FAS/CD95, DR5, FAS ligands and caspase-8) rather than senescence (Sheikh and Fornace, 2000; Aubrey et al., 2018; Mijit et al., 2020). Besides the above mentioned RCD, radiotherapy can induce autophagy and necroptosis. Since autophagy has both pro-survival and pro-cell death properties, controversial and not completely elucidated is its role in IR response (Hu et al., 2016). Similarly, also the role of necroptosis in radiation response is ambiguous (Adjemian et al., 2020).

ATM activated by DNA damage increases p53 expression that reduces the levels of SLC7A11 via a repressing interaction with SLC7A11 promoter or by stimulating USP7-mediated proteasome degradation of SLC7A11, in turn leading to ferroptosis (Kang et al., 2019; Wang et al., 2019). Similarly, p53 induces ferroptosis by stimulating the expression of SAT1, GLS2 or ferredoxin reductase (FDXR) (Hu et al., 2010; Ou et al., 2016; Zhang et al., 2017). In addition, p53 controls the expression of MDM2 that, via regulating lipid metabolism and FSP1 expression, favors ferroptosis (Venkatesh et al., 2020). Conversely, ferroptosis is attenuated upon p53-mediated upregulation of p21. Metabolic stress induced by cystine deprivation stimulates the p53-p21 axis preserving GSH levels and attenuating ferroptosis (Tarangelo et al., 2018). Another protein involved in IR-induced ferroptosis is the AMP-activated protein Kinase (AMPK) (Lei et al., 2020; Ye et al., 2020). This protein can either stimulate or inhibit ferroptosis. By stimulating the phosphorylation of beclin 1, which in turn favors the downregulation of Xc−, activated AMPK induces ferroptosis (Song et al., 2018). In the other hand, AMPK activates the biosynthesis of PUFA containing phospholipids inhibiting ferroptosis (Lee et al., 2020). IR stimulates the expression of heme oxygenase 1 (HMOX1) and FR, which trigger the release of iron and in such a way the induction of ferroptosis (Chiang et al., 2018). Conversely, the exposure to IR upregulates FR heavy chain (FTH1) and reduces oxidative stress in turn attenuating ferroptosis and promoting radiation resistance (Choudhary et al., 2020). These findings indicates an intersection between cellular pathways implicated in DNA damage response and RCD, which includes, besides ferroptosis, the immunogenic cell death (ICD) mechanisms embracing apoptosis, necroptosis and autophagy. Upon radiotherapy-mediated ICD stimulation, T-cells recruited into the tumor microenvironment (TME) promote ferroptosis (Lang et al., 2019).

3.1 Combination strategies for enhancing ionizing radiation antitumor activity and for overcoming radiation resistance

Radiation resistance of tumors is an urgent clinical problem responsible for treatment failure. The understanding of the molecular mechanisms subtending radiation resistance is critical for setting up medical strategies, including drug combinations, aimed at improving rediotherapy response (Table 1).

Radiotherapy is used for the clinical management of patients with different tumor types including nasopharyngeal carcinoma (NPC) and the development of radiation resistance is the main cause of treatment failure in NPC-suffering patients. Huang et al. report that these patients show increased expression of m6A mRNA demethylase fat mass and obesity-associated protein (FTO) and that this feature correlates with radiation resistance and poor prognosis (Huang et al., 2023). In support of this observation is the finding that increased levels of FTO characterize NPC cell lines resistant to IR (C666-1R, HONE1R) compared to the corresponding sensitive counterparts (C666-1, HONE1). NPC cells exposed to IR show morphological changes typical of ferroptosis, increased MDA levels and reduced GSH cellular content. The treatment with FB23-2 (a FTO inhibitor) counteracts this behavior, which is reversed following FTO overexpression or upon exposure to ferrostatin-1. Moreover, the IR response of resistant cells is significantly improved by FB23-2 treatment. The exposure to IR and FB23-2 increases DNA damage *in vitro* and this observation is corroborated *in vivo* in xenograft HNE1R-bearing mice. The authors speculate that a link exists between FTO and OTU deubiquitinase, ubiquitin aldehyde binding 1 (OTUB1). Molecularly, via its demethylase activity, FTO produces m6A modification of the OTUB1 transcript stimulating the expression of OTUB1 protein and its interaction with SLC7A11, in turn activating SLC7A11 and leading to ferroptosis inhibition and radiation resistance. These interpretations are supported *in vivo* in xenograft HONE1R-bearing mice and PDX-mouse models exposed to the combination erastin/IR. Compared to IR alone, the combination with the ferroptosis inducer erastin enhances the radiosensitivity of HONE1R tumors.

Another key protein implicated in radiation resistance by inhibiting ferroptosis is angiopoietin-like 4 (ANGPTL4) (Zhang et al., 2022). High levels of ANGPTL4 associate with poor prognosis of patients suffering from lung adenocarcinoma and adrenocortical carcinoma. A549 and H1299 lung cancer cell lines cultured under hypoxic condition show an increased expression of ANGPTL4 and radiation resistance. Moreover, compared to cells cultured under physiologic conditions, hypoxic cells show higher levels of ANGPTL4 accumulated into released exososmes. Upon silencing of ANGPTL4, A549 cells restore the sensitivity to IR, while reacquire IR resistance after ANGPTL4 ectopic expression. The relationship between ANGPTL4 and ferroptosis is demonstrated in ANGPTL4-overexpressing cells cultured under normoxia, which show increased expression of GPX4, SLC7A11, FTH1, and FTL (e.g., reduced ferroptosis and enhanced radiation resistance). Conversely, the above ferroptosis-associated proteins are decreased in

TABLE 1 Combination strategies for enhancing ferroptosis induced by ionizing radiation.

Tumor type	Cell lines	Pathway involved	*In vivo* evaluation	Combination strategy	References
Nasopharyngeal carcinoma	C666-1	FTO/OTUB1/SLC7A11	HONE1R	IR/FB23-2	Huang et al. (2023)
	HONE1				
	C666-1R				
	HONE1R				
Lung cancer	A549	ANGPL4/GPX4/SLC7A11	A549	IR/ANGPTL4 enriched exosomes	Zhang et al. (2022)
	H1299				
Hepatocellular carcinoma	SK-Hep	SOCS2/SLC7A11	SK-Hep-1 SK-Hep-1R	IR/SOCS2-overexpressing plasmid	Chen et al. (2023)
	HepG2				
	SK-Hep-1R				
	HepG2-1R				
Hepatocellular carcinoma	HepG2	COMMD10/HIF1α/ SLC7A11	HepG2	IR/Cu chelator	Yang et al. (2022)
	MHCC-97H				
Oral squamous cell carcinoma	SCC15-S	GPX4	SCC15-R	IR/Hyperbaric oxygen (HBO)	Liu et al. (2022)
	SCC15-R				
Colorectal cancer	MC38	ATF3-SLC7A11-GPX4	MC38	IR/niraparib	Shen et al. (2022)
	CT26				
	HT29				
Esophageal squamous cell carcinoma	KYSE30	SCD1	N.D.	IR/MF-438	Luo et al. (2022)
	KYSE70				
	KYSE140				
	KYSE150				
	KYSE410				
	KYSE450				
	KYSE510				

N.D., not defined.

ANGPTL4-silenced cells cultured under hypoxic conditions (e.g., increased ferroptosis and radiosensitivity). *In vivo* experiments in xenograft A549-bearing mice treated with ANGPTL4 enriched exosomes and exposed to IR support *in vitro* data confirming the relationship between radiation resistance and ferroptosis.

Radiation resistance accounts for the failure of radiotherapy in hepatocellular carcinoma (HCC) as well and Chen and colleagues have studied the role played by ferroptosis in radiosensitizing HCC using a panel of radiosensitive (SK-Hep and HepG2) and radioresistant (SK-Hep-1R and HepG2-1R) HCC cell lines (Chen et al., 2023). By comparing the gene expression profiles of SK-Hep and SK-Hep-1R cells, SOCS2, and SMOX genes were identified as differentially expressed. The expression of SOCS2 gene was reduced in SK-Hep-1R, while SMOX was increased. Gene expression data from GEPIA and HCCDB databases and Kaplan-Meier (K-M) analysis showed that low expression of SOCS2 and high expression of SMOX correlate with poor prognosis of HCC patients. The radiation resistance observed in resistant cells is overcome upon SOCS2 ectopic expression. Conversely, radiation resistance is enhanced in SK-Hep and HepG2 cells following SOCS2 silencing. *In vivo* experiments confirm the *in vitro* results. Moreover, immunohistochemical staining of irradiated explanted tumors shows an increased expression of SOCS2 paralleled by a modulation of ferroptosis markers, including a downregulation of GPX4 and SLC7A11, and an increased expression of 4-HNE. This observation is confirmed in a set of clinical tissues in which the levels of ferroptosis markers correlate with radiotherapy response. Co-immunoprecipitation assays demonstrate a protein interaction between SOCS2 and SLC7A11. Following the protein interaction, the E3-ubiquitin ligase activity of SCOS2 allows ubiquitination and proteasomal degradation of SLC7A11 leading to ferroptosis.

Iron homeostasis is controlled by copper (Cu) and elevated levels of this micronutrient impact on tumorigenesis, resistance to treatments and prognosis of HCC suffering patients (Yang et al., 2022). HepG2 and MHCC-97H cells exposed to IR downregulates the copper metabolism MURR1 domain 10 (COMMD10) increasing the cellular accumulation of Cu and leading to radiation resistance. These results are corroborated by gain and

loss of function experiments performed in a panel of HCC cell lines showing that increased COMMD10 levels parallel with reduced cellular accumulation of Cu and radisensitivity. Conversely, reduced expression of COMMD10 increases Cu accumulation leading to radiation resistance. The role played by Cu in tumor growth is confirmed *in vivo* in HepG2-bearing mice fed with Cu-rich food upon irradiation. Compared to mice fed under normal conditions, animals fed with Cu-rich food show increased tumor volume, which is reduced following the administration of a Cu chelator. Moreover, immunohistochemistry analysis of HCC clinical samples shows that the levels of COMMD10 in patients sensitive to radiotherapy are higher than that measured in samples from radioresistant subjects. Proteomic analysis performed in HepG2 and COMMD10-depleted HepG2 cells reveals a differential expression of genes implicated in cell death. These findings, together with the observation that the treatment with ferrostatin-1 and liproxstatin-1 increases the growth of COMMD10 overexperring cells, indicate that ferroptosis is critical for radiosensitivity. Based on the observation that the sequence of the promoter of SLC7A11 contains binding sites for HIF1-α, the authors propose an interplay between COMMD10, SLC7A11, and HIF1-α as a molecular mechanism supporting the cellular response. By interacting with HIF1-α, COMMD10 impedes HIF1-α nuclear translocation and reduces SLC7A11 expression. The IR-mediated reduced expression of COMMD10 favors the cellular accumulation of Cu that stabilizes HIF1-α and inhibits its ubiquitin degradation. Following nuclear translocation, HIF1-α stimulates CER and SLC7A11 transcription inhibiting ferroptosis.

The effect of the co-exposure of IR and hyperbaric oxygen (HBO) on oral squamous cell carcinoma (OSCC) cells is studied by Liu and co-workers (Liu et al., 2022). Compared to the exposure to IR, the combination IR/HBO increases the cytotoxicity in SCC15-S cells, which is only in minimal part mediated by apoptosis. Conversely, the combination enhances the levels of ferroptosis markers (iron, ROS and MDA). Upon IR exposure, cells increase the levels of ACSL4 and SLC7A11 (two ferroptosis promoters) as well as that of GPX4 (a ferroptosis blocker), the latter being the major factor accounting for radiation resistance. The treatment with IR/HBO is ineffective on ACSL4 and SLC7A11 levels, while reduces the expression of GPX4 and in such a way shifts the equilibrium towards the induction of ferroptosis. These findings are corroborated by the observation that the transfection of SCC15-S cells with GPX4-overexpressing plasmid or the treatment with ferrostatin-1 reverse the effects of the combination. The authors also show that IR/HBO exposure sensitizes the radio-resistant SCC15-R cells to IR. Although less sensitive to ferroptosis, SCC15-R cells exposed to the combination significantly reduce the expression of GPX4 in turn favoring ferroptosis, and these results are confirmed *in vivo* in xenograft SCC15-R-bearing mice. Compared to mice treated with IR, animals exposed to IR/HBO show a significant reduction in tumor growth. In support of the ferroptosis induction as a mechanism of tumor growth delay is the observation that the treatment with ferrostatin-1 counteracts the antitumor activity of IR/HBO exposure. A deeper investigation on clinical samples (tumor and normal tissues as well as serum) from 38 OSCC patients shows that, compared to adjacent normal oral tissues, the expression of GPX4 is increased in tumors. In addition, the serum levels of GPX4 in cancer patients are increased in comparison to healthy donors. Of note, high levels of GPX4 (e.g., reduced ferroptosis) are accompanied with poor chemo-radiotherapy outcome.

Another interesting combination for sensitizing colorectal cancer (CC) to IR is proposed by Shen and colleagues (Shen et al., 2022). To protect themselves against DNA damages, cancer cells stimulate poly (ADP-ribose) polymerase (PARP)-1 and PARP-2 activities favoring the activation of DNA repair pathways. This scenario supports the rational of combining radiotherapy with PARP inhibitors (PARPi) to potentiate IR-mediated DNA damage and in turn increasing cell death. Compared to CC cell lines (murine MC38 and CT26 cells as well as human HT29 cells) exposed to IR, cells exposed to the combination of the PARPi niraparib with IR show increased levels of DNA DSBs. The combination significantly increases the cell death *in vitro* and enhances antitumor effects *in vivo*. The exposure to PARPi induces the cyclic GMP-AMP synthase (cGAS) and stimulator of interferon genes (STING), allowing the activation of cGAS-STING-TBK1-IRF3 signaling that stimulates IFNB1 transcription and the release of IFNβ, CXCL10, CCL5, and MX1. These findings are also observed *in vivo* in M38 tumor-bearing mice. The role played by cGAS is corroborated by the observation that cGAS-silenced M38 cells are less sensitive to the combination treatment. The levels of ferroptosis markers (increased MDA and PTGS2 levels, reduced SLC7A11 and GPX4 expression) reflect the induction of ferroptosis as a mechanism of cell death. The analysis of the gene expression of cGAS-silenced M38 cells in comparison to cGAS normal expressing cells supports a critical role for the activating transcription factor 3 (ATF3) and underlines the existence of a ATF3-SLC7A11-GPX4 axis controlling ferroptosis induction upon exposure to IR and niraparib. In addition, cGAS depletion in M38 tumor-bearing mice abolishes the IR-induced infiltration of CD8+T, CD8+GZMB + T-cells leading to reduced antitumor efficacy, thus corroborating the role of cGAS for the combination efficacy. The analysis of tumor samples before and after radiotherapy from 32 patients affected by CC reveals that increased expression of cGAS, ATF3, and PTGS2 as well as an high density of CD8+T-cells associate with a high disease-free survival rate.

The enzyme stearoyl-CoA desaturase (SCD1) catalyzes the formation of oleic acid and palmitoleic acid and plays a critical role in IR response. Increased levels of SCD1 are observed in a panel of esophageal squamous cell carcinoma (ESCC) cell lines and the targeting of SCD1 by MF-438 is pursued by Luo and colleagues for increasing IR potency (Luo et al., 2022). Cells treated with MF-438 reduce cell growth and the combined exposure to IR and subtoxic concentrations of MF-438 results in synergistic antiproliferative activity. The synergism is attenuated upon silencing of SCD1 as well as following exposure to the ferroptosis inhibitor RLS3. The MF-438-mediated inhibition of SCD1 increases lipid peroxidation, ATP and HMGB1 release into the extracellular compartment, and this behavior is enhanced upon exposure to the combination IR/MF-438. Since similar results are observed in cells exposed to the combination IR/RLS3, it is likely that the induction of ferroptosis is the key mechanism of antitumor activity. These observations are corroborated by the finding that cells exposed to exogenous oleic acid or palmitoleic acid undergo ferroptosis. *In vitro* data are confirmed *in vivo* in ESCC-bearing mice exposed to IR/MF-438. The authors analyze the expression of SCD1 in ESCC patients from

TABLE 2 Nano-systems for enhancing the antitumor activity of ionizing radiation.

Nano-system	Type of metal	Cell lines	*In vivo* evaluation	References
HPNPs	Iron	Mouse melanoma B16F10 cells	Mouse melanoma B16F10 tumors	Lin et al. (2023)
		Mouse normal L929 fibroblasts		
FPH	Iron	Mouse mammary carcinoma 4T1 cells	Mouse mammary 4T1 tumors	Hou et al. (2023)
		Mouse RAW264.7 macrophages		
Fe_2O_3@TA-Pt	Iron	Mouse mammary carcinoma 4T1 cells	Mouse mammary 4T1 tumors	Jiang et al. (2022)
		Normal human HUVEC cells		
GOD@FeN_4-SAzyme	Iron	Mouse mammary carcinoma 4T1 cells	Mouse mammary 4T1 tumors	Zhu et al. (2022)
SPIONC	Iron	Human lung cancer NCI-H460 cells	Human lung cancer NCI-H460 tumors	Li et al. (2022)
iCoDMSN	Cobalt	Mouse mammary carcinoma 4T1 cells	Mouse mammary 4T1 tumors	Zhao et al. (2023)
		Human breast cancer MCF-7 cells		
		Human lung cancer A549 cells		
		Human colorectal cancer Caco-2 cells		
		Human gastric carcinoma SGC-7901 cells		
AGulX	Gadolinium	Human breast cancer MDA-MB-231 cells	Human breast cancer MDA-MB-231 tumors	Sun et al. (2022)
		Human breast cancer MDA-MB-468 cells		
3a	Gold	Human cervical carcinoma HeLa cells	Human cervical carcinoma HeLa cells transplanted in zebrafish	Yang et al. (2022)
		Human cervical carcinoma SiHa cells		
PBmB-DOX	Bismuth	Mouse mammary carcinoma 4T1 cells	Mouse mammary 4T1 tumors	Hou et al. (2022)

GEPIA database and stratify them in high and low expression groups. Compared to normal epithelium, SCD1 is significantly increased in tumor tissues and high SCD1 expressing patients experience a shorter disease-free survival.

3.2 Nano-systems for enhancing ionizing radiation antitumor activity

Another strategy for potentiating IR-mediated ferroptosis induction implies the use of metal-based nanoparticles (NPs) (Table 2). These NPs exploit the enhanced permeability retention effect to selectively induce ferroptosis in tumors. The tumor selectivity is also enhanced by the in local IR exposure, and these features allow reduced treatment toxicity.

3.2.1 Iron-based nanosystems

Lin and coworkers have assembled hemin, PX-12 (a TRX-1 inhibitor) and human serum albumin to built HPNPs (Lin et al., 2023). These NPs are stable in physiologic solution and in blood and rapidly release PX-12 under acidic conditions (e.g., pH 5). Acidic conditions, recapitulating acidic TME, favor the production of OH• by HPNPs and stimulate Fenton reaction. *In vitro* experiments performed in mouse melanoma B16F10 cells and normal mouse L929 fibroblasts show that HPNPs are better internalized in tumor compared to normal cells. The combination HPNPs/radiotherapy improves ROS production leading to increased cytotoxicity with respect to HPNPs administered alone. Besides the increased ROS production (mediated by both hemin and radiotherapy), the combination HPNPs/radiotherapy implements MDA, reduces the levels of antioxidants (GSH and TRX-1) and attenuates the GPX4 activity, in turn stimulating ferroptosis. These findings are corroborated by the observation that the treatment with ferrostatin-1 counteracts this behavior. *In vivo* experiments in B16F10 tumor-suffering mice demonstrate that HPNPs are biocompatible. Moreover, compared to animals treated with HPNPs, the tumor growth of mice exposed to the combination HPNPs/radiotherapy is significantly reduced. *Ex vivo* analysis evidences reduced GSH and GPX4 levels as well as increased MDA content in tumors exposed to the combination with respect to those treated with HPNPs alone.

To potentiate radiotherapy efficacy in breast cancer, Hou et al. propose multifunctional NPs composed by a shell of platinum decorated with hyaluronic acid (HA) encapsulating a core of Fe(III)-polydopamine (FPH) (Hou et al. 2023). FPH are stable at pH 7.4 and show photothermal properties upon 808 nm irradiation. Conversely, in acidic conditions NPs dissociate and release Fe^{3+}. The red-ox reaction Fe^{3+}/Fe^{2+} converts GSH into GSSG allowing GSH depletion and H_2O_2 hydrolysis producing O_2 and OH• (Fenton reaction). Since the depletion of GSH is increased at 50°C, it is conceivable that the photothermal-mediated hyperthermia improves antitumor potency of FPH. An additional property of FPH is their ability to produce O_2 by catalyzing the hydrolysis of

H_2O_2 by Pt nanoenzyme. *In vitro* experiments carried out in mouse 4T1 breast cancer cells and in RAW264.7 macrophage cells show a preferential accumulation of FPH in cancer cells, likely dependent on the interaction of HA with CD44. In addition, compared to the treatment with FPH, near infrared radiation (NIR, 808 nm) or IR alone, the exposure to FPH/NIR and FPH/IR significantly potentiates cytotoxicity in 4T1 cells. The improved cytotoxicity observed in cells treated with the combinations correlates with increased depletion of GSH levels and increased ROS and DNA damages. This behavior is counteracted by the treatment with ferrostatin-1. *In vivo* experiments performed in 4T1 tumor-bearing mice corroborate *in vitro* results and demonstrate the biocompatibility of FPH. NIR absorbance, Pt-mediated X-ray attenuation and enhanced permeability retention-mediated tumor selectivity render FPH a very useful tool for imaging as well.

Fe_2O_3@TA-Pt are NPs containing a core of Fe_2O_3 covered by platinum and tannic acid (TA-Pt) (Jiang et al., 2022). Fe_2O_3@TA-Pt are stable in mouse serum, while acidic pH (5.5), mimicking TME, favors the disassembling of the TA-Pt envelop releasing Fe_2O_3. In presence of H_2O_2, which is abundant in TME, Fe^{3+} is converted in Fe^{2+} generating O_2 and OH• (Fenton reaction). Fe_2O_3@TA-Pt better accumulate into 4T1 cells with respect to normal HUVEC cells, and this observation correlates with the increased cytotoxicity in tumor cells. The analysis of the DNA damage upon NPs exposure reveals that, besides the ROS-mediated DNA damage, Pt-DNA adducts, which reflect the release of the Pt by NPs, are observed. Additionally, Fe_2O_3@TA-Pt treatment enhances the radiotherapy sensitivity of 4T1 cells and potentiates ferroptosis induction, as demonstrated by the reduced levels of GSH and GPX4 observed upon combination exposure. *In vivo* experiments in 4T1 tumor-bearing mice show the preferential accumulation of NPs in liver and tumor. Moreover, the tumor volume of mice exposed to radiotherapy upon treatment with Fe_2O_3@TA-Pt is significantly reduced with respect to that of animals singly treated with NPs or radiotherapy. The combination Fe_2O_3@TA-Pt/IR is well tolerated with no signs of toxicity, reduces the tumor recurrence as well as the pulmonary metastasis and enhances the survival of mice.

Single-atom nanozymes (SAzymes) are enzyme-based drugs containing a single metal atom in their active sites that are interesting for anticancer therapy. Critical for the antitumor properties of these nano-systems is the presence into the TME of a specific enzymatic activity as well as H_2O_2. Zhu et al. (2022) have engineered a SAzyme based on FeN_4 and glucose oxidase (GOD) (GOD@FeN_4-SAzyme) for radio-enzymatic therapy. The elevated glucose level in tumor over the normal cells allows the production of H_2O_2 via GOD of the GOD@FeN_4-SAzyme and this results in sustained production of OH• and O_2 as well as in GSH depletion. The enzymatic cascade triggered by GOD is enhanced by IR, which favor the conversion Fe^{3+}/Fe^{2+} implementing the generation of OH• and potentiating apoptosis and ferroptosis. Cytotoxic experiments performed in 4T1 cells show that the killing activity of GOD@FeN_4-SAzyme is enhanced upon exposure to IR. Compared to the treatment with GOD@FeN_4-SAzyme or IR separately, the combination GOD@FeN_4-SAzyme/IR significantly increases the DNA damages (increased γ-H2AX signals) as well as ferroptosis (increased lipid peroxidation and OH•, reduced GSH and GPX4 levels accompanied by mitochondria membrane alterations). Besides ferroptosis, treated 4T1 cells show apoptosis induction (e.g., PARP and caspase 3 activation). Intravenous and intratumoral injection are used for *in vivo* administration of GOD@FeN_4-SAzyme in 4T1-tumor bearing mice. Magnetic resonance imaging (MRI) reveals that GOD@FeN_4-SAzyme accumulate into the tumor. Compared to the exposure to GOD@FeN_4-SAzyme or IR, a significant reduction of tumor volume is observed in animals treated with the combination GOD@FeN_4-SAzyme/IR. *Ex vivo* investigation recapitulates *in vitro* findings (e.g., increased γ-H2Ax and reduced GSH). GOD@FeN_4-SAzyme are biocompatible and the combination is well tolerated as well.

The pH-sensitive supramagnetic iron oxide nano-clusters (SPIONC) are proposed by Li et al. (2022) for enhancing radiation sensitivity in lung cancer. Under acidic conditions, which recapitulate TME and intracellular compartment conditions, SPIONC decompose and generate OH• via Fenton reaction. SPIONC efficiently accumulate in NCI-H460 cells. Compared to SPIONC or IR individual exposure, the combination SPIONC/IR is more effective in inhibiting cell proliferation. Cells exposed to the combination increase iron, lipid peroxides, ROS and γ-H2AX levels. These features reflect apoptosis (reduced expression of Bcl2 and increased caspase 3 activation) and ferroptosis induction (reduced expression of SLC7A11 and GPX4). The involvement of ferroptosis in SPIONC/IR response of tumor cells is corroborated by the observation that the pre-treatment with ferrostatin-1 attenuates cytotoxicity. *In vivo* experiments in orthotopic mice model of NCI-H460 cells in which SPIONC are injected by both intravenous and intra-tracheal delivery show that intra-tracheal delivery is to prefer for MRI analysis. Moreover, the exposure to the combination SPIONC/IR results in increased tumor volume inhibition and survival rate with respect to the administration of SPIONC or IR separately. No important toxic side effects are reported upon treatment. The analysis of explanted tumors from euthanized mice confirms the molecular alterations observed *in vitro*.

3.2.2 Nano-systems based on cobalt, gadolinium, gold, and bismuth

Another ferroptosis-stimulating nano-system has been recently proposed by Zhao and colleagues (Zhao et al., 2023). Starting from the observation that high level of cobalt (Co) in tumors associates with a good prognosis, the authors have engineered Co oxide nanodots by assembling bovine serum albumin and $CoCl_2$. These nanodots are conjugated with iRGD peptides and encapsulated into dentritic mesoporus silica nanoparticles (iCoDMSN). Acidic conditions stimulate the release of Co^{2+} by iCoDMSN and the presence of iRGD favors their tumor penetration. iCoDMSN are cytotoxic on a panel of different tumor cell lines, including murine 4T1 cells and human MCF-7 breast cancer cells, human A549 lung cancer cells, human Caco-2 colorectal cancer cells and human SGC-7901gastric carcinoma cells. Therefore, these nanostructures show interesting photoacoustic imaging ability under 808 nm irradiation and *in vivo* experiments in 4T1-tumor bearing mice show that iCoDMSN are well tolerated (e.g., no important signs of liver and kidney toxicity), preferentially co-localize with lysosomes and that iRGD favors tumor accumulation. Proteomic studies performed on 4T1 cells exposed to iCoDMSN underline that ferroptosis pathways play a critical role for cell response. These findings are supported by the increased lipid peroxidation, MDA and iron levels observed in iCoDMSN-treated 4T1 cells, and by the observation that this behavior is counteracted upon exposure to ferrostatin-1.

Proteomic analysis also underlines an increased level of HMOX1, which controls Fe^{2+} accumulation and ferroptosis induction by increasing the expression of TFR as well as by reducing solute carrier family 40 member 1 (SLC40A1). Upon treatment, accumulated iCoDMSN perturb the KEAP1/NRF2/HMOX1 axis. This axis is governed by the level of nuclear factor erythroid 2-related factor 2 (NRF2, Bellezza et al., 2018), which is a transcription factor for HMOX1. These results are confirmed *in vivo* in 4T1-tumor bearing mice exposed to the combination iCoDMSN/radiotherapy. Compared to mice treated with iCoDMSN, a increased tumor volume inhibition and survival rate are observed in mice treated with iCoDMSN/radiotherapy. *Ex vivo* analysis confirms the results obtained *in vitro* (reduced KEAP1, increased NRF2, HMOX1, iron, and MDA).

Aimed at overcoming radiation resistance and reducing radiotherapy damages to normal tissues, Sun and colleagues have proposed gadolinium (Gd)-based NPs (AGulX) (Sun et al., 2022). AGulX are based on polysiloxane covering Gd entrapped by the chelator dodecane tetraacetic acid (DOTA) moieties that functionalize the polysiloxane. Upon IR exposure, AGulX produce secondary and Auger electrons as well as free radicals. These NPs are under clinical investigation in brain, lung and pancreatic cancers. In the study by Sun et al., AGulX are evaluated in triple negative breast cancer cells (MDA-MB-231 and MDA-MB-468 cell lines) *in vitro* and *in vivo*. Compared to the treatment with AGulX or IR, the combination AGulX/IR reduces cell growth as well as cell migration and invasion capability. Additionally, cells exposed to the combination enhance ROS production, DNA damage (increased number of γ-H2AX foci) as well as G2/M cell-cycle arrest. Molecularly, the combination stimulates the phosphorylation of ATR and Chk1 (e.g., G2/M block) and reduces the phosphorylation of ATM and Chk2 (e.g., reduced homologous recombination repair ability). Moreover, by diminishing the activation of the MRN-ATM-Chk2 axis, the combination also impairs the non homologous end-joining, which is reflected by the reduced phosphorylation of p53 and BRCA1. Besides apoptosis induction (e.g., PARP and caspase 3 activation), cells exposed to AGulX/IR reduce the expression of NRF2 favoring ferroptosis by attenuating SLC7A11 activity, in turn reducing GSH synthesis and GPX4 activity. The increased levels of lipid perixidation and MDA support the induction of ferroptosis as a mechanism of cell death. These findings are confirmed by the observation that ferroptosis is attenuated by the siRNA-mediated silencing of NRF2, SLC7A11 and GPX4 as well as by the treatment with ferrostatin-1. The *in vitro* results parallel the *in vivo* observations in MDA-MB-231 tumor-bearing mice. No important signs of toxicity are reported in treated animals.

A series of metal-biotin-conjugated nano-structures based on different metals endowed with radiosensitizer properties is proposed by Yang and colleagues (Yang et al., 2022). Among the different nano-systems, the gold derivative 3a is selected for further investigations. 3a contains a biotin moiety for favoring tumor selectivity and uptake, a triply bonded dicarbon alkynyl amide linker joining biotin to Au, which is hidden by a lipophilic phosphine residue to increase membrane solubility. Compared to the auranofin (the reference), 3a shows similar antiproliferative potency on human cervical carcinoma HeLa and SiHa cells. Moreover, the tumor selectivity of 3a, which is dependent on biotin, is supported by the observation that 3a uptake is higher in Hela cells (expressing high levels of biotin receptor) with respect to normal human cervical epithelial H8 cells (expressing low levels of the receptor). Au-containing compounds, including auranofin, inhibit thioredoxin reductases (TRXR) and 3a-treated cells show reduced TRXR enzymatic activity. This finding is corroborated by docking studies showing that Au binds the selenium of the TRXR. The inhibition of the detoxification properties of TRXR stimulates ROS production and favors G2/M cell-cycle arrest as well as apoptosis (e.g., reduced Bcl2, increased Bax and alteration of the mitochondria membrane potential). Gene expression analysis performed on HeLa cells exposed to 3a shows a differential expression of genes involved in ferroptosis, including TXNRD1, HMOX1, SLC7A11, GCLM, FTH1, FTL, GPX1, GPX1P1, and GPX4. The exposure of HeLa cells to IR following 3a treatment stimulates DNA damage (increased γ-H2AX levels) and downregulates GPX4 expression, leading to reduced cell survival. This behavior is counteracted by the exposure to N-acetyl L-cysteine or ferrostatin-1. The radiosensitizing properties of 3a are confirmed *in vivo* in zebrafish transplanted with Hela cells exposed to the combination 3a/IR.

Along this way, Hou et al. have reported the synthesis and the antitumor properties of PBmB-DOX NPs (Hou et al., 2022). PBmB-DOX include a core of Bi_2S_3 covered by PEGylated doxorubicin (DOX). Moreover, PBmB-DOX contain-Mn-O- bonds that are sensitive to high GSH level, which is typical of the TME, allowing tumor selectivity and release of DOX under acidic conditions. The PBmB-DOX disassembling mediated by high levels of GSH favors the release of Mn^{2+} that, besides stimulating Fenton reaction and potentiating DOX-mediated antitumor activity, allows magnetic resonance contrast enhancement. The downregulation of GSH reduces 4T1 cell proliferation, while no important changes are evidenced in the growth of normal PBmB-DOX-treated HUVECs cells. The depletion of GSH upon treatment reduces the expression of GPX4 and increases lipid peroxidation. PBmB-DOX are more potent than free DOX on 4T1 cells and, compared to the exposure to IR or PBmB-DOX as single treatments, the combination PBmB-DOX/IR increases the amount of γ-H2AX foci. *In vivo* studies in 4T1 tumor-bearing mice demonstrate that PBmB-DOX are biocompatible with no important toxic effects reported for major organs, and that they preferentially accumulate into the tumor. Longer circulation time in plasma is reported for PBmB-DOX with respect to free DOX, and PBmB-DOX more efficiently suppress tumor growth with respect to free DOX. The exposure to IR upon PBmB-DOX treatment significantly improves antitumor activity with no important signs of toxicity. Histological analysis of tumors explanted from mice shows increased expression of γ-H2AX and reduced GPX4 levels following the exposure to the combination. Lastly, a remarkable signal enhancement in tumor is evidenced in MRI after 6 h post-injection of PBmB-DOX, thus confirming the theranostic properties of the nano-system.

4 Ionizing radiation-associated gene signatures

Recently, results from investigations focused on the studies of ferroptosis-associated gene signatures for predicting radiotherapy patient outcomes have been reported (Table 3).

TABLE 3 Gene signatures associated to ionizing radiation.

Gene signature	Tumor types	Cell line validation	Pathway involved	References
MAPK1	Malignant glioblastoma	U87	IL-17	Xie et al. (2022)
ZEB1		U251	Cytokine-cytokine receptor interaction	
MAP1LC3A			TNF signaling pathways	
HSPB1			DCs	
CA9			Macrophages	
STAT3			TIL	
TNFAIP3			Treg cells	
SCL7A11	Breast cancer	MCF7	SLC7A11/ESR1	Liu et al. (2022)
		ZR-75-1	SLC7A11/NEDD4L	
		MDA-MB-231		
ACSL3	Prostate cancer	No	Epithelial–mesenchymal transition	Feng et al. (2022)
EPAS1			Allograft rejection	
FASN			Fc gamma R-mediated phagocytosis	
GSTP1			TGF beta signaling	
LDHB			ECM receptor interaction	
NEDD4L			Adipocytokine signaling	
			Androgen response	
			Notch signalling	

The combination of temozolomide and radiotherapy is used for the treatment of malignant glioblastoma (GBM). Though effective, the combination is not curative and the identification of radiosensitive-associated biomarkers is an urgent need for predicting prognosis and therapy outcome. In the study by Xie et al. (2022), expression profiles of genes involved in radiation response and ferroptosis-associated pathways of GBM patients and healthy subjects from The Cancer Genome Atlas (TCGA) database are analyzed. Among the differentially expressed genes (DEGs) intersecting the two pathways, seven genes (MAPK1, ZEB1, MAP1LC3A, HSPB1, CA9, STAT3, and TNFAIP3) overlap and the analysis of the protein-protein interaction network indicates STAT3 as the hub gene. The application of the Least Absolute Shrinkage and Selection Operator (LASSO) and Cox regression analysis defines a risk score that stratifies patients in low- and high-risk groups. Patients in the high-risk group show low overall survival (OS) and high mortality. Receiver Operating Characteristic (ROC) curve and K-M analysis confirm the power of the signature in predicting patients' survival. The prognostic model is validated by data from Chinese Glioma Genome Atlas (CGGA) database used as an external independent validation cohort. Functional enrichment analyses defined by Gene Ontology (GO) and Kyoto Encyclopedia of Genes and Genomes (KEGG) as well as immune cell infiltration patterns analysis from single-sample Gene Set Enrichment Analysis (ssGSEA) allow the identification of the most represented pathways in high-risk group, including IL-17, cytokine-cytokine receptor interaction, TNF signaling pathways, DCs, macrophages, Tumor-infiltrating lymphocytes (TIL) and Treg cells. *In vitro* experiments performed in glioblastoma U87 and U251 cells treated with the combination erastin/IR support the relationship between radiosensitivity and ferroptosis.

Gene expression profiles of breast cancer and normal tissues as well as the survival and clinical information from TCGA database are analyzed by Liu and colleagues (Liu et al., 2022). Among the DEGs associated with ferroptosis, SLC7A11 is the most upregulated in tumors compared to normal tissues. Numerous clinic-pathologic properties associate with SLC7A11 levels, including the expression of estrogen receptor (ER). ER-positive tissues show lower levels of SLC7A11 (e.g., increased ferroptosis) with respect to ER-negative samples. The univariate Cox regression for OS model demonstrates that high SLC7A11 levels associate with worse OS. *In vitro* experiments carried out in a panel of breast cancer cell lines (ER-positive MCF7 and ZR-75-1 as well as ER-negative MDA-MB-231) treated with ferrostatin-1 or erastin in combination with IR support the critical role played by SLC7A11 in regulating IR-induced ferroptosis in ER-positive cells. The study also shows a positive correlation between the expression of estrogen receptor 1 (ESR1) and SLC7A11 and the analysis by K-M predicts poor prognosis for patients with high levels of ESR1. Molecularly, IR exposure stimulates the expression of ESR1 that, in turn, increases SLC7A11 levels attenuating ferroptosis. This finding is supported by the observation that upon ESR1/SLC7A11 knockdown in ER-

positive cells, IR-induced ferroptosis is enhanced. Immunoprecipitation assay revels that no direct protein-protein interaction occurs between ESR1 and SLC7A11. Conversely, a protein interaction involving SLC7A11 and the E3 ubiquitin ligase neural precursor cell expressed developmentally downregulated gene 4-like (NEDD4L) is critical for stimulating the proteasome-mediated degradation of SLC7A11. Based on these findings, the authors suggest that two pathways, including ESR1/SLC7A11 and SLC7A11/NEDD4L, control SLC7A11 level and regulate ferroptosis induced by IR exposure.

By analyzing expression data (mRNA and lncRNA) from Gene Expression Omnibus (GEO) database of normal and prostate cancer tissues of patients treated with radical radiotherapy and intersecting them with ferroptosis-related genes, Feng and co-workers construct a gene signature, including ACSL3, EPAS1, FASN, GSTP1, LDHB, and NEDD4L. This signature allows the definition of a ferroptosis-related gene prognostic index (FGPI) useful for predicting biochemical recurrence (BR) and radiation resistance of prostate cancer suffering patients (Feng et al., 2022). FGPI allows the stratification of the patients in high- and low-risk groups. Although ROC curve poorly discriminates BR patients from patients who do not experience BR, it evidences that FGPI potentially reflects radiation resistance. Indeed, compared to no BR patients, a significant higher FGPI is observed for BR patients treated with radical radiotherapy. The application of the K-M curve shows that FGPI is an independent risk factor for biochemically relapse (BCR) and metastasis-free survival (MFS) in patients treated with radical radiotherapy. Moreover, compared to low-risk, high-risk group patients treated with radical prostatectomy are at higher risk of metastasis. The application of the GeneMANIA database and ceRNA network assigns a critical role to lnRNAPART1 in controlling ACSL3 and EPAS1 expression via a intricate crosstalk involving 60 different miRNAs. Gene Set Enrichment Analysis (GSEA) shows differences in pathway enrichment in high-risk (epithelial–mesenchymal transition, allograft rejection, Fc gamma R-mediated phagocytosis, TGF beta signaling pathway, and extracellular matrix receptor interaction) with respect to low-risk patients (adipocytokine signaling pathway, androgen response and notch signalling). Drug and immunologic analysis as well as TME analysis resulting from the application of dedicated softwares, which consider the expression of ACSL3 and EPAS1, underline potential sensitivity to nine drugs (OSI-027, OSI-930, PAC-1, PHA-793887, PI-103, PIK-93, SNX-2112, TPCA-1, and UNC0638) for high-risk patients. Compared to no BR patients, BR patients group shows lower expression levels of METTL14, which predict sensitivity to methylating agents, and higher expression of PDCD1LG2 (PD-L2) and CD96. However, only CD96 is significantly associated with BCR-free survival. Regarding the results of TME analysis, cancer-related fibroblasts, macrophages, stromal score, immune score, estimate score, and tumor purity are risk factors for BCR closely associated to BCR-free survival.

5 Conclusion

Although radiotherapy is the first choice for the treatment of different tumors types, the development of radiation resistance impairs its effectiveness and medical strategies aimed at overcoming this drawback are urgent. Among these strategies, the combination of IR with ferrptosis inducers proved to synergize thus potentiating radiotherapy. Moreover, since the activation of defense cellular pathways in response to IR exposure attenuates radiotherapy effectiveness, deeper investigations aimed at studying the involved pathways as well as at developing ferroptosis inducers or novel combinatorial strategies are intriguing ways to pave for combating radiation resistance. Besides the use of small molecules inducing ferroptosis, the combination of IR with nano-systems endowed with both diagnostic and therapeutic potential is promising. In spite of their capability to overcome the resistance to apoptosis developed by tumors exposed to conventional chemotherapeutics, ferroptosis inducers show drawbacks typical of small molecules, including low solubility, limited tumor targeting, and toxic side effects that have often impeded their clinical evaluation. These drawbacks have been tackled by NPs that, functioning like a “Trojan horse”, localize into the tumors via the enhanced permeability retention effect and are entered into the therapeutics armamentarium for fighting tumors. NPs ameliorate the circulation time of encapsulated drugs and stimulate anticancer immunity at the tumor site. Specific decoration aimed at targeting peculiar tumor-expressing molecules as well as exploiting non physiologic conditions typical of TME potentiate the tumor selectivity of NPs. Tumor targeting is also in part guaranteed by the local irradiation of the tumor. NPs are designed to disassemble themselves under peculiar conditions (e.g., the acidic pH as well as the presence of specific enzymes), ameliorating the selectivity of the cargo release. Therefore, the magnetic properties of the metal composing the structure of the NPs account for their theranostics potential. Among the combinations including small molecules here reported, only IR/niraparib is currently under investigation in phase I-II clinical trials (https://www.clinicaltrials.gov) in triple negative breast cancer (NCT03945721 and NCT04837209), pancreatic tumors (NCT04409002), prostate cancer (NCT04194554, NCT04037254), glioblastoma (NCT05666349) and head and neck squamous cell carcinoma (NCT05784012) patients. Regarding the clinical studies exploiting NPs, although all the NPs considered have been tested *in vivo* showing interesting antitumor profile, only AGluX is under phase I-II clinical evaluation in patients with brain tumors and brain metastasis, gynecologic cancers, non small cell lung cancers, and pancreatic cancers (NCT04899908, NCT03308604, NCT02820454, NCT04789486, NCT03818386, and NCT04784221. https://www.clinicaltrials.gov). Lastly, the continuous implementation of the gene signatures predicting IR response via ferroptosis-mediated cell death is expected to positively impact on patient`s health.

In conclusion, despite the preclinical success achieved with the combination strategies, additional efforts and clinical investigations are required in the future to demonstrate their safety profile as well as their antitumor effectiveness.

Author contributions

GB and NZ wrote the review manuscript. All authors contributed to the article and approved the submitted version.

Funding

The APC was funded by Ricerca Corrente from Italian Ministry of Health.

Acknowledgments

This work was supported by Ricerca Corrente funds from Italian Ministry of Health.

Conflict of interest

The authors declare that the research was conducted in the absence of any commercial or financial relationships that could be construed as a potential conflict of interest.

Publisher's note

References

Adjemian, S., Oltean, T., Martens, S., Wiernicki, B., Goossens, V., Vanden Berghe, T., et al. (2020). Ionizing radiation results in a mixture of cellular outcomes including mitotic catastrophe, senescence, methuosis, and iron-dependent cell death. *Cell Death Dis.* 11, 1003. doi:10.1038/s41419-020-03209-y

Aubrey, B. J., Kelly, G. L., Janic, A., Herold, M. J., and Strasser, A. (2018). How does p53 induce apoptosis and how does this relate to p53-mediated tumour suppression? *Cell Death Differ.* 25, 104–113. doi:10.1038/cdd.2017.169

Azzam, E. I., Jay-Gerin, J. P., and Pain, D. (2012). Ionizing radiation-induced metabolic oxidative stress and prolonged cell injury. *Cancer Lett.* 327, 48–60. doi:10.1016/j.canlet.2011.12.012

Baidoo, K. E., Yong, K., and Brechbiel, M. W. (2013). Molecular pathways: Targeted α-particle radiation therapy. *Clin. Cancer Res.* 19, 530–537. doi:10.1158/1078-0432.CCR-12-0298

Bellezza, I., Giambanco, I., Minelli, A., and Donato, R. (2018). Nrf2-Keap1 signaling in oxidative and reductive stress. *Biochim. Biophys. Acta Mol. Cell Res.* 1865, 721–733. doi:10.1016/j.bbamcr.2018.02.010

Bersuker, K., Hendricks, J. M., Li, Z., Magtanong, L., Ford, B., Tang, P. H., et al. (2019). The CoQ oxidoreductase FSP1 acts parallel to GPX4 to inhibit ferroptosis. *Nature* 575, 688–692. doi:10.1038/s41586-019-1705-2

Bieging, K. T., Mello, S. S., and Attardi, L. D. (2014). Unravelling mechanisms of p53-mediated tumour suppression. *Nat. Rev. Cancer* 14, 359–370. doi:10.1038/nrc3711

Chen, Q., Zheng, W., Guan, J., Liu, H., Dan, Y., Zhu, L., et al. (2023). SOCS2-enhanced ubiquitination of SLC7A11 promotes ferroptosis and radiosensitization in hepatocellular carcinoma. *Cell Death Differ.* 30, 137–151. doi:10.1038/s41418-022-01051-7

Chiang, S. K., Chen, S. E., and Chang, L. C. (2018). A dual role of heme oxygenase-1 in cancer cells. *Int. J. Mol. Sci.* 20, 39. doi:10.3390/ijms20010039

Choudhary, S., Burns, S. C., Mirsafian, H., Li, W., Vo, D. T., Qiao, M., et al. (2020). Genomic analyses of early responses to radiation inglioblastoma reveal new alterations at transcription,splicing, and translation levels. *Sci. Rep.* 10, 8979. doi:10.1038/s41598-020-65638-1

D'Herde, K., and Krysko, D. V. (2017). Ferroptosis: Oxidized PEs trigger death. *Nat. Chem. Biol.* 13, 4–5. doi:10.1038/nchembio.2261

Delaney, G., Jacob, S., Featherstone, C., and Barton, M. (2005). The role of radiotherapy in cancer treatment: Estimating optimal utilization from a review of evidence-based clinical guidelines. *Cancer* 104, 1129–1137. doi:10.1002/cncr.21324

Dixon, S. J., Lemberg, K. M., Lamprecht, M. R., Skouta, R., Zaitsev, E. M., Gleason, C. E., et al. (2012). Ferroptosis: An iron-dependent form of nonapoptotic cell death. *Cell* 149, 1060–1072. doi:10.1016/j.cell.2012.03.042

Doll, S., and Conrad, M. (2017). Iron and ferroptosis: A still ill-defined liaison. *IUBMB Life* 69, 423–434. doi:10.1002/iub.1616

Doll, S., Freitas, F. P., Shah, R., Aldrovandi, M., da Silva, M. C., Ingold, I., et al. (2019). FSP1 is a glutathione-independent ferroptosis suppressor. *Nature* 575, 693–698. doi:10.1038/s41586-019-1707-0

Feng, D., Shi, X., Xiong, Q., Zhang, F., Li, D., Wei, W., et al. (2022). A ferroptosis-related gene prognostic index associated with biochemical recurrence and radiation resistance for patients with prostate cancer undergoing radical radiotherapy. *Front. Cell Dev. Biol.* 10, 803766. doi:10.3389/fcell.2022.803766

Feng, H., and Stockwell, B. R. (2018). Unsolved mysteries: How does lipid peroxidation cause ferroptosis? *PLoS Biol.* 16, e2006203. doi:10.1371/journal.pbio.2006203

Friedmann Angeli, J. P., Krysko, D. V., and Conrad, M. (2019). Ferroptosis at the crossroads of cancer-acquired drug resistance and immune evasion. *Nat. Rev. Cancer* 19, 405–414. doi:10.1038/s41568-019-0149-1

Galluzzi, L., Vitale, I., Aaronson, S. A., Abrams, J. M., Adam, D., Agostinis, P., et al. (2018). Molecular mechanisms of cell death: Recommendations of the nomenclature committee on cell death. *Cell Death Differ.* 25, 486–541. doi:10.1038/s41418-017-0012-4

Gaschler, M. M., and Stockwell, B. R. (2017). Lipid peroxidation in cell death. *Biochem. Biophys. Res. Commun.* 482, 419–425. doi:10.1016/j.bbrc.2016.10.086

Hassannia, B., Vandenabeele, P., and Vanden Berghe, T. (2019). Targeting ferroptosis to iron out cancer. *Cancer Cell* 35, 830–849. doi:10.1016/j.ccell.2019.04.002

Hou, M., Zhu, K., Hu, H., Zheng, S., Wu, Z., Ren, Y., et al. (2022). Rapid synthesis of 'yolk-shell'-like nanosystem for MR molecular and chemo-radio sensitization. *J. Control Release* 347, 55–67. doi:10.1016/j.jconrel.2022.04.033

Hou, Y. K., Zhang, Z. J., Li, R. T., Peng, J., Chen, S. Y., Yue, Y. R., et al. (2023). Remodeling the tumor microenvironment with core-shell nanosensitizer featuring dual-modal imaging and multimodal therapy for breast cancer. *ACS Appl. Mater Interfaces* 15, 2602–2616. doi:10.1021/acsami.2c17691

Hu, L., Wang, H., Huang, L., Zhao, Y., and Wang, J. (2016). Crosstalk between autophagy and intracellular radiation response (Review). *Int. J. Oncol.* 49, 2217–2226. doi:10.3892/ijo.2016.3719

Hu, W., Zhang, C., Wu, R., Sun, Y., Levine, A., and Feng, Z. (2010). Glutaminase 2, a novel p53 target gene regulating energy metabolism and antioxidant function. *Proc. Natl. Acad. Sci. U. S. A.* 107, 7455–7460. doi:10.1073/pnas.1001006107

Huang, R. X., and Zhou, P. K. (2020). DNA damage response signaling pathways and targets for radiotherapy sensitization in cancer. *Signal Transduct. Target Ther.* 5, 60. doi:10.1038/s41392-020-0150-x

Huang, W. M., Li, Z. X., Wu, Y. H., Shi, Z. L., Mi, J. L., Hu, K., et al. (2023). m6A demethylase FTO renders radioresistance of nasopharyngeal carcinoma via promoting OTUB1-mediated anti-ferroptosis. *Transl. Oncol.* 27, 101576. doi:10.1016/j.tranon.2022.101576

Jaffray, D. A. (2012). Image-guided radiotherapy: From current concept to future perspectives. *Nat. Rev. Clin. Oncol.* 9, 688–699. doi:10.1038/nrclinonc.2012.194

Jennis, M., Kung, C. P., Basu, S., Budina-Kolomets, A., Leu, J. I., Khaku, S., et al. (2016). An African-specific polymorphism in the TP53 gene impairs p53 tumor suppressor function in a mouse model. *Genes Dev.* 30, 918–930. doi:10.1101/gad.275891.115

Jiang, L., Kon, N., Li, T., Wang, S. J., Su, T., Hibshoosh, H., et al. (2015). Ferroptosis as a p53-mediated activity during tumour suppression. *Nature* 520, 57–62. doi:10.1038/nature14344

Jiang, W., Wei, L., Chen, B., Luo, X., Xu, P., Cai, J., et al. (2022). Platinum prodrug nanoparticles inhibiting tumor recurrence and metastasis by concurrent chemoradiotherapy. *J. Nanobiotechnology* 20, 129. doi:10.1186/s12951-022-01322-y

Kang, R., Kroemer, G., and Tang, D. (2019). The tumor suppressor protein p53 and the ferroptosis network. *Free Radic. Biol. Med.* 133, 162–168. doi:10.1016/j.freeradbiomed.2018.05.074

Kryukov, G. V., Castellano, S., Novoselov, S. V., Lobanov, A. V., Zehtab, O., Guigó, R., et al. (2003). Characterization of mammalian selenoproteomes. *Science* 300, 1439–1443. doi:10.1126/science.1083516

Lang, X., Green, M. D., Wang, W., Yu, J., Choi, J. E., Jiang, L., et al. (2019). Radiotherapy and immunotherapy promote tumoral lipid oxidation and ferroptosis via synergistic repression of SLC7A11. *Cancer Discov.* 9, 1673–1685. doi:10.1158/2159-8290.CD-19-0338

Lee, H., Zandkarimi, F., Zhang, Y., Meena, J. K., Kim, J., Zhuang, L., et al. (2020). Energy-stress-mediated AMPK activation inhibits ferroptosis. *Nat. Cell Biol.* 22, 225–234. doi:10.1038/s41556-020-0461-8

Lei, G., Mao, C., Yan, Y., Zhuang, L., and Gan, B. (2021). Ferroptosis, radiotherapy, and combination therapeutic strategies. *Protein Cell* 12, 836–857. doi:10.1007/s13238-021-00841-y

Lei, G., Zhang, Y., Koppula, P., Liu, X., Zhang, J., Lin, S. H., et al. (2020). The role of ferroptosis in ionizing radiation-induced cell death and tumor suppression. *Cell Res.* 30, 146–162. doi:10.1038/s41422-019-0263-3

Lei, G., Zhuang, L., and Gan, B. (2022). Targeting ferroptosis as a vulnerability in cancer. *Nat. Rev. Cancer* 22, 381–396. doi:10.1038/s41568-022-00459-0

Lei, P., Bai, T., and Sun, Y. (2019). Mechanisms of ferroptosis and relations with regulated cell death: A review. *Front. Physiol.* 10, 139. doi:10.3389/fphys.2019.00139

Li, Y., Yang, J., Gu, G., Guo, X., He, C., Sun, J., et al. (2022). Pulmonary delivery of theranostic nanoclusters for lung cancer ferroptosis with enhanced chemodynamic/radiation synergistic therapy. *Nano Lett.* 22, 963–972. doi:10.1021/acs.nanolett.1c03786

Liang, C., Zhang, X., Yang, M., and Dong, X. (2019). Recent progress in ferroptosis inducers for cancer therapy. *Adv. Mater* 31, e1904197. doi:10.1002/adma.201904197

Lin, L. S., Song, J., Song, L., Ke, K., Liu, Y., Zhou, Z., et al. (2018). Simultaneous fenton-like ion delivery and glutathione depletion by MnO2 -based nanoagent to enhance chemodynamic therapy. *Angew. Chem. Int. Ed. Engl.* 57, 4902–4906. doi:10.1002/anie.201712027

Lin, Y., Chen, X., Yu, C., Xu, G., Nie, X., Cheng, Y., et al. (2023). Radiotherapy-mediated redox homeostasis-controllable nanomedicine for enhanced ferroptosis sensitivity in tumor therapy. *Acta Biomater.* S1742-7061 (23), 300–311. doi:10.1016/j.actbio.2023.01.022

Liu, J., An, W., Zhao, Q., Liu, Z., Jiang, Y., Li, H., et al. (2022). Hyperbaric oxygen enhances X-ray induced ferroptosis in oral squamous cell carcinoma cells. *Oral Dis.* 2022. doi:10.1111/odi.14461

Liu, R., Liu, L., Bian, Y., Zhang, S., Wang, Y., Chen, H., et al. (2022). The dual regulation effects of ESR1/nedd4l on SLC7A11 in breast cancer under ionizing radiation. *Front. Cell Dev. Biol.* 9, 772380. doi:10.3389/fcell.2021.772380

Luo, H., Wang, X., Song, S., Wang, Y., Dan, Q., and Ge, H. (2022). Targeting stearoyl-coa desaturase enhances radiation induced ferroptosis and immunogenic cell death in esophageal squamous cell carcinoma. *Oncoimmunology* 11, 2101769. doi:10.1080/2162402X.2022.2101769

Maier, P., HartmannWenz, L,F., and Herskind, C. (2016). Cellular pathways in response to ionizing radiation and their targetability for tumor radiosensitization. *Int. J. Mol. Sci.* 17, 102. doi:10.3390/ijms17010102

Mancias, J. D., Wang, X., Gygi, S. P., Harper, J. W., and Kimmelman, A. C. (2014). Quantitative proteomics identifies NCOA4 as the cargo receptor mediating ferritinophagy. *Nature* 509, 105–109. PMID: 24695223. doi:10.1038/nature13148

Mijit, M., Caracciolo, V., Melillo, A., Amicarelli, F., and Giordano, A. (2020). Role of p53 in the regulation of cellular senescence. *Biomolecules* 10, 420. doi:10.3390/biom10030420

Ou, Y., Wang, S. J., Li, D., Chu, B., and Gu, W. (2016). Activation of SAT1 engages polyamine metabolism with p53-mediated ferroptotic responses. *Proc. Natl. Acad. Sci. U. S. A.* 113, E6806–E6812. doi:10.1073/pnas.1607152113

Reisz, J. A., Bansal, N., Qian, J., Zhao, W., and Furdui, C. M. (2014). Effects of ionizing radiation on biological molecules-mechanisms of damage and emerging methods of detection. *Antioxid. Redox Signal* 21, 260–292. doi:10.1089/ars.2013.5489

Sabin, R. J., and Anderson, R. M. (2011). Cellular Senescence - its role in cancer and the response to ionizing radiation. *Genome Integr.* 2, 7. doi:10.1186/2041-9414-2-7

Seibt, T. M., Proneth, B., and Conrad, M. (2019). Role of GPX4 in ferroptosis and its pharmacological implication. *Free Radic. Biol. Med.* 133, 144–152. doi:10.1016/j.freeradbiomed.2018.09.014

Shah, R., Margison, K., and Pratt, D. A. (2017). The potency of diarylamine radical-trapping antioxidants as inhibitors of ferroptosis underscores the role of autoxidation in the mechanism of cell death. *ACS Chem. Biol.* 12, 2538–2545. doi:10.1021/acschembio.7b00730

Sheikh, M. S., and Fornace, A. J. (2000). Death and decoy receptors and p53-mediated apoptosis. *Leukemia* 14, 1509–1513. doi:10.1038/sj.leu.2401865

Shen, D., Luo, J., Chen, L., Ma, W., Mao, X., Zhang, Y., et al. (2022). PARPi treatment enhances radiotherapy-induced ferroptosis and antitumor immune responses via the cGAS signaling pathway in colorectal cancer. *Cancer Lett.* 550, 215919. doi:10.1016/j.canlet.2022.215919

Song, X., Zhu, S., Chen, P., Hou, W., Wen, Q., Liu, J., et al. (2018). AMPK-mediated BECN1 phosphorylation promotes ferroptosis by directly blocking system Xc- activity. *Curr. Biol.* 28, 2388–2399. doi:10.1016/j.cub.2018.05.094

Stockwell, B. R., Friedmann Angeli, J. P., Bayir, H., Bush, A. I., Conrad, M., Dixon, S. J., et al. (2017). Ferroptosis: A regulated cell death nexus linking metabolism, redox biology, and disease. *Cell* 171, 273–285. doi:10.1016/j.cell.2017.09.021

Sun, H., Cai, H., Xu, C., Zhai, H., Lux, F., Xie, Y., et al. (2022). AGuIX nanoparticles enhance ionizing radiation-induced ferroptosis on tumor cells by targeting the NRF2-GPX4 signaling pathway. *J. Nanobiotechnology* 20, 449. doi:10.1186/s12951-022-01654-9

Tang, D., Kang, R., Berghe, T. V., Vandenabeele, P., and Kroemer, G. (2019). The molecular machinery of regulated cell death. *Cell Res.* 29, 347–364. doi:10.1038/s41422-019-0164-5

Tang, M., Chen, Z., Wu, D., and Chen, L. (2018). Ferritinophagy/ferroptosis: Iron-related newcomers in human diseases. *J. Cell Physiol.* 233, 9179–9190. doi:10.1002/jcp.26954

Tarangelo, A., Magtanong, L., Bieging-Rolett, K. T., Li, Y., Ye, J., Attardi, L. D., et al. (2018). p53 suppresses metabolic stress-induced ferroptosis in cancer cells. *Cell Rep.* 22, 569–575. doi:10.1016/j.celrep.2017.12.077

Torti, S. V., and Torti, F. M. (2019). Winning the war with iron. *Nat. Nanotechnol.* 14, 499–500. doi:10.1038/s41565-019-0419-9

Trujillo-Alonso, V., Pratt, E. C., Zong, H., Lara-Martinez, A., Kaittanis, C., Rabie, M. O., et al. (2019). FDA-approved ferumoxytol displays anti-leukaemia efficacy against cells with low ferroportin levels. *Nat. Nanotechnol.* 14, 616–622. doi:10.1038/s41565-019-0406-1

Vanden Berghe, T., Vanlangenakker, N., Parthoens, E., Deckers, W., Devos, M., Festjens, N., et al. (2010). Necroptosis, necrosis and secondary necrosis converge on similar cellular disintegration features. *Cell Death Differ.* 17, 922–930. doi:10.1038/cdd.2009.184

Venkatesh, D., O'Brien, N. A., Zandkarimi, F., Tong, D. R., Stokes, M. E., Dunn, D. E., et al. (2020). MDM2 and MDMX promote ferroptosis by PPARα-mediated lipid remodeling. *Genes Dev.* 34, 526–543. doi:10.1101/gad.334219.119

Wang, Y., Yang, L., Zhang, X., Cui, W., Liu, Y., Sun, Q. R., et al. (2019). Epigenetic regulation of ferroptosis by H2B monoubiquitination and p53. *EMBO Rep.* 20, e47563. doi:10.15252/embr.201847563

Wenzel, S. E., Tyurina, Y. Y., Zhao, J., St Croix, C. M., Dar, H. H., Mao, G., et al. (2017). PEBP1 wardens ferroptosis by enabling lipoxygenase generation of lipid death signals. *Cell* 171, 628–641. doi:10.1016/j.cell.2017.09.044

Xie, L., Song, X., Yu, J., Guo, W., Wei, L., Liu, Y., et al. (2011). Solute carrier protein family may involve in radiation-induced radioresistance of non-small cell lung cancer. *J. Cancer Res. Clin. Oncol.* 137, 1739–1747. doi:10.1007/s00432-011-1050-9

Xie, Y., Xiao, Y., Liu, Y., Lu, X., Wang, Z., Sun, S., et al. (2022). Construction of a novel radiosensitivity- and ferroptosis-associated gene signature for prognosis prediction in gliomas. *J. Cancer* 13, 2683–2693. doi:10.7150/jca.72893

Yang, M., Wu, X., Hu, J., Wang, Y., Wang, Y., Zhang, L., et al. (2022). COMMD10 inhibits HIF1α/CP loop to enhance ferroptosis and radiosensitivity by disrupting Cu-Fe balance in hepatocellular carcinoma. *J. Hepatol.* 76, 1138–1150. doi:10.1016/j.jhep.2022.01.009

Yang, W. S., Kim, K. J., Gaschler, M. M., Patel, M., Shchepinov, M. S., and Stockwell, B. R. (2016). Peroxidation of polyunsaturated fatty acids by lipoxygenases drives ferroptosis. *Proc. Natl. Acad. Sci. U. S. A.* 113, E4966–E4975. doi:10.1073/pnas.1603244113

Yang, W. S., and Stockwell, B. R. (2008). Synthetic lethal screening identifies compounds activating iron-dependent, nonapoptotic cell death in oncogenic-RAS-harboring cancer cells. *Chem. Biol.* 15, 234–245. doi:10.1016/j.chembiol.2008.02.010

Yang, Z., Huang, S., Liu, Y., Chang, X., Liang, Y., Li, X., et al. (2022). Biotin-Targeted Au(I) radiosensitizer for cancer synergistic therapy by intervening with redox homeostasis and inducing ferroptosis. *J. Med. Chem.* 65, 8401–8415. doi:10.1021/acs.jmedchem.2c00300

Ye, L. F., Chaudhary, K. R., Zandkarimi, F., Harken, A. D., Kinslow, C. J., Upadhyayula, P. S., et al. (2020). Radiation-induced lipid peroxidation triggers ferroptosis and synergizes with ferroptosis inducers. *ACS Chem. Biol.* 15, 469–484. doi:10.1021/acschembio.9b00939

Yuan, H., Li, X., Zhang, X., Kang, R., and Tang, D. (2016). Identification of ACSL4 as a biomarker and contributor of ferroptosis. *Biochem. Biophys. Res. Commun.* 478, 1338–1343. doi:10.1016/j.bbrc.2016.08.124

Zhang, Y., Liu, X., Zeng, L., Zhao, X., Chen, Q., Pan, Y., et al. (2022). Exosomal protein angiopoietin-like 4 mediated radioresistance of lung cancer by inhibiting ferroptosis under hypoxic microenvironment. *Br. J. Cancer* 127, 1760–1772. doi:10.1038/s41416-022-01956-7

Zhang, Y., Qian, Y., Zhang, J., Yan, W., Jung, Y. S., Chen, M., et al. (2017). Ferredoxin reductase is critical for p53-dependent tumor suppression via iron regulatory protein 2. *Genes Dev.* 31, 1243–1256. doi:10.1101/gad.299388.117

Zhang, Y., Shi, J., Liu, X., Feng, L., Gong, Z., Koppula, P., et al. (2018). BAP1 links metabolic regulation of ferroptosis to tumour suppression. *Nat. Cell Biol.* 20, 1181–1192. doi:10.1038/s41556-018-0178-0

Zhao, J., Chen, Y., Xiong, T., Han, S., Li, C., He, Y., et al. (2023). Clustered cobalt nanodots initiate ferroptosis by upregulating heme oxygenase 1 for radiotherapy sensitization. *Small* 19, e2206415. doi:10.1002/smll.202206415

Zheng, J., and Conrad, M. (2020). The metabolic underpinnings of ferroptosis. *Cell Metab.* 32, 920–937. doi:10.1016/j.cmet.2020.10.011

Zhu, X., Wu, J., Liu, R., Xiang, H., Zhang, W., Chang, Q., et al. (2022). Engineering single-atom iron nanozymes with radiation-enhanced self-cascade catalysis and self-supplied H2O2 for radio-enzymatic therapy. *ACS Nano* 16, 18849–18862. doi:10.1021/acsnano.2c07691

frontiers | Frontiers in Molecular Biosciences

TYPE Review
PUBLISHED 29 June 2023
DOI 10.3389/fmolb.2023.1229710

OPEN ACCESS

EDITED BY
Yanqing Liu,
Columbia University, United States

REVIEWED BY
Jingjie Yi,
Columbia University, United States
Yue Liu,
The University of Texas at Austin, United States
Bowen Tang,
PTC Therapeutics, United States

*CORRESPONDENCE
McKale R. Montgomery,
mckale.montgomery@okstate.edu

RECEIVED 26 May 2023
ACCEPTED 21 June 2023
PUBLISHED 29 June 2023

CITATION
Cardona CJ and Montgomery MR (2023), Iron regulatory proteins: players or pawns in ferroptosis and cancer?
Front. Mol. Biosci. 10:1229710.
doi: 10.3389/fmolb.2023.1229710

Iron regulatory proteins: players or pawns in ferroptosis and cancer?

Cameron J. Cardona and McKale R. Montgomery*

Department of Nutritional Sciences, Oklahoma State University, Stillwater, OK, United States

Cells require iron for essential functions like energy production and signaling. However, iron can also engage in free radical formation and promote cell proliferation thereby contributing to both tumor initiation and growth. Thus, the amount of iron within the body and in individual cells is tightly regulated. At the cellular level, iron homeostasis is maintained post-transcriptionally by iron regulatory proteins (IRPs). Ferroptosis is an iron-dependent form of programmed cell death with vast chemotherapeutic potential, yet while IRP-dependent targets have established roles in ferroptosis, our understanding of the contributions of IRPs themselves is still in its infancy. In this review, we present the growing circumstantial evidence suggesting that IRPs play critical roles in the adaptive response to ferroptosis and ferroptotic cell death and describe how this knowledge can be leveraged to target neoplastic iron dysregulation more effectively.

KEYWORDS

iron homeostasis, cancer, iron-sulfur cluster biogenesis, programmed cell death, reactive oxygen species, lipid peroxidation

1 Introduction

Iron is an essential metal for all forms of life; in fact, a large portion of the Earth itself is made of iron, making it the most abundant element on the planet (Sheftel et al., 2012). The essentiality of iron has led to its long-established role in medicine. Since the 1500s, iron has been used by physicians to treat a wide range of medical ailments (Beutler, 2002). Iron primarily exists in two forms: a reduced ferrous (Fe^{2+}) form and an oxidized ferric (Fe^{3+}) form. In its ferrous form, iron is highly reactive, interacting with hydrogen peroxide to form reactive oxygen species (ROS) and ferric iron (Vogt et al., 2021). The importance of iron homeostasis in the prevention of human disease is well recognized and is exemplified by paitents with the hereditary iron overload disorder hemochromatosis. Individuals with hemochromatosis are at increased risk for diabetes, hematologic malignancies, colorectal and gastric cancers, as well as cirrhosis and hepatocellular carcinoma, which account for nearly 20%–30% of deaths for patients with untreated or poorly controlled hemochromatosis (Bradbear et al., 1985; Nelson et al., 1995; Pietrangelo, 2010).

Despite this potential danger, iron is necessary for DNA synthesis, cell signaling, and cellular respiration, among other functions (Vogt et al., 2021), so insufficient iron availability is also very deleterious (Camaschella, 2019). Iron deficiency is primarily caused by inadequate dietary intake, but can be secondary to infection, inflammation, and genetic disorders. The primary symptoms of iron deficiency are fatigue and reduced work capacity, but when severe, iron deficiency is also associated with impaired cognititive development and increased risk of child and maternal mortality and is a major cause of disability

worldwide (Kassebaum et al., 2014; Camaschella, 2019; The Lancet, 2019). As such, both systemic and cellular iron homeostasis need to be tightly regulated to maintain health and prevent disease (Chifman et al., 2014).

Absorption of iron is regulated via secretion of the hormone hepcidin (Meynard et al., 2014) and cellular iron levels are mediated post-transcriptionally by iron regulatory proteins (IRPs) (Chifman et al., 2014). Hepcidin maintains systemic iron homeostasis by controlling the movement of iron from the enterocyte into circulation (Meynard et al., 2014). IRPs function by sensing intracellular iron levels and binding to iron responsive elements (IRE) in the untranslated regions (UTRs) of the mRNA encoding many of the proteins involved in cellular iron homeostasis (Anderson et al., 2012). Depending on the location of the IRE, IRP binding can have two vastly different effects (Anderson et al., 2012). Binding of IRPs to IREs in the 5′ UTR results in translation inhibition and binding in the 3' UTR results in mRNA stabilization (Wallander et al., 2006).

Ferroptosis is a form of iron-dependent cell death, that is, the result of excess lipid peroxidation (Dixon et al., 2012; Stockwell, 2022). Under normal conditions, endogenous antioxidants such as Glutathione peroxidase 4 (GPX4) can alleviate these lipid peroxides (Lee et al., 2021; Stockwell, 2022). Cysteine is imported into the cell via solute carrier family 7 member 11 (SLC7A11), one half of the antiporter system Xc^- (Stockwell, 2022). This cysteine is then converted to cystine prior to its incorporation into glutathione (GSH) (Stockwell, 2022). GPX4 then oxidizes GSH to reduce lipid peroxides to lipid alcohols (Stockwell, 2022). Disruption of any part of these endogenous antioxidant regulatory systems is sufficient to trigger ferroptosis (Lee et al., 2021).

Oxidation in ferroptosis can occur via both iron-based auto-oxidation or enzymatic-mediated mechanisms (Lee et al., 2021). Non-enzymatic auto-oxidation is the result of Fenton-like chemistry, in which ferrous (Fe^{2+}) iron reacts directly with oxygen leading to the formation of ferric (Fe^{3+}) iron and a radical (Dixon et al., 2012; Lee et al., 2021). Multiple iron-containing oxidation enzymes can also lead to the development of ROS (Lee et al., 2021). However, the role of iron metabolism in ferroptosis has only just begun to be elucidated and the roles of many iron-related proteins have yet to be described. While increased mitochondrial iron import (Yuan et al., 2016) and inhibition of iron sulfur cluster biogenesis have been shown to increase ferroptosis sensitivity in cancer cells (Novera et al., 2020), cellular iron accumulation is associated with resistance to ferroptosis in neuronal and senescent cell types (Wang et al., 2016; Masaldan et al., 2018). These findings indicate that the role of iron in ferroptosis is complex and likely context- and cell-type dependent.

2 Dietary iron metabolism and systemic iron homeostasis

In the diet, iron is present as both heme and non-heme iron (Abbaspour et al., 2014). Non-heme iron is primarily found in plant sources, while heme iron comes directly from the myoglobin and hemoglobin in animal products (Abbaspour et al., 2014). These two forms of iron have drastically different bioavailabilities, with maximum bioavailabilities of 10 and 30-percent, respectively (Skolmowska and Głąbska, 2019). Although there is no regulated pathway for the excretion of iron, absorption of at least 1–2 mg of iron daily by enterocytes in the duodenum is necessary to directly replace iron lost through the death of skin and intestinal cells, sweat, and menstruation (Wallander et al., 2006; Anderson et al., 2012; Chifman et al., 2014). Thus, the recommended dietary allowance for iron in male and female individuals is set at 8 mg/day and 18 mg/day, respectively, to account for low bioavailability and increased loss in females.

Elemental iron from non-heme sources enters the enterocyte through solute carrier family 11 member 2 (SLC11A2, also known as divalent metal transporter I (DMT1)), a transport protein, that is, able to transport ferrous iron (Yanatori and Kishi, 2019). However, at this point dietary non-heme iron is in the ferric form, so it has to be reduced by the ferric reductase, cytochrome b reductase 1 (CYBRD1) prior to its absorption (Chifman et al., 2014). Though heme iron transporters have been described, the primary dietary heme iron transporter has yet to be identified (Muckenthaler et al., 2017). Inside the cell, iron is released from heme via the action of heme oxygenase 1 (HMOX1) and joins non-heme iron in the labile iron pool (Chifman et al., 2014). This iron can now be used by the enterocytes (Abbaspour et al., 2014), stored in the iron storage protein, ferritin (Chifman et al., 2014; Plays et al., 2021) or exported to the rest of the body via solute carrier family 40 member 1 (SLC40A1), also known as ferroportin (Sheftel et al., 2012). Because ferroportin only exports ferric iron, ferrous iron must first be oxidized by hephaestin (HEPH), a membrane-anchored multicopper ferroxidase (Deshpande et al., 2017). After movement through SLC40A1, iron binds the iron transport protein transferrin (TF), enters the plasma, and is transported to other cells throughout the body (Chifman et al., 2014). When iron levels are adequate, hepcidin antimicrobial peptide (HAMP), commonly referred to as hepcidin, is excreted by the liver and blocks the export of iron by promoting SLC40A1 internalization and degradation (Meynard et al., 2014). Due to the short lifespan of enterocytes, the remaining iron is inevitably lost when these cells are sloughed off and excreted in the feces (Anderson et al., 2012).

Two major destinations for TF-bound iron leaving the small intestine are the liver and bone marrow (Chifman et al., 2014; Meynard et al., 2014). The liver has two major iron-related functions—Iron storage and regulation of systemic iron homeostasis via HAMP (Meynard et al., 2014). Hepatocytes internalize iron via the proteins transferrin receptor and transferrin receptor 2 (TFRC, TFR2) and the homeostatic iron regulator (HFE) (Chifman et al., 2014). Transcription of hepcidin is regulated through a process in which bone-morphogenic protein six (BMP6) binds its receptor, triggering the phosphorylation of receptor mediated SMAD homolog (R-SMAD) (Meynard et al., 2014). This results in SMAD family members 1, 5 and 8 (SMAD1, SMAD5, SMAD8), forming a complex with SMAD 4, resulting in downstream suppression of hepcidin secretion (Meynard et al., 2014; Xiao et al., 2020; Xu et al., 2021). Hepcidin is primarily regulated in response to iron availability, but can also be triggered by inflammation, hypoxia and the rate of erythrocyte formation (Chifman et al., 2014). Hepatic iron stores can vary significantly based on gender and a variety of other factors (Pietrangelo, 2016). Because of its role in iron storage, multiple diseases occur due to the storage of excess iron in the liver

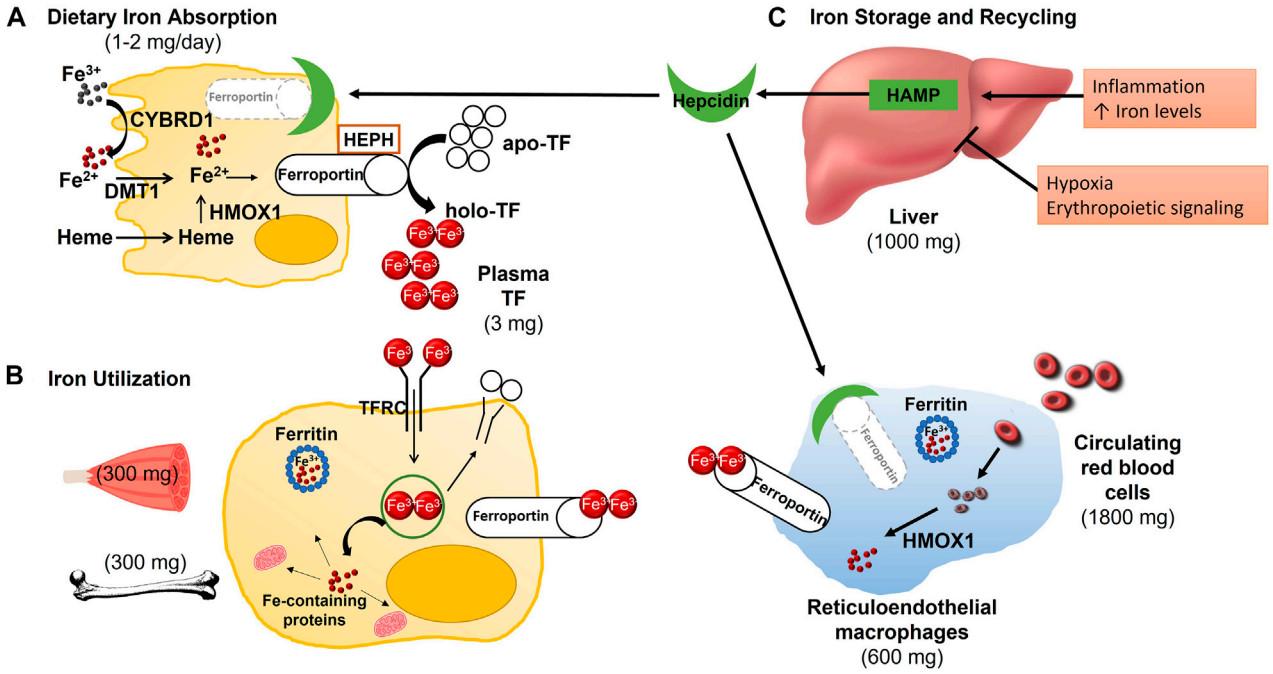

FIGURE 1
Absorption, Distribution and Metabolism of Iron. **(A)** Each day, 1–2 mg of iron are absorbed in the duodenum. Ferric, non-heme iron must first be reduced by duodenal cytochrome B (CYBRD1) to be transported into the enterocyte via divalent metal transporter 1 (DMT1). Dietary heme iron enters the enterocyte via an unknown transporter where the iron is then released from heme by heme oxygenase (HMOX1), joining non-heme iron in the labile iron pool. If not needed by the enterocyte, the ferrous iron is released into circulation, by exiting the cell through ferroportin. Following export across the basolateral membrane, ferrous iron is oxidized by hephaestin (HEPH) before it is bound to transferrin (TF) for transport to various tissues. **(B)** Transferrin-bound iron binds to transferrin receptor (TFRC) on the cell surface where the TF/TFRC complex is internalized though receptor-mediated endocytosis. The acidic pH of the endosome results in the release of iron from TF so that it can be pumped into the cytoplasm, most likely through DMT1. TF and TFRC are recycled back to the cell surface where they dissociate upon encountering a neutral pH. Inside the cell, iron can be stored in ferritin, utilized for iron-dependent processes such as the synthesis of myoglobin in skeletal muscle or erythropoiesis in the bone marrow, or exported back into circulation via ferroportin. **(C)** Whole-body iron homeostasis is maintained though the hepatic synthesis of hepcidin (HAMP) and the efficient recycling of senescent red blood cells by reticuloendothelial macrophages. In response to inflammation and increased iron availability, hepcidin production is increased. The binding of hepcidin to ferroportin at the cell surface of enterocytes and macrophages leads to its internalization and degradation, subsequently diminishing iron absorption and release from stores, respectively. Hepcidin production is decreased in response to hypoxia and enhanced erythropoiesis to increase iron uptake and availability.

(Pietrangelo, 2016). Although symptoms of these diseases are similar, they are the result of a variety of pathophysiologies, including genetic or acquired loss of hepcidin, inhibition of hepcidin function and loss of ferroportin (Pietrangelo, 2016).

Another major destination for iron in the body is the erythroid bone marrow (Chifman et al., 2014). Here, iron is essential for erythropoiesis as it is a major component of hemoglobin (Kautz and Nemeth, 2014). Iron enters erythroblasts via TFRC-mediated endocytosis and the mitochondria through the protein solute carrier family 25 member 37 (SLC25A37), also known as mitoferrin-1 (Chifman et al., 2014). In both the cytosol and mitochondria, it is used for heme formation, prior to being combined with the globin chains synthesized in the cytoplasm to form hemoglobin (Anderson et al., 2012; Chung et al., 2012; Farid et al., 2022). Once mature erythrocytes become senescent, their iron can be recycled by macrophages of the reticuloendothelial system (RES) (Chifman et al., 2014). RES macrophages phagocytose erythrocytes forming an erythrophagolysosome (EPL) that travels through the cytoplasm to the endoplasmic reticulum (ER) (Sheftel et al., 2012). The ER is then able to recruit HMOX1 (Sheftel et al., 2012) which frees iron for use by the macrophage or export to other cells through ferroportin (Chifman et al., 2014). This system is well described; however, the exact mechanism by which iron leaves the EPL has yet to be elucidated (Sheftel et al., 2012). Most iron used by the body is maintained through this efficient iron recycling system involving the bone marrow, erythroblasts, and reticuloendothelial macrophages (Winn et al., 2020). Figure 1 illustrates how iron status is sensed by the liver to regulate iron absorption, recycling, and distribution throughout the body.

3 IRP-mediated control of cellular iron metabolism and homeostasis

Across the body, the movement of iron into and out of cells must be tightly regulated. Cellular iron metabolism and homeostasis are regulated by the binding of iron regulatory proteins (IRPs), aconitase 1 (ACO1, also known as IRP1) and iron response element binding protein 2 (IREB2, also known as IRP2) to iron-responsive elements (IRE) in the untranslated regions (UTRs) of the mRNA of many iron related proteins (Anderson et al., 2012). The IRE is a stem looped portion of the mRNA containing the sequence

CAGUG followed by uracil or cytosine, that is, around 28 nucleotides in length (Wallander et al., 2006). This region is highly conserved across IRE containing mRNAs (Wallander et al., 2006). IREs can be located in either the 3′ or 5′ UTRs of mRNA, with 5′IRE-IRP binding resulting in translational repression, and 3′IRE-IRP binding inhibiting endonucleolytic degradation (Wallander et al., 2006; Anderson et al., 2012). Classic examples of 5′IRE containing mRNAs include those involved in the storage (FTH1, FTL) and export (SLC40A1) of iron and examples of 3′IRE containing mRNAs include those involved in the import (TFRC, SLC11A2) of iron (Chifman et al., 2014). In 2011, Sanchez and colleagues (Sanchez et al., 2011) identified over 30 additional IRE containing mRNAs using immunoselection and microarrays.

Although IRP1 and IRP2 are similar in structure, they do have significant differences in the way they sense iron and bind to IREs (Volz, 2008). IRP1 exists in two forms: a cytosolic aconitase isoform that doesn't bind IREs, or an RNA binding form, that binds IREs with a high affinity (Anderson et al., 2012). In conditions where adequate iron is available, assembly of an Fe-S cluster confers enzymatic activity, whereas under low iron conditions, disassembly of the Fe-S cluster promotes IRE binding (Wallander et al., 2006). IRP1 is also able to respond to multiple non-iron inputs including the presence of reactive oxygen and nitrogen species, the presence of heme compounds and phosphorylation of the serine it the 138th position (Volz, 2008; Anderson et al., 2012), all of which result in the disassembly of the Fe-S cluster, allowing for IRE binding (Volz, 2008). In addition to these multiple feedback loops, the ubiquitin E3 ligase responsible for iron-induced proteasomal degradation of IRP2 has been shown to also ubiquitinate IRP1 (Anderson et al., 2012).

Despite having almost sixty-percent similarity to IRP1, IRP2 lacks an Fe-S cluster and is primarily regulated by alterations in protein stability (Volz, 2008). IRP2's degradation occurs in response to ubiquitination by its E3 ubiquitin ligase, F-box and leucin-rich repeat protein 5 (FBLX5), a protein with a hemerythrin-like domain in its N-terminal that allows it to sense the presence of iron and oxygen in the cell (Ruiz and Bruick, 2014). During times where iron is limiting or the occurrence of hypoxia, the hemerythrin-like domain conformationally changes FBXL5, resulting in increased stability and IRP2-IRE binding activity (Ruiz and Bruick, 2014). IRP2 also differs from IRP1 in that it has a 73 amino acid sequence rich in cysteine, glycine, lysine, and proline (Volz, 2008). Residues in this domain can be oxidized by heme, allowing the protein RANBP2-type and C3HC4-type zinc finger containing 1 [RBCK1, also known as heme-oxidized IRP2 ubiquitin ligase (HOIL-1)] to mark it for degradation in response to heme availability (Anderson et al., 2012). Additionally, IRP2 has been shown to have altered IRE binding affinity at different stages in the cell cycle as phosphorylation at the 157th position during the G2/M transition results in an inability to bind IREs (Wallander et al., 2008).

In response to low iron, the IRE binding activity of both IRP1 and IRP2 are increased, leading to ferritin degradation and TFRC stabilization in an attempt to increase cellular iron content (Anderson et al., 2012). Circulating transferrin bound to iron is then able to bind to its receptor, found on the cell surface, resulting in receptor mediated endocytosis, during which a clathrin coated sorting endosome is formed (Sheftel et al., 2012). This endosome contains a v-ATPase pump, that is, able to manipulate the pH of the endosome, resulting in a pH of around 5.6 (Sheftel et al., 2012; Ogun and Adeyinka, 2022). At this low pH, iron is released from transferrin (Sheftel et al., 2012), allowing both TF and TFRC to return to the cell surface (Chifman et al., 2014). Within the endosome, ferric iron is reduced back to its ferrous form by a member of the six transmembrane epithelial antigen of the prostate (STEAP) family prior to its export into the cytoplasmic labile iron pool through DMT1, where it is made available to the cell or stored in ferritin (Sheftel et al., 2012).

Inside of the cell, iron can be used for a variety of cellular processes, including hemoglobin synthesis, cell signaling, iron-sulfur cluster group formation, energy production, DNA synthesis, and cell respiration (Abbaspour et al., 2014). Because of it's potential to form toxic free radicals, iron, that is, not used by the cell or exported, is stored in the iron storage protein ferritin, a nanocage made up of various repeats of light and heavy chains that can oxidize and store up to 5,000 molecules of iron (Plays et al., 2021). The heavy chains are responsible for oxidation of iron prior to storage in the light chains (Plays et al., 2021). When the cell develops an increased need for iron, autophagosomes and autolysosomes are utilized to free ferritin bound iron for use through a nuclear receptor activated 4 (NCOA4) mediated process known as ferritinophagy (Liu et al., 2022). This process is IRP-independent and a secondary pathway through which ferritin is degraded (Liu et al., 2022).

Movement of iron within the cell is achieved by chaperone proteins, such as poly (rC)-binding protein 1 (PCBP1), which allow iron to move throughout the cell without contributing to ROS formation (Patel et al., 2021). In some cells, ferrous iron in the labile iron pool can be transported through the membrane transport protein ferroportin into the plasma, where it is almost immediately bound to transferrin (Sheftel et al., 2012; Chifman et al., 2014). Prior to this export, it must be oxidized back to its ferric form, as discussed previously. The binding of iron to transferrin is possible because of the presence of a carbonate in transferrin that contains a charge opposite that of ferric iron (Ogun and Adeyinka, 2022). This process is essential to allow transferrin to safely move iron throughout the body without forming toxic free radicals (Chifman et al., 2014).

4 Ferroptosis

In 2012, Scott Dixon and colleagues in the Stockwell lab described a novel form of regulated cell death they coined ferroptosis due to its dependence on iron availability (Dixon et al., 2012). Ferroptosis occurs as the result of the iron-dependent accumulation of lipid reactive oxygen species (ROS) and results in shrunken mitochondria with thickened membranes (Dixon et al., 2012). The description of ferroptosis as an alternative form of programmed cell death has resulted in a booming new area of research across many chronic diseases including cancer, neurodegeneration, and cardiovascular diseases (Stockwell, 2022). Key to understanding the therapeutic potential of ferroptosis in health and disease is the availability of two agents of ferroptosis induction characterized in the original description of ferroptosis: erastin and RAS-selective lethal 3 (RSL3) (Dixon et al., 2012).

Erastin induces ferroptosis by blocking the function of SLC7A11 resulting in downstream interruption of glutathione

(GSH) production, and subsequently GPX4 synthesis (Dixon et al., 2014). RSL3 induces ferroptosis by directly binding to and inhibiting the function of GPX4 (Yang et al., 2014). Ferroptosis then occurs as the result of excess lipid peroxidation, beyond the capacity of the endogenous lipophilic antioxidant glutathione peroxidase 4 (GPX4) to repair them (Stockwell, 2022). The ensuing lipid ROS accumulation leads to altered function and membrane destruction, resulting in cell death (Lee et al., 2021).

GPX4 is an endogenous antioxidant that selectively targets lipids (Lee et al., 2021; Stockwell, 2022). The canonical GPX4 production pathway begins with system Xc^-, which refers to the two membrane transport proteins solute carrier family 3 member 2 (SLC3A2) and solute carrier family 7 member 11 (SLC7A11) (Stockwell, 2022). These proteins function as antiporters, responsible for the import of cystine and export of glutamate, respectively (Lu et al., 2017). Inside of the cell, cystine is reduced to two cysteines which are incorporated into GSH prior to its oxidation by GPX4 to reduce lipid peroxides to lipid alcohols (Lu et al., 2017; Stockwell, 2022). As such, exogenous lipophilic antioxidants can be used to prevent ferroptosis (Lee et al., 2021). The two most commonly used examples are liproxstatin-1 (Lip-1) and ferrostatin-1 (Fer-1) (Zilka et al., 2017; Stockwell, 2022). Both of these function as radical trapping antioxidants (RTAs), meaning that they prevent autooxidation rather than influencing the activity of the oxidases contributing to lipid peroxide formation (Zilka et al., 2017). Other inhibitors of ferroptosis also exist, for example: probucol, an antioxidant drug used to treat dyslipidemia (Yamashita et al., 2015), is able to inhibit ferroptosis (Stockwell, 2022). Additionally, selenium, nitroxide, iron chelators like deferoxamine (DFO) and even, at very high doses, necrostatin-1, a necrosis inhibitor, have been shown to inhibit ferroptosis (Stockwell, 2022).

Since the generation of lipid ROS is the main mechanism of damage leading to cell death by ferroptosis, lipid metabolism plays a critical role in ferroptosis. Phospholipids that contain polyunsaturated fatty acid (PUFA-PLs) are at an especially high risk for peroxidation, particularly PUFAs containing adrenic or arachidonic acids (Lee et al., 2021; Stockwell, 2022). This role applies specifically to membrane-incorporated PUFA-PLs, as the oxidation of PUFAs that are not membrane anchored and incorporated into PUFA-PLs do not contribute to ferroptosis (Lee et al., 2021). The lipid metabolism protein, achaete-scute family belch transcription factor 4 (ASCL4), which incorporates long chain fatty acids and acyl-CoA into fatty acid esters prior to phospholipid generation by lysophosphatidylcholine acyltransferase 3 (LPCAT3) is an important mediator between lipid metabolism and ferroptosis (Doll et al., 2017). In breast cancer cells, decreased or increased ASCL4 expression is associated with reduced or augmented ferroptosis sensitivity, respectively (Lee et al., 2021). Additionally, monounsaturated fatty acids have been shown to be ferroptosis protective, possibly due to competition with PUFAs for phospholipid synthesis (Lee et al., 2021).

There are two main mechanisms of lipid peroxidation in ferroptosis: enzyme-mediated and auto-oxidation (Lee et al., 2021). Enzymatic oxidation is the result of the action of many iron containing proteins, including lipoxygenases (LOXs), cytochrome P450 oxidoreductase (POR), and nicotinamide adenine dinucleotide phosphate (NADPH) oxidases (NOXs) (Lee et al., 2021). LOXs function by oxidizing PUFAs to PUFA lipid hyperoxides (Kuhn et al., 2015). Increased POR activity is hypothesized to accelerate the conversion of ferrous iron in its heme group to ferric iron and *vice versa*, either promoting or directly contributing to lipid peroxidation (Lee et al., 2021). Finally, NOXs generate lipid superoxides through a reaction in which NADPH and oxygen are converted to a hydrogen, a superoxide radical, and $NADP^+$ (Panday et al., 2015). Non-enzymatic auto-oxidation occurs as the result of Fenton chemistry whereby ferrous iron and hydrogen peroxide (H_2O_2) react resulting in hydroxyl radicals and ferric iron, amongst other products (Dixon et al., 2012; Lee et al., 2021).

When ferroptosis was originally described, it was demonstrated that iron chelation and supplementation decreased and increased ferroptosis, respectively (Dixon et al., 2012). Thus, the name, ferroptosis, was inspired by the essentiality of available redox-active iron for any of the above-mentioned processes to occur. Li et al. (2017) demonstrated that exposure to excess levels of both hemoglobin and ferrous iron resulted in ferroptosis. The authors showed that excess hemoglobin results in increased lipid peroxide accumulation as a result of GPX4 inhibition (Li et al., 2017). It is important to note that increased total cellular iron is not necessary for ferroptosis, as release of iron from ferritin can be ferroptosis promoting (Quiles del Rey and Mancias, 2019). Despite these findings, the role of iron metabolism in ferroptosis is only beginning to be elucidated and the functions of many proteins involved in iron metabolism in ferroptosis remain poorly understood.

5 Iron and IRPs in ferroptosis

Ferroptosis is driven by extensive iron-dependent accumulation of lipid reactive oxygen species (ROS), which ultimately commits cells to death (Dixon et al., 2012). Importantly, IRPs, the principal regulators of cellular iron homeostasis themselves are also regulated by iron availability and reactive oxygen species (Anderson et al., 2012), yet our understanding of how the IRP-IRE-system contributes to iron accumulation during ferroptotic cell death is still in its infancy. Investigations into the roles of IRPs in ferroptosis are made complicated however because even though IRP1 and IRP2 are ubiquitously expressed (Meyron-Holtz et al., 2004a), their relative expression levels differ in cell type and tissue-dependent manners, and they can display distinct biological roles under different physiologic conditions (Meyron-Holtz et al., 2004b).

It is currently understood that uptake of transferrin-bound iron, via the IRP target TFRC, is necessary for ferroptosis and that RNAi knockdown of TFRC decreases ferroptosis sensitivity (Gao et al., 2015). Nevertheless, the question as to why TFRC would continue to import iron following ferroptosis induction at the cost of cell death remains. Research into TFRC regulation during ferroptosis induction has led to conflicting findings. Wang et al. (2016) reported reduced TFRC expression after erastin treatment. Such results are consistent with an appropriate cell response, wherein IRPs sense a relative cellular iron overload and decrease mRNA binding to reduce TFRC expression and subsequent cellular iron uptake (Wang et al., 2016).

Conversely, however, Alvarez et al. (2017) reported increased TFRC expression following erastin treatment. The authors

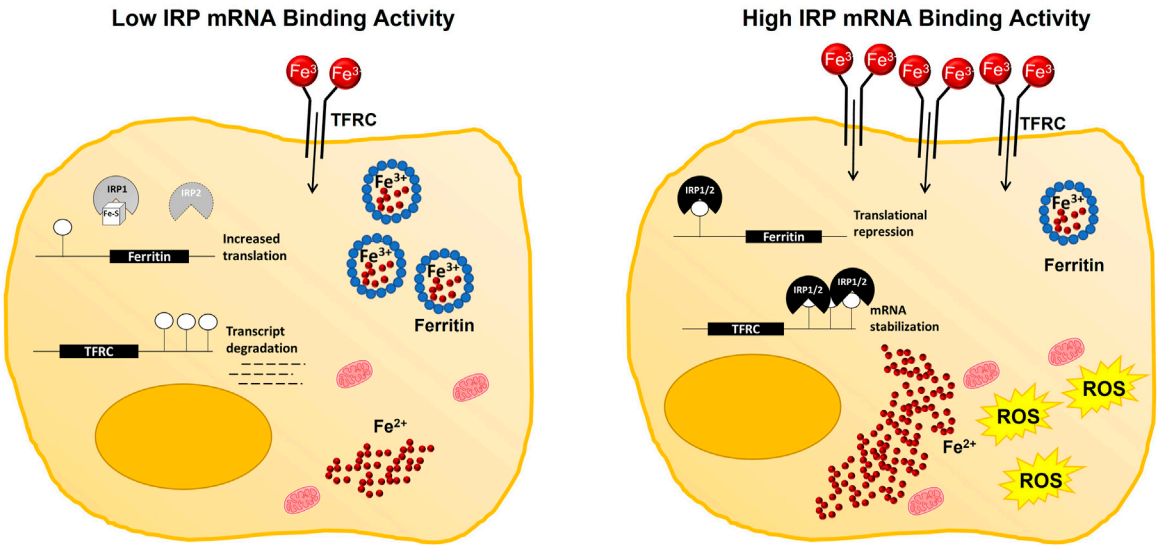

FIGURE 2
Working model of IRP-mediated contributions to cellular iron availability during ferroptosis. Under iron replete conditions, IRP mRNA binding activity is decreased. Subsequently, iron uptake by TFRC is reduced, while storage of iron in ferritin is increased to maintain a relatively small pool of labile iron within the cell. Whereas, under iron deficient conditions, or with impaired Fe-S cluster biogenesis, IRP mRNA binding activity is increased, reducing the capacity of the cell to safely store iron in ferritin while simultaneously promoting iron uptake by increasing TFRC abundance. Increased IRP mRNA binding activity then facilitates ferroptotic cell death by increasing the size of the labile iron pool and enabling ROS production.

speculated that the increase in TFRC expression is the result of decreased Fe-S biogenesis/stability and the ensuing increase in IRP1 mRNA binding activity (Alvarez et al., 2017). Nonetheless, neither IRP1 nor IRP2 expression or activity were assessed in either of these studies. Given the essentiality of iron availability to the effectiveness of ferroptosis activation, there is a fundamental need to understand the contribution of this major iron regulatory system to ferroptosis to fully harness its therapeutic potential.

IRP2 was first identified as a critical ferroptosis regulatory gene using a high-throughput shRNA screening library in the seminal work by Dixon et al. (2012). A strength of this work was that these findings were then validated by shRNA knockdown of IRP2 and its negative regulatory E3 ubiquitin ligase FBXL5, which resulted in reduced and enhanced sensitivity to ferroptosis induction, respectively. However, IRP2 mRNA binding activity was not assessed, and oxidized IRPs will not bind IRE (Henderson and Kuhn, 1995; Zumbrennen et al., 2009), so it cannot be assumed that increased levels of IRP2 protein expression indicates active IRE binding. Indeed, the effects on downstream IRP2 targets were inconsistent with functional changes in IRP2 mRNA binding activity (Dixon et al., 2012). This raises the possibility that in ferroptosis, IRP2 may be functioning independently of its canonical role in mRNA binding.

In support of this hypothesis, changes in IRP mRNA binding activity do not always predict differences in ferroptosis sensitivity (Thompson et al., 2020). The context-dependent differences in IRP involvement are likely multifaceted. Factors such as mode of ferroptosis induction (Gryzik et al., 2021), metabolic state of the cell (Novera et al., 2020), and differences in endogenous antioxidant capacities (Cardona et al., 2022) that influence the ability to handle a given amount of labile iron could all contribute to IRP responsiveness. Regardless, increased IRP-IRE binding activity (Chen et al., 2020), and even the increased expression of either IRP1 (Yao et al., 2021; Zhang et al., 2022) or IRP2 (Li et al., 2020) alone have been shown to augment ferroptosis sensitivity (Figure 2).

Fe-S cluster biogenesis is also another critical link between IRP-dependent control of cellular iron homeostasis and ferroptotic cell death as both cysteine deprivation and glutathione depletion promote ferroptosis and diminish Fe-S cluster biogenesis (Sipos et al., 2002; Novera et al., 2020). The formation, or lack thereof then, of an Fe-S cluster into IRP1 determines its role within the cell. When intracellular iron levels are low, IRP1 regulates iron homeostasis through its mRNA binding activity, but under iron adequate conditions, IRP1 primarily exists in an Fe-S cluster containing enzymatic form (Meyron-Holtz et al., 2004a).

The most common means of inducing ferroptosis include inhibiting system xc^-, and thus preventing cysteine import and glutathione production, or directly inhibiting GPX4 activity. As such, a negative impact on Fe-S cluster biogenesis, and subsequent promotion of IRP1 mRNA binding activity has been assumed by a number of investigators (Yuan et al., 2016; Terzi et al., 2021; Zhang et al., 2022), but has only been indirectly assessed by measuring changes in aconitase activity (Novera et al., 2020; Yao et al., 2021). The accumulation of mitochondrial iron however is also consistent with the hypothesis that ferroptosis induction disrupts Fe-S biogenesis and promotes IRP1 mRNA binding activity (Sipos et al., 2002; Yuan et al., 2016; Novera et al., 2020). Moreover, stabilization of the mitochondrial membrane protein, CDGSH iron sulfur domain 1 (CISD1), which can aid in the repair of oxidatively damaged IRP1 Fe-S clusters, has been shown to inhibit ferroptosis by decreasing mitochondrial lipid peroxidation (Yuan et al., 2016). Thus, current evidence does at least support a role for IRP1 mRNA binding activity in contributing to ferroptotic cell death, but it appears to be due to a pathologic disturbance of Fe-S biosynthesis rather than a response to changes in cellular iron.

It has also been hypothesized that IRP1 expression can be modulated to avoid cell death by ferroptosis (Zhang et al., 2022). Zhang et al. (2022) found that enolase 1 (ENO1), an enzyme involved in glycolysis is able to bind IRP1 mRNA and recruit CCR4-NOT transcription complex subunit 6 (CNOT6), a protein that utilizes its nuclease domain to degrade IRP1 mRNA (Zhang et al., 2022). The authors of the study also reported that expression of solute carrier family 25 member 37 (SLC25A37), also referred to as mitoferrin-1 (MFRN1), the protein responsible for import of iron into the mitochondria, is decreased in response to ENO1 (Zhang et al., 2022). Additionally, they showed that decreased SLC25A37 expression led to decreased ROS formation, leading to the hypothesis that ENO1 regulated an IRP1-SLC25A37 axis to alter ferroptosis sensitivity (Zhang et al., 2022). These findings support another role for IRP1 in ferroptosis.

Intriguingly however, disruption of Fe-S cluster biogenesis by cysteine deprivation in ovarian clear cell carcinoma cell lines only led to ferroptotic cell death in cells which were relying more heavily on glycolysis for energy production (Novera et al., 2020). Whereas cells that were depending more heavily on oxidative phosphorylation appeared to succumb to apoptosis (Novera et al., 2020). The authors postulated the observed differences in cell death may be due to the high use of Fe-S containing proteins to complete oxidative metabolism, and thus metabolic state may be important to consider when assessing the role of IRPs in ferroptosis (Novera et al., 2020). Given the preferences for glycolytic energy production in many tumor cell types, these findings suggest disruption of Fe-S cluster assembly and perturbation of IRP function could be used to further augment ferroptosis sensitivity cancer.

Previous work indicates that in addition to the control of IRP1 function, IRP2 stability is also dependent upon Fe-S cluster assembly proteins (Stehling et al., 2013), but this has only recently been explored in the context of ferroptosis (Terzi et al., 2021). In both reports though, IRP2 stability and mRNA binding activity were increased upon inhibition of cytosolic Fe-S protein assembly. This suggests that activation of ferroptosis by restricting cysteine and glutathione availability would also mimic an iron starvation response by increasing the mRNA binding activity of both IRP1 and IRP2. However, the mRNA binding activity of neither IRP1 nor IRP2 has been fully characterized following treatment with traditional ferroptosis inducing agents such as erastin or RSL3.

Some artemisinin derivatives like artemether (ART) and dihydroartemisinin (DAT) can also be ferroptosis inductive (Chen et al., 2020; Li et al., 2020), and one way these compounds may promote ferroptosis is by increasing IRP mRNA binding activity (Chen et al., 2020; Li et al., 2020). In 2020, when studying ART as a potential liver fibrosis treatment, Li et al. (2020) found that ART induced ferroptosis through IRP2. They reported a dose dependent increase in IRP2 expression in response to ART treatment and that IRP2 knockdown significantly decreased ART's ability to induce ferroptosis (Li et al., 2020). Intriguingly, labile iron within the cell may also bind directly to DAT. In this form, the DAT-iron complex retains iron's redox potential but is unable to alter IRP activity (Chen et al., 2020). Thus, artemisinin derivatives may be particularly useful in combination with other small molecule inducers of ferroptosis.

6 IRPs in cancer and ferroptosis

In cancer, IRP signaling can be corrupted in an effort to acquire sufficient iron to support rapid cell proliferation. For example, IRP2 overexpression in breast cancer results in increased TFRC expression, decreased ferritin expression, and subsequently an increased labile iron pool (Wang et al., 2014). Increased expression of TFRC was also found to have worse clinical prognosis in patients that had renal cell carcinoma (Greene et al., 2017). As mentioned above, increased expression of TFRC is typically mediated by increased IRP mRNA binding activity, but overexpression of IRP1 was actually found to decrease tumor growth *in vivo* (Chen et al., 2007). Thus, despite their similar roles in the maintenance of iron homeostasis, IRP1 and IRP2 exhibit opposing phenotypes in the reduction and promotion of tumor growth, respectively.

The disparate effects of IRP1 *versus* IRP2 expression in cancer outcomes may be partially explained by the specific 73 amino acid insert in IRP2 that structurally distinguishes it from IRP1. Indeed, overexpression of wild-type IRP2 significantly increased tumor burden in a mouse xenograft model, but when a mutant version IRP2 lacking the 73 amino acid insert was overexpressed in the same model, this response was blunted (Maffettone et al., 2010). Intriguingly, the expression of canonical IRP targets was largely unaffected in tumors expressing either the wild-type or mutant version of IRP, but rather wild-type IRP2 bearing tumors displayed increased levels of MYC proto-oncogene, bHLH transcription factor (MYC) and mitogen-activated protein kinase 1/3 (MAPK1/3) phosphorylation. These findings suggest that IRP2 may promote tumor development independently of its role in iron metabolism.

IRP2 has also been implicated in tumor progression via its capacity to suppress translation of the tumor suppressor gene, tumor protein p53 (TP53) (Zhang et al., 2017). However, this regulation seems to function in a highly regulated feedback loop as TP53 inactivation of the IRE-IRP system can also facilitate tumor cell growth arrest by restricting cellular iron availability (Zhang et al., 2008). This work was recently expanded upon by the discovery that wild-type TP53 can specifically modulate IRP1 RNA binding activity via the transcriptional regulation of the iron-sulfur cluster assembly enzyme (ISCU) (Funauchi et al., 2015). The importance of the iron-TP53 feedback loop in tumor suppression is further supported by the findings that decreased ISCU expression in human liver cancer tissues is associated with TP53 mutations (Funauchi et al., 2015).

As TP53 is the most commonly mutated gene in all of human cancers, our lab then asked the question as to how IRP1 and IRP2 are regulated in cancer cells harboring distinct TP53 mutation types. We found that induction of mutant TP53 expression significantly reduced ferredoxin reductase (FDXR) expression, and that this reduced expression was associated with impaired mitochondrial Fe-S cluster biogenesis and altered IRP function in response to changes in cellular iron availability (Clarke et al., 2019). Notably, proper FDXR signaling has also been shown to be essential for IRP2 mediated control of TP53-dependent tumor suppression (Zhang et al., 2017). In humans, FDXR is critical for Fe-S cluster biogenesis and its reduction is associated with misregulation of cellular iron homeostasis (Shi et al., 2012). As such, ferroptosis induction has been proposed as a way to therapeutically target

tumor cells expressing distinct mutant TP53 subtypes (Thompson et al., 2020).

Fe-S cluster containing proteins are also essential components of energy metabolism and DNA repair enzymes, and their impaired assembly could significantly impact tumor progression. Intriguingly, the antidiabetic drug pioglitazone was recently shown to inhibit iron transfer into the mitochondria by stabilizing the [2Fe-2S] cluster in CDGSH iron sulfur domain 1 (CISD1) (Zuris et al., 2011). It was then proposed that an unrecognized benefit of pioglitazone use for diabetic patients might be reduced ROS production as a result of decreased mitochondrial iron availability. However, an unintended consequence of this mitochondrial iron restriction could be diminished ferroptosis sensitivity. Indeed, Yuan et al. (2016) demonstrated that pioglitozone diminishes ferroptotic cell death in a CISD1-dependent manner by protecting against mitochondrial iron accumulation. Continued investigations are needed to delineate how pioglitazone influences cellular IRP mRNA binding activity, and how this influence could impact ferroptosis sensitivity.

7 Conclusion

Cancer cells are extravagant users of iron, and as such, much effort has been devoted to taking advantage of cancers cells' "iron addiction" by restricting iron availability (Lui et al., 2015). However, these approaches are confounded by the essential nature of iron for noncancerous cells as well. Ferroptosis has been described as a novel approach to exploiting the toxic nature of iron to promote programmed cell death, but again the toxic potential of iron for all cell types must be considered. Given the essentiality of the IRP-IRE system to the maintenance of iron homeostasis, and the growing body of evidence implicating the key players of this system in ferroptotic cell death, delineating the specific roles of IRP1 and IRP2 in ferroptosis is of fundamental importance to fully harness its chemotherapeutic potential.

Author contributions

CC and MM contributed equally to reviewing and interpreting the relevant literature, drafting, and editing the manuscript. All authors contributed to the article and approved the submitted version.

Funding

This research was supported by the National Institutes of Health, National Cancer Institute grant R03 CA259595 and the National Institute on Aging grant R03 AG077299.

Conflict of interest

The authors declare that the research was conducted in the absence of any commercial or financial relationships that could be construed as a potential conflict of interest.

Publisher's note

References

Abbaspour, N., Hurrell, R., and Kelishadi, R. (2014). Review on iron and its importance for human health. *J. Res. Med. Sci.* 19 (2), 164–174.

Alvarez, S. W., Sviderskiy, V. O., Terzi, E. M., Papagiannakopoulos, T., Moreira, A. L., Adams, S., et al. (2017). NFS1 undergoes positive selection in lung tumours and protects cells from ferroptosis. *Nature* 551 (7682), 639–643. doi:10.1038/nature24637

Anderson, C. P., Shen, M., Eisenstein, R. S., and Leibold, E. A. (2012). Mammalian iron metabolism and its control by iron regulatory proteins. *Biochim. Biophys. Acta* 1823 (9), 1468–1483. doi:10.1016/j.bbamcr.2012.05.010

Beutler, E. (2002). History of iron in medicine. *Blood Cells Mol. Dis.* 29 (3), 297–308. doi:10.1006/bcmd.2002.0560

Bradbear, R. A., Bain, C., Siskind, V., Schofield, F. D., Webb, S., Axelsen, E. M., et al. (1985). Cohort study of internal malignancy in genetic hemochromatosis and other chronic nonalcoholic liver diseases. *J. Natl. Cancer Inst.* 75 (1), 81–84. doi:10.1093/jnci/75.1.81

Camaschella, C. (2019). Iron deficiency. *Blood, J. Am. Soc. Hematol.* 133 (1), 30–39. doi:10.1182/blood-2018-05-815944

Cardona, C. J., Hermann, E. R., Kouplen, K. N., Hartson, S. D., and Montgomery, M. R. (2022). Differences in antioxidant and lipid handling protein expression influence how cells expressing distinct mutant TP53 subtypes maintain iron homeostasis. *Cells* 11 (13), 2064. doi:10.3390/cells11132064

Chen, G., Fillebeen, C., Wang, J., and Pantopoulos, K. (2007). Overexpression of iron regulatory protein 1 suppresses growth of tumor xenografts. *Carcinogenesis* 28 (4), 785–791. doi:10.1093/carcin/bgl210

Chen, G. Q., Benthani, F. A., Wu, J., Liang, D., Bian, Z. X., and Jiang, X. (2020). Artemisinin compounds sensitize cancer cells to ferroptosis by regulating iron homeostasis. *Cell Death Differ.* 27 (1), 242–254. doi:10.1038/s41418-019-0352-3

Chifman, J., Laubenbacher, R., and Torti, S. V. (2014). A systems biology approach to iron metabolism. *Adv. Exp. Med. Biol.* 844, 201–225. doi:10.1007/978-1-4939-2095-2_10

Chung, J., Chen, C., and Paw, B. H. (2012). Heme metabolism and erythropoiesis. *Curr. Opin. Hematol.* 19 (3), 156–162. doi:10.1097/MOH.0b013e328351c48b

Clarke, S. L., Thompson, L. R., Dandekar, E., Srinivasan, A., and Montgomery, M. R. (2019). Distinct TP53 mutation subtypes differentially influence cellular iron metabolism. *Nutrients* 11 (9), 2144. doi:10.3390/nu11092144

Deshpande, C. N., Xin, V., Lu, Y., Savage, T., Anderson, G. J., and Jormakka, M. (2017). Large scale expression and purification of secreted mouse hephaestin. *PLoS One* 12 (9), e0184366. doi:10.1371/journal.pone.0184366

Dixon, S. J., Lemberg, K. M., Lamprecht, M. R., Skouta, R., Zaitsev, E. M., Gleason, C. E., et al. (2012). Ferroptosis: An iron-dependent form of nonapoptotic cell death. *Cell* 149 (5), 1060–1072. doi:10.1016/j.cell.2012.03.042

Dixon, S. J., Patel, D. N., Welsch, M., Skouta, R., Lee, E. D., Hayano, M., et al. (2014). Pharmacological inhibition of cystine–glutamate exchange induces endoplasmic reticulum stress and ferroptosis. *eLife* 3, e02523. doi:10.7554/eLife.02523

Doll, S., Proneth, B., Tyurina, Y. Y., Panzilius, E., Kobayashi, S., Ingold, I., et al. (2017). ACSL4 dictates ferroptosis sensitivity by shaping cellular lipid composition. *Nat. Chem. Biol.* 13 (1), 91–98. doi:10.1038/nchembio.2239

Farid, Y., Bowman, N. S., and Lecat, P. (2022). "Biochemistry, hemoglobin synthesis," in *StatPearls* (Treasure Island (FL): StatPearls Publishing LLC). StatPearls Publishing Copyright © 2022.

Funauchi, Y., Tanikawa, C., Yi Lo, P. H., Mori, J., Daigo, Y., Takano, A., et al. (2015). Regulation of iron homeostasis by the p53-ISCU pathway. *Sci. Rep.* 5, 16497. doi:10.1038/srep16497

Gao, M., Monian, P., Quadri, N., Ramasamy, R., and Jiang, X. (2015). Glutaminolysis and transferrin regulate ferroptosis. *Mol. Cell* 59 (2), 298–308. doi:10.1016/j.molcel.2015.06.011

Greene, C. J., Attwood, K., Sharma, N. J., Gross, K. W., Smith, G. J., Xu, B., et al. (2017). Transferrin receptor 1 upregulation in primary tumor and downregulation in benign kidney is associated with progression and mortality in renal cell carcinoma patients. *Oncotarget* 8 (63), 107052–107075. doi:10.18632/oncotarget.22323

Gryzik, M., Asperti, M., Denardo, A., Arosio, P., and Poli, M. (2021). NCOA4-mediated ferritinophagy promotes ferroptosis induced by erastin, but not by RSL3 in HeLa cells. *Biochim. Biophys. Acta Mol. Cell Res.* 1868 (2), 118913. doi:10.1016/j.bbamcr.2020.118913

Henderson, B. R., and Kuhn, L. C. (1995). Differential modulation of the RNA-binding proteins IRP-1 and IRP-2 in response to iron. IRP-2 inactivation requires translation of another protein. *J. Biol. Chem.* 270 (35), 20509–20515. doi:10.1074/jbc.270.35.20509

Kassebaum, N. J., Jasrasaria, R., Naghavi, M., Wulf, S. K., Johns, N., Lozano, R., et al. (2014). A systematic analysis of global anemia burden from 1990 to 2010. *Blood* 123 (5), 615–624. doi:10.1182/blood-2013-06-508325

Kautz, L., and Nemeth, E. (2014). Molecular liaisons between erythropoiesis and iron metabolism. *Blood* 124 (4), 479–482. doi:10.1182/blood-2014-05-516252

Kuhn, H., Banthiya, S., and van Leyen, K. (2015). Mammalian lipoxygenases and their biological relevance. *Biochim. Biophys. Acta* 1851 (4), 308–330. doi:10.1016/j.bbalip.2014.10.002

Lee, J. Y., Kim, W. K., Bae, K. H., Lee, S. C., and Lee, E. W. (2021). Lipid metabolism and ferroptosis. *Biol. (Basel)* 10 (3), 184. doi:10.3390/biology10030184

Li, Q., Han, X., Lan, X., Gao, Y., Wan, J., Durham, F., et al. (2017). Inhibition of neuronal ferroptosis protects hemorrhagic brain. *JCI insight* 2 (7), e90777. doi:10.1172/jci.insight.90777

Li, Y., Jin, C., Shen, M., Wang, Z., Tan, S., Chen, A., et al. (2020). Iron regulatory protein 2 is required for artemether -mediated anti-hepatic fibrosis through ferroptosis pathway. *Free Radic. Biol. Med.* 160, 845–859. doi:10.1016/j.freeradbiomed.2020.09.008

Liu, M. Z., Kong, N., Zhang, G. Y., Xu, Q., Xu, Y., Ke, P., et al. (2022). The critical role of ferritinophagy in human disease. *Front. Pharmacol.* 13, 933732. doi:10.3389/fphar.2022.933732

Lu, B., Chen, X. B., Ying, M. D., He, Q. J., Cao, J., and Yang, B. (2017). The role of ferroptosis in cancer development and treatment response. *Front. Pharmacol.* 8, 992. doi:10.3389/fphar.2017.00992

Lui, G. Y., Kovacevic, Z., Richardson, V., Merlot, A. M., Kalinowski, D. S., and Richardson, D. R. (2015). Targeting cancer by binding iron: Dissecting cellular signaling pathways. *Oncotarget* 6 (22), 18748–18779. doi:10.18632/oncotarget.4349

Maffettone, C., Chen, G., Drozdov, I., Ouzounis, C., and Pantopoulos, K. (2010). Tumorigenic properties of iron regulatory protein 2 (IRP2) mediated by its specific 73-amino acids insert. *PLoS One* 5 (4), e10163. doi:10.1371/journal.pone.0010163

Masaldan, S., Clatworthy, S. A. S., Gamell, C., Meggyesy, P. M., Rigopoulos, A. T., Haupt, S., et al. (2018). Iron accumulation in senescent cells is coupled with impaired ferritinophagy and inhibition of ferroptosis. *Redox Biol.* 14, 100–115. doi:10.1016/j.redox.2017.08.015

Meynard, D., Babitt, J. L., and Lin, H. Y. (2014). The liver: Conductor of systemic iron balance. *Blood* 123 (2), 168–176. doi:10.1182/blood-2013-06-427757

Meyron-Holtz, E. G., Ghosh, M. C., Iwai, K., LaVaute, T., Brazzolotto, X., Berger, U. V., et al. (2004a). Genetic ablations of iron regulatory proteins 1 and 2 reveal why iron regulatory protein 2 dominates iron homeostasis. *EMBO J.* 23 (2), 386–395. doi:10.1038/sj.emboj.7600041

Meyron-Holtz, E. G., Ghosh, M. C., and Rouault, T. A. (2004b). Mammalian tissue oxygen levels modulate iron-regulatory protein activities *in vivo*. *Science* 306 (5704), 2087–2090. doi:10.1126/science.1103786

Muckenthaler, M. U., Rivella, S., Hentze, M. W., and Galy, B. (2017). A red carpet for iron metabolism. *Cell* 168 (3), 344–361. doi:10.1016/j.cell.2016.12.034

Nelson, R. L., Davis, F. G., Persky, V., and Becker, E. (1995). Risk of neoplastic and other diseases among people with heterozygosity for hereditary hemochromatosis. *Cancer* 76 (5), 875–879. doi:10.1002/1097-0142(19950901)76:5<875:aid-cncr2820760523>3.0.co;2-q

Novera, W., Lee, Z.-W., Nin, D. S., Dai, M. Z.-Y., Binte Idres, S., Wu, H., et al. (2020). Cysteine deprivation targets ovarian clear cell carcinoma via oxidative stress and iron–sulfur cluster biogenesis deficit. *Antioxidants redox Signal.* 33 (17), 1191–1208. doi:10.1089/ars.2019.7850

Ogun, A. S., and Adeyinka, A. (2022). "Biochemistry, transferrin," in *StatPearls* (Treasure Island (FL): StatPearls Publishing LLC). StatPearls Publishing Copyright © 2022.

Panday, A., Sahoo, M. K., Osorio, D., and Batra, S. (2015). NADPH oxidases: An overview from structure to innate immunity-associated pathologies. *Cell Mol. Immunol.* 12 (1), 5–23. doi:10.1038/cmi.2014.89

Patel, S. J., Protchenko, O., Shakoury-Elizeh, M., Baratz, E., Jadhav, S., and Philpott, C. C. (2021). The iron chaperone and nucleic acid-binding activities of poly(rC)-binding protein 1 are separable and independently essential. *Proc. Natl. Acad. Sci. U. S. A.* 118 (25), e2104666118. doi:10.1073/pnas.2104666118

Pietrangelo, A. (2010). Hereditary hemochromatosis: Pathogenesis, diagnosis, and treatment. *Gastroenterology* 139 (2), 393–408, 408.e1-2. doi:10.1053/j.gastro.2010.06.013

Pietrangelo, A. (2016). Iron and the liver. *Liver Int.* 36, 116–123. doi:10.1111/liv.13020

Plays, M., Müller, S., and Rodriguez, R. (2021). Chemistry and biology of ferritin. *Metallomics* 13 (5), mfab021. doi:10.1093/mtomcs/mfab021

Quiles del Rey, M., and Mancias, J. D. (2019). NCOA4-mediated ferritinophagy: A potential link to neurodegeneration. *Front. Neurosci.* 13, 238. doi:10.3389/fnins.2019.00238

Ruiz, J. C., and Bruick, R. K. (2014). F-Box and leucine-rich repeat protein 5 (FBXL5): Sensing intracellular iron and oxygen. *J. Inorg. Biochem.* 133, 73–77. doi:10.1016/j.jinorgbio.2014.01.015

Sanchez, M., Galy, B., Schwanhaeusser, B., Blake, J., Bähr-Ivacevic, T., Benes, V., et al. (2011). Iron regulatory protein-1 and -2: Transcriptome-wide definition of binding mRNAs and shaping of the cellular proteome by iron regulatory proteins. *Blood* 118 (22), e168–e179. doi:10.1182/blood-2011-04-343541

Sheftel, A. D., Mason, A. B., and Ponka, P. (2012). The long history of iron in the Universe and in health and disease. *Biochim. Biophys. Acta* 1820 (3), 161–187. doi:10.1016/j.bbagen.2011.08.002

Shi, Y., Ghosh, M., Kovtunovych, G., Crooks, D. R., and Rouault, T. A. (2012). Both human ferredoxins 1 and 2 and ferredoxin reductase are important for iron-sulfur cluster biogenesis. *Biochim. Biophys. Acta* 1823 (2), 484–492. doi:10.1016/j.bbamcr.2011.11.002

Sipos, K., Lange, H., Fekete, Z., Ullmann, P., Lill, R., and Kispal, G. (2002). Maturation of cytosolic iron-sulfur proteins requires glutathione. *J. Biol. Chem.* 277 (30), 26944–26949. doi:10.1074/jbc.M200677200

Skolmowska, D., and Głąbska, D. (2019). Analysis of heme and non-heme iron intake and iron dietary sources in adolescent menstruating females in a national polish sample. *Nutrients* 11 (5), 1049. doi:10.3390/nu11051049

Stehling, O., Mascarenhas, J., Vashisht, A. A., Sheftel, A. D., Niggemeyer, B., Rosser, R., et al. (2013). Human CIA2A-FAM96A and CIA2B-FAM96B integrate iron homeostasis and maturation of different subsets of cytosolic-nuclear iron-sulfur proteins. *Cell Metab.* 18 (2), 187–198. doi:10.1016/j.cmet.2013.06.015

Stockwell, B. R. (2022). Ferroptosis turns 10: Emerging mechanisms, physiological functions, and therapeutic applications. *Cell* 185 (14), 2401–2421. doi:10.1016/j.cell.2022.06.003

Terzi, E. M., Sviderskiy, V. O., Alvarez, S. W., Whiten, G. C., and Possemato, R. (2021). Iron-sulfur cluster deficiency can be sensed by IRP2 and regulates iron homeostasis and sensitivity to ferroptosis independent of IRP1 and FBXL5. *Sci. Adv.* 7 (22), eabg4302. doi:10.1126/sciadv.abg4302

The Lancet (2019). *Anaemia—level 1 impairment [online]*. The Lancet (Accessed June 12, 2023).

Thompson, L. R., Oliveira, T. G., Hermann, E. R., Chowanadisai, W., Clarke, S. L., and Montgomery, M. R. (2020). Distinct TP53 mutation types exhibit increased sensitivity to ferroptosis independently of changes in iron regulatory protein activity. *Int. J. Mol. Sci.* 21 (18), 6751. doi:10.3390/ijms21186751

Vogt, A.-C. S., Arsiwala, T., Mohsen, M., Vogel, M., Manolova, V., and Bachmann, M. F. (2021). On iron metabolism and its regulation. *Int. J. Mol. Sci.* 22 (9), 4591. doi:10.3390/ijms22094591

Volz, K. (2008). The functional duality of iron regulatory protein 1. *Curr. Opin. Struct. Biol.* 18 (1), 106–111. doi:10.1016/j.sbi.2007.12.010

Wallander, M. L., Leibold, E. A., and Eisenstein, R. S. (2006). Molecular control of vertebrate iron homeostasis by iron regulatory proteins. *Biochim. Biophys. Acta* 1763 (7), 668–689. doi:10.1016/j.bbamcr.2006.05.004

Wallander, M. L., Zumbrennen, K. B., Rodansky, E. S., Romney, S. J., and Leibold, E. A. (2008). Iron-independent phosphorylation of iron regulatory protein 2 regulates ferritin during the cell cycle. *J. Biol. Chem.* 283 (35), 23589–23598. doi:10.1074/jbc.M803005200

Wang, W., Deng, Z., Hatcher, H., Miller, L. D., Di, X., Tesfay, L., et al. (2014). IRP2 regulates breast tumor growth. *Cancer Res.* 74 (2), 497–507. doi:10.1158/0008-5472.CAN-13-1224

Wang, Y. Q., Chang, S. Y., Wu, Q., Gou, Y. J., Jia, L., Cui, Y. M., et al. (2016). The protective role of mitochondrial ferritin on erastin-induced ferroptosis. *Front. Aging Neurosci.* 8, 308. doi:10.3389/fnagi.2016.00308

Winn, N. C., Volk, K. M., and Hasty, A. H. (2020). Regulation of tissue iron homeostasis: The macrophage "ferrostat. *JCI Insight* 5 (2), e132964. doi:10.1172/jci.insight.132964

Xiao, X., Alfaro-Magallanes, V. M., and Babitt, J. L. (2020). Bone morphogenic proteins in iron homeostasis. *Bone* 138, 115495. doi:10.1016/j.bone.2020.115495

Xu, Y., Alfaro-Magallanes, V. M., and Babitt, J. L. (2021). Physiological and pathophysiological mechanisms of hepcidin regulation: Clinical implications for iron disorders. *Br. J. Haematol.* 193 (5), 882–893. doi:10.1111/bjh.17252

Yamashita, S., Masuda, D., and Matsuzawa, Y. (2015). Did we abandon probucol too soon? *Curr. Opin. Lipidol.* 26 (4), 304–316. doi:10.1097/MOL.0000000000000199

Yanatori, I., and Kishi, F. (2019). DMT1 and iron transport. *Free Radic. Biol. Med.* 133, 55–63. doi:10.1016/j.freeradbiomed.2018.07.020

Yang, W. S., SriRamaratnam, R., Welsch, M. E., Shimada, K., Skouta, R., Viswanathan, V. S., et al. (2014). Regulation of ferroptotic cancer cell death by GPX4. *Cell* 156 (1-2), 317–331. doi:10.1016/j.cell.2013.12.010

Yao, F., Cui, X., Zhang, Y., Bei, Z., Wang, H., Zhao, D., et al. (2021). Iron regulatory protein 1 promotes ferroptosis by sustaining cellular iron homeostasis in melanoma. *Oncol. Lett.* 22 (3), 657. doi:10.3892/ol.2021.12918

Yuan, H., Li, X., Zhang, X., Kang, R., and Tang, D. (2016). CISD1 inhibits ferroptosis by protection against mitochondrial lipid peroxidation. *Biochem. Biophys. Res. Commun.* 478 (2), 838–844. doi:10.1016/j.bbrc.2016.08.034

Zhang, F., Wang, W., Tsuji, Y., Torti, S. V., and Torti, F. M. (2008). Post-transcriptional modulation of iron homeostasis during p53-dependent growth arrest. *J. Biol. Chem.* 283 (49), 33911–33918. doi:10.1074/jbc.M806432200

Zhang, Y., Qian, Y., Zhang, J., Yan, W., Jung, Y. S., Chen, M., et al. (2017). Ferredoxin reductase is critical for p53-dependent tumor suppression via iron regulatory protein 2. *Genes Dev.* 31 (12), 1243–1256. doi:10.1101/gad.299388.117

Zhang, T., Sun, L., Hao, Y., Suo, C., Shen, S., Wei, H., et al. (2022). ENO1 suppresses cancer cell ferroptosis by degrading the mRNA of iron regulatory protein 1. *Nat. Cancer* 3 (1), 75–89. doi:10.1038/s43018-021-00299-1

Zilka, O., Shah, R., Li, B., Friedmann Angeli, J. P., Griesser, M., Conrad, M., et al. (2017). On the mechanism of cytoprotection by ferrostatin-1 and liproxstatin-1 and the role of lipid peroxidation in ferroptotic cell death. *ACS Cent. Sci.* 3 (3), 232–243. doi:10.1021/acscentsci.7b00028

Zumbrennen, K. B., Wallander, M. L., Romney, S. J., and Leibold, E. A. (2009). Cysteine oxidation regulates the RNA-binding activity of iron regulatory protein 2. *Mol. Cell Biol.* 29 (8), 2219–2229. doi:10.1128/mcb.00004-09

Zuris, J. A., Harir, Y., Conlan, A. R., Shvartsman, M., Michaeli, D., Tamir, S., et al. (2011). Facile transfer of [2Fe-2S] clusters from the diabetes drug target mitoNEET to an apo-acceptor protein. *Proc. Natl. Acad. Sci. U. S. A.* 108 (32), 13047–13052. doi:10.1073/pnas.1109986108

frontiers | Frontiers in Molecular Biosciences

TYPE Review
PUBLISHED 04 July 2023
DOI 10.3389/fmolb.2023.1223493

OPEN ACCESS

EDITED BY
Yanqing Liu,
Columbia University, United States

REVIEWED BY
Xudong Wang,
University of Pennsylvania, United States
Ran Tao,
Texas A&M University Baylor College of Dentistry, United States

*CORRESPONDENCE
Qiaoling Liu,
1134447805@qq.com
Tianming Wang,
wangtianming@njmu.edu.cn

RECEIVED 16 May 2023
ACCEPTED 22 June 2023
PUBLISHED 04 July 2023

CITATION
Lai W, Chen J, Wang T and Liu Q (2023), Crosstalk between ferroptosis and steroid hormone signaling in gynecologic cancers.
Front. Mol. Biosci. 10:1223493.
doi: 10.3389/fmolb.2023.1223493

Crosstalk between ferroptosis and steroid hormone signaling in gynecologic cancers

Wen Lai[1], Jianquan Chen[2], Tianming Wang[2]* and Qiaoling Liu[1]*

[1]Department of Obstetrics and Gynecology, The Affiliated Jiangning Hospital with Nanjing Medical University, Nanjing, China, [2]Central Laboratory, Translational Medicine Research Center, The Affiliated Jiangning Hospital with Nanjing Medical University, Nanjing, China

Ferroptosis is a novel types of regulated cell death and is widely studied in cancers and many other diseases in recent years. It is characterized by iron accumulation and intense lipid peroxidation that ultimately inducing oxidative damage. So far, signaling pathways related to ferroptosis are involved in all aspects of determining cell fate, including oxidative phosphorylation, metal-ion transport, energy metabolism and cholesterol synthesis progress, et al. Recently, accumulated studies have demonstrated that ferroptosis is associated with gynecological oncology related to steroid hormone signaling. This review trends to summarize the mechanisms and applications of ferroptosis in cancers related to estrogen and progesterone, which is expected to provide a theoretical basis for the prevention and treatment of gynecologic cancers.

KEYWORDS

ferroptosis, lipid peroxidation, gynecologic cancers, estrogen, progesterone

1 Introduction

Ferroptosis is a unique iron-dependent non-apoptotic cell death and is considered as one of the most widely studied regulated cell death types in the last decade. The concept of ferroptosis is first proposed by Dixon et al., in 2012, they triggered ferroptosis with erastin (a selective lethal small molecule drug targeting the oncogenic *RAS*) and described its major features (Dixon et al., 2012). During ferroptosis, the outer mitochondrial membrane is ruptured and the mitochondrial cristae reduction is commonly observed in mitochondrial morphology. The regulation of ferroptosis is associated with iron homeostasis and lipid metabolism (Li et al., 2020). Multiple factors caused Fe^{2+} accumulation that generates numerous reactive oxygen species (ROS) from hydrogen peroxide through the Fenton reaction and lead to ferroptosis. Lipid peroxidation is considered as the primary driver of ferroptosis (Gaschler and Stockwell, 2017; Kagan et al., 2017). Either the depletion of glutathione (GSH) or reduction of glutathione peroxidase 4 (GPX4) activity would attenuate lipid peroxide metabolism, increase ROS level and cause ferroptosis. The molecular mechanism of ferroptosis is involved in a complex regulation network such as system xc−-GSH-GPX4 pathway, serotransferrin-mediated iron uptake, unsaturated fatty acid-mediated lipid peroxidation, and cholesterol synthesis related mevalonate pathway, et al. (Figure 1). We are interested in the crosstalk between ferroptosis and steroid hormone signaling pathway in gynecologic cancers. Here this review trends to summarize the molecular mechanisms of ferroptosis on steroid hormone signaling pathway and its applications in gynecologic cancers.

2 Molecular mechanism of ferroptosis

Ferroptosis occurs mainly by targeting two pathways (extrinsic and intrinsic pathways) (Tang and Kroemer, 2020). In the extrinsic pathway, ferroptosis begins with the inhibition of cystine/glutamic acid transporter (system xc−) or with the activity of the serotransferrin (TF)-mediated iron uptake. In the intrinsic pathway, it is activated by blocking intracellular antioxidant enzyme such as GPX 4 (Chen et al., 2021a).

2.1 System xc−-GSH-GPX4 pathway

System xc−-GSH-GPX4 pathway is the main defense system to antiferroptosis. The system xc− is comprised of two subunits: solute carrier family 7 member 11(SLC7A11) and solute carrier family 3 members 2 (SLC3A2) (Sato et al., 2000). After the exchange of Cysteine and Cystine, system xc− maintains the GSH generation in a continuous reactions (Lewerenz et al., 2013). In mammalian cells, one of the most important functions of system xc− is mediating Cystine transport by glutamate reverse transportation. Cystine is convert to cysteine, then cysteine is catalyzed by glutamate-cysteine ligase (GCL) and glutathione synthetase (GSS) for GSH synthesis (Bayır et al., 2020). SLC7A11 is commonly used as the target of system xc−. SLC7A11 promotes the expression of GPX4 through the mTORC-4EBP1 signaling pathway (Zhang YY. et al., 2021). Up-regulating the expression of system xc− is involved in the enhanced chemoresistance and tumor growth (Ishimoto et al., 2011; Habib et al., 2015). Inhibiting SLC7A11 causes GSH depletion (Dixon et al., 2012). Down-regulating system xc− by targeting TP53 (Jiang et al., 2015; Liu S. et al., 2022), NFE2L2 (Chen et al., 2017), BAP1 (Zhang et al., 2018), BECN1 or OTUB1(Song et al., 2018), can reduce GSH synthesis, enhance ROS generation, and result in ferroptosis. GPX4 belongs to GSH peroxidases and it is an antiferroptotic molecular (Seibt et al., 2019). It reduces the generation of phospholipid hydroperoxide and converts it to phospholipid alcohol. The GPX4 activity is depended on the presence of GSH and selenium, which finally affect ferroptosis (Ingold et al., 2018). Some small molecular compounds can inhibit GPX4 activity directly or indirectly to induce ferroptosis, and some other compounds can lead to the degradation of GPX4 (Yang et al., 2014; Shimada et al., 2016). High expression level of GPX4 is correlated with bad prognosis in breast cancer (BC) patients, and the GPX4 reduction enhances the sensitivity of cancer cells to cisplatin (Zhang et al., 2020).

2.2 Serotransferrin-mediated iron uptake

Intracellular Fe^{2+} accumulation is one of central events to induce ferroptosis. The increased iron uptake and the reduced iron storage as well as the limited iron efflux can induce ferroptosis (Chen X. et al., 2020). Iron metabolism capability determines cell susceptibility to ferroptosis by regulating cell labile iron (LIP). Increasing LIP could enhance the Fenton reaction so as to produce more hydroxyl radicals (Feng et al., 2020). The iron-loaded Serotransferrin (TF) binds to Transferrin receptor protein 1 (TFRC) locating in cytomembrane and forms a TF-TFRC complex (Yang and Stockwell, 2008; Wang Y. et al., 2020). The complex releases iron (Fe^{2+}) into the cytoplasm mediated by solute carrier family 11 member 2 (SLC11A2) (Montalbetti et al., 2013; Gao et al., 2015). The intracellular free iron is stored as a ferritin-Fe^{3+} complex (Muhoberac and Vidal, 2019) and this complex releases Fe^{2+} through a ferritinophagy manner (Park and Chung, 2019). Ferritinophagy is an autophagy-dependent degradation of ferritin progress. During ferritinophagy, the ferritin-Fe^{3+} complex is mediated by nuclear receptor coactivator 4 (NCOA4) to degrade in autolysosome and releases Fe^{2+}, which increases cell sensitivity to ferroptosis (Mancias et al., 2014; Mancias et al., 2015; Gatica et al., 2018; Liang et al., 2022). Enhancing iron output or increasing ferritin output can suppress ferritinophagy. The iron output is mediated by solute carrier family 40 member 1 (SLC40A1) in cytomembrane, the ferritin output is mediated by exosome, both of them are able to inhibit ferroptosis (Geng et al., 2018; Brown et al., 2019).

2.3 Unsaturated fatty acid-mediated lipid peroxidation

The unsaturated fatty acids-mediated lipid peroxidation is an important pathway to induce lipid peroxidation and ferroptosis. The intracellular free fatty acids are mainly generated from two ways: the first way is the fatty acid *de novo* synthesis mediated by Acetyl-CoA carboxylase (ACAC); the second way is the fatty acid release derived from lipid droplet (LD). In the fatty acid *de novo* synthesis progress, acetyl-CoA is catalyzed by ACAC to malonyl-CoA, and then is subjected to a continuous polymerization into fatty acids (Batchuluun et al., 2022). In this progress, several major enzymes (including ACLY, ACSs, ACC, FASN, and SCD1) are involved in fatty acid generation (Li et al., 2022). The excess free fatty acids are usually synthesized into triacylglycerols (TAGs), which are mainly stored in LD. Multiple enzymes regulate LD formation and LD catabolism: during LD formation, GPAT, AGPAT, Lipin and DGAT are required (Tan et al., 2014; Onal et al., 2017); during LD catabolism, ATGL, HSL and MGL are the rate-limiting enzymes of lipolysis that catalyze LD into fatty acids step-by-step (Zechner et al., 2012; Missaglia et al., 2019; Wang T. et al., 2020); in addition to lipolysis, an autophagy-dependent progress referred to lipophagy also has a function of LD breakdown mediated by acid lipases in the autolysosome (Kaur and Debnath, 2015; Schott et al., 2019). The polyunsaturated fatty acids (PUFAs), either from ACAC-mediated *de novo* synthesis or LD breakdown, are able to trigger ferroptosis. In this progress, long-chain fatty acid–CoA ligase 4 (ACSL4) and lysophospholipid acyltransferase 5 (LPCAT3) are required. Combining with CoA, ACSL4 catalyzes the free arachidonic acid (AA) or adrenergic acid (Ada), which is most likely to undergo peroxidation, to form AA-CoA or Ada-CoA (Yuan et al., 2016; Doll et al., 2017; Kagan et al., 2017). LPCAT3 promotes PUFA-CoA and phospholipid (PL) to form into PUFA-PL, enhances lipid peroxidation and induces ferroptosis (Dixon et al., 2015; Chen et al., 2021a).

2.4 Mevalonate (MVA) pathway

Cholesterol can be produced by receptor-mediated LDL-cholesterol uptake or cholesterol *de novo* synthesis. In cholesterol

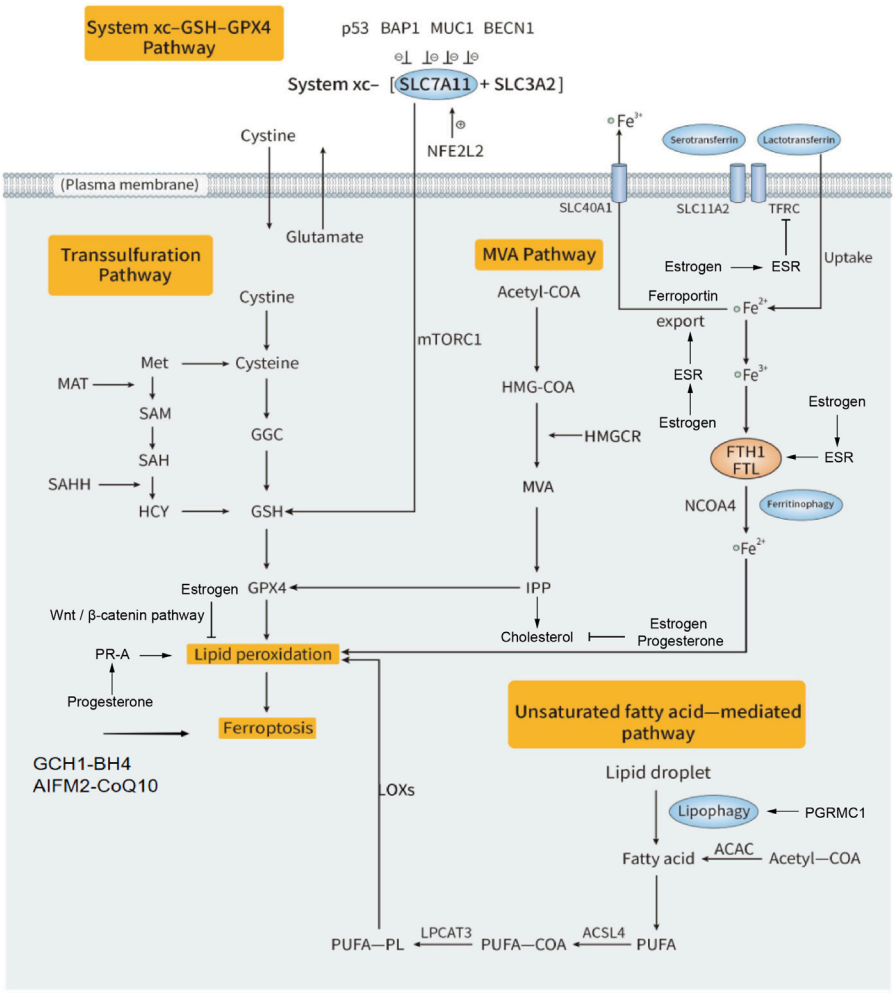

FIGURE 1
Regulation mechanisms of estrogen and progesterone on ferroptosis in gynecologic cancers. Ferroptosis is driven by iron-dependent lipid peroxidation. There are multiple molecular mechanisms involved in the regulation of ferroptosis. Iron-loaded TF-TFRC complexes releases Fe^{2+} into the cytoplasm via SLC11A2. The intracellular free iron is stored as Fe^{3+}-ferritin complex. The autophagy-dependent ferritinophagy is mediated by NCOA4 for degradation of ferritin at lysosome to release Fe^{2+}. The excess Fe^{2+} induces lipid peroxidation via Fenton reaction. PUFAs, which are mainly from ACAC-mediated fatty acid synthesis or by the lipophagy, also can induce ferroptosis. PUFAs convert to PUFA-PL by ACSL4 and LPCAT3, finally induce lipid peroxidation. The system xc−-GSH-GPX4 pathway mainly acts as a defense system so as to antiferroptosis. In this pathway, cystine enters the cell and is oxidized to cysteine, with the action of GCL and GSS, GSH is synthesized and catalyzed by GPX4 to antiferroptosis. IPP, a metabolic intermediate from MVA pathway related to cholesterol synthesis, can enhance GPX4 activity and cause antiferroptotic effect. Transsulfuration pathway, GCH1-BH4 pathway and AIFM 2-CoQ10 pathway also have unique mechanisms to antiferroptosis. Estrogen binds to ESR and reduces free iron by inhibition of TFRC and ferritin or by promotion of ferroportin. Estrogen can also suppress lipid peroxidation through Wnt/β-catenin pathway. Progesterone enhances lipid peroxidation via its receptor PR-A. The other progesterone receptor PGRMC1 also mediated lipophagy to increase ROS generation. Both estrogen and progesterone supplement can inhibit cholesterol synthesis, which regulates GPX4 in turn.

biosynthesis pathway, three molecules of acetyl-CoA are catalyzed by HMG-CoA synthase into 3-hydroxy-3-methylglutaryl-CoA (HMG-CoA). This CoA-derivative is then converted to Mevalonate (MVA) through a reduction reaction by HMG-CoA reductase (HMGCR), which is a rate-limiting enzyme for cholesterol biosynthesis (Liao et al., 2016; Ni et al., 2021). In the next step, MVA forms isopentenyl diphosphate (IPP) via phosphorylation and decarboxylation (Kuzuyama and Seto, 2012; Bathaie et al., 2017). With catalytic action of the endoplasmic reticulum cyclase and oxygenase, IPP is catalyzed into squalene, then into lanosterol, and is finally converted to cholesterol through multiple steps. In addition, IPP also has a function of antiferroptosis, it promotes the expression of GPX4 to defend lipid peroxidation so as to inhibit ferroptosis (Warner et al., 2000; Ingold et al., 2018). Statins can also reduce GPX4 and inhibit ferroptosis by targeting HMGCR activity through MVA pathway (Yu et al., 2017).

2.5 Other pathways

Besides the system xc−, cysteine can also be produced through the thiolation. The transsulfuration pathway is another antioxidant process that inhibits lipid peroxidation. In this pathway, methionine is converted by methionine adenosyltransferase to S-adenosylmethionine

and is further converted to S-adenosylhomocysteine (SAH). The S-adenosylhomocysteine hydrolase (SAHH) hydrolyzed SAH to the cysteine precursor homocysteine (HCY) (Chen et al., 2016). It is reported that increasing DJ-1 (an oxidative stress-related protein) promotes the stability of SAHH activity and HCY synthesis through this pathway (Cao et al., 2020). Knockdown of Cysteine-tRNA synthetases (CARS), which is a molecular that links cysteine to tRNA for protein translation, promotes transsulfuration, enhances cysteine synthesis, increases GSH, and inhibits ferroptosis (Yao and Fox, 2013; Hayano et al., 2016).

In addition, Apoptosis-inducing factor mitochondrion-associated 2 (AIFM2)-Coenzyme Q10 (CoQ10) axis is another antiferroptosis pathway. AIFM2 (also known as FSP1) is a NADP-dependent oxidoreductase of CoQ10 (Wei et al., 2020). CoQ10 is a lipophilic compound and is considered as a lipophilic free radical scavenger. It is reported that overexpressing AIFM2 inhibited ferroptosis and positively correlated with ferroptosis resistance in many cancers (Bersuker et al., 2019).

Similarly, the GCH1-BH4 pathway is reported to inhibit lipid peroxidation and defend ferroptosis (Kraft et al., 2020). Tetrahydrobiopterin (BH4) is an integral part of the antioxidant system and GTP cyclohydrolase-1 (GCH1) is the rate-limiting enzyme in the synthesis of BH4 (Latremoliere and Costigan, 2011; Cronin et al., 2018). GCH1 selectively inhibited the peroxidation of certain PUFA-PL, overexpressing GCH1 rescues ferroptosis induced by RSL-3 (a GPX4 inhibitor) in mouse fibroblasts.

3 Steroid hormone and steroid hormone signaling

3.1 Steroid hormone synthesis

It is well known that the main substrate for estrogen and progesterone synthesis is cholesterol. The receptor-mediated LDL-cholesterol uptake and cholesterol *de novo* synthesis is the major source of cholesterol. In the progress of receptor-mediated LDL-cholesterol uptake, after endocytosis, the cholesterol ester is cleaved by acid lipase in lysosome, free cholesterol is then transferred onto NPC intracellular cholesterol transporter 1 (NPC1) which is located in lysosomal membrane, and followed by a further transport to other organelles (Pfeffer, 2019). Cholesterol also could be generated through cholesterol *de novo* synthesis pathway. In this pathway, HMG-CoA, which is condensed from acetyl-CoA, is then reduced to MVA by HMGCR, and is further phosphorylated and decarboxylated into IPP. IPP is used to generate cholesterol through multiple steps (Kuzuyama and Seto, 2012; Liao et al., 2016; Bathaie et al., 2017; Ni et al., 2021). Then, as for substrate of steroid hormone synthesis, cholesterol could be catalyzed into estrogen and progesterone. Cholesterol enters into mitochondria, it is then catalyzed to pregnenolone by a cytochrome P450 monooxygenase referred to Cholesterol side-chain cleavage enzyme (CYP11A1 or P450scc) through hydroxylation of the side-chain and cleavage (Strushkevich et al., 2011). Pregnenolone or progesterone could be hydroxylated by Steroid 17-alpha-hydroxylase/17,20 lyase (CYP17A1 or P450c17) to form 17-alpha hydroxy metabolites. Then 17-OH pregnenolone is converted to dehydroepiandrosterone (DHEA) and finally forms estrogens (Auchus et al., 1998; Miller, 2002; DeVore and Scott, 2012; Petrunak et al., 2014; Yoshimoto et al., 2016) (Figure 2). Steroid hormones also have the capability to regulate intracellular cholesterol level in turn. A previously study referred to the effect of steroid hormone on cholesterol synthesis, has demonstrated that the inhibition of cholesterol synthesis could be found in the treatment of many steroids (DHEA, beta-estradiol, pregnenolone, progesterone and deoxycorticosterone included) (Metherall et al., 1996).

3.2 Steroid hormone signaling pathway

Estrogen is mainly generated by granulosa cells of ovaries (Fuentes and Silveyra, 2019). It maintains normal physiological function such as reproductive system development, body metabolism level regulation, immune regulation and a variety of sex hormone-driven cancers (Baker et al., 2017; Kumar and Goyal, 2021). Estrogen encompasses four estrogenic steroid hormones (estrone, 17-beta-estradiol (E_2), estriol and estetrol). Among the four terms, E_2 has the highest affinity of estrogen receptors (ERs) (Russell et al., 2019). ERs are divided into two categories: nuclear receptor type and membranous receptor type. The nuclear receptors mainly contain ESR1 (also called ERα) and ESR2 (also named ERβ), while the membranous receptor is G protein-coupled estrogen receptor (GPER1). ESR1 and ESR2 are highly homologous in the amino acid sequence of their DNA binding domain (96%) and the ligand binding domain (55%) (Kuiper and Gustafsson, 1997). ESR1 locates in epithelial and muscle cells of the uterus and vagina, epithelial and stromal cells of the breast, germinal epithelium of the ovary, and testicular interstitial cells (Pelletier and El-Alfy, 2000). ESR2 has a broad distribution of tissues, including the gastrointestinal tract, lung, and brain (Younes and Homma, 2011). They trigger different transcriptional responses and have opposite effects to determine the cell fate (Kwon et al., 2020). In the genomic effects of estrogen-mediated signaling, estrogen binds to ESR1 or ESR2, forms a estrogen-receptor complex, and regulates the transcription of downstream genes in the nucleus by interaction with estrogen response elements (EREs) directly or by tethering to Sp-1 and Ap-1 (Fuentes and Silveyra, 2019; Chen P. et al., 2022). Under physiological condition, estrogen regulates a variety of cellular processes such as autophagy, proliferation, apoptosis, survival, differentiation, and vasodilation. It also regulates Ca^{2+} mobilization, PI3K signaling, and MAPK pathway through membrane-bound ERs with a non-genomic effect (Chen YC. et al., 2022).

In addition to estrogen, progesterone also plays an important role in gynecologic cancers (Kim et al., 2013). Progesterone is a natural progestin, it is produced from follicular granulosa cells after reaching the luteinizing hormone (LH) peak in the middle of the menstrual cycle, and is mainly produced by the corpus luteum and placenta (Bulletti et al., 2022). Besides the functions of maintaining the implantation of embryonic endometrium and sustain pregnancy, progesterone has multiple biological effects such as utero-relaxation and neuroprotection (Bulletti et al., 1993; Jodhka et al., 2009). In animal models, progesterone affects cognitive ability and suggests its potential role of cognitive ability in human (particularly more relevant for women) (Henderson, 2018). Classical progesterone signaling pathway can be activated by the steroid hormone progesterone through nuclear progesterone receptor (nPR), which has two major isoforms (PR-A and PR-B) (Ali et al., 2023). PR-A is necessary for

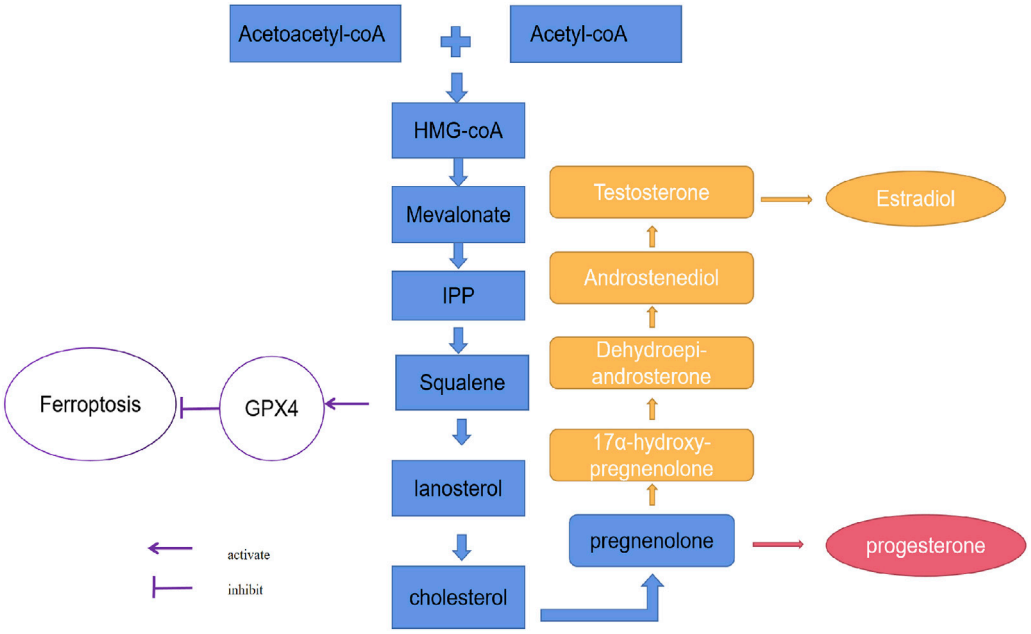

FIGURE 2
The relationship between ferroptosis and the synthesis of estrogen and progesterone. The synthesis of estrogen and progesterone depends on cholesterol. Three molecules of acetyl-CoA condense successively to form HMG-CoA. HMG-CoA is then reduced to MVA by HMGCR, and is further phosphorylated and decarboxylated to form IPP. IPP is condensed to produce squalene and then squalene forms lanosterol by the catalysis of endoplasmic reticulum cyclase and oxygenase, finally lanosterol is converted to cholesterol. Cholesterol enters into mitochondria and converts to pregnenolone by P450scc. Then 17-OH pregnenolone is converted to DHEA and finally forms estrogen.

uterine development and PR-B is necessary for mammary gland development (Conneely and Lydon, 2000). The two isoforms can form a homodimer or heterodimer, and regulate the transcription of downstream genes in the nucleus by interaction with progesterone response elements directly or by tethering to Sp-1 and Ap-1 (Tsai et al., 1988; Tseng et al., 2003; Daniel et al., 2011). Progesterone also activates non-classical pathway via non-nuclear PR containing progesterone receptor membrane component 1 (PGRMC1) and progesterone receptor membrane component 2 (PGRMC2). Numerous studies in endometriosis (EMs) have shown the association of progesterone and iron overload (Van Langendonckt et al., 2002; Van Langendonckt et al., 2004; Lousse et al., 2009). In addition, progesterone takes part in ferroptosis by affecting protein-protein interaction. Progesterone targets Fibulin-1 (FBLN1) in the process of endometrial stromal cells (ESCs) decidualization, FBLN1 interacts with EGF-containing fibrin-like extracellular matrix protein 1 (EFEMP1) and affects the stability of EFEMP1. Silencing of *EFEMP1* inhibits the effect of FBLN1 on ferroptosis (Wan et al., 2022).

4 Crosstalk in gynecologic cancers

4.1 Steroid hormone signaling and gynecologic cancers

Ovarian cancer (OVCA) is one of the most lethal malignancies, including epithelial tumor, sexual cord-mesenchymal tumor and germ cell tumor. The epithelial OVCA is most common among all the OVCA types with less than 50% on the 5-year relative survival rate (Torre et al., 2018). High estrogen level is often observed in patients with OVCA, and the estrogen receptor is also high expressed in OVCAs (Mungenast and Thalhammer, 2014; Englert-Golon et al., 2021; Xu et al., 2022). High progesterone level also increases the risk of OVCA. The progesterone signaling promotes the development of high-grade serous carcinoma into metastatic OVCA via BRCA1/DNA repair signaling pathway (Kim et al., 2020).

Endometrial cancer (EC) is the sixth most common cancer in the world. In the United States, its incidence rate increases year by year. The prognosis of patients with recurrent EC and clinical histological detection of aggressive EC is usually limited (Siegel et al., 2019). Surgery, radiotherapy and chemotherapy are the current approach for EC treatment, but have unsatisfactory effects. Estrogen stimulates EC proliferation, while progesterone inhibits it. In estrogen-dependent EC, ESR1 is high expressed, it interacts with GPER and promotes the proliferation of EC cells via PI3K signaling pathway and MAPK signaling pathway (Yu et al., 2022). Progesterone acts to antagonize estrogen in EC. PR is mainly expressed in epithelial cells and stromal cells. It inhibits the proliferation of EC cells with a paracrine manner (Kim et al., 2013; Gompel, 2020).

Cervical cancer (CC) is also most common in women, and almost all cases of cervical squamous cell carcinoma can be attributed to the infection of human papillomavirus (HPV). Basing on their carcinogenic potential, HPVs are classified as low-risk HPV (lrHPV) or high-risk HPV (hrHPV) (Bedell et al., 2020). About 67% of HPV infections will be eliminated within 12 months without intervention and the eliminated rate would reach 90% within 24 months, however, the remaining HPV infections might have high persistent potential (Plummer et al., 2007). Persistent HPV

infection will lead to an abnormal proliferation in the lesion region named cervical intraepithelial neoepithelial neoplasia (CIN). According to pathological grade, CIN is classified as CINI, II, and III, or is classified as low-grade squamous intraepithelial lesion (LSIL) and high-grade squamous intraepithelial lesion (HSIL). CINI corresponds to LSIL or dysplasia, CINII and most CINII correspond to HSIL or moderate and severe dysplasia (Jayshree, 2021). CC is a non-estrogen-dependent cancer. But estrogen coordinates with HPV by increasing the DNA double-strand breaks (DSBs), then it promotes proliferation of CC cells through G protein-coupled receptor 30 (GPR30) signaling pathway (Ogawa et al., 2023). The estrogen receptor ESR1 is expressed higher in the nucleus of squamous epithelium than that in cervical lesions. And the expression of ESR1 in squamous epithelium is higher than that in the cervical glands. Progesterone receptor is important for suppression of CC occurrence, low expression of PR may increase the risk of CC, activating PR by medroxyprogesterone acetate reduces the occurrence of CC (Park et al., 2021; Baik et al., 2022). Notably, PGRMC1 has been reported to promote migration of CC cells, siRNA-mediated *PGRMC1* knockdown reduces the proliferation of CC cells and inhibits the migration ability of CC cells (Shih et al., 2019).

Besides to gynecologic cancers, breast cancer (BC) is considered to be the most relative cancer of steroid hormone signaling. BC is one of the highest incidence cancers in the world (Duggan et al., 2021). The breast has a unique microenvironment containing a large number of adipocytes. Thus, hormone signaling and lipid metabolism capability may be involved in the invasion and metastasis of BC. In hormone-dependent BC, estrogen has a high level in BC and it can induce DNA damage by metabolites (Starek-Świechowicz et al., 2021). Estrogen activates PI3K signaling pathway by ERs to promote cell proliferation of BC cells where ERs is highly expressed (Vasan et al., 2019). Progesterone influences early events in the occurrence of BC. PR-B mediates the proliferation of BC cells related to progesterone and it also regulates the actions of extranuclear signaling of PRs (Trabert et al., 2020).

4.2 Steroid hormone signaling and ferroptosis

The relation between ferroptosis and steroid hormone signaling has been studied in a variety of cancer types from molecular mechanism to the development of targeted therapeutic drug. Activation of estrogen-related receptor gamma (ESRRG) may enhance the effect of ferroptosis in HCC cells with sorafenib-resistant (Kim et al., 2022). Increasing PGRMC1 expression promotes fatty acid oxidation and enhances the sensitivity of paclitaxel-tolerant cancer cells (PCC) to ferroptosis in head and neck cancer (You JH. et al., 2021). It is well known that most gynecologic cancers (including EC, CC and OVCA) are driven by sex hormone (Baker et al., 2017), so deeply understanding the crosstalk between ferroptosis and steroid hormone signaling is helpful for tumor-targeted therapy in gynecologic cancers. In molecular mechanism, the effect of steroid hormone signaling on ferroptosis is complex (Figure 1). Firstly, steroid hormone signaling is able to regulate iron homeostasis. Secondly, abnormal steroid hormone level may affect the endogenous antioxidant capacity.

In most of gynecologic cancers, estrogen disrupts intracellular iron level and promotes free iron export into systemic circulation. Hepcidin is an important regulator of systemic iron balance. A previous study on female mouse model has reported that estrogen can reduce the expression of hepcidin (Yang et al., 2020). An *in vivo* study has reported that serum hepcidin levels declines more than 40% after E_2 treatment in females (Lehtihet et al., 2016). Estrogen represses hepcidin expression via ERE of its promoter region; ovariectomizing reduces serum iron level in mice, but elevates the tissue iron level (Hou et al., 2012). Besides to hepcidin, estrogen also affects iron uptake and iron export in multiple gynecologic cancer types (Bajbouj et al., 2019; Riera Leal et al., 2020). Ovarian clear cell carcinoma (CCC) is a most common OVCA type. Among endometriosis-associated OVCA (EAOC), the positive percentage of ESR in CCC is only 8%, which is lower than the other OVCA types (Lai et al., 2013). In a previously study of CCC, it is found that free iron levels in endometriotic cysts and CCCs are both higher than that in nonendometriotic benign cysts (Yamaguchi et al., 2008). In doxorubicin-treated OVCA cells and BC cells, E_2 inhibits the expression of TFRC but promotes that of ferroportin and ferritin (Bajbouj et al., 2019). In BCs, from a study of ferroptosis induced by sulfasalazine, it is reported that the expression level of TFRC in ER-positive BCs is much lower than that in the ER-negative BCs, and ESR1 knockdown increases TFRC expression (Yu et al., 2019). From a meta-analysis of CC patients in China, the result indicates that high serum iron levels may have a protective function for CC patients (Chen S. et al., 2020). In CC cell lines, the effect of E_2 that it reduces free iron and intracellular ferritin level is only found in HaCaT cells (Riera Leal et al., 2020). However, this effect is not found in some other CC cell types (HeLa, SiHa and C33A) (Riera Leal et al., 2020). Progesterone is another important steroid sex hormone with a function of maintaining iron level, but sometimes its effect on iron regulation is contradictory. In zebrafish model, progesterone promotes the degradation of ferroportin and enhances the transcriptional expression of hepcidin (Li et al., 2016). PGRMC1, rather than the classical PRs, mediates the activity of SRC family kinases to promote hepcidin biosynthesis, and this effect can be rescued by the inhibition of SRC family kinase (Li et al., 2016). Moreover, PGRMC1 is found expressed higher in triple-negative BC (TNBC) than that in the other BC subtypes. Overexpression of *PGRMC1* reduces free iron level and inhibits ferroptosis by binding to intracellular iron; the inhibition of PGRMC1 enhances sensitivity of BC cells (MDA-MB231) to ferroptosis inducer (Zhao et al., 2023).

Abnormal steroid hormone level also affects antioxidant capacity of cancer cells so as to regulate their sensitivity to ferroptosis. For instance, IPP, an intermediate product in cholesterol synthesis, could defend ferroptosis by promoting GPX4 activity (Warner et al., 2000; Ingold et al., 2018); while inhibiting HMGCR activity by statins could also inhibit GPX4 through the same pathway (Yu et al., 2017). Moreover, increasing Sterol regulatory element-binding protein 2 (SREBP2), which promotes cholesterol synthesis by targeting HMGCR, could also suppress ferroptosis (Hong et al., 2021). Because steroid hormones (E_2 and progesterone) have been proven to inhibit cholesterol synthesis (Metherall et al., 1996), thus, steroid hormone may act to antiferroptosis. Estrogen has been reported to protect against oxidative stress by promoting the expression of mitochondrial antioxidant enzymes (SOD2, GPXs), increasing antioxidants and reducing free radicals in many organs and cells (Irwin et al., 2008; Vina and Borras, 2010). In CC cells, E_2 reduces NO level and MDA level (final product of the lipid peroxidation). This effect could be reversed by metformin treatment (Riera Leal

et al., 2020). It can also inhibit oxidative stress through Wnt/β-catenin signaling pathway in ovarian endometrioid adenocarcinoma (Wu et al., 2007). Progesterone is reported to increase ROS level in sperm and fallopian tube fibroblasts (Gimeno-Martos et al., 2020; Wu et al., 2023). Progesterone induces ROS generation and suppresses OVCA via its receptor PR-A (Wu et al., 2017). Fallopian tube (FT) is well known as the origin of high-grade serous ovarian cancer, and defective p53 is considered as an early event in the FT epithelium-to-OVCA transition. After progesterone treatment, combining with more ROS generation, necroptosis is activated via TNF-α/RIPK1/RIPK3/MLKL pathway in p53-defective human FT fimbrial epithelial cell line (FE25 cells). The antioxidant Necrox-2 and acetylcysteine could rescue this effect (Wu et al., 2017).

Simply elevating iron level may lead to an unexpected effect. From a study of ECOA, the authors indicate that iron-induced oxidative stress may promote the production of the antioxidants, and follow by apoptosis-resistance malignant transformation of endometriosis (Kobayashi et al., 2019). A recent study also reports that persistent and mild ferroptosis increases the expression of antioxidant genes and promotes initiation of HPV-positive CC (Wang T. et al., 2022). Iron deprivation with iron chelators represses HPV E6/E7 oncogene expression and has profound antiproliferative effects in HPV-positive CC cells (HeLa and SiHa) (Braun et al., 2020). Thus, targeting ferroptosis for killing serous gynecologic cancer cells should consider their respective features (steroid hormones and the expression levels of their receptors).

4.3 Ferroptosis in gynecologic cancers

Ferroptosis is important for repressing the occurrence, development and metastasis of gynecologic cancers (Fan et al., 2022). In OVCA, a lot of studies have proven that enhancing lipid peroxidation is important for inhibiting OVCA cells, providing us with an emerging strategy for the OVCA treatment (Park et al., 2018; Zhao et al., 2019; Zhao X. et al., 2022). Resent study has indicated that drug-resistant OVCA cells are vulnerable to GPX4 inhibition, the ferroptosis inducer (RSL3) suppress the viability of drug-resistant OVCA cells but less affect the parental cells (Hangauer et al., 2017). Another study has proven that inhibition of monounsaturated fatty acids generation by the blockage of SCD1 sensitizes OVCA cells to RSL3 (Tesfay et al., 2019). Moreover, the inhibition of ROS generation through the Nrf2/heme oxygenase 1 (HMOX1) signaling pathway, promotes the cell proliferation of cisplatin-resistant OVCA cells (Sun et al., 2019). All the studies suggest that the drug resistance of OVCA cells depends on the endogenic antioxidant system. Ferroptosis is also proved to have a synergistic effect with chemotherapy, radiotherapy and immunotherapy in killing OVCA cells (Zhao H. et al., 2022). Ferroptosis can be induced in OVCA cells by artesunate in a ROS-dependent manner, transferrin pretreatment enhances this effect and ferrostatin-1 can rescue (Greenshields et al., 2017). Basing on the effect of ferroptosis in OVCA, a scoring system related to ferroptosis genes is used to predict the prognosis of OVCA patients (You Y. et al., 2021). Thus, there are convincing evidences to show a closely relationship of OVCA and ferroptosis.

Ferroptosis is found in SILs from patients with hrHPV infection and persistent ferroptosis contributes to an anti-ferroptosis effect in CC (Wang T. et al., 2022). In addition, more ROS generation is found in cancer cells because the cancer cells require large amount of nutrients for rapid proliferation (Wang et al., 2019). So, cancer cells increase the antioxidant activity to maintain the redox balance and prevent from cell death caused by high level of ROS. Lipid peroxidation is one of the most obvious features of ferroptosis, and its importance in CC has been proven in many studies, providing us with new insight for CC treatment by targeting ferroptosis (Jelić et al., 2018; Jelic et al., 2021).

Recently, the study on the relation between ferroptosis and EC gets many attentions. Basing on the expression profiles of cancer genomic database, some research teams have described the characteristics of ferroptosis-related genes in EC, and further provided evidences to describe the relationship between ferroptosis and the immune microenvironment, suggesting that ferroptosis-related genes could be used for the prognosis prediction of EC (Liu J. et al., 2021; Weijiao et al., 2021; Liu L. et al., 2022). A recently study has identified a centrosome microtubule-binding protein Centrosome spindle pole-associated protein (CSPP1), which functions in cell cycle-dependent cytoskeletal tissue and ciliation, to be a potential biomarker of ferroptosis, providing a novel target for the diagnosis, prognosis and therapy of EC (Wang W. et al., 2022). Another study has shown that ETS transcription factor ELK1 (ELK1) is upregulated in EC cells, and it binds to the promoter of GPX4 to antiferroptosis, indicating the ELK1/GPX4 axis might be a potential therapeutic target to develop drugs for EC (Wei et al., 2022).

Besides to gynecologic cancers, numerous studies of ferroptosis on the development and treatment of BC have been reported. And ferroptosis is considered to be a potential and valuable research direction for the treatment of BC (Sui et al., 2022). Some randomized controlled studies have reported that TF level is positively related to the incidence of ER-negative BC (Hou et al., 2021); the dietary iron supplementation is negatively correlated with the risk of BC; but in the postmenopausal women, heme iron is positively correlated with the risk of ER-positive and/or PR-positive BC (Chang et al., 2020). Iron transport protein and hepcidin have protective functions for BC patients (Pinnix et al., 2010), and the expression of TFRC is positively related to the quantity of immunocytes in BC patients (Chen et al., 2021b). Interferon -γ (IFN-γ) secreted from immunocytes suppress the cystine-uptake by reducing SLC7A11 (a ferroptosis related gene) in BC cells, followed by a lipid peroxidation and ferroptosis (Wang W. et al., 2019). In BC tissues, *SLC7A11* expresses higher than that in adjacent normal tissues. From a study of IR on BC, it is positively correlated with ESR1. ESR1 promotes SLC7A11 expression early after IR, either ESR1 or SLC7A11 knockdown enhances ferroptosis induced by IR in the ER-positive BC cells (Liu R. et al., 2021). It is reported that ESR1 inhibition enhances the sensitivity of ER-positive BC cells to ionizing radiation (IR) by inducing ferroptosis (Liu and Gu 2022). Drugs such as siramesine and lapatinib can reduce GSH level, increase ROS generation, and induce ferroptosis in BC cells (Ma et al., 2017). MUC1-C is able to interact with CD44v (CD44 variant) to stable the system xc–, increase GSH level and result in antiferroptosis in BC cells (Hasegawa et al., 2016). Notably, drug-resistant BC cells exhibits a dependence of GPX4 activity, thus,

targeting GPX4 to induce ferroptosis might potentially overcome drug-resistant BC (Hangauer et al., 2017). A recently study has developed a series of small molecules that trigger to ferroptosis, and verified the effect on selectively killing drug-resistant BC stem cell-like cells (bCSC) with mesenchymal phenotypes *in vitro* (Taylor et al., 2019).

5 Tumor therapy in gynecologic cancers

5.1 Steroid hormone-targeted tumor therapy

The hormone-targeted therapy in BC can be divided into three broad categories. The first category is selective estrogen receptor modulator (SERM), which functions by binding to ER to block estrogen, including Tamoxifen, Toremifene and Fulvestrant. Tamoxifen is most commonly used in ER + BC (Legha, 1988; Yang et al., 2013), Toremifene has a comparable efficacy of Tamoxifen (Zhou et al., 2011), and Fulvestrant is the latest generation of ER inhibitor for the treatment of ER + BC (Chen P. et al., 2022). The second category is aromatase inhibitors, which functions to inhibit estrogen synthesis, including Letrozole (Mukherjee et al., 2022), Anastrozole (Nabholtz, 2006), and Exemestane (Wang Y. et al., 2022). The third category is the progesterone analogue, which functions to active PRs, including megestrol and medroxyprogesterone. Megestrol acetate (MA) is one of the first pregnancy promotors to be evaluated for hormonal treatment of advanced BC (Sedlacek, 1988). Some clinical trials have shown that luteinizing hormone releasing hormone receptor antagonists, such as Goserrelin, are also effective for BC (Moore et al., 2015).

Basing on the steroid hormone signaling characteristics of gynecological cancers, there are a lot of steroid hormone-targeted drugs applied for cancer therapy. Letrozole (an aromatase inhibitors) is used for the treatment of low-grade serous ovarian cancer and high-grade serous ovarian cancer by inhibition of estrogen generation (Heinzelmann-Schwarz et al., 2018). Besides Letrozole, there are some the third-generation aromatase inhibitors such as Anastrozole and Exemestane. Fulvestrant has a high affinity of ER and downregulates its expression. Fluvestrant is effective for in patients with disease recurrence after endocrine therapy, some ongoing clinical trials suggest that Fluvestrant may be effective in OVCA (Bidard et al., 2022; Cristofanilli et al., 2022).

Because CC is a non-hormone-responsive cancer, steroid hormone-targeted tumor therapy is not common in CC. But there are some studies which have reported the relation between long-term oral contraceptives and the increasing risk of CC (Chung et al., 2010), which reminds us to concerned about the use of hormone replacement therapy in patients with CC.

For the treatment of EC, steroid hormone-targeted drugs are usually applied in well-differentiated endometrioid adenocarcinoma, young women with early stage EC who need to maintain fertility, and patients with advanced, recurrent, or inoperable EC. Medroxyprogesterone acetate (MPA) and MA are high-potency progesterone drugs that commonly used in EC, Levonorgestrel-releasing intrauterine device (LNG-IUD) also appears to be an alternative therapy in patients who do not tolerate oral therapy (Garzon et al., 2021; Zhao H. et al., 2022; Markowska et al., 2022). The application of SERM, gonadotropin-releasing hormone agonist (GnRH agonist) (Emons and Gründker, 2021) or aromatase inhibitors is good option for the treatment of EC (Zhang et al., 2019; Markowska et al., 2022). Tamoxifen is a selective estrogen receptor modulator that is effective for low-toxicity advanced or recurrent EC (Emons et al., 2020). Some clinical trials suggest that Fluvestrant is effective for EC (Battista and Schmidt, 2016; Bogliolo et al., 2017) and other aromatase inhibitors (letrozole, anastrozole) also have meaningful efficacy in patients with recurrent EC (Slomovitz et al., 2015; Heudel et al., 2022; Slomovitz et al., 2022).

5.2 Ferroptosis-targeted tumor therapy

There is a good application prospect of ferroptosis induced by the blockage of endogenous antioxidant system or by the regulation of intracellular free iron level in immunotherapy, radiation therapy and drug treatment of gynecologic cancers (Table 1). For example, MA-resistant EC cells are susceptible to ferroptosis (Murakami et al., 2023); Carboplatin is effective for estrogen-resistant BC (Larsen et al., 2012). Immune checkpoint inhibitor (ICI) has made unprecedented breakthrough in some cancer types (Hernandez et al., 2022), however, due to lack of tumor-infiltrating lymphocytes, numerous cancer types with poor prognosis after ICI immunotherapy remain. A recent study has reported that $CD8^{+}$T cells release cytokines to induce ferroptosis in OVCA cells (ID8) by suppressing system xc−, restraining cystine uptake, and enhancing lipid peroxidation (Wang K. et al., 2019). For radiation therapy (RT), there are plenty of evidences supporting its association with ferroptosis in cancers from multiple organs, including breast, ovarian, vulvar, and melanoma (Lang et al., 2019; Lei et al., 2020; Ye et al., 2020). Ionizing radiation (IR) inhibits system xc− in an ATM-dependent manner, which is a core component of DNA damage/repair systems (Matsuoka et al., 2007). In addition, Olaparib (a PARP inhibitor) can repress system xc− and induces ferroptosis in OVCA cells (Zhang et al., 2021a).

Artemisinin is proposed to promote free radical generation by Fe^{2+} (Li and Zhou, 2010). Its safety on intravenous or intravaginal administration in patients with advanced solid tumors (NCT 02353026) and cervical intraepithelial neoplasias (NCT 02354534) have been evaluated (Chen et al., 2021c; von Hagens et al., 2017). Artesunate (ART) can promote ferritinophagy to release free iron, and thus induce ferroptosis (Eling et al., 2015; Ooko et al., 2015; Lin et al., 2016; Du et al., 2019). ART-conjugated phosphorescence rhenium (I) complexes can promote ROS generation and induce ferroptosis in OVCA and CC cells (Shield et al., 2009; Greenshields et al., 2017; Ye et al., 2021). Sorafenib is able to inhibit GSH and promote ROS generation in CC cells (Wang C. et al., 2021). Quinones inhibits cell growth of EC cells by inducing ferroptosis through both iron regulation and blockage of endogenous antioxidant system (Zhang et al., 2021b).

In addition, unsaturated fatty acid-mediated lipid peroxidation could be activated by IR, leading to ferroptosis in BC cells (MCF-7) (Lei et al., 2020). Sulfasalazine (SSZ) has recently been recognized as

TABLE 1 List of ferroptosis-targeted tumor therapy drugs in gynecologic cancers.

Tumor	Drug	Mechanism of action	References
Cervical Cancer	Artemisinin	Promote free radical generation by Fe^{2+} and selectively reduces ESR1 level	Li and Zhou (2010)
	ART-conjugated phosphorescence rhenium (I) complexes	Inactivate GPX4, promote ROS generation and induce ferroptosis	Greenshields et al. (2017)
			Ye et al. (2021)
			Shield et al. (2009)
	Sorafenib	Inhibit GSH and promote ROS generation	Wang et al. (2021b)
Ovarian Cancer	Olaparib	Repress system xc− to induce ferroptosis	Zhang et al. (2021a)
	Artesunate	Promote ferritinophagy to release Fe^{2+}	Du et al. (2019)
			Eling et al. (2015)
			Lin et al. (2016)
			Ooko et al. (2015)
	ART-conjugated phosphorescence rhenium (I) complexes	Inactivate GPX4, promote ROS generation and induce ferroptosis	Greenshields et al. (2017)
			Ye et al. (2021)
			Shield et al. (2009)
	Immune checkpoint inhibitors	Promote $CD8^+$T cells to release cytokines that trigger ferroptosis by suppressing system xc− and enhancing lipid peroxidation	Wang et al. (2019a)
Endometrial Cancer	Quinones	Inhibit system xc−, affect iron level via the regulation of heme oxygenase and transferrin	Zhang et al. (2021b)
Breast Cancer	Sulfasalazine	Inhibit system xc− and disrupt circadian rhythms of TFRC expression	Babu and Muckenthaler (2016)
			Yoshida (2015)
			Yoshida (2018)
			Okazaki et al. (2017)
	Statins (Atorvastatin and Fluvastatin)	Inhibit GPX4 and CoQ10 through MVA pathway	Shimada et al. (2016)
			Viswanathan et al. (2017)
			Bjarnadottir et al. (2013)
			Garwood et al. (2010)
	Lapatinib (a tyrosine kinase inhibitor)	Promote ferritinophagy with autophagy-dependent manner	Ma et al. (2017)
	Vitamin C	Promote ferritinophagy to release Fe^{2+} and increase ROS level by Fenton reaction	Wang et al. (2021a)
			Singh et al. (2013)

a system xc− inhibitor (Babu and Muckenthaler, 2016). It affects iron metabolism by disruption of circadian rhythms of TFRC expression (Yoshida, 2015; Okazaki et al., 2017; Yoshida, 2018). SSZ has been planned to be administered for clinical therapy of patients with BC and chronic pain from a Phase I clinical trial (NCT03847311). Statins can inhibit GPX4 and CoQ10 through MVA pathway, which triggers ferroptosis (Shimada et al., 2016; Viswanathan et al., 2017). Atorvastatin and fluvastatin also have antiproliferative effects on the BC cells with high expressing *HMGCR* (Garwood et al., 2010; Bjarnadottir et al., 2013). Lapatinib (a tyrosine kinase inhibitor) is reported to induce ferroptosis by activation of autophagy-dependent ferritinophagy in BC cells (Ma et al., 2017). Vitamin C can promote ferritinophagy for the release of free iron and to increase ROS level by Fenton reaction (Wang C. et al., 2021). It is reported to inhibit BC by targeting miR-93-Nrf2 axis (Singh et al., 2013).

Furthermore, steroid hormone-targeted therapy combining with ferroptosis inducer is applied in some gynecologic cancers with drug resistance. More than 30 years ago, the treatment of cisplatin, doxorubicin, cyclophosphamide, and MA is used for recurrent and metastatic EC (Hoffman et al., 1989). Besides the effect on ferroptosis, Artemisinin selectively reduces ESR1 level. The

tamoxifen–artemisinin hybrids and estrogen–artemisinin hybrid compounds are highly active against BC cells (MCF-7) (Fröhlich et al., 2020).

6 Future perspective and conclusion

Gynecologic cancers are the most common malignant cancers in women. They affect thousands of lives and have attracted public attention due to the increased incidence rate worldwide. As a new type of RCD, ferroptosis has become a hot-spot issue in cancer research. In the past decade, there have been many studies on various aspects of ferroptosis, including molecular mechanisms, metabolic pathways, regulatory factors and tumor-related signaling pathways. Although some studies have proposed the importance of ferroptosis in gynecologic cancers, however, the underlying molecular mechanisms involved in ferroptosis and the occurrence and development of gynecological cancers have not yet been fully elucidated. We should also notice the relationship between steroid hormone signaling and ferroptosis in gynecologic cancers. The steroid hormone levels are distinct due to gynecologic cancer types, and the expression levels of steroid hormone receptors also have great difference. We examined the expression levels of steroid hormone signaling-related genes (ESR1, ESR2, PR and PGRMC1) in gynecologic cancer tissues and their adjacent samples from TCGA RNA seq data (Supplementary Figure S1). From the TCGA RNA seq data of CC with 317 patients documented, we found that ESR1 and PR were decreased in primary tumors and metastatic tumors compared to that in normal tissues, while ESR2 and PGRMC1 were increased in metastatic tumors compared to that in normal tissues and primary tumors. From the TCGA RNA seq data of OVCA with 758 patients documented, we did not find significant difference of the four genes between primary tumors and recurrent tumors. From the TCGA RNA seq data of EC with 606 patients documented, PR was decreased in primary tumors compared to that in normal tissues, while the other genes were not changed. From the TCGA RNA seq data of BC with 1,284 patients documented, ESR1 was increased in primary tumors and metastatic tumors compared to that in normal tissues, while ESR2 was decreased in primary tumors and metastatic tumors. In addition, ESR2 was found a low expression level in CC, OVCA and EC tissues. All the four genes were expressed much higher in BC tissues than that of CC, OVCA and EC tissues (Supplementary Figure S1). We next examined the expression levels of ferroptosis-related genes (GPX4, TFRC, HMGCR and ACSL4) in gynecologic cancer tissues and their adjacent samples from TCGA RNA seq data. From the TCGA RNA seq data of CC, we found that GPX4, TFRC and HMGCR were increased in primary tumors and metastatic tumors compared to that in normal tissues, while ACSL4 was decreased (Supplementary Figure S2). From the TCGA RNA seq data of OVCA, only ACSL4 was increased in recurrent tumors compared to that in primary tumors. From the TCGA RNA seq data of EC, we found that GPX4, TFRC and HMGCR were increased in primary tumors compared to that in normal tissues, while ACSL4 was not changed. From the TCGA RNA seq data of BC, only ACSL4 was decreased in primary tumors and metastatic tumors compared to that in normal tissues, while the other genes were not changed (Supplementary Figure S2).

It is important to select the best manner to trigger ferroptosis basing on the expression levels of ferroptosis-genes and characteristic of steroid hormone signaling in gynecologic cancers. In OVCA, due to the high expression of ER and low expression of PR, inhibition of estrogen signaling or activation of non-classical progesterone signaling pathway mediated by PGRMC1 are beneficial to ferroptosis. PGRMC1 has been reported to induce ferroptosis by enhancing LD lipolysis in other cell type, thus increasing unsaturated fatty acid generation to enhance lipid peroxidation and inhibiting GPX4 to reduce the antioxidant ability of OVCA cells may induce ferroptosis.

During CC development, we should also notice the function of PGRMC1 rather than ESR1 and PR. Although serotransferrin-mediated iron uptake is increased and PGRMC1 can promote LD lipolysis, but the decrease of ACSL4 may weaken this effect. The activation of the MVA pathway and the elevated GPX4 expression may constitute a strong antioxidant defense system against ferroptosis. Thus, stains and GPX4-targeted drugs may have a better treatment effect to trigger ferroptosis in CC.

In EC, due to the high expression of ESR1, PR and PGRMC1, inhibition of estrogen signaling or activation of progesterone signaling may have good effect for inducing ferroptosis. Basing on the elevated expression of TFRC and HMGCR in EC, drugs enhancing ferritinophagy and inhibiting the MVA pathway may induce ferroptosis of EC cells.

During the progress of BC development, both inhibition of estrogen signaling and enhance of progesterone signaling are necessary. Although the decrease of ACSL4 may weaken ferroptosis, enhanced LD lipolysis is still beneficial in promoting ferroptosis because the breast is rich in fat. In addition, stains and GPX4-targeted drugs may also have good treatment effect in BC. Thus, basing on the features of ferroptosis and steroid hormone signaling, the combination of steroid hormone-targeted tumor therapy and ferroptosis-targeted tumor therapy is expected to solve the problem of drug-resistance and may further enhance therapeutic efficiency of gynecologic cancers.

How to use the ferroptosis mechanism for tumor-targeted therapy still has a long way to go in gynecologic cancers. In the future, we hope to investigate the regulatory mechanism of ferroptosis on the estrogen and progesterone signaling pathways in order to provide a theoretical basis for the prevention and treatment of gynecological cancers.

Author contributions

WL and TW wrote the manuscript and were involved with submission; JC and QL were involved with project concept; WL, JC, and QL performed data collection; WL and TW revised the manuscript and were responsible for final approval; All authors contributed to the article and approved the submitted version.

Funding

This work is supported by Open Project of Jiangsu Biobank of Clinical Resources (Grant/Award Number: TC2021B013) and the Nanjing Healthcare Science and Technology Development Special Funded Project (Grant/Award Number: YKK20197).

Conflict of interest

The authors declare that the research was conducted in the absence of any commercial or financial relationships that could be construed as a potential conflict of interest.

Publisher's note

All claims expressed in this article are solely those of the authors and do not necessarily represent those of their affiliated organizations, or those of the publisher, the editors and the reviewers. Any product that may be evaluated in this article, or claim that may be made by its manufacturer, is not guaranteed or endorsed by the publisher.

Supplementary material

The Supplementary Material for this article can be found online at: https://www.frontiersin.org/articles/10.3389/fmolb.2023.1223493/full#supplementary-material

References

Ali, M., Ciebiera, M., Vafaei, S., Alkhrait, S., Chen, H. Y., Chiang, Y. F., et al. (2023). Progesterone signaling and uterine fibroid pathogenesis; molecular mechanisms and potential therapeutics. *Cells* 12 (8), 1117. doi:10.3390/cells12081117

Auchus, R. J., Lee, T. C., and Miller, W. L. (1998). Cytochrome b5 augments the 17,20-lyase activity of human P450c17 without direct electron transfer. *J. Biol. Chem.* 273 (6), 3158–3165. doi:10.1074/jbc.273.6.3158

Babu, K. R., and Muckenthaler, M. U. (2016). miR-20a regulates expression of the iron exporter ferroportin in lung cancer. *J. Mol. Med. Berl.* 94 (3), 347–359. doi:10.1007/s00109-015-1362-3

Baik, S., Mehta, F. F., Unsal, E., Park, Y., and Chung, S. H. (2022). Estrogen inhibits epithelial progesterone receptor-dependent progestin therapy efficacy in a mouse model of cervical cancer. *Am. J. Pathol.* 192 (2), 353–360. doi:10.1016/j.ajpath.2021.10.008

Bajbouj, K., Shafarin, J., and Hamad, M. (2019). Estrogen-dependent disruption of intracellular iron metabolism augments the cytotoxic effects of doxorubicin in select breast and ovarian cancer cells. *Cancer Manag. Res.* 11, 4655–4668. doi:10.2147/CMAR.S204852

Baker, J. M., Al-Nakkash, L., and Herbst-Kralovetz, M. M. (2017). Estrogen-gut microbiome axis: Physiological and clinical implications. *Maturitas* 103, 45–53. doi:10.1016/j.maturitas.2017.06.025

Batchuluun, B., Pinkosky, S. L., and Steinberg, G. R. (2022). Lipogenesis inhibitors: Therapeutic opportunities and challenges. *Nat. Rev. Drug Discov.* 21 (4), 283–305. doi:10.1038/s41573-021-00367-2

Bathaie, S. Z., Ashrafi, M., Azizian, M., and Tamanoi, F. (2017). Mevalonate pathway and human cancers. *Curr. Mol. Pharmacol.* 10 (2), 77–85. doi:10.2174/1874467209666160112123205

Battista, M. J., and Schmidt, M. (2016). Fulvestrant for the treatment of endometrial cancer. *Expert Opin. Investig. Drugs* 25 (4), 475–483. doi:10.1517/13543784.2016.1154532

Bayır, H., Anthonymuthu, T. S., Tyurina, Y. Y., Patel, S. J., Amoscato, A. A., Lamade, A. M., et al. (2020). Achieving life through death: Redox biology of lipid peroxidation in ferroptosis. *Cell Chem. Biol.* 27 (4), 387–408. doi:10.1016/j.chembiol.2020.03.014

Bedell, S. L., Goldstein, L. S., and Goldstein, A. R. (2020). Cervical cancer screening: Past, present, and future. *Sex. Med. Rev.* 8 (1), 28–37. doi:10.1016/j.sxmr.2019.09.005

Bersuker, K., Hendricks, J. M., Li, Z., Magtanong, L., Ford, B., Tang, P. H., et al. (2019). The CoQ oxidoreductase FSP1 acts parallel to GPX4 to inhibit ferroptosis. *Nature* 575 (7784), 688–692. doi:10.1038/s41586-019-1705-2

Bidard, F. C., Hardy-Bessard, A. C., Dalenc, F., Bachelot, T., Pierga, J. Y., de la Motte Rouge, T., et al. (2022). Switch to fulvestrant and palbociclib versus no switch in advanced breast cancer with rising ESR1 mutation during aromatase inhibitor and palbociclib therapy (PADA-1): A randomised, open-label, multicentre, phase 3 trial. *Lancet Oncol.* 23 (11), 1367–1377. doi:10.1016/S1470-2045(22)00555-1

Bjarnadottir, O., Romero, Q., Bendahl, P. O., Jirström, K., Rydén, L., Loman, N., et al. (2013). Targeting HMG-CoA reductase with statins in a window-of-opportunity breast cancer trial. *Breast Cancer Res. Treat.* 138 (2), 499–508. doi:10.1007/s10549-013-2473-6

Bogliolo, S., Cassani, C., Dominoni, M., Orlandini, A., Ferrero, S., Iacobone, A. D., et al. (2017). The role of fulvestrant in endometrial cancer. *Expert Opin. Drug Metab. Toxicol.* 13 (5), 537–544. doi:10.1080/17425255.2016.1244264

Braun, J. A., Herrmann, A. L., Blase, J. I., Frensemeier, K., Bulkescher, J., Scheffner, M., et al. (2020). Effects of the antifungal agent ciclopirox in HPV-positive cancer cells: Repression of viral E6/E7 oncogene expression and induction of senescence and apoptosis. *Int. J. cancer* 146 (2), 461–474. doi:10.1002/ijc.32709

Brown, C. W., Amante, J. J., Chhoy, P., Elaimy, A. L., Liu, H., Zhu, L. J., et al. (2019). Prominin2 drives ferroptosis resistance by stimulating iron export. *Dev. Cell* 51 (5), 575–586.e4. doi:10.1016/j.devcel.2019.10.007

Bulletti, C., Bulletti, F. M., Sciorio, R., and Guido, M. (2022). Progesterone: The key factor of the beginning of life. *Int. J. Mol. Sci.* 23 (22), 14138. doi:10.3390/ijms232214138

Bulletti, C., Prefetto, R. A., Bazzocchi, G., Romero, R., Mimmi, P., Polli, V., et al. (1993). Electromechanical activities of human uteri during extra-corporeal perfusion with ovarian steroids. *Hum. Reprod.* 8 (10), 1558–1563. doi:10.1093/oxfordjournals.humrep.a137891

Cao, J., Chen, X., Jiang, L., Lu, B., Yuan, M., Zhu, D., et al. (2020). DJ-1 suppresses ferroptosis through preserving the activity of S-adenosyl homocysteine hydrolase. *Nat. Commun.* 11 (1), 1251. doi:10.1038/s41467-020-15109-y

Chang, V. C., Cotterchio, M., Bondy, S. J., and Kotsopoulos, J. (2020). Iron intake, oxidative stress-related genes and breast cancer risk. *Int. J. Cancer* 147 (5), 1354–1373. doi:10.1002/ijc.32906

Chen, D., Tavana, O., Chu, B., Erber, L., Chen, Y., Baer, R., et al. (2017). NRF2 is a major target of ARF in p53-independent tumor suppression. *Mol. Cell* 68 (1), 224–232.e4. doi:10.1016/j.molcel.2017.09.009

Chen, F., Fan, Y., Hou, J., Liu, B., Zhang, B., Shang, Y., et al. (2021c). Integrated analysis identifies TfR1 as a prognostic biomarker which correlates with immune infiltration in breast cancer. *Aging (Albany NY)* 13 (17), 21671–21699. doi:10.18632/aging.203512

Chen, H., Liu, S., Ji, L., Wu, T., Ji, Y., Zhou, Y., et al. (2016). Folic acid supplementation mitigates alzheimer's disease by reducing inflammation: A randomized controlled trial. *Mediat. Inflamm.* 2016, 5912146. doi:10.1155/2016/5912146

Chen, P., Li, B., and Ou-Yang, L. (2022a). Role of estrogen receptors in health and disease. *Front. Endocrinol.* 13, 839005. doi:10.3389/fendo.2022.839005

Chen, S., Shen, L., Luo, S., Lan, X., and Wang, L. (2020b). Association between serum iron levels and the risk of cervical cancer in Chinese: A meta-analysis. *J. Int. Med. Res.* 48 (3), 300060519882804. doi:10.1177/0300060519882804

Chen, X., Kang, R., Kroemer, G., and Tang, D. (2021b). Broadening horizons: The role of ferroptosis in cancer. *Nat. Rev. Clin. Oncol.* 18 (5), 280–296. doi:10.1038/s41571-020-00462-0

Chen, X., Li, J., Kang, R., Klionsky, D. J., and Tang, D. (2021a). Ferroptosis: Machinery and regulation. *Autophagy* 17 (9), 2054–2081. doi:10.1080/15548627.2020.1810918

Chen, X., Yu, C., Kang, R., and Tang, D. (2020a). Iron metabolism in ferroptosis. *Front. Cell Dev. Biol.* 8, 590226. doi:10.3389/fcell.2020.590226

Chen, Y. C., Yu, J., Metcalfe, C., De Bruyn, T., Gelzleichter, T., Malhi, V., et al. (2022b). Latest generation estrogen receptor degraders for the treatment of hormone receptor-positive breast cancer. *Expert Opin. Investig. Drugs* 31 (6), 515–529. doi:10.1080/13543784.2021.1983542

Chung, S. H., Franceschi, S., and Lambert, P. F. (2010). Estrogen and ERalpha: Culprits in cervical cancer? *Trends Endocrinol. metabolism TEM* 21 (8), 504–511. doi:10.1016/j.tem.2010.03.005

Conneely, O. M., and Lydon, J. P. (2000). Progesterone receptors in reproduction: Functional impact of the A and B isoforms. *Steroids* 65 (10-11), 571–577. doi:10.1016/s0039-128x(00)00115-x

Cristofanilli, M., Rugo, H. S., Im, S. A., Slamon, D. J., Harbeck, N., Bondarenko, I., et al. (2022). Overall survival with palbociclib and fulvestrant in women with HR+/HER2- ABC: Updated exploratory analyses of PALOMA-3, a double-blind, phase III randomized study. *Clin. cancer Res. official J. Am. Assoc. Cancer Res.* 28 (16), 3433–3442. doi:10.1158/1078-0432.CCR-22-0305

Cronin, S. J. F., Seehus, C., Weidinger, A., Talbot, S., Reissig, S., Seifert, M., et al. (2018). The metabolite BH4 controls T cell proliferation in autoimmunity and cancer. *Nature* 563 (7732), 564–568. doi:10.1038/s41586-018-0701-2

Daniel, A. R., Hagan, C. R., and Lange, C. A. (2011). Progesterone receptor action: Defining a role in breast cancer. *Expert Rev. Endocrinol. metabolism* 6 (3), 359–369. doi:10.1586/eem.11.25

DeVore, N. M., and Scott, E. E. (2012). Structures of cytochrome P450 17A1 with prostate cancer drugs abiraterone and TOK-001. *Nature* 482 (7383), 116–119. doi:10.1038/nature10743

Dixon, S. J., Lemberg, K. M., Lamprecht, M. R., Skouta, R., Zaitsev, E. M., Gleason, C. E., et al. (2012). Ferroptosis: An iron-dependent form of nonapoptotic cell death. *Cell* 149 (5), 1060–1072. doi:10.1016/j.cell.2012.03.042

Dixon, S. J., Winter, G. E., Musavi, L. S., Lee, E. D., Snijder, B., Rebsamen, M., et al. (2015). Human haploid cell genetics reveals roles for lipid metabolism genes in nonapoptotic cell death. *ACS Chem. Biol.* 10 (7), 1604–1609. doi:10.1021/acschembio.5b00245

Doll, S., Proneth, B., Tyurina, Y. Y., Panzilius, E., Kobayashi, S., Ingold, I., et al. (2017). ACSL4 dictates ferroptosis sensitivity by shaping cellular lipid composition. *Nat. Chem. Biol.* 13 (1), 91–98. doi:10.1038/nchembio.2239

Du, J., Wang, T., Li, Y., Zhou, Y., Wang, X., Yu, X., et al. (2019). DHA inhibits proliferation and induces ferroptosis of leukemia cells through autophagy dependent degradation of ferritin. *Free Radic. Biol. Med.* 131, 356–369. doi:10.1016/j.freeradbiomed.2018.12.011

Duggan, C., Trapani, D., Ilbawi, A. M., Fidarova, E., Laversanne, M., Curigliano, G., et al. (2021). National health system characteristics, breast cancer stage at diagnosis, and breast cancer mortality: A population-based analysis. *Lancet Oncol.* 22 (11), 1632–1642. doi:10.1016/S1470-2045(21)00462-9

Eling, N., Reuter, L., Hazin, J., Hamacher-Brady, A., and Brady, N. R. (2015). Identification of artesunate as a specific activator of ferroptosis in pancreatic cancer cells. *Oncoscience* 2 (5), 517–532. doi:10.18632/oncoscience.160

Emons, G., and Gründker, C. (2021). Role of gonadotropin-releasing hormone (GnRH) in ovarian cancer. *Cells* 10 (2), 437. doi:10.3390/cells10020437

Emons, G., Mustea, A., and Tempfer, C. (2020). Tamoxifen and endometrial cancer: A janus-headed drug. *Cancers (Basel)* 12 (9), 2535. doi:10.3390/cancers12092535

Englert-Golon, M., Andrusiewicz, M., Żbikowska, A., Chmielewska, M., Sajdak, S., and Kotwicka, M. (2021). Altered expression of ESR1, ESR2, PELP1 and c-SRC genes is associated with ovarian cancer manifestation. *Int. J. Mol. Sci.* 22 (12), 6216. doi:10.3390/ijms22126216

Fan, R., Sun, Y., Wang, M., Wang, Q., Jiang, A., and Yang, T. (2022). New insights on ferroptosis and gynecological malignancies. *Front. Mol. Biosci.* 9, 921298. doi:10.3389/fmolb.2022.921298

Feng, H., Schorpp, K., Jin, J., Yozwiak, C. E., Hoffstrom, B. G., Decker, A. M., et al. (2020). Transferrin receptor is a specific ferroptosis marker. *Cell Rep.* 30 (10), 3411–3423.e7. doi:10.1016/j.celrep.2020.02.049

Fröhlich, T., Mai, C., Bogautdinov, R. P., Morozkina, S. N., Shavva, A. G., Friedrich, O., et al. (2020). Synthesis of tamoxifen-artemisinin and estrogen-artemisinin hybrids highly potent against breast and prostate cancer. *ChemMedChem* 15 (15), 1473–1479. doi:10.1002/cmdc.202000174

Fuentes, N., and Silveyra, P. (2019). Estrogen receptor signaling mechanisms. *Adv. protein Chem. Struct. Biol.* 116, 135–170. doi:10.1016/bs.apcsb.2019.01.001

Gao, M., Monian, P., Quadri, N., Ramasamy, R., and Jiang, X. (2015). Glutaminolysis and transferrin regulate ferroptosis. *Mol. Cell* 59 (2), 298–308. doi:10.1016/j.molcel.2015.06.011

Garwood, E. R., Kumar, A. S., Baehner, F. L., Moore, D. H., Au, A., Hylton, N., et al. (2010). Fluvastatin reduces proliferation and increases apoptosis in women with high grade breast cancer. *Breast Cancer Res. Treat.* 119 (1), 137–144. doi:10.1007/s10549-009-0507-x

Garzon, S., Uccella, S., Zorzato, P. C., Bosco, M., Franchi, M. P., Student, V., et al. (2021). Fertility-sparing management for endometrial cancer: Review of the literature. *Minerva Med.* 112 (1), 55–69. doi:10.23736/S0026-4806.20.07072-X

Gaschler, M. M., and Stockwell, B. R. (2017). Lipid peroxidation in cell death. *Biochem. Biophys. Res. Commun.* 482 (3), 419–425. doi:10.1016/j.bbrc.2016.10.086

Gatica, D., Lahiri, V., and Klionsky, D. J. (2018). Cargo recognition and degradation by selective autophagy. *Nat. Cell Biol.* 20 (3), 233–242. doi:10.1038/s41556-018-0037-z

Geng, N., Shi, B. J., Li, S. L., Zhong, Z. Y., Li, Y. C., Xua, W. L., et al. (2018). Knockdown of ferroportin accelerates erastin-induced ferroptosis in neuroblastoma cells. *Eur. Rev. Med. Pharmacol. Sci.* 22 (12), 3826–3836. doi:10.26355/eurrev_201806_15267

Gimeno-Martos, S., Miguel-Jimenez, S., Casao, A., Cebrián-Pérez, J. A., Muiño-Blanco, T., and Pérez-Pe, R. (2020). Underlying molecular mechanism in the modulation of the ram sperm acrosome reaction by progesterone and 17β-estradiol. *Animal reproduction Sci.* 221, 106567. doi:10.1016/j.anireprosci.2020.106567

Gompel, A. (2020). Progesterone and endometrial cancer. *Best. Pract. Res. Clin. Obstet. Gynaecol.* 69, 95–107. doi:10.1016/j.bpobgyn.2020.05.003

Greenshields, A. L., Shepherd, T. G., and Hoskin, D. W. (2017). Contribution of reactive oxygen species to ovarian cancer cell growth arrest and killing by the anti-malarial drug artesunate. *Mol. Carcinog.* 56 (1), 75–93. doi:10.1002/mc.22474

Habib, E., Linher-Melville, K., Lin, H. X., and Singh, G. (2015). Expression of xCT and activity of system xc(-) are regulated by NRF2 in human breast cancer cells in response to oxidative stress. *Redox Biol.* 5, 33–42. doi:10.1016/j.redox.2015.03.003

Hangauer, M. J., Viswanathan, V. S., Ryan, M. J., Bole, D., Eaton, J. K., Matov, A., et al. (2017). Drug-tolerant persister cancer cells are vulnerable to GPX4 inhibition. *Nature* 551 (7679), 247–250. doi:10.1038/nature24297

Hasegawa, M., Takahashi, H., Rajabi, H., Alam, M., Suzuki, Y., Yin, L., et al. (2016). Functional interactions of the cystine/glutamate antiporter, CD44v and MUC1-C oncoprotein in triple-negative breast cancer cells. *Oncotarget* 7 (11), 11756–11769. doi:10.18632/oncotarget.7598

Hayano, M., Yang, W. S., Corn, C. K., Pagano, N. C., and Stockwell, B. R. (2016). Loss of cysteinyl-tRNA synthetase (CARS) induces the transsulfuration pathway and inhibits ferroptosis induced by cystine deprivation. *Cell Death Differ.* 23 (2), 270–278. doi:10.1038/cdd.2015.93

Heinzelmann-Schwarz, V., Knipprath Meszaros, A., Stadlmann, S., Jacob, F., Schoetzau, A., Russell, K., et al. (2018). Letrozole may be a valuable maintenance treatment in high-grade serous ovarian cancer patients. *Gynecol. Oncol.* 148 (1), 79–85. doi:10.1016/j.ygyno.2017.10.036

Henderson, V. W. (2018). Progesterone and human cognition. *Climacteric* 21 (4), 333–340. doi:10.1080/13697137.2018.1476484

Hernandez, R., Põder, J., LaPorte, K. M., and Malek, T. R. (2022). Engineering IL-2 for immunotherapy of autoimmunity and cancer. *Nat. Rev. Immunol.* 22 (10), 614–628. doi:10.1038/s41577-022-00680-w

Heudel, P., Frenel, J. S., Dalban, C., Bazan, F., Joly, F., Arnaud, A., et al. (2022). Safety and efficacy of the mTOR inhibitor, vistusertib, combined with anastrozole in patients with hormone receptor-positive recurrent or metastatic endometrial cancer: The VICTORIA multicenter, open-label, phase 1/2 randomized clinical trial. *JAMA Oncol.* 8 (7), 1001–1009. doi:10.1001/jamaoncol.2022.1047

Hoffman, M. S., Roberts, W. S., Cavanagh, D., Praphat, H., Solomon, P., and Lyman, G. H. (1989). Treatment of recurrent and metastatic endometrial cancer with cisplatin, doxorubicin, cyclophosphamide, and megestrol acetate. *Gynecol. Oncol.* 35 (1), 75–77. doi:10.1016/0090-8258(89)90016-4

Hong, X., Roh, W., Sullivan, R. J., Wong, K. H. K., Wittner, B. S., Guo, H., et al. (2021). The lipogenic regulator SREBP2 induces transferrin in circulating melanoma cells and suppresses ferroptosis. *Cancer Discov.* 11 (3), 678–695. doi:10.1158/2159-8290.CD-19-1500

Hou, C., Hou, Q., Xie, X., Wang, H., Chen, Y., Lu, T., et al. (2021). Serum iron status and the risk of breast cancer in the European population: A two-sample mendelian randomisation study. *Genes Nutr.* 16 (1), 9. doi:10.1186/s12263-021-00691-7

Hou, Y., Zhang, S., Wang, L., Li, J., Qu, G., He, J., et al. (2012). Estrogen regulates iron homeostasis through governing hepatic hepcidin expression via an estrogen response element. *Gene* 511 (2), 398–403. doi:10.1016/j.gene.2012.09.060

Ingold, I., Berndt, C., Schmitt, S., Doll, S., Poschmann, G., Buday, K., et al. (2018). Selenium utilization by GPX4 is required to prevent hydroperoxide-induced ferroptosis. *Cell* 172 (3), 409–422.e21. doi:10.1016/j.cell.2017.11.048

Irwin, R. W., Yao, J., Hamilton, R. T., Cadenas, E., Brinton, R. D., and Nilsen, J. (2008). Progesterone and estrogen regulate oxidative metabolism in brain mitochondria. *Endocrinology* 149 (6), 3167–3175. doi:10.1210/en.2007-1227

Ishimoto, T., Nagano, O., Yae, T., Tamada, M., Motohara, T., Oshima, H., et al. (2011). CD44 variant regulates redox status in cancer cells by stabilizing the xCT subunit of system xc(-) and thereby promotes tumor growth. *Cancer Cell* 19 (3), 387–400. doi:10.1016/j.ccr.2011.01.038

Jayshree, R. S. (2021). The immune microenvironment in human papilloma virus-induced cervical lesions-evidence for estrogen as an immunomodulator. *Front. Cell Infect. Microbiol.* 11, 649815. doi:10.3389/fcimb.2021.649815

Jelić, M., Mandić, A., Kladar, N., Sudji, J., Božin, B., and Srdjenović, B. (2018). Lipid peroxidation, antioxidative defense and level of 8-hydroxy-2-deoxyguanosine in cervical cancer patients. *J. Med. Biochem.* 37 (3), 336–345. doi:10.1515/jomb-2017-0053

Jelic, M. D., Mandic, A. D., Maricic, S. M., and Srdjenovic, B. U. (2021). Oxidative stress and its role in cancer. *J. Cancer Res. Ther.* 17 (1), 22–28. doi:10.4103/jcrt.JCRT_862_16

Jiang, L., Kon, N., Li, T., Wang, S. J., Su, T., Hibshoosh, H., et al. (2015). Ferroptosis as a p53-mediated activity during tumour suppression. *Nature* 520 (7545), 57–62. doi:10.1038/nature14344

Jodhka, P. K., Kaur, P., Underwood, W., Lydon, J. P., and Singh, M. (2009). The differences in neuroprotective efficacy of progesterone and medroxyprogesterone acetate correlate with their effects on brain-derived neurotrophic factor expression. *Endocrinology* 150 (7), 3162–3168. doi:10.1210/en.2008-1247

Kagan, V. E., Mao, G., Qu, F., Angeli, J. P. F., Doll, S., Croix, C. S., et al. (2017). Oxidized arachidonic and arsenic PEs navigate cells to ferroptosis. *Nat. Chem. Biol.* 13 (1), 81–90. doi:10.1038/nchembio.2238

Kaur, J., and Debnath, J. (2015). Autophagy at the crossroads of catabolism and anabolism. *Nat. Rev. Mol. Cell Biol.* 16 (8), 461–472. doi:10.1038/nrm4024

Kim, D. H., Kim, M. J., Kim, N. Y., Lee, S., Byun, J. K., Yun, J. W., et al. (2022). DN200434, an orally available inverse agonist of estrogen-related receptor γ, induces ferroptosis in sorafenib-resistant hepatocellular carcinoma. *BMB Rep.* 55 (11), 547–552. doi:10.5483/BMBRep.2022.55.11.089

Kim, J. J., Kurita, T., and Bulun, S. E. (2013). Progesterone action in endometrial cancer, endometriosis, uterine fibroids, and breast cancer. *Endocr. Rev.* 34 (1), 130–162. doi:10.1210/er.2012-1043

Kim, O., Park, E. Y., Kwon, S. Y., Shin, S., Emerson, R. E., Shin, Y. H., et al. (2020). Targeting progesterone signaling prevents metastatic ovarian cancer. *Proc. Natl. Acad. Sci. U. S. A.* 117 (50), 31993–32004. doi:10.1073/pnas.2013595117

Kobayashi, H., Yamada, Y., Kawahara, N., Ogawa, K., and Yoshimoto, C. (2019). Integrating modern approaches to pathogenetic concepts of malignant transformation of endometriosis. *Oncol. Rep.* 41 (3), 1729–1738. doi:10.3892/or.2018.6946

Kraft, V. A. N., Bezjian, C. T., Pfeiffer, S., Ringelstetter, L., Müller, C., Zandkarimi, F., et al. (2020). GTP cyclohydrolase 1/tetrahydrobiopterin counteract ferroptosis through lipid remodeling. *ACS Cent. Sci.* 6 (1), 41–53. doi:10.1021/acscentsci.9b01063

Kuiper, G. G., and Gustafsson, J. A. (1997). The novel estrogen receptor-beta subtype: Potential role in the cell- and promoter-specific actions of estrogens and anti-estrogens. *FEBS Lett.* 410 (1), 87–90. doi:10.1016/s0014-5793(97)00413-4

Kumar, R. S., and Goyal, N. (2021). Estrogens as regulator of hematopoietic stem cell, immune cells and bone biology. *Life Sci.* 269, 119091. doi:10.1016/j.lfs.2021.119091

Kuzuyama, T., and Seto, H. (2012). Two distinct pathways for essential metabolic precursors for isoprenoid biosynthesis. *Proc. Jpn. Acad. Ser. B Phys. Biol. Sci.* 88 (3), 41–52. doi:10.2183/pjab.88.41

Kwon, S., Ahn, S. H., Jeong, W. J., Jung, Y. H., Bae, Y. J., Paik, J. H., et al. (2020). Estrogen receptor α as a predictive biomarker for survival in human papillomavirus-positive oropharyngeal squamous cell carcinoma. *J. Transl. Med.* 18 (1), 240. doi:10.1186/s12967-020-02396-8

Lai, C. R., Hsu, C. Y., Chen, Y. J., Yen, M. S., Chao, K. C., and Li, A. F. Y. (2013). Ovarian cancers arising from endometriosis: A microenvironmental biomarker study including ER, HNF1ß, p53, PTEN, BAF250a, and COX-2. *J. Chin. Med. Assoc. JCMA* 76 (11), 629–634. doi:10.1016/j.jcma.2013.07.008

Lang, X., Green, M. D., Wang, W., Yu, J., Choi, J. E., Jiang, L., et al. (2019). Radiotherapy and immunotherapy promote tumoral lipid oxidation and ferroptosis via synergistic repression of SLC7A11. *Cancer Discov.* 9 (12), 1673–1685. doi:10.1158/2159-8290.CD-19-0338

Larsen, M. S., Yde, C. W., Christensen, I. J., and Lykkesfeldt, A. E. (2012). Carboplatin treatment of antiestrogen-resistant breast cancer cells. *Int. J. Oncol.* 41 (5), 1863–1870. doi:10.3892/ijo.2012.1623

Latremoliere, A., and Costigan, M. (2011). GCH1, BH4 and pain. *Curr. Pharm. Biotechnol.* 12 (10), 1728–1741. doi:10.2174/138920111798357393

Legha, S. S. (1988). Tamoxifen in the treatment of breast cancer. *Ann. Intern Med.* 109 (3), 219–228. doi:10.7326/0003-4819-109-3-219

Lehtihet, M., Bonde, Y., Beckman, L., Berinder, K., Hoybye, C., Rudling, M., et al. (2016). Circulating hepcidin-25 is reduced by endogenous estrogen in humans. *PloS one* 11 (2), e0148802. doi:10.1371/journal.pone.0148802

Lei, G., Zhang, Y., Koppula, P., Liu, X., Zhang, J., Lin, S. H., et al. (2020). The role of ferroptosis in ionizing radiation-induced cell death and tumor suppression. *Cell Res.* 30 (2), 146–162. doi:10.1038/s41422-019-0263-3

Lewerenz, J., Hewett, S. J., Huang, Y., Lambros, M., Gout, P. W., Kalivas, P. W., et al. (2013). The cystine/glutamate antiporter system x(c)(-) in health and disease: From molecular mechanisms to novel therapeutic opportunities. *Antioxid. Redox Signal* 18 (5), 522–555. doi:10.1089/ars.2011.4391

Li, C., Zhang, L., Qiu, Z., Deng, W., and Wang, W. (2022). Key molecules of fatty acid metabolism in gastric cancer. *Biomolecules* 12 (5), 706. doi:10.3390/biom12050706

Li, J., Cao, F., Yin, H. L., Huang, Z. J., Lin, Z. T., Mao, N., et al. (2020). Ferroptosis: Past, present and future. *Cell death Dis.* 11 (2), 88. doi:10.1038/s41419-020-2298-2

Li, J., and Zhou, B. (2010). Biological actions of artemisinin: Insights from medicinal chemistry studies. *Molecules* 15 (3), 1378–1397. doi:10.3390/molecules15031378

Li, X., Rhee, D. K., Malhotra, R., Mayeur, C., Hurst, L. A., Ager, E., et al. (2016). Progesterone receptor membrane component-1 regulates hepcidin biosynthesis. *J. Clin. investigation* 126 (1), 389–401. doi:10.1172/JCI83831

Liang, L., Wang, H., Yao, J., Wei, Q., Lu, Y., Wang, T., et al. (2022). NPC1 deficiency contributes to autophagy-dependent ferritinophagy in HEI-OC1 auditory cells. *Front. Mol. Biosci.* 9, 952608. doi:10.3389/fmolb.2022.952608

Liao, P., Hemmerlin, A., Bach, T. J., and Chye, M. L. (2016). The potential of the mevalonate pathway for enhanced isoprenoid production. *Biotechnol. Adv.* 34 (5), 697–713. doi:10.1016/j.biotechadv.2016.03.005

Lin, R., Zhang, Z., Chen, L., Zhou, Y., Zou, P., Feng, C., et al. (2016). Dihydroartemisinin (DHA) induces ferroptosis and causes cell cycle arrest in head and neck carcinoma cells. *Cancer Lett.* 381 (1), 165–175. doi:10.1016/j.canlet.2016.07.033

Liu, J., Wang, Y., Meng, H., Yin, Y., Zhu, H., and Ni, T. (2021a). Identification of the prognostic signature associated with tumor immune microenvironment of uterine corpus endometrial carcinoma based on ferroptosis-related genes. *Front. Cell Dev. Biol.* 9, 735013. doi:10.3389/fcell.2021.735013

Liu, L., Zhang, C., Qu, S., Liu, R., Chen, H., Liang, Z., et al. (2022b). ESR1 inhibits ionizing radiation-induced ferroptosis in breast cancer cells via the NEDD4L/CD71 pathway. *Arch. Biochem. Biophys.* 725, 109299. doi:10.1016/j.abb.2022.109299

Liu, R., Liu, L., Bian, Y., Zhang, S., Wang, Y., Chen, H., et al. (2021b). The dual regulation effects of ESR1/nedd4l on SLC7A11 in breast cancer under ionizing radiation. *Front. Cell Dev. Biol.* 9, 772380. doi:10.3389/fcell.2021.772380

Liu, S., Zhang, Q., Liu, W., and Huang, X. (2022a). Prediction of prognosis in patients with endometrial carcinoma and immune microenvironment estimation based on ferroptosis-related genes. *Front. Mol. Biosci.* 9, 916689. doi:10.3389/fmolb.2022.916689

Liu, Y., and Gu, W. (2022). p53 in ferroptosis regulation: the new weapon for the old guardian. *Cell Death Differ.* 29 (5), 895–910. doi:10.1038/s41418-022-00943-y

Lousse, J. C., Defrere, S., Van Langendonckt, A., Gras, J., González-Ramos, R., Colette, S., et al. (2009). Iron storage is significantly increased in peritoneal macrophages of endometriosis patients and correlates with iron overload in peritoneal fluid. *Fertil. Steril.* 91 (5), 1668–1675. doi:10.1016/j.fertnstert.2008.02.103

Ma, S., Dielschneider, R. F., Henson, E. S., Xiao, W., Choquette, T. R., Blankstein, A. R., et al. (2017). Ferroptosis and autophagy induced cell death occur independently after siramesine and lapatinib treatment in breast cancer cells. *PLoS One* 12 (8), e0182921. doi:10.1371/journal.pone.0182921

Mancias, J. D., Pontano Vaites, L., Nissim, S., Biancur, D. E., Kim, A. J., Wang, X., et al. (2015). Ferritinophagy via NCOA4 is required for erythropoiesis and is regulated by iron dependent HERC2-mediated proteolysis. *Elife* 4, e10308. doi:10.7554/eLife.10308

Mancias, J. D., Wang, X., Gygi, S. P., Harper, J. W., and Kimmelman, A. C. (2014). Quantitative proteomics identifies NCOA4 as the cargo receptor mediating ferritinophagy. *Nature* 509 (7498), 105–109. doi:10.1038/nature13148

Markowska, A., Chudecka-Głaz, A., Pityński, K., Baranowski, W., Markowska, J., and Sawicki, W. (2022). Endometrial cancer management in young women. *Cancers (Basel)* 14 (8), 1922. doi:10.3390/cancers14081922

Matsuoka, S., Ballif, B. A., Smogorzewska, A., McDonald, E. R., 3rd, Hurov, K. E., Luo, J., et al. (2007). ATM and ATR substrate analysis reveals extensive protein networks responsive to DNA damage. *Science* 316 (5828), 1160–1166. doi:10.1126/science.1140321

Metherall, J. E., Li, H., and Waugh, K. (1996). Role of multidrug resistance P-glycoproteins in cholesterol biosynthesis. *J. Biol. Chem.* 271 (5), 2634–2640. doi:10.1074/jbc.271.5.2634

Miller, W. L. (2002). Androgen biosynthesis from cholesterol to DHEA. *Mol. Cell Endocrinol.* 198 (1-2), 7–14. doi:10.1016/s0303-7207(02)00363-5

Missaglia, S., Coleman, R. A., Mordente, A., and Tavian, D. (2019). Neutral lipid storage diseases as cellular model to study lipid droplet function. *Cells* 8 (2), 187. doi:10.3390/cells8020187

Montalbetti, N., Simonin, A., Kovacs, G., and Hediger, M. A. (2013). Mammalian iron transporters: Families SLC11 and SLC40. *Mol. Asp. Med.* 34 (2-3), 270–287. doi:10.1016/j.mam.2013.01.002

Moore, H. C., Unger, J. M., Phillips, K. A., Boyle, F., Hitre, E., Porter, D., et al. (2015). Goserelin for ovarian protection during breast-cancer adjuvant chemotherapy. *N. Engl. J. Med.* 372 (10), 923–932. doi:10.1056/NEJMoa1413204

Muhoberac, B. B., and Vidal, R. (2019). Iron, ferritin, hereditary ferritinopathy, and neurodegeneration. *Front. Neurosci.* 13, 1195. doi:10.3389/fnins.2019.01195

Mukherjee, A. G., Wanjari, U. R., Nagarajan, D., K K, V., V, A., P, J. P., et al. (2022). Letrozole: Pharmacology, toxicity and potential therapeutic effects. *Life Sci.* 310, 121074. doi:10.1016/j.lfs.2022.121074

Mungenast, F., and Thalhammer, T. (2014). Estrogen biosynthesis and action in ovarian cancer. *Front. Endocrinol.* 5, 192. doi:10.3389/fendo.2014.00192

Murakami, H., Hayashi, M., Terada, S., and Ohmichi, M. (2023). Medroxyprogesterone acetate-resistant endometrial cancer cells are susceptible to ferroptosis inducers. *Life Sci.* 325, 121753. doi:10.1016/j.lfs.2023.121753

Nabholtz, J. M. (2006). Role of anastrozole across the breast cancer continuum: From advanced to early disease and prevention. *Oncology* 70 (1), 1–12. doi:10.1159/000091180

Ni, W., Mo, H., Liu, Y., Xu, Y., Qin, C., Zhou, Y., et al. (2021). Targeting cholesterol biosynthesis promotes anti-tumor immunity by inhibiting long noncoding RNA SNHG29-mediated YAP activation. *Mol. Ther.* 29 (10), 2995–3010. doi:10.1016/j.ymthe.2021.05.012

Ogawa, M., Hashimoto, K., Kitano, S., Yamashita, S., Toda, A., Nakamura, K., et al. (2023). Estrogen induces genomic instability in high-risk HPV-infected cervix and promotes the carcinogenesis of cervical adenocarcinoma. *Biochem. Biophys. Res. Commun.* 659, 80–90. doi:10.1016/j.bbrc.2023.04.009

Okazaki, F., Matsunaga, N., Hamamura, K., Suzuki, K., Nakao, T., Okazaki, H., et al. (2017). Administering xCT inhibitors based on circadian clock improves antitumor effects. *Cancer Res.* 77 (23), 6603–6613. doi:10.1158/0008-5472.CAN-17-0720

Onal, G., Kutlu, O., Gozuacik, D., and Dokmeci Emre, S. (2017). Lipid droplets in health and disease. *Lipids health Dis.* 16 (1), 128. doi:10.1186/s12944-017-0521-7

Ooko, E., Saeed, M. E., Kadioglu, O., Sarvi, S., Colak, M., Elmasaoudi, K., et al. (2015). Artemisinin derivatives induce iron-dependent cell death (ferroptosis) in tumor cells. *Phytomedicine* 22 (11), 1045–1054. doi:10.1016/j.phymed.2015.08.002

Park, E., and Chung, S. W. (2019). ROS-mediated autophagy increases intracellular iron levels and ferroptosis by ferritin and transferrin receptor regulation. *Cell death Dis.* 10 (11), 822. doi:10.1038/s41419-019-2064-5

Park, S., Lim, W., Jeong, W., Bazer, F. W., Lee, D., and Song, G. (2018). Sideroxylon (Callistemon lanceolatus) suppressed cell proliferation and increased apoptosis in ovarian cancer cells accompanied by mitochondrial dysfunction, the generation of reactive oxygen species, and an increase of lipid peroxidation. *J. Cell Physiol.* 233 (11), 8597–8604. doi:10.1002/jcp.26540

Park, Y., Baik, S., Ho, C., Lin, C. Y., and Chung, S. H. (2021). Progesterone receptor is a haploinsufficient tumor-suppressor gene in cervical cancer. *Mol. Cancer Res.* 19 (1), 42–47. doi:10.1158/1541-7786.MCR-20-0704

Pelletier, G., and El-Alfy, M. (2000). Immunocytochemical localization of estrogen receptors alpha and beta in the human reproductive organs. *J. Clin. Endocrinol. Metab.* 85 (12), 4835–4840. doi:10.1210/jcem.85.12.7029

Petrunak, E. M., DeVore, N. M., Porubsky, P. R., and Scott, E. E. (2014). Structures of human steroidogenic cytochrome P450 17A1 with substrates. *J. Biol. Chem.* 289 (47), 32952–32964. doi:10.1074/jbc.M114.610998

Pfeffer, S. R. (2019). NPC intracellular cholesterol transporter 1 (NPC1)-mediated cholesterol export from lysosomes. *J. Biol. Chem.* 294 (5), 1706–1709. doi:10.1074/jbc.TM118.004165

Pinnix, Z. K., Miller, L. D., Wang, W., D'Agostino, R., Jr, Kute, T., Willingham, M. C., et al. (2010). Ferroportin and iron regulation in breast cancer progression and prognosis. *Sci. Transl. Med.* 2 (43), 43ra56. doi:10.1126/scitranslmed.3001127

Plummer, M., Schiffman, M., Castle, P. E., Maucort-Boulch, D., and Wheeler, C. M. (2007). A 2-year prospective study of human papillomavirus persistence among women with a cytological diagnosis of atypical squamous cells of undetermined significance or low-grade squamous intraepithelial lesion. *J. Infect. Dis.* 195 (11), 1582–1589. doi:10.1086/516784

Riera Leal, A., Ortiz-Lazareno, P. C., Jave-Suarez, L. F., Ramírez De Arellano, A., Aguilar-Lemarroy, A., Ortiz-García, Y. M., et al. (2020). 17β-estradiol-induced mitochondrial dysfunction and Warburg effect in cervical cancer cells allow cell survival under metabolic stress. *Int. J. Oncol.* 56 (1), 33–46. doi:10.3892/ijo.2019.4912

Russell, J. K., Jones, C. K., and Newhouse, P. A. (2019). The role of estrogen in brain and cognitive aging. *Neurother. J. Am. Soc. Exp. Neurother.* 16 (3), 649–665. doi:10.1007/s13311-019-00766-9

Sato, H., Tamba, M., Kuriyama-Matsumura, K., Okuno, S., and Bannai, S. (2000). Molecular cloning and expression of human xCT, the light chain of amino acid transport system xc. *Antioxid. Redox Signal* 2 (4), 665–671. doi:10.1089/ars.2000.2.4-665

Schott, M. B., Weller, S. G., Schulze, R. J., Krueger, E. W., Drizyte-Miller, K., Casey, C. A., et al. (2019). Lipid droplet size directs lipolysis and lipophagy catabolism in hepatocytes. *J. Cell Biol.* 218 (10), 3320–3335. doi:10.1083/jcb.201803153

Sedlacek, S. M. (1988). An overview of megestrol acetate for the treatment of advanced breast cancer. *Semin. Oncol.* 15 (2), 3–13.

Seibt, T. M., Proneth, B., and Conrad, M. (2019). Role of GPX4 in ferroptosis and its pharmacological implication. *Free Radic. Biol. Med.* 133, 144–152. doi:10.1016/j.freeradbiomed.2018.09.014

Shield, K., Ackland, M. L., Ahmed, N., and Rice, G. E. (2009). Multicellular spheroids in ovarian cancer metastases: Biology and pathology. *Gynecol. Oncol.* 113 (1), 143–148. doi:10.1016/j.ygyno.2008.11.032

Shih, C. C., Chou, H. C., Chen, Y. J., Kuo, W. H., Chan, C. H., Lin, Y. C., et al. (2019). Role of PGRMC1 in cell physiology of cervical cancer. *Life Sci.* 231, 116541. doi:10.1016/j.lfs.2019.06.016

Shimada, K., Skouta, R., Kaplan, A., Yang, W. S., Hayano, M., Dixon, S. J., et al. (2016). Global survey of cell death mechanisms reveals metabolic regulation of ferroptosis. *Nat. Chem. Biol.* 12 (7), 497–503. doi:10.1038/nchembio.2079

Siegel, R. L., Miller, K. D., and Jemal, A. (2019). Cancer statistics. *CA Cancer J. Clin.* 69(1), 7–34. doi:10.3322/caac.21551

Singh, B., Ronghe, A. M., Chatterjee, A., Bhat, N. K., and Bhat, H. K. (2013). MicroRNA-93 regulates NRF2 expression and is associated with breast carcinogenesis. *Carcinogenesis* 34 (5), 1165–1172. doi:10.1093/carcin/bgt026

Slomovitz, B. M., Filiaci, V. L., Walker, J. L., Taub, M. C., Finkelstein, K. A., Moroney, J. W., et al. (2022). A randomized phase II trial of everolimus and letrozole or hormonal therapy in women with advanced, persistent or recurrent endometrial carcinoma: A gog foundation study. *Gynecol. Oncol.* 164 (3), 481–491. doi:10.1016/j.ygyno.2021.12.031

Slomovitz, B. M., Jiang, Y., Yates, M. S., Soliman, P. T., Johnston, T., Nowakowski, M., et al. (2015). Phase II study of everolimus and letrozole in patients with recurrent endometrial carcinoma. *J. Clin. Oncol.* 33 (8), 930–936. doi:10.1200/JCO.2014.58.3401

Song, X., Zhu, S., Chen, P., Hou, W., Wen, Q., Liu, J., et al. (2018). AMPK-mediated BECN1 phosphorylation promotes ferroptosis by directly blocking system X(c)(-) activity. *Curr. Biol.* 28 (15), 2388–2399.e5. doi:10.1016/j.cub.2018.05.094

Starek-Świechowicz, B., Budziszewska, B., and Starek, A. (2021). Endogenous estrogens-breast cancer and chemoprevention. *Pharmacol. Rep.* 73 (6), 1497–1512. doi:10.1007/s43440-021-00317-0

Strushkevich, N., MacKenzie, F., Cherkesova, T., Grabovec, I., Usanov, S., and Park, H. W. (2011). Structural basis for pregnenolone biosynthesis by the mitochondrial monooxygenase system. *Proc. Natl. Acad. Sci. U. S. A.* 108 (25), 10139–10143. doi:10.1073/pnas.1019441108

Sui, S., Xu, S., and Pang, D. (2022). Emerging role of ferroptosis in breast cancer: New dawn for overcoming tumor progression. *Pharmacol. Ther.* 232, 107992. doi:10.1016/j.pharmthera.2021.107992

Sun, X., Wang, S., Gai, J., Guan, J., Li, J., Li, Y., et al. (2019). SIRT5 promotes cisplatin resistance in ovarian cancer by suppressing DNA damage in a ROS-dependent manner via regulation of the Nrf2/HO-1 pathway. *Front. Oncol.* 9, 754. doi:10.3389/fonc.2019.00754

Tan, J. S., Seow, C. J., Goh, V. J., and Silver, D. L. (2014). Recent advances in understanding proteins involved in lipid droplet formation, growth and fusion. *J. Genet. genomics = Yi chuan xue bao* 41 (5), 251–259. doi:10.1016/j.jgg.2014.03.003

Tang, D., and Kroemer, G. (2020). *Ferroptosis. Curr. Biol. Cb.* 30 (21), R1292–R1297. doi:10.1016/j.cub.2020.09.068

Taylor, W. R., Fedorka, S. R., Gad, I., Shah, R., Alqahtani, H. D., Koranne, R., et al. (2019). Small-molecule ferroptotic agents with potential to selectively target cancer stem cells. *Sci. Rep.* 9 (1), 5926. doi:10.1038/s41598-019-42251-5

Tesfay, L., Paul, B. T., Konstorum, A., Deng, Z., Cox, A. O., Lee, J., et al. (2019). Stearoyl-CoA desaturase 1 protects ovarian cancer cells from ferroptotic cell death. *Cancer Res.* 79 (20), 5355–5366. doi:10.1158/0008-5472.CAN-19-0369

Torre, L. A., Trabert, B., DeSantis, C. E., Miller, K. D., Samimi, G., Runowicz, C. D., et al. (2018). Ovarian cancer statistics. *CA Cancer J. Clin.* 68(4):284–296. doi:10.3322/caac.21456

Trabert, B., Sherman, M. E., Kannan, N., and Stanczyk, F. Z. (2020). Progesterone and breast cancer. *Endocr. Rev.* 41 (2), 320–344. doi:10.1210/endrev/bnz001

Tsai, S. Y., Carlstedt-Duke, J., Weigel, N. L., Dahlman, K., Gustafsson, J. A., Tsai, M. J., et al. (1988). Molecular interactions of steroid hormone receptor with its enhancer element: Evidence for receptor dimer formation. *Cell* 55 (2), 361–369. doi:10.1016/0092-8674(88)90059-1

Tseng, L., Tang, M., Wang, Z., and Mazella, J. (2003). Progesterone receptor (hPR) upregulates the fibronectin promoter activity in human decidual fibroblasts. *DNA Cell Biol.* 22 (10), 633–640. doi:10.1089/104454903770238102

Van Langendonckt, A., Casanas-Roux, F., and Donnez, J. (2002). Iron overload in the peritoneal cavity of women with pelvic endometriosis. *Fertil. Steril.* 78 (4), 712–718. doi:10.1016/s0015-0282(02)03346-0

Van Langendonckt, A., Casanas-Roux, F., Eggermont, J., and Donnez, J. (2004). Characterization of iron deposition in endometriotic lesions induced in the nude mouse model. *Hum. Reprod.* 19 (6), 1265–1271. doi:10.1093/humrep/deh182

Vasan, N., Toska, E., and Scaltriti, M. (2019). Overview of the relevance of PI3K pathway in HR-positive breast cancer. *Ann. Oncol.* 30 (10), x3–x11. doi:10.1093/annonc/mdz281

Vina, J., and Borras, C. (2010). Women live longer than men: Understanding molecular mechanisms offers opportunities to intervene by using estrogenic compounds. *Antioxidants redox Signal.* 13 (3), 269–278. doi:10.1089/ars.2009.2952

Viswanathan, V. S., Ryan, M. J., Dhruv, H. D., Gill, S., Eichhoff, O. M., Seashore-Ludlow, B., et al. (2017). Dependency of a therapy-resistant state of cancer cells on a lipid peroxidase pathway. *Nature* 547 (7664), 453–457. doi:10.1038/nature23007

von Hagens, C., Walter-Sack, I., Goeckenjan, M., Osburg, J., Storch-Hagenlocher, B., Sertel, S., et al. (2017). Prospective open uncontrolled phase I study to define a well-tolerated dose of oral artesunate as add-on therapy in patients with metastatic breast cancer (ARTIC M33/2). *Breast Cancer Res. Treat.* 164 (2), 359–369. doi:10.1007/s10549-017-4261-1

Wan, Y., Song, Y., Chen, J., Kong, J., Gu, C., Huang, J., et al. (2022). Upregulated fibulin-1 increased endometrial stromal cell viability and migration by repressing EFEMP1-dependent ferroptosis in endometriosis. *Biomed. Res. Int.* 2022, 4809415. doi:10.1155/2022/4809415

Wang, C., Zeng, J., Li, L. J., Xue, M., and He, S. L. (2021a). Cdc25A inhibits autophagy-mediated ferroptosis by upregulating ErbB2 through PKM2 dephosphorylation in cervical cancer cells. *Cell death Dis.* 12 (11), 1055. doi:10.1038/s41419-021-04342-y

Wang, K., Jiang, J., Lei, Y., Zhou, S., Wei, Y., and Huang, C. (2019a). Targeting metabolic-redox circuits for cancer therapy. *Trends Biochem. Sci.* 44 (5), 401–414. doi:10.1016/j.tibs.2019.01.001

Wang, T., Gong, M., Cao, Y., Zhao, C., Lu, Y., Zhou, Y., et al. (2022a). Persistent ferroptosis promotes cervical squamous intraepithelial lesion development and oncogenesis by regulating KRAS expression in patients with high risk-HPV infection. *Cell death Discov.* 8 (1), 201. doi:10.1038/s41420-022-01013-5

Wang, T., Wei, Q., Liang, L., Tang, X., Yao, J., Lu, Y., et al. (2020b). OSBPL2 is required for the binding of COPB1 to ATGL and the regulation of lipid droplet lipolysis. *iScience* 23 (7), 101252. doi:10.1016/j.isci.2020.101252

Wang, W., Green, M., Choi, J. E., Gijón, M., Kennedy, P. D., Johnson, J. K., et al. (2019b). CD8(+) T cells regulate tumour ferroptosis during cancer immunotherapy. *Nature* 569 (7755), 270–274. doi:10.1038/s41586-019-1170-y

Wang, W., Zhang, J., Wang, Y., Xu, Y., and Zhang, S. (2022b). Identifies microtubule-binding protein CSPP1 as a novel cancer biomarker associated with ferroptosis and tumor microenvironment. *Comput. Struct. Biotechnol. J.* 20, 3322–3335. doi:10.1016/j.csbj.2022.06.046

Wang, X., Xu, S., Zhang, L., Cheng, X., Yu, H., Bao, J., et al. (2021b). Vitamin C induces ferroptosis in anaplastic thyroid cancer cells by ferritinophagy activation. *Biochem. Biophys. Res. Commun.* 551, 46–53. doi:10.1016/j.bbrc.2021.02.126

Wang, Y., Jing, F., and Wang, H. (2022c). Role of Exemestane in the treatment of estrogen-receptor-positive breast cancer: A narrative review of recent evidence. *Adv. Ther.* 39 (2), 862–891. doi:10.1007/s12325-021-01924-2

Wang, Y., Liu, Y., Liu, J., Kang, R., and Tang, D. (2020a). NEDD4L-mediated LTF protein degradation limits ferroptosis. *Biochem. biophysical Res. Commun.* 531 (4), 581–587. doi:10.1016/j.bbrc.2020.07.032

Warner, G. J., Berry, M. J., Moustafa, M. E., Carlson, B. A., Hatfield, D. L., and Faust, J. R. (2000). Inhibition of selenoprotein synthesis by selenocysteine tRNA[Ser]Sec lacking isopentenyladenosine. *J. Biol. Chem.* 275 (36), 28110–28119. doi:10.1074/jbc.M001280200

Wei, S., Yu, Z., Shi, R., An, L., Zhang, Q., Zhang, Q., et al. (2022). GPX4 suppresses ferroptosis to promote malignant progression of endometrial carcinoma via transcriptional activation by ELK1. *BMC Cancer* 22 (1), 881. doi:10.1186/s12885-022-09986-3

Wei, X., Yi, X., Zhu, X. H., and Jiang, D. S. (2020). Posttranslational modifications in ferroptosis. *Oxid. Med. Cell Longev.* 2020, 8832043. doi:10.1155/2020/8832043

Weijiao, Y., Fuchun, L., Mengjie, C., Xiaoqing, Q., Hao, L., Yuan, L., et al. (2021). Immune infiltration and a ferroptosis-associated gene signature for predicting the prognosis of patients with endometrial cancer. *Aging* 13 (12), 16713–16732. doi:10.18632/aging.203190

Wu, N., Zhang, X., Wang, Z., Fang, C., and Li, H. (2023). Progesterone prevents HGSOC by promoting precancerous cell pyroptosis via inducing fibroblast paracrine. *iScience* 26 (4), 106523. doi:10.1016/j.isci.2023.106523

Wu, N. Y., Huang, H. S., Chao, T. H., Chou, H. M., Fang, C., Qin, C. Z., et al. (2017). Progesterone prevents high-grade serous ovarian cancer by inducing necroptosis of p53-defective fallopian tube epithelial cells. *Cell Rep.* 18 (11), 2557–2565. doi:10.1016/j.celrep.2017.02.049

Wu, R., Hendrix-Lucas, N., Kuick, R., Zhai, Y., Schwartz, D. R., Akyol, A., et al. (2007). Mouse model of human ovarian endometrioid adenocarcinoma based on somatic defects in the Wnt/beta-catenin and PI3K/Pten signaling pathways. *Cancer Cell* 11 (4), 321–333. doi:10.1016/j.ccr.2007.02.016

Xu, X. L., Huang, Z. Y., Yu, K., Li, J., Fu, X. W., and Deng, S. L. (2022). Estrogen biosynthesis and signal transduction in ovarian disease. *Front. Endocrinol. (Lausanne).* 13, 827032. doi:10.3389/fendo.2022.827032

Yamaguchi, K., Mandai, M., Toyokuni, S., Hamanishi, J., Higuchi, T., Takakura, K., et al. (2008). Contents of endometriotic cysts, especially the high concentration of free iron, are a possible cause of carcinogenesis in the cysts through the iron-induced persistent oxidative stress. *Clin. cancer Res.* 14 (1), 32–40. doi:10.1158/1078-0432.CCR-07-1614

Yang, G., Nowsheen, S., Aziz, K., and Georgakilas, A. G. (2013). Toxicity and adverse effects of Tamoxifen and other anti-estrogen drugs. *Pharmacol. Ther.* 139 (3), 392–404. doi:10.1016/j.pharmthera.2013.05.005

Yang, L., Wang, H., Yang, X., Wu, Q., An, P., Jin, X., et al. (2020). Auranofin mitigates systemic iron overload and induces ferroptosis via distinct mechanisms. *Signal Transduct. Target Ther.* 5 (1), 138. doi:10.1038/s41392-020-00253-0

Yang, W. S., SriRamaratnam, R., Welsch, M. E., Shimada, K., Skouta, R., Viswanathan, V. S., et al. (2014). Regulation of ferroptotic cancer cell death by GPX4. *Cell* 156 (1-2), 317–331. doi:10.1016/j.cell.2013.12.010

Yang, W. S., and Stockwell, B. R. (2008). Synthetic lethal screening identifies compounds activating iron-dependent, nonapoptotic cell death in oncogenic-RAS-harboring cancer cells. *Chem. Biol.* 15 (3), 234–245. doi:10.1016/j.chembiol.2008.02.010

Yao, P., and Fox, P. L. (2013). Aminoacyl-tRNA synthetases in medicine and disease. *EMBO Mol. Med.* 5 (3), 332–343. doi:10.1002/emmm.201100626

Ye, L. F., Chaudhary, K. R., Zandkarimi, F., Harken, A. D., Kinslow, C. J., Upadhyayula, P. S., et al. (2020). Radiation-induced lipid peroxidation triggers ferroptosis and synergizes with ferroptosis inducers. *ACS Chem. Biol.* 15 (2), 469–484. doi:10.1021/acschembio.9b00939

Ye, R. R., Chen, B. C., Lu, J. J., Ma, X. R., and Li, R. T. (2021). Phosphorescent rhenium(I) complexes conjugated with artesunate: Mitochondrial targeting and apoptosis-ferroptosis dual induction. *J. Inorg. Biochem.* 223, 111537. doi:10.1016/j.jinorgbio.2021.111537

Yoshida, G. J. (2018). Emerging roles of Myc in stem cell biology and novel tumor therapies. *J. Exp. Clin. Cancer Res.* 37 (1), 173. doi:10.1186/s13046-018-0835-y

Yoshida, G. J. (2015). Metabolic reprogramming: The emerging concept and associated therapeutic strategies. *J. Exp. Clin. Cancer Res.* 34, 111. doi:10.1186/s13046-015-0221-y

Yoshimoto, F. K., Gonzalez, E., Auchus, R. J., and Guengerich, F. P. (2016). Mechanism of 17α,20-lyase and new hydroxylation reactions of human cytochrome P450 17A1: 18O labeling and oxygen surrogate evidence for a role of a perferryl oxygen. *J. Biol. Chem.* 291 (33), 17143–17164. doi:10.1074/jbc.M116.732966

You, J. H., Lee, J., and Roh, J. L. (2021a). PGRMC1-dependent lipophagy promotes ferroptosis in paclitaxel-tolerant persister cancer cells. *J. Exp. Clin. Cancer Res.* 40 (1), 350. doi:10.1186/s13046-021-02168-2

You, Y., Fan, Q., Huang, J., Wu, Y., Lin, H., and Zhang, Q. (2021b). Ferroptosis-related gene signature promotes ovarian cancer by influencing immune infiltration and invasion. *J. Oncol.* 2021, 9915312. doi:10.1155/2021/9915312

Younes, M., and Honma, N. (2011). Estrogen receptor β. *Arch. Pathol. Lab. Med.* 135 (1), 63–66. doi:10.5858/2010-0448-RAR.1

Yu, H., Guo, P., Xie, X., Wang, Y., and Chen, G. (2017). Ferroptosis, a new form of cell death, and its relationships with tumourous diseases. *J. Cell Mol. Med.* 21 (4), 648–657. doi:10.1111/jcmm.13008

Yu, H., Yang, C., Jian, L., Guo, S., Chen, R., Li, K., et al. (2019). Sulfasalazine-induced ferroptosis in breast cancer cells is reduced by the inhibitory effect of estrogen receptor on the transferrin receptor. *Oncol. Rep.* 42 (2), 826–838. doi:10.3892/or.2019.7189

Yu, K., Huang, Z. Y., Xu, X. L., Li, J., Fu, X. W., and Deng, S. L. (2022). Estrogen receptor function: Impact on the human endometrium. *Front. Endocrinol. (Lausanne).* 13, 827724. doi:10.3389/fendo.2022.827724

Yuan, H., Li, X., Zhang, X., Kang, R., and Tang, D. (2016). Identification of ACSL4 as a biomarker and contributor of ferroptosis. *Biochem. Biophys. Res. Commun.* 478 (3), 1338–1343. doi:10.1016/j.bbrc.2016.08.124

Zechner, R., Zimmermann, R., Eichmann, T. O., Kohlwein, S. D., Haemmerle, G., Lass, A., et al. (2012). FAT SIGNALS-lipases and lipolysis in lipid metabolism and signaling. *Cell metab.* 15 (3), 279–291. doi:10.1016/j.cmet.2011.12.018

Zhang, X., Sui, S., Wang, L., Li, H., Zhang, L., Xu, S., et al. (2020). Inhibition of tumor propellant glutathione peroxidase 4 induces ferroptosis in cancer cells and enhances anticancer effect of cisplatin. *J. Cell Physiol.* 235 (4), 3425–3437. doi:10.1002/jcp.29232

Zhang, Y., Shi, J., Liu, X., Feng, L., Gong, Z., Koppula, P., et al. (2018). BAP1 links metabolic regulation of ferroptosis to tumour suppression. *Nat. Cell Biol.* 20 (10), 1181–1192. doi:10.1038/s41556-018-0178-0

Zhang, Y., Swanda, R. V., Nie, L., Liu, X., Wang, C., Lee, H., et al. (2021a). mTORC1 couples cyst(e)ine availability with GPX4 protein synthesis and ferroptosis regulation. *Nat. Commun.* 12 (1), 1589. doi:10.1038/s41467-021-21841-w

Zhang, Y., Xia, M., Zhou, Z., Hu, X., Wang, J., Zhang, M., et al. (2021b). p53 promoted ferroptosis in ovarian cancer cells treated with human serum incubated-superparamagnetic iron oxides. *Int. J. nanomedicine* 16, 283–296. doi:10.2147/IJN.S282489

Zhang, Y. Y., Ni, Z. J., Elam, E., Zhang, F., Thakur, K., Wang, S., et al. (2021c). Juglone, a novel activator of ferroptosis, induces cell death in endometrial carcinoma Ishikawa cells. *Food & Funct.* 12 (11), 4947–4959. doi:10.1039/d1fo00790d

Zhang, Z., Huang, H., Feng, F., Wang, J., and Cheng, N. (2019). A pilot study of gonadotropin-releasing hormone agonist combined with aromatase inhibitor as fertility-sparing treatment in obese patients with endometrial cancer. *J. Gynecol. Oncol.* 30 (4), e61. doi:10.3802/jgo.2019.30.e61

Zhao, G., Cardenas, H., and Matei, D. (2019). Ovarian cancer-why lipids matter. *Cancers (Basel)* 11 (12), 1870. doi:10.3390/cancers11121870

Zhao, H., Xu, Y., and Shang, H. (2022a). Ferroptosis: A new promising target for ovarian cancer therapy. *Int. J. Med. Sci.* 19 (13), 1847–1855. doi:10.7150/ijms.76480

Zhao, X., Niu, J., Shi, C., and Liu, Z. (2022b). Levonorgestrel-releasing intrauterine device plus metformin, or megestrol acetate plus metformin for fertility-sparing treatment of atypical endometrial hyperplasia and early endometrial carcinoma: A prospective, randomized, blind-endpoint design trial protocol. *Reprod. Health* 19 (1), 206. doi:10.1186/s12978-022-01513-8

Zhao, Y., Ruan, X., Cheng, J., Xu, X., Gu, M., and Mueck, A. O. (2023). PGRMC1 promotes triple-negative breast cancer cell growth via suppressing ferroptosis. *Climacteric* 26 (2), 135–142. doi:10.1080/13697137.2023.2170225

Zhou, W. B., Ding, Q., Chen, L., Liu, X. A., and Wang, S. (2011). Toremifene is an effective and safe alternative to tamoxifen in adjuvant endocrine therapy for breast cancer: Results of four randomized trials. *Breast Cancer Res. Treat.* 128 (3), 625–631. doi:10.1007/s10549-011-1556-5

Frontiers in
Molecular Biosciences

Explores biological processes in living organisms on a molecular scale

Focuses on the molecular mechanisms underpinning and regulating biological processes in organisms across all branches of life.

Discover the latest Research Topics

See more →

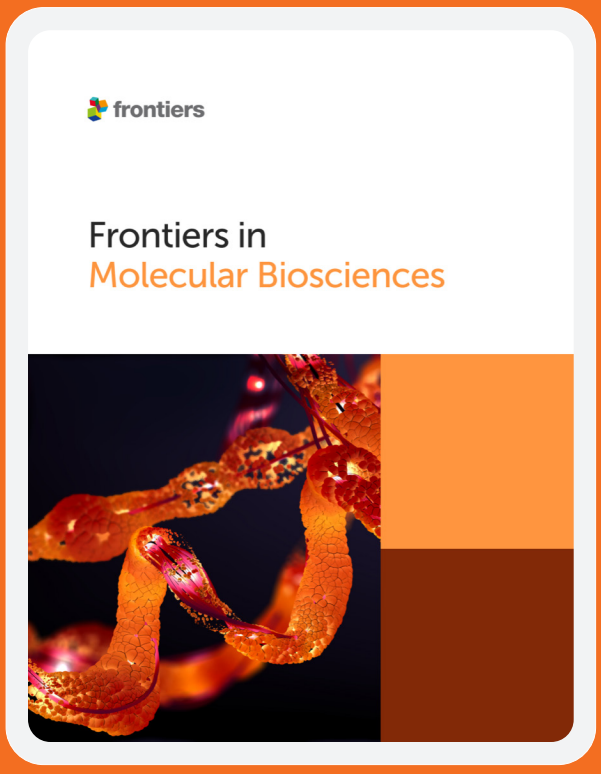

Frontiers

Avenue du Tribunal-Fédéral 34
1005 Lausanne, Switzerland
frontiersin.org

Contact us

+41 (0)21 510 17 00
frontiersin.org/about/contact